# Insights in

# neuro-oncology and neurosurgical oncology 2021

**Edited by**
David D. Eisenstat and Erik P. Sulman

**Published in**
Frontiers in Oncology

## About Frontiers

Frontiers is more than just an open access publisher of scholarly articles: it is a pioneering approach to the world of academia, radically improving the way scholarly research is managed. The grand vision of Frontiers is a world where all people have an equal opportunity to seek, share and generate knowledge. Frontiers provides immediate and permanent online open access to all its publications, but this alone is not enough to realize our grand goals.

## Frontiers journal series

The Frontiers journal series is a multi-tier and interdisciplinary set of open-access, online journals, promising a paradigm shift from the current review, selection and dissemination processes in academic publishing. All Frontiers journals are driven by researchers for researchers; therefore, they constitute a service to the scholarly community. At the same time, the *Frontiers journal series* operates on a revolutionary invention, the tiered publishing system, initially addressing specific communities of scholars, and gradually climbing up to broader public understanding, thus serving the interests of the lay society, too.

## Dedication to quality

Each Frontiers article is a landmark of the highest quality, thanks to genuinely collaborative interactions between authors and review editors, who include some of the world's best academicians. Research must be certified by peers before entering a stream of knowledge that may eventually reach the public - and shape society; therefore, Frontiers only applies the most rigorous and unbiased reviews. Frontiers revolutionizes research publishing by freely delivering the most outstanding research, evaluated with no bias from both the academic and social point of view. By applying the most advanced information technologies, Frontiers is catapulting scholarly publishing into a new generation.

## What are Frontiers Research Topics?

Frontiers Research Topics are very popular trademarks of the *Frontiers journals series*: they are collections of at least ten articles, all centered on a particular subject. With their unique mix of varied contributions from Original Research to Review Articles, Frontiers Research Topics unify the most influential researchers, the latest key findings and historical advances in a hot research area.

Find out more on how to host your own Frontiers Research Topic or contribute to one as an author by contacting the Frontiers editorial office: frontiersin.org/about/contact

# Insights in neuro-oncology and neurosurgical oncology: 2021

**Topic editors**

David D. Eisenstat — Murdoch Childrens Research Institute, Royal Children's Hospital, Australia

Erik P. Sulman — New York University, United States

# Table of
# contents

**frontiers** | Frontiers in Oncology

# Editorial: Insights in neuro-oncology and neurosurgical oncology: 2021

Erik P. Sulman[1,2,3,4]* and David D. Eisenstat[1,5,6,7]*

[1]Section of Neuro-oncology & Neurosurgical Oncology, Frontiers in Oncology and Frontiers in Neurology, Lausanne, Switzerland, [2]Department of Radiation Oncology, NYU Grossman School of Medicine, New York, NY, United States, [3]Brain and Spine Tumor Center, Laura and Isaac Perlmutter Cancer Center, New York NY, United States, [4]Department of Radiation Oncology, NYU Langone Health, New York, NY, United States, [5]Children's Cancer Centre, Royal Children's Hospital, Parkville, VIC, Australia, [6]Department of Stem Cell Biology, Murdoch Children's Research Institute, Parkville, VIC, Australia, [7]Department of Paediatrics, University of Melbourne, Parkville, VIC, Australia

Editorial on the Research Topic
Insights in neuro-oncology and neurosurgical oncology: 2021

The Frontiers Research Topic titled ***Insights in Neuro-Oncology and Neurosurgical Oncology: 2021*** includes a collection of 18 articles published from May 2021 to March 2022. The topics summarize our understanding of as well as key advances in the field of Neuro-Oncology, covering a variety of subjects focused on primary central nervous system (CNS) tumors, such as biomarkers and diagnostics, model systems, anatomic and surgical considerations, and novel approaches to therapeutics. A comprehensive review of brain metastases is also included.

## Insights into biomarkers and diagnostics in neuro-oncology

In 2018, Capper et al. introduced DNA methylation profiling for CNS tumors, significantly improving our capacity to correctly categorize and diagnose brain tumors in children and adults (1). More recently, the fifth edition of the World Health Organization (WHO) Classification of Tumours of the Central Nervous System was published, integrating tumor histology, tumor grade (where applicable), tumor markers, and molecular genetics (2).

Zreik et al. studied disparities in the reporting of 1p/19 co-deletions (codel) in oligodendroglial tumors before and after the introduction of the fourth version of the WHO CNS classification in 2016 through an analysis of the National Cancer Database. Interestingly, the reported rate of codel testing increased from ~45% in 2011 to nearly 60% in 2017. Furthermore, those with a reported test result received adjuvant therapy

with an OR of 1.73. However, significant disparities were observed by geography as well as ethnicity and race.

Cell surface markers are characterized in two separate studies. Lu et al. investigate the impact of tumor purity and focus on the role of CD3E, a novel immune biomarker, in the tumor microenvironment of low-grade gliomas (LGG) of adults using the TCGA and GEO databases, with validation in a real-world cohort of 100 Asian patients. The prognostic utility of the cell surface expressed and well-described glioma stem cell marker, CD133, in adult high-grade gliomas (HGG) is assessed in a systematic review provided by Shadbad et al. The authors conclude that using a 10% cut-off, overexpression of CD133 protein was associated with a very poor progression-free survival (PFS) linked to tumor progression/recurrence.

In an interesting report, Prasad et al. describe a multi-generational family with germline BAP1-inactivating mutations resulting in meningiomas with rhabdoid features. Rhabdoid meningiomas are classified as WHO Grade III meningiomas and have a variable prognosis. Germline mutations of the tumor suppressor gene BAP1 are linked to a rare tumor predisposition syndrome and affected patients are at very high risk of melanoma and mesothelioma. The authors recommend that germline testing be offered for patients with meningiomas harboring BAP1-inactivating mutations.

## Neuroanatomic and neurosurgical insights

In this group of six manuscripts, insights were provided into diverse topics regarding specific neuroanatomic considerations, imaging adjuncts, and localized therapies. Skardelly et al.s assess the extent of resection (EOR) and residual tumor volume in a retrospective, multicenter cohort study of adult patients with glioblastoma (GBM). The authors developed a nomogram validated in a separate patient cohort that can be applied in clinical practice and incorporated into prospective non-randomized clinical trials where EOR could introduce bias in the outcomes concerning PFS and overall survival (OS). Feng et al. apply Enhanced Recovery After Surgery (ERAS) principles regarding rehabilitation, quality of life, and survivorship in 50 brain tumor patients experiencing craniotomy. Although postoperative recovery was enhanced in this patient cohort, the authors recommend multicenter collaborative studies in order to confirm that ERAS can enhance patient prognosis while concomitantly reducing postoperative complications.

Surgical approaches to tumors located in in or originating from the fourth ventricle were the focus of Onorini et al., who studied 92 consecutive pediatric patients treated at a single center by one pediatric neurosurgeon who used either telovelar (51 patients) or transvermian (41 patients) surgical approaches to tumor resection. In this single-center study, a relatively low rate (11%) of cerebellar

mutism (also referred to as posterior fossa syndrome) was noted, and there were no significant differences between either surgical strategy. The authors advocate training in and the application of either neurosurgical approach to tumors localized to the fourth ventricle, individualized to tumor anatomy, infiltration of the vermis, and lateral or upwards extension. Li et al. discuss advances in the neurosurgical approach to parasellar meningiomas, incorporating preoperative imaging and protection of the cerebral arteries and their perforating branches, which can be compressed, encased, or, rarely, invaded by these extra-axial tumors. The authors promote the use of a bidirectional dissection technique.

Gao et al. present an interesting manuscript regarding glioma-associated epilepsy (GAE) and the emerging application of radiomics in neuro-oncology in a cohort of 166 adult patients with frontal gliomas. In addition to identifying 17 specific MR imaging features, the authors also consider the influence of patient age and tumor grade in an integrated clinical-radiomics predictive model.

The application of laser interstitial thermal therapy (LITT) as a minimally invasive adjunct to surgery is explored by Noh et al.. During LITT, continuous real-time temperature mapping was conducted using magnetic resonance thermometry. The authors studied 17 patients, paying specific attention to the contribution of signal dropout, an artifact of biopsy that often precedes LITT. Within this group, 6 of the 17 patients had biopsies with artifacts due to the presence of blood or air that affected the thresholds of thermal damage at tumor borders.

## Considerations on pathogenesis and disease modeling

Two publications included in this article collection focus on GBM tumor heterogeneity and the subventricular zone (SVZ), respectively. Comba et al. explore spatiotemporal heterogeneity in glioblastomas in a timely review of the influence of the molecular genetic features of the tumor, the tumor microenvironment (including non-transformed neuronal and glial cells, immune, mesenchymal, and stem cells), and dynamic qualities within the tumor itself. The authors discuss the contributions of more recently adopted platforms including machine learning in histopathology, single-cell transcriptomics, and spatial transcriptomics. Data acquisition using these technologies will better inform our preclinical models with translational implications, including high-throughput drug screening.

Beiriger et al. compare neural stem/precursor cells (NSC) resident to the adult SVZ and glioma stem cells (GSC), which are both implicated in the pathogenesis of gliomas. The authors review several in vitro and in vivo model systems and include human brain and/or GBM organoids as important emerging model systems in the study of the contributions of NSC and

GSC, thereby reframing our approaches toward improving preclinical translational research in the laboratory.

## Considerations for the use of tumor treating fields in neuro-oncology

Two articles discuss insights into the efficacy of tumor treating fields (TTF), an FDA-approved treatment adjunct for adults with glioblastoma, which is being explored for other treatment indications in children and adults with brain and other solid tumors. The effect of the corticosteroid dexamethasone (DXM) on TTF is addressed by Linder et al. The authors use GBM cell lines treated with DXM and either radiotherapy or TTF *in vitro*. In addition, they perform a retrospective analysis of GBM patients who received TTF +/- DXM. The authors conclude that concomitant DXM with TTF did not affect the efficacy of TTF *in vitro* or in clinical practice. The impact of the ongoing COVID-19 pandemic on the use of TTF is the focus of a separate contribution by Gatson et al., who summarize an expert panel discussion, which took place during the early months of the pandemic. Since TTF is administered by a portable device that is used in the home and is not known for additional immunosuppressive effects over and above the intrinsic effects of the tumor itself, the authors recommend that specific patient populations, especially the elderly and those with co-morbidities, may benefit from TTF-mediated therapies.

## Treatment advances using viral gene, immune checkpoint, and CAR T-cell mediated therapies

A major focus in neuro-oncology reflects ongoing efforts to advance our understanding and utilization of therapies that harness the immune system. Viral-mediated gene therapies for GBM are reviewed by Li et al. The authors summarize several viral vectors and their potential or current use in viral gene therapy, including retroviruses, lentiviruses, adenoviruses, herpes simplex virus (HSV), and oncolytic viruses; many of these vectors are under active investigation in clinical trials in neuro-oncology. Combined immune checkpoint inhibitor therapy applied to meningeal melanoma, a relatively uncommon tumor entity belonging to the class of primary melanocytic tumors of the CNS, is presented by Burgos et al.

Burns et al. summarize current efforts in the laboratory and the clinic to use CAR T-cell therapies, which have already been adopted for some hematopoietic malignancies expressing CD19, in the treatment of very challenging pediatric brain tumors, especially diffuse midline gliomas with Histone H3K27 alterations, which are relatively prevalent in children. Methods of application (intraventricular, intra-tumoral, intravenous), CAR T-cell design,

target identification, and characterization, targeting one or more antigens (i.e., multivalent CARs), cytokine release syndrome and other CAR T-cell associated toxicities, and combinatorial therapies with kinase and other small molecule inhibitors and/or immune checkpoint inhibitors are all under active investigation.

## Insights into brain metastases

Finally, Li et al. provide a comprehensive review of brain metastases (intracranial metastatic disease or IMD) in adults for which the application of improved molecular genetics-based diagnostics, neuroimaging, minimally invasive surgery, novel local therapies, improvements in radiation therapy (stereotactic radiosurgery, hippocampal sparing whole brain radiotherapy, etc.), neurocognitive rehabilitation strategies, and the application of either targeted and/or immunotherapies offer some hope to those patients with very poor prognoses overall. Specific sections of this review article focus on breast cancer, NSCLC, and melanoma, given their relative contributions to IMD in adults.

## Concluding remarks

Despite significant progress in neuro-oncology translational and clinical research, we have yet to fully realize the potential of improved diagnostic platforms; advances in therapy from surgery; radiation; and other local or systemic therapies, including targeted, viral gene, or immunotherapies. Given the high priority of this combined effort, the neuro-oncology community has mapped out an ambitious agenda for improving both the duration and quality of survival for our pediatric and adult patients with primary or secondary tumors of the central nervous system. However, we will have to continue our collective journey to achieve these worthy goals.

## Author contributions

ES and DE conceptualized and co-wrote the manuscript. Both authors approved the final version.

## Funding

## Conflict of interest

The authors declare that the editorial was conducted in the absence of any commercial or financial relationships that could be construed as a potential conflict of interest.

## Publisher's note

All claims expressed in this article are solely those of the authors and do not necessarily represent those of their affiliated organizations, or those of the publisher, the editors and the reviewers. Any product that may be evaluated in this article, or claim that may be made by its manufacturer, is not guaranteed or endorsed by the publisher.

## References

1. Capper D, Jones D, Sill M, Hovestadt V, Schrimpf D, Sturm D, et al. DNA Methylation-based classification of central nervous system tumours. *Nature* (2018) 555(7697):469–74. doi: 10.1038/nature26000

2. Louis DN, Perry A, Wesseling P, Brat DJ, Cree IA, Figarella-Branger D, et al. The 2021 WHO classification of tumors of the central nervous system: a summary. *Neuro Oncol* (2021) 23(8):1231–51. doi: 10.1093/neuonc/noab106

# Tumor Treating Fields for Glioblastoma Therapy During the COVID-19 Pandemic

Na Tosha N. Gatson[1,2], Jill Barnholtz-Sloan[3], Jan Drappatz[4], Roger Henriksson[5], Andreas F. Hottinger[6], Piet Hinoul[7], Carol Kruchko[8], Vinay K. Puduvalli[9], David D. Tran[10], Eric T. Wong[11] and Martin Glas[12]*

[1] Division of Neuro-Oncology, Department of Neurology, Geisinger Health, Neuroscience & Cancer Institutes, Danville, PA & Geisinger Commonwealth School of Medicine, Scranton, PA, United States, [2] Neuro-Oncology, Banner MD Anderson Cancer Center, Phoenix, AZ, United States, [3] Department of Population and Quantitative Health Sciences, Case Western Reserve University School of Medicine & Research and Education, University Hospitals of Cleveland, Cleveland, OH, United States, [4] Hillman Cancer Center, Department of Medicine and Neurology, University of Pittsburgh, Pittsburgh, PA, United States, [5] Department of Radiation Sciences & Oncology at the University of Umeå, Umeå, Sweden, [6] Departments of Clinical Neurosciences & Oncology, Lausanne University Hospital (CHUV), Lausanne, Switzerland, [7] Global Medical Affairs, Novocure Inc., New York, NY, United States, [8] Central Brain Tumor Registry of the United States (CBTRUS), Hinsdale, IL, United States, [9] Department of Neuro-Oncology, The University of Texas MD Anderson Cancer Center, Houston, TX, United States, [10] Lillian S. Wells Department of Neurosurgery and Preston A. Wells, Jr. Brain Tumor Center at the McKnight Brain Institute of the University of Florida College of Medicine, Gainesville, FL, United States, [11] Department of Neurology, Beth Israel Deaconess Medical Center, Harvard Medical School, Boston, MA, United States, [12] Division of Clinical Neurooncology, Department of Neurology and German Cancer Consortium (DKTK) Partner Site, University Hospital Essen, University Duisburg-Essen, Essen, Germany

**Background:** The COVID-19 pandemic has placed excessive strain on health care systems and is especially evident in treatment decision-making for cancer patients. Glioblastoma (GBM) patients are among the most vulnerable due to increased incidence in the elderly and the short survival time. A virtual meeting was convened on May 9, 2020 with a panel of neuro-oncology experts with experience using Tumor Treating Fields (TTFields). The objective was to assess the risk-to-benefit ratio and provide guidance for using TTFields in GBM during the COVID-19 pandemic.

**Panel Discussion:** Topics discussed included support and delivery of TTFields during the COVID-19 pandemic, concomitant use of TTFields with chemotherapy, and any potential impact of TTFields on the immune system in an intrinsically immunosuppressed GBM population. Special consideration was given to TTFields' use in elderly patients and in combination with radiotherapy regimens. Finally, the panel discussed the need to better capture data on COVID-19–positive brain tumor patients to analyze longitudinal outcomes and changes in treatment decision-making during the pandemic.

**Expert Opinion:** TTFields is a portable home-use device which can be managed via telemedicine and safely used in GBM patients during the COVID-19 pandemic. TTFields has no known immunosuppressive effects which is important during a crisis where other treatment methods might be limited, especially for elderly patients with multiple co-morbidities. It is too early to estimate the full impact of COVID-19 on the global healthcare

system and on patient outcomes and the panel strongly recommended collaboration with existing cancer COVID-19 registries to follow CNS tumor patients.

**Keywords: COVID-19, tumor treating fields, glioblastoma, recurrent glioblastoma, elderly**

## INTRODUCTION

The global case-fatality ratio for COVID-19 in confirmed cases was 2.1% as of January 11, 2021 (1), and the rate increases to 22.4% in the cancer population (2). GBM patients are considered a vulnerable patient population during the ongoing COVID-19 pandemic mainly due to the increased incidence of GBM in the elderly population (3), treatment related immunosuppression, and the requirement for frequent hospital visits. Importantly, the >65-year-old age group is expected to increase over the next two decades in the USA, Canada, Australia, and Europe (4). Various groups of experts have already published recommendations and considerations concerning the treatment of patients with high grade glioma during the early stages of the COVID-19 pandemic (5, 6). Elderly patients have a significantly higher risk of mortality when infected with COVID-19 (7) as do patients with multiple co-morbidities, common in the elderly population (8), especially obesity and hypertension (9–11).

Recently published recommendations for care of brain tumor patients with COVID-19 focus on the need to continue essential treatments such as surgery, but to carefully assess the need for full cycles of radiation therapy as well as the timing of immunosuppressive agents such as temozolomide (TMZ) and steroids (5, 6). Strict adherence to physical distancing rules is reinforced by these recommendations as the safety of both patients and health care providers is of utmost priority. As such, in-person patient visits to health care facilities should be reduced to a safe minimum to minimize potential exposure of the patient and to ensure adequate safety of the ongoing treatment.

The aforementioned recommendations to treat patients with brain tumors in the context of the COVID-19 pandemic (5, 6) focused on general recommendations and not on specific therapies such as TTFields. TTFields is an established treatment modality for newly diagnosed GBM, the most common type of primary malignant brain tumor in adults (3), and is delivered using Optune®, a portable home-use medical device. TTFields are low intensity, intermediate frequency (200 kHz) alternating electric fields that disrupt cancer cell division (12, 13). The large Phase 3 randomized control trial, EF-14, has demonstrated TTFields efficacy for GBM: TTFields combined with TMZ significantly increased overall survival *vs* TMZ alone in patients with newly diagnosed GBM (14) without deterioration in quality of life (QoL) (15).

The recently published SNO/EANO consensus article (16) summarizes the role of TTFields in newly diagnosed GBM patients aged 18 to 70 years with good functional status as compared to poor performing newly diagnosed GBM patients aged ≥ 65 to 70 years, and evaluated both MGMT-methylated and unmethylated patients in both groups (**Figure 1**).

TTFields has no known suppressive effect on the immune system, and may be a reliable treatment modality in times of a health pandemic when other treatment methods that require in-person visits to the hospital/doctor are limited. In-person monthly visits by device support specialists (DSS) are critical to provide patient-education and training for proper use of new and replacement equipment, array placement, and appropriate follow-up on usage. These practices required review during the pandemic to better comply with physical distancing recommendations. Bernhardt et al. noted that TTFields therapy regimen is generally associated with a low relative likelihood of having viral exposure. (5) Still, device delivery and support has been transitioned to include virtual and telemedicine practices which allow for safer physical distancing with fewer in-person encounters.

International experts in the field of neuro-oncology with TTFields experience were convened by Novocure to provide guidance and discuss available data on TTFields use in both newly diagnosed GBM and recurrent GBM in the context of the COVID-19 pandemic. This paper provides an opinion from an expert panel for a risk-benefit based decision regarding the inclusion of TTFields therapy to treat GBM during the COVID-19 pandemic.

## METHODS

### Expert Panel Discussion

A virtual meeting with a panel of multinational experts was conducted on May 9, 2020. The panel was chosen by specialists in GBM treatment with TTFields experience, and consisted of 7 neuro-oncologists (including two internal medicine specialists and one surgeon), an epidemiologist, a radiation-oncologist, President of the Central Brain Tumor Registry of the United States (CBTRUS), and Novocure's Head of Global Medical Affairs. In addition to the panel members, further discussions were held with other researchers, statisticians, and COVID-19 cancer registry developers relevant to the neuro-oncology community after the advisory board meeting.

### Objectives of the Panel Discussion

The purpose of this expert panel discussion was to gain insights on:

1. Treatment challenges and selection during the COVID-19 pandemic
2. Safety profile of TTFields as observed by the attendees
3. Clinical and patient experiences using TTFields during the pandemic
4. Opportunities to expand awareness and education on TTFields safety profile
5. TTFields use in clinical trials during the pandemic
6. Future directions in research and treatment guidelines in cancer COVID-19 patients
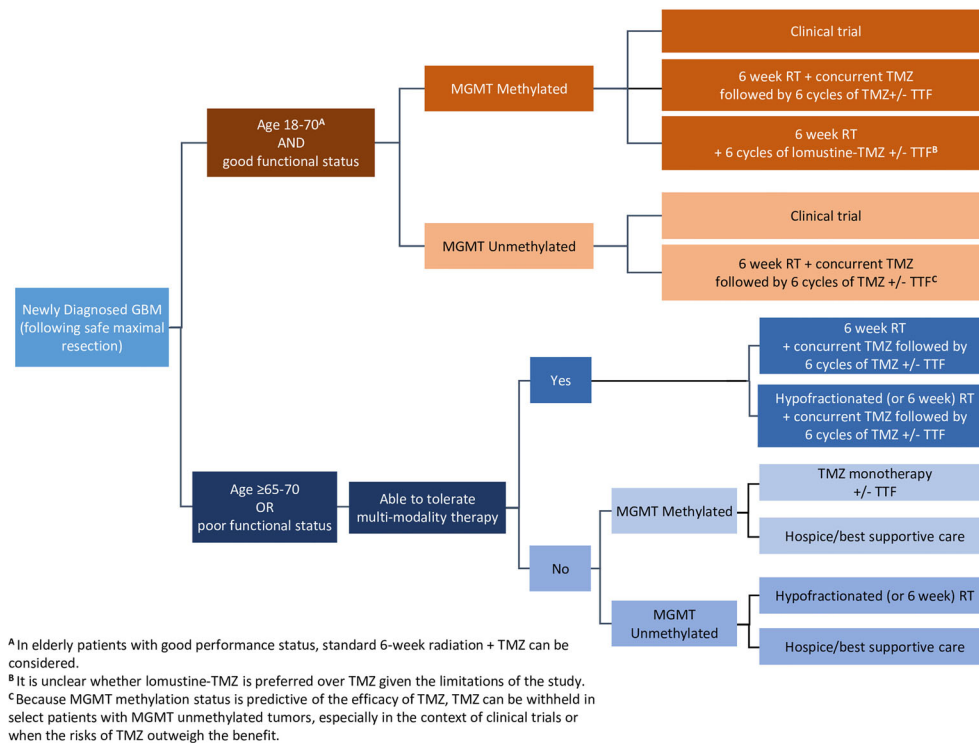
**FIGURE 1** | Wen, et al. Adult glioblastoma management: a Society for Neuro-Oncology (SNO) and European Society of Neuro-Oncology (EANO) consensus review. Neuro-Oncology. 2020;22(8):1073–1113. DOI: 10.1093/neuonc/noaa106. *Adapted and reprinted by permission of Oxford University Press on behalf of the Society for Neuro-Oncology.* GBM, glioblastoma; MGMT, O(6)-methylguanine-DNA methyltransferase; RT, radiation therapy; TMZ, temozolomide; TTF, Tumor Treating Fields. *Disclaimer: OUP and SNO are not responsible or in any way liable for the accuracy of the adaptation. Licensee is solely responsible for the adaptation in this publication/reprint.*

## DISCUSSION

### TTFields Impact on the Immune System

Given that GBM patients are in a baseline immune compromised state (17) and undergo additional immune suppression related to standard of care chemo- and radiotherapies, it was noted that the use of adjuvant TTFields therapy poses no known additional risk. Recent preclinical investigations have demonstrated that TTFields induced immunogenic (tumor) cell-death and potentially enhances the anti-tumor effects of the anti-PD-1 immune checkpoint inhibitor when used in combination (18). There were no observed negative in vivo effects on immune system function in tested mouse models (18). In these experiments, pulmonary regions were treated with TTFields and the frequency of T-cells (CD8+, Tregs, CD4+), dendritic cells, and macrophages were investigated (18). Hematopoiesis has been demonstrated to be unaffected by TTFields as hematopoietic stems cells, residing in the bone marrow, are shielded due to the high bone impedance resulting in significantly lower field intensities (19). Diamant *et al.* reported no impact on T-cell counts secondary to TTFields (20). In vitro studies of T-cell functionality such as induced cytotoxic degranulation and direct cytotoxic activity were not inhibited

by TTFields (20). Taken together, the preclinical data, to date, suggests that TTFields do not induce local and systemic immunosuppressive effects and supports a favorable clinical safety profile for TTFields. The combination of TTFields with an immune-checkpoint inhibitor (anti PD-1) and TMZ is currently under investigation for newly diagnosed GBM (2-THE-TOP trial) (21), and available preliminary safety results suggest that the combination therapy is well tolerated.

### Concomitant Use of Chemotherapy and TTFields

GBM patients may be intrinsically immunosuppressed as demonstrated by reduced CD4/CD8 counts (22). Standard treatments such as TMZ, dexamethasone, and lomustine (CCNU, Gleostine) have been reported to further hamper the adaptive immune system by reducing the CD4/CD8 counts (23, 24). Importantly, the CeTeG trial evaluated combined use of TMZ and CCNU without noting increased infection rates (25), which challenges the overall immunosuppressive impact of these chemotherapy regimens. However, immune competence against infection have more to do with the innate than the adaptive immune system (26, 27). While the benefit of TMZ in MGMT-

promoter-unmethylated patients has been debated (28), many have continued its use in this patient population despite pandemic concerns. Overall, the pandemic has not driven indications for major modifications in the use of standard chemotherapeutic regimens in GBM care.

The randomized phase III EF-11 trial investigated safety of TTFields as monotherapy (n=116) in recurrent GBM patients compared to best standard of care (BSC; n=91). Patients receiving TTFields in the EF-11 trial had fewer blood and lymphatic system disorders (4.3% TTFields alone *versus* 18.7% BSC), infections (4.3% TTFields alone *versus* 12.1% BSC) and respiratory, thoracic, and mediastinal disorders (6.0% TTFields alone *versus* 11.0% BSC) (29, 30). Of note, the EF-14 trial demonstrated similar toxicity profiles between the TTFields plus second-line therapy *versus* second-line therapy alone following the first progression (31). In addition to the phase III clinical trials, retrospective investigations of TTFields in combination with other therapies (i.e. TMZ and CCNU) found no increase in adverse events (AE) in newly diagnosed GBM (32) nor in TTFields plus CCNU in recurrent GBM (33).

In recurrent GBM (TTFields used as monotherapy) (30) and newly diagnosed GBM (TTFields plus TMZ) (14), the most common TTFields-related AE was skin reaction beneath the arrays, with no significant increase in systemic AEs, including blood and lymphatic system disorders. In many cases, skin reaction can be prevented and managed at home via telemedicine assessment and appropriate use of topical therapies as noted in the skin reaction guidelines (34). Therefore, treatment of skin reactions can take place in compliance with physical distancing regulations. Additionally, patients who receive TTFields treatment consistently report no deterioration in quality of life (15, 30).

## TTFields in Elderly Patients

In a recent real world evidence study in England covering approximately 40% of the population, increasing age was strongly associated with risk of COVID-19–related mortality (fully adjusted hazard ratios per age group: 40 to 49 years, 0.3 *vs* 50 to 59 years, 1.0 *vs* 60 to 69 years, 2.4 *vs* 70 to 79 years, 6.1 vs 80+ years, 20.6) (7). The efficacy of TTFields in elderly newly diagnosed GBM patients (age ≥ 65) was also investigated in the EF-14 trial, and this subgroup analysis indicated that TTFields in combination with TMZ (n=89) was associated with significantly increased survival compared to TMZ alone (n=45) (17.4 months versus 13.7 months; HR, 0.51; 95% CI, 0.33–0.77) (14). Both data from the EF14 study (n=134) (35) as well as the recently published global post-marketing surveillance analysis of TTFields (n=2,887 elderly patients out of 11,029 total patients) (36) demonstrated a comparable safety profile between the elderly subgroup and non-elderly subgroups treated with TTFields plus TMZ. Specifically, the most common TTFields-related AE, skin reaction, was comparable in elderly, adult, and pediatric subgroups, with an incidence of 36%, 34%, and 37% respectively. The incidence of infections was <1% in all groups (36), and so addition of TTFields in high-risk elderly GBM patients is not expected to be associated with poorer outcomes in the context of COVID-19.

## TTFields and Radiation Therapy

Use of TTFields with radiation induced cellular DNA damage demonstrated synergistic effects *in vitro* (37, 38). Currently, TTFields is approved for use in newly diagnosed GBM in combination with adjuvant TMZ initiated after completion of chemoradiation (i.e. in concert with the current GBM standard of care). There was agreement among the experts that there is no objective data to suggest that radiation dose or schedule negatively impacts the efficacy of TTFields and, presumably, TTFields could also be offered after hypofractionated chemoradiotherapy when indicated.

A pilot trial by Bokstein et al. (39) demonstrated the feasibility and safety of TTFields administered concurrently with radiotherapy and TMZ in newly diagnosed GBM patients. Several ongoing newly diagnosed GBM clinical trials are investigating the safety and efficacy of this concurrent triple-modality therapy, and include: (1) the phase II study conducted in Israel (40), (2) the German PriCoTTF phase II study (41), and (3) the global phase III study EF-32/TRIDENT (42). A phase II study, GERAS, will enroll elderly patients, who will receive TTFields and concomitant hypofractionated radiation therapy and will provide additional insights into the use of TTFields in this patient population (43).

## TTFields Therapy Delivery and Support During the COVID-19 Pandemic

Patients on TTFields undergo routine home-based technical support and education at the start of TTFields and follow up with monthly home-based visits for usage downloads. A recent publication raised important concerns regarding the potential risk of DSS breach of pandemic physical distancing restrictions during these patient interactions (5). This panel reaffirmed the importance of minimizing exposure risks to COVID-19 for both patients and support specialists and supports the measures to reduce infectious exposure risks, such as: (1) DSS to offer virtual treatment starts; (2) DSS to follow strict protocols for wearing full personal protective equipment (PPE) including mask, glasses, gloves, and a disposable gown for all necessary in-person visits; (3) Allowing temporary approval to obtain verbal patient consent via telemedicine for TTFields therapy; (4) Adapting the monthly DSS visit to be completed virtually with device replacements either by shipping (in the US) or non-contact home front door delivery (in Europe); and (5) Availability of new software in the US, called MyLink™, which enables patients to remotely download monthly usage reports.

## TTFields and Conduct of Clinical Trials During the COVID-19 Pandemic

The experts indicated that some medical centers have seen an increase in TTFields' acceptance and use due to limitations for patient enrollment in many non-TTFields clinical trials. The expert panel agreed that TTFields provides safe and effective practices for newly diagnosed as well as established and recurrent GBM patients on clinical trials which limits exposure risks during the COVID-19 pandemic. The fact that TTFields

treatment can be initiated and maintained at home was identified as an advantage when comparing TTFields-based GBM clinical trials with other treatment modalities which might require the in-person patient visits to medical facilities. An expert panelist involved in ongoing TTFields-based clinical trials noted its recommendation for continued recruitment based on the overall favorable safety profile of TTFields.

## Cancer COVID-19 Pandemic Registries and Brain Tumor Patients

Multiple national and international COVID-19 registries have been established since the onset of the COVID-19 pandemic. Important to this effort are the cancer and COVID-19 registries aimed at assessing epidemiological, demographic, and practice and treatment outcomes as well as identifying cancer health disparities uncovered by the COVID-19 pandemic; CCC19 (44), NCI NCCAPS (45), ASCO (46), and ESMO-CoCARE (47). There is some degree of overlap within these registries, but each has specific regulatory constraints and data collection objectives which increases the potential for wide variability in data reporting.

Our expert panel discussed the potential for better alignment with these registries, aiming to increase the representation of central nervous system tumor patients and garner participation from the pertinent neuro-oncology community. Several experts have worked closely with the COVID-19 and Cancer Consortium (CCC19) (44) to begin evaluating the COVID-19 impact on brain tumor patient care and outcomes. The CCC19 (North America) is one of the largest inclusive cancer COVID-19 registries and has partnered with the European Society for Medical Oncology Registries (ESMO-CoCARE (47), covering Europe and Asia) to increase the rate of data collection by combining coverage of their respective participating sites across the world.

## CONCLUSION

TTFields is a treatment modality for newly diagnosed and recurrent GBM that can be safely administered during the current COVID-19 pandemic when other treatment methods are limited. Since TTFields has no known suppressive effect on the immune system and is an established treatment modality with a proven safety profile, it should be considered in times when immunosuppression and other point of care critical factors such as physical distancing and travel reduction are of concern. As TTFields is a portable home-use device it involves no treatment-related travel thereby avoiding additional hospital exposure. Furthermore, the most common skin-related adverse events can be managed in the home via telemedicine. Clinical trial enrollment with TTFields have continued relatively unaffected. The expert panel further concluded that it is currently too early to see the full impact of COVID-19 on GBM patients and strongly recommended establishing support via the cancer and COVID-19 registries (**Table 1**).

We recognize that there are non-safety issues that might limit brain tumor patient's access to use of the TTFields device during

**TABLE 1** | Summary of Key Points: Based on expert panel opinion.

**Summary of Key Points**

- Safer practices for TTFields patient assessment and education as well as safer device delivery and replacement have been instituted to meet the physical distancing recommendations during the COVID-19 pandemic.
- For established patients—TTFields can be safely continued during the COVID-19 pandemic
- For new patients—TTFields can be safety initiated during the COVID-19 pandemic
- TTFields clinical trials participation should be continued and encouraged provided there is appropriate clinical/research support during the COVID-19 pandemic.
- Continuous assessment of treatment practices and outcomes for GBM patients during the COVID-19 pandemic is of critical importance to the field of Neuro-Oncology. Affiliation with the established COVID-19 and cancer registries is important to capture these data.

the COVID-19 pandemic. One important limitation might be due to out-of-pocket expense to the patient and/or the already challenged healthcare system during this crisis. While the cost impact on therapeutic access was outside of the scope of this panel discussion, we agree this is an important issue to consider and should be studied further.

## DATA AVAILABILITY STATEMENT

The original contributions presented in the study are included in the article material. Further inquiries can be directed to the corresponding author.

## AUTHOR CONTRIBUTIONS

## FUNDING

## ACKNOWLEDGMENTS

# REFERENCES

1. *John Hopkins Coronavirus Resource Center*. Available at: https://coronavirus.jhu.edu/ (Accessed August 21, 2020).

2. Zhang H, Han H, He T, Labbe KE, Hernandez AV, Chen H, et al. Clinical Characteristics and Outcomes of COVID-19–Infected Cancer Patients: A Systematic Review and Meta-Analysis. *J Natl Cancer Inst* (2021) 113(4):371–80. doi: 10.1093/jnci/djaa168

3. Ostrom QT, Cioffi G, Gittleman H, Patil N, Waite K, Kruchko C, et al. CBTRUS Statistical Report: Primary Brain and Other Central Nervous System Tumors Diagnosed in the United States in 2012-2016. *Neuro Oncol* (2019) 21 (Suppl_5):v1–100. doi: 10.1093/neuonc/noz150

4. Minniti G, Lombardi G, Paolini S. Glioblastoma in Elderly Patients: Current Management and Future Perspectives. *Cancers* (2019) 11:336. doi: 10.3390/cancers11030336

5. Bernhardt D, Wick W, Weiss SE, Sahgal A, Lo SS, Suh JH, et al. Neuro-Oncology Management During the COVID19 Pandemic With a Focus on WHO Grade III and IV Gliomas. *Neuro Oncol* (2020) 22(7):928–35. doi: 10.1093/neuonc/noaa113

6. Mohile NA, Blakeley JO, Gatson NTN, Hottinger AF, Lassman AB, Ney DE, et al. Urgent Considerations for the Neurooncologic Treatment of Patients With Gliomas During the COVID-19 Pandemic. *Neuro Oncol* (2020) 22 (7):912–7. doi: 10.1093/neuonc/noaa090

7. Williamson EJ, Walker AJ, Bhaskaran K, Bacon S, Bates C, Morton CE, et al. Factors Associated With COVID-19-Related Death Using Opensafely. *Nature* (2020) 584:430–6. doi: 10.1038/s41586-020-2521-4

8. Barnett K, Mercer SW, Norbury M, Watt G, Wyke S, Guthrie B. Epidemiology of Multimorbidity and Implications for Health Care, Research, and Medical Education: A Cross-Sectional Study. *Lancet* (2012) 380:37–43. doi: 10.1016/S0140-6736(12)60240-2

9. Richardson S, Hirsch JS, Narasimhan M, Crawford JM, McGinn T, Davidson KW, et al. Presenting Characteristics, Comorbidities, and Outcomes Among 5700 Patients Hospitalized With COVID-19 in the New York City Area. *JAMA* (2020) 323(20):2052–9. doi: 10.1001/jama.2020.6775

10. Hussain A, Mahawar K, Xia Z, Yang W, EL-Hasani S. Obesity and Mortality of COVID-19. Meta-Analysis. *Obes Res Clin Pract* (2020) 14(4):295–300. doi: 10.1016/j.orcp.2020.07.002

11. de Almeda-Pititto B, Dualib PM, Zajdenverg L, Dantas JR, de Souza F, Rodacki M, et al. Severity and Mortality of COVID 19 in Patients With Diabetes, Hypertension and Cardiovascular Disease: A Meta-Analysis. *Diabetol Metab Syndr* (2020) 12:75. doi: 10.1186/s13098-020-00586-4

12. Mun EJ, Babiker HM, Weinberg U, Kirson ED, VonHoff DD. Tumor-Treating Fields: A Fourth Modality in Cancer Treatment. *Clin Cancer Res* (2018) 24 (2):266–75. doi: 10.1158/10780432.CCR-17-1117

13. Ghiaseddin AP, Shin D, Melnick K, Tran D. Tumor Treating Fields in the Management of Patients With Malignant Gliomas. *Curr Treat Options Oncol* (2020) 21(9):76. doi: 10.1007/s11864-020-00773-5

14. Stupp R, Taillibert S, Kanner A, Read W, Steinberg D, Lhermitte B, et al. Effect of Tumor-Treating Fields Plus Maintenance Temozolomide Vs Maintenance Temozolomide Alone on Survival in Patients With Glioblastoma: A Randomized Clinical Trial. *JAMA* (2017) 318(23):2306–16. doi: 10.1001/jama.2017.18718

15. Taphoorn MJB, Dirven L, Kanner AA, Lany-Shahaf G, Weinberg U, Taillibert S, et al. Influence of Treatment With Tumor-Treating Fields on Health-Related Quality of Life of Patients With Newly Diagnosed Glioblastoma: A Secondary Analysis of a Randomized Clinical Trial. *JAMA Oncol* (2018) 4 (4):495–504. doi: 10.1001/jamaoncol.2017.5082

16. Wen PY, Weller W, Lee EQ, Alexander BM, Barnholtz-Sloan JS, Barthel FP, et al. Glioblastoma in Adults: A Society for Neurooncology (SNO) and European Society of Neuro-Oncology (EANO) Consensus Review on Current Management and Future Directions. *Neuro Oncol* (2020) 22 (8):1073–113. doi: 10.1093/neuonc/noaa106

17. Ladomersky E, Scholtens DM, Kocherginsky M, Hibler EA, Bartom ET, Otto-Meyer S, et al. The Coincidence Between Increasing Age, Immunosuppression, and the Incidence of Patients With Glioblastoma. *Front Pharmacol* (2019) 10:200. doi: 10.3389/fphar.2019.00200

18. Voloshin T, Kaynan N, Davidi S, Porat Y, Shteingauz A, Schneiderman RS, et al. Tumor-Treating Fields (Ttfields) Induce Immunogenic Cell Death

Resulting in Enhanced Antitumor Efficacy When Combined With Anti-PD-1 Therapy. *Cancer Immunol Immunother* (2020) 69(7):1191–204. doi: 10.1007/s00262-020-02534-7

19. Kirson ED, Ddbaly V, Tovarys F, Vymazal J, Soustiel JF, Itzhaki A, et al. Alternating Electric Fields Arrest Cell Proliferation in Animal Tumor Models and Human Brain Tumors. *Proc Natl Acad Sci* (2007) 104(24):10152–7. doi: 10.1073/pnas.0702916104

20. Diamant G, Simchony H, Shiloach T, Globerson-Levin A, Gasri Plotnitsky L, Eshhar Z, et al. P12.05 Evaluating the Compatibility of Tumor Treating Electric Fields With Key Antitumoral Immune Functions. *Neuro Oncol* (2019) 21(suppl_3):iii60. doi: 10.1093/neuonc/noz126.216

21. Tran D, Warren S, Allen A, Sampson D, Chen D, Thomas N, et al. Phase 2 Open-Labeled Study of Adjuvant Temozolomide Plus Tumor Treating Fields Plus Pembrolizumab in Patients With Newly Diagnosed Glioblastoma (2-the-TOP). *Neuro Oncol* (2019) 21(Suppl_6):vi10. doi: 10.1093/neuonc/noz175.038

22. Chongsathidkiet P, Jackson C, Koyama S, Loebel F, Cui X, Farber SH, et al. Sequestration of T Cells in Bone Marrow in the Setting of Glioblastoma and Other Intracranial Tumors. *Nat Med* (2018) 24(9):1459–68. doi: 10.1038/s41591-018-0135-2

23. Grossman SA, Ye X, Lesser G, Sloan A, Carraway H, Desideri S, et al. Immunosuppression in Patients With High-Grade Gliomas Treated With Radiation and Temozolomide. *Clin Cancer Res* (2011) 17(16):5473– 5480. doi: 10.1158/1078-0432.CCR-11-0774

24. Capper D, von Deimling A, Brandes AA, Carpentier AF, Kesari S, Sepulveda-Sanchez JM, et al. Biomarker and Histopathology Evaluation of Patients With Recurrent Glioblastoma Treated With Galunisertib, Lomustine, or the Combination of Galunisertib and Lomustine. *Int J Mol Sci* (2017) 18(5):995. doi: 10.3390/ijms18050995

25. Herrlinger U, Tzaridis T, Mack F, Sloan A, Carraway H, Desideri S, et al. Lomustine-Temozolomide Combination Therapy Versus Standard Temozolomide Therapy in Patients With Newly Diagnosed Glioblastoma With Methylated MGMT Promoter (Ceteg/NOA–09): A Randomised, Open-Label, Phase 3 Trial. *Lancet* (2019) 393(10172):678–88. doi: 10.1016/S0140-6736(18)31791-4

26. Hosseini A, Hashemi V, Shomali N, Asghari F, Gharibi T, Akbari M, et al. Innate and Adaptive Immune Responses Against Coronavirus. *BioMed Pharmacother* (2020) 132:110859. doi: 10.1016/j.biopha.2020.110859

27. Carty M, Guy C, Bowie AG. Detection of Viral Infections by Innate Immunity. *Biochem Pharmacol* (2021) 183:114316. doi: 10.1016/j.bcp.2020.114316

28. Hegi ME, Diserens A-C, Gorlia T, Hamou M-F, de Tribolet N, Weller M, et al. MGMT Gene Silencing and Benefit From Temozolomide in Glioblastoma. *N Engl J Med* (2005) 352(10):997–1003. doi: 10.1056/NEJMoa043331

29. *Optune Instructions for Use*. Available at: https://www.optune.com/hcp/instructions-foruse (Accessed August 21, 2020).

30. Stupp R, Wong ET, Kanner AA, Steinberg D, Engelhard H, Heidecke V, et al. Novottf-100A Versus Physician's Choice Chemotherapy in Recurrent Glioblastoma: A Randomised Phase III Trial of a Novel Treatment Modality. *Eur J Cancer* (2012) 48(14):2192–202. doi: 10.1016/j.ejca.2012.04.011

31. Kesari S, Ram Z. EF-14 Trial Investigators. Tumor-Treating Fields Plus Chemotherapy Versus Chemotherapy Alone for Glioblastoma At First Recurrence: A Post Hoc Analysis of the EF-14 Trial. *CNS Oncol* (2017) 6 (3):185–93. doi: 10.2217/cns-2016–0049

32. Lazaridis L, Schäfer N, Teuber-Hanselmann S, Blau T, Schmidt T, Oster C, et al. Tumour Treating Fields (Ttfields) in Combination With Lomustine and Temozolomide in Patients With Newly Diagnosed Glioblastoma. *J Cancer Res Clin Oncol* (2020) 146(3):787–92. doi: 10.1007/s00432-019-03106-8

33. Kinzel A, Lavy-Shahaf G, Kirson E. P01.065 Tumor Treating Fields (Ttfields) in Combination With Lomustine (CCNU) in the EF-14 Phase 3 Clinical Study - a Safety Analysis. *Neuro Oncol* (2018) 20(suppl_3):iii244. doi: 10.1093/neuonc/noy139.107

34. Lacouture ME, Anadkat J, Ballo MT, Iwamoto F, Jeyapalan SA, La Rocca RV, et al. Prevention and Management of Dermatologic Adverse Events Associated With Tumor Treating Fields in Patients With Glioblastoma. *Front Oncol* (2020) 10:1045. doi: 10.3389/fonc.2020.01045

35. Ram Z, Kim CY, Zhu JJ. Efficacy of Tumor Treating Fields (Ttfields) in Elderly Patients With Newly Diagnosed Glioblastoma (GBM): Sub-Group Analysis of the Phase III EF-14 Trial. *J Clin Oncol* (2020) 38(15_Suppl):e24019. doi: 10.1200/JCO.2020.38.15_suppl.e24019

36. Shi W, Blumenthal DT, Oberheim Bush NA, Kebir S, Lukas RV, Muragaki Y, et al. Global Post-Marketing Safety Surveillance of Tumor Treating Fields (Ttfields) in Patients With High-Grade Glioma in Clinical Practice. *J Neurooncol* (2020) 148(3):489–500. doi: 10.1007/s11060-020-03540-6

37. Giladi M, Munster M, Schneiderman RS, Kebir S, Lukas RV, Muragaki Y, et al. Tumor Treating Fields (Ttfields) Delay DNA Damage Repair Following Radiation Treatment of Glioma Cells. *Radiat Oncol* (2017) 12(1):206. doi: 10.1186/s13014-017-0941-6

38. Kim EH, Kim YJ, Song HS, Jeong YK, Lee JY, Sung J, et al. Biological Effect of an Alternating Electric Field on Cell Proliferation and Synergistic Antimitotic Effect in Combination With Ionizing Radiation. *Oncotarget* (2016) 7 (38):62267–79. doi: 10.18632/oncotarget.11407

39. Bokstein F, Blumenthal D, Limon D, Harosh CB, Ram Z, Grossman R. Concurrent Tumor Treating Fields (Ttfields) and Radiation Therapy for Newly Diagnosed Glioblastoma: A Prospective Safety and Feasibility Study. *Front Oncol* (2020) 10:411. doi: 10.3389/fonc.2020.00411

40. Bokstein F, Blumenthal D, Limon D, Harosh CB, Ram Z, Grossman R. Abstract CT206: Concurrent Tumor Treating Fields (Ttfields) and Radiation Therapy for Newly Diagnosed Glioblastoma: A Safety and Feasibility Study. *Cancer Res* (2020) 80(16 Supplement):CT206–6. doi: 10.1158/1538-7445.AM2020-CT206

41. Kebir S, Lazaridis L, Schmidt T, Oster C, Pierscianek D, Guberina N, et al. Abstract CT106: Pricottf Trial: A Phase I/II Trial of Ttfields Prior and Concomitant to Radiotherapy in Newly Diagnosed Glioblastoma. *Cancer Res* (2020) 80(16 Supplement):CT106–6. doi: 10.1158/1538-7445.AM2020-CT106

42. Shi W, Kleinberg L, Jeyapalan SA, Goldlust SA, Nagpal S, Reardon DA, et al. Phase III TRIDENT Trial: Radiation and Temozolomide +/- Tumor Treating Fields in Newly Diagnosed Glioblastoma. *J Clin Oncol* (2020) 38(15_suppl): TPS2580. doi: 10.1200/JCO.2020.38.15_suppl.TPS2580

43. Höne SJ, Krisam J, Jäkel C, Schmitt D, Lang K, El Shafie R, et al. P05.07 Effect of Tumor-Treating Fields Plus Short-Course Radiation With or Without Temozolomide in Elderly Patients With Glioblastoma (GERAS Trial). *Neuro Oncol* (2019) 21(Suppl_3):iii35. doi: 10.1093/neuonc/noz126.121

44. The COVID-19 and Cancer Consortium. Available at: https://ccc19.org/ (Accessed August 21, 2020).

45. National Institutes of Health, National Cancer Institute. *NCI COVID-19 in Cancer Patients Study (NCCAPS)*. Available at: https://www.cancer.gov/ research/keyinitiatives/covid-19/coronavirus-research-initiatives/nccaps (Accessed August 21, 2020).

46. American Society of Clinical Oncology. *ASCO Survey on COVID-19 in Oncology (ASCO) Registry*. Available at: https://www.asco.org/asco-coronavirusinformation/coronavirus-registry (Accessed August 21, 2020).

47. European Society for Medical Oncology. *ESMO-Cocare Registry* . Available at: https://www.esmo.org/covid-19-and-cancer/collaborating-on-registries-studies-andsurveys/esmo-cocare-registry (Accessed August 21, 2020).

# Viral Gene Therapy for Glioblastoma Multiforme: A Promising Hope for the Current Dilemma

Junsheng Li [1,2,3,4,5], Wen Wang [1,2,3,4,5], Jia Wang [1,2,3,4,5], Yong Cao [1,2,3,4,5], Shuo Wang [1,2,3,4,5] and Jizong Zhao [1,2,3,4,5,6]*

[1] Department of Neurosurgery, Beijing Tiantan Hospital, Capital Medical University, Beijing, China, [2] China National Clinical Research Center for Neurological Diseases, Beijing, China, [3] Center of Stroke, Beijing Institute for Brain Disorders, Beijing, China, [4] Beijing Key Laboratory of Translational Medicine for Cerebrovascular Disease, Beijing, China, [5] Beijing Translational Engineering Center for 3D Printer in Clinical Neuroscience, Beijing, China, [6] Savaid Medical School, University of the Chinese Academy of Sciences, Beijing, China

Glioblastoma multiforme (GBM), as one of the most common malignant brain tumors, was limited in its treatment effectiveness with current options. Its invasive and infiltrative features led to tumor recurrence and poor prognosis. Effective treatment and survival improvement have always been a challenge. With the exploration of genetic mutations and molecular pathways in neuro-oncology, gene therapy is becoming a promising therapeutic approach. Therapeutic genes are delivered into target cells with viral vectors to act specific antitumor effects, which can be used in gene delivery, play an oncolysis effect, and induce host immune response. The application of engineering technology makes the virus vector used in genetics a more prospective future. Recent advances in viral gene therapy offer hope for treating brain tumors. In this review, we discuss the types and designs of viruses as well as their study progress and potential applications in the treatment of GBM. Although still under research, viral gene therapy is promising to be a new therapeutic approach for GBM treatment in the future.

Keywords: gene therapy, viral therapy, glioblastoma multiforme, viral vector, treatment strategy

## INTRODUCTION

Glioblastoma multiforme (GBM) is one of the most common primary brain tumors in adults (1, 2), mainly derived from astrocytes (3, 4). The World Health Organization (WHO) classification in 2016 defined GBM as grade IV, which leads to a high degree of malignancy and mortality. The current standard treatment for GBM includes maximum surgical resection, radiotherapy, and chemotherapy (5–7). However, the complete resection of GBM has been challenging due to the invasive growth pattern and the functional area involvement. It has been almost inevitable that the tumor-infiltrating parenchyma tissue eventually relapsed even after surgical resection (8, 9). The resistance to chemotherapy drug temozolomide (TMZ) was mainly caused by O6-methylguanine-DNA methyltransferase over-expression, mismatch repair and base excision repair (10–12). The molecules mediated GBM chemoresistance, including P-glycoprotein, multidrug-resistance protein transporters, and DNA repair enzymes (13). Furthermore, the inefficient delivery across the

blood-brain barrier (BBB) limited the entry of therapeutic drugs into the central nervous system (CNS) (14–16). Glioblastoma stem cells supported tumor self-renewal which contributed to GBM resistance to radiotherapy (17–19). So even with standard treatment, the outcome of patients with GBM was still very poor. The median survival of patients diagnosed with GBM was just about 15 months (20–22). The clinical use of additional therapies, including local adjuvant therapy with Carmustine wafers and tumor-angiogenesis inhibition with Bevacizumab, were tried to improve the outcome (23–26). However, the survival rate was still less than 5% within five years of diagnosis (27, 28).

Therefore, the application of new treatment methods to get rid of the limitations of conventional treatment has been necessary. Growing evidence has proved that tumor is a kind of genetic disease (29, 30). With the exploration in the treatment of other diseases, viral gene therapy has brought hope for the treatment of GBM (31–33). Both wild-type viruses and engineered viruses could be used for viral gene therapy. Non-lytic viruses were used for gene therapy and lytic viruses exert anti-tumor effects by inducing tumor cell lysis (34). Moreover, the lytic viruses exposed GBM antigens to the host immune system which stimulated a specific immune response to tumor cells (35). The natural sensitivity of GBM cells to virus infection has made viral therapy a promising prospect. The viral vectors were designed according to the characteristic of target cells, the size of therapeutic gene, and the ability of long-term gene expression. In this review, we will focus on the types of viral vectors and demonstrate the versatility of gene therapy for GBM treatment. In this review, we will focus on the types of viral vectors (**Table 1**) and demonstrate the versatility of gene therapy for GBM treatment.

# VIRAL VECTORS

## Retrovirus

Because of the special biological characteristics, retrovirus vectors were first attempted in gene therapy for glioma. Replicating retroviral vectors were able to deliver the prodrug activator genes, which were also called suicide genes, into tumor cells and integrate into host genomes (36, 37). When a prodrug was given, the protein expressed by the gene could convert the non-toxic drug into a cytotoxic substance, which led to GBM cell death (38). Even as tumor cells escape the killing of cytotoxic drugs, they could also be used as an integrated retrovirus set and continue to play a role in the events of GBM recurrence (39). Therefore, this method was also known as "suicide gene therapy". In the initial clinical trial, the therapeutic effect of retroviral vectors encoding herpes simplex virus thymidine kinase (HSV-tk) on malignant brain tumors was evaluated. The researchers found that HSV-tk could convert ganciclovir (GCV) into an active form of GCV triphosphate, which inhibited DNA replication and cell division in tumor cells, resulting in an

**TABLE 1 |** Modifications and mechanisms of the viral vectors used for GBM gene therapy.

| Viral vector | Agent | Modification | Mechanism |
|---|---|---|---|
| Retrovirus | HSV-tk | suicide gene therapy, thymidine kinase (TK) gene transfer | converting ganciclovir (GCV) into active form GCV triphosphate |
| | TOCA511 | suicide gene therapy, cytosine deaminase (CD) gene transfer | converting 5-fluorocytosine (5-FC) into active antineoplastic 5-fluorouracil (5-FU) |
| Lentivirus | shRNA-lentivirus | sh-Bcl2 and S-TRAIL transfer | down-regulating Bcl-2 and inducing S-TRAIL expression |
| | sh-SirT1 lentivirus | sh-SirT1 transfer | silencing SirT1 in CD133+ cells to improve radiotherapeutic sensitivity |
| | miR-100 lentivirus | miR-100 transfer | regulating FGFR3 to inhibit tumor growth and increase sensitivity to chemotherapy |
| | GAS1-PT*EN* lentivirus | growth arrest specific 1 (GAS1) and phosphatase and tensin homolog (PTEN) gene transfer | expressing GAS1 and PTEN equally to perform superimposed anti-tumor effect |
| Adenovirus | ONYX-015 | E1B gene deletion | replicating in p53 pathway altered tumor cells |
| | Delta-24 | E1A gene partial deletion, Delta-24 RGD: Arg- Gly-Asp peptide sequence incorporation | replicating in Rb/p16 tumor suppressor pathway defective GBM cells Delta-24 RGD: expressing αv integrins to enhance infectivity |
| Herpes simplex virus | HSV1716 | RL1 gene (γ34.5) loci deletion | targeting cells with defects in PKR pathway |
| | C134 | RL1 gene (γ34.5) loci deletion, human cytomegalovirus IRS1 gene transfer | expressing IRS1 protein to enhance replication |
| | G207 | RL1 (γ34.5) and UL39 gene deletion | inhibiting viral replication in non-dividing cells |
| | rQNestin34.5v.2 | RL1 gene (γ34.5) loci deletion, RL1 gene under control of nestin promoter. | replicating in PKR-deficient, nestin-positive tumor cells |
| Oncolytic virus | Pelareorep (REOLYSIN) | wild-type reovirus | replicating specifically in Ras pathway activated tumor cells |
| | TG6002 | ribonucleotide reductase genes deletion vaccinia, suicide gene therapy, FCU1 gene transfer | direct oncolysis effect and prodrug conversion |
| | H-1PV | wild-type parvovirus | clathrin-mediated endocytosis, DNA damage response, and cell-cycle arrest |
| | PVS-RIPO | poliovirus-rhinovirus chimera | restrict replicating in CD155-expressing tumor cells |

anti-tumor effect (40). However, the results also indicated the limitations in transfection inefficiency of retroviral vectors was inefficient (41).

Retroviral vector TOCA511 has been used to deliver cytosine deaminase (CD) gene into tumor cells (42). CD enzyme converted the prodrug 5-fluorocytosine (5-FC) to active antineoplastic 5-fluorouracil (5-FU) which caused the death of tumor cells. The preclinical studies observed that TOCA511 did not lead to widespread or uncontrolled replication, which proved the safety of TOCA511 treatment. The safety and activity of TOCA511 were further supported by molecular analyses (43). Moreover, another study found that in addition to direct cytotoxic effects, TOCA511 could also be used as a radiosensitizing agent (44). TOCA511 could increase the intratumor concentration of 5-FU and induce T cell-mediated antitumor immunity (45, 46). TOCA 511 has been shown to be safe and provide a significant survival benefit in the clinical trial (47). Recent results from the Phase III clinical trial showed that TOCA511 treatment significantly improved survival in patients with two or more recurrences (48).

## Lentivirus

Lentiviruses belonged to the retroviridae family (49, 50). Exogenous genes or shRNAs could be effectively integrated into the genomes of dividing or non-dividing cells to achieve the effect of persistent expression of the target sequence (51). Compared with retroviral vectors, lentiviral vectors were more stable and less prone to insertion mutation. The active transportation of pre-integration complex through the nucleopore was the unique mechanism of lentiviral vectors (52). Researchers constructed a lentiviral vector expressing shRNA to downregulate Bcl-2 and S-TRAIL to induce apoptosis in glioma cells. The result showed that lentivirus-mediated apoptosis resulted in an increase in the expression of activated caspase-3 and caspase-7, which accelerated the apoptosis of tumor cells (53). The transfection of target genes by lentiviral vectors could improve sensitivity of GBM to radiotherapy. The CD133$^+$ cells in GBM were resistant to radiotherapy. A study down-regulated the expression of sirtuin 1(SirT1) in CD133$^+$ by a lentiviral vector expressing shRNA (sh-SirT1). The results showed that the silence of SirT1 significantly enhanced the inhibition of tumor growth by radiotherapy and improved the mean survival rate of GBM (54).

Specific miRNAs were proved to be associated with the increase of proliferation, invasiveness, angiogenesis, and apoptosis resistance in GBM. A study has shown that with the transfection of lentiviral vectors, the overexpression of miR-100 significantly inhibited the growth and migration of GBM, and increased the sensitivity to chemotherapy. And the delivered miR-100 played an anti-tumor effect on GBM by regulating FGFR3 directly (55). The latest genome editing technology could also be used for GBM treatment by lentiviral vector transfection. It has shown that editing the sequence of vascular laminin-411 overexpressed in GBM could suppress tumor growth and improve survival of GBM (56). Researchers constructed lentiviral vectors with an equal expression of growth arrest specific 1 (GAS1) and phosphatase and tensin homolog (PTEN) *via* the versatility of expression cassettes allocation. Both of the transgenes were regulated by the same promoter. The result showed that the anti-tumor effect of GAS1 could be superimposed with the inhibitory effect of PTEN on Akt pathway, and this could significantly inhibit the growth of GBM (57).

## Adenovirus

Adenovirus is a non-enveloped double-stranded DNA virus (58, 59). Adenoviruses selected for gene therapy were serotypes 2 and 5 (60). Adenoviral vectors used coxsackie-adenovirus receptor (CAR) to mediate cell tropism and internalize adenovirus vectors by the interactions between penton protein and host cell surface integrins (61–63). After endocytosis into the tumor cells, adenoviruses did not integrate into the host genome and remained episomal while gene expression (64).

The E1 and E3 regions of adenovirus genome were conventionally deleted to eliminate the expression-related toxicity by adenovirus infection. The latest generation of adenoviral vectors could minimize the anti-adenovirus immune response by removing all the endogenous virus coding regions to induce more stable transgene expression (65). The deficiency of non-replicative adenoviruses was that episomes might be diluted due to cell division, resulting in a rapid decline in transgene expression. Conditional replication adenoviruses, as tumor-specific agents, were designed to selectively replicate within and kill the tumor cells (66). Moreover, the replicated transgenes could spread the therapeutic effect to other neighboring tumor cells. The genetically modified adenovirus ONYX-015 was a recombinant chimeric Ad2 and Ad5 vector with selective replication ability. The protein encoded by adenovirus E1B gene interacted with tumor suppressor p53 and the transcriptional activity was blocked (67). Due to the decreased expression of p53 in GBM, ONYX-015 was able to replicate effectively. Previous studies showed that ONYX-015 administration was safe and effective (68). And the phase I clinical trial has shown that no serious adverse events were observed in patients treated with ONYX-015 and ONYX-015 therapy could significantly inhibit tumor growth (69).

Delta-24 was designed to selectively replicate in cells deficient in the Rb/p16 tumor suppressor pathway. The deletion of retinoblastoma (Rb) binding domain fragment in E1A gene inhibited the interaction between E1A and Rb. Rb protein negatively regulates cell growth by blocking E2F. Rb/p16 tumor suppressor pathway deficiency likely occurred in GBM cells, which made it possible for Delta-24 selective replication in GBM cells but not in the normal cells (70). Furthermore, it was difficult for adenoviral vectors transfection due to the poor expression of CAR in tumor cells, which reduced the therapeutic effect. By mortifying an Arg- Gly-Asp peptide sequence in the HI loop of the fiber, the vectors were allowed to bind αv integrins to enter the tumor cells, thus enhancing the infectivity of the virus (71). Delta-24 and its modified versions have shown encouraging results in clinical trials (72).

## Herpes Simplex Virus

Herpes simplex viral vectors used for gene therapy were mainly modified from Herpes Simplex virus type 1 (HSV-1), an

enveloped double-stranded DNA virus (73). Due to the neurotropic nature, HSV vectors are attractive for gene transduction in central nervous system tumors. The 152kbp genome length made it possible to carry a sufficient payload (68).

RL1 gene (γ34.5) was a necessary gene for effective replication of HSV. RL1 gene encodes The Infected Cell Protein 34.5 (ICP34.5), also known as Neurovirulence factor ICP34.5, was encoded by RL1. Phosphorylation of translation initiation factor eIF2α by protein kinase R (PKR) inhibited the translation process and blocked the production of viral proteins. Moreover, PKR could activate transcription factor NF-κB by inducing the degradation of negative regulator IκB to stimulate the antiviral immune response. ICP34.5 reversed this process by activating phosphatase-1α (74). The PKR pathway was often inhibited in GBM, so it did not restrict the replication of HSV vectors with the modification of ICP 34.5. For example, the recombinant vector HSV1716 removed both copies of RL1 to allow its selective replication in tumor cells (75). Clinical studies have proved that HSV-1716 can effectively improve the survival of patients (76, 77). C134 vectors deleted RL1 gene and inserted human cytomegalovirus IRS1 gene to enhance replication (78).

Another important gene UL39 encoded the large subunit of ribonucleotide reductase (RR), also known as ICP6. This protein converts ribonucleotide into deoxyribonucleotide allowing viral DNA replication, and the UL39-deficient vectors were unable to replicate in non-dividing cells. However, the host ribonucleotide reductase could compensate for the function loss of viral RR in dividing cells. Combining the two mechanisms above, the deletion of RL1 gene in G207 allowed the virus to target GBM cells, and the mutation in UL39 gene eliminated the replication in normal non-dividing cells (79). The result of the clinical studies has shown the safety of G207 in GBM treatment, and the favorable therapeutic effect of the combination with G207 and radiotherapy in recurrent GBM treatment (80, 81). Due to the specific up-regulation of nestin promoter in gliomas, rQNestin34.5v.2 vectors were designed within an insertion with a copy of RL1 gene under the transcriptional control of nestin promoter. The combination of the vectors and cyclophosphamide was proved to increase virus replication in tumors and improve the survival rate of patients (82).

## Oncolytic Virus

Oncolytic viruses had dual anti-tumor effects, which not only destroyed tumor cells directly but activated tumor-specific immune response. Current clinical trials have demonstrated the feasibility of OV-specific tumor infection. By selective transfection and replication (83, 84), tumor cell lysis was induced without damage to normal cells. Furthermore, oncolytic viruses were also able to infect tumor vascular endothelial cells, inhibit tumor-related angiogenesis, and cause hypoxic death of tumor cells (85). Meanwhile, oncolytic viruses induced systemic anti-tumor immunity by releasing tumor-associated antigens (86).

In addition to wild-type viruses, engineered viruses could also be used as oncolytic viruses, including reovirus, vaccinia virus, parvovirus, poliovirus, vaccinia virus, Newcastle disease virus, etc. And the anti-tumor immunity could be further enhanced by

encoding cytokines, chemokines, and tumor-associated antigens (87). Currently, types of viruses have been involved in clinical trials to verify the safety and therapeutic effectiveness. Reovirus was a non-enveloped wild-type oncolytic virus with double-stranded RNA genome. Reovirus Pelareorep (REOLYSIN) could replicate specifically in Ras pathway activated tumor cells (88). In the phase I clinical trial, no treatment-related adverse reactions after intratumoral injection of reovirus were observed (89). Reovirus therapy could lead to tumor leukocyte infiltration and an increase in the expression of IFN, caspase 3, and PD-L1 (90). As an enveloped double-stranded DNA virus, the vaccinia virus did not rely on cell receptors, but membrane fusion to enter cells. Its rapid replication cycle and strong ability of intercellular transmission made it a promising candidate for viral therapy (91). TG6002 was modified from vaccinia virus, which was designed as a combination of direct oncolysis effect and prodrug conversion function. It mainly replicated in tumor cells and transformed 5-FC into 5-FU. Its safety and oncolytic activity have been confirmed in a large number of preclinical studies (68). Parvovirus was a single-stranded DNA virus. As a kind of parvovirus, H-1PV bound to the receptors on the surface of host cells and entered within endocytosis mediated by clathrin, inducing DNA damage and cell cycle arrest (92). The result of clinical trials showed that H-1PV could cross the BBB to reach the tumor and enhance the immunogenicity in tumor microenvironment (93, 94). Poliovirus was a kind of encapsidated viruses with a single strand RNA. Poliovirus infected tumor cells by binding the cell adhesion molecule CD-155 expressed in GBM (95). The phase I clinical trial showed that PVS-RIPO (poliovirus-rhinovirus chimera) immunotherapy significantly improved the survival rate of GBM patients (96).

## GENE THERAPY

Gene therapy achieved the purpose of treatment by delivering therapeutic genes or manipulating disease-related genes into target cells. Based on the related therapeutic strategies, gene therapy has been divided into suicide gene therapy, oncolytic viral gene therapy, tumor suppressor gene therapy, immuno-stimulatory therapy, and tumor microenvironmental regulation therapy (97, 98). Suicide gene therapy and oncolytic viral gene therapy have been described above. The main function of tumor suppressor genes included cell signal transduction and epigenetic regulation, negative regulation of cell cycle, negative regulator expression, regulation related to stem cell proliferation, and DNA mismatch repair. Studies have shown that Rb, p53, PTEN, CDKN2A, and other tumor suppressor genes played an important role in effective GBM inhibition. However, the related clinical trials on tumor suppressor gene therapy were limited. IFN-β (interferon β) inhibited the growth and invasion of GBM with the effects of anti-tumor immune modulation, anti-proliferation, and anti-angiogenesis (99). IFN-β gene delivered by viral vectors showed a widespread expression and distribution in astrocytes and endothelial cells. A phase I clinical trial showed local inflammation and tumor necrosis in IFN-β treatment (100). The intra-tumor injection of angiostatin could effectively inhibit tumor

growth and vascularization (101, 102). Therefore, anti-angiogenic genes and tumor extracellular matrix regulatory genes made it possible to treat GBM *via* modulating tumor microenvironment.

## DISCUSSION

Glioblastoma has been a common, highly aggressive, and heterogeneous brain tumor. The infiltration of GBM to the surrounding tissue made it impossible to eliminate by surgical intervention. The inefficient delivery of BBB reduced the therapeutic effect of chemotherapy. The abnormal vascularization promoted the proliferation of tumor cells. And immunosuppressive status in tumor microenvironment severely limited the anti-tumor response to GBM. Therefore, we urgently need new treatment strategies to face the challenges of this disease and improve the prognosis of patients. Gene therapy aimed to treat GBM by targeting and regulating oncogenes and tumor suppressor genes in tumor cells. The latest understanding of genetic material and molecular alteration provided an accurate theoretical basis for gene therapy. Due to the high transfection efficiency and the development of vector engineering techniques, viruses were widely used in the researches of GBM gene therapy. Viral vectors-mediated gene therapy could be combined with current treatment methods to improve therapeutic outcomes. The transmission of suicide genes has been evaluated in clinical trials to overcome the resistance of chemotherapy. HSV-tk and TOCA511 converted the prodrugs into active form and mediate the anti-tumor response. The transfection of sh-siRT1 vectors in CD133+ GBM cells significantly improved the resistance to radiotherapy. The extensive replication of oncolytic viruses in tumor cells, including ONYX-015, Delta-24, and PVS-RIPO, led to cytolysis and induced an anti-tumor immune response. Furthermore, the expression of cytokines could enhance the therapeutic effectiveness of viral vectors by improving anti-tumor immunity. However, there are still some concerns that need to resolve in viral gene therapy before its application in clinical therapy. The first is the transduction efficiency and expression stability of target genes. As we mentioned, the

expression level of receptors and the efficiency of membrane fusion affected the entry of the virus into tumor cells. How well the viruses entered the cells would determine the effectiveness of gene therapy. Non-replicative viruses, including adenoviral vectors, were not integrated into the host genome, the expression level of the transgenes might decrease with cell divisions. Secondly, viral vectors needed to be further optimized to improve tumor targeting especially in radiotherapy and chemotherapy-resistant GBM cells, and avoid entering normal cells. Multiforme implied that heterogeneity existed among the GBM cells within the same tumor. It has been necessary to explore the common mechanism of viral replication. Moreover, the use of engineering technology to eliminate the immunogenicity of virus was worth considering, which could avoid antiviral immunity. Currently, several preclinical trials and clinical trials have proved the safety of viral therapy. However, the effectiveness of its treatment in clinical trials was still unclear, so large clinical trials have been needed. Undeniably, viral gene therapy provided a new therapeutic approach and perspective in GBM treatment.

## CONCLUSION

Viral gene therapy has shown strong therapeutic potential in GBM treatment. In the future, studies need to focus on the therapeutic efficacy and monitor adverse events before viral vectors widely use in clinical practice. Furthermore, the combination of viral gene therapy with other new treatment methods needs further research. Although the road ahead may be challenging, gene therapy has brought new hope for patients with GBM.

## AUTHOR CONTRIBUTIONS

All authors listed have made a substantial, direct, and intellectual contribution to the work, and approved it for publication.

## REFERENCES

1. Tan A, Ashley D, López G, Malinzak M, Friedman H, Khasraw M. Management of Glioblastoma: State of the Art and Future Directions. *CA: Cancer J Clin* (2020) 70(4):299–312. doi: 10.3322/caac.21613
2. Nagle V, Henry K, Hertz C, Graham M, Campos C, Parada L, et al. Imaging Tumor-Infiltrating Lymphocytes in Brain Tumors With [Cu]Cu-NOTA-Anti-CD8 PET. *Clin Cancer Res an Off J Am Assoc Cancer Res* (2021) 27:1958–66. doi: 10.1158/1078-0432.ccr-20-3243
3. Richard S. Explicating the Pivotal Pathogenic, Diagnostic, and Therapeutic Biomarker Potentials of Myeloid-Derived Suppressor Cells in Glioblastoma. *Dis Markers* (2020) 2020:8844313. doi: 10.1155/2020/8844313
4. Akter M, Lim J, Choi E, Han I. Non-Thermal Biocompatible Plasma Jet Induction of Apoptosis in Brain Cancer Cells. *Cells* (2021) 10(2):236. doi: 10.3390/cells10020236
5. Thomas A, Brennan C, DeAngelis L, Omuro A. Emerging Therapies for Glioblastoma. *JAMA Neurol* (2014) 71(11):1437–44. doi: 10.1001/jamaneurol.2014.1701

6. Batich K, Mitchell D, Healy P, Herndon J, Sampson J. Once, Twice, Three Times a Finding: Reproducibility of Dendritic Cell Vaccine Trials Targeting Cytomegalovirus in Glioblastoma. *Clin Cancer Res an Off J Am Assoc Cancer Res* (2020) 26(20):5297–303. doi: 10.1158/1078-0432.ccr-20-1082
7. Vasilev A, Sofi R, Rahman R, Smith S, Teschemacher A, Kasparov S. Using Light for Therapy of Glioblastoma Multiforme (GBM). *Brain Sci* (2020) 10(2):75. doi: 10.3390/brainsci10020075
8. Wick W, Osswald M, Wick A, Winkler F. Treatment of Glioblastoma in Adults. *Ther Adv Neurological Disord* (2018) 11:1756286418790452. doi: 10.1177/1756286418790452
9. Birzu C, French P, Caccese M, Cerretti G, Idbaih A, Zagonel V, et al. Recurrent Glioblastoma: From Molecular Landscape to New Treatment Perspectives. *Cancers* (2020) 13(1):47. doi: 10.3390/cancers13010047
10. Cabrini G, Fabbri E, Lo Nigro C, Dechecchi MC, Gambari R. Regulation of Expression of O6-Methylguanine-DNA Methyltransferase and the Treatment of Glioblastoma (Review). *Int J Oncol* (2015) 47(2):417–28. doi: 10.3892/ijo.2015.3026

11. Lee SY. Temozolomide Resistance in Glioblastoma Multiforme. *Genes Dis* (2016) 3(3):198–210. doi: 10.1016/j.gendis.2016.04.007

12. Binabaj MM, Bahrami A, ShahidSales S, Joodi M, Joudi Mashhad M, Hassanian SM, et al. The Prognostic Value of MGMT Promoter Methylation in Glioblastoma: A Meta-Analysis of Clinical Trials. *J Cell Physiol* (2018) 233(1):378–86. doi: 10.1002/jcp.25896

13. Lu C, Shervington A. Chemoresistance in Gliomas. *Mol Cell Biochem* (2008) 312:71–80. doi: 10.1007/s11010-008-9722-8

14. Dréan A, Goldwirt L, Verreault M, Canney M, Schmitt C, Guehennec J, et al. Blood-Brain Barrier, Cytotoxic Chemotherapies and Glioblastoma. *Expert Rev Neurother* (2016) 16(11):1285–300. doi: 10.1080/14737175.2016.1202761

15. Da Ros M, De Gregorio V, Iorio AL, Giunti L, Guidi M, de Martino M, et al. Glioblastoma Chemoresistance: The Double Play by Microenvironment and Blood-Brain Barrier. *Int J Mol Sci* (2018) 19(10):2879. doi: 10.3390/ijms19102879

16. Vengoji R, Ponnusamy MP, Rachagani S, Mahapatra S, Batra SK, Shonka N, et al. Novel Therapies Hijack the Blood-Brain Barrier to Eradicate Glioblastoma Cancer Stem Cells. *Carcinogenesis* (2019) 40(1):2–14. doi: 10.1093/carcin/bgy171

17. Pointer KB, Clark PA, Zorniak M, Alrfaei BM, Kuo JS. Glioblastoma Cancer Stem Cells: Biomarker and Therapeutic Advances. *Neurochemistry Int* (2014) 71:1–7. doi: 10.1016/j.neuint.2014.03.005

18. Alifieris C, Trafalis DT. Glioblastoma Multiforme: Pathogenesis and Treatment. *Pharmacol Ther* (2015) 152:63–82. doi: 10.1016/j.pharmthera.2015.05.005

19. Bernstock JD, Mooney JH, Ilyas A, Chagoya G, Estevez-Ordonez D, Ibrahim A, et al. Molecular and Cellular Intratumoral Heterogeneity in Primary Glioblastoma: Clinical and Translational Implications. *J Neurosurgery* (2019) 133:611–946. doi: 10.3171/2019.5.jns19364

20. Thakkar JP, Dolecek TA, Horbinski C, Ostrom QT, Lightner DD, Barnholtz-Sloan JS, et al. Epidemiologic and Molecular Prognostic Review of Glioblastoma. *Cancer epidemiology Biomarkers Prev Publ Am Assoc Cancer Research cosponsored by Am Soc Prev Oncol* (2014) 23(10):1985–96. doi: 10.1158/1055-9965.epi-14-0275

21. Riley MM, San P, Lok E, Swanson KD, Wong ET. The Clinical Application of Tumor Treating Fields Therapy in Glioblastoma. *J Visualized Experiments JoVE* (2019) 146. doi: 10.3791/58937

22. Benitez J, Finlay D, Castanza A, Parisian A, Ma J, Longobardi C, et al. Pten Deficiency Leads to Proteasome Addiction, a Novel Vulnerability in Glioblastoma. *Neuro-Oncology* (2021). doi: 10.1093/neuonc/noab001

23. Roux A, Peeters S, Zanello M, Bou Nassif R, Abi Lahoud G, Dezamis E, et al. Extent of Resection and Carmustine Wafer Implantation Safely Improve Survival in Patients With a Newly Diagnosed Glioblastoma: A Single Center Experience of the Current Practice. *J Neuro-Oncology* (2017) 135(1):83–92. doi: 10.1007/s11060-017-2551-4

24. Akiyama Y, Kimura Y, Enatsu R, Mikami T, Wanibuchi M, Mikuni N. Advantages and Disadvantages of Combined Chemotherapy With Carmustine Wafer and Bevacizumab in Patients With Newly Diagnosed Glioblastoma: A Single-Institutional Experience. *World Neurosurgery* (2018) 113:e508–e14. doi: 10.1016/j.wneu.2018.02.070

25. Anthony C, Mladkova-Suchy N, Adamson D. The Evolving Role of Antiangiogenic Therapies in Glioblastoma Multiforme: Current Clinical Significance and Future Potential. *Expert Opin investigational Drugs* (2019) 28(9):787–97. doi: 10.1080/13543784.2019.1650019

26. Xiao ZZ, Wang ZF, Lan T, Huang WH, Zhao YH, Ma C, et al. Carmustine as a Supplementary Therapeutic Option for Glioblastoma: A Systematic Review and Meta-Analysis. *Front Neurol* (2020) 11:1036. doi: 10.3389/fneur.2020.01036

27. Batash R, Asna N, Schaffer P, Francis N, Schaffer M. Glioblastoma Multiforme, Diagnosis and Treatment; Recent Literature Review. *Curr medicinal Chem* (2017) 24(27):3002–9. doi: 10.2174/0929867324666170516123206

28. Burri SH, Gondi V, Brown PD, Mehta MP. The Evolving Role of Tumor Treating Fields in Managing Glioblastoma: Guide for Oncologists. *Am J Clin Oncol* (2018) 41(2):191–6. doi: 10.1097/coc.0000000000000395

29. Jovčevska I. Sequencing the Next Generation of Glioblastomas. *Crit Rev Clin Lab Sci* (2018) 55(4):264–82. doi: 10.1080/10408363.2018.1462759

30. Le Rhun E, Preusser M, Roth P, Reardon DA, van den Bent M, Wen P, et al. Molecular Targeted Therapy of Glioblastoma. *Cancer Treat Rev* (2019) 80:101896. doi: 10.1016/j.ctrv.2019.101896

31. Bansal K, Engelhard HH. Gene Therapy for Brain Tumors. *Curr Oncol Rep* (2000) 2(5):463–72. doi: 10.1007/s11912-000-0067-z

32. Kroeger KM, Muhammad AK, Baker GJ, Assi H, Wibowo MK, Xiong W, et al. Gene Therapy and Virotherapy: Novel Therapeutic Approaches for Brain Tumors. *Discovery Med* (2010) 10(53):293–304.

33. Assi H, Candolfi M, Baker G, Mineharu Y, Lowenstein PR, Castro MG. Gene Therapy for Brain Tumors: Basic Developments and Clinical Implementation. *Neurosci Lett* (2012) 527(2):71–7. doi: 10.1016/j.neulet.2012.08.003

34. Immidisetti A, Nwagwu C, Adamson D, Patel N, Carbonell A. Clinically Explored Virus-Based Therapies for the Treatment of Recurrent High-Grade Glioma in Adults. *Biomedicines* (2021) 9(2):138. doi: 10.3390/biomedicines9020138

35. Saha D, Martuza RL, Rabkin SD. Oncolytic Herpes Simplex Virus Immunovirotherapy in Combination With Immune Checkpoint Blockade to Treat Glioblastoma. *Immunotherapy* (2018) 10(9):779–86. doi: 10.2217/imt-2018-0009

36. Di Meco F, Benedetti S, Colombo MP, Finocchiaro G. Perspectives for the Gene Therapy of Malignant Gliomas by Suicide Gene Transfer. *J neurosurgical Sci* (1997) 41(3):227–34.

37. Tai CK, Kasahara N. Replication-Competent Retrovirus Vectors for Cancer Gene Therapy. *Front Bioscience* (2008) 13:3083–95. doi: 10.2741/2910

38. Culver KW, Ram Z, Wallbridge S, Ishii H, Oldfield EH, Blaese RM. In Vivo Gene Transfer With Retroviral Vector-Producer Cells for Treatment of Experimental Brain Tumors. *Science* (5063) 1992 256:1550–2. doi: 10.1126/science.1317968

39. Haddad AF, Young JS, Mummaneni NV, Kasahara N, Aghi MK. Immunologic Aspects of Viral Therapy for Glioblastoma and Implications for Interactions With Immunotherapies. *J Neuro-Oncology* (2021) 152:1–13. doi: 10.1007/s11060-020-03684-5

40. Rainov NG. A Phase III Clinical Evaluation of Herpes Simplex Virus Type 1 Thymidine Kinase and Ganciclovir Gene Therapy as an Adjuvant to Surgical Resection and Radiation in Adults With Previously Untreated Glioblastoma Multiforme. *Hum Gene Ther* (2000) 11(17):2389–401. doi: 10.1089/104303400750038499

41. Ram Z, Culver KW, Oshiro EM, Viola JJ, DeVroom HL, Otto E, et al. Therapy of Malignant Brain Tumors by Intratumoral Implantation of Retroviral Vector-Producing Cells. *Nat Med* (1997) 3(12):1354–61. doi: 10.1038/nm1297-1354

42. Perez OD, Logg CR, Hiraoka K, Diago O, Burnett R, Inagaki A, et al. Design and Selection of Toca 511 for Clinical Use: Modified Retroviral Replicating Vector With Improved Stability and Gene Expression. *Mol Ther J Am Soc Gene Ther* (2012) 20(9):1689–98. doi: 10.1038/mt.2012.83

43. Hogan DJ, Zhu JJ, Diago OR, Gammon D, Haghighi A, Lu G, et al. Molecular Analyses Support the Safety and Activity of Retroviral Replicating Vector Toca 511 in Patients. *Clin Cancer Res* (2018) 24 (19):4680–93. doi: 10.1158/1078-0432.ccr-18-0619

44. Takahashi M, Valdes G, Hiraoka K, Inagaki A, Kamijima S, Micewicz E, et al. Radiosensitization of Gliomas by Intracellular Generation of 5-Fluorouracil Potentiates Prodrug Activator Gene Therapy With a Retroviral Replicating Vector. *Cancer Gene Ther* (2014) 21(10):405–10. doi: 10.1038/cgt.2014.38

45. Hiraoka K, Inagaki A, Kato Y, Huang TT, Mitchell LA, Kamijima S, et al. Retroviral Replicating Vector-Mediated Gene Therapy Achieves Long-Term Control of Tumor Recurrence and Leads to Durable Anticancer Immunity. *Neuro Oncol* (2017) 19(7):918–29. doi: 10.1093/neuonc/nox038

46. Mitchell LA, Lopez Espinoza F, Mendoza D, Kato Y, Inagaki A, Hiraoka K, et al. Toca 511 Gene Transfer and Treatment With the Prodrug, 5-Fluorocytosine, Promotes Durable Antitumor Immunity in a Mouse Glioma Model. *Neuro Oncol* (2017) 19(7):930–9. doi: 10.1093/neuonc/nox037

47. Cloughesy TF, Landolfi J, Hogan DJ, Bloomfield S, Carter B, Chen CC, et al. Phase 1 Trial of Vocimagene Amiretrorepvec and 5-Fluorocytosine for Recurrent High-Grade Glioma. *Sci Trans Med* (2016) 8(341):341ra75. doi: 10.1126/scitranslmed.aad9784

48. Cloughesy TF, Petrecca K, Walbert T, Butowski N, Salacz M, Perry J, et al. Effect of Vocimagene Amiretrorepvec in Combination With Flucytosine Vs Standard of Care on Survival Following Tumor Resection in Patients With

Recurrent High-Grade Glioma: A Randomized Clinical Trial. *JAMA Oncol* (2020) 6(12):1939–46. doi: 10.1001/jamaoncol.2020.3161

49. Lesnik EA, Sampath R, Ecker DJ. Rev Response Elements (RRE) in Lentiviruses: An Rnamotif Algorithm-Based Strategy for RRE Prediction. *Medicinal Res Rev* (2002) 22(6):617–36. doi: 10.1002/med.10027

50. Moreira AS, Cavaco DG, Faria TQ, Alves PM, Carrondo MJT, Peixoto C. Advances in Lentivirus Purification. *Biotechnol J* (2021) 16(1):e2000019. doi: 10.1002/biot.202000019

51. McCarron A, Donnelley M, McIntyre C, Parsons D. Challenges of Up-Scaling Lentivirus Production and Processing. *J Biotechnol* (2016) 240:23–30. doi: 10.1016/j.jbiotec.2016.10.016

52. Manikandan C, Kaushik A, Sen D. Viral Vector: Potential Therapeutic for Glioblastoma Multiforme. *Cancer Gene Ther* (2020) 27(5):270–9. doi: 10.1038/s41417-019-0124-8

53. Kock N, Kasmieh R, Weissleder R, Shah K. Tumor Therapy Mediated by Lentiviral Expression of Shbcl-2 and S-TRAIL. *Neoplasia (New York NY)* (2007) 9(5):435–42. doi: 10.1593/neo.07223

54. Chang CJ, Hsu CC, Yung MC, Chen KY, Tzao C, Wu WF, et al. Enhanced Radiosensitivity and Radiation-Induced Apoptosis in Glioma CD133-Positive Cells by Knockdown of Sirt1 Expression. *Biochem Biophys Res Commun* (2009) 380(2):236–42. doi: 10.1016/j.bbrc.2009.01.040

55. Luan Y, Zhang S, Zuo L, Zhou L. Overexpression of Mir-100 Inhibits Cell Proliferation, Migration, and Chemosensity in Human Glioblastoma Through FGFR3. *OncoTargets Ther* (2015) 8:3391–400. doi: 10.2147/ott.s85677

56. Sun T, Patil R, Galstyan A, Klymyshyn D, Ding H, Chesnokova A, et al. Blockade of a Laminin-411-Notch Axis With CRISPR/Cas9 or a Nanobioconjugate Inhibits Glioblastoma Growth Through Tumor-Microenvironment Cross-Talk. *Cancer Res* (2019) 79(6):1239–51. doi: 10.1158/0008-5472.can-18-2725

57. Sánchez-Hernández L, Hernández-Soto J, Vergara P, González RO, Segovia J. Additive Effects of the Combined Expression of Soluble Forms of GAS1 and PTEN Inhibiting Glioblastoma Growth. *Gene Ther* (2018) 25(6):439–49. doi: 10.1038/s41434-018-0020-0

58. Hall K, Blair Zajdel ME, Blair GE. Unity and Diversity in the Human Adenoviruses: Exploiting Alternative Entry Pathways for Gene Therapy. *Biochem J* (2010) 431(3):321–36. doi: 10.1042/bj20100766

59. Yang TC, Maluf NK. Characterization of the Non-Specific DNA Binding Properties of the Adenoviral Iva2 Protein. *Biophys Chem* (2014) 193-194:1–8. doi: 10.1016/j.bpc.2014.06.005

60. Volpers C, Kochanek S. Adenoviral Vectors for Gene Transfer and Therapy. *J Gene Med* (2004) 6 Suppl 1:S164–71. doi: 10.1002/jgm.496

61. Bergelson JM, Cunningham JA, Droguett G, Kurt-Jones EA, Krithivas A, Hong JS, et al. Isolation of a Common Receptor for Coxsackie B Viruses and Adenoviruses 2 and 5. *Science* (5304) 1997) 275:1320–3. doi: 10.1126/science.275.5304.1320

62. Zhang Y, Bergelson JM. Adenovirus Receptors. *J Virol* (2005) 79(19):12125–31. doi: 10.1128/jvi.79.19.12125-12131.2005

63. Stasiak AC, Stehle T. Human Adenovirus Binding to Host Cell Receptors: A Structural View. *Med Microbiol Immunol* (2020) 209(3):325–33. doi: 10.1007/s00430-019-00645-2

64. Castro MG, Candolfi M, Wilson TJ, Calinescu A, Paran C, Kamran N, et al. Adenoviral Vector-Mediated Gene Therapy for Gliomas: Coming of Age. *Expert Opin Biol Ther* (2014) 14(9):1241–57. doi: 10.1517/14712598.2014.915307

65. Kochanek S. High-Capacity Adenoviral Vectors for Gene Transfer and Somatic Gene Therapy. *Hum Gene Ther* (1999) 10(15):2451–9. doi: 10.1089/10430349950016807

66. Nandi S, Lesniak M. Adenoviral Virotherapy for Malignant Brain Tumors. *Expert Opin Biol Ther* (2009) 9(6):737–47. doi: 10.1517/14712590902988451

67. McCormick F. Interactions Between Adenovirus Proteins and the P53 Pathway: The Development of ONYX-015. *Semin Cancer Biol* (2000) 10(6):453–9. doi: 10.1006/scbi.2000.0336

68. Rius-Rocabert S, García-Romero N, García A, Ayuso-Sacido A, Nistal-Villan E. Oncolytic Virotherapy in Glioma Tumors. *Int J Mol Sci* (2020) 21(20):7604. doi: 10.3390/ijms21207604

69. Chiocca EA, Abbed KM, Tatter S, Louis DN, Hochberg FH, Barker F, et al. A Phase I Open-Label, Dose-Escalation, Multi-Institutional Trial of Injection With an E1B-Attenuated Adenovirus, ONYX-015, Into the Peritumoral Region of Recurrent Malignant Gliomas, in the Adjuvant Setting. *Mol Ther J Am Soc Gene Ther* (2004) 10(5):958–66. doi: 10.1016/j.ymthe.2004.07.021

70. Fueyo J, Gomez-Manzano C, Alemany R, Lee PS, McDonnell TJ, Mitlianga P, et al. A Mutant Oncolytic Adenovirus Targeting the Rb Pathway Produces Anti-Glioma Effect in Vivo. *Oncogene* (2000) 19(1):2–12. doi: 10.1038/sj.onc.1203251

71. Philbrick B, Adamson DC. DNX-2401: An Investigational Drug for the Treatment of Recurrent Glioblastoma. *Expert Opin Investig Drugs* (2019) 28(12):1041–9. doi: 10.1080/13543784.2019.1694000

72. Lamfers ML, Grill J, Dirven CM, Van Beusechem VW, Geoerger B, Van Den Berg J, et al. Potential of the Conditionally Replicative Adenovirus Ad5-Delta24RGD in the Treatment of Malignant Gliomas and Its Enhanced Effect With Radiotherapy. *Cancer Res* (2002) 62(20):5736–42.

73. Ahmad I, Wilson DW. HSV-1 Cytoplasmic Envelopment and Egress. *Int J Mol Sci* (2020) 21(17):5969. doi: 10.3390/ijms21175969

74. Grandi P, Peruzzi P, Reinhart B, Cohen JB, Chiocca EA, Glorioso JC. Design and Application of Oncolytic HSV Vectors for Glioblastoma Therapy. *Expert Rev Neurother* (2009) 9(4):505–17. doi: 10.1586/ern.09.9

75. Streby KA, Geller JI, Currier MA, Warren PS, Racadio JM, Towbin AJ, et al. Intratumoral Injection of HSV1716, an Oncolytic Herpes Virus, is Safe and Shows Evidence of Immune Response and Viral Replication in Young Cancer Patients. *Clin Cancer Res* (2017) 23(14):3566–74. doi: 10.1158/1078-0432.ccr-16-2900

76. Rampling R, Cruickshank G, Papanastassiou V, Nicoll J, Hadley D, Brennan D, et al. Toxicity Evaluation of Replication-Competent Herpes Simplex Virus (ICP 34.5 Null Mutant 1716) in Patients With Recurrent Malignant Glioma. *Gene Ther* (2000) 7(10):859–66. doi: 10.1038/sj.gt.3301184

77. Harrow S, Papanastassiou V, Harland J, Mabbs R, Petty R, Fraser M, et al. HSV1716 Injection Into the Brain Adjacent to Tumour Following Surgical Resection of High-Grade Glioma: Safety Data and Long-Term Survival. *Gene Ther* (2004) 11(22):1648–58. doi: 10.1038/sj.gt.3302289

78. Cassady KA, Bauer DF, Roth J, Chambers MR, Shoeb T, Coleman J, et al. Pre-Clinical Assessment of C134, a Chimeric Oncolytic Herpes Simplex Virus, in Mice and Non-Human Primates. *Mol Ther Oncolytics* (2017) 5:1–10. doi: 10.1016/j.omto.2017.02.001

79. Cinatl J Jr, Michaelis M, Driever PH, Cinatl J, Hrabeta J, Suhan T, et al. Multimutated Herpes Simplex Virus G207 is a Potent Inhibitor of Angiogenesis. *Neoplasia (New York NY)* (2004) 6(6):725–35. doi: 10.1593/neo.04265

80. Markert JM, Liechty PG, Wang W, Gaston S, Braz E, Karrasch M, et al. Phase Ib Trial of Mutant Herpes Simplex Virus G207 Inoculated Pre-and Post-Tumor Resection for Recurrent GBM. *Mol Ther J Am Soc Gene Ther* (2009) 17(1):199–207. doi: 10.1038/mt.2008.228

81. Markert JM, Razdan SN, Kuo HC, Cantor A, Knoll A, Karrasch M, et al. A Phase 1 Trial of Oncolytic HSV-1, G207, Given in Combination With Radiation for Recurrent GBM Demonstrates Safety and Radiographic Responses. *Mol Ther J Am Soc Gene Ther* (2014) 22(5):1048–55. doi: 10.1038/mt.2014.22

82. Chiocca EA, Nakashima H, Kasai K, Fernandez SA, Oglesbee M. Preclinical Toxicology of Rqnestin34.5v.2: An Oncolytic Herpes Virus With Transcriptional Regulation of the ICP34.5 Neurovirulence Gene. *Mol Ther Methods Clin Dev* (2020) 17:871–93. doi: 10.1016/j.omtm.2020.03.028

83. Bartlett DL, Liu Z, Sathaiah M, Ravindranathan R, Guo Z, He Y, et al. Oncolytic Viruses as Therapeutic Cancer Vaccines. *Mol Cancer* (2013) 12(1):103. doi: 10.1186/1476-4598-12-103

84. Foreman PM, Friedman GK, Cassady KA, Markert JM. Oncolytic Virotherapy for the Treatment of Malignant Glioma. *Neurother J Am Soc Exp Neurother* (2017) 14(2):333–44. doi: 10.1007/s13311-017-0516-0

85. Breitbach CJ, Paterson JM, Lemay CG, Falls TJ, McGuire A, Parato KA, et al. Targeted Inflammation During Oncolytic Virus Therapy Severely Compromises Tumor Blood Flow. *Mol Ther J Am Soc Gene Ther* (2007) 15(9):1686–93. doi: 10.1038/sj.6300215

86. Workenhe ST, Mossman KL. Oncolytic Virotherapy and Immunogenic Cancer Cell Death: Sharpening the Sword for Improved Cancer Treatment Strategies. *Mol Ther J Am Soc Gene Ther* (2014) 22(2):251–6. doi: 10.1038/mt.2013.220

87. Chiocca EA, Rabkin SD. Oncolytic Viruses and Their Application to Cancer Immunotherapy. *Cancer Immunol Res* (2014) 2(4):295–300. doi: 10.1158/2326-6066.cir-14-0015

88. Biederer C, Ries S, Brandts CH, McCormick F. Replication-Selective Viruses for Cancer Therapy. *J Mol Med (Berlin Germany)* (2002) 80(3):163–75. doi: 10.1007/s00109-001-0295-1

89. Forsyth P, Roldán G, George D, Wallace C, Palmer CA, Morris D, et al. A Phase I Trial of Intratumoral Administration of Reovirus in Patients With Histologically Confirmed Recurrent Malignant Gliomas. *Mol Ther J Am Soc Gene Ther* (2008) 16(3):627–32. doi: 10.1038/sj.mt.6300403

90. Samson A, Scott KJ, Taggart D, West EJ, Wilson E, Nuovo GJ, et al. Intravenous Delivery of Oncolytic Reovirus to Brain Tumor Patients Immunologically Primes for Subsequent Checkpoint Blockade. *Sci Trans Med* (2018) 10(422):7577. doi: 10.1126/scitranslmed.aam7577

91. Thorne SH, Bartlett DL, Kirn DH. The Use of Oncolytic Vaccinia Viruses in the Treatment of Cancer: A New Role for an Old Ally? *Curr Gene Ther* (2005) 5(4):429–43. doi: 10.2174/1566523054546215

92. Vihinen-Ranta M, Suikkanen S, Parrish CR. Pathways of Cell Infection by Parvoviruses and Adeno-Associated Viruses. *J Virol* (2004) 78(13):6709–14. doi: 10.1128/jvi.78.13.6709-6714.2004

93. Geletneky K, Hajda J, Angelova AL, Leuchs B, Capper D, Bartsch AJ, et al. Oncolytic H-1 Parvovirus Shows Safety and Signs of Immunogenic Activity in a First Phase I/IIa Glioblastoma Trial. *Mol Ther J Am Soc Gene Ther* (2017) 25(12):2620–34. doi: 10.1016/j.ymthe.2017.08.016

94. Angelova AL, Barf M, Geletneky K, Unterberg A, Rommelaere J. Immunotherapeutic Potential of Oncolytic H-1 Parvovirus: Hints of Glioblastoma Microenvironment Conversion Towards Immunogenicity. *Viruses* (2017) 9(12):382. doi: 10.3390/v9120382

95. Merrill MK, Bernhardt G, Sampson JH, Wikstrand CJ, Bigner DD, Gromeier M. Poliovirus Receptor CD155-Targeted Oncolysis of Glioma. *Neuro Oncol* (2004) 6(3):208–17. doi: 10.1215/s1152851703000577

96. Desjardins A, Gromeier M, Herndon JE,2, Beaubier N, Bolognesi DP, Friedman AH, et al. Recurrent Glioblastoma Treated With Recombinant Poliovirus. *New Engl J Med* (2018) 379(2):150–61. doi: 10.1056/NEJMoa1716435

97. Kamran N, Calinescu A, Candolfi M, Chandran M, Mineharu Y, Asad A, et al. Recent Advances and Future of Immunotherapy for Glioblastoma. *Expert Opin Biol Ther* (2016) 16(10):1245–64. doi: 10.1080/14712598.2016.1212012

98. Zhang H, Wang R, Yu Y, Liu J, Luo T, Fan F. Glioblastoma Treatment Modalities Besides Surgery. *J Cancer* (2019) 10(20):4793–806. doi: 10.7150/jca.32475

99. GuhaSarkar D, Su Q, Gao G, Sena-Esteves M. Systemic AAV9-Ifnβ Gene Delivery Treats Highly Invasive Glioblastoma. *Neuro-Oncology* (2016) 18(11):1508–18. doi: 10.1093/neuonc/now097

100. Yoshida J, Mizuno M, Fujii M, Kajita Y, Nakahara N, Hatano M, et al. Human Gene Therapy for Malignant Gliomas (Glioblastoma Multiforme and Anaplastic Astrocytoma) by in Vivo Transduction With Human Interferon Beta Gene Using Cationic Liposomes. *Hum Gene Ther* (2004) 15(1):77–86. doi: 10.1089/10430340460732472

101. Tanaka T, Cao Y, Folkman J, Fine H. Viral Vector-Targeted Antiangiogenic Gene Therapy Utilizing an Angiostatin Complementary DNA. *Cancer Res* (1998) 58(15):3362–9.

102. Szentirmai O, Baker C, Bullain S, Lin N, Takahashi M, Folkman J, et al. Successful Inhibition of Intracranial Human Glioblastoma Multiforme Xenograft Growth Via Systemic Adenoviral Delivery of Soluble Endostatin and Soluble Vascular Endothelial Growth Factor Receptor-2: Laboratory Investigation. *J neurosurgery* (2008) 108(5):979–88. doi: 10.3171/jns/2008/108/5/0979

OPEN ACCESS

*Edited by:*
Sandro M. Krieg,
Technical University of Munich,
Germany

*Reviewed by:*
Josef Vymazal,
Na Homolce Hospital, Czechia
Carsten Hagemann,
Julius Maximilian University of
Würzburg, Germany

*\*Correspondence:*
Benedikt Linder
Linder@med.uni-frankfurt.de
Daniel Dubinski
danieldubinski@gmail.com

*†Present address:*
Daniel Dubinski,
Department of Neurosurgery,
University Hospital Rostock,
Rostock, Germany

‡These authors share first authorship

§These authors share last authorship

# Dexamethasone Treatment Limits Efficacy of Radiation, but Does Not Interfere With Glioma Cell Death Induced by Tumor Treating Fields

Benedikt Linder [1‡], Abigail Schiesl [1‡], Martin Voss [2], Franz Rödel [3], Stephanie Hehlgans [3], Ömer Güllülü [3], Volker Seifert [4], Donat Kögel [1], Christian Senft [4§] and Daniel Dubinski [1,4\*†§]

[1] Experimental Neurosurgery, Neuroscience Center, Goethe University Hospital, Frankfurt, Germany, [2] Dr. Senckenberg Institute of Neurooncology, Goethe University Hospital, Frankfurt, Germany, [3] Department of Radiotherapy and Oncology, Goethe University Hospital Frankfurt, Frankfurt, Germany, [4] Department of Neurosurgery, Goethe University Hospital, Frankfurt, Germany

**Purpose:** Dexamethasone (Dex) is the most common corticosteroid to treat edema in glioblastoma (GBM) patients. Recent studies identified the addition of Dex to radiation therapy (RT) to be associated with poor survival. Independently, Tumor Treating Fields (TTFields) provides a novel anti-cancer modality for patients with primary and recurrent GBM. Whether Dex influences the efficacy of TTFields, however, remains elusive.

**Methods:** Human GBM cell lines MZ54 and U251 were treated with RT or TTFields in combination with Dex and the effects on cell counts and cell death were determined *via* flow cytometry. We further performed a retrospective analysis of GBM patients with TTFields treatment +/- concomitant Dex and analysed its impact on progression-free (PFS) and overall survival (OS).

**Results:** The addition of Dex significantly reduced the efficacy of RT in U251, but not in MZ54 cells. TTFields (200 kHz/250 kHz) induced massive cell death in both cell lines. Concomitant treatment of TTFields and Dex did not reduce the overall efficacy of TTFields. Further, in our retrospective clinical analysis, we found that the addition of Dex to TTFields therapy did not influence PFS nor OS.

**Conclusion:** Our translational investigation indicates that the efficacy of TTFields therapy in patients with GBM and GBM cell lines is not affected by the addition of Dex.

Keywords: brain cancer, TTFields, corticosteroids, dexamethasone, glioma, survival, translational investigation

# INTRODUCTION

## Dexamethasone Administration for Vasogenic Edema Management in Patients With Glioblastoma

Patients suffering from glioblastoma (GBM) usually are afflicted with perilesional edema that is caused by a tumor-induced disruption of the blood brain barrier (BBB) (1). Defective astrocytes lead to the impairment of endothelial tight junctions on the one hand and tumor-produced vascular endothelial growth factor (VEGF) that increases vessel permeability on the other hand resulting in the diffusion of fluid into the extracellular brain parenchyma with a consequent increase of intracranial pressure (ICP) (2). The resulting perilesional edema is the major contributor to patient's neurologic deficits. Corticosteroids reduce the permeability of tumor vessels by upregulating tight junctions and inducing the transcription of several genes that are involved in stabilization of the BBB (e.g. occludin, NF-κB, VE-cadherin etc) (3). In the clinical practice, Dexamethasone (Dex) has become the corticoid of choice for brain tumor-associated cerebral edema due to its fast and effective alleviation of perilesional edemas, long half-life, low mineralocorticoid activity and the reduction of nausea. Despite its routine clinical use, the lack of prospective clinical studies impairs the implementation of a standard dosage protocol. Usually, the orally administered dosage ranges from daily 2 to 20 mg Dex (4).

## Unfavorable Clinical Effects of Concomitant Dex Administration in GBM

Given the fact that perilesional edemas are a major cause of mortality in GBM patients, their treatment is indispensable. However, long-term Dex ingestion also leads to numerous well characterized clinical side effects including insomnia, psychiatric alterations, tremor, hyperglycemia, muscle atrophy, cushingoid appearance, hypertension, gastrointestinal perforation and immunosuppression (1). Furthermore, recent studies identified concomitant Dex administration as a risk factor for an impaired progression-free (PFS) and overall survival (OS) of patients suffering from GBM. A retrospective clinical study of 73 GBM patients demonstrated that Dex administration concomitant to radiation therapy (RT) leads to a reduction of the OS from 22.6 to 12.7 months (4). Furthermore, a multicentre retrospective analysis of more than 2000 GBM patients identified Dex as an independent risk factor for poor outcome, even after adjusting for extent of resection, initial treatment, age and Karnofsky Performance Score (KPS) (5). Another study demonstrated that patients with Dex-induced leucocytosis (DIL) had decreased OS and PFS and showed a significant reduction of tumor-infiltrating leukocytes and lymphocytes (6).

## Experimental Effects of Dex Administration in Preclinical Studies

The molecular effects of Dex on GBM cells as described in previous studies are pleiotropic and partially conflicting, possibly related to context-dependent effects in different tumors/cell models and experimental setups. Accordingly, Dex was shown either to inhibit or to stimulate the proliferation of glioma cells *in vitro*. Previous data further suggest a time-dependent and dosage-dependent antiproliferative effect of Dex (7, 8). Moreover, Dex administration was associated with reduced glioma cell invasion, primarily caused by decreased transcription of metalloproteases (9). On the other hand, Dex decreased the efficacy of chemotherapy by counteracting an alkylating agents induced apoptosis in primary GBM cell lines (10). The addition of Dex to glioma stem cells led to increased proliferation and invasion (2). In addition, Dex treatment leads to a decreased hypoxia-sensitivity in primary glioma cell lines, presumably by downregulation of VEGF (11).

## TTFields in GBM Therapy

TTFields (Optune, Novocure LTD) is a new type of cancer treatment modality that has been shown to significantly improve outcome in GBM patients in combination with radio-chemotherapy and was approved for newly diagnosed and recurrent GBM (12). TTFields create alternating electric fields with varying frequencies between 50 to 400 kHz and its efficacy is dependent on the cell type, size and orientation (13). Two pairs of juxtapositioned transduced arrays placed on the patient's skin, deliver a locoregional antiproliferative and cell-killing effect on mitotic glioma cells by interfering with the cell's mitotic apparatus (disruption of the polymerization of highly dynamic microtubules and septin filaments). This electromechanical cell cycle intervention leads to abnormal chromosome segregation and consecutive cell death (14). However, recent studies explored further mechanisms of action including the inhibition of the DNA damage response (DDR) by altered expression of DNA repair genes in the BRCA1 pathway and impaired cellular migration and invasion (15). Furthermore, TTFields increased immunogenic cell death in combination with anti-PD1 therapy presumably by increasing the amount of CD45+ tumor infiltrating cells.

## Aim of This Study

To date, Dex remains the gold standard of edema treatment in the clinical setting due to its highly effective resolution of perilesional edema and fast improvement of patient's neurologic deficits despite the unfavorable long-term consequences. Previous studies identified the addition of Dex to increased radio resistance and poor outcome in glioma therapy. Furthermore, TTFields therapy is a novel effective treatment modality that shows improved survival in GBM therapy and is now widely used in the clinical setting. Yet, the effects of concomitant Dex administration during TTFields therapy remain unknown. We thus conducted this translational study to analyse the effects of Dex on TTFields efficacy in patients with GBM and GBM cell lines.

# MATERIALS AND METHODS

## Patients and Data Collection

For this study, an ethical approval was obtained from ethics committee of the University hospital Frankfurt am Main (Identification number: 20-676). As a non-interventional, retrospective single-center study no patient consent was necessary.

## Patient Cohort

In total, 26 GBM patients that were treated at the Department of Neurosurgery, University Hospital, Goethe University Frankfurt am Main and received TTFields treatment between November 2015 and September 2019 were retrospectively analysed. According the EF 14 trial the inclusion criteria was pathological GBM verification, age over 18 years, Karnofsky scale ≥ 70, received maximal debulking surgery and radiotherapy concomitant with Temozolomide (45-70Gy). Further inclusion criteria were the application of TTFields (Novocure, LTD). Patients in the Dexamethasone cohort were identified as presence of Dexamethasone medication at the beginning of TTFields treatment and the dosage ranged between 0.5 and 4mg/d. Patient characteristics that were extracted from the medical chart included sex, age, MGMT methylation status, date of starting and ending TTFields therapy, date of surgery, date of death or date of last contact and the date of tumor progression. Tumor progression was defined as the date of cranial MRI with progressive disease according to the RANO 18 criteria and/or the assessment of the local interdisciplinary neurooncological tumor board (16).

## Clinical Application of TTFields

Within the framework of this trial, TTFields were started after completion of radiochemotherapy. The alternating electric fields were delivered (≥ 18 hours/d) via 4 transducer arrays on the shaved scalp. Temozolomide was administered (150-200 mg/m2) for 5 days per 28-day cycle (6-12 cycles) (12).

## GBM Cell Lines and Culture

U251-MG (U251) and MZ-54 (17), two adherent human Glioblastoma wild type cell lines were used. Both cell lines were maintained in DMEM Glutamax Media (Sigma-Aldrich) supplemented with 10% heat-inactivated FCS (Invitrogen) and 1% Penicillin/Streptomycin (Invitrogen). For cultivation, cells were kept in an incubator at 37°C and a 5% $CO_2$ atmosphere. We passaged the cells weekly at a ratio of 1:10 for MZ-54 or 1:20 for U251 using Trypsin (Sigma, Aldrich) as detachment solution. A 100mg/10ml Dex stock injection solution (Jenapharm) was added after media change in final half-maximal inhibitory concentrations (IC50) of 65 µM for MZ-54 cells and 165 µM for U251 cells. Dex was kept at 4°C in a light sealed Falcon.

## TTFields Application

TTFields were applied according to the protocol described by Porat et al. (17) with minor modifications to the experimental setup. 10.000 cells per dish were seeded on 24 mm² coverslips in 500µl DMEM medium placed at the bottom of the ceramic TTFields dishes. After overnight incubation at 37°C, the medium was removed and replaced with fresh 2 ml DMEM medium with or without Dex. The TTFields dishes were covered with Parafilm (Sigma-Aldrich) manually before starting TTFields treatment. Cells were then subjected to electric field treatment at 250 kHz for MZ-54 and 200 kHz for U251 and expected intensities between 1.48 V/cm – 1.41 V/cm for 24h, 48h and 72h using the Inovitro™ system (Novocure Haifa, Israel). The TTFields dishes were kept inside an incubator at 20°C - 21°C, since the Novocure device produces excessive heat (18). After harvesting and Annexin/PI staining, the effects of TTFields on cell death induction and cell count were analysed by a BD Accuri C6 (BD Biosciences, Franklin Lakes, New Jersey, USA) fluorescence-activated cell-sorting device (FACS).

## Frequency Scan

For the determination of the optimal frequency, TTFields were administered as described in Porat et al. (17), on MZ-54 cells at different frequencies ranging from 200 kHz, 250 kHz, 300 kHz to 350 kHz for a duration of 72 h. Cell death and cell count were then determined via flow cytometry. For U251 cells, we worked with 200 kHz as optimal frequency as used in previous studies (19).

## Cell Viability Assay

The IC50 concentration of Dex were determined for four different cell lines (U251 and MZ-54) using the MTT-Assay. For this purpose, cells were plated at 5.000 cells/well in 96-well plates and a day later subjected to 72 h Dex treatment at increasing concentrations: 0 µM, 0.2 µM, 1 µM, 5 µM, 10 µM, 50 µM, 100 µM, 250 µM, 500 µM, 1 mM. Cells were cultivated at 37°C. At time points 0 h, 24 h, 48 h, 72 h the cell confluence was measured using the Tecan reader. For the determination of cell viability, 20 µl of 5 mg/ml MTT-Tetrazolium salt (3-[4,5-Dimethylthiazol-2-yl]-2,5-diphenyltetrazolium bromide) (Sigma-Aldrich) was added to each well after treatment. After allowing cells to incubate for 3 h at 37°C, the media containing MTT was carefully removed and 100 µl isopropanol/HCl solution (1ml HCl in 24 ml Isopropanol) was added to each well with gently mixing for 20 min to dissolve the formazan crystals and fixate the cells. The photometrical absorption was measured using a Tecan Spark plate reader (Tecan) at a wavelength of 560 nm.

## IC50 Calculations

The IC50 value is the concentration of a drug in which cell viability is inhibited to 50% of the control. The IC50 was determined by nonlinear regression analysis in GraphPad Prism (Version 7, GraphPad Software) using the function "log (inhibitor) vs. response (three parameters) of the data derived from the MTT measurement after normalizing the data from solvent-treated cells to 100% using the "remove baseline" function.

## Flow Cytometry

After the treatment period the medium was removed, and wells were washed with PBS. Cells were next trypsinized and incubated for 10 min at 37°C. PBS was added to the cells to stop trypsin reaction, washed twice, and then transferred into FACS tubes. The FACS tubes were centrifuged for 3 minutes at 195 x g to form pellets. After discarding the supernatant, cells were stained with 0.8 µl Propidium Iodide (Sigma-Aldrich, 10 µg/ml) and 0.8 µl Annexin V-APC (BD Pharmingen #550475) in 50 µl FACS-Buffer, mixed and incubated in the dark for 10 min at room temperature. Flow cytometric determination of cell death

was performed by counting of 10.000 cells on an Acurri C6 (Becton Dikinson).

## Irradiation Procedures

Cells were plated in 12 well-plates and then pre-treated with or without Dex for 24 h prior to radiation. Irradiation (IR) was performed using a linear accelerator with 6 MV photon energy, 100 cm focus to isocentre distance and a dose rate of 6 Gy/min (Elekta, Crawley, UK) at the Department of Radiation Therapy (University Hospital Frankfurt, Frankfurt, Germany). GBM cells were irradiated at room temperature with a dose of 10, 20, 30, 40 Gy. Afterwards cells were incubated with or without Dex for another 48 h and 72 h at 37°C. Control cells underwent the same experimental conditions.

## Statistical Analysis

Statistical analysis was done using GraphPad Prism 7 (GraphPad Software, La Jolla CA, USA). The minimum level of statistical significance was set at $p \leq 0.05$. Significances were marked as follows: $p \leq 0.05$: *, $p \leq 0.01$: **, $p \leq 0.001$: ***, $p<0.0001$: ****, n.s. not significant. Significances are depicted between control and treatments or as indicated. To estimate the survival rates, the Kaplan-Meier analysis was used. The differences between curves were assessed using the log-rank test. Progression-free survival (PFS) was defined as the time from diagnosis to first recurrence or death. Overall survival (OS) was defined as the time of first presentation to death. The applied statistical test is denoted in the respective figure legend.

## RESULTS

In order to test our hypothesis whether Dex affects the efficacy of TTFields-treatment we first determined the response of the cells towards Dex. For this purpose, we treated the cells with increasing concentrations of Dex, ranging from 0.2 μM to 1000 μM and measured cell viability after 72 h using MTT assays (**Figure 1A**). Afterwards we determined the IC50 values using non-linear regression analyses and obtained an IC50 of 65 and 165 μM for MZ-54 and U251, respectively. This concentration reflects the frequently used clinical dosage of 4-16 mg/d. Next, we aimed to determine the optimal TTFields frequency for MZ-54 cells. Thus, we performed a frequency scan using 200, 250, 300 and 350 kHz of MZ-54 cells and measured cell death (**Figure 1B**) and cell count (**Figure 1C**). This approach revealed that the optimal frequency for MZ-54 cells is 250 kHz. For U251 cells we adopted the best frequency available from the literature at 200 kHz (20).

As outlined above, recently, it was shown that Dex can protect GBM cells from radiation-induced cell death *in vitro* (5). Therefore, we first wanted to test whether these effects using our cell models. For this purpose, we pre-treated MZ-54 and U251 GBM cells with Dex for 24 h before radiation treatment consisting of 10, 20, 30 and 40 Gy (**Figure 2**). After 48 h and 72 h after irradiation, cell death, and that after cell counts were determined *via* flow cytometry. These experiments showed that in MZ-54 cells (**Figures 2A, B**) increasing doses of radiation resulted in increased cell death, whereas after 72 h the amount of
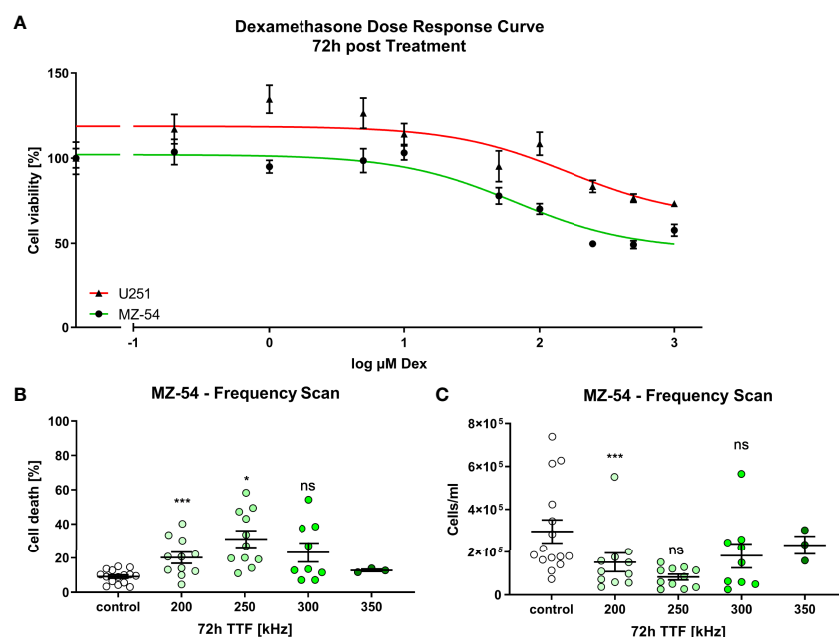


**FIGURE 1** | **(A)** Non-linear regression (log (inhibitor) *vs.* response (three parameters)) of MZ-54 (green) and U251 (red) 72h after treatment with increasing concentrations of Dex and determining cell viability using MTT Assay. The half-maximal inhibitory concentration was determined at 65 μM and 165 μM for MZ-54 and U251, respectively. **(B)** FACS-based measurement of cell death of MZ-54 cells 72h after Tumor Treating Field (TTFields) application at the depicted frequency. **(C)** FACS-based measurement of cell count derived from the same measurement as in **(B)**. The optimal frequency of 250 kHz was selected for MZ-54 cells. ns, not significant; *p < 0.05; **p < 0.01; ***p < 0.001; One-Way ANOVA with Dunnett's multiple comparison test (GraphPad Prism 7).
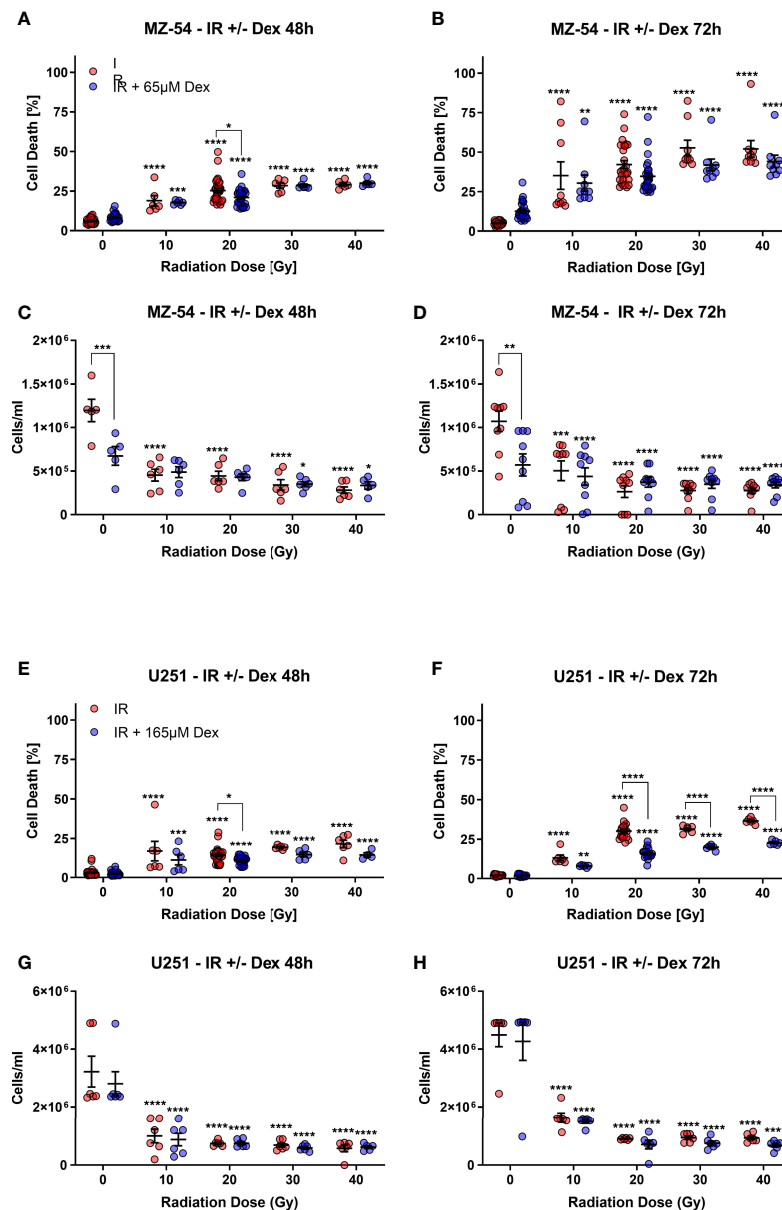
**FIGURE 2** | FACS-based measurement of **(A, B)** cell death and **(C, D)** cell count of MZ-54 GBM cells after 24h pre-treatment with Dex and irradiation (IR). The measurements were conducted **(A, C)** 48h and **(B, D)** 72h after IR-treatment. MZ-54 show dose-dependent increases in cell death and concomitant decreases in cell counts, with no discernible effect through the addition of Dex. FACS-based measurement of **(E, F)** cell death and **(G, H)** cell count after **(E, G)** 48h and **(F, H)** 72h of U251 GBM cells treated accordingly show similar IR-dose-dependent increases and decrease in cell death and cell count respectively. Note that U251 cells are protected from IR-induced cell death after additional Dex-treatment. *p < 0.05; **p < 0.01; ***p < 0.001; ****p < 0.0001; Two-Way ANOVA with Dunnett's multiple comparison test (GraphPad Prism 7).

cell death was higher compared to 48 h. The addition of Dex had almost no statistically significant effect on cell death in MZ-54, except for 20 Gy after 48 h, where a moderate cell death rescue was observed. These observations are further corroborated by our analyses of the cell counts (**Figures 2C, D**). Here, we observed after both timepoints a Dex-induced decrease in cell number in non-irradiated control cells. In contrast, IR-treatment effectively and dose-dependently reduced the amount of cells

significantly, but an additional Dex-treatment had no further inhibiting effect. U251 (**Figures 2E–H**) also showed a dose-dependent increase in cell death (**Figures 2E, F**) and reduction in cell number (**Figures 2G, H**) with stronger effects at the later time point. Dex alone had no discernible effect on either cell death or cell count in non-irradiated cells, whereas it could rescue cell death at 20 Gy IR after 48 h and even more pronounced at doses higher than 20 Gy after 72 h.

Next, we wondered if Dex has a similar effect on cell death induction of TTFields treatment. For this purpose, we treated the cells with IC50 concentrations of Dex and simultaneously commenced TTFields treatment (**Figure 3**) for 24, 48 and 72 h and measured cell death and cell counts *via* flow cytometry. This analysis revealed that in treated MZ-54 cells (**Figure 3A**) no cell death occurred at 24 h, whereas after 48 and 72 h cell death was very pronounced. The addition of Dex had neither a discernible effect on TTFields efficacy nor on its own. For U251 (**Figure 3B**), we could determine a significant induction of cell death after 24 h of treatment, which was strongly increased after 48 h and 72 h. The concurrent addition of Dex had no effect on cell death induction after 24 h and 48 h, but resulted in a moderate, yet significant, prevention of cell death after 72 h. Conversely, we also analysed cell count from our FACS data (**Figure 3C**). This analysis revealed that after 24h of treatment a slight downward-trend using Dex alone and TTFields alone for MZ-54 can be observed, which culminates in a significant reduced cell number in the combined treatment. At later time points (48h and 72h), the growth-inhibitory effects of Dex and TTFields became even more apparent, whereas TTFields treatment was more effective than Dex. The combined treatment showed slightly less cell numbers after 48h; however, this difference did not reach statistical significance and after 72h no difference was visible. Similar results regarding TTFields and combination treatment were obtained in U251 (**Figure 3D**), which can both effectively reduce the cell number with the effect being most pronounced after 72h. In contrast, Dex single treatment had no effect on cell number after any time point, which is in line with the reduced sensitivity observed using the dose-response curve, that MZ-54 are more sensitive towards Dex. Based on these results we

concluded that Dex does not interfere with TTFields treatment *in vitro*. We further concluded that TTFields treatment may exhibit cell death to a greater extent compared to IR-treatment, especially in IR-resistant cell models such as U251.

To crosscheck these findings in the clinical setting, we analysed the characteristics and clinical outcome of 26 patients that were treated for primary GBM in our University Hospital according to the EF-14 trial ([12]). During the TTFields therapy 10 patients received Dex and 16 patients had no concomitant Dex administration. The median Dex dosage was 2 mg (SD: 1.45). Male to female ratio was non-significant in our cohort (60% male in the Dex group *vs.* 75% in the Dex negative group). Median age was also statistically non-significant between the cohort (55 years in the Dex *vs.* 50 years in the Dex negative group). Furthermore, MGMT promotor methylation was observed in 50% of the patients in the Dex group *vs.* 44% in the Dex negative group. Finally, the median TTFields treatment time in days and the median day from operation to TTFields therapy was not-significant between the two cohort (**Table 1**). In addition, PFS was 9 months in the Dex cohort *vs.* 11 in patients without Dex treatment and thus not statistically significant. OS was 15 months in the Dex cohort *vs.* 18 months in patients without Dex again not reaching a level of significance (**Figure 4** and **Table 1**).

## DISCUSSION

We aimed to determine whether concomitant Dex administration affects TTFields efficacy. We choose a translational approach to answer this question and found that Dex administration during TTFields application has no negative effect on the antitumor
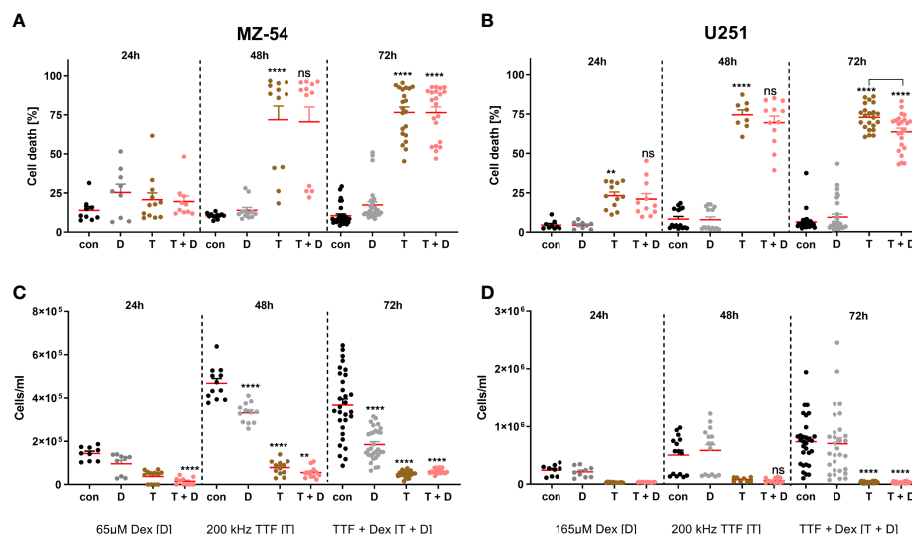


**FIGURE 3** | FACS-based measurement of **(A, B)** cell death and **(C, D)** cell count of **(A, C)** MZ-54 and **(B, D)** U251 GBM cells after treatment with the IC50 of Dex and Tumor Treating Field (TTFields) application at the optimal frequency for 24, 48 and 72h. Effective cell death induction can be appreciated after 48h using TTFields and TTFields + Dex in both GBM cell lines with a concomitant decrease in cell count. Note the MZ-54 also display reduced cell counts after 48h and 72h after Dex alone and U251 already display significantly induced cell death after 24h. *p < 0.05; **p < 0.01; ***p < 0.001; ****p < 0.0001; ns, non significant. One-Way ANOVA with Tukey's multiple comparison test (GraphPad Prism 7). Con, control; D, dex; T, TTFields; T + D, TTFields + Dex.

TABLE 1 | Baseline characteristics of GBM cohort stratified by Dex administration during TTFields treatment.

| Numbers | Dex =10 | no Dex =16 | p-value |
|---|---|---|---|
| **Sex** | | | |
| Male (n) | 6 (60%) | 12 (75%) | n.s. |
| Female (n) | 4 (40%) | 4 (25%) | n.s. |
| **Median age** | | | |
| Years | 55 (23-75) | 50 (27-68) | n.s. |
| **MGMT status** | | | |
| Methylated | 5 (50%) | 7 (44%) | n.s. |
| Unmethylated | 5 (50%) | 9 (56%) | n.s. |
| **IDH-1 status** | | | |
| Wildtype | 9 (90%) | 16 (100%) | n.s. |
| Mutated | 1 (10%) | 0 (0%) | n.s. |
| **P 53** | | | |
| Wildtype | 6 (60%) | 6 (38%) | n.s. |
| Mutated | 4 (40%) | 10 (62%) | n.s. |
| **Survival** | | | |
| Progression-free survival in months (range) | 9 (5-28) | 11 (5-39) | n.s. |
| Overall survival in months (range) | 15 (8-32) | 18 (7-39) | n.s. |
| **Median TTFields application in days** | 177 (21-260) | 92 (59-409) | n.s. |
| **Median Days from operation to TTFields** | 163.5 (46.9) | 175.5 (64.3) | n.s. |

*ns, non significant.*

capacity *in vitro* and in a retrospective clinical evaluation. On the other hand, our *in vitro* results confirm the accumulating evidence against the usage of Dex during RT.

The addition of Dex during RT resulted a significantly increased radio-resistance in U251 GBM cells, whereas for MZ54 cells only a small tendency after 72h of treatment is apparent. These findings underscore the context-dependency of DEX effects that was also observed in other studies (5). This is in accordance with a clinical observation of Shields et al., who showed that Dex usage during RT was correlated with reduced OS and PFS (4). Additionally, Pitter et al., described Dex-induced anti-proliferative effects that may confer protection from radiotherapy-induced genotoxic stress, by inducing cell cycle arrest (5). In line with the mentioned research, our analysis confirm that Dex pre-treatment leads to a significant RT-induced cell death resistance in both GBM cell lines. Interestingly, this observed resistance does not occur when analysing the cell count, although an RT-dependent reduction in cell count can be observed. RT, first induces cell cycle arrest, which can ultimately lead to cell death if RT-induced damages cannot be restored and the cells proceed to cell cycle. Thus, we reason that

the combined cell cycle arrest by Dex and RT more potently prevents the cells from escaping this cell cycle arrest, and therefore protects them from cell death.

On the other hand, *in vitro* TTFields application (200 kHz/ 250 kHz) for 72 h induced massive cell death in U251 and MZ54 cell lines. The frequency and efficacy of *in vitro* TTFields application is in line with the literature (17), while the higher frequency of MZ54 cells likely is due to their increased size compared to U251 cells.

In the clinical setting however, Dex weaning in symptomatic patients is problematic and administration is often maintained thorough adjuvant therapy. Therefore, the main question was whether concomitant Dex administration reduces TTFields efficacy analogous to RT in GBM. Adjusted for the optimal frequency and Dex concentration, the addition of Dex to TTFields showed no significant impact on cell death in MZ-54 and U251 cells. Complimentary, the retrospective analysis of GBM patients showed no significant impact on PFS and OS. Our study revealed no contraindication of Dex usage in GBM patients during TTFields application. However, these results should be evaluated in lager prospective clinical trials.
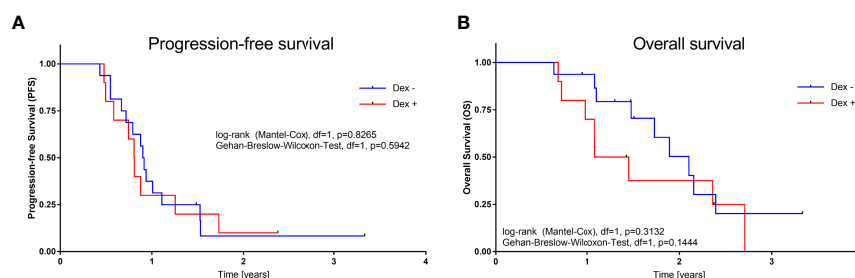


**FIGURE 4 | (A)** Kaplan–Meier plots for progression-free survival **(A)**, and overall survival **(B)** stratified by Dex administration during TTFields treatment. P-values calculated from log-rank and Gehan-Breslow-Wilcoxon-test) (GraphPad Prism 7).

To answer the impending question why TTFields efficacy is not alternated by Dex is challenging. Wong et al. described their retrospective analysis of phase III registration trial comparing TTFields *vs* chemotherapy in recurrent GBM patients. Their unsupervised mathematical algorithm showed that a Dex dose higher than 4.1 mg per day was associated with reduced OS in the TTFields-treated cohort. Peripheral blood lymphocyte counts were independent of Dex application but positively correlated with patient's outcome. The group therefore concludes that dexamethasone exerted a profound interference on the therapeutic effects of TTFields therapy (21). The median Dex dosage in our cohort was 2 mg and accordingly under the proposed cut-off. Collectively these data suggest that there could be a therapeutic window for concomitant DEX treatment without major effects on TTFields efficacy that can be used for the benefit of the GBM patients. We did not analyse peripheral blood lymphocytes which makes it difficult to oppose our studies. However, as TTFields are a local tumor therapy and its systemic effects remain elusive, we advocate the point of local antitumoral TTFields effect unaffected by Dex. The TTFields induced disruption of the mitotic chromosomes spatial order which results in asymmetric chromosome segregation and aneuploidy is supposedly not counteracted by systemic Dex administration.

Nevertheless, several studies identified high Dex dosage as prognostically unfavourable in GBM. We therefore advocate consequent Dex weaning where possible but our data indicates that concomitant application during TTFields therapy is not associated with poor efficacy and outcome.

Our study has several strengths and weaknesses. First, we analysed two cell lines, which cannot exclude different results in other cultivated GBM cells. As such, future research should include further cell lines including primary ones. As a strength,

our investigation is the first study to answer the question of Dex effects by a translational approach and both *in vitro* and retrospective clinical findings resulted in coherent results. The obvious limitation of the clinical finding is the single centre character, the small sample size and the retrospective design. As this part is of observational character, confounding, selection bias, reverse causation and uncontrolled statistical error risk cannot be excluded. However, further prospective randomized trials with large cohorts are necessary to confirm our findings.

## CONCLUSION

This study provides the first evidence that concomitant Dex administration is not associated with reduced TTFields efficacy nor affects patient's outcome in GBM therapy.

## DATA AVAILABILITY STATEMENT

The raw data supporting the conclusions of this article will be made available by the authors, without undue reservation.

## AUTHOR CONTRIBUTIONS

BL and AS collected the data. DD and BL wrote the first draft. DK, CS, and DD supervised the manuscript. All authors supplied additional information, edited the manuscript, and contributed to critical review and revision of the manuscript. All authors contributed to the article and approved the submitted version.

## REFERENCES

1. Dubinski D, Hattingen E, Senft C, Seifert V, Peters KG, Reiss Y, et al. Controversial Roles for Dexamethasone in Glioblastoma – Opportunities for Novel Vascular Targeting Therapies. *J Cereb Blood Flow Metab* (2019) 39:1460–8. doi: 10.1177/0271678X19859847

2. Luedi MM, Singh SK, Mosley JC, Hassan ISA, Hatami M, Gumin J, et al. Dexamethasone-Mediated Oncogenicity In Vitro and in an Animal Model of Glioblastoma. *J Neurosurg* (2018) 129:1–10. doi: 10.3171/2017.7.JNS17668

3. Plate KH, Scholz A, Dumont DJ. Tumor Angiogenesis and Anti-Angiogenic Therapy in Malignant Gliomas Revisited. *Acta Neuropathol* (2012) 124:763–75. doi: 10.1007/s00401-012-1066-5

4. Shields LBE, Shelton BJ, Shearer AJ, Chen L, Sun DA, Parsons S, et al. Dexamethasone Administration During Definitive Radiation and Temozolomide Renders a Poor Prognosis in a Retrospective Analysis of Newly Diagnosed Glioblastoma Patients. *Radiat Oncol* (2015) 10:222. doi: 10.1186/s13014-015-0527-0

5. Pitter KL, Tamagno I, Alikhanyan K, Hosni-Ahmed A, Pattwell SS, Donnola S, et al. Corticosteroids Compromise Survival in Glioblastoma. *Brain* (2016) 139:1458–71. doi: 10.1093/brain/aww046

6. Dubinski D, Won S-Y, Gessler F, Quick-Weller J, Behmanesh B, Bernatz S, et al. Dexamethasone-Induced Leukocytosis is Associated With Poor Survival in Newly Diagnosed Glioblastoma. *J Neurooncol* (2018) 137:503–10. doi: 10.1007/s11060-018-2761-4

7. Liles WC, Dale DC, Klebanoff SJ. Glucocorticoids Inhibit Apoptosis of Human Neutrophils. *Blood* (1995) 86:3181–8. doi: 10.1182/blood.V86.8.3181.bloodjournal8683181

8. Kaup B, Schindler I, Knüpfer H, Schlenzka A, Preiß R, Knüpfer MM. Time-Dependent Inhibition of Glioblastoma Cell Proliferation by Dexamethasone. *J Neurooncol* (2001) 51:105–10. doi: 10.1023/A:1010684921099

9. Lin Y-M, Jan H-J, Lee C-C, Tao H-Y, Shih Y-L, Wei H-W, et al. Dexamethasone Reduced Invasiveness of Human Malignant Glioblastoma Cells Through a MAPK Phosphatase-1 (MKP-1) Dependent Mechanism. *Eur J Pharmacol* (2008) 593:1–9. doi: 10.1016/j.ejphar.2008.06.111

10. Sur P, Sribnick EA, Patel SJ, Ray SK, Banik NL. Dexamethasone Decreases Temozolomide-Induced Apoptosis in Human Glioblastoma T98G Cells. *Glia* (2005) 50:160–7. doi: 10.1002/glia.20168

11. Machein MR, Kullmer J, Fiebich BL, Plate KH, Warnke PC. Vascular Endothelial Growth Factor Expression, Vascular Volume, and, Capillary Permeability in Human Brain Tumors. *Neurosurgery* (1999) 44:732–40. doi: 10.1097/00006123-199904000-00022

12. Stupp R, Taillibert S, Kanner A, Read W, Steinberg DM, Lhermitte B, et al. Effect of Tumor-Treating Fields Plus Maintenance Temozolomide vs Maintenance Temozolomide Alone on Survival in Patients With Glioblastoma. *JAMA* (2017) 318:2306. doi: 10.1001/jama.2017.18718

13. Kirson ED, Dbalý V, Tovaryš F, Vymazal J, Soustiel JF, Itzhaki A, et al. Alternating Electric Fields Arrest Cell Proliferation in Animal Tumor Models and Human Brain Tumors. *Proc Natl Acad Sci U S A* (2007) 104:10152–7. doi: 10.1073/pnas.0702916104

14. Silginer M, Weller M, Stupp R, Roth P. Biological Activity of Tumor-Treating Fields in Preclinical Glioma Models. *Cell Death Dis* (2017) 8:e2753–3. doi: 10.1038/cddis.2017.171

15. Karanam NK, Srinivasan K, Ding L, Sishc B, Saha D, Story MD. Tumor-Treating Fields Elicit a Conditional Vulnerability to Ionizing Radiation *Via*

the Downregulation of BRCA1 Signaling and Reduced DNA Double-Strand Break Repair Capacity in Non-Small Cell Lung Cancer Cell Lines. *Cell Death Dis* (2017) 8:e2711. doi: 10.1038/cddis.2017.136

16. Wen PY, Chang SM, Van Den Bent MJ, Vogelbaum MA, Macdonald DR, Lee EQ. Response Assessment in Neuro-Oncology Clinical Trials. *J Clin Oncol* (2017) 35:2439–49. doi: 10.1200/JCO.2017.72.7511

17. Porat Y, Giladi M, Schneiderman RS, Blat R, Shteingauz A, Zeevi E, et al. Determining the Optimal Inhibitory Frequency for Cancerous Cells Using Tumor Treating Fields (TTFields). *J Vis Exp* (2017) 2017:e55820. doi: 10.3791/55820

18. Giladi M, Munster M, Schneiderman RS, Voloshin T, Porat Y, Blat R, et al. Tumor Treating Fields (TTFields) Delay DNA Damage Repair Following Radiation Treatment of Glioma Cells. *Radiat Oncol* (2017) 12:206. doi: 10.1186/s13014-017-0941-6

19. Shteingauz A, Porat Y, Voloshin T, Schneiderman RS, Munster M, Zeevi E, et al. AMPK-Dependent Autophagy Upregulation Serves as a Survival Mechanism in Response to Tumor Treating Fields (TTFields). *Cell Death Dis* (2018) 9:1074. doi: 10.1038/s41419-018-1085-9

20. Hetschko H, Voss V, Seifert V, Prehn JHM, Kögel D. Upregulation of DR5 by Proteasome Inhibitors Potently Sensitizes Glioma Cells to TRAIL-Induced Apoptosis. *FEBS J* (2008) 275:1925–36. doi: 10.1111/j.1742-4658.2008.06351.x

21. Wong ET, Lok E, Gautam S, Swanson KD. Dexamethasone Exerts Profound Immunologic Interference on Treatment Efficacy for Recurrent Glioblastoma. *Br J Cancer* (2015) 113:232–41. doi: 10.1038/bjc.2015.238

# Uncovering Spatiotemporal Heterogeneity of High-Grade Gliomas: From Disease Biology to Therapeutic Implications

Andrea Comba [1,2,3], Syed M. Faisal [1,2,3], Maria Luisa Varela [1,2,3], Todd Hollon [1], Wajd N. Al-Holou [1], Yoshie Umemura [1], Felipe J. Nunez [4], Sebastien Motsch [5], Maria G. Castro [1,2,3] and Pedro R. Lowenstein [1,2,3]*

[1] Department of Neurosurgery, University of Michigan Medical School, Ann Arbor, MI, United States, [2] Department of Cell and Developmental Biology, University of Michigan Medical School, Ann Arbor, MI, United States, [3] Rogel Cancer Center, University of Michigan Medical School, Ann Arbor, MI, United States, [4] Laboratory of Molecular and Cellular Therapy, Fundación Instituto Leloir, Buenos Aires, Argentina, [5] School of Mathematical and Statistical Sciences, Arizona State University, Tempe, AZ, United States

Glioblastomas (GBM) are the most common and aggressive tumors of the central nervous system. Rapid tumor growth and diffuse infiltration into healthy brain tissue, along with high intratumoral heterogeneity, challenge therapeutic efficacy and prognosis. A better understanding of spatiotemporal tumor heterogeneity at the histological, cellular, molecular, and dynamic levels would accelerate the development of novel treatments for this devastating brain cancer. Histologically, GBM is characterized by nuclear atypia, cellular pleomorphism, necrosis, microvascular proliferation, and pseudopalisades. At the cellular level, the glioma microenvironment comprises a heterogeneous landscape of cell populations, including tumor cells, non-transformed/reactive glial and neural cells, immune cells, mesenchymal cells, and stem cells, which support tumor growth and invasion through complex network crosstalk. Genomic and transcriptomic analyses of gliomas have revealed significant inter and intratumoral heterogeneity and insights into their molecular pathogenesis. Moreover, recent evidence suggests that diverse dynamics of collective motion patterns exist in glioma tumors, which correlate with histological features. We hypothesize that glioma heterogeneity is not stochastic, but rather arises from organized and dynamic attributes, which favor glioma malignancy and influences treatment regimens. This review highlights the importance of an integrative approach of glioma histopathological features, single-cell and spatially resolved transcriptomic and cellular dynamics to understand tumor heterogeneity and maximize therapeutic effects.

**Keywords:** glioblastoma multiforme, heterogeneity, tumor microenvironment, dynamic, spatial resolution, deep learning, precision oncology

# INTRODUCTION

Glioblastoma (GBM) is the most common malignant primary brain tumor in adults, occurring most commonly in the $6^{th}$ to $7^{th}$ decade of life (1). GBM is classified by World Health Organization (WHO) as an astrocytic grade IV tumor, which commonly presents as a heterogeneously enhanced mass by neuroimaging. Microvascular proliferation, hypercellularity, nuclear atypia, pseudopalisades, cellular pleomorphism, and necrosis are hallmarks of GBM histopathology (2).

The prognosis for GBM is relatively poor and universally fatal, with a median overall survival of approximately 16 months from the time of diagnosis. $O^6$-methylguanine-DNA methyl transferase (*MGMT*) promotor methylation is detected in about a third of GBM, and is prognostic of a better survival outcome, and predictive of better treatment response to alkylating chemotherapy. Isocitrate dehydrogenase 1 (IDH1) mutations, which are associated with more favorable outcome, represent a new tumor group termed 'adult-type, diffuse glioma, IDH-mutant, astrocytoma, grades 2-4', while glioblastoma is now reserved to the 'adult-type, diffuse glioma, IDH1 wildtype' (3–6). The current standard of care for GBM utilizes methods that are agnostic of molecular GBM phenotypes. They comprise an initial, maximally safe surgical resection, followed by conformal radiotherapy with concurrent oral temozolomide chemotherapy, followed by adjuvant temozolomide therapy. In addition, the use of tumor treatment fields has been introduced to the treatment of adult diffuse gliomas, though it is not considered part of standard of care (7, 8). Historically, each of the standard of care measures only adds a few months to survival. Although bevacizumab improves progression free survival, there is no evidence, at this time, that standard of care second line treatment improves overall survival (9, 10).

Advancement in GBM treatments is urgently needed; however, treating GBM faces numerous challenges due to, but not limited to, temporal and spatial tumor heterogeneity, altered cellular metabolism, and the unique immunosuppressive glioma microenvironment (11, 12). Immunotherapies and molecularly targeted personalized medicine have recently advanced the field of oncology in many cancer types; however, targeted agents against recurrent EGFR mutations and immune checkpoint inhibitors have so far not improved overall survival for GBM patients (13–19).

Moreover, assessing the treatment response holds significant importance to developing better GBM treatments. However, it can be quite difficult to differentiate tumor progression from inflammatory or necrotic changes associated with treatment, such as chemoradiation and immunotherapy, making neuroradiographic assessment suboptimal in these cases (20, 21). The blood-brain-barrier hinders drugs from reaching the tumor site, and also limits the utility of liquid biopsy (22). The lack of optimal surrogate markers of survival to effectively assess treatment efficacy is a paramount challenge the neuro-oncology community faces when evaluating potential new therapies (23). These challenges suggest that advanced, integrated histological, cellular, and molecular characterization with spatial resolution can provide insights for therapeutic interventions and predict clinical outcomes for GBM patients. Herein, we will review the recent advances made towards these integrated approaches.

# MOLECULAR GENETICS AND EPIGENETIC ALTERATIONS IN GLIOMA

GBMs differ in histologic features, malignancy grade, and molecular alterations. Recently, the presence and distribution of genetic/epigenetic alterations have been added as criteria to classify gliomas, refining the histological WHO classification, which previously defined these tumors as glial in origin (24–26). Recurrent IDH1 point mutations, which have been identified as contributors to gliomagenesis (27, 28), is used to classify gliomas and represents a major division of mutant IDH1 gliomas from wild-type-IDH1 (wt-IDH1) gliomas. wt-IDH1 gliomas, WHO grade IV, high grade gliomas (HGG) (12, 24, 29), present with several genomic alterations and higher somatic mutation frequency versus low grade gliomas (LGG) (30, 31). In adults, wt-IDH1 gliomas retain ATRX activity, and typically co-exhibit *TP53* and *TERT* promoter (*TERT*p) mutations. In addition, wt-IDH1 gliomas can harbor alterations in regulators of the RTK-RAS-PI3K signaling cascade, including EGFR amplification, as well as mutations or deletions to tumor-suppressor genes *PTEN* and *CDKN2A/B*, and alterations to chromosomes 7 and 10 (12, 24, 25, 31). IDH1 mutation, usually at arginine 132 (R132H), occurs in the vast majority of diffuse LGG (WHO grade II), and occurs also in a LGG that has recurred as GBM (WHO grade IV) (29, 32–35). IDH1-R132H, which is associated with better prognosis in glioma, catalyzes 2-hydroxyglutarate production, prompting epigenetic reprogramming of the glioma transcriptome (29, 32, 36–39).

A subgroup of adult-type diffuse mutant IDH1 gliomas which harbor 1p/19q chromosomal co-deletions (1p/19q-codel) and *TERT* promoter mutation are now classified as oligodendrogliomas (6, 40). Epigenetics alterations are a remarkable feature of gliomas with clinical significance. DNA methylation in CpG islands define the CpG island methylator phenotype (G-CIMP), a hallmark of mutant-IDH1 glioma, which is linked to better prognosis (41, 42). On the other hand, demethylation in *CXCR4*, *TBX18*, *SP5*, and *TMEM22* genes are related with tumor initiation and progression in GBM (43). Analyzing methylation profiles of TCGA data identified DNA methylation clusters designated subtypes LGm1 to LGm6, which were linked to molecular glioma subclasses and WHO grades (32). Also, methylation of CpG islands in the MGMT promoter predicts a better response to DNA alkylating agents (44). Recently, a novel methylation subgroup of IDH-WT GBM was introduced. This group differs from known molecular subgroups in terms of methylation and copy number profile with a distinct histological appearance and molecular signature (45).

In addition, different histone mutations are associated with pediatric brain tumors. Various studies have shown a high frequency of two-point mutations in the genes of the histone variants H3.3 "H3F3A", and to a lesser extent H3.1 "HIST1H3B", which result in substitution of lysine at position 27 with methionine (K27M) or glycine at position 34 with arginine or

valine (G34V/R). Further reports highlighted the association of K27M mutation with midline gliomas (MLG) and G34V/R mutation with gliomas of the cerebral hemispheres (46–48). In this context, epigenetic modifications to histone tails by methylation or acetylation in gliomas impact gene expression and, therefore, tumor characteristics (38, 49, 50). Identification of these alterations have been useful for predicting prognosis of glioma patients (51) and for developing therapeutics agents targeting regulators of histone modifications, such as DNA methyltransferase (DNMT) inhibitors and histone deacetylase inhibitors (HDACIs) (52).

As a consequence of the genetic alterations that classify gliomas, significant signaling pathways are altered. This includes activation of the growth factor receptor tyrosine kinase (RTK) pathways as result of PDGF and EGFR overexpression (53, 54). The frequent activation of RAS, PI3K/PTEN/AKT, RB/CDKN2A-p16INK4a, and TP53/MDM2/MDM4/CDKN2A-p14ARF pathways are implicated in glioma proliferation (55, 56). On the other hand, the anaplastic features of HGG/GBM can be boosted by NOTCH signaling activation, which is related with hypoxia and PI3K/AKT/ mTOR and ERK/MAPK pathways (57). Other alterations in glioma cell signaling include metabolic (58), cell differentiation (59), and DNA repair (38, 60) pathways, all with the therapeutic implications.

## HGG INTERTUMORAL AND INTRATUMORAL MOLECULAR HETEROGENEITY

HGG/GBM are characterized by high intertumoral and intratumoral heterogeneity. This heterogeneity is observed at different inter-related levels (histological, cellular and molecular) and is one of the main features that hinders tumor treatment (**Figure 1**). Molecular unsupervised transcriptome analysis of GBM revealed different tumor clusters, highlighting the prominent intertumoral heterogeneity. Different studies over the past 15 years have attempted to classify GBM into molecular subtypes. Back in 2006, Phillips et al. reported the molecular gene expression profile of 76 HGGs, defining signatures from a set of 35 genes, which characterized 3 different subtypes: Proneural, Proliferative, and Mesenchymal. They found a correlation between molecular subtypes and histological tumor grade. Also, Mesenchymal and Proliferative tumors showed a markedly inferior prognosis compared to Proneural (61). Subsequent studies carried out by Verhaak et al. used integrated, multidimensional genomic data and DNA copy number to define a more robust gene expression-based molecular GBM classification into 3 confirmed subtypes with a signature from 210 genes per subtype (53). Overall, aberrations and gene expression of *EGFR*, *NF1*, and *PDGFRA* define Classical, Mesenchymal, and Proneural subtypes, respectively. Specifically, the Classical subtype exhibited chromosome 7 amplification associated with high-level EGFR amplification. This subtype also lacked distinct additional genetic abnormalities in TP53, NF1, PDGFRA, or IDH1, but affected expression of genes, such as FGFR3, PDGFA, EGFR, AKT2, and NES. The Mesenchymal subtype displayed focal hemizygous deletions of a

region at 17q11.2, containing the gene NF1. This subtype was associated with greater necrosis and inflammatory infiltrates, which was linked to higher expression of tumor necrosis factor and NF-kB pathway genes, such as TRADD, RELB, and TNFRSF1A. Some of the most relevant differentially expressed genes of Mesenchymal tumors were CASP1/4/5/8, ILR4, CHI3L1, TRADD, TLR2/4, and RELB, among others. The Proneural subtype was defined by PDGFRA and TP53 alterations and IDH1point mutations and differential expression of DLL3, NKX2-2, SOX2, ERBB3, and OLIG2 (53).

Using DNA methylation profiles from 396 GBMs, Brennan et al. in 2013 identified six methylation clusters. They found that Cluster M1 (60%) was enriched in Mesenchymal subtype, Cluster M3 (58%) was enriched in Classical subtype, and the G-CIMP cluster was enriched in Proneural subtype. They observed that the Mesenchymal subtype expressed higher levels of endothelial markers, such as CD31 and VEGFR2, in concordance with Phillips et al. (61) and inflammation markers, such as fibronectin and COX2. On the other hand, the Proneural subtype was associated with somatic mutations to genes such as IDH1, TP53, ATRX, and MYC, and the Classical subtype with EGFR amplifications or mutations (31).

Lastly, in 2017, Wang et al. postulated GBM-specific intertumoral heterogeneity, and defined 3 tumor-intrinsic transcriptional subtypes from transcriptomic analysis of wt-IDH GBM samples, derivative neurospheres, and single-glioma-cell gene expression profiles (62, 63). Subtypes were designated as Proneural, Mesenchymal, and Classical using a 50-gene expression signature per subtype, which represented a 42 to 54% overlap with previous studies (53). The 50-gene expression signature by subtype could be summarized by the most relevant genes from each group. The Mesenchymal subtype overexpresses BCL3, TGFBI, ITGB1, LOX, COL1A2, VDR, IL6, and MMP7, the Proneural subtype has increased expression of GARBR3, HOXD3, ERBB3, SOX10, CDKN1C, PDGFRA, HDAC2, and EPHB1. Finally, the Classical subtype was characterized by overexpression of PTPRA, ELOVL2, SOX9, PAX6, CDH4, SEPT11, MEOX2, and FGFR3, among others.

A new study by Garofano, L. et al. postulates a novel pathway-based stratification of GBM that uncovers new subtypes with potential prognostic relevance, namely mitochondrial (MTC), glycolytic/plurimetabolic (GPM), proliferative/progenitor (PPR), and neuronal (NEU) (64).

In another study, Neftel et al. showed that glioma subtypes are associate with a set of cellular states that define 4 different groups: NPC-like (neural progenitor like), OPC-like (oligodendrocyte progenitor like), AC-like (Astrocyte like) and MES-like (mesenchymal like). The frequency of each steady-state is modulated by specific genetic modifications (CDK4, PDGFRA, EGFR and NF1); in addition, each single tumor can contain a diversity of states maintained by cellular plasticity (65).

Although similarities and discrepancies surround glioma subtype classification, the Mesenchymal subtype is one of the steadiest subtypes, when analyzing human GBM tissues, GBM xenograft models, and derivative GBM stem cells (53, 61, 66, 67).

In addition to the vast molecular intertumoral heterogeneity, GBM also exhibit high heterogeneity within the same tumor

**FIGURE 1 |** Continued
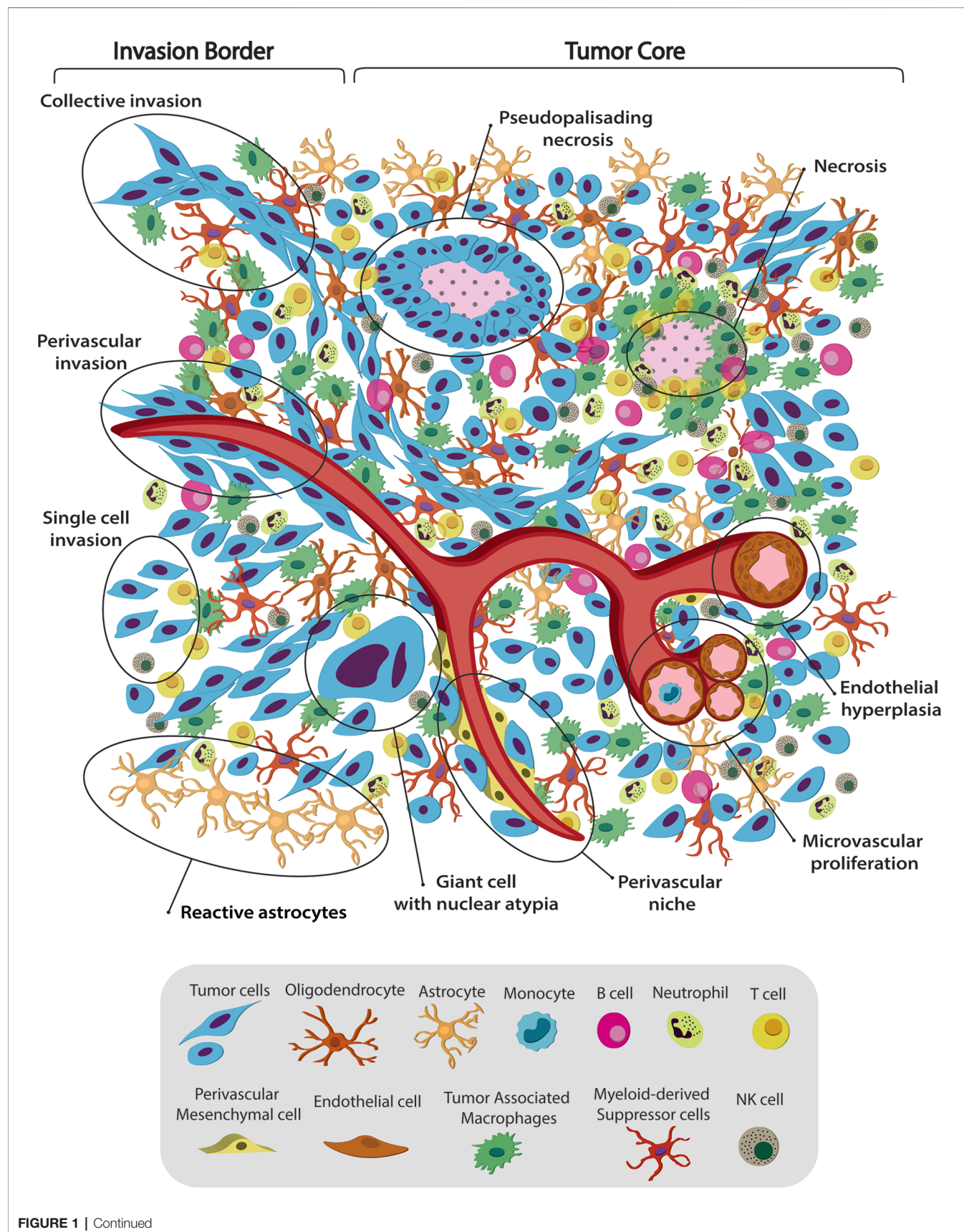
**FIGURE 1** | Spatiotemporal complex intratumoral heterogeneity of GBM. GBM intratumoral heterogeneity at the histological, cellular and dynamic level is illustrated. The schematic representation of the gliomas TME highlights the spatio-temporal heterogeneity at the histological, dynamic, and cellular level. We indicate various hallmarks of GBM. (1) Pseudopalisading necrosis in GBM is characterized by garland-like organization of tumor cells at the edge of areas of tumor necrosis. Glioma cells migrate away from hypoxic regions and invade into healthy tissue at the infiltrating edge. (2) Endothelial hyperplasia represents the vascular lesions characterized by the proliferation of endothelial cells. Glomeruloid vessels and extensive endothelial multilayering result from the endothelial hyperplasia characteristic of GBM. (3) Microvascular proliferation appears as glomeruloid tufts of multilayered endothelial cells together with smooth muscle cells and pericytes. VEGF release from the surrounding necrosis tissue acts on nearby vessels to cause vascular hyperplasia, including microvascular proliferation. (4) Scattered large pleomorphic glioma cells represent multinucleated giant cells with generalized nuclear atypia. (5) Poorly vascularized regions of the tumor become hypoxic and necrotic. At the dynamic level GMB displays different migratory patterns. (6) The tumor–brain interface is characterized by an invasive edge that harbors invasive glioma cells that migrate along white matter tracts or extracellular matrix fibers to infiltrate the brain either as collective invasion (i.e., connected elongated cells infiltrating the brain parenchyma), or (7) Single-cell invasion characterized by amoeboid movements, weak intercellular adhesions, and random movement. (8) Glioma cells are shown to also invade collectively using the perivascular space. Perivascular glioma cells quickly invade the perivascular space as a conduit for invasion. Bottom panel shows the striking cellular heterogeneity of GBM, being composed of both neoplastic cells and nonmalignant cells. It includes several phenotypes of tumor cells, such as rounded cells and mesenchymal-like cells, as well as nonmalignant cells, that form the tumor microenvironment (TME) and make up 50% of the tumor mass. TME is composed of normal brain residents: neurons, astrocytes, oligodendrocytes and microglia; endothelial cells from the vasculature, surrounded by perivascular-mesenchymal cells; and immune system infiltrating cells. 95% of the TME are tumor associated macrophages (TAM), derived either from circulating monocytes or microglia. The remaining 5% are mainly dendritic cells, with smaller contributions of T cells, B cells, NK cells and neutrophils. Understanding tumor heterogeneity composition allows to employ better antitumor therapies.

mass, showing histologically and molecularly dissimilar areas (**Figure 1**). Research studies using tumor sampling from different anatomical locations demonstrated that 60% (6/10) of tumors presented two or three different subtypes within the same tumor (68). Other studies showed that molecular subtypes correlate with histological features. Mesenchymal tumor was associated with hypoxic and perinecrotic areas and high microvascular proliferative zones, while Classical was related to vascular and invasive zones. Tumors with these two characteristics had the worst prognosis (69).

Single-cell RNA-Seq (scRNA-Seq) analysis has emerged as an important approach to dissect the cellular and molecular profile of complex tumors compared to bulk conventional analysis. scRNA-Seq has yielded insights into phenotypic and genotypic differences resulting from tumor cells, the relation with the neural lineages, and the tumor microenvironment, and subpopulations of transformed cells in these extremely heterogeneous tumors (63, 70–72). Analysis of scRNA-Seq suggested that GBM consist of a combination of tumor cells with different GBM subtype footprints (63). Patel et al. analyzed intratumoral heterogeneity by single-cell full-length transcriptomes (SMART-Seq) of isolated cells from five freshly resected human wt-IDH/EGFR amplified GBM depleted of CD45+ cells. They observed a genetic correlation between individual cells and transcriptional intratumoral heterogeneity within the same tumor. They also observed mosaic protein expression of common signaling pathways affected in GBM, such as EGFR, PDGFRA, PDGFA, FGFR1, FGF1, NOTCH2, and JAG1. Interestingly, all tumors contained heterogeneous combinations of individual cells corresponding to different TCGA defined subtypes. They observed that intratumoral subtype heterogeneity imparted significant insights into GBM biology and prognosis, where extensive heterogeneity was associated with reduced survival. Tumors highly heterogeneous for different subtypes or displaying Mesenchymal signatures had poorer outcome than pure Proneural GBM (63). On the other hand, Wang et al. reported multiple activation of different subtypes associated with intratumoral heterogeneity. They suggested that only 8% of the TCGA samples activated more than one transcriptional subtype, displaying low simplicity

scores, while GBM samples with a single subtype had higher simplicity scores. Using this approach, they demonstrated that samples with high simplicity scores had significant survival differences between Mesenchymal and non-Mesenchymal tumors. They concluded that the intratumoral heterogeneity at single-cell level is captured in the transcriptional signature of the bulk tumor (66).

A recent study suggested that tumoral classification pays little attention to the importance of existing intratumoral heterogeneity. They focused on regional architecture of the tumor by analyzing different tumor areas using 9 immunoreactivity biomarkers relevant for GBM. They found that 3 of the 5 pathophysiologically relevant clusters, transformed neuronal, highly proliferative, and mesenchymal stem cell regions, correlated with the 3 tumor subtypes described by Phillips et al. Particularly the Mesenchymal subtype was characterized by high vimentin and nestin expression levels (73). All together, these studies highlight the complexity of GBM molecular signatures and emphasize the importance of considering intratumoral heterogeneity to understand tumor growth and invasion, and develop novel antitumor strategies.

# GLIOMA TUMOR MICROENVIRONMENT AND CELLULAR HETEROGENEITY

Gliomas are a complex composition of both malignant and nonmalignant cells. Nonmalignant cells, including microglia, astrocytes, macrophages, lymphocytes, endothelial, and other cells, collectively constitute the tumor microenvironment (TME), making up ~50% of GBM tumor mass as shown in **Figure 1** (71). The vast majority of GBM infiltrate can be classified as either macrophage or microglia (~95%), with the remaining population comprised primarily of dendritic cells (~4.5%) (71). Darmanis et al. found that transcriptionally distinct immune cells residing in the core increased tumor growth, survival, and invasion by inhibiting inflammation, increasing angiogenesis, and extracellular matrix remodeling (71). Microglia are the predominant resident immune cells in the healthy brain; however, under pathological conditions, brain parenchyma recruits circulating monocytes, which differentiate

into macrophages (74, 75). Tumor-associated macrophages (TAM) play key roles in promoting invasion, angiogenesis, metastasis, and immune suppression (76). They can originate from two distinct lineages: tissue-resident microglia (CD45^{lo} MG-TAM) or monocytes recruited from peripheral circulation (CD45^{hi} M-TAM) (77–79). LGG tend to have more MG-TAM, while HGG are enriched in M-TAM (80). Recent work has described that in GBM TAMs within the tumor core mostly originate from the bone marrow derived pool whereas those in the tumor periphery are largely derived from microglial cells (81). These findings correlate with transcriptomic data (71) and reviewed in (79). TAM populations can also be subdivided into activation state phenotypes: Unstimulated M0, classically activated M1, and alternatively activated M2 (17, 74). The M1 phenotype is anti-tumorigenic and is present at lower levels in GBM infiltrate, while the M2 phenotype is pro-tumorigenic and more abundant, correlating with shorter survival (82). It has been shown that resident microglia are crucial modulatory cell population playing a central role in regulation of vascular homeostasis and angiogenesis and represent an alternative source of pro-angiogenic growth factors and cytokines (79, 83). CXCL2 is expressed in several cell types present in GBM such us endothelial cells, glioma cells, T cells, mast cells and myeloid cells, and its expression level has been correlated with GBM aggressiveness (84). Isolated microglia/macrophages from glioma produce a variety of pro-angiogenic molecules as well as high level of CXCL2 (83). CXCL2/IL8/CXCR2 axis has showed to be involved in maintaining GBM angiogenesis (85, 86). The CXCR2 antagonist SB225002 has shown inhibition in tumor growth, and led to reduced number of TAMs as well as tumor vessels (85, 86). Malignant cells recruit microglia and macrophages to the tumor, where they acquire an M2 phenotype and contribute to an immunosuppressive TME. One of the main factors recruiting TAM is the chemo-attractant, colony-stimulating factor (CSF), which is also a critical for macrophage function. Attenuating the interaction between CSF-1 and its receptor by employing target inhibitors reduces TAM numbers at the tumor site and impairs glioma invasion (87).

Although they have an abundance of TAM, gliomas are defined as immunogenically "cold" because they have low levels of infiltrating T cells (17, 88). Lymphocyte infiltrate present in the TME are CD4+ T helper, CD8+ T cytotoxic, and Tregs, with CD4+ cells more numerous than CD8+ (89). High Treg levels in GBM suppress the function of antigen-presenting cells and inhibit T cell proliferation, contributing to tumor evasion (90). Tregs may be immunosuppressive by employing immune checkpoints molecules, such as CTLA-4 and PD-L1 (17, 19, 91, 92). Also, recent work showed that inhibition of the CLEC2D-CD161 pathway may provide synergistic therapeutic benefit when combined with PD-1 blockade by enhancing the anti-tumor function infiltrating T cells in GBM of distinct T cell populations (93).

Myeloid-derived suppressor cells (MDSC) are found extensively in GBM TME (94). They are a heterogeneous population of immature myeloid cells formed from myeloid progenitors and macrophage, granulocyte, and dendritic cell precursors. However, MDSC do have some common features, such as their myeloid

origin, immature state, and, most importantly, the ability to convert immune responses from a Th1 to a Th2 phenotype, which potently inhibits CD4+ and CD8+ T cells and fosters an immunosuppressive TME (95). Inhibiting COX2 reduces MDSC recruitment and increases cytotoxic T cell levels (96).

Elevated tumor-associated neutrophil (TAN) infiltration correlates with lower survival, suggesting that neutrophil infiltrate contributes to immunosuppression (97), and subsequent tumorigenesis and tumor growth. Elevated neutrophil CXCL8 expression boosts recruitment, and is found in high levels in gliomas (98). Disrupting the interaction of CXCL8 with its receptors, CXCR1 and CXCR2, is a possible approach for dismantling neutrophil infiltration and its associated immune suppression. In addition to TAM, MDSC, TAN, and Tregs, Bregs also suppress the immune response in GBM by interacting with other TME cells to augment immunosuppression (99). Glioma cells can induce a phenotype switch from B cells to Bregs, which contributes to Tregs recruitment and suppression of CD8+ T cells (100, 101).

There are also non-immune cell components of the GBM TME, which contribute to tumor progression. A common histologic feature of glioma is reactive astrocytosis, in which tumor-associated astrocytes are more proliferative, have JAK–STAT pathway activation, and CD274 expression (102). Astrocytes, as wells as microglia, secrete anti-inflammatory cytokines, contributing to an immunosuppressive environment (102). A pro-tumorigenic function has also been described for neurons, by either paracrine or autocrine mechanisms (103), as well as through functional synaptic integrations (104). Even though oligodendrocytes are detected in relatively high numbers by scRNA-Seq of glioma clinical samples, their role in glioma pathology has yet to be determined.

Stromal components, such as endothelial cells, and pericyte/ mesenchymal stem cells (MSC), also play a role in tumor formation and progression. MSC are a small population characterized by self-renewal, expression of stemness markers, and multi-lineage differentiation properties (105). Tumor cells hijack neural development mechanisms, shifting MSC into glioblastoma stem cells (GSC), which possess tumor-propagating potential and are resistant to radiotherapy and chemotherapies (105, 106). Since MSC cells share expression markers with pericytes and are mainly localized around blood vessels (107), it is difficult to differentiate MSCs from pericytes (108). Up till now, there is no exclusive set of expression markers that differentiates MSC from pericytes, making it difficult to distinguish between them.

As outlined in this section, the interactions between glioma cells and constituents of the TME play key roles in tumor growth and progression. A deeper understanding of the dynamics of these interactions would bring us a step closer to designing effective treatments.

# TUMORAL DYNAMIC HETEROGENEITY PATTERNS ACROSS HISTOLOGIC FEATURES

Gliomas are characterized by intratumoral heterogeneity and diffuse invasion into the healthy parenchyma. In doing so,

gliomas use various motility patterns, *i.e.*, single cell invasion or collective invasion (**Figure 1**) (109–113). Tumor growth and invasion is usually considered to be a stochastic. However, whether tumor growth actually results from random processes, or whether gliomas self-organize to promote tumor growth and invasion is not well understood. Thus, the existence of organized dynamic structures in tumors, and what role they may play in tumor progression remains poorly elucidated (114). We recently characterized the complex dynamics of glioma cells in both the tumor core and at the tumor invasive borders, using mouse glioma explants from genetically engineered mouse models (111, 113). We recently found that collective motion of tumor cells can be identified histologically as fascicles of aligned spindle-like and mesenchymal-like tumor cells. For simplicity, we propose to refer to these fascicles as oncostreams. Together with their capacity for collective motion, our data indicate that they likely contribute to tumor malignant behavior. Thus, we interpret oncostreams to be histological structures that represent areas of collective motion (113). As our data indicate that oncostream density correlates with tumor malignancy, we suggest that they are characteristic pathological components of gliomas. Oncostreams display two main types of collective motion, as defined elsewhere by us (112): (i) streams (↑↓) = cells move in both directions, (ii) flocks (↑↑) = cells move mostly in one direction. Cells that move without a preferred direction are defined as swarms and are histologically identified as areas of round cells. We recently showed, using agent-based mathematical modeling, that interactions between individual cells are sufficient to produce these large-scale patterns of collective motion (112). Collective motion patterns have been observed during normal development and also in pathological conditions, such as epithelial to mesenchymal transitions in cancers, followed by metastasis to distant organs (115–117). Directionally correlated cell movement within the tumor core have been also observed in recent studies using *ex vivo* explants of spontaneous intestinal carcinoma. Staneva et al. provided detailed mathematical support for the existence of dynamic patterns, such as *currents* and *vortices*. Their currents are homologues to our *flocks*, since cells move in one single direction in both descriptions (118). Equally, studies of *in vivo* motility of human glioma cell invasion within immune-suppressed animals, indicate complex motility patterns at the tumor border (118). Interestingly, these authors determined that cells can actually move towards and away from the tumor, using two types of invasion patterns at the glioma border, the *invasive margin* of multicellular invading groups of cells, and the *diffuse infiltration* of single cells. *Swarms*, in our descriptions, correspond to diffuse infiltration, since these cells present with an increased speed and less directionality in both studies, whereas the invasive margin corresponds to our directional collective motion patterns (119). The role of collective dynamic patterns within glioma tumors has not been addressed in detail so far. A better understanding of glioma dynamic heterogeneity, taking into account its constituent histological features and their underlying molecular basis, are essential to provide a more accurate picture of gliomas. We believe that the eventual pharmacological disruption of collective glioma dynamic patterns will inhibit glioma growth and progression, and will become a novel treatment approach.

## THE GBM MOLECULAR LANDSCAPE: CURRENT AND FUTURES PERSPECTIVES IN METHODOLOGIES TO ANALYZE GBM WITH SPATIAL RESOLUTION

Molecular studies of bulk tumors or scRNA-Seq studies disclose the complex cellular and molecular heterogeneity of GBM, but lack the spatial dimension of tumor tissue. The spatial heterogeneity of glioma tumors is not just regulated by the mixture of genotypic profile of individual cells, but rather is shaped by the crosstalk between tumor and TME cells in different tumor areas. Understanding how the molecular heterogeneity relates to the classical histological GBM hallmarks would provide invaluable information for integrated characterization, diagnosis, and treatment (**Figure 2**).

In recent years, *in situ* spatially characterized tissue analysis using state of the art technology, such as spatial transcriptomics or multiplex protein expression, opened up new paths to study in greater detail the cellular and molecular heterogeneity in the context of intact tumor tissue including GBM (121, 122). These technologies span tissue laser capture microdissection (LCM) combined with *ex situ* RNA-Seq analysis, *in situ* DNA oligonucleotide barcoding followed by *ex situ* sequencing, and computationally assigned spatial information to expression and imaging methods based on fluorescence *in situ* hybridization (FISH) or *in situ* sequencing (ISS) (123). Methodology parameters, such as sample type and processing, number of detected genes, experimental throughput, and spatial resolution need to be considered before selecting the appropriate method.

Some studies using spatially resolved transcriptomic analysis demonstrated the importance of these technology for examining spatial heterogeneity of the glioma TME. Laser scanning microdissection and RNA-Seq analysis assigned genomic alterations and gene expression patterns to specific GBM histological hallmarks, including tumor infiltration, pseudopalisades cells around necrotic areas, and cellular tumor and microvascular proliferation (69). This Ivy Glioblastoma Atlas project (IvyGAP) combined spatial molecular information with histological features and the clinical database from the patients' cohort, providing deeper understanding of tumor heterogeneity. Intratumoral microenvironment-specific expression from the IvyGAP atlas also advocated potential therapeutic avenues by identifying brain tumor initiating cells and target genes within individual anatomical regions (124, 125). Our recent study proposed an improved laser scanning microdissection methodology to study the gene expression pattern of multicellular mesenchymal-like structures within the glioma tumor core and at the invasion front (113, 125–128).

Novel studies have recently provided new perspectives in the analysis of proteomics, metabolomics, and lipidomics in different cancers (129–131). In GBM, Gularyan et al. describe developing the TOF-SIMS (time-of-flight secondary ion mass spectrometry) methodology to detect protein expression and metabolites in paraffin or frozen glioma sections with spatial resolution (132). This allowed morphological differentiation of diverse regions in patient-derived tumors, which correlated with clinically relevant

**FIGURE 2** | Schematic illustration of the integrative translational preclinical and clinical workflow for translational implications. **(A)** First, clinical information is collected including the MRI and specific glioma grade type. **(B)** Following surgery, neuropathological studies are used for both histopathological assessment and investigation of intratumoral heterogeneity. The histopathology images in **Figure 2B** are modified from Figures 1.34A, 1.35A,B, 1.41A in Chapter 1 Astrocyte Tumors, in IARC, and Otmar D. Wiestler. WHO Classification of Tumours of the Central Nervous System: WHO Classification of Tumours of the Central Nervous System (4th Edition), edited by David N. Louis, World Health Organization, 2006 (120). **(C)** Next, multiregional studies of the surgical samples can be harnessed to determine molecular targets within GBM employing bulk RNA-seq, scRNA-seq and spatially resolved transcriptomics. scRNA-seq method examines heterogeneity at very detailed resolution. The precision treatments are assessed according to tumor heterogeneity evaluation and potential pharmacological sensitivities. **(D)** Prediction of histopathological features based on a novel artificial intelligence analysis of histological data will further aid clinical decisions. Furthermore, intratumoral heterogeneity assessment based on advanced imaging and machine-learning predictions should be carried out to monitor spatio-temporal heterogeneity dynamically and treatment. **(E)** GBM patient derived glioma cells, neurospheres and organoids can be exploited for preclinical modeling and perform pharmacological drug screening using *in-vitro* and *ex-vivo* assays. Patient derived organoids model the parental tissue and can be used to complement standard molecular pathology to understand mechanisms of resistance and can be applied to numerous functional assays such as: tumor cell survival, proliferation and self-renewal, and *ex-vivo* invasion/migration assays to identify pharmacological agent to target glioma invasion. Integrative GBM analysis attempts to improve predictive outcomes and treatments for GBM.

data, *i.e.*, tumor grade, survival, to study GBM. Employing these emerging methodologies that combine histopathology with next generation sequencing or metabolomics are essential for translational applications, which identify novel potential targets in glioma tumors. These approaches could generate a new understanding of glioma behavior, uncovering the heterogeneity in functions, dynamics, and interrelation of tumor cells with TME cells (**Figure 2**).

## COMPUTATIONAL DEEP LEARNING ANALYSIS AND NOVEL IMAGING TECHNOLOGIES APPLIED TO TUMOR HETEROGENEITY

The recent breakthroughs in artificial intelligence (AI), specifically deep neural networks, have resulted in major advances in glioma radiomics and digital pathology. Given a

sufficiently large amount of training data, deep neural networks can identify the optimal set of image features to achieve high performance on a specific task, such as image classification. For example, deep neural networks can classify tumors harboring isocitrate dehydrogenase-1/2 (IDH1/2) mutations versus wt-IDH1/2 from brain magnetic resonance imaging (MRI) (133, 134). Similar methods have been applied to diagnose 1p/19q co-deletion and *MGMT* promotor methylation status (135).

Over the previous decade, digital pathology has experienced a renaissance due to two major factors: (1) the availability of large, public pathology datasets (136) and (2) major breakthroughs in computer vision methods. The application of deep neural networks to the analysis and interpretation of whole-slide images (WSI) has ushered in a new era of digital pathology in cancer (137–140). Efficient whole-slide scanning and digital pathology tools have allowed for quantitative microscopic analysis of tumor heterogeneity (141). Tumor microscopy provides essential phenotypic and microenvironment features

not characterized by molecular profiling or -omics data. The spatial relationships between tumor-associated stroma and tumor infiltration can be directly visualized at single-cell resolution using digital pathology (**Figure 2**).

Our group is currently investigating using optical microscopy and AI to rapidly characterize fresh glioma specimens (138, 142–144). By combining stimulated Raman histology, a rapid, label-free optical imaging method, with deep neural networks, we can automate glioma classification and grading in under 2 minutes. Moreover, we can detect regions of dense, viable tumor infiltration in primary and recurrent tumors.

## GLIOMA HETEROGENEITY AND TME IN CLINICAL THERAPEUTIC RESISTANCE

Within individual tumors, there is significant heterogeneity at the TME level, wherein unique spatial niches harbor numerous cell populations (65, 145–148). These niches are dynamic and adjust to environmental pressures, such as treatment. Indeed, recent data reinforces this adaptive remodeling within tumors. Neftel et al. showed that gene expression in GBM is driven by four different cellular states, which are dynamic and driven by genetic, epigenetic, and microenvironmental factors (65). Even unique genetic subclones were found to exist within all 4 cellular states. Longitudinal assessment of paired patient specimens has revealed unique patterns of clonal evolution with standard of care treatment, highlighting evidence that rare resistant subclones often exist within the initial tumors that are often responsible for treatment resistance (149, 150).

The clinical implication of such profound dynamic cellular and microenvironmental heterogeneity is vast. How does one target a tumor with various subtypes of dynamic gene expression wherein local TMEs maintain and protect tumor cells? With this understanding, it is not unexpected that single target therapies have largely failed in GBM. For example, EGFR alterations are common GBM driver mutations, most frequently as the EGFRvIII variant, which results in a detectable antigen. Clinical trial results of rindopepimut, a peptide vaccine targeting this variant, were disappointing and found that patients who progressed through treatment lost EGFRvIII expression (18, 151, 152). SRC and SRC family kinases (SFKs) have a broad and important role in numerous signaling pathways, which promote GBM tumor growth and invasion; however, a clinical trial assessing Dasatinib, a potent SFK inhibitor, failed to meet its clinical endpoint (153, 154). Similar results occurred from targeting KIT amplification or mutation with Imatinib (155, 156) and TGFβ inhibitors (157, 158), amongst others. The most well-known failure of a single targeted therapy is bevacizumab, a monoclonal antibody against the vascular endothelial growth factor (VEGF), which is highly expressed in GBM and associated with endothelial cell proliferation and angiogenesis (9, 10). Despite an initial imaging response, patient survival did not improve. On the other hand, there are targeted therapies that have shown some promising results, such as targeting BRAFv600e mutations, although using single agents often results in recurrence, which has led to targeting BRAF combined with MEK inhibition (131, 159). In spite of many new

therapeutic approaches being in clinical trials, so far, unfortunately, none has shown efficacy in randomized control double blinded Phase III clinical trials (16, 17, 160)

Overall, results from targeted therapy have been disappointing, although there may be numerous reasons why certain therapies were unsuccessful. Despite positive findings in murine models, penetrance across the human blood brain barrier and activity within the brain at the clinical drug dosages are rarely validated. Perhaps the dosage required for penetration and efficacy in humans is not utilized, or not attainable. This further emphasizes the need for phase 0 studies assessing drug penetration and response in human studies. Furthermore, clinical trials may have failed to properly enrich patients likely to benefit; thus, identifying appropriate biomarkers may lead to better patient selection.

Nevertheless, the most likely failure of our current treatment strategies is a lack of understanding of the significant dynamic tumor heterogeneity, which drives therapeutic resistance. However, it is yet unclear how clinical therapeutics can be altered to target this intra and intertumoral heterogeneity. We must consider therapies that address multiple resistance pathways, including immune-based therapies that may target multiple tumor antigens (19, 161–163), or therapies targeting common metabolic and physiological pathways, which may improve chances of success (164, 165). Furthermore, greater effort in developing preclinical models and clinical studies to understand spatial heterogeneity, tumor recurrence, and evolutionary trajectories in GBM are vital (**Figure 2**).

## PRECISION ONCOLOGY FOR GLIOMAS: TARGETING SPATIAL HETEROGENEITY

Cancer therapies have evolved from traditional chemotherapy and radiotherapy options to more personalized and focused approaches. We have seen remarkable progress in recent years, especially in pancreatic, prostate, and ovarian cancers. Precision oncology leverages genetic alterations and molecular markers present in the patient tumor to deliver a personalized therapeutic regimen (166). The progress of precision medicine essentially relies on identifying targetable biological features in tumors (167). This presents a significant challenge, especially for GBM, which is highly heterogeneous. Glioma cells vary in their morphology, underlying gene expression, and genetic mutational landscape (168). Consequently, any chosen therapeutic target may be expressed by most, but not all, cells, resulting in incomplete tumor eradication.

Mutant IDH status, *MGMT* promoter methylation status, BRAF mutation, and upregulated PI3K/AKT/mTOR signaling pathway have drawn attention as actionable alterations in LGG patients (35, 169–171). Adult brain tumors have seen some progress with precision medicine approaches, especially targeting BRAF, H3K27 demethylation, and NTRK fusions (170, 172, 173). Targeting DNA repair mechanisms with PARP inhibitors, and mutant IDH enzyme and gene fusions with appropriate inhibitors holds potential for treating GBM patients with such genetic alterations (171, 172, 174–176). Identification of several markers relevant to GBM diagnostics

using liquid biopsies with NGS for circulating free DNA and/or circulating tumor cells could be used in molecular diagnosis of cytological specimens and potential administration of innovative precision therapy (177, 178).

Nevertheless, spatial and temporal heterogeneity is a critical challenge that the neuro-oncology field must address before precision oncology can be considered a viable option for brain tumor patients (62, 69, 179, 180). Spatial heterogeneity in GBM resected tumors is recognized in transcriptional atlases, where genomic alterations and gene expression patterns vary between the leading edge, infiltrating tumor, cellular tumor, pseudopalisading cells around necrosis, and microvascular proliferation regions (69). To explain the evolution of multiple GBMs (M-GBMs), Lee et al. proposed a multiverse model based on extensive bulk and single-cell RNAseq data (62). They demonstrated that M-GBMs are more genetically diverse than nearby tumors and genetic similarity between multiregional samples correlates with treatment response. Furthermore, enrichment of *PIK3CA* mutations in M-GBMs, as well as the effects of PAM inhibitors, which are more selective in patient-derived glioma cells. Their findings support the truncal target hypothesis, which states that truncal mutations can help guide more effective therapies (62). Recently, it has been shown within a single GBM tumor, that intratumoral spatial heterogeneity of Bruton's Tyrosine kinase activity in tumor core versus edge cells showed distinct therapeutic responses (181).

Glioma-initiating cells (early-branched, ancestor-like tumor cells) at tumor edges receive signals from the tumor core, which promotes their malignancy (182–184). Evidence from several murine tumor models supports the Edge-to-Core progression theory (182). However, it is unclear if this hypothesis universally describes the development of primary GBM. Brain tumor cells at the edge reside in a distinct environment from the tumor core, interacting with various somatic cells, including neurons, astrocytes, vascular endothelial cells, and immune cells (104, 185–188). These tumor-associated somatic cells may contain cellular populations that can activate or suppress tumor cells. Multi-OMICs studies have established largely distinct signaling pathways activated in edge- and core-located tumor cells viz., Esm1/endocan, Bruton's Tyrosine Kinase, nitrogen metabolism. Thus, developing spatially distinct therapeutic modalities for GBM is a critical challenge (181, 182, 189–191). Understanding the phenotypic complexities of patient tumor cells will necessitate molecular investigation to develop effective precision treatments for gliomas (**Figure 2**).

## CONCLUSIONS

Over the last few years, tumor heterogeneity has come to the forefront as a *bona fide* hallmark of tumor biology, including tumor dynamics, migration, and invasion. In the particular case of GBM, heterogeneity is present at the anatomical, histological, functional, molecular, vascular, and immune levels. The complex spatiotemporal structure of brain tumors is likely a major contributor to the difficulties of treating these tumors since treatments may not be equally effective across heterogeneous tumor areas. The presence of heterogeneity means that

treatments should be tailored to target microenvironments, since the tumor cell characteristics and their microenvironments vary by tumor location. However, it has been difficult to factor tumor heterogeneity into treatment design.

Heterogeneity in the extracellular matrix, tumor dynamics, and immune compartments are current areas of active research, as these determinants of tumor growth and treatment resistance have not been given adequate consideration so far. For example, the role of collagen in brain tumor growth remains poorly understood, as are the factors that render these tumors resistant to immune checkpoint inhibitors. Equally, the dynamic nature of these tumors has consequences for our understanding of tumor invasion into healthy brain, and the interactions of immune cytotoxic lymphocytes with tumor cells. The invasive areas of the tumor border are also highly variable, demonstrating that heterogeneity needs to be considered across all tumor locations. Invasion is the major determinant of tumor progression and patient death, highlighting the importance of characterizing its histological, functional, molecular, vascular, and immune heterogeneity across the temporal spectrum. We predict that future therapeutic approaches will need to be effective across different tumor areas, spatially, functionally, and molecularly, to improve the overall treatment efficacy for GBM.

## AUTHOR CONTRIBUTIONS

## FUNDING

## ACKNOWLEDGMENTS

# REFERENCES

1. Ostrom QT, Patil N, Cioffi G, Waite K, Kruchko C, Barnholtz-Sloan JS. CBTRUS Statistical Report: Primary Brain and Other Central Nervous System Tumors Diagnosed in the United States in 2013-2017. *Neuro Oncol* (2020) 22(12 Suppl 2):iv1–iv96. doi: 10.1093/neuonc/noaa200

2. Louis DN, Ohgaki H, Wiestler OD, Cavenee WK. *Classification of Tumours of the Central Nervous System*, Revised 4th edition. World Health Organization and International Agency for Research on Cancer (2016). p. 1–408.

3. Singer LS, Feldman AZ, Buerki RA, Horbinski CM, Lukas RV, Stupp R. The Impact of the Molecular Classification of Glioblastoma on the Interpretation of Therapeutic Clinical Trial Results. *Chin Clin Oncol* (2021). doi: 10.21037/cco-21-33

4. Brat DJ, Aldape K, Colman H, Figrarella-Branger D, Fuller GN, Giannini C, et al. cIMPACT-NOW Update 5: Recommended Grading Criteria and Terminologies for IDH-Mutant Astrocytomas. *Acta Neuropathol* (2020) 139(3):603–8. doi: 10.1007/s00401-020-02127-9

5. Louis DN, Wesseling P, Aldape K, Brat DJ, Capper D, Cree IA, et al. cIMPACT-NOW Update 6: New Entity and Diagnostic Principle Recommendations of the cIMPACT-Utrecht Meeting on Future CNS Tumor Classification and Grading. *Brain Pathol* (2020) 30(4):844–56. doi: 10.1111/bpa.12832

6. Louis DN, Perry A, Wesseling P, Brat DJ, Cree IA, Figarella-Branger D, et al. The 2021 WHO Classification of Tumors of the Central Nervous System: A Summary. *Neuro Oncol* (2021) 23:1–21. doi: 10.1093/neuonc/noab106

7. Stupp R, Mason WP, van den Bent MJ, Weller M, Fisher B, Taphoorn MJ, et al. Radiotherapy Plus Concomitant and Adjuvant Temozolomide for Glioblastoma. *N Engl J Med* (2005) 352(10):987–96. doi: 10.1056/NEJMoa043330

8. Stupp R, Taillibert S, Kanner A, Read W, Steinberg D, Lhermitte B, et al. Effect of Tumor-Treating Fields Plus Maintenance Temozolomide vs Maintenance Temozolomide Alone on Survival in Patients With Glioblastoma: A Randomized Clinical Trial. *Jama* (2017) 318(23):2306–16. doi: 10.1001/jama.2017.18718

9. Chinot OL, Wick W, Mason W, Henriksson R, Saran F, Nishikawa R, et al. Bevacizumab Plus Radiotherapy-Temozolomide for Newly Diagnosed Glioblastoma. *N Engl J Med* (2014) 370(8):709–22. doi: 10.1056/NEJMoa1308345

10. Gilbert MR, Dignam JJ, Armstrong TS, Wefel JS, Blumenthal DT, Vogelbaum MA, et al. A Randomized Trial of Bevacizumab for Newly Diagnosed Glioblastoma. *N Engl J Med* (2014) 370(8):699–708. doi: 10.1056/NEJMoa1308573

11. Luengo A, Gui DY, Vander Heiden MG. Targeting Metabolism for Cancer Therapy. *Cell Chem Biol* (2017) 24(9):1161–80. doi: 10.1016/j.chembiol.2017.08.028

12. Reifenberger G, Wirsching HG, Knobbe-Thomsen CB, Weller M. Advances in the Molecular Genetics of Gliomas - Implications for Classification and Therapy. *Nat Rev Clin Oncol* (2017) 14(7):434–52. doi: 10.1038/nrclinonc.2016.204

13. Corso CD, Bindra RS. Success and Failures of Combined Modalities in Glioblastoma Multiforme: Old Problems and New Directions. *Semin Radiat Oncol* (2016) 26(4):281–98. doi: 10.1016/j.semradonc.2016.06.003

14. McGranahan T, Therkelsen KE, Ahmad S, Nagpal S. Current State of Immunotherapy for Treatment of Glioblastoma. *Curr Treat Options Oncol* (2019) 20(3):24–. doi: 10.1007/s11864-019-0619-4

15. Westphal M, Maire CL, Lamszus K. EGFR as a Target for Glioblastoma Treatment: An Unfulfilled Promise. *CNS Drugs* (2017) 31(9):723–35. doi: 10.1007/s40263-017-0456-6

16. Aldape K, Brindle KM, Chesler L, Chopra R, Gajjar A, Gilbert MR, et al. Challenges to Curing Primary Brain Tumours. *Nat Rev Clin Oncol* (2019) 16(8):509–20. doi: 10.1038/s41571-019-0177-5

17. Chuntova P, Chow F, Watchmaker PB, Galvez M, Heimberger AB, Newell EW, et al. Unique Challenges for Glioblastoma Immunotherapy-Discussions Across Neuro-Oncology and Non-Neuro-Oncology Experts in Cancer Immunology. Meeting Report From the 2019 SNO Immuno-Oncology Think Tank. *Neuro Oncol* (2021) 23(3):356–75. doi: 10.1093/neuonc/noaa277

18. Reardon DA, Desjardins A, Vredenburgh JJ, O'Rourke DM, Tran DD, Fink KL, et al. Rindopepimut With Bevacizumab for Patients With Relapsed EGFRvIII-Expressing Glioblastoma (ReACT): Results of a Double-Blind Randomized Phase II Trial. *Clin Cancer Res* (2020) 26(7):1586–94. doi: 10.1158/1078-0432.CCR-18-1140

19. Cloughesy TF, Mochizuki AY, Orpilla JR, Hugo W, Lee AH, Davidson TB, et al. Neoadjuvant Anti-PD-1 Immunotherapy Promotes a Survival Benefit With Intratumoral and Systemic Immune Responses in Recurrent Glioblastoma. *Nat Med* (2019) 25(3):477–86. doi: 10.1038/s41591-018-0337-7

20. Ellingson BM, Wen PY, Cloughesy TF. Modified Criteria for Radiographic Response Assessment in Glioblastoma Clinical Trials. *Neurotherapeutics* (2017) 14(2):307–20. doi: 10.1007/s13311-016-0507-6

21. Okada H, Weller M, Huang R, Finocchiaro G, Gilbert MR, Wick W, et al. Immunotherapy Response Assessment in Neuro-Oncology: A Report of the RANO Working Group. *Lancet Oncol* (2015) 16(15):e534–e42. doi: 10.1016/S1470-2045(15)00088-1

22. Nevel KS, Wilcox JA, Robell LJ, Umemura Y. The Utility of Liquid Biopsy in Central Nervous System Malignancies. *Curr Oncol Rep* (2018) 20(8):60. doi: 10.1007/s11912-018-0706-x

23. Chuntova P, Chow F, Watchmaker P, Galvez M, Heimberger AB, Newell EW, et al. Unique Challenges for Glioblastoma Immunotherapy - Discussions Across Neuro-Oncology and Non-Neuro-Oncology Experts in Cancer Immunology. *Neuro Oncol* (2020) 23(3):356–75. doi: 10.1093/neuonc/noaa277

24. Louis DN, Perry A, Reifenberger G, von Deimling A, Figarella-Branger D, Cavenee WK, et al. The 2016 World Health Organization Classification of Tumors of the Central Nervous System: A Summary. *Acta Neuropathol* (2016) 131(6):803–20. doi: 10.1007/s00401-016-1545-1

25. Masui K, Mischel PS, Reifenberger G. Molecular Classification of Gliomas. *Handb Clin Neurol* (2016) 134:97–120. doi: 10.1016/B978-0-12-802997-8.00006-2

26. Wesseling P, Capper D. WHO 2016 Classification of Gliomas. *Neuropathol Appl Neurobiol* (2018) 44(2):139–50. doi: 10.1111/nan.12432

27. Mazor T, Chesnelong C, Pankov A, Jalbert LE, Hong C, Hayes J, et al. Clonal Expansion and Epigenetic Reprogramming Following Deletion or Amplification of Mutant IDH1. *Proc Natl Acad Sci USA* (2017) 114(40):10743–8. doi: 10.1073/pnas.1708914114

28. Watanabe T, Nobusawa S, Kleihues P, Ohgaki H. IDH1 Mutations Are Early Events in the Development of Astrocytomas and Oligodendrogliomas. *Am J Pathol* (2009) 174(4):1149–53. doi: 10.2353/ajpath.2009.080958

29. Cancer Genome Atlas Research N, Brat DJ, Verhaak RG, Aldape KD, Yung WK, Salama SR, et al. Comprehensive, Integrative Genomic Analysis of Diffuse Lower-Grade Gliomas. *N Engl J Med* (2015) 372(26):2481–98. doi: 10.1056/NEJMoa1402121

30. Lawrence MS, Stojanov P, Polak P, Kryukov GV, Cibulskis K, Sivachenko A, et al. Mutational Heterogeneity in Cancer and the Search for New Cancer-Associated Genes. *Nature* (2013) 499(7457):214–8. doi: 10.1038/nature12213

31. Brennan CW, Verhaak RG, McKenna A, Campos B, Noushmehr H, Salama SR, et al. The Somatic Genomic Landscape of Glioblastoma. *Cell* (2013) 155(2):462–77. doi: 10.1016/j.cell.2013.09.034

32. Ceccarelli M, Barthel FP, Malta TM, Sabedot TS, Salama SR, Murray BA, et al. Molecular Profiling Reveals Biologically Discrete Subsets and Pathways of Progression in Diffuse Glioma. *Cell* (2016) 164(3):550–63. doi: 10.1016/j.cell.2015.12.028

33. Delgado-Lopez PD, Corrales-Garcia EM, Martino J, Lastra-Aras E, Duenas-Polo MT. Diffuse Low-Grade Glioma: A Review on the New Molecular Classification, Natural History and Current Management Strategies. *Clin Transl Oncol* (2017) 19(8):931–44. doi: 10.1007/s12094-017-1631-4

34. Ostrom QT, Gittleman H, Truitt G, Boscia A, Kruchko C, Barnholtz-Sloan JS. CBTRUS Statistical Report: Primary Brain and Other Central Nervous System Tumors Diagnosed in the United States in 2011-2015. *Neuro Oncol* (2018) 20(suppl_4):iv1–iv86. doi: 10.1093/neuonc/noy131

35. Bai H, Harmanci AS, Erson-Omay EZ, Li J, Coskun S, Simon M, et al. Integrated Genomic Characterization of IDH1-Mutant Glioma Malignant Progression. *Nat Genet* (2016) 48(1):59–66. doi: 10.1038/ng.3457

36. Parsons DW, Jones S, Zhang X, Lin JC, Leary RJ, Angenendt P, et al. An Integrated Genomic Analysis of Human Glioblastoma Multiforme. *Science* (2008) 321(5897):1807–12. doi: 10.1126/science.1164382

37. Dang L, White DW, Gross S, Bennett BD, Bittinger MA, Driggers EM, et al. Cancer-Associated IDH1 Mutations Produce 2-Hydroxyglutarate. *Nature* (2009) 462(7274):739–44. doi: 10.1038/nature08617

38. Nunez FJ, Mendez FM, Kadiyala P, Alghamri MS, Savelieff MG, Garcia-Fabiani MB, et al. IDH1-R132H Acts as a Tumor Suppressor in Glioma *Via* Epigenetic Up-Regulation of the DNA Damage Response. *Sci Transl Med* (2019) 11(479):eaaq1427. doi: 10.1126/scitranslmed.aaq1427

39. Yan H, Parsons DW, Jin G, McLendon R, Rasheed BA, Yuan W, et al. IDH1 and IDH2 Mutations in Gliomas. *N Engl J Med* (2009) 360(8):765–73. doi: 10.1056/NEJMoa0808710

40. Arita H, Matsushita Y, Machida R, Yamasaki K, Hata N, Ohno M, et al. TERT Promoter Mutation Confers Favorable Prognosis Regardless of 1p/19q Status in Adult Diffuse Gliomas With IDH1/2 Mutations. *Acta Neuropathol Commun* (2020) 8(1):201. doi: 10.1186/s40478-020-01078-2

41. Noushmehr H, Weisenberger DJ, Diefes K, Phillips HS, Pujara K, Berman BP, et al. Identification of a CpG Island Methylator Phenotype That Defines a Distinct Subgroup of Glioma. *Cancer Cell* (2010) 17(5):510–22. doi: 10.1016/S1040-1741(10)79529-4

42. Wiestler B, Capper D, Sill M, Jones DT, Hovestadt V, Sturm D, et al. Integrated DNA Methylation and Copy-Number Profiling Identify Three Clinically and Biologically Relevant Groups of Anaplastic Glioma. *Acta Neuropathol* (2014) 128(4):561–71. doi: 10.1007/s00401-014-1315-x

43. Zhang YH, Li Z, Zeng T, Pan X, Chen L, Liu D, et al. Distinguishing Glioblastoma Subtypes by Methylation Signatures. *Front Genet* (2020) 11:604336. doi: 10.3389/fgene.2020.604336

44. Wick W, Weller M, van den Bent M, Sanson M, Weiler M, von Deimling A, et al. MGMT Testing–the Challenges for Biomarker-Based Glioma Treatment. *Nat Rev Neurol* (2014) 10(7):372–85. doi: 10.1038/nrneurol.2014.100

45. Suwala AK, Stichel D, Schrimpf D, Maas SLN, Sill M, Dohmen H, et al. Glioblastomas With Primitive Neuronal Component Harbor a Distinct Methylation and Copy-Number Profile With Inactivation of TP53, PTEN, and RB1. *Acta Neuropathol* (2021) 142(1):179–89. doi: 10.1007/s00401-021-02302-6

46. Khuong-Quang DA, Buczkowicz P, Rakopoulos P, Liu XY, Fontebasso AM, Bouffet E, et al. K27M Mutation in Histone H3.3 Defines Clinically and Biologically Distinct Subgroups of Pediatric Diffuse Intrinsic Pontine Gliomas. *Acta Neuropathol* (2012) 124(3):439–47. doi: 10.1007/s00401-012-0998-0

47. Schwartzentruber J, Korshunov A, Liu XY, Jones DT, Pfaff E, Jacob K, et al. Driver Mutations in Histone H3.3 and Chromatin Remodelling Genes in Paediatric Glioblastoma. *Nature* (2012) 482(7384):226–31. doi: 10.1038/nature10833

48. Kallappagoudar S, Yadav RK, Lowe BR, Partridge JF. Histone H3 Mutations–a Special Role for H3.3 in Tumorigenesis? *Chromosoma* (2015) 124(2):177–89. doi: 10.1007/s00412-015-0510-4

49. Funato K, Smith RC, Saito Y, Tabar V. Dissecting The Impact Of Regional Identity And The Oncogenic Role Of Human-Specific Notch2nl In an Hesc Model of H3.3g34r-Mutant Glioma. *Cell Stem Cell* (2018) 28: (5):894–905.e7. doi: 10.1016/j.stem.2021.02.003

50. Kim YZ. Altered Histone Modifications in Gliomas. *Brain Tumor Res Treat* (2014) 2(1):7–21. doi: 10.14791/btrt.2014.2.1.7

51. Liu B-L, Cheng J-X, Zhang X, Wang R, Zhang W, Lin H, et al. Global Histone Modification Patterns as Prognostic Markers to Classify Glioma Patients. *Cancer Epidemiol Biomarkers Prev* (2010) 19(11):2888–96. doi: 10.1158/1055-9965.EPI-10-0454

52. Zang L, Kondengaden SM, Che F, Wang L, Heng X. Potential Epigenetic-Based Therapeutic Targets for Glioma. *Front Mol Neurosci* (2018) 11:408. doi: 10.3389/fnmol.2018.00408

53. Verhaak RG, Hoadley KA, Purdom E, Wang V, Qi Y, Wilkerson MD, et al. Integrated Genomic Analysis Identifies Clinically Relevant Subtypes of Glioblastoma Characterized by Abnormalities in PDGFRA, IDH1, EGFR, and NF1. *Cancer Cell* (2010) 17(1):98–110. doi: 10.1016/j.ccr.2009.12.020

54. Nazarenko I, Hede SM, He X, Hedren A, Thompson J, Lindstrom MS, et al. PDGF and PDGF Receptors in Glioma. *Ups J Med Sci* (2012) 117(2):99–112. doi: 10.3109/03009734.2012.665097

55. Nakada M, Kita D, Watanabe T, Hayashi Y, Teng L, Pyko IV, et al. Aberrant Signaling Pathways in Glioma. *Cancers (Basel)* (2011) 3(3):3242–78. doi: 10.3390/cancers3033242

56. Crespo I, Vital AL, Gonzalez-Tablas M, Patino Mdel C, Otero A, Lopes MC, et al. Molecular and Genomic Alterations in Glioblastoma Multiforme. *Am J Pathol* (2015) 185(7):1820–33. doi: 10.1016/j.ajpath.2015.02.023

57. Gersey Z, Osiason AD, Bloom L, Shah S, Thompson JW, Bregy A, et al. Therapeutic Targeting of the Notch Pathway in Glioblastoma Multiforme. *World Neurosurg* (2019) 131:252–63.e2. doi: 10.1016/j.wneu.2019.07.180

58. Bi J, Chowdhry S, Wu S, Zhang W, Masui K, Mischel PS. Altered Cellular Metabolism in Gliomas - An Emerging Landscape of Actionable Co-Dependency Targets. *Nat Rev Cancer* (2020) 20(1):57–70. doi: 10.1038/s41568-019-0226-5

59. Rohle D, Popovici-Muller J, Palaskas N, Turcan S, Grommes C, Campos C, et al. An Inhibitor of Mutant IDH1 Delays Growth and Promotes Differentiation of Glioma Cells. *Science* (2013) 340(6132):626–30. doi: 10.1126/science.1236062

60. Sulkowski PL, Corso CD, Robinson ND, Scanlon SE, Purshouse KR, Bai H, et al. 2-Hydroxyglutarate Produced by Neomorphic IDH Mutations Suppresses Homologous Recombination and Induces PARP Inhibitor Sensitivity. *Sci Transl Med* (2017) 9(375):eaal2463. doi: 10.1126/scitranslmed.aal2463

61. Phillips HS, Kharbanda S, Chen R, Forrest WF, Soriano RH, Wu TD, et al. Molecular Subclasses of High-Grade Glioma Predict Prognosis, Delineate a Pattern of Disease Progression, and Resemble Stages in Neurogenesis. *Cancer Cell* (2006) 9(3):157–73. doi: 10.1016/j.ccr.2006.02.019

62. Lee JK, Wang J, Sa JK, Ladewig E, Lee HO, Lee IH, et al. Spatiotemporal Genomic Architecture Informs Precision Oncology in Glioblastoma. *Nat Genet* (2017) 49(4):594–9. doi: 10.1038/ng.3806

63. Patel AP, Tirosh I, Trombetta JJ, Shalek AK, Gillespie SM, Wakimoto H, et al. Single-Cell RNA-Seq Highlights Intratumoral Heterogeneity in Primary Glioblastoma. *Science* (2014) 344(6190):1396–401. doi: 10.1126/science.1254257

64. Garofano L, Migliozzi S, Oh YT, D'Angelo F, Najac RD, Ko A, et al. Pathway-Based Classification of Glioblastoma Uncovers a Mitochondrial Subtype With Therapeutic Vulnerabilities. *Nat Cancer* (2021) 2(2):141–56. doi: 10.1038/s43018-020-00159-4

65. Neftel C, Laffy J, Filbin MG, Hara T, Shore ME, Rahme GJ, et al. An Integrative Model of Cellular States, Plasticity, and Genetics for Glioblastoma. *Cell* (2019) 178(4):835–49.e21. doi: 10.1016/j.cell.2019.06.024

66. Wang Q, Hu B, Hu X, Kim H, Squatrito M, Scarpace L, et al. Tumor Evolution of Glioma-Intrinsic Gene Expression Subtypes Associates With Immunological Changes in the Microenvironment. *Cancer Cell* (2017) 32(1):42–56 e6. doi: 10.1016/j.ccell.2017.06.003

67. Bhat KPL, Balasubramaniyan V, Vaillant B, Ezhilarasan R, Hummelink K, Hollingsworth F, et al. Mesenchymal Differentiation Mediated by NF-kappaB Promotes Radiation Resistance in Glioblastoma. *Cancer Cell* (2013) 24(3):331–46. doi: 10.1016/j.ccr.2013.08.001

68. Sottoriva A, Spiteri I, Piccirillo SG, Touloumis A, Collins VP, Marioni JC, et al. Intratumor Heterogeneity in Human Glioblastoma Reflects Cancer Evolutionary Dynamics. *Proc Natl Acad Sci USA* (2013) 110(10):4009–14. doi: 10.1073/pnas.1219747110

69. Puchalski RB, Shah N, Miller J, Dalley R, Nomura SR, Yoon JG, et al. An Anatomic Transcriptional Atlas of Human Glioblastoma. *Science* (2018) 360(6389):660–3. doi: 10.1126/science.aaf2666

70. Pang B, Xu J, Hu J, Guo F, Wan L, Cheng M, et al. Single-Cell RNA-Seq Reveals the Invasive Trajectory and Molecular Cascades Underlying Glioblastoma Progression. *Mol Oncol* (2019) 13(12):2588–603. doi: 10.1002/1878-0261.12569

71. Darmanis S, Sloan SA, Croote D, Mignardi M, Chernikova S, Samghababi P, et al. Single-Cell RNA-Seq Analysis of Infiltrating Neoplastic Cells at the Migrating Front of Human Glioblastoma. *Cell Rep* (2017) 21(5):1399–410. doi: 10.1016/j.celrep.2017.10.030

72. Xiong Z, Yang Q, Li X. Effect of Intra- and Inter-Tumoral Heterogeneity on Molecular Characteristics of Primary IDH-Wild Type Glioblastoma Revealed by Single-Cell Analysis. *CNS Neurosci Ther* (2020) 26(9):981–9. doi: 10.1111/cns.13396

73. Bergmann N, Delbridge C, Gempt J, Feuchtinger A, Walch A, Schirmer L, et al. The Intratumoral Heterogeneity Reflects the Intertumoral Subtypes of Glioblastoma Multiforme: A Regional Immunohistochemistry Analysis. *Front Oncol* (2020) 10:494. doi: 10.3389/fonc.2020.00494

74. Hambardzumyan D, Gutmann DH, Kettenmann H. The Role of Microglia and Macrophages in Glioma Maintenance and Progression. *Nat Neurosci* (2016) 19(1):20–7. doi: 10.1038/nn.4185

75. Quail DF, Joyce JA. The Microenvironmental Landscape of Brain Tumors. *Cancer Cell* (2017) 31(3):326–41. doi: 10.1016/j.ccell.2017.02.009

76. Mantovani A, Marchesi F, Malesci A, Laghi L, Allavena P. Tumour-Associated Macrophages as Treatment Targets in Oncology. *Nat Rev Clin Oncol* (2017) 14(7):399–416. doi: 10.1038/nrclinonc.2016.217

77. Chen Z, Feng X, Herting CJ, Garcia VA, Nie K, Pong WW, et al. Cellular and Molecular Identity of Tumor-Associated Macrophages in Glioblastoma. *Cancer Res* (2017) 77(9):2266–78. doi: 10.1158/0008-5472.CAN-16-2310

78. Bowman RL, Klemm F, Akkari L, Pyonteck SM, Sevenich L, Quail DF, et al. Macrophage Ontogeny Underlies Differences in Tumor-Specific Education in Brain Malignancies. *Cell Rep* (2016) 17(9):2445–59. doi: 10.1016/j.celrep.2016.10.052

79. Brandenburg S, Blank A, Bungert AD, Vajkoczy P. Distinction of Microglia and Macrophages in Glioblastoma: Close Relatives, Different Tasks? *Int J Mol Sci* (2020) 22(1):eabc2511. doi: 10.3390/ijms22010194

80. Venteicher AS, Tirosh I, Hebert C, Yizhak K, Neftel C, Filbin MG, et al. Decoupling Genetics, Lineages, and Microenvironment in IDH-Mutant Gliomas by Single-Cell RNA-Seq. *Science* (2017) 355(6332):eaai8478. doi: 10.1126/science.aai8478

81. Landry AP, Balas M, Alli S, Spears J, Zador Z. Distinct Regional Ontogeny and Activation of Tumor Associated Macrophages in Human Glioblastoma. *Sci Rep* (2020) 10(1):19542. doi: 10.1038/s41598-020-76657-3

82. Tian Y, Ke Y, Ma Y. High Expression of Stromal Signatures Correlated With Macrophage Infiltration, Angiogenesis and Poor Prognosis in Glioma Microenvironment. *PeerJ* (2020) 8:e9038. doi: 10.7717/peerj.9038

83. Brandenburg S, Muller A, Turkowski K, Radev YT, Rot S, Schmidt C, et al. Resident Microglia Rather Than Peripheral Macrophages Promote Vascularization in Brain Tumors and Are Source of Alternative Pro-Angiogenic Factors. *Acta Neuropathol* (2016) 131(3):365–78. doi: 10.1007/s00401-015-1529-6

84. Hu J, Zhao Q, Kong LY, Wang J, Yan J, Xia X, et al. Regulation of Tumor Immune Suppression and Cancer Cell Survival by CXCL1/2 Elevation in Glioblastoma Multiforme. *Sci Adv* (2021) 7(5):eabc2511. doi: 10.1126/sciadv.abc2511

85. Urbantat RM, Blank A, Kremenetskaia I, Vajkoczy P, Acker G, Brandenburg S. The CXCL2/IL8/CXCR2 Pathway Is Relevant for Brain Tumor Malignancy and Endothelial Cell Function. *Int J Mol Sci* (2021) 22(5):2634. doi: 10.3390/ijms22052634

86. Acker G, Zollfrank J, Jelgersma C, Nieminen-Kelha M, Kremenetskaia I, Mueller S, et al. The CXCR2/CXCL2 Signalling Pathway - An Alternative Therapeutic Approach in High-Grade Glioma. *Eur J Cancer* (2020) 126:106–15. doi: 10.1016/j.ejca.2019.12.005

87. Pyonteck SM, Akkari L, Schuhmacher AJ, Bowman RL, Sevenich L, Quail DF, et al. CSF-1R Inhibition Alters Macrophage Polarization and Blocks Glioma Progression. *Nat Med* (2013) 19(10):1264–72. doi: 10.1038/nm.3337

88. Klemm F, Maas RR, Bowman RL, Kornete M, Soukup K, Nassiri S, et al. Interrogation of the Microenvironmental Landscape in Brain Tumors Reveals Disease-Specific Alterations of Immune Cells. *Cell* (2020) 181(7):1643–60 e17. doi: 10.1016/j.cell.2020.05.007

89. Gieryng A, Pszczolkowska D, Walentynowicz KA, Rajan WD, Kaminska B. Immune Microenvironment of Gliomas. *Lab Invest* (2017) 97(5):498–518. doi: 10.1038/labinvest.2017.19

90. Takeuchi Y, Nishikawa H. Roles of Regulatory T Cells in Cancer Immunity. *Int Immunol* (2016) 28(8):401–9. doi: 10.1093/intimm/dxw025

91. Atabani SF, Thio CL, Divanovic S, Trompette A, Belkaid Y, Thomas DL, et al. Association of CTLA4 Polymorphism With Regulatory T Cell Frequency. *Eur J Immunol* (2005) 35(7):2157–62. doi: 10.1002/eji.200526168

92. Jacobs JF, Idema AJ, Bol KF, Nierkens S, Grauer OM, Wesseling P, et al. Regulatory T Cells and the PD-L1/PD-1 Pathway Mediate Immune Suppression in Malignant Human Brain Tumors. *Neuro Oncol* (2009) 11(4):394–402. doi: 10.1215/15228517-2008-104

93. Mathewson ND, Ashenberg O, Tirosh I, Gritsch S, Perez EM, Marx S, et al. Inhibitory CD161 Receptor Identified in Glioma-Infiltrating T Cells by Single-Cell RNA Analysis. *Cell* (2021) 184(5):1281–98.e26. doi: 10.1016/j.cell.2021.01.022

94. Kamran N, Kadiyala P, Saxena M, Candolfi M, Li Y, Moreno-Ayala MA, et al. Immunosuppressive Myeloid Cells' Blockade in the Glioma Microenvironment Enhances the Efficacy of Immune-Stimulatory Gene Therapy. *Mol Ther* (2017) 25(1):232–48. doi: 10.1016/j.ymthe.2016.10.003

95. Kast RE, Hill QA, Wion D, Mellstedt H, Focosi D, Karpel-Massler G, et al. Glioblastoma-Synthesized G-CSF and GM-CSF Contribute to Growth and Immunosuppression: Potential Therapeutic Benefit From Dapsone, Fenofibrate, and Ribavirin. *Tumour Biol* (2017) 39(5):1010428317699797. doi: 10.1177/1010428317699797

96. Fujita M, Kohanbash G, Fellows-Mayle W, Hamilton RL, Komohara Y, Decker SA, et al. COX-2 Blockade Suppresses Gliomagenesis by Inhibiting Myeloid-Derived Suppressor Cells. *Cancer Res* (2011) 71(7):2664–74. doi: 10.1158/0008-5472.CAN-10-3055

97. Han S, Liu Y, Li Q, Li Z, Hou H, Wu A. Pre-Treatment Neutrophil-to-Lymphocyte Ratio Is Associated With Neutrophil and T-Cell Infiltration and Predicts Clinical Outcome in Patients With Glioblastoma. *BMC Cancer* (2015) 15:617. doi: 10.1186/s12885-015-1629-7

98. Nasser MW, Raghuwanshi SK, Grant DJ, Jala VR, Rajarathnam K, Richardson RM. Differential Activation and Regulation of CXCR1 and CXCR2 by CXCL8 Monomer and Dimer. *J Immunol* (2009) 183(5):3425–32. doi: 10.4049/jimmunol.0900305

99. Fremd C, Schuetz F, Sohn C, Beckhove P, Domschke C. B Cell-Regulated Immune Responses in Tumor Models and Cancer Patients. *Oncoimmunology* (2013) 2(7):e25443. doi: 10.4161/onci.25443

100. Humphries W, Wei J, Sampson JH, Heimberger AB. The Role of Tregs in Glioma-Mediated Immunosuppression: Potential Target for Intervention. *Neurosurg Clin N Am* (2010) 21(1):125–37. doi: 10.1016/j.nec.2009.08.012

101. Han S, Feng S, Ren M, Ma E, Wang X, Xu L, et al. Glioma Cell-Derived Placental Growth Factor Induces Regulatory B Cells. *Int J Biochem Cell Biol* (2014) 57:63–8. doi: 10.1016/j.biocel.2014.10.005

102. Henrik Heiland D, Ravi VM, Behringer SP, Frenking JH, Wurm J, Joseph K, et al. Tumor-Associated Reactive Astrocytes Aid the Evolution of Immunosuppressive Environment in Glioblastoma. *Nat Commun* (2019) 10(1):2541. doi: 10.1038/s41467-019-10493-6

103. Venkatesh HS, Tam LT, Woo PJ, Lennon J, Nagaraja S, Gillespie SM, et al. Targeting Neuronal Activity-Regulated Neuroligin-3 Dependency in High-Grade Glioma. *Nature* (2017) 549(7673):533–7. doi: 10.1038/nature24014

104. Venkatesh HS, Morishita W, Geraghty AC, Silverbush D, Gillespie SM, Arzt M, et al. Electrical and Synaptic Integration of Glioma Into Neural Circuits. *Nature* (2019) 573(7775):539–45. doi: 10.1038/s41586-019-1563-y

105. Lathia JD, Mack SC, Mulkearns-Hubert EE, Valentim CL, Rich JN. Cancer Stem Cells in Glioblastoma. *Genes Dev* (2015) 29(12):1203–17. doi: 10.1101/gad.261982.115

106. Parada LF, Dirks PB, Wechsler-Reya RJ. Brain Tumor Stem Cells Remain in Play. *J Clin Oncol* (2017) 35(21):2428–31. doi: 10.1200/JCO.2017.73.9540

107. Svensson A, Ozen I, Genove G, Paul G, Bengzon J. Endogenous Brain Pericytes are Widely Activated and Contribute to Mouse Glioma Microvasculature. *PloS One* (2015) 10(4):e0123553. doi: 10.1371/journal.pone.0123553

108. Crisan M, Yap S, Casteilla L, Chen CW, Corselli M, Park TS, et al. A Perivascular Origin for Mesenchymal Stem Cells in Multiple Human Organs. *Cell Stem Cell* (2008) 3(3):301–13. doi: 10.1016/j.stem.2008.07.003

109. Baker GJ, Yadav VN, Motsch S, Koschmann C, Calinescu AA, Mineharu Y, et al. Mechanisms of Glioma Formation: Iterative Perivascular Glioma Growth and Invasion Leads to Tumor Progression, VEGF-Independent Vascularization, and Resistance to Antiangiogenic Therapy. *Neoplasia* (2014) 16(7):543–61. doi: 10.1016/j.neo.2014.06.003

110. Gritsenko PG, Friedl P. Adaptive Adhesion Systems Mediate Glioma Cell Invasion in Complex Environments. *J Cell Sci* (2018) 131(15):jcs216382. doi: 10.1242/jcs.216382

111. Comba A, Zamler D, Argento AE, Koschmann C, Nunez FJ, Edwards M, et al. CSIG-11. Oncostreams: Novel Structures that Specify Gliomas' Self-Organization, Are Anatomically Discrete, Functionally Unique, and Molecularly Distinct. *Neuro Oncol* (2017) 19(suppl_6):vi52–vi. doi: 10.1093/neuonc/nox168.206

112. Jamous S, Comba A, Lowenstein PR, Motsch S. Self-Organization in Brain Tumors: How Cell Morphology and Cell Density Influence Glioma Pattern Formation. *PloS Comput Biol* (2020) 16(5):e1007611. doi: 10.1371/journal.pcbi.1007611

113. Comba A, Motsch S, Dunn PJ, Hollon TC, Argento AE, Zamler DB, et al. Spatiotemporal Analysis of Glioma Heterogeneity Reveals Col1A1 as an Actionable Target to Disrupt Tumor Mesenchymal Differentiation, Invasion

and Malignancy. *bioRxiv* (2021) 2020.12.01.404970. doi: 10.1101/2020.12.01.404970

114. Xavier da Silveira Dos Santos A, Liberali P. From Single Cells to Tissue Self-Organization. *FEBS J* (2019) 286(8):1495–513. doi: 10.1111/febs.14694

115. Rørth P. Fellow Travellers: Emergent Properties of Collective Cell Migration. *EMBO Rep* (2012) 13(11):984–91. doi: 10.1038/embor.2012.149

116. Méhes E, Vicsek T. Collective Motion of Cells: From Experiments to Models. *Integr Biol (Camb)* (2014) 6(9):831–54. doi: 10.1039/C4IB00115J

117. Szabó A, Mayor R. Mechanisms of Neural Crest Migration. *Annu Rev Genet* (2018) 52:43–63. doi: 10.1146/annurev-genet-120417-031559

118. Staneva R, El Marjou F, Barbazan J, Krndija D, Richon S, Clark AG, et al. Cancer Cells in the Tumor Core Exhibit Spatially Coordinated Migration Patterns. *J Cell Sci* (2019) 132(6):jcs220277. doi: 10.1242/jcs.220277

119. Alieva M, Leidgens V, Riemenschneider MJ, Klein CA, Hau P, van Rheenen J. Intravital Imaging of Glioma Border Morphology Reveals Distinctive Cellular Dynamics and Contribution to Tumor Cell Invasion. *Sci Rep* (2019) 9(1):2054. doi: 10.1038/s41598-019-38625-4

120. IARC, Wiestler DO. WHO Classification of Tumours of the Central Nervous System: WHO Classification of Tumours of the Central Nervous System (4th Edition), Louis DN, ed., Lyon France: World Health Organization. (2006) Chapter 1: Astrocytic Tumors. p. 13-52.

121. Vickovic S, Eraslan G, Salmen F, Klughammer J, Stenbeck L, Schapiro D, et al. High-Definition Spatial Transcriptomics for *in Situ* Tissue Profiling. *Nat Methods* (2019) 16(10):987–90. doi: 10.1038/s41592-019-0548-y

122. Lein E, Borm LE, Linnarsson S. The Promise of Spatial Transcriptomics for Neuroscience in the Era of Molecular Cell Typing. *Science (New York NY)* (2017) 358(6359):64–9. doi: 10.1126/science.aan6827

123. Maniatis S, Petrescu J, Phatnani H. Spatially Resolved Transcriptomics and its Applications in Cancer. *Curr Opin Genet Dev* (2021) 66:70–7. doi: 10.1016/j.gde.2020.12.002

124. Miller TE, Liau BB, Wallace LC, Morton AR, Xie Q, Dixit D, et al. Transcription Elongation Factors Represent *In Vivo* Cancer Dependencies in Glioblastoma. *Nature* (2017) 547(7663):355–9. doi: 10.1038/nature23000

125. Yu D, Khan OF, Suva ML, Dong B, Panek WK, Xiao T, et al. Multiplexed RNAi Therapy Against Brain Tumor-Initiating Cells *Via* Lipopolymeric Nanoparticle Infusion Delays Glioblastoma Progression. *Proc Natl Acad Sci USA* (2017) 114(30):E6147–E56. doi: 10.1073/pnas.1701911114

126. Comba A, Zamler D B, Dunn P, Argento A, Kadiyala P, Nand Yadav V, et al. CSIG-08. Dynamics of Glioma Growth: Self-Organization Guides the Patterning of the Extracellular Matrix and Regulates Tumor Progression. *Neuro Oncol* (2018) 20(suppl_6):vi44–vi. doi: 10.1093/neuonc/noy148.174

127. Comba A, Dunn P, Argento AE, Kadiyala P, Motsch S, Kish P, et al. 3131 Oncostreams: Novel Dynamics Pathological Multicellular Structures Involved in Glioblatoma Growth and Invasion. *J Clin Trans Sci* (2019) 3 (s1):111–. doi: 10.1017/cts.2019.253

128. Comba A, Dunn PJ, Kish PE, Kadiyala P, Kahana A, Castro MG, et al. Laser Capture Microdissection of Glioma Subregions for Spatial and Molecular Characterization of Intratumoral Heterogeneity, Oncostreams, and Invasion. *J Vis Exp* (2020) 158:e60939. doi: 10.3791/60939

129. Boyle ST, Mittal P, Kaur G, Hoffmann P, Samuel MS, Klingler-Hoffmann M. Uncovering Tumor-Stroma Inter-Relationships Using MALDI Mass Spectrometry Imaging. *J Proteome Res* (2020) 19(10):4093–103. doi: 10.1021/acs.jproteome.0c00511

130. Keren L, Bosse M, Marquez D, Angoshtari R, Jain S, Varma S, et al. A Structured Tumor-Immune Microenvironment in Triple Negative Breast Cancer Revealed by Multiplexed Ion Beam Imaging. *Cell* (2018) 174 (6):1373–87.e19. doi: 10.1016/j.cell.2018.08.039

131. Keren L, Bosse M, Thompson S, Risom T, Vijayaragavan K, McCaffrey E, et al. MIBI-TOF: A Multiplexed Imaging Platform Relates Cellular Phenotypes and Tissue Structure. *Sci Adv* (2019) 5(10):eaax5851. doi: 10.1126/sciadv.aax5851

132. Gularyan SK, Gulin AA, Anufrieva KS, Shender VO, Shakhparonov MI, Bastola S, et al. Investigation of Inter- and Intratumoral Heterogeneity of Glioblastoma Using TOF-SIMS. *Mol Cell Proteomics* (2020) 19(6):960–70. doi: 10.1074/mcp.RA120.001986

133. Chang K, Bai HX, Zhou H, Su C, Bi WL, Agbodza E, et al. Residual Convolutional Neural Network for the Determination of IDH Status in Low- and High-Grade Gliomas From MR Imaging. *Clin Cancer Res* (2018) 24(5):1073–81. doi: 10.1158/1078-0432.CCR-17-2236

134. Bangalore Yoganananda CG, Shah BR, Vejdani-Jahromi M, Nalawade SS, Murugesan GK, Yu FF, et al. A Novel Fully Automated MRI-Based Deep-Learning Method for Classification of IDH Mutation Status in Brain Gliomas. *Neuro Oncol* (2020) 22(3):402–11. doi: 10.1101/757385

135. Chang P, Grinband J, Weinberg BD, Bardis M, Khy M, Cadena G, et al. Deep-Learning Convolutional Neural Networks Accurately Classify Genetic Mutations in Gliomas. *AJNR Am J Neuroradiol* (2018) 39(7):1201–7. doi: 10.3174/ajnr.A5667

136. Clark K, Vendt B, Smith K, Freymann J, Kirby J, Koppel P, et al. The Cancer Imaging Archive (TCIA): Maintaining and Operating a Public Information Repository. *J Digit Imaging* (2013) 26(6):1045–57. doi: 10.1007/s10278-013-9622-7

137. Niazi MKK, Parwani AV, Gurcan MN. Digital Pathology and Artificial Intelligence. *Lancet Oncol* (2019) 20(5):e253–e61. doi: 10.1016/S1470-2045 (19)30154-8

138. Hollon TC, Pandian B, Adapa AR, Urias E, Save AV, Khalsa SSS, et al. Near Real-Time Intraoperative Brain Tumor Diagnosis Using Stimulated Raman Histology and Deep Neural Networks. *Nat Med* (2020) 26(1):52–8. doi: 10.1038/s41591-019-0715-9

139. Coudray N, Ocampo PS, Sakellaropoulos T, Narula N, Snuderl M, Fenyo D, et al. Classification and Mutation Prediction From Non-Small Cell Lung Cancer Histopathology Images Using Deep Learning. *Nat Med* (2018) 24 (10):1559–67. doi: 10.1038/s41591-018-0177-5

140. Pantanowitz L, Quiroga-Garza GM, Bien L, Heled R, Laifenfeld D, Linhart C, et al. An Artificial Intelligence Algorithm for Prostate Cancer Diagnosis in Whole Slide Images of Core Needle Biopsies: A Blinded Clinical Validation and Deployment Study. *Lancet Digit Health* (2020) 2(8):e407–e16. doi: 10.1016/S2589-7500(20)30159-X

141. Heindl A, Nawaz S, Yuan Y. Mapping Spatial Heterogeneity in the Tumor Microenvironment: A New Era for Digital Pathology. *Lab Invest* (2015) 95 (4):377–84. doi: 10.1038/labinvest.2014.155

142. Hollon TC, Pandian B, Urias E, Save AV, Adapa AR, Srinivasan S, et al. Rapid, Label-Free Detection of Diffuse Glioma Recurrence Using Intraoperative Stimulated Raman Histology and Deep Neural Networks. *Neuro Oncol* (2020) 23(1):144–55. doi: 10.1093/neuonc/noaa162.

143. Orringer DA, Pandian B, Niknafs YS, Hollon TC, Boyle J, Lewis S, et al. Rapid Intraoperative Histology of Unprocessed Surgical Specimens *Via* Fibre-Laser-Based Stimulated Raman Scattering Microscopy. *Nat BioMed Eng* (2017) 1:0027. doi: 10.1038/s41551-016-0027

144. Hollon TC, Lewis S, Pandian B, Niknafs YS, Garrard MR, Garton H, et al. Rapid Intraoperative Diagnosis of Pediatric Brain Tumors Using Stimulated Raman Histology. *Cancer Res* (2018) 78(1):278–89. doi: 10.1158/0008-5472.CAN-17-1974

145. Wang X, Prager BC, Wu Q, Kim LJY, Gimple RC, Shi Y, et al. Reciprocal Signaling Between Glioblastoma Stem Cells and Differentiated Tumor Cells Promotes Malignant Progression. *Cell Stem Cell* (2018) 22(4):514–28.e5. doi: 10.1016/j.stem.2018.03.011

146. Hambardzumyan D, Bergers G. Glioblastoma: Defining Tumor Niches. *Trends Cancer* (2015) 1(4):252–65. doi: 10.1016/j.trecan.2015.10.009

147. Osuka S, Van Meir EG. Overcoming Therapeutic Resistance in Glioblastoma: The Way Forward. *J Clin Invest* (2017) 127(2):415–26. doi: 10.1172/JCI89587

148. Calabrese C, Poppleton H, Kocak M, Hogg TL, Fuller C, Hamner B, et al. A Perivascular Niche for Brain Tumor Stem Cells. *Cancer Cell* (2007) 11(1):69–82. doi: 10.1016/j.ccr.2006.11.020

149. Wang J, Cazzato E, Ladewig E, Frattini V, Rosenbloom DI, Zairis S, et al. Clonal Evolution of Glioblastoma Under Therapy. *Nat Genet* (2016) 48 (7):768–76. doi: 10.1038/ng.3590

150. Kim H, Zheng S, Amini SS, Virk SM, Mikkelsen T, Brat DJ, et al. Whole-Genome and Multisector Exome Sequencing of Primary and Post-Treatment Glioblastoma Reveals Patterns of Tumor Evolution. *Genome Res* (2015) 25 (3):316–27. doi: 10.1101/gr.180612.114

151. Binder DC, Ladomersky E, Lenzen A, Zhai L, Lauing KL, Otto-Meyer SD, et al. Lessons Learned From Rindopepimut Treatment in Patients With EGFRvIII-Expressing Glioblastoma. *Transl Cancer Res* (2018) 7(Suppl 4): S510–S3. doi: 10.21037/tcr.2018.03.36

152. Weller M, Butowski N, Tran DD, Recht LD, Lim M, Hirte H, et al. Rindopepimut With Temozolomide for Patients With Newly Diagnosed, EGFRvIII-Expressing Glioblastoma (ACT IV): A Randomised, Double-Blind, International Phase 3 Trial. *Lancet Oncol* (2017) 18(10):1373–85. doi: 10.1016/S1470-2045(17)30517-X

153. Schiff D, Sarkaria J. Dasatinib in Recurrent Glioblastoma: Failure as a Teacher. *Neuro Oncol* (2015) 17(7):910–1. doi: 10.1093/neuonc/nov086

154. Lassman AB, Pugh SL, Gilbert MR, Aldape KD, Geinoz S, Beumer JH, et al. Phase 2 Trial of Dasatinib in Target-Selected Patients With Recurrent Glioblastoma (RTOG 0627). *Neuro Oncol* (2015) 17(7):992–8. doi: 10.1093/neuonc/nov011

155. Raymond E, Brandes AA, Dittrich C, Fumoleau P, Coudert B, Clement PM, et al. Phase II Study of Imatinib in Patients With Recurrent Gliomas of Various Histologies: A European Organisation for Research and Treatment of Cancer Brain Tumor Group Study. *J Clin Oncol* (2008) 26(28):4659–65. doi: 10.1200/JCO.2008.16.9235

156. Frolov A, Evans IM, Li N, Sidlauskas K, Paliashvili K, Lockwood N, et al. Imatinib and Nilotinib Increase Glioblastoma Cell Invasion *Via* Abl-Independent Stimulation of p130Cas and FAK Signalling. *Sci Rep* (2016) 6:27378. doi: 10.1038/srep27378

157. Capper D, von Deimling A, Brandes AA, Carpentier AF, Kesari S, Sepulveda-Sanchez JM, et al. Biomarker and Histopathology Evaluation of Patients With Recurrent Glioblastoma Treated With Galunisertib, Lomustine, or the Combination of Galunisertib and Lomustine. *Int J Mol Sci* (2017) 18(5):995. doi: 10.3390/ijms18050995

158. Brandes AA, Carpentier AF, Kesari S, Sepulveda-Sanchez JM, Wheeler HR, Chinot O, et al. A Phase II Randomized Study of Galunisertib Monotherapy or Galunisertib Plus Lomustine Compared With Lomustine Monotherapy in Patients With Recurrent Glioblastoma. *Neuro Oncol* (2016) 18(8):1146–56. doi: 10.1093/neuonc/now009

159. Kushnirsky M, Feun LG, Gultekin SH, de la Fuente MI. Prolonged Complete Response With Combined Dabrafenib and Trametinib After BRAF Inhibitor Failure in BRAF-Mutant Glioblastoma. *JCO Precis Oncol* (2020) 4: PO.19.00272. doi: 10.1200/PO.19.00272

160. Wen PY, Weller M, Lee EQ, Alexander BM, Barnholtz-Sloan JS, Barthel FP, et al. Glioblastoma in Adults: A Society for Neuro-Oncology (SNO) and European Society of Neuro-Oncology (EANO) Consensus Review on Current Management and Future Directions. *Neuro Oncol* (2020) 22 (8):1073–113. doi: 10.1093/neuonc/noaa106

161. Castro MG, Candolfi M, Wilson TJ, Calinescu A, Paran C, Kamran N, et al. Adenoviral Vector-Mediated Gene Therapy for Gliomas: Coming of Age. *Expert Opin Biol Ther* (2014) 14(9):1241–57. doi: 10.1517/14712598.2014. 915307

162. Garcia-Fabiani MB, Ventosa M, Comba A, Candolfi M, Nicola Candia AJ, Alghamri MS, et al. Immunotherapy for Gliomas: Shedding Light on Progress in Preclinical and Clinical Development. *Expert Opin Investig Drugs* (2020) 29(7):659–84. doi: 10.1080/13543784.2020.1768528

163. Bell JC, Ilkow CS. A Viro-Immunotherapy Triple Play for the Treatment of Glioblastoma. *Cancer Cell* (2017) 32(2):133–4. doi: 10.1016/j.ccell.2017. 07.012

164. Zhou W, Yao Y, Scott AJ, Wilder-Romans K, Dresser JJ, Werner CK, et al. Purine Metabolism Regulates DNA Repair and Therapy Resistance in Glioblastoma. *Nat Commun* (2020) 11(1):3811. doi: 10.1101/2020.03.26. 010140

165. Conde J, Pumroy RA, Baker C, Rodrigues T, Guerreiro A, Sousa BB, et al. Allosteric Antagonist Modulation of TRPV2 by Piperlongumine Impairs Glioblastoma Progression. *ACS Cent Sci* (2021) 7(5):868–81. doi: 10.1021/acscentsci.1c00070

166. Ghiaseddin A, Hoang Minh LB, Janiszewska M, Shin D, Wick W, Mitchell DA, et al. Adult Precision Medicine: Learning From the Past to Enhance the Future. *Neurooncol Adv* (2021) 3(1):vdaa145. doi: 10.1093/noajnl/vdaa145

167. Ippen FM, Colman H, van den Bent MJ, Brastianos PK. Precision Medicine for Primary Central Nervous System Tumors: Are We There Yet? *Am Soc Clin Oncol Educ Book* (2018) 38:158–67. doi: 10.1200/EDBK_199247

168. Prados MD, Byron SA, Tran NL, Phillips JJ, Molinaro AM, Ligon KL, et al. Toward Precision Medicine in Glioblastoma: The Promise and the Challenges. *Neuro Oncol* (2015) 17(8):1051–63. doi: 10.1093/neuonc/nov031

169. Hegi ME, Diserens AC, Gorlia T, Hamou MF, de Tribolet N, Weller M, et al. MGMT Gene Silencing and Benefit From Temozolomide in Glioblastoma. *N Engl J Med* (2005) 352(10):997–1003. doi: 10.1056/NEJMoa043331

170. Kaley T, Touat M, Subbiah V, Hollebecque A, Rodon J, Lockhart AC, et al. BRAF Inhibition in BRAF(V600)-Mutant Gliomas: Results From the VE-BASKET Study. *J Clin Oncol* (2018) 36(35):3477–84. doi: 10.1200/JCO.2018.78.9990

171. Molenaar RJ, Botman D, Smits MA, Hira VV, van Lith SA, Stap J, et al. Radioprotection of IDH1-Mutated Cancer Cells by the IDH1-Mutant Inhibitor AGI-5198. *Cancer Res* (2015) 75(22):4790–802. doi: 10.1158/0008-5472.CAN-14-3603

172. Gambella A, Senetta R, Collemi G, Vallero SG, Monticelli M, Cofano F, et al. NTRK Fusions in Central Nervous System Tumors: A Rare, But Worthy Target. *Int J Mol Sci* (2020) 21(3):753. doi: 10.3390/ijms21030753

173. Hashizume R, Andor N, Ihara Y, Lerner R, Gan H, Chen X, et al. Pharmacologic Inhibition of Histone Demethylation as a Therapy for Pediatric Brainstem Glioma. *Nat Med* (2014) 20(12):1394–6. doi: 10.1038/nm.3716

174. Jagtap P, Szabo C. Poly(ADP-Ribose) Polymerase and the Therapeutic Effects of its Inhibitors. *Nat Rev Drug Discov* (2005) 4(5):421–40. doi: 10.1038/nrd1718

175. Johannessen TC, Prestegarden L, Grudic A, Hegi ME, Tysnes BB, Bjerkvig R. The DNA Repair Protein ALKBH2 Mediates Temozolomide Resistance in Human Glioblastoma Cells. *Neuro Oncol* (2013) 15(3):269–78. doi: 10.1093/neuonc/nos301

176. Wang P, Wu J, Ma S, Zhang L, Yao J, Hoadley KA, et al. Oncometabolite D-2-Hydroxyglutarate Inhibits ALKBH DNA Repair Enzymes and Sensitizes IDH Mutant Cells to Alkylating Agents. *Cell Rep* (2015) 13(11):2353–61. doi: 10.1016/j.celrep.2015.11.029

177. Kolostova K, Pospisilova E, Pavlickova V, Bartos R, Sames M, Pawlak I, et al. Next Generation Sequencing of Glioblastoma Circulating Tumor Cells: Non-Invasive Solution for Disease Monitoring. *Am J Transl Res* (2021) 13 (5):4489–99.

178. Schnabel E, Knoll M, Schwager C, Warta R, Mock A, Campos B, et al. Prognostic Value of microRNA-221/2 and 17-92 Families in Primary Glioblastoma Patients Treated With Postoperative Radiotherapy. *Int J Mol Sci* (2021) 22(6):2960. doi: 10.3390/ijms22062960

179. Nikbakht H, Panditharatna E, Mikael LG, Li R, Gayden T, Osmond M, et al. Spatial and Temporal Homogeneity of Driver Mutations in Diffuse Intrinsic Pontine Glioma. *Nat Commun* (2016) 7:11185. doi: 10.1038/ncomms11185

180. Dincer C, Kaya T, Keskin O, Gursoy A, Tuncbag N. 3D Spatial Organization and Network-Guided Comparison of Mutation Profiles in Glioblastoma Reveals Similarities Across Patients. *PloS Comput Biol* (2019) 15(9): e1006789. doi: 10.1371/journal.pcbi.1006789

181. Ibrahim AN, Yamashita D, Anderson JC, Abdelrashid M, Alwakeal A, Estevez-Ordonez D, et al. Intratumoral Spatial Heterogeneity of BTK Kinomic Activity Dictates Distinct Therapeutic Response Within a Single Glioblastoma Tumor. *J Neurosurg* (2019) 18:1–12. doi: 10.3171/2019.7. JNS191376

182. Bastola S, Pavlyukov MS, Yamashita D, Ghosh S, Cho H, Kagaya N, et al. Glioma-Initiating Cells at Tumor Edge Gain Signals From Tumor Core Cells to Promote Their Malignancy. *Nat Commun* (2020) 11(1):4660. doi: 10.1038/s41467-020-18189-y

183. Spiteri I, Caravagna G, Cresswell GD, Vatsiou A, Nichol D, Acar A, et al. Evolutionary Dynamics of Residual Disease in Human Glioblastoma. *Ann Oncol* (2019) 30(3):456–63. doi: 10.1093/annonc/mdy506

184. Lee JH, Lee JE, Kahng JY, Kim SH, Park JS, Yoon SJ, et al. Human Glioblastoma Arises From Subventricular Zone Cells With Low-Level Driver Mutations. *Nature* (2018) 560(7717):243–7. doi: 10.1038/s41586-018-0389-3

185. Venkataramani V, Tanev DI, Strahle C, Studier-Fischer A, Fankhauser L, Kessler T, et al. Glutamatergic Synaptic Input to Glioma Cells Drives Brain Tumour Progression. *Nature* (2019) 573(7775):532–8. doi: 10.1038/s41586-019-1564-x

186. Zeng Q, Michael IP, Zhang P, Saghafinia S, Knott G, Jiao W, et al. Synaptic Proximity Enables NMDAR Signalling to Promote Brain Metastasis. *Nature* (2019) 573(7775):526–31. doi: 10.1038/s41586-019-1576-6

187. Iser IC, Lenz G, Wink MR. EMT-Like Process in Glioblastomas and Reactive Astrocytes. *Neurochem Int* (2019) 122:139–43. doi: 10.1016/j.neuint.2018.11.016

188. Castro BA, Flanigan P, Jahangiri A, Hoffman D, Chen W, Kuang R, et al. Macrophage Migration Inhibitory Factor Downregulation: A Novel Mechanism of Resistance to Anti-Angiogenic Therapy. *Oncogene* (2017) 36(26):3749–59. doi: 10.1038/onc.2017.1

189. Li C, Cho HJ, Yamashita D, Abdelrashid M, Chen Q, Bastola S, et al. Tumor Edge-to-Core Transition Promotes Malignancy in Primary-to-Recurrent Glioblastoma Progression in a PLAGL1/CD109-Mediated Mechanism. *Neurooncol Adv* (2020) 2(1):vdaa163. doi: 10.1093/noajnl/vdaa163

190. Pavlyukov MS, Yu H, Bastola S, Minata M, Shender VO, Lee Y, et al. Apoptotic Cell-Derived Extracellular Vesicles Promote Malignancy of Glioblastoma *Via* Intercellular Transfer of Splicing Factors. *Cancer Cell* (2018) 34(1):119–35.e10. doi: 10.1016/j.ccell.2018.05.012

191. Yamashita D, Bernstock JD, Elsayed G, Sadahiro H, Mohyeldin A, Chagoya G, et al. Targeting Glioma-Initiating Cells *via* the Tyrosine Metabolic Pathway. *J Neurosurg* (2020) 134(3):721–32. doi: 10.3171/2019.11.JNS192028.

ORIGINAL RESEARCH

# Germline BAP1 Mutation in a Family With Multi-Generational Meningioma With Rhabdoid Features: A Case Series and Literature Review

Rahul N. Prasad[1], Ulysses G. Gardner[2], Alexander Yaney[1], Daniel M. Prevedello[3], Daniel C. Koboldt[4], Diana L. Thomas[5], Elaine R. Mardis[4] and Joshua D. Palmer[1]*

[1] Department of Radiation Oncology, The Ohio State University Comprehensive Cancer Center-Arthur G. James Cancer Hospital and Richard J. Solove Research Institute, Columbus, OH, United States, [2] Boonshoft School of Medicine, Wright State University, Dayton, OH, United States, [3] Department of Neurosurgery, The Ohio State University Comprehensive Cancer Center-Arthur G. James Cancer Hospital and Richard J. Solove Research Institute, Columbus, OH, United States, [4] The Steve and Cindy Rasmussen Institute for Genomic Medicine, Nationwide Children's Hospital, Columbus, OH, United States, [5] Department of Pathology, The Ohio State University Comprehensive Cancer Center-Arthur G. James Cancer Hospital and Richard J. Solove Research Institute, Columbus, OH, United States

Meningioma is the most common primary brain tumor, and recurrence risk increases with increasing WHO Grade from I to III. Rhabdoid meningiomas are a subset of WHO Grade III tumors with rhabdoid cells, a high proliferation index, and other malignant features that follow an aggressive clinical course. Some meningiomas with rhabdoid features either only focally or without other malignant features are classified as lower grade yet still recur early. Recently, inactivating mutations in the tumor suppressor gene BAP1 have been associated with poorer prognosis in rhabdoid meningioma and meningioma with rhabdoid features, and germline mutations have been linked to a hereditary tumor predisposition syndrome (TPDS) predisposing patients primarily to melanoma and mesothelioma. We present the first report of a familial BAP1 inactivating mutation identified after multiple generations of a family presented with meningiomas with rhabdoid features instead of with previously described BAP1 loss-associated malignancies. A 24-year-old female presented with a Grade II meningioma with rhabdoid and papillary features treated with subtotal resection, adjuvant external beam radiation therapy, and salvage gamma knife radiosurgery six years later. Around that time, her mother presented with a meningioma with rhabdoid and papillary features managed with resection and adjuvant radiation therapy. Germline testing was positive for a pathogenic BAP1 mutation in both patients. Sequencing of both tumors demonstrated biallelic BAP1 inactivation via the combination of germline BAP1 mutation and either loss of heterozygosity or somatic mutation. No additional mutations implicated in oncogenesis

were noted from either patient's germline or tumor sequencing, suggesting that the inactivation of *BAP1* was responsible for pathogenesis. These cases demonstrate the importance of routine *BAP1* tumor testing in meningioma with rhabdoid features regardless of grade, germline testing for patients with *BAP1* inactivated tumors, and tailored cancer screening in this population.

## INTRODUCTION

Meningioma is the most common primary brain tumor, and recurrence risk increases with increasing WHO Grade from I to III (1). Rhabdoid meningiomas are a subset of WHO grade III tumors that predominantly consist of rhabdoid cells similar to other rhabdoid tumors (such as atypical teratoid rhabdoid tumor) and have a high proliferation index and other histologic features of malignancy (2, 3). These cases usually follow an aggressive clinical course, so traditional grading has excellent prognostic value. On the other hand, some meningiomas show rhabdoid features only focally and/or lack other features of malignancy (high mitotic rate, brain invasion, necrosis, macronucleoli, sheet-like growth, and hypercellularity). The WHO suggests these tumors be graded as usual with an added descriptor of "with rhaboid features". These cases are thought to be less aggressive but closer follow-up may be warranted as notably some behave aggressively (2, 3).

Recently, inactivating mutations in the tumor suppressor gene *BAP1* that codes for the breast cancer (BRCA)1-associated protein, an important member of many vital pathways including DNA damage signaling and repair (4), have been associated with significantly decreased time to recurrence in patients with rhabdoid meningioma and meningioma with rhabdoid features (5, 6). Patients with a familial germline mutation in *BAP1* display a hereditary tumor predisposition syndrome (TPDS) leading to early onset malignancy – most frequently melanoma, mesothelioma, and renal cell carcinoma (6–9). Prior retrospective analyses and case series have discovered familial *BAP1* TPDS after patients presented with these malignancies, and in some cases, close relatives were later found to have meningiomas. However, to our best knowledge, we present the first report of an inherited *BAP1* inactivating mutation identified after several generations of a family presented with meningioma with rhabdoid features instead of with previously documented *BAP1* loss-associated cancers (7–9). We review these patients' diagnoses, molecular profiling results, and management in the context of the literature to demonstrate the importance of *BAP1* tumor testing in meningioma with rhabdoid features regardless of grade, germline testing for patients with *BAP1* inactivated tumors, and tailored cancer screening in this population. Informed consent was obtained from both patients, and the institutional review board approved this study.

## CASE DESCRIPTION

A 24-year-old female (Patient A) presented with decreased left facial sensation, blurry vision, left-sided frontal headaches, and pain with mastication of 3 months' duration refractory to symptom-directed medical management. Physical exam revealed left masticator weakness, diminished sensation in the left V1-V3 distribution, and a decreased left-sided corneal reflex but was otherwise unremarkable. **Figures 1A–D** depicts a timeline for this patient presentation. Magnetic resonance imaging (MRI) of the brain with contrast revealed an infiltrating, contrast enhancing, roughly 5-cm mass centered in the left parasellar region with compression of the left temporal lobe, cavernous sinus, pons, and trigeminal nerve (**Figure 1A**). The patient underwent a left orbital frontal craniotomy with middle cranial fossa resection resulting in subtotal resection of the tumor. Pathologic evaluation revealed a meningothelial tumor composed of polygonal cells with mildly pleomorphic oval nuclei, abundant eosinophilic cytoplasm, and conspicuous cell borders. Many of the tumor cells showed eccentrically placed nuclei and round cytoplasmic inclusions of hypereosinophilic material consistent with rhabdoid morphology (**Figure 2A**). A significant component of papillary architecture was also present (**Figure 2B**). Mitoses were counted at 3 per 10 high power fields. The tumor cells showed diffuse immunoreactivity for EMA (**Figure 2C**) and vimentin (**Figure 2D**). There was complete loss of BAP-1 immunoreactivity in the tumor cells (**Figure 2E**) with appropriate internal positive controls (endothelial cells, inflammatory cells, etc.). The tumor cells showed focal staining for cytokeratin AE1/AE3. GFAP, S100, desmin, Melan-A, and HMB45 were negative. The Ki-67 proliferation index was 15%. Ultrastructural studies (electron microscopy) confirmed the presence of cytoplasmic whorls of intermediate filaments in many of the tumor cells (**Figure 2F**). Despite the rhabdoid and papillary features, in the absence of other malignant features (increased mitoses, necrosis, brain invasion, etc.), a diagnosis of atypical meningioma, WHO grade II, was ultimately made. Postoperative MRI brain demonstrated significant surgical decompression with residual enhancement along the left petroclinoid ligament and region of the cavernous sinus (**Figure 1B**).

Because of the subtotal resection of Grade II disease, adjuvant radiation therapy was recommended to 5940 cGy in 33 daily fractions. The patient was simulated in the supine position with an aquaplast mask for head and neck immobilization. To delineate treatment volumes, preoperative and postoperative
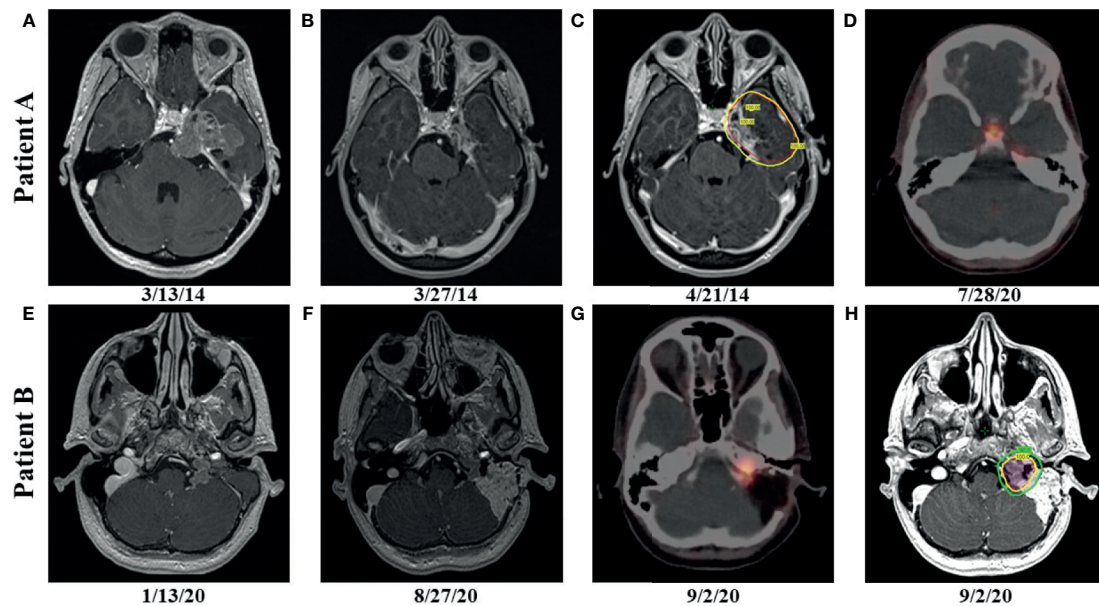
**FIGURE 1** | Patient A: preoperative, axial T1 postcontrast weighted magnetic resonance (MRI) imaging showing enhancing disease **(A)**; postoperative, axial T1 postcontrast weighted MRI imaging showing enhancing, residual disease **(B)**; radiation therapy (RT) planning using volumetric arc therapy (VMAT) resulted in excellent coverage of the planning target volume (PTV) (red) by the 100% isodose line (yellow) corresponding to 5940 cGy **(C)**; follow up gallium-68 dotatate positron emission tomography (PET) after more than 6 years showing hypermetabolic, recurrent disease in the left tentorial leaflet and physiologic uptake in the pituitary **(D)**; Patient B: preoperative, axial T1 postcontrast weighted MRI imaging showing enhancing disease **(E)**; postoperative, axial T1 postcontrast weighted MRI imaging showing enhancing, residual disease **(F)**; postoperative PET showing hypermetabolic, residual disease **(G)**; RT planning using VMAT resulted in excellent coverage of the 6000 cGy (red) and 5400 cGy (blue) PTVs by the 100% (yellow) and 90% (green) isodose lines, respectively **(H)**.

T1-weighted axial postcontrast MRI imaging was fused to the computed tomography (CT) simulation scan. A preoperative gross tumor volume (GTV) was created to ensure that the clinical target volume (CTV) consisting of the residual contrast enhancing disease and postoperative bed appropriately covered the extent of the macroscopic and potential microscopic disease. An anisotropic expansion of 0-8 mm from the CTV was used to create a planning target volume (PTV) accounting for daily setup uncertainty while respecting dose constraints to the optic structures and brainstem (max dose less than or equal to 5400 cGy) (**Figure 1C**). Treatment was delivered using volumetric modulated arc therapy (VMAT) with 4 six MV arcs. RT was well tolerated with no significant adverse effects. The patient did well initially, but noted increasing headaches of several months duration over 6 years after resection. MRI brain with contrast showed increased nodular enhancement along the anterior margin of the left tentorial leaflet correlating with increased uptake on gallium-68 dotatate positron emission tomography (PET) imaging (**Figure 1D**). She underwent gamma knife radiosurgery to the recurrent disease to 22 Gy prescribed to the 50% isodose line.

Around the same time, the 57-yo mother (Patient B) of Patient A presented with a 1-year history of left-sided, progressive hearing loss and pulsatile tinnitus refractory to symptom-directed medical management. On physical exam, she displayed left-sided conducting hearing loss without other

abnormalities. **Figures 1E–H** depicts a timeline for this patient presentation. MRI Brain with contrast revealed a roughly 2.6 cm, enhancing left skull base mass involving the cerebellar-medullary angle cistern and centered around the jugular fossa with a tympanic component protruding into the middle ear cavity (**Figure 1E**). A left middle ear biopsy was consistent with meningioma with positive staining for EMA. She underwent a left tympanoplasty mastoidectomy resulting in subtotal resection of the tumor. Pathologic evaluation confirmed a meningioma with nearly identical appearance to the tumor of Patient A. Rhabdoid features were noted including eccentrically placed nuclei and abundant eosinophilic cytoplasm (**Figure 3A**). Papillary architecture with epithelioid cells arranged in perivascular papillae was also noted (**Figure 3B**). Mitoses were very rare (less than 1 per 10 high power fields). In support of the diagnosis, the tumor cells were immunoreactive for EMA (**Figure 3C**), vimentin (**Figure 3D**), and progesterone receptor (patchy; **Figure 3E**). The tumor cells showed diffuse loss of immunoreactivity for BAP-1 (**Figure 3F**). The tumor cells were also focally positive for S100, calponin, AE1/3, MNF116, CAM 5.2, CD138, SMA, and desmin. SHDHB, CD138, CD99, Melan-A, HMB-45, synaptophysin, and nuclear STAT6 were negative. Interestingly, SSTR2 immunostain was negative despite previous reports describing expression in most meningiomas including Grade II and III meningiomas (10, 11). The Ki-67 proliferation index was 10%. The tumor displayed infrequent mitoses (1 per
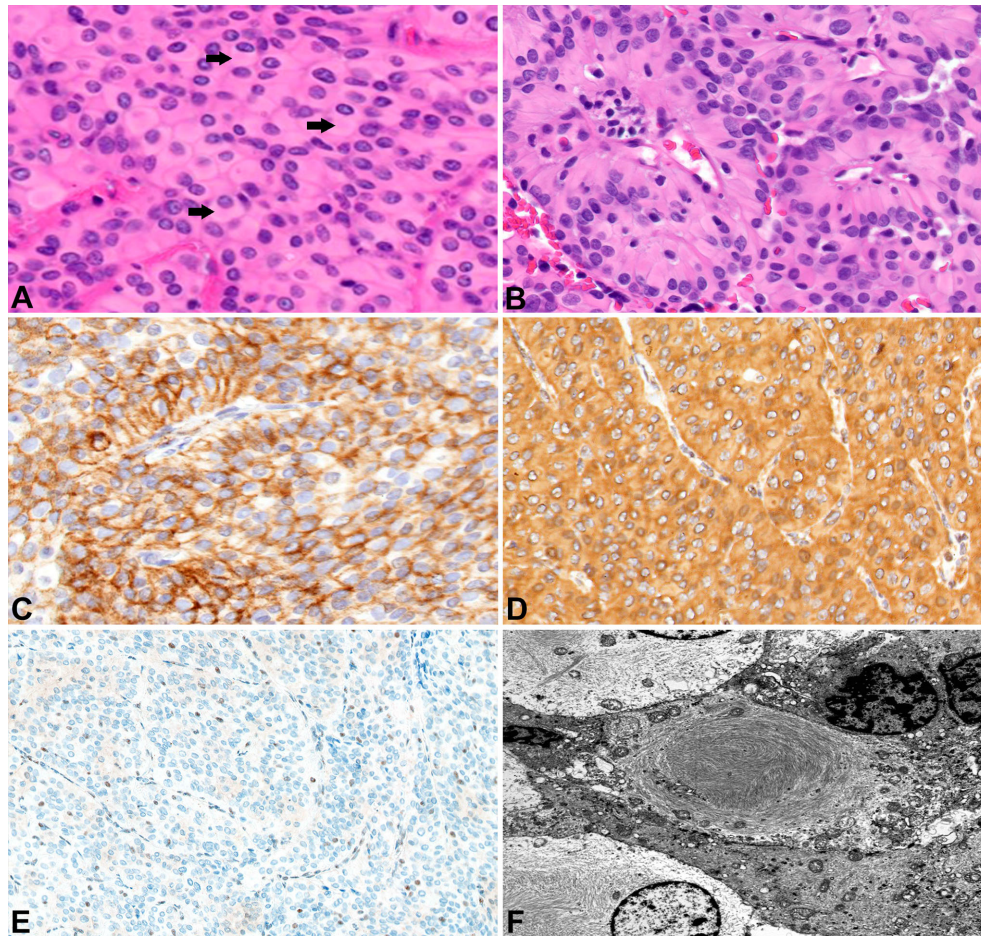
**FIGURE 2** | Surgical pathology for Patient A H&E stained sections show numerous rhabdoid tumor cells with cytoplasmic hypereosinophilic inclusions (arrows) (400x) **(A)**. Papillary features are also readily apparent (200x) **(B)**. EMA highlights the tumor cells (200x) **(C)**. The tumors cells label for vimentin (200x) **(D)**. There is loss of BAP-1 immunoreactivity in the tumor cells with appropriate internal positive controls (endothelial cells) (100x) **(E)**. Ultrastructural studies revealed cytoplasmic whorls of intermediate filaments **(F)**.

10 per HPF) and otherwise lacked anaplastic features. Postoperative MRI revealed residual tumor projecting into the cerebellomedullary angle, extending into the cerebellomedullary cistern and left jugular foramen, and tracking along the carotid sheath (**Figure 1F**) with corresponding increased uptake on gallium-68 dotatate PET (**Figure 1G**).

Because of the rhabdoid features potentially portending higher risk of recurrence, adjuvant radiation therapy to 6000 cGy in 30 fractions was recommended after the subtotal resection. The patient was simulated in the supine position with an aquaplast mask for head and neck immobilization. The postoperative PET as well as T1-weighted axial postcontrast and T2 flair MRI sequences were fused to the CT simulation scan and used to delineate a GTV encompassing the residual tumor. The GTV was expanded 0.3 cm to create a CTV and another 0.3 cm to create a PTV that was prescribed 5400 cGy in 30 fractions. A higher dose PTV receiving 6000 cGy in 30 fractions *via* a simultaneous integrated boost was created using a 0.2 cm expansion from the GTV that was then cropped off the left cranial nerves VII and VIII. The brainstem was constrained to a max dose of less than 5400 cGy, and the left cochlea and fifth, seventh, and eighth cranial nerves were to receive a mean dose of less than 5000 cGy. Treatment was delivered *via* VMAT with 3 six MV arcs (**Figure 1H**) and was well tolerated with no significant adverse events.

Due to the strong family history of meningioma with rhabdoid features and patient age at presentation, germline genetic testing was recommended. The daughter tested positive for a pathogenic *BAP1* variant (NM_004656.4:c.1777C>T, (p.Gln593*) with no other cancer susceptibility loci found mutated (CancerNext-Expanded, Ambry Genetics) (12, 13). Her mother subsequently tested positive for the same germline mutation. The c.1777C>T variant maps to exon 14 of *BAP1* and is predicted to introduce a nonsense change at amino acid 593. It has been reported as pathogenic by multiple clinical laboratories (ClinVar ID: 422219). The premature termination resulting from
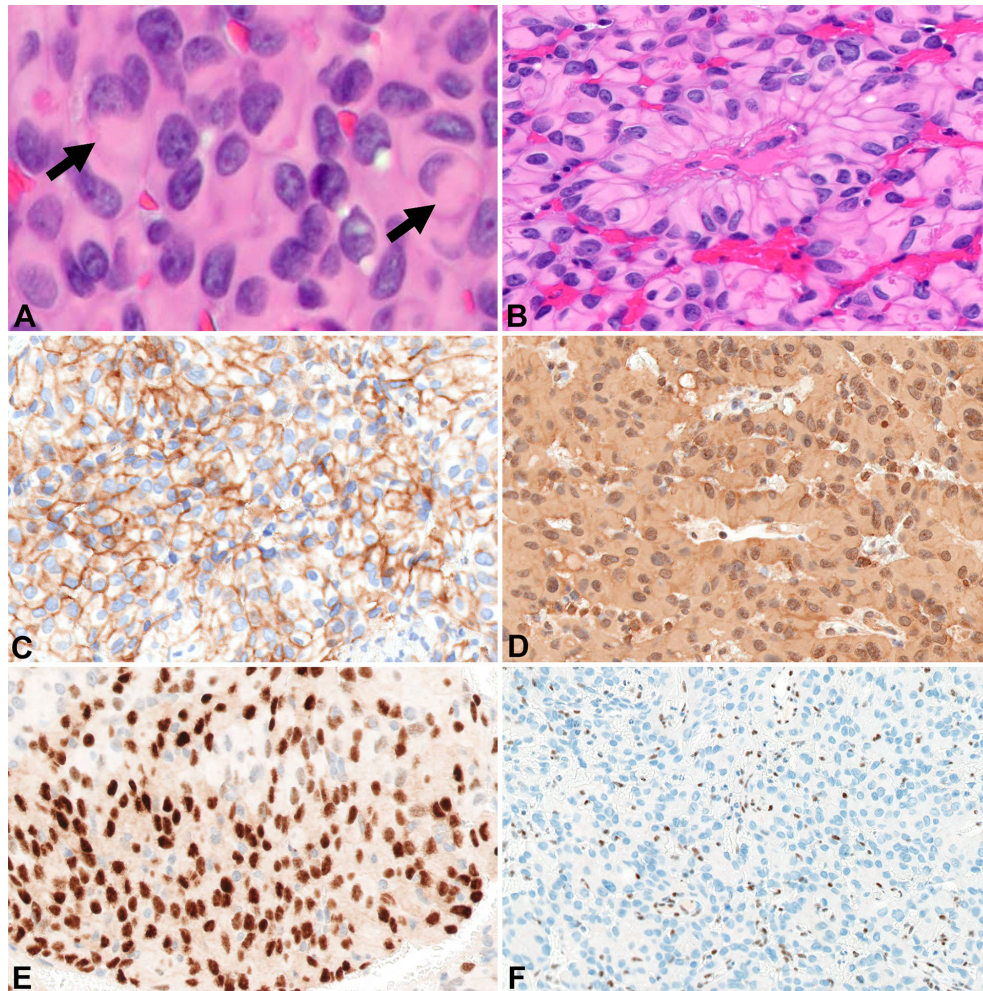
**FIGURE 3** | Surgical pathology for Patient B H&E stained sections show areas of rhabdoid tumor cells with cytoplasmic hypereosinophilic inclusions (arrows) (400x) **(A)**. Papillary arrangement of tumor cells (200x) **(B)**. EMA highlights the tumor cells (200x) **(C)**. Tumor cells are diffusely positive for vimentin (200x) **(D)**. Focal immunoreactivity for progesterone receptor in the tumor cells (200x) **(E)**. Diffuse loss of BAP-1 immunoreactivity in the tumor cells with appropriate internal controls (100x) **(F)**.

this variant would remove the BRCA1-binding domain (residues 594-657) (14). A previous study of a family with autosomal dominant, early-onset melanocytic neoplasms demonstrated that tumors which are biallelic for this variant show no BAP1 protein expression by immunohistochemistry. These findings suggest a loss-of-function effect mediated by nonsense-mediated mRNA decay (15).

We submitted our interpretation of the variant to the ClinVar database [Accession: SCV001748998.1 (Submitted: Jul 09, 2021)]. A family history of kidney cancer at age of 52 in Patient B's sister was discovered as well as lung cancer in patient B's father (**Supplementary Figure 1**). No family history of malignancy was noted on Patient A's father's side of the family. We performed exome capture (IDT xGen Exome Research Panel v2.0 enhanced with the xGenCNV Backbone Panel and Cancer spike-in) and sequencing (NovaSeq6000) on tumor DNA and matched peripheral blood mononuclear cells from both mother and daughter (**Supplementary Document 1**). Analyses of these data supported the previous finding of germline *BAP1* (p.Gln593*) mutation in both tumors. The second inactivating somatic mutation in *BAP1* in Patient A's tumor occurred through an 11-base pair frameshift mutation NM_004656.4:c.1092_1102del (p.His364GlnfsTer30) consistent with a loss of function *BAP1* variant (**Figures 4A, B**). By contrast, Patient B's tumor exhibited LOH across the entirety of chromosome 3 including the second *BAP1* allele (**Figures 4C, D**). Patient A's tumor had an additional 3 somatic coding mutations, and Patient B's displayed an additional 18 somatic coding mutations (**Supplementary Table 1**). However, none of these mutations occurred in known cancer genes or in genes associated with meningioma (12) besides a missense somatic mutation in PIK3CA in the tumor of patient B. Mutations in PIK3CA have
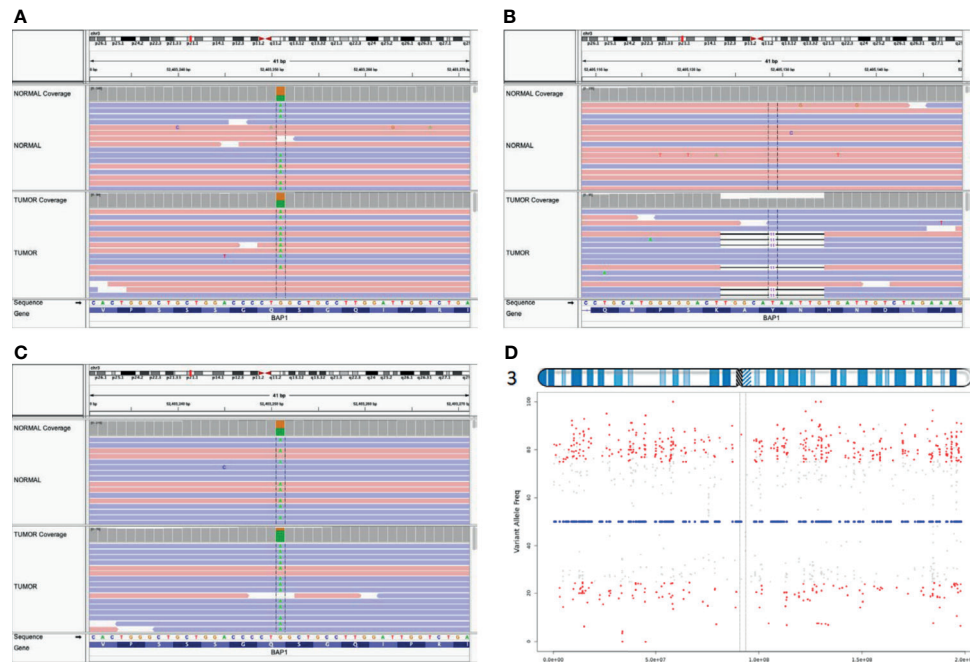
**FIGURE 4** | Biallelic inactivation of BAP1 by differing mechanisms. Aligned sequence data from Patient A show the pathogenic BAP1 variant is heterozygous in the germline (top track) and tumor (bottom track) **(A)**; the second hit is a somatic frameshift mutation **(B)**. In contrast, aligned sequence data from Patient B **(C)** show the germline variant approaching homozygosity in the tumor **(D)**. VarScan tumor allele frequency plot for heterozygous germline variants on chromosome 3 of Patient B indicates chromosome-level LOH across chromosome 3.

been previously associated with meningioma (16–18). This raises the possibility for genetic cooperation with BAP1-driven pathogenicity in tumor B, but this particular mutation has not been previously noted to be pathogenic.

At present, more than 7 years post- resection, Patient A has no clinical or radiographic evidence of newly recurrent or progressive disease. Nine months post-resection, Patient B displays no clinical or radiographic evidence of disease.

## DISCUSSION

We have highlighted the first account of a familial *BAP1* inactivating mutation identified after multiple generations of a family presented with meningioma with rhabdoid features instead of presenting with previously described malignancies (4, 7–9, 19). *BAP1* codes for the (BRCA)1-associated protein which is integral to many cellular pathways including DNA damage signaling and repair, and inactivating mutations of this tumor suppressor gene are oncogenic (4). Patients with germline mutations display a TPDS phenotype leading to early onset malignancy, most frequently melanoma, mesothelioma, and renal cell carcinoma (4, 6–9, 19). Prior case series have documented inherited germline mutations after patients presented with these cancers (7–9). One report identified a germline *BAP1* truncating mutation, c.799 C>T (p.Gln267*),

in a patient presenting with uveal melanoma leading to biallelic inactivation of *BAP1* with associated loss of function in this patient's tumor as well as in a lung adenocarcinoma and meningioma in 2 additional relatives (7). Another case series highlighted a family presenting with multiple mesotheliomas and melanocytic tumors found to have an inherited germline *BAP1* mutation (c.1948T>A (p.Tyr646*); two of the family members developed meningiomas in addition to their mesotheliomas (8). A larger series documented several families presenting with melanoma and mesothelioma secondary to an inherited *BAP1* (p.Asp404*) germline truncating mutation, and one case of papillary meningioma was identified by autopsy (9). These authors incidentally noted several cases of meningioma in patients with germline *BAP1* mutations, but our case series is unique in identifying the presence of a familial *BAP1* mutation directly through patient presentation with meningioma with rhabdoid features rather than mesothelioma, uveal melanoma, or cutaneous malignancy. One case of pediatric rhabdoid meningioma in a patient found to have a germline *BAP1* mutation has been previously reported, but the mutation may have been sporadic as no cancers were reported in the patient's siblings or parents' generation, genetic testing was not conducted for any family members, and no other meningiomas were identified in this family (20).

A detailed family history was unremarkable for cancer other than rapidly fatal cases of kidney cancer in Patient B's sister at

the age of 52 and lung cancer in Patient B's father at age 59. Patient B's father had no known risk factors associated with lung cancer. Given the relatively young age at which these fatal cancers were diagnosed, it is plausible that one or both of these deceased family members carried an undiagnosed germline *BAP1* mutation. Regardless, our case series provide further support for the need for referral for genetic testing for patients presenting with *BAP1* mutated rhabdoid meningioma. A recent genetic analysis and literature review suggested germline testing for patients with 2 more or *BAP1* TPDS associated tumors, a single tumor with unusually young age at presentation, or a family history (21). Due to the rarity of this condition, prospective experience is not available to guide screening guidelines for patients with a germline mutation. However, referral for annual dermatologic and ophthalmological screening should be considered due to retrospective data showing a high risk of uveal and cutaneous melanoma (6, 21). Even young family members should consider genetic testing as uveal and ocular melanomas may present as early as in the teenage years (6, 21). Screening renal ultrasound, MRI, or urinalysis for renal cell carcinoma could also be considered (21), as these patients are prone to renal cell carcinoma and *BAP1* mutated renal tumors appear to grow at a faster rate than kidney cancers driven by other mutations such as in von Hippel-Lindau disease (19).

Recently, inactivating *BAP1* mutations have been linked to significantly reduced time to recurrence in both Grade III rhabdoid and lower grade meningioma with rhabdoid features (26 months *versus* 116 months, $p < 0.001$, hazard ratio 12.89) (5, 6). Characteristic features of a Grade III rhabdoid meningioma include rhabdoid components in combination with malignant features such as high mitotic rate, brain invasion, necrosis, macronucleoli, sheet-like growth, or hypercellularity. These grade III meningiomas tend to behave with an aggressiveness consistent with their high grade. In contrast, outcomes for lower grade meningiomas with rhabdoid features are mixed (2, 3). Tumors receive this designation if either rhabdoid components are only focal or the previously noted aggressive features are lacking. Although some of these lower grade tumors are less aggressive (2, 3), an analysis by Shankar et al. noted that a subset with BAP1 inactivation recurred far earlier (5, 6). Despite not meeting the full criteria for Grade III rhabdoid meningioma, both patients' meningioma with rhabdoid features in our study displayed biallelic *BAP1* inactivation *via* an inherited germline *BAP1* (p.Gln593*) mutation and biallelic inactivation by different somatic mechanisms. Neither tumor contained mutations in additional genes associated with meningioma (such as *NF2* and *AKT1*) (6) or malignancy, strongly implicating *BAP1* inactivation in disease pathogenesis. Patient A had a relatively aggressive disease course consistent with previously reported experiences in rhabdoid meningioma. Her *BAP1* mutated meningioma recurred after roughly 6 years, or well before the median time to recurrence expected for a *BAP1* wild type rhabdoid meningioma as reported by Shankar et al. (5). Although Patient B has no evidence of recurrence 9 months after resection, further follow up is needed. Meningiomas with

rhabdoid histopathologic features appear to encompass a diverse genetic spectrum, and *BAP1* function may be just as important, if not more so, than morphology. At this time, *BAP1* inactivation is not routinely tested for in rhabdoid meningioma let alone meningioma with rhabdoid features (6). Thus, neither patient was screened for malignancies at the time of diagnosis with meningioma. Fortunately, neither patient has yet developed a cancer despite an 85-100% lifetime risk (6, 21). However, upfront tumor testing for *BAP1* inactivation may have aided with prognostication and introduction of timely screening for melanoma and other malignancy.

Besides the relatively limited follow up for Patient B, additional limitations of this case series include that germline genetic testing for asymptomatic family members was not available, and surgical pathology was not accessible to pursue tumor sequencing for family members previously deceased secondary to malignancy. Regardless, we present the first report of a familial *BAP1* inactivation TPDS identified after multiple generations of a family presented with meningioma with rhabdoid features instead of presenting with malignancies. Inactivating *BAP1* mutations have been associated with inferior outcomes in rhabdoid meningioma and meningioma with rhabdoid features, and routine tumor testing for this mutation may aid prognostication in lower grade tumors with rhabdoid features. Because germline mutations produce a TPDS, genetic testing should be offered to patients found to have *BAP1* inactivated tumors. Despite a lack prospective evidence to inform guidelines for screening for malignancy in this population, surveillance for ocular and cutaneous melanoma for patients carrying this germline mutation should be considered based upon elevated rates of disease in retrospective series. Given the paucity of available data to guide management of this rare condition, additional work is needed to determine the optimal diagnostic and management strategy for *BAP1* mutated meningioma with rhabdoid features and develop consensus guidelines for screening patients with inactivating germline mutations for malignancy.

## DATA AVAILABILITY STATEMENT

The original contributions presented in the study are included in the article/**Supplementary Material**. Further inquiries can be directed to the corresponding author.

## ETHICS STATEMENT

The studies involving human participants were reviewed and approved by Except, patient written consent obtained. The patients/participants provided their written informed consent to participate in this study.

## AUTHOR CONTRIBUTIONS

## ACKNOWLEDGMENTS

## SUPPLEMENTARY MATERIAL

## REFERENCES

1. Louis DN, Perry A, Reifenberger G, von Deimling A, Figarella-Branger D, Cavenee WK, et al. The 2016 World Health Organization Classification of Tumors of the Central Nervous System: A Summary. *Acta Neuropathol* (2016) 131(6):803–20. doi: 10.1007/s00401-016-1545-1

2. Vaubel RA, Chen SG, Raleigh DR, Link MJ, Chicoine MR, Barani I, et al. Meningiomas With Rhabdoid Features Lacking Other Histologic Features of Malignancy: A Study of 44 Cases and Review of the Literature. *J Neuropathol Exp Neurol* (2016) 75(1):44–52. doi: 10.1093/jnen/nlv006

3. Wu Y-T, Ho J-T, Lin Y-J, Lin J-W. Rhabdoid Papillary Meningioma: A Clinicopathologic Case Series Study. *Neuropathology* (2011) 31(6):599–605. doi: 10.1111/j.1440-1789.2011.01201.x

4. Carbone M, Harbour JW, Brugarolas J, Bononi A, Pagano I, Dey A, et al. Biological Mechanisms and Clinical Significance of BAP1 Mutations in Human Cancer. *Cancer Discovery* (2020) 10(8):1103–20. doi: 10.1158/2159-8290.CD-19-1220

5. Shankar GM, Abedalthagafi M, Vaubel RA, Merrill PH, Nayyar N, Gill CM, et al. Germline and Somatic BAP1 Mutations in High-Grade Rhabdoid Meningiomas. *Neuro Oncol* (2017) 19(4):535–45. doi: 10.1093/neuonc/now235

6. Shankar GM, Santagata S. BAP1 Mutations in High-Grade Meningioma: Implications for Patient Care. *Neuro Oncol* (2017) 19(11):1447–56. doi: 10.1093/neuonc/nox094

7. Abdel-Rahman MH, Pilarski R, Cebulla CM, Massengill JB, Christopher BN, Boru G, et al. Germline BAP1 Mutation Predisposes to Uveal Melanoma, Lung Adenocarcinoma, Meningioma, and Other Cancers. *J Med Genet* (2011) 48(12):856–9. doi: 10.1136/jmedgenet-2011-100156

8. Cheung M, Kadariya Y, Talarchek J, Pei J, Ohar JA, Kayaleh OR, et al. Germline BAP1 Mutation in a Family With High Incidence of Multiple Primary Cancers and a Potential Gene–Environment Interaction. *Cancer Letters* (2015) 369(2):261–5. doi: 10.1016/j.canlet.2015.09.011

9. Wadt K a W, Aoude LG, Johansson P, Solinas A, Pritchard A, Crainic O, et al. A Recurrent Germline BAP1 Mutation and Extension of the BAP1 Tumor Predisposition Spectrum to Include Basal Cell Carcinoma. *Clin Genet* (2015) 88(3):267–72. doi: 10.1111/cge.12501

10. Barresi V, Alafaci C, Salpietro F, Tuccari G. Sstr2A Immunohistochemical Expression in Human Meningiomas: Is There a Correlation With the Histological Grade, Proliferation or Microvessel Density? *Oncol Rep* (2008) 20(3):485–92. doi: 10.3892/or_00000032

11. Silva CB de O, Ongaratti BR, Trott G, Haag T, Ferreira NP, Leães CGS, et al. Expression of Somatostatin Receptors (SSTR1-SSTR5) in Meningiomas and its Clinicopathological Significance. *Int J Clin Exp Pathol* (2015) 8 (10):13185–92.

12. Fountain DM, Smith MJ, O'Leary C, Pathmanaban ON, Roncaroli F, Bobola N, et al. The Spatial Phenotype of Genotypically Distinct Meningiomas Demonstrate Potential Implications of the Embryology of the Meninges. *Oncogene* (2021) 40(5):875–84. doi: 10.1038/s41388-020-01568-6

13. Kukuyan A-M, Sementino E, Kadariya Y, Menges CW, Cheung M, Tan Y, et al. Inactivation of Bap1 Cooperates With Losses of Nf2 and Cdkn2a to Drive the Development of Pleural Malignant Mesothelioma in Conditional Mouse Models. *Cancer Res* (2019) 79(16):4113–23. doi: 10.1158/0008-5472.CAN-18-4093

14. Haugh AM, Njauw C-N, Bubley JA, Verzì AE, Zhang B, Kudalkar E, et al. Genotypic and Phenotypic Features of BAP1 Cancer Syndrome: A Report of 8 New Families and Review of Cases in the Literature. *JAMA Dermatol* (2017) 153(10):999–1006. doi: 10.1001/jamadermatol.2017.2330

15. McDonnell KJ, Gallanis GT, Heller KA, Melas M, Idos GE, Culver JO, et al. A Novel BAP1 Mutation is Associated With Melanocytic Neoplasms and Thyroid Cancer. *Cancer Genet* (2016) 209(3):75–81. doi: 10.1016/j.cancergen.2015.12.007

16. Abedalthagafi M, Bi WL, Aizer AA, Merrill PH, Brewster R, Agarwalla PK, et al. Oncogenic PI3K Mutations are as Common as AKT1 and SMO Mutations in Meningioma. *Neuro Oncol* (2016) 18(5):649–55. doi: 10.1093/neuonc/nov316

17. Pang JC, Chung NYF, Chan NHL, Poon WS, Thomas T, Ng H. Rare Mutation of PIK3CA in Meningiomas. *Acta Neuropathol* (2006) 111(3):284–5. doi: 10.1007/s00401-005-0021-0

18. Zadeh G, Karimi S, Aldape KD. PIK3CA Mutations in Meningioma. *Neuro Oncol* (2016) 18(5):603–4. doi: 10.1093/neuonc/now029

19. Ball MW, An JY, Gomella PT, Gautam R, Ricketts CJ, Vocke CD, et al. Growth Rates of Genetically Defined Renal Tumors: Implications for Active Surveillance and Intervention. *JCO* (2020) 38(11):1146–53. doi: 10.1200/JCO.19.02263

20. Ravanpay AC, Barkley A, White-Dzuro GA, Cimino PJ, Gonzalez-Cuyar LF, Lockwood C, et al. Giant Pediatric Rhabdoid Meningioma Associated With a Germline BAP1 Pathogenic Variation: A Rare Clinical Case. *World Neurosurgery* (2018) 119:402–15. doi: 10.1016/j.wneu.2018.06.227

21. Chau C, van Doorn R, van Poppelen NM, van der Stoep N, Mensenkamp AR, Sijmons RH, et al. Families With BAP1-Tumor Predisposition Syndrome in the Netherlands: Path to Identification and a Proposal for Genetic Screening Guidelines. *Cancers (Basel)* (2019) 11(8):1114. doi: 10.3390/cancers11081114

# The Prognostic Value of CD133 in Predicting the Relapse and Recurrence Pattern of High-Grade Gliomas on MRI: A Meta-Analysis

*Mahdi Abdoli Shadbad [1,2], Negar Hosseinkhani [2], Zahra Asadzadeh [2], Oronzo Brunetti [3], Nicola Silvestris [3,4*†] and Behzad Baradaran [2,5,6*†]*

[1] Student Research Committee, Tabriz University of Medical Sciences, Tabriz, Iran, [2] Immunology Research Center, Tabriz University of Medical Sciences, Tabriz, Iran, [3] Medical Oncology Unit, IRCCS IstitutoTumori "Giovanni Paolo II" of Bari, Bari, Italy, [4] Department of Biomedical Sciences and Human Oncology, University of Bari "Aldo Moro", Bari, Italy, [5] Department of Immunology, Tabriz University of Medical Sciences, Tabriz, Iran, [6] Pharmaceutical Analysis Research Center, Tabriz University of Medical Sciences, Tabriz, Iran

**Background:** Cancer stem cells have been implicated in tumor relapse, tumor invasion, and cancer therapy resistance in high-grade gliomas; thus, characterizing cancer stem cell-related markers can help determine the prognosis of affected patients. Preclinical studies have reported that CD133 is implicated in tumor recurrence and cancer therapy resistance in high-grade gliomas; however, clinical studies have reported inconclusive results regarding its prognostic value in patients with high-grade gliomas.

**Methods:** We systematically searched the PubMed, Scopus, Web of Science, and Embase databases to obtain peer-reviewed studies published before March 10, 2021. Then, we conducted the current systematic review and meta-analysis based on the preferred reporting items for systematic reviews and meta-analyses (PRISMA) statements. By applying the random-effect model, the effect size of studies investigating the progression-free survival (PFS), time to local recurrence (TTL), and time to distant recurrence (TTD) were calculated using RevMan version 5.4. The heterogeneity between the included studies was studied by the $I^2$ index and Cochran's Q test. Egger test was performed on funnel plots to investigate the potential asymmetry and publication bias among the included studies using CMA version 2.

**Results:** With the 10% cut-off, CD133 protein overexpression is associated with the inferior PFS of patients with high-grade gliomas. Increased CD133 protein expression is associated with sooner distant tumor recurrence on MRI in glioblastoma patients and patients with high-grade gliomas and improved TTL on MRI in glioblastoma patients.

**Conclusion:** Based on the current evidence from 1086 patients with high-grade gliomas, CD133 overexpression is a valuable marker to predict tumor relapse and tumor recurrence patterns in patients with high-grade gliomas.

**Keywords:** CD133, high-grade gliomas, high-grade gliomas relapse, high-grade gliomas recurrence pattern, progression-free survival, time to local recurrence, time to distant recurrence, magnetic resonance imaging

## INTRODUCTION

Gliomas are among the frequently diagnosed primary brain tumors; however, the prognosis of affected patients is not favorable. Indeed, tumor recurrence and cancer therapy resistance have posed daunting challenges for patients with high-grade gliomas (1). Therefore, a better understanding of the biology of high-grade gliomas might pave the way for introducing novel biomarkers that can predict the prognosis of affected patients.

Cancer stem cells are a small population of tumor bulk that has been introduced as the main culprit of tumor relapse. The stemness and self-renewal features of these tumoral cells can give rise to a malignant tumor after the initial therapy. Besides tumor development, cancer stem cells can facilitate tumor migration (2–4). These tumor-initiating cells have also been implicated in chemoresistance. Indeed, the overexpression of aldehyde dehydrogenase-I, stimulated DNA repair mechanisms, reduced chemotherapeutic agents influx, and increased their efflux are among the proposed mechanisms for cancer stem cells-mediated chemoresistance in high-grade gliomas (5). It has been reported that these cells can stimulate the Wnt/β-catenin pathway, leading to stemness, increased invasion, and proliferation in high-grade gliomas (6, 7). Wickström et al. have indicated that the stimulation of the Wnt/β-catenin pathway is highly associated with temozolomide resistance in glioblastoma *via* activating MGMT (8).

Preclinical findings have indicated that CD133 is overexpressed in cancer stem cells of high-grade gliomas. It has been shown that CD133 can activate the Wnt/β-catenin pathway, maintaining the cancer stem cell population in glioblastoma. Indeed, the expression level of Wnt/β-catenin-related signals in CD133-positive cancer stem cells has been substantially increased compared to differentiated CD133-negative glioblastoma cells (9). Growing evidence indicates that CD133 can increase proliferation, induce cancer therapy resistance, and maintain stemness in glioblastoma (10–13). Despite the critical roles of CD133 in tumor development, there is a controversy about the prognostic value of CD133 in predicting tumor relapse and its recurrence pattern in high-grade gliomas (14–17).

Herein, the current study aims to determine the prognostic value of CD133 in predicting tumor relapse and tumor recurrence patterns in patients with high-grade gliomas. The results of this current study can be translated into clinical practice to predict tumor recurrence and its patterns in patients with high-grade gliomas.

## METHODS

This study was performed according to the PRISMA statements (18).

### Search Strategy

The PubMed, Scopus, Web of Science, and Embase databases were systematically searched to obtain peer-reviewed records published before March 10, 2021, with the following keywords: ("CD133" OR "prominin-1" OR "AC133" OR "AC133 antigen" OR "PROML1" OR "AC133 antigen" OR "prominin-like protein 1" OR "CORD12" OR "RP41" OR "MSTP061" OR "MCDR2" OR "STGD4" OR "prominin 1" OR "prominin (mouse)-like 1" OR "HProminin" OR "PROM1" OR "antigen AC133" OR "CD133 antigen") and ("glioblastoma" OR "glioblastoma multiforme" OR "high-grade glioma" OR "high grade glioma" OR "anaplastic" OR "anaplastic astrocytoma" OR "astrocytoma" OR "grade III glioma" OR "grade IV glioma") and ("local recurrence" OR "distant recurrence" OR "local relapse" OR "distant relapse" OR "local recurrent" OR "distant recurrent" OR "local-recurrence" OR "distant-recurrence" OR "local-relapse" OR "distant-relapse" OR "local-recurrent" OR "distant-recurrent" OR "LRFS" OR "local recurrence-free survival" OR "distant recurrence-free survival" OR "DRFS" OR "local recurrence free survival" OR "distant recurrence free survival" OR "local-recurrence-free survival" OR "distant-recurrence-free survival" OR "DRFS" OR "local-recurrence free survival" OR "distant-recurrence free survival" OR "relapse-free survival" OR "recurrence-free survival" OR "relapse free survival" OR "recurrence free survival" OR "RFS" OR "local relapse-free survival" OR "local relapse free survival" OR "local-relapse-free survival" OR "local-relapse free survival" OR "distant relapse free survival" OR "distant relapse-free survival" OR "distant-relapse-free survival" OR "distant-relapse free survival" OR "time to progression" OR "time-to-progression" OR "time to-progression" OR "time-to progression" OR "TTP" OR "progression-free survival" OR "PFS" OR "progression free survival" OR "disease free survival" OR "disease-free survival" OR "DFS" OR "distant recurrence-free interval" OR "distant recurrence free interval" OR "distant-recurrence free interval" OR "distant-recurrence-free interval" OR "recurrence-free interval" OR "recurrence free interval" OR "DDFS" OR "distant disease-free survival" OR "distant disease free survival" OR "distant-disease free survival" OR "distant-disease-free survival" OR "IDFS" OR "invasive disease-free survival" OR "invasive disease free survival" OR "invasive-disease free survival" OR "invasive-disease-free survival" OR "prognosis" OR "prognostic" OR "prognoses"). We incorporated the Emtree and MeSH terms to increase the sensitivity of our systematic search.

### Definition of Recurrence Pattern Indices

To investigate the prognostic value of CD133 expression in determining relapse and recurrence patterns of high-grade gliomas, we investigated the association between the protein expression of CD133 with TTL, TTD, and PFS. Local recurrence is defined as a new enhanced lesion on MRI contiguous (< 3cm) the resection site, and distant recurrence is defined as a new enhanced lesion on MRI away (> 3cm) from the resection site (16, 17, 19).

### Study Selection and Data Extraction

After the systematic search, the retrieved studies were screened in two phases. In the first phase, the obtained papers were independently reviewed by two authors (M.A.S and N.H)

based on their titles and abstracts. In the second phase, the full text of the records and their supplementary data were independently reviewed by the same authors for consideration to be included in the current meta-analysis. Any disagreements were resolved *via* consulting with B.B and consensus.

## The Inclusion and the Exclusion Criteria

Studies with the following eligibility criteria were included in the current meta-analysis: (1) clinical studies, (2) investigations with the objectives of studying the association between CD133 expression with the relapse and the recurrence pattern-related survival indices, i.e., TTL, TTD, and PFS, in patients with high-grade gliomas, (3) studies that investigated the protein expression of CD133 in high-grade gliomas, and (4) studies that were published in English.

Records with the following criteria were excluded from the meta-analysis: (1) studies that failed to fulfill the inclusion criteria as mentioned above, (2) studies that only investigated the mRNA expression of CD133, rather than protein expression of CD133, (3) investigations that did not provide the prognostic data regarding the CD133 expression, (4) meeting abstracts, (5) duplicated records, (6) book chapters, (7) preclinical studies, (8) review articles, and (9) studies that were solely based on bioinformatics.

## Data Extraction

The following data were extracted from the included studies: (1) the first author and the year of publication, (2) the sample size, (3) the country, (4) the glioma grade, (5) the measured end-point, (6) the detection method, (7) cut-off for considering CD133 expression as high, and (8) the HR and the 95% confidence interval (CI) of measured PFS, TTD, and TTL.

## Evaluating the Quality of Included Studies

We assessed the quality of the included studies to facilitate the translation of our obtained results into routine practice. The quality of included studies has been evaluated according to the Hayden et al. checklist (20).

## Statistical Analysis

We used RevMan version 5.4 to conduct our meta-analyses. The common effect sizes were calculated as HR to assess the association between the protein expression of CD133 with the relapse and the recurrence pattern of high-grade gliomas in affected patients. Since there might be unpublished investigations regarding this topic, we applied the random-effect model. Like our previous investigation, the standard chi-squared test (Cochran Q test) and $I^2$ index were used to assess the possible heterogeneity among the included studies (21). The values over 50% for the $I^2$ index were considered as high heterogeneity. To visualize the potential asymmetry and publication bias, we provided funnel plots using CMA version 2. Besides, we performed the Egger test to evaluate the potential publication bias in an objective manner.

# RESULTS

## The Results of the Systematic Review

We obtained 992 records from PubMed (*n*=179), and Web of Science (*n*=201), Embase (*n*=286), and Scopus (*n*=326). After removing duplicated studies, the title and the abstracts of the remaining studies were screened. In the second phase, the full text of the remaining 36 studies and their supplementary data were reviewed for consideration to be included in the current meta-analysis. Following the exclusion of the 24 studies, we extracted the data from the remaining 12 studies. The flowchart of our systematic review process is demonstrated in **Figure 1**. The characteristics of the included studies are shown in **Table 1**.

The included studies have been published between 2008 to 2020. The included studies concerning the PFS of affected patients have applied different cut-offs for considering protein CD133 expression as high. However, the studies investigating CD133 protein expression with TTL and TTD have applied a unified method and cut-off (**Table 1**).

## The Protein Expression of CD133 and PFS of Patients With High-Grade Gliomas

Our results have indicated that increased protein expression of CD133 is significantly associated with the inferior PFS of patients with high-grade gliomas (HR = 1.72, 95% CI: 1.22 – 2.42, P = 0.002). Our results have also indicated a high and significant heterogeneity between the included studies ($I^2$ = 65%, P = 0.003) (**Figure 2**). Therefore, the meta-analyses of the included studies based on CD133 protein overexpression cut-offs have been conducted to address the high and significant heterogeneity.

### The Protein Expression of CD133 and PFS of Patients With High-Grade Gliomas With 2% Cut-Off

Our results have demonstrated that the protein overexpression of CD133 with 2% cut-off is not significantly associated with the inferior PFS of patients with high-grade gliomas (HR = 1.25, 95% CI: 0.75 – 2.10, P = 0.39). Our results have also indicated no significant heterogeneity between the included studies ($I^2$ = 47%, P = 0.15) (**Figure 3**).

### The Protein Expression of CD133 and PFS of Patients With High-Grade Gliomas With 10% Cut-Off

Our results have demonstrated that the protein overexpression of CD133 with 10% cut-off is significantly associated with the inferior PFS of patients with high-grade gliomas (HR = 1.82, 95% CI: 1.10 – 3.01, P = 0.02). Besides, our results have shown no significant heterogeneity between the included studies ($I^2$ = 15%, P = 0.31) (**Figure 4**).

### The Protein Expression of CD133 and PFS of Patients With High-Grade Gliomas With 50% Cut-Off

Our study has shown that the protein overexpression of CD133 with 50% cut-off is not significantly associated with the inferior PFS of patients with high-grade gliomas (HR = 1.37, 95% CI: 0.86 – 2.18, P = 0.19). Our results have also shown no significant heterogeneity between the included studies ($I^2$ = 0%, P = 0.52) (**Figure 5**).

**FIGURE 1** | The flowchart of literature identification, inclusion, and exclusion in the current systematic review.
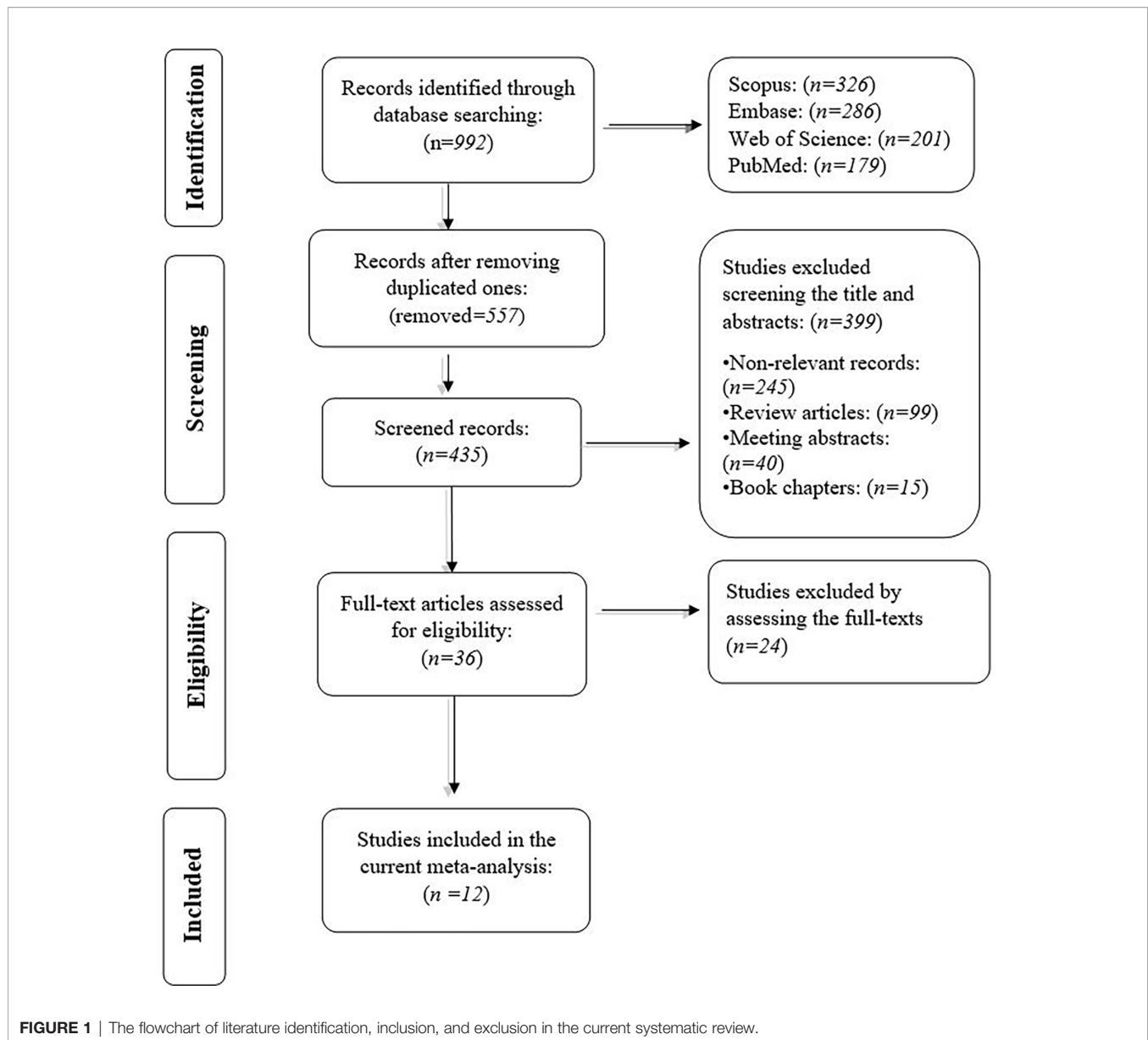
**TABLE 1** | The characteristics of the twelve included studies.

| No. | First author, year | Country | Sample size | Glioma grade | Endpoint | Detection method | Cut-off |
|-----|--------------------|---------|-------------|--------------|----------|------------------|---------|
| 1 | Tetsu Yamaki, 2020 (17) | Japan | 167 | IV | TTD and TTL | The integration of IHC with Western blot | Ratio>1 |
| 2 | Yasuo Iwadate, 2017 (15) | Japan | 70 | IV | PFS | IHC | 10% |
| 3 | Yasuo Iwadate, 2016 (14) | Japan | 80 | IV | PFS | IHC | 10% |
| 4 | Ichiyo Shibahara, 2015 (16) | Japan | 86 | III | TTD and TTL | The integration of IHC with Western blot | Ratio > 1 |
| 5 | Rikke H Dahlrot, 2014 (22) | Denmark | 211 | III and IV | PFS | Immunofluorescence | 2% |
| 6 | Jung Ha Shin, 2013 (23) | South Korea | 67 | IV | PFS | IHC | 50% |
| 7 | Ichiyo Shibahara, 2013 (19) | Japan | 112 | IV | TTD and TTL | The integration of IHC with Western blot | Ratio > 1 |
| 8 | Consolación Melguizo, 2012 (24) | Spain and Italy | 78 | IV | PFS | IHC | 25% |
| 9 | Kyung-Jung Kim, 2011 (25) | South Korea | 88 | IV | PFS | IHC | 50% |
| 10 | JIE HE, 2011 (26) | China | 59 | III and IV | PFS | IHC | 10% |
| 11 | Roberto Pallini, 2008 (27) | Italy | 44 | IV | PFS | Immunofluorescence | 2% |
| 12 | Felix Zeppernick, 2008 (28) | Germany | 24 | III | PFS | IHC | 1% |

*TTD, time to distant recurrence; TTL, time to local recurrence; PFS, progression-free survival, and IHC, immunohistochemistry.*

**FIGURE 2** | The forest plot of studies evaluating the prognostic value of CD133 overexpression in determining the PFS of patients with high-grade gliomas; Rikke H Dahlrot (IV) pertains to the Dahlrot et al.'s study on patients with grade IV gliomas, and Rikke H Dahlrot pertains to the Dahlrot et al.'s study on patients with grade III gliomas.



**FIGURE 3** | The forest plot of studies evaluating the prognostic value of CD133 overexpression in determining the PFS of patients with high-grade gliomas (with 2% cut-off); Rikke H Dahlrot (IV) pertains to the Dahlrot et al.'s study on patients with grade IV gliomas, and Rikke H Dahlrot pertains to the Dahlrot et al.'s study on patients with grade III gliomas.

## The Protein Expression of CD133 and TTD of Glioblastoma Patients

The current study has shown that increased protein expression of CD133 is significantly associated with sooner distant recurrence of gliomas in glioblastoma patients (HR = 3.32, 95% CI: 1.81 – 6.07, P = 0.0001). Besides, we have found no significant heterogeneity between the included studies ($I^2$ = 0%, P = 0.73) (**Figure 6**).

## The Protein Expression of CD133 and TTD of Patients With High-Grade Gliomas

Our results have demonstrated that increased protein expression of CD133 is significantly associated with a shorter time of distant tumor recurrence in patients with high-grade gliomas (HR = 2.49, 95% CI: 1.25 – 4.95, P = 0.009). Besides, we have found no significant heterogeneity between the included studies ($I^2$ = 33%, P = 0.22) (**Figure 7**).



**FIGURE 4** | The forest plot of studies evaluating the prognostic value of CD133 overexpression in determining the PFS of patients with high-grade gliomas (with 10% cut-off).

**FIGURE 5** | The forest plot of studies evaluating the prognostic value of CD133 overexpression in determining the PFS of patients with high-grade gliomas (with 50% cut-off).

## The Protein Expression of CD133 and TTL of Glioblastoma Patients

The current meta-analysis has indicated that elevated protein expression of CD133 is significantly associated with improved TTL in glioblastoma patients (HR = 0.47, 95% CI: 0.33 – 0.68, P < 0.0001). Besides, we have found no significant heterogeneity between the included studies ($I^2$ = 0%, P = 0.66) (**Figure 8**).

## The Protein Expression of CD133 and TTL of Patients With High-Grade Gliomas

Our results have shown that increased protein expression of CD133 is significantly associated with favorable TTL in patients with high-grade gliomas (HR = 0.57, 95% CI: 0.34 – 0.94, P = 0.03). Besides, we have found no significant heterogeneity between the included studies ($I^2$ = 45%, P = 0.16) (**Figure 9**).

## The Evaluation of Potential Bias in the Included Studies

We assessed the quality of included studies based on the Hayden et al. statements. Three studies have shown bias in the confounding measurement and account; however, collectively, there has been no considerable bias that can affect the obtained results (**Table 2**).

## Evaluating Potential Publication Bias

Based on our results, there has been no significant publication bias in our obtained results regarding the prognostic value of CD133 overexpression in patients with high-grade gliomas, the prognostic value of CD133 overexpression in patients with high-grade gliomas with 2% cut-off, the prognostic value of CD133 overexpression in patients with high-grade gliomas with 10% cut-off, and the TTD of patients with high-grade gliomas

(**Figures 1S–4S**). However, our results have demonstrated significant publication bias in the studies evaluating the TTL of patients with high-grade gliomas (**Figure 5S**).

## DISCUSSION

Although multiple clinical studies have investigated the prognostic value of CD133 in predictive tumor relapse and recurrence patterns in patients with high-grade gliomas, the published results are inconclusive. Therefore, it is necessary to clarify its prognostic value in predicting tumor relapse and recurrence patterns in patients with high-grade gliomas.

As a transmembrane glycoprotein, CD133 has been implicated in glioblastoma growth (11). In 2004, Singh et al. reported that only brain tumor cells with CD133-positive phenotype could initiate tumor development in mice brains (29). Liu et al. have indicated that CD133-positive glioblastoma cells overexpress the genes involved in inhibiting apoptosis and promoting stemness, i.e., Nestin, CD90, CD44, MGMT, CXCR4, and Musashi-1 (30). Furthermore, CD133 can confer radioresistance to glioblastoma cells and promote radiation-induced DNA damage repair (12). Besides radioresistance, CD133 upregulation has been associated with chemoresistance. Poon et al. have shown that there has been a strong association between adducin 3, a cytoskeletal factor linked with chemoresistance, with CD133. Indeed, this co-expression has been highly associated with a temozolomide-resistant state in glioblastoma cells (31). Consistent with this, Nakai et al. have reported a remarkable association between CD133 and MDR1 in glioblastoma cells and resected glioblastoma tissues, indicating the critical role of CD133 in maintaining chemoresistance (32).
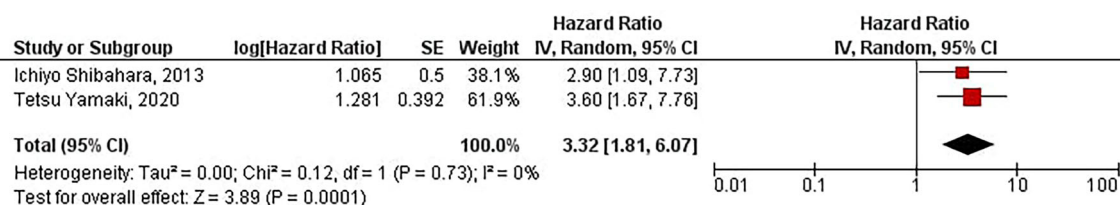


**FIGURE 6** | The forest plot of studies evaluating the prognostic value of CD133 in determining the TTD of glioblastoma patients.
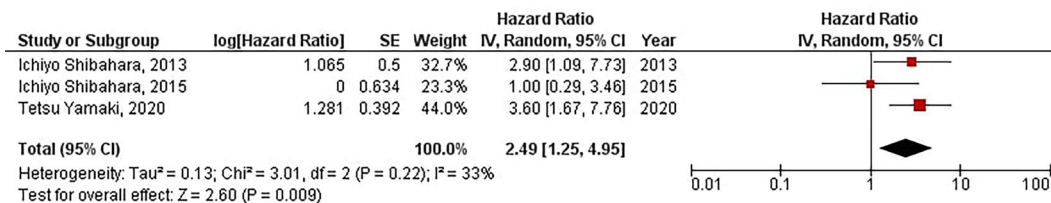
**FIGURE 7** | The forest plot of studies evaluating the prognostic value of CD133 in determining the TTD of patients with high-grade gliomas.
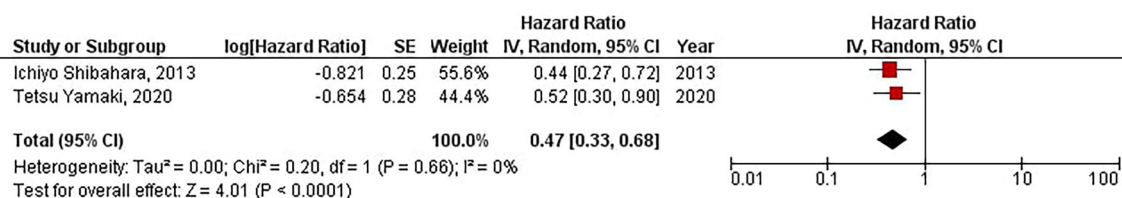


**FIGURE 8** | The forest plot of studies evaluating the prognostic value of CD133 in determining the TTL of glioblastoma patients.

Therefore, CD133 can be considered a critical factor in chemo/radioresistance development in glioblastoma, which can reproduce glioma after initial therapy.

Our results have indicated that increased protein expression of CD133 is significantly associated with the inferior PFS of patients with high-grade gliomas (HR = 1.72, 95% CI: 1.22 – 2.42, P = 0.002). However, the high heterogeneity between studies has urged us to conduct meta-analyses based on the cut-offs of CD133 protein expression ($I^2$ = 65%, P = 0.003) (**Figure 2**). Our results have demonstrated that with the threshold of 10%, CD133 protein overexpression is significantly associated with the inferior PFS of affected patients (HR = 1.82, 95% CI: 1.10 – 3.01, P = 0.02). Consistent with our observed results, Wang et al. have also indicated that protein/gene overexpression of CD133 is associated with the inferior PFS of patients with low-grade patients (33). Although it has been previously shown that CD133 overexpression is associated with worsened PFS of glioma patients, those results are based on pooling the protein and gene expression of CD133, which can be misleading (33).

Besides, pooling data from low-grade gliomas and high-grade gliomas can also lead to misleading results (34). Moreover, without defining the cut-off for considering CD133 expression as overexpressed, the clinical translation of these kinds of studies might be at stake. In contrast, with including recently published studies and analyzing the protein expression of CD133 based on glioma grades and their defined cut-offs, the current updated study indicates that CD133 overexpression with 10% cut-off is associated with the inferior PFS in patients with high-grade gliomas.

For the first time, our meta-analysis has shown that increased protein expression of CD133 is associated with the inferior TTD of patients with glioblastoma and high-grade glioma patients (HR = 3.32, 95% CI: 1.81 – 6.07, P = 0.0001, and HR = 1.64, 95% CI: 1.18 – 2.29, P = 0.003, respectively). Indeed, our results have indicated that upregulated protein expression of CD133 is associated with sooner distant tumor relapse in glioblastoma and high-grade glioma patients. Besides, our results have demonstrated that increased protein expression of CD133 is



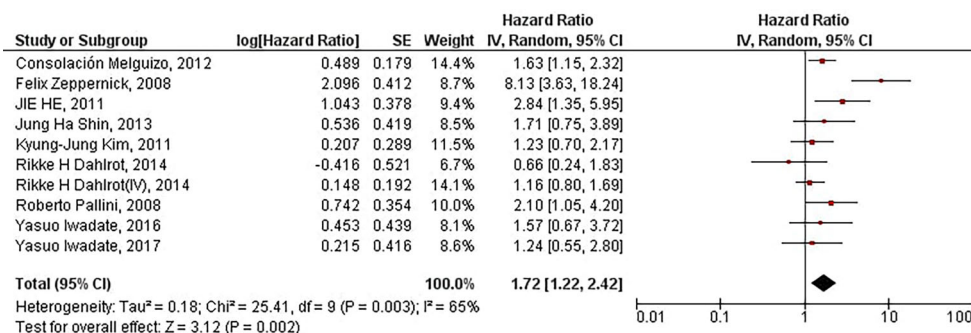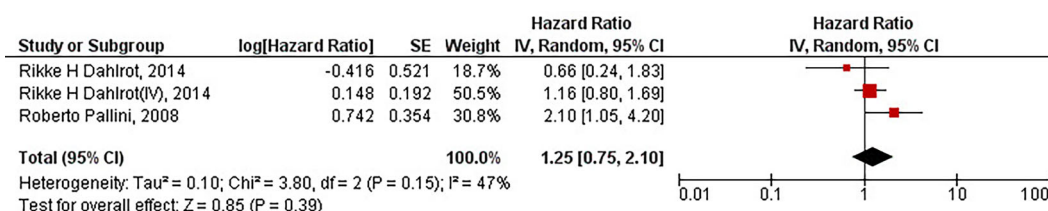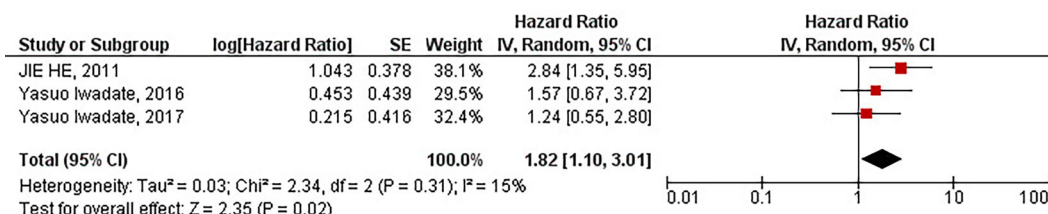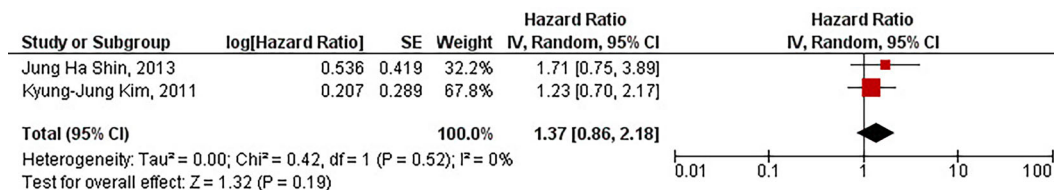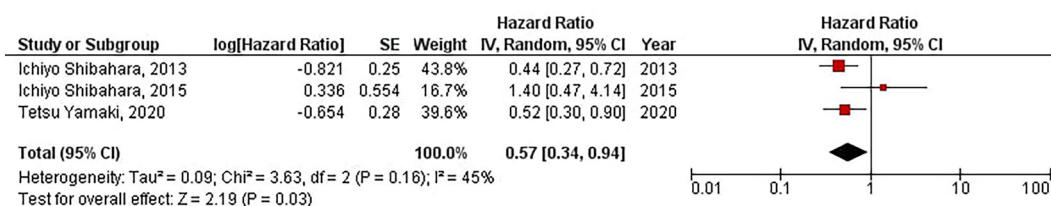**FIGURE 9** | The forest plot of studies evaluating the prognostic value of CD133 in determining the TTL of patients with high-grade gliomas.

| First author and the year of publication | Study participation | Study attrition | Prognostic factor measurement | Outcome measurement | Confounding measurement and account | Analysis |
|---|---|---|---|---|---|---|
| Tetsu Yamaki, 2020 (17) | *** | *** | *** | *** | *** | *** |
| Yasuo Iwadate, 2017 (15) | *** | *** | *** | *** | *** | *** |
| Yasuo Iwadate, 2016 (14) | *** | *** | *** | *** | *** | *** |
| Ichiyo Shibahara, 2015 (16) | *** | *** | ** | *** | *** | *** |
| Rikke H Dahlrot, 2014 (22) | *** | *** | *** | *** | * | ** |
| Jung Ha Shin, 2013 (23) | *** | *** | *** | *** | *** | *** |
| Ichiyo Shibahara, 2013 (19) | *** | *** | *** | *** | *** | *** |
| Consolación Melguizo 2012 (24) | *** | *** | *** | *** | * | ** |
| Kyung-Jung Kim, 2011 (25) | *** | *** | *** | *** | *** | *** |
| JIE HE, 2011 (26) | *** | *** | *** | * | * | *** |
| Roberto Pallini, 2008 (27) | *** | *** | *** | *** | *** | *** |
| Felix Zeppernick, 2008 (28) | *** | ** | *** | *** | *** | *** |

*\*\*\*Bias might not present; \*\*Bias might be partly present; \*Bias might be present.*

associated with the improved TTL of glioblastoma patients (HR = 0.47, 95% CI: 0.33 – 0.68, P < 0.0001). Although our study has also indicated that elevated protein expression of CD133 is associated with favorable TTL of patients with high-grade gliomas (HR = 0.57, 95% CI: 0.35 – 0.94, P = 0.03), there has been significant publication bias among the included studies (**Figure 5S**). Thus, further investigations are required for evaluating the association between increased CD133 protein expression with the TTL of these patients. Collectively, our results have indicated that increased protein expression of CD133 is associated with sooner distant recurrence of glioblastoma and high-grade gliomas on MRI. Also, increased protein expression of CD133 is associated with improved TTL of glioblastomas on MRI. Therefore, the protein expression of CD133 can be a valuable prognostic factor for predicting the recurrence patterns of glioblastoma and high-grade gliomas in affected patients.

The current study has several limitations. First, we only included the studies that were published in English. Its second limitation stems from the nature of cohort studies that, unlike randomized clinical trials, all the confounding variables cannot be addressed. Nevertheless, the current study has several strengths as well. First, for the first time, our study has sorted out the prognostic value of protein expression of CD133, as the functional form of CD133, in predicting the relapse and recurrence pattern of high-grade gliomas based on defined cut-offs. Second, our study has linked a cancer stem cell marker and preclinical findings with clinical and imaging findings, which pave the way for more investigations to correlate the cancer stem markers with imaging findings.

## CONCLUSION

With a 10% cut-off, increased protein expression of CD133 is associated with the inferior PFS of patients with high-grade gliomas. Besides, the increased protein expression of CD133 is associated with sooner distant tumor recurrence and improved TTL of glioblastomas. Also, we have found that elevated protein

expression of CD133 is associated with a shorter time of distant tumor recurrence in affected patients with high-grade gliomas. Overall, the protein overexpression of CD133 can be a valuable prognostic biomarker for predicting the relapse and recurrence pattern of high-grade gliomas.

## DATA AVAILABILITY STATEMENT

The original contributions presented in the study are included in the article/**Supplementary Material**. Further inquiries can be directed to the corresponding authors.

## AUTHOR CONTRIBUTIONS

All authors contributed to the article and approved the submitted version. MA has come up with the research question, selected the studies, extracted the data, analyzed the data, and wrote most of the manuscript. NH has selected the studies, interpreted the results, and provided the tables. ZA and OB have critically reviewed the paper, improved the quality of the manuscript. NS and BB have supervised the study and critically reviewed the manuscript.

## ACKNOWLEDGMENTS

## SUPPLEMENTARY MATERIAL

The Supplementary Material for this article can be found online at: https://www.frontiersin.org/articles/10.3389/fonc.2021.722833/full#supplementary-material

# REFERENCES

1. Hanif F, Muzaffar K, Perveen K, Malhi SM, Simjee SU. Glioblastoma Multiforme: A Review of its Epidemiology and Pathogenesis Through Clinical Presentation and Treatment. *Asian Pacif J Cancer Prevent: APJCP* (2017) 18(1):3.

2. Najafzadeh B, Asadzadeh Z, Motafakker Azad R, Mokhtarzadeh A, Baghbanzadeh A, Alemohammad H, et al. The Oncogenic Potential of NANOG: An Important Cancer Induction Mediator. *J Cell Physiol* (2021) 236(4):2443–58. doi: 10.1002/jcp.30063

3. Lathia JD, Mack SC, Mulkearns-Hubert EE, Valentim CL, Rich JN. Cancer Stem Cells in Glioblastoma. *Genes Dev* (2015) 29(12):1203–17. doi: 10.1101/gad.261982.115

4. Yaghobi Z, Movassaghpour A, Talebi M, Shadbad MA, Hajiasgharzadeh K, Pourvahdani S, et al. The Role of CD44 in Cancer Chemoresistance: A Concise Review. *Eur J Pharmacol* (2021) 174147.

5. Sharifzad F, Ghavami S, Verdi J, Mardpour S, Sisakht MM, Azizi Z, et al. Glioblastoma Cancer Stem Cell Biology: Potential Theranostic Targets. *Drug Resist Updates* (2019) 42:35–45. doi: 10.1016/j.drup.2018.03.003

6. Lee Y, Lee J-K, Ahn SH, Lee J, Nam D-H. WNT Signaling in Glioblastoma and Therapeutic Opportunities. *Lab Invest* (2016) 96(2):137–50. doi: 10.1038/labinvest.2015.140

7. Derakhshani A, Rostami Z, Safarpour H, Shadbad MA, Nourbakhsh NS, Argentiero A, et al. From Oncogenic Signaling Pathways to Single-Cell Sequencing of Immune Cells: Changing the Landscape of Cancer Immunotherapy. *Molecules* (2021) 26(8):2278.

8. Wickström M, Dyberg C, Milosevic J, Einvik C, Calero R, Sveinbjörnsson B, et al. Wnt/β-Catenin Pathway Regulates MGMT Gene Expression in Cancer and Inhibition of Wnt Signalling Prevents Chemoresistance. *Nat Commun* (2015) 6(1):1–10.

9. Behrooz AB, Syahir A. Could We Address the Interplay Between CD133, Wnt/β-Catenin, and TERT Signaling Pathways as a Potential Target for Glioblastoma Therapy? *Front Oncol* (2021) 11:1049. doi: 10.3389/fonc.2021.642719

10. Manoranjan B, Chokshi C, Venugopal C, Subapanditha M, Savage N, Tatari N, et al. A CD133-AKT-Wnt Signaling Axis Drives Glioblastoma Brain Tumor-Initiating Cells. *Oncogene* (2020) 39(7):1590–9. doi: 10.1038/s41388-019-1086-x

11. Yao J, Zhang T, Ren J, Yu M, Wu G. Effect of CD133/prominin-1 Antisense Oligodeoxynucleotide on *In Vitro* Growth Characteristics of Huh-7 Human Hepatocarcinoma Cells and U251 Human Glioma Cells. *Oncol Rep* (2009) 22(4):781–7.

12. Bao S, Wu Q, McLendon RE, Hao Y, Shi Q, Hjelmeland AB, et al. Glioma Stem Cells Promote Radioresistance by Preferential Activation of the DNA Damage Response. *Nature* (2006) 444(7120):756–60. doi: 10.1038/nature05236

13. Bi C-L, Fang J-S, Chen F-H, Wang Y-J, Wu J. Chemoresistance of CD133 (+) Tumor Stem Cells From Human Brain Glioma. *Zhong Nan Da Xue Xue Bao Yi Xue Ban= J Cent South Univ Med Sci* (2007) 32(4):568–73.

14. Iwadate Y, Matsutani T, Hirono S, Shinozaki N, Saeki N. Transforming Growth Factor-β and Stem Cell Markers Are Highly Expressed Around Necrotic Areas in Glioblastoma. *J Neuro Oncol* (2016) 129(1):101–7. doi: 10.1007/s11060-016-2145-6

15. Iwadate Y, Suganami A, Tamura Y, Matsutani T, Hirono S, Shinozaki N, et al. The Pluripotent Stem-Cell Marker Alkaline Phosphatase Is Highly Expressed in Refractory Glioblastoma With DNA Hypomethylation. *Neurosurgery* (2017) 80(2):248–56. doi: 10.1093/neuros/nyw026

16. Shibahara I, Sonoda Y, Shoji T, Kanamori M, Saito R, Inoue T, et al. Malignant Clinical Features of Anaplastic Gliomas Without IDH Mutation. *Neuro-Oncology* (2015) 17(1):136–44. doi: 10.1093/neuonc/nou112

17. Yamaki T, Shibahra I, K-i M, Kanemura Y, Konta T, Kanamori M, et al. Relationships Between Recurrence Patterns and Subventricular Zone Involvement or CD133 Expression in Glioblastoma. *J Neuro Oncol* (2020) 146(3):489–99. doi: 10.1007/s11060-019-03381-y

18. Moher D, Liberati A, Tetzlaff J, Altman DG, Group P. Preferred Reporting Items for Systematic Reviews and Meta-Analyses: The PRISMA Statement. *PloS Med* (2009) 6(7):e1000097.

19. Shibahara I, Sonoda Y, Saito R, Kanamori M, Yamashita Y, Kumabe T, et al. The Expression Status of CD133 Is Associated With the Pattern and Timing of Primary Glioblastoma Recurrence. *Neuro-Oncology* (2013) 15(9):1151–9. doi: 10.1093/neuonc/not066

20. Hayden JA, Côté P, Bombardier C. Evaluation of the Quality of Prognosis Studies in Systematic Reviews. *Ann Internal Med* (2006) 144(6):427–37. doi: 10.7326/0003-4819-144-6-200603210-00010

21. Lotfinejad P, Asghari Jafarabadi M, Abdoli Shadbad M, Kazemi T, Pashazadeh F, Sandoghchian Shotorbani S, et al. Prognostic Role and Clinical Significance of Tumor-Infiltrating Lymphocyte (TIL) and Programmed Death Ligand 1 (PD-L1) Expression in Triple-Negative Breast Cancer (TNBC): A Systematic Review and Meta-Analysis Study. *Diagnostics* (2020) 10(9):704. doi: 10.3390/diagnostics10090704

22. Dahlrot RH, Hansen S, Jensen SS, Schrøder HD, Hjelmborg J, Kristensen BW. Clinical Value of CD133 and Nestin in Patients With Glioma: A Population-Based Study. *Int J Clin Exp Pathol* (2014) 7(7):3739.

23. Shin JH, Lee YS, Hong Y-K, Kang CS. Correlation Between the Prognostic Value and the Expression of the Stem Cell Marker CD133 and Isocitrate Dehydrogenase1 in Glioblastomas. *J Neuro Oncol* (2013) 115(3):333–41. doi: 10.1007/s11060-013-1234-z

24. Melguizo C, Prados J, González B, Ortiz R, Concha A, Alvarez PJ, et al. MGMT Promoter Methylation Status and MGMT and CD133 Immunohistochemical Expression as Prognostic Markers in Glioblastoma Patients Treated With Temozolomide Plus Radiotherapy. *J Trans Med* (2012) 10(1):1–11. doi: 10.1186/1479-5876-10-250

25. Kim KJ, Lee KH, Kim HS, Moon KS, Jung TY, Jung S, et al. The Presence of Stem Cell Marker-Expressing Cells Is Not Prognostically Significant in Glioblastomas. *Neuropathology* (2011) 31(5):494–502. doi: 10.1111/j.1440-1789.2010.01194.x

26. He J, Shan Z, Li L, Liu F, Liu Z, Song M, et al. Expression of Glioma Stem Cell Marker CD133 and O6-Methylguanine-DNA Methyltransferase Is Associated With Resistance to Radiotherapy in Gliomas. *Oncol Rep* (2011) 26(5):1305–13. doi: 10.3892/or.2011.1393

27. Pallini R, Ricci-Vitiani L, Banna GL, Signore M, Lombardi D, Todaro M, et al. Cancer Stem Cell Analysis and Clinical Outcome in Patients With Glioblastoma Multiforme. *Clin Cancer Res* (2008) 14(24):8205–12. doi: 10.1158/1078-0432.CCR-08-0644

28. Zeppernick F, Ahmadi R, Campos B, Dictus C, Helmke BM, Becker N, et al. Stem Cell Marker CD133 Affects Clinical Outcome in Glioma Patients. *Clin Cancer Res* (2008) 14(1):123–9. doi: 10.1158/1078-0432.CCR-07-0932

29. Singh SK, Hawkins C, Clarke ID, Squire JA, Bayani J, Hide T, et al. Identification of Human Brain Tumour Initiating Cells. *Nature* (2004) 432(7015):396–401. doi: 10.1038/nature03128

30. Liu G, Yuan X, Zeng Z, Tunici P, Ng H, Abdulkadir IR, et al. Analysis of Gene Expression and Chemoresistance of CD133+ Cancer Stem Cells in Glioblastoma. *Mol Cancer* (2006) 5(1):1–12.

31. Poon M-W, Zhuang JTF, Wong STS, Sun S, Zhang X-Q, Leung GKK. Co-Expression of Cytoskeletal Protein Adducin 3 and CD133 in Neurospheres and a Temozolomide-Resistant Subclone of Glioblastoma. *Anticancer Res* (2015) 35(12):6487–95.

32. Nakai E, Park K, Yawata T, Chihara T, Kumazawa A, Nakabayashi H, et al. Enhanced MDR1 Expression and Chemoresistance of Cancer Stem Cells Derived From Glioblastoma. *Cancer Invest* (2009) 27(9):901–8. doi: 10.3109/07357900801946679

33. Wang Y, Zhao G, Yu T. CD133 Expression may be Useful as a Prognostic Indicator in Glioblastoma Multiforme: A Meta-Analysis. *Int J Clin Exp Pathol* (2016) 9(12):12407–14.

34. Han M, Guo L, Zhang Y, Huang B, Chen A, Chen W, et al. Clinicopathological and Prognostic Significance of CD133 in Glioma Patients: A Meta-Analysis. *Mol Neurobiol* (2016) 53(1):720–7. doi: 10.1007/s12035-014-9018-9

**Conflict of Interest:** The authors declare that the research was conducted in the absence of any commercial or financial relationships that could be construed as a potential conflict of interest.

**Publisher's Note:** All claims expressed in this article are solely those of the authors and do not necessarily represent those of their affiliated organizations, or those of the publisher, the editors and the reviewers. Any product that may be evaluated in this article, or claim that may be made by its manufacturer, is not guaranteed or endorsed by the publisher.

# Malignant Tumor Purity Reveals the Driven and Prognostic Role of *CD3E* in Low-Grade Glioma Microenvironment

Xiuqin Lu[1†], Chuanyu Li[2†], Wenhao Xu[3†], Yuanyuan Wu[4†], Jian Wang[5], Shuxian Chen[6], Hailiang Zhang[3], Huadong Huang[2*], Haineng Huang[2*] and Wangrui Liu[1,2*]

[1] Department of Nursing and Health Management, Shanghai University of Medicine & Health Sciences, Shanghai, China, [2] Department of Neurosurgery, Affiliated Hospital of Youjiang Medical University for Nationalities, Guangxi, China, [3] Department of Urology, Fudan University Shanghai Cancer Center, Shanghai Medical University, Fudan University, Shanghai, China, [4] Department of Gastroenterology, Naval Medical Center of People's Liberation Army (PLA) of China, Naval Military Medical University, Shanghai, China, [5] Department of Transplantation, Xinhua Hospital Affiliated to Shanghai Jiao Tong University School of Medicine, Shanghai, China, [6] Department of Oncology, Xinhua Hospital Affiliated to Shanghai Jiao Tong University School of Medicine, Shanghai, China

The tumor microenvironment (TME) contributes to the initiation and progression of many neoplasms. However, the impact of low-grade glioma (LGG) purity on carcinogenesis remains to be elucidated. We selected 509 LGG patients with available genomic and clinical information from the TCGA database. The percentage of tumor infiltrating immune cells and the tumor purity of LGG were evaluated using the ESTIMATE and CIBERSORT algorithms. Stromal-related genes were screened through Cox regression, and protein-protein interaction analyses and survival-related genes were selected in 487 LGG patients from GEO database. Hub genes involved in LGG purity were then identified and functionally annotated using bioinformatics analyses. Prognostic implications were validated in 100 patients from an Asian real-world cohort. Elevated tumor purity burden, immune scores, and stromal scores were significantly associated with poor outcomes and increased grade in LGG patients from the TCGA cohort. In addition, *CD3E* was selected with the most significant prognostic value (Hazard Ratio=1.552, *P*<0.001). Differentially expressed genes screened according to *CD3E* expression were mainly involved in stromal related activities. Additionally, significantly increased *CD3E* expression was found in 100 LGG samples from the validation cohort compared with adjacent normal brain tissues. High *CD3E* expression could serve as an independent prognostic indicator for survival of LGG patients and promotes malignant cellular biological behaviors of LGG. In conclusion, tumor purity has a considerable impact on the clinical, genomic, and biological status of LGG. *CD3E*, the gene for novel membrane immune biomarker deeply affecting tumor purity, may help to evaluate the prognosis and develop individual immunotherapy strategies for LGG patients. Evaluating the ratio of differential tumor purity and *CD3E* expression levels may provide novel insights into the complex structure of the LGG microenvironment and targeted drug development.

**Keywords: tumor microenvironment, tumor purity, CD3E, low-grade glioma, prognosis, immune infiltrations**

# BACKGROUND

The treatment and prognosis of glioma are relatively limited because the understanding of immune gene regulation and carcinogenesis is incomplete (1, 2). In the United States, the annual incidence of pediatric low-grade glioma (LGG) is 1.3-2.1 cases per 100,000 people, while adult LGG is more common with an estimated 9.1-12.5 cases per 100,000 people (3, 4). Glioblastoma multiforme (Grade IV) is the second most common primary intracranial tumor, and the most common malignant tumor of the central nervous system. GBM accounts for 15.4% of all primary brain tumors and 45.6% of primary malignant brain tumors. Grade I gliomas are essentially benign and respectable (5). A large number of clinical studies have found that the survival rate of LGG patients is low, and many patients have a sharp decline in survival time from tumor deterioration in the later stage (6). The high recurrence and malignancy rates of LGG are detrimental to patients (7, 8). Investigating approaches to maintain the quality of life of LGG patients while prolonging their overall survival (OS) has become a common focus for clinicians and researchers (9–12).

The rapid development of modern bioinformatics and phenotyping has provided great convenience to our research (13–15). Recent work has suggested that the tumor microenvironment (TME) can facilitate the development of tumors (16, 17). The interactions between cancer cells, stromal cells, and recruited immune cells promote the invasion and metastasis of a variety of cancers, as well as cell proliferation, anti-apoptosis signals, and evasion of immune surveillance. This significantly impacts the treatment and prognosis of cancer patients (18, 19). The TME is mainly composed of resident stromal cells and recruited immune cells (20), which affect tumor blood vessel growth and tumor proliferation, respectively. Additionally, tumor-infiltrating immune cells (TICs) in the TME can be used to determine patient prognosis (21), and the related immune genes have an impact on cancer patient survival (22, 23). This correlation has led to improvements in immune-based treatment methods to create immune checkpoint inhibitors and identify prognostic biomarkers for tumor patients (24–26). These studies suggest that the various immune responses of the LGG TME may change the purity of the tumor, thereby affecting the invasive and metastatic abilities of LGG. There is a reported strong connection between LGG and the TME. The higher the stromal and immune scores of LGG display, the lower the purity and higher the aggressiveness of the tumor show. Low glioma purity shows a strong immunophenotype and suggests a poor prognosis (27). Thus, clinicians and basic science researchers are required to identify tumor purities that accurately reflect the LGG heterogeneity and complex role of the microenvironment, which may also help to discover novel biomarkers of LGG.

We selected 509 LGG patients from The Cancer Genome Atlas (TCGA) dataset and calculated the percentage of TICs and tumor purity of each LGG tumor through ESTIMATE and CIBERSORT calculation methods. We also calculated the ratio of immune and matrix components and selected the inter-sample screening in the Gene Expression Omnibus (GEO). LGG genes associated with prognosis were identified and the predictive biomarker *CD3E* was found. The T cell antigen receptor epsilon subunit (*CD3E*) gene is located on chromosome 11q23.3, composed of nine exons, and is associated with autosomal recessive hereditary early-onset immunodeficiency 18 phenotype, which is a severe combined immunodeficiency variant (27). Moreover, *CD3E* is overexpressed in certain solid tumors and is associated with immunity (28, 29). Among the differentially expressed genes (DEGs) produced by comparing immunological and matrix components in LGG samples, we determined that *CD3E* is a potential indicator of TME status changes in LGG. This gene may affect the tumor microenvironment of LGG by regulating T cells, which may be completely different from the tumor microenvironment of other organs outside the skull. The higher the expression of *CD3E* is, the worse the prognosis of LGG patients is.

# METHODS

## Data Collection

This study included 509 patients from TCGA (30) database and 487 patients from GEO (30, 31) databases (three datasets, GSE107850 on GPL14951, GSE26576 on GPL6801 and GPL570, GSE20395 on GPL9183, were selected as the second testing cohort for further analysis) two independent testing cohorts. To further improve the clinical value of the study, a total of 100 LGG patients, who underwent surgery in Affiliated Hospital of YouJiang Medical University for Nationalities (AHYMUN, Baise, China) from June 2014 to July 2019, were enrolled in this study. Clinical data of LGG patients that may affect the OS and disease-free survival (DFS) were collected, including age, gender, epilepsy history, capsular invasion Karnofsky score and tumor envelope infiltration.

LGG patients with available RNA sequencing data from the Cancer Genome Atlas (TCGA) database (https://tcga-data.nci. nih.gov/tcga/) were consecutively recruited for the analyses from UCSC Xena (http://xena.ucsc.edu/). UCSC Xena is an online exploration tool for public and private, multi-omic and clinical/phenotype data, and provided level 3 data from TCGA databases. The gene expression profile was measured experimentally using the Illumina HiSeq 2000 RNA Sequencing platform by the University of North Carolina TCGA genome characterization center.

## Tumor Purity Calculation

R software (32) (version 4.0.0) was used to estimate the proportion of TME immune cells and stromal cells in each LGG sample. We use the ssGSEA algorithm to calculate ImmuneScore, StromalScore and ESTIMATEScore (33, 34).

---

**Abbreviations:** AHYMUN, Affiliated Hospital of YouJiang Medical University for Nationalities; GEO, Gene Expression Omnibus; GO, Gene Ontology; GSEA, Gene Set Enrichment Analysis; HR, hazard ratio; IHC, immunohistochemistry; KEGG, Kyoto Encyclopedia of Genes and Genomes; LGG, Low grade glioma; OS, overall survival; PPI, Protein-protein interaction; TCGA, the Cancer Genome Atlas; TIC, tumor-infiltrating immune cells; TME, tumor microenvironment.

The CIBERSORT algorithm is used to calculate the proportion of immune cells in LGG (35).

## Totally 1,068 LGG Patients Included From Online Public and Real-World Cohorts

This study included 509 patients from TCGA database and 487 patients from GEO database (GSE107850, GSE60898, GSE26576) as two independent testing cohorts. To further improve the clinical value of the study, a total of 100 LGG patients, who underwent surgery in Affiliated Hospital of YouJiang Medical University for Nationalities (AHYMUN) from June 2014 to July 2019, were enrolled in this study. Clinical data of LGG patients that may affect the OS and disease-free survival (DFS) were collected, including age, gender, epilepsy history, capsular invasion Karnofsky score and tumor envelope infiltration. Tissue samples were collected during surgery and available from AHYMUN tissue bank. IHC staining of CD3E was performed using a mouse monoclonal anti-CD3E antibody (1:800, ab16669, Abcam, USA) in 100 LGG samples. Positive or negative staining of CD3E protein in a FFPE slide was independently evaluated as previously described (36).

## Screening for Differential Expressed Genes

Using "LIMMA" (37) in R software, standardize the data and perform differential expression analysis. Put the relevant code into R, and analyze the DEGs in LGG samples and normal brain tissue samples through the limma software package. $P$ value < 0.05 and Log2FC > 1 was set as the threshold for identifying Clinical-related DEGs.

## Screening for Immune and Stromal Related DEGs

According to the median of the Immune score and the Stromal score, we grouped high and low samples, so as to screen out the TME related genes that highly involved in heterogeneity of tumor immune environment. The 509 LGG samples in the TCGA database were marked as high or low. Use package limma to conduct differential analysis of gene expression, and generate Stromal related DEGs by comparing high and low score samples. Stromal related DEGs (high/low score group) and false discovery rate < 0.05 with a fold change greater than 1 after log2 conversion were considered significant. We calculated the TIC value in all LGG data by the CIBERSORT method, and the samples with $P$ < 0.05 can be further analyzed.

## Functional Enrichment Analysis

The protein-protein interaction (PPI) network is constructed from the STRING (38) database. All gene interaction networks were drawn by Cytoscape (version 3.8.0.) (39). We performed gene ontology (GO) enrichment analysis of DEGs through R software, and determined the biological processes (BPs), cell components (CCs) and molecular functions (MFs) of each gene (40). We also performed Kyoto Encyclopedia of Genes and Genomes (KEGG) enrichment analysis to show enrichment for related genes (41). We use GSEA software (vision 4.0.3) to analyze the entire transcriptome of all tumor samples (42), and only genomes with p<0.05 are considered important.

## Immunohistochemistry

Immunohistochemistry streptavidin peroxidase method was used to detect the expression of *CD3E* in tumor, immune and stromal cells from LGG and adjacent normal tissues (43). Immunostaining of CD3E was performed using a rabbit monoclonal anti-CD3E antibody (1:1000, ab237721, Abcam). Positive or negative staining of a certain protein in one FFPE slide was independently assessed by two experienced clinicians, and determined as follows. The LGG samples were scored according to the degree of cell staining intensity and density. Intensity score: 0, cytoplasmic yellow particles; 1, light brown particles; 2, obvious brown particles; 3, a large number of dark brown particles. Density score (according to the percentage of positive cells): 0, 0%, 1, <10%, 2.11%-50%, 3, 51-80%, 4, 80%. The final IHC score is calculated by multiplying the two scores.

## Single-Cell Datasets Processing and Collection

Tumor Immune Single-cell Hub (TISCH, http://tisch.comp-genomics.org/home/) is used to screen for scRNA-seq datasets with detailed cell-type annotation at the single-cell level focusing on tumor microenvironment across different cancers. GSE131928 10X (n = 9, number of cells = 13,553), GSE131928 Smartseq2 (n = 28, number of cells = 7,930), GSE135437 (n = 19, number of cells = 12,559), GSE139448 (n = 3, number of cells = 12,152), GSE141982 (n = 2. Number of cells = 526) and GSE148842 (n = 7, number of cells = 111,397) were enrolled with correlation analysis between CD3E expression and abundance of immune cells infiltrations.

## Cells and Plasmids

Two human glioma cell lines (N9, N33) were cultured in Dulbecco's modified Eagle medium: nutrient mixture F-12 (DMEM: F12, 01-172-1ACS, Biological Industries) and 10% fetal bovine serum (FBS), 04-001-1A, Bioindustry). CD3E siRNA duplexes were transfected using Lipofectamine 3000 reagent (Invitrogen, USA) according to the manufacturer's protocol. Cells were used for further analyses after transfection for 48 h. The sequences of siRNA duplexes are listed below: siRNA1#: 5'-UUCUUCAUUACCAUCUUGCCC-3', siRNA2#: 5'-UAAAUACCACCCAUUUCUUCAU-3'.

## Western Blot

After the specified treatment, the cells were harvested and lysed in RIPA buffer and quantified by the bicinchoninic acid assay kit (Pierce, USA). The total protein was separated by sodium dodecyl sulfate polyacrylamide gel electrophoresis (SDS-PAGE) under denaturing conditions and transferred to a nitrocellulose filter (NC) membrane. The membrane was incubated with blocking buffer for 2 hours at room temperature and then with the primary antibody anti-CD3E (1:1000, ab237721, Abcam) overnight at 4°C. Then, the protein was visualized using ECL plus western blotting detection reagents (Biosciences) and detected with an enhanced chemiluminescence kit.

## Cell Counting Kit-8 Assay

100 microliters of N9 and N33 cell suspension ($5 \times 10^4$) were added to each well of a 96-well plate, with triple wells in each group. The culture plate was placed in the incubator for pre-culture for 24 hours until the cells stick to the culture dish. Then, we add different concentrations of culture medium to the wells for 24 hours, and add normal and high-sugar medium to the culture plate. After 24 hours, 10 µl CCK-8 solution (#CK04; Dojindo, Japan) was added to each well, and then incubate for 2 hours.

## Transwell Assay

Cell invasion ability was assessed using the Transwell chamber (BD Biosciences). A total of $2 \times 10^5$ cells were plated on top of a polycarbonate Transwell filter with 200 mL serum-free medium. The lower compartment is filled with 500 mL of complete medium (1640 + 10% fetal bovine serum). After 24 hours, cells in the upper chamber were removed with cotton swabs, and cells on the underside were fixed with 4% paraformaldehyde for 10 minutes at room temperature. After been washed and air drying, stained cells in four randomly selected fields were photographed and counted under a light microscope (Olympus, Tokyo, Japan).

## Statistical Analysis

In this study, R (Version 3.3.2) and RStudio (Version 1.2) were utilized to perform most data analyses, including Cox regression analyses (44), Kaplan-Meier plots (45), risk plots, PPI network and functional annotations. All tests were two-sided and *p*-value less than 0.05 were taken as significant. The scatter plot was used to represent the differential expression of CD3E in normal and LGG tissues. The primary endpoint, the overall survival of patients who survived specific period of time, which was determined based on the length of time from the date of surgery to the date of death or the date of the last follow-up. Disease-free survival as a secondary endpoint refers to the length of time from the start of curative treatment for which no disease can be found to the date of progression to the date of starting second-line treatment or starting treatment.

## RESULTS

As shown in **Figure 1**, this work was conducted in three stages. To estimate the proportion of TICs and tumor purity in LGG samples, transcriptome RNA-seq data from 516 patients were downloaded from TCGA, after which ESTIMATE and CIBERSORT algorithms were performed. DEGs shared by ImmuneScore and StromalScore were used to construct a PPI network. Significant hub genes in the PPI network were evaluated using univariate Cox regression cross-analysis. Additionally, we selected a qualified dataset from the GEO database and conducted a differential analysis to obtain clinical-related DEGs. Then, any associations between the DEGs and LGG patient survival rates were evaluated and screened. Next, *CD3E* was identified and validated as the most relevant gene after combining the two datasets of DEGs. Further

studies focused on the impact of *CD3E* on survival, GSEA, and correlation with TICs. Functional annotations of neighboring genes and clinical validation of *CD3E* were performed. Finally, we entered the research conclusions in our own AHYMUN center for clinical cohort study.

## TME-Related Scores Are Related to Survival of LGG Patients

To confirm whether the proportion of cells in the TME and tumor purity can affect the survival time of LGG patients, we calculated ImmuneScore, StromalScore, and ESTIMATEScore and generated a Kaplan-Meier survival curve. The Score was positively associated to the higher the proportion of the corresponding component in the TME. The sum of ImmuneScore and StromalScore is ESTIMATEScore, which also reflects tumor purity. **Figure 2** shows how the TME scores are related to overall survival. ImmuneScore ($P = 0.003$), StromalScore ($P < 0.001$), and ESTIMATEScore ($P = 0.006$) values were positively correlated with OS. These results indicate that the prognosis of LGG patients can be inferred based on the estimated matrix score and help to develop a personalized treatment plan.

## TME-Related Scores Are Related to the Clinical Features of LGG Patients

We combined the corresponding clinical information of TCGA LGG patients with the above calculated scores to determine whether the LGG TME and tumor purity are related to the patient's clinical characteristics. ImmuneScore positively correlated with high grade LGG (**Figures 3A–C**, $P < 0.001$), StromalScore also positively correlated with high grade LGG (**Figures 3D–F**, $P < 0.001$), and ESTIMATEScore accompanied with high grade LGG (**Figures 3G–I**, $P < 0.001$). These results indicate that tumor purity and the ESTIMATE scores in the TME are related to the deterioration of LGG. The higher the ESTIMATE scores in the TME, the lower the purity of the tumor and the worse the prognosis of LGG patients.

## Enrichment Analyses of Stromal Related DEGs

To determine the exact changes in the genetic profiles of immune and matrix components in the TME, we used the two packages "limma" (46) and "pheatmap" (47, 48) for analysis, we set the filter conditions to "fdrFilter = 0.05, logFCfilter = 1.5", by reading the expression input file, deleting the normal sample, reading the score file, according to the score The median value groups the samples, performs difference analysis, and outputs the differences of all genes, and then screens out genes that affect survival. We compared high- and low-scoring samples based on the median value (**Figure 4**). We obtained 518 DEGs from StromalScore, which contained 461 upregulated genes and 57 downregulated genes (**Figure 4A**). We also obtained 297 DEGs through ImmuneScore, with 201 upregulated genes and 96 downregulated genes (**Figure 4B**). Through a Venn diagram, we determined that 199 upregulated genes with high scores and 19 downregulated genes with low scores were contained in both ImmuneScore and
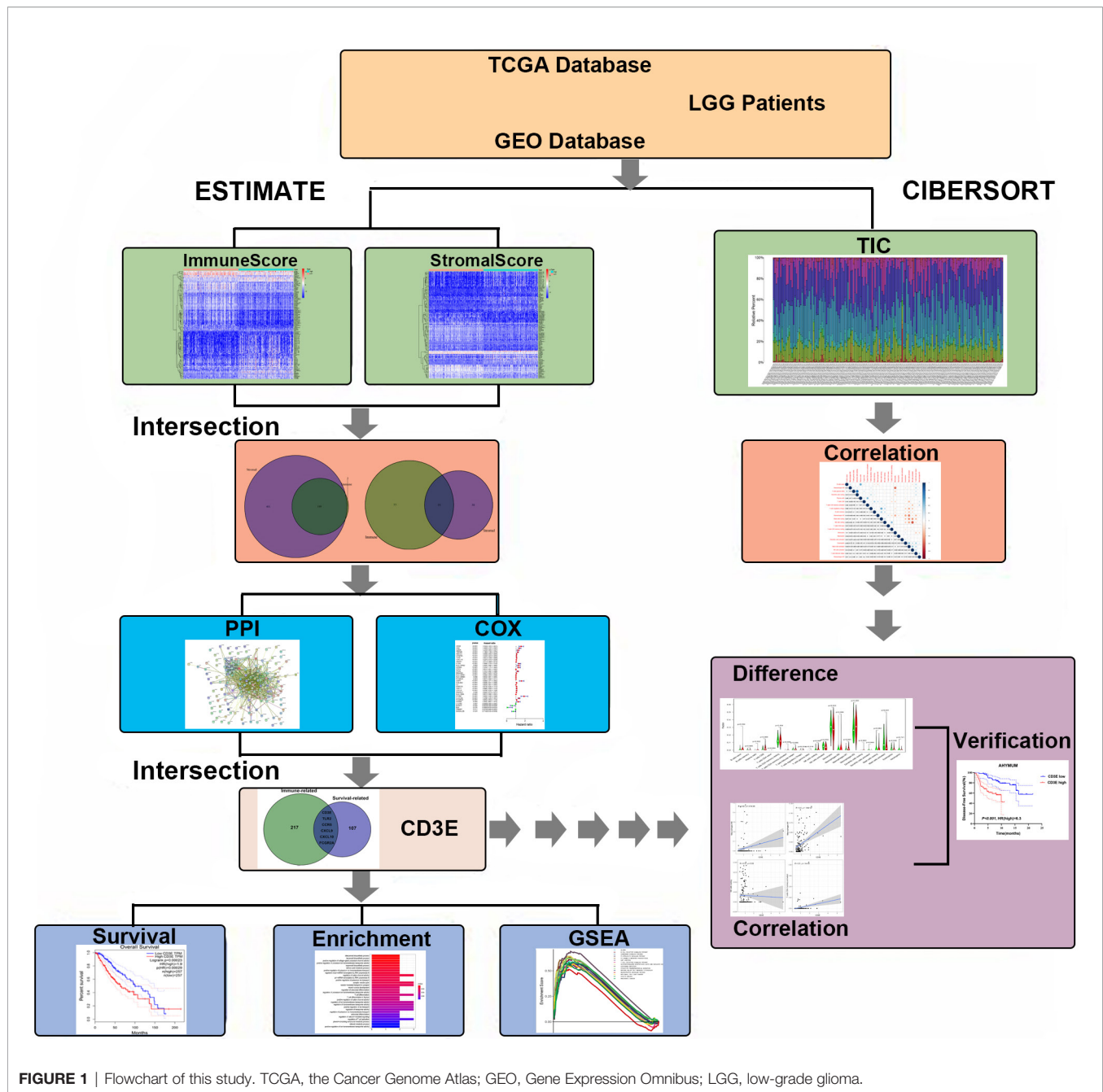
**FIGURE 1** | Flowchart of this study. TCGA, the Cancer Genome Atlas; GEO, Gene Expression Omnibus; LGG, low-grade glioma.

StromalScore (**Figures 5A, B**). These 223 stromal related DEGs may play a decisive role in the LGG TME. Through GO enrichment and KEGG analyses, we found that the biological functions of these genes are mainly related to immunity (**Figures 5C, D**).

## Identification of Key Stromal Related Genes

To further study the underlying mechanisms of the abovementioned genes and determine which were most crucial, we generated a PPI network diagram through String. The

interactions between the genes are shown in **Figure 6A**. We selected the top 30 genes ranked by the number of nodes and plotted them as a bar graph (**Figure 6B**). We performed univariate Cox regression analysis on stromal related DEGs and LGG patient survival to determine which genes are most high risk for LGG patients and which are low risk (**Figure 6C**). Finally, we combined the main nodes in the PPI diagram and the top 75 genes ranked by *P* value to analyze them, and obtained 30 intersecting genes. (**Figure 6D**). These genes are significantly related to the prognosis of LGG.

**FIGURE 2** | Correlation of scores with the survival of patients with LGG. **(A)** Kaplan-Meier survival analysis for LGG patients grouped into high or low score in ImmuneScore determined by the comparison with the median, *P* = 0.003. **(B)** Kaplan–Meier survival curve for StromalScore, p < 0.001. **(C)** Survival analysis with Kaplan–Meier method for LGG patients grouped by ESTIMATEScore, P = 0.006.
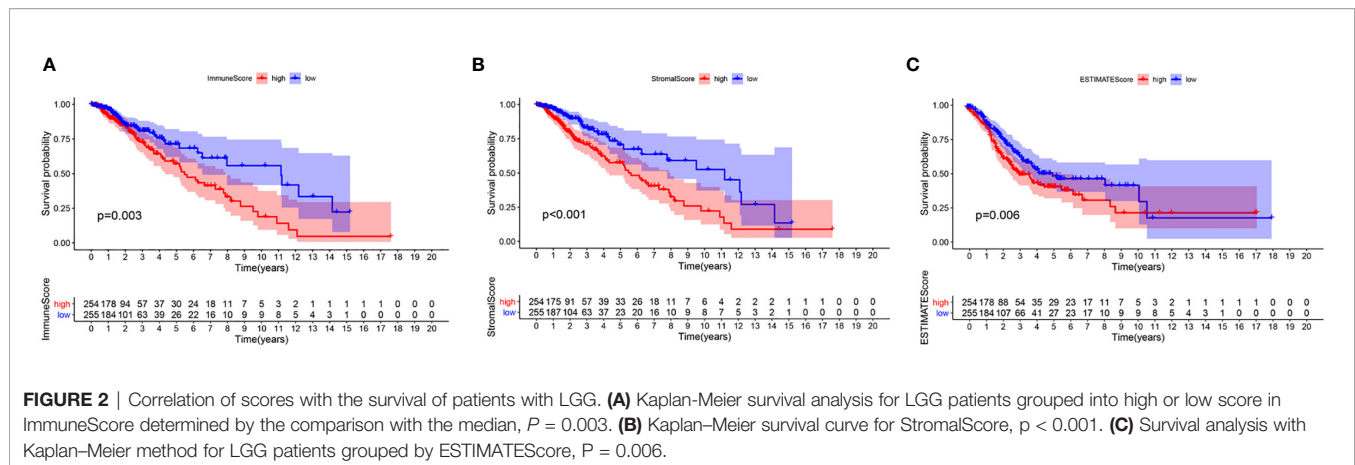
## Filtering Clinical-Related DEGs to Identify a Target Gene

We used the R language package "limma" (46) to screen the genes that affect survival in three GEO sets (GSE107850, GSE60898, GSE26576). We screened 114 clinical-related DEGs (*P* < 0.001) that were significantly related to survival from a group of 13,299 genes and compared them with the previous stromal related DEGs to obtain seven genes: *CD3E, TLR2, CCR5, CXCL9, CXCL10, FCGR2A*, and *ITGAL* (**Figure 6E**). We mapped the PPI network for these seven genes (**Figure 6F**). 78.89% of terms were in co-expression (lavender line), 7.65% of terms were shared protein domains (yellow line), 7.11% of terms were in co-localization (deep blue line), and 7.11% of terms were predicted (khaki line). We also performed GO and KEGG pathway analyses on these seven genes, finding that the genes were related to immune diseases and the inflammatory response (**Figure 6G**).

Next, in order to reduce system bias and select multiple cohorts with large samples to increase the rigor of the research, we also screened the clinically relevant genes in the GEO database. We selected a suitable data set from the GEO database for clinical analysis (GSE107850, GSE60898, GSE26576), comparing it with the immune-related genes, based on the hazard ratio (HR) value of each gene and the survival-related P value, we targeted CD3E for further study.

We divided the dataset into high and low expression groups according to the median *CD3E* expression value and screened using "log fold change = 0.5, and *P* < 0.05". A total of 114 related differential genes were obtained. The 15 genes with the most significant up-regulation and the 11 genes with the most significant down-regulation were selected for further analysis (**Table S1**), which were visualized with a volcano map (**Figure 7A**) and heat map (**Figure 7B**).

## Correlation Analyses of Clinical-Related DEGs and Functional Enrichment Analysis of CD3E in LGG

As illustrated in **Figure 7C**, gene-gene interactions between clinical-related DEGs were analyzed. 95.20% of terms were in co-expression (lavender line) and 4.80% terms were in co-localization (deep blue line). We then conducted a biological function enrichment analysis of clinical-related DEGs. The results showed that enrichments of biological processes included positive regulation of voltage-gated potassium channel activity, positive regulation of potassium ion transmembrane transporter activity, and regulation of pri-miRNA transcription by RNA polymerase II (pol II) (**Figure 7D**); enrichments of cellular components included ion glutamatergic synapse, apical plasma membrane, and apical part of cell (**Figure 7E**); enrichments of molecular functions included oxidoreductase activity, calmodulin binding, and copper ion binding (**Figure 7F**). Enrichments in KEGG pathway analysis were glioma, tyrosine metabolism, and citrate cycle (**Figure 7G**).

We correlated the 20 most significantly up-regulated genes and the 20 most significantly down-regulated genes with *CD3E*. As shown in **Figure 7H**, red represents a positive correlation and green represents a negative correlation. The deeper of the color indicated the greater the relevance. *CD3E* was positively correlated with *LILRB4, UPK1A*, and *REM1*, and negatively correlated with *RIT2, OGDHL*, and *KCNC2* (**Figure 7H**).

Besides, as shown in **Figures S1A, B**, we identified 866 up-regulated genes and 256 down-regulated genes based on top 25% high (G1) and low (G2) CD3E expression in total 256 LGG patients from TCGA using Limma R package with |LogFC| > 2, *P* < 0.05. GO and KEGG enrichment could effectively suggest gene functions and associated high-level genome functional information in **Figures S1C, F**. In addition of this role of signal transduction in T-cell activation and proliferation, CD3E plays an essential role in correct T-cell development, neutrophil activation involved in immune responses, cell adhesion molecules and extracellular matrix organization, thus reshaping suppressive TME and promoting malignant behaviors of LGG.

## *CD3E* Expression Is Negatively Related to LGG Patient Survival

*CD3E* is an epsilon subunit of the T cell antigen receptor. According to the *CD3E* expression median value, all LGG

**FIGURE 3** | Correlation of ImmuneScore and StromalScore with clinicopathological staging characteristics. **(A, D, G)** Distribution of ImmuneScore, StromalScore, and ESTIMATEScore in age. $P$ = 0.6, 0.067, and 0.32. **(B, E, H)** Distribution of three kinds of scores in gender. $P$ = 0.31, 0.28, 0.28. **(C, F, I)** Distribution of scores in grade. $P < 0.001$.
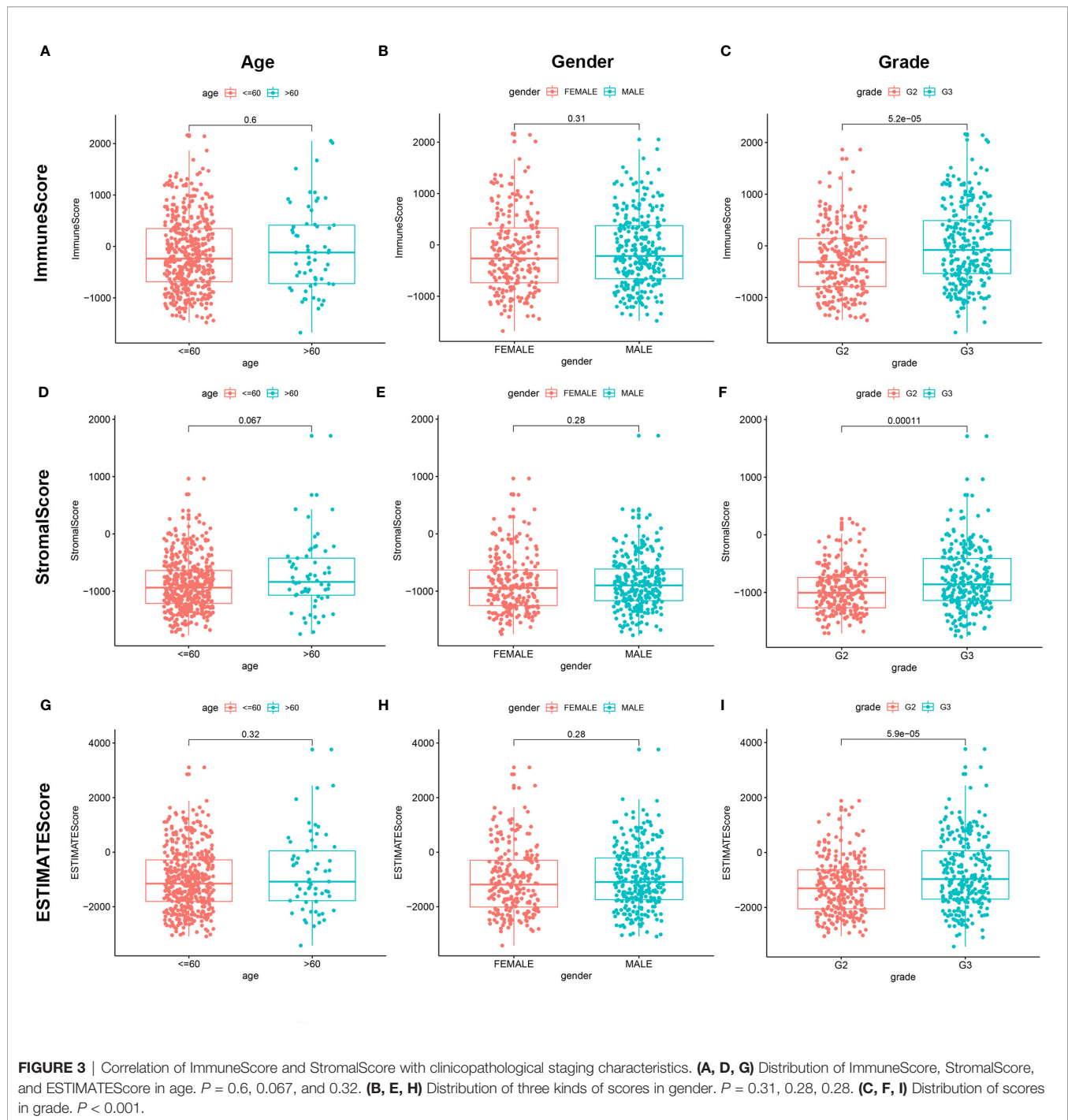
samples were divided into *CD3E* high and low expression groups. Analysis of the TCGA data ($P$ = 0.000637; **Figure 8A**) and GEO data ($P < 0.001$; **Figure 8B**) suggested that the survival rate of LGG patients with high *CD3E* expression was lower than those with low *CD3E* expression. Interestingly, after a literature review and pan-cancer statistical tests (16, 49), we found that *CD3E* may have an opposite prognostic effect in gliomas than in most other tumors (**Figure 8C**). Moreover, it is only in the two head tumors

of uveal melanoma and LGG that the higher the expression is, the worse the prognosis is (**Figure S2**). Finally, we studied the difference in *CD3E* expression between Grade II and Grade III patients in the TCGA cohort. We found that patients with higher grades had higher expression levels of *CD3E* and worse prognosis in the clinic (**Figure 8D**).

At the same time, we conducted a subgroup analysis of different clinical characteristics on clinical data to eliminate

**FIGURE 4** | Heatmaps, Venn plots for DEGs. **(A)** Heatmap for DEGs generated by comparison of the high score group vs. the low score group in ImmuneScore. Row name of heatmap is the gene name, and column name is the ID of samples which not shown in plot. Differentially expressed genes were determined by Wilcoxon rank sum test with q = 0.05 and fold-change > 1 after log2 transformation as the significance threshold. **(B)** Heatmap for DEGs in StromalScore, similar with **(A)**.



**FIGURE 5** | Up-regulated and down-regulated and enrichment analysis of GO and KEGG. **(A, B)** Venn plots showing common up-regulated and down-regulated DEGs shared by ImmuneScore and StromalScore. **(C, D)** GO and KEGG enrichment analysis for DEGs.

**FIGURE 6** | Protein–protein interaction network and univariate COX. **(A)** Interaction network constructed with String. **(B)** The top 30 genes ordered by the number of nodes. **(C)** Univariate COX regression analysis with DEGs was done, listing the top significant factors with *P* < 0.001. **(D)** Venn plot showing the common factors shared by nodes in PPI and top significant factors in univariate COX. **(E)** Venn plot showing the common factors shared by nodes in Stromal related DEGs and Clinical-related DEGs. **(F)** Interaction network constructed with 7 genes. **(G)** GO and KEGG pathway analyses on 7 genes.

clinical bias. We found that the effect of CD3E is still the same in LGG patients with different clinical characteristics (**Figure S3**). Then, we explored differential *CD3E* expression based on the histological subtypes of LGG. Significantly elevated *CD3E*

expression was found in astrocytoma samples ($n$ = 194) compared with oligoastrocytoma samples ($n$ = 130, $P$ = 6.43 × $10^{-4}$) or oligodendroglioma samples ($n$ = 130, $P$ = 6.4187 × $10^{-4}$) (**Figure S4**).
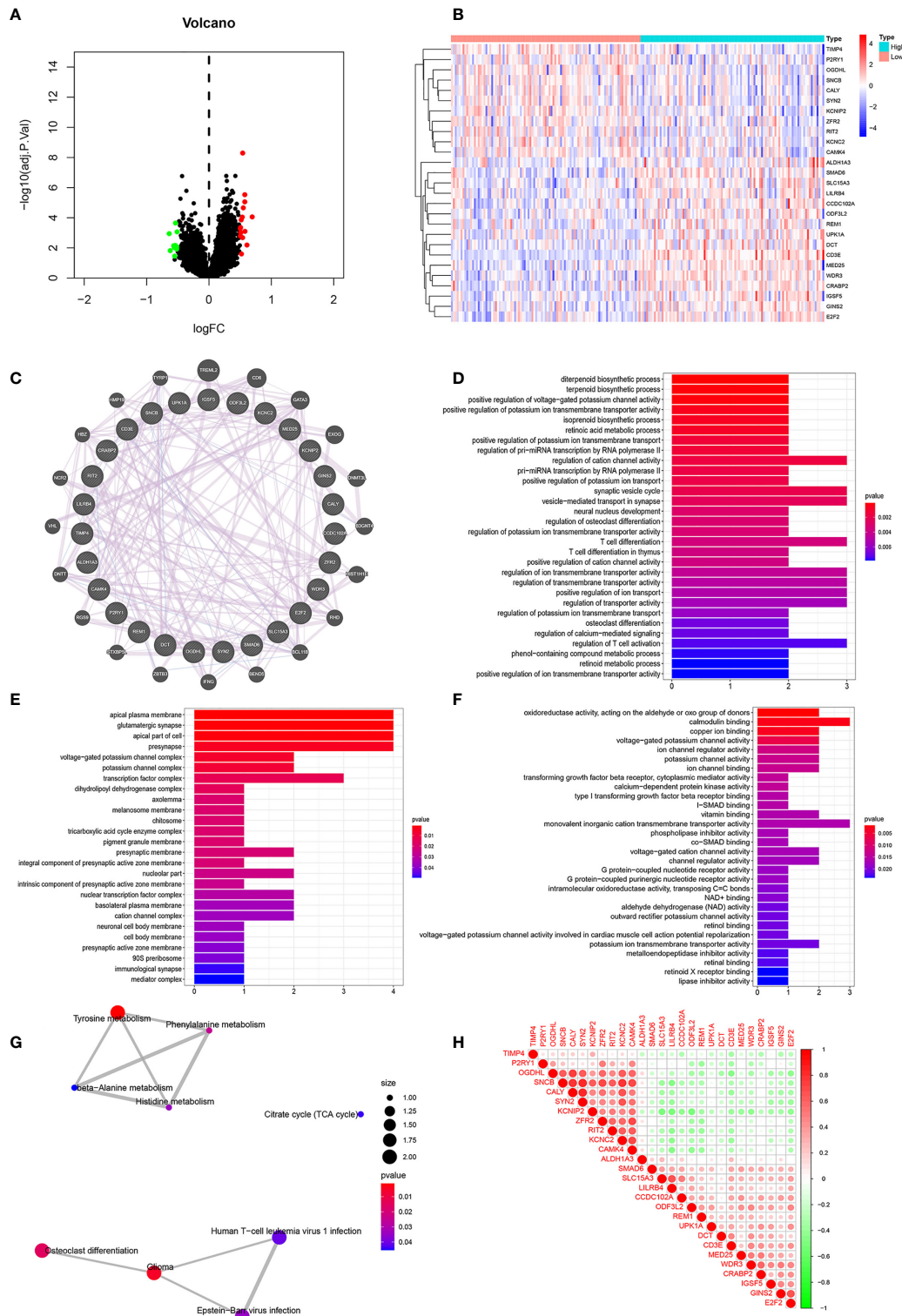
**FIGURE 7** | Correlation Analyses of Clinical-Related DEGs **(A)** The volcano map of Clinical-Related DEGs. **(B)** The heat map of Clinical-Related DEGs. **(C)** PPI of Clinical-Related DEGs. co-expression (lavender line), co-localization (deep blue line). **(D)** The enrichments of biological processes of DEGs. **(E)** The enrichments of cellular components of DEGs. **(F)** The enrichments of molecular functions of DEGs. **(G)** The enrichments in KEGG pathway of DEGs. **(H)** The 20 most significantly up-regulated genes and the 20 most significantly down-regulated genes with *CD3E*. Red color was for positive correlation, and green color represented a negative correlation. The deeper the color indicated the greater the relevance.
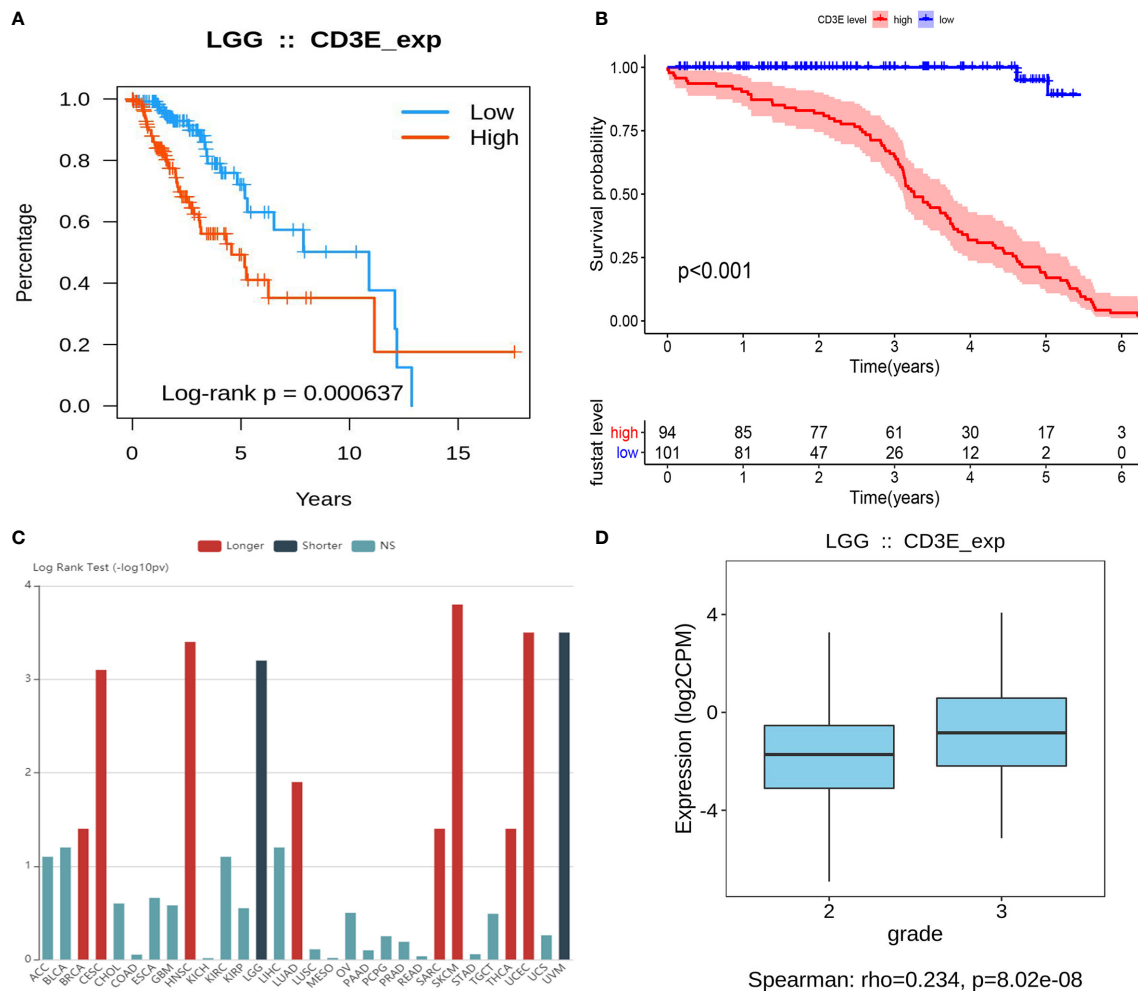
**FIGURE 8** | Relationship between *CD3E* expression and survival of LGG patients **(A)** Relationship between *CD3E* expression and survival of LGG patients in the TCGA database (*P* = 0.000637). **(B)** Relationship between *CD3E* expression and survival of LGG patients in the GSE database (*P* < 0.001). **(C)** CD3E might have completely opposite prognostic effect of CD3E in gliomas than that of most other tumors. **(D)** The relationship between *CD3E* expression and survival of LGG patients.

## Correlation of *CD3E* With the Proportion of TICs

We used the CIBERSORT algorithm to analyze the proportion of TICs for 22 immune cells in LGG to further study the correlation between *CD3E* and the immune microenvironment of LGG. (**Figures 9A, B**). Considering that *CD3E* expression is negatively correlated with the survival rate of LGG patients, we performed GSEA analysis on the high expression group. We found that the genes in the *CD3E* high expression group mainly participated in stromal related activities, such as the B cell receptor signaling pathway, chemokine signaling pathway, and T cell receiver signaling pathway (**Figure 9C**). Furthermore, *CD3E* was positively related to glioma and immune cell response. These results suggest that *CD3E* may be a potential indicator of TME status for LGG.

We found that the expression of *CD3E* is related to 10 groups of TICs in LGG (**Figure 10**). Seven kinds of TICs were positively

correlated with *CD3E* expression, including M0 macrophages, M1 macrophages, resting mast cells, resting NK cells, CD4^{+} memory activated T cells, CD8^{+} T cells, and regulatory T cells. Three kinds of TICs were negatively correlated with *CD3E* expression, including eosinophils, monocytes, and activated NK cells. Then, we calculated the relationship between the abundance of tumor infiltrating lymphocytes and the expression, copy number, methylation, or mutation of *CD3E* in LGG (**Figure S5**). These results suggest that *CD3E* is related to the immune activity of the TME, thereby affecting the tumor purity of LGG.

Next, we aimed to investigate predictive role of CD3E expression in predicting responses to immune checkpoint inhibitors of LGG using Tumor Immune Dysfunction and Exclusion (TIDE) algorithm. Interestingly, we found that TIDE score was significantly higher in CD3E^{high} group compared with CD3E^{low} group in 255 LGG patients (*P* = 0.001), suggesting poor
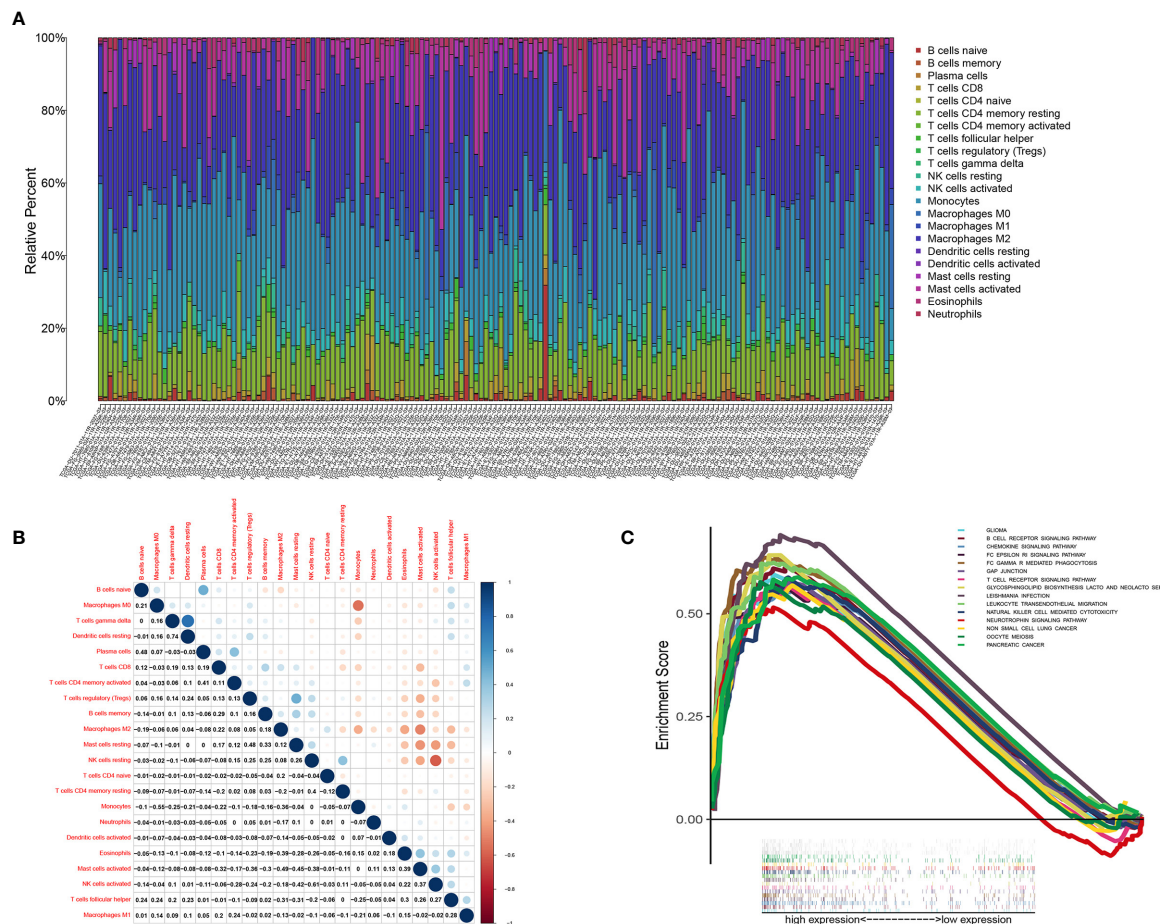
**FIGURE 9** | TIC profile in tumor samples and correlation analysis. **(A)** Barplot showing the proportion of 22 kinds of TICs in LGG tumor samples. Column names of plot were sample ID. **(B)** Heatmap showing the correlation between 22 kinds of TICs and numeric in each tiny box indicating the p value of correlation between two kinds of cells. The shade of each tiny color box represented corresponding correlation value between two cells, and Pearson coefficient was used for significance test. **(C)** GSEA for samples with high *CD3E* expression.

prognosis of LGG patients with high CD3E expression and the poor tolerance of immune checkpoint inhibitor therapy (**Figure S6**).

## Single Cell Analysis of CD3E in Brain Tumors

To further explore the mechanism by which CD3E promotes tumor immune evasion in brain tissue and LGG, we performed complex bioinformatics work including functional enrichment and GSEA analyses. The results suggested that CD3E is more likely to participate in T cell-regulated immune deficiency as one of its important roles in the formation of the TCR. Next, we enrolled six glioma single-cell sequencing datasets from GEO analysis (GSE131928 10X, GSE131928 Smartseq2, GSE135437, GSE139448, GSE141982, and GSE148842), which suggested significantly elevated *CD3E* expression in CD8$^+$ T cells, especially the exhaustive T cells. Therefore, we hypothesize that CD3E possibly contributes to an immune evasion mechanism in brain tumors by leading to T cell dysfunction (**Figure 11**).

## Clinicopathological Features Related to *CD3E* Expression

To verify *CD3E* expression in LGG, we performed immunohistochemistry (IHC) (**Figures 12A, B**). The scatter plot of the IHC scores revealed that *CD3E* expression increased in LGG tissues in the AHYMUN cohort ($P < 0.01$). In **Table 1**, we show that higher *CD3E* expression correlates with patient age ($P = 0.027$), grade ($P < 0.001$), microvascular invasion ($P = 0.009$), history of epilepsy ($P < 0.001$), and Karnofsky score ($P = 0.002$). We believe this indicates that the higher the expression of *CD3E* in patients, the worse the prognosis.

## Cox Regression Analysis

We used univariate Cox regression analysis to demonstrate the relationship between *CD3E* and AHYMUN patients and found that *CD3E* is not significantly related to age and gender (**Figure 12C**). In the multivariate model, we also found that patients in the high expression group had worse OS (HR = 3.22; $P = 0.001$). Moreover, in the AHNTU cohort, the microvascular

**FIGURE 10** | Correlation of TICs proportion with *CD3E* expression. **(A)** Violin plot showed the ratio differentiation of 22 kinds of immune cells between LGG tumor samples with low or high *CD3E* expression relative to the median of *CD3E* expression level, and Wilcoxon rank sum was used for the significance test. **(B)** Venn plot displayed ten kinds of TICs correlated with *CD3E* expression codetermined by difference and correlation tests displayed in violin and scatter plots, respectively. **(C)** Scatter plot showed the correlation of 14 kinds of TICs proportion with the *CD3E* expression (*P* < 0.05). The red line in each plot was fitted linear model indicating the proportion tropism of the immune cell along with *CD3E* expression, and Pearson coefficient was used for the correlation test.

invasion (HR = 1.52; *P* = 0.024), the presence of capsular infiltration (HR = 1.63; *P* = 0.016), and the Karnofsky scores (ref < 80) (HR = 1.46; *P* = 0.023) were associated with low OS (**Table 2**).

We found that the patient's gender and epilepsy history were not related to DFS (**Figure 12D**). We found through Cox analysis that the high expression of the *CD3E* gene caused a significant decrease in OS (HR = 4.33; *P* < 0.001) (**Table S1**). Grade, capsular infiltration, microvascular invasion, and Karnofsky scores were related to OS (*P* < 0.05). As seen in **Figures 12E, F**, the higher the *CD3E* expression level, the lower the OS and DFS of LGG patients.

## Down-Regulation of CD3E Inhibits Cell Proliferation and Invasion Abilities in N9 and N33 Cells

To explore biological malignancy of CD3E in LGG, we used siRNA methods to restrain the expression of CD3E. Western blot showed that CD3E protein expression was markedly decreased after siRNA-CD3E transfection, compared with the negative control group (**Figures 13A, B**). CCK8 assay showed that the decreased CD3E expression significantly inhibited cell proliferation in N9 and N33 cells (**Figures 13C–E**). Still, we found that when expression of CD3E was inhibited, the invasion

ability of N9 and N33 cell lines was significantly reduced compared with normal genitive control group (**Figure 13E**). Taken together, down-regulated CD3E expression significantly restrained LGG cells proliferation and invasion capacities, thus may reducing the malignant biological behaviors and aggressive progression of LGG.

## DISCUSSION

In this study, we first screened the immune genes related to the TME in LGG patients from the TCGA database. Next, we screened genes related to the prognosis of LGG patients from GEO. After combining the above genes, we determined *CD3E* to be the main target gene. Then, we conducted a series of bioinformatics analyses and verified the research results at our own center. We found that *CD3E* may be an indicator gene of the TME status of LGG patients and, by affecting the TME of LGG, can thereby change the tumor purity and affect the prognosis of patients.

The combination of the cancer cell genotype, its gene expression pattern, and the influence of the TME determines the tumor's adaptability, evolution, and resistance to treatment (50). In recent years, studies using TCGA and GSE have mapped the genetic picture and overall expression status of numerous
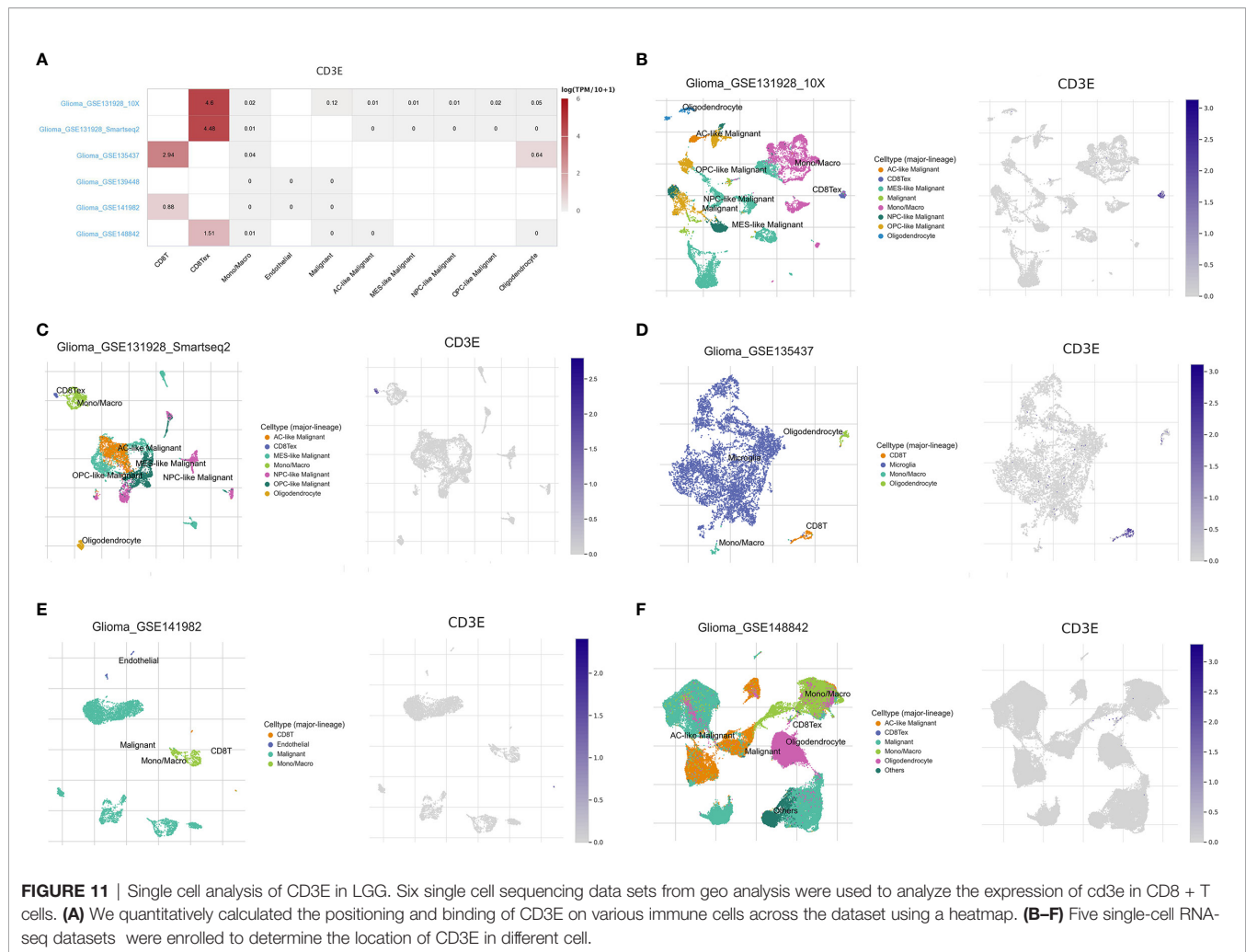
**FIGURE 11** | Single cell analysis of CD3E in LGG. Six single cell sequencing data sets from geo analysis were used to analyze the expression of cd3e in CD8 + T cells. **(A)** We quantitatively calculated the positioning and binding of CD3E on various immune cells across the dataset using a heatmap. **(B–F)** Five single-cell RNA-seq datasets were enrolled to determine the location of CD3E in different cell.

tumors, identified driver mutations, and defined tumor subtypes based on specific transcription profiles (51, 52).

LGG is a common brain tumor, and the prognosis of patients with WHO grade II and III is normally poor (53). However, surgery, radiation therapy, or chemotherapy (usually using temozolomide) often cannot improve the prognosis and survival of patients (54, 55). The reasons for the lack of progress include the growth of invasive tumors in basic organs, which limits the utility of local therapies. Additionally, the protection of tumor cells by the blood-brain barrier limits the drug concentration, while the blood-tumor barrier protects tumor cells (56). When pursuing immune-based glioblastoma treatment methods, the unique immune environment of the central nervous system needs to be considered (57–59). Therefore, we need to study novel LGG immunotherapy candidates. Here, we began with the transcriptional analysis of LGG data in TCGA and found that the decreased expression of *CD3E* is closely related to poor prognosis of patients. Therefore, *CD3E* is a potential prognostic indicator and treatment target in LGG patients.

Yoshihara et al. developed an algorithm for evaluating tumor purity (60), using gene expression data to evaluate the presence of antigen cells and the penetration of immune cells in tumor

samples. The evaluation algorithm proved to be a robust tumor fine prediction algorithm. Previous studies have shown that low tumor purity is associated with poor prognosis in colon cancer, gastric cancer and glioma (27, 61). However, there are few studies on specific genes that affect tumor purity and thus affect LGG. Our research shows that the purity of tumors affected by CD3E plays an important role in predicting the prognosis and genomic status of LGG. The higher the expression of CD3E, the lower the purity of LGG tumors, which is associated with enhanced immune escape and poor prognosis, suggesting that patients with low-purity LGG may benefit more from immunotherapy. In order to better understand TME and make better clinical decisions, further research on tumor purity is needed.

*CD3E* encodes the polypeptide CD3-ϵ, which together with the CD3-γ, -δ and -ZETA and T-cell receptor α/β and γ/δ T cell receptor heterodimer -CD3 complex. The complex plays an important role in coupling antigen recognition to several intracellular signal transduction pathways, so defects in *CD3E* can lead to immunodeficiency (62). CD3E role as a biological component that is functionally important for T cell receptor signaling for proper immunity. This is why the molecule appeared to be increased and as they proposed that would
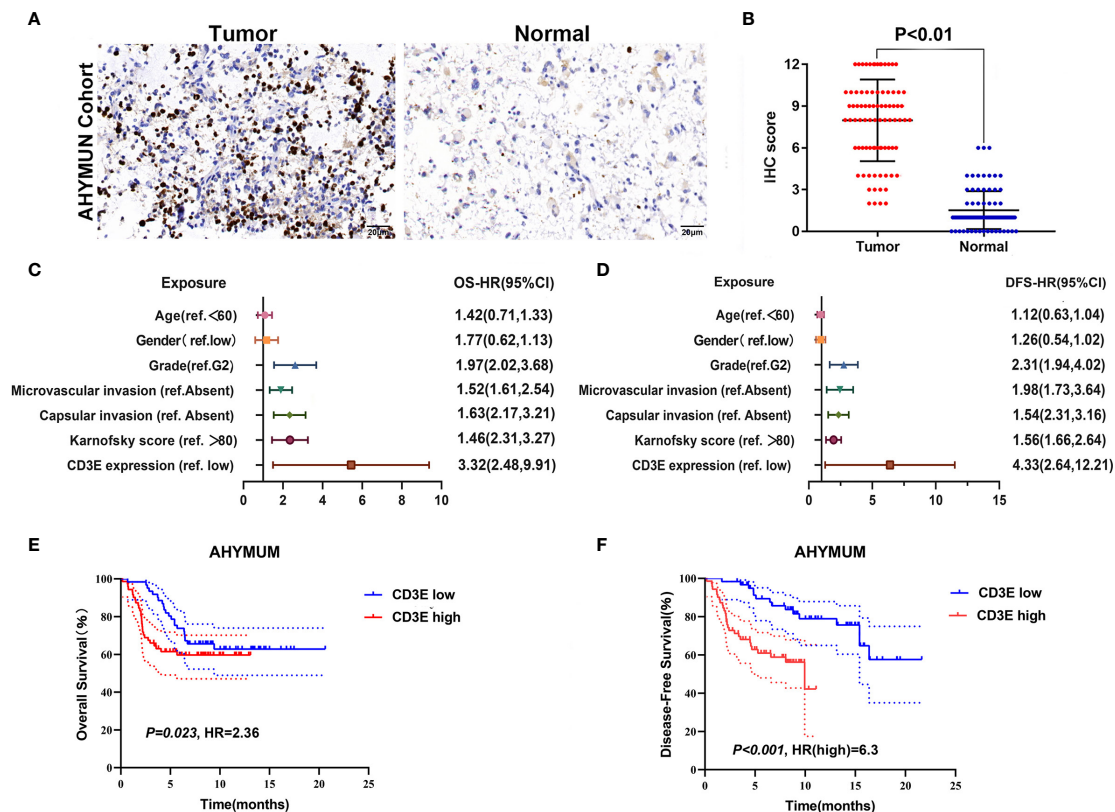
**FIGURE 12** | The relationship between *CD3E* gene and LGG prognosis was further verified. **(A)** IHC on collected LGG tissue. **(B)** The scatter plot of the IHC scores (*P* < 0.01). **(C, D)** Forest plots were used to visualize the univariate Cox regression analysis of OS and DFS in the AHYMUM cohorts. **(E, F)** Survival curves showed that LGG patients with elevated *CD3E* expression levels in the AHYMUN cohort showed poorer OS (*P* = 0.023) and poorer DFS (*P* < 0.001).

relate to a poorer prognosis. In fact, the more T cells in the tissue would mean that T cell immunity occurs there to act against tumor cells as ones would expect. However, there are many T cell subsets most of which have CD3E as the TCR/CD3 complex component, yet they perform different function ranging from protection (e.g., CD4 and CD8 T cells against viruses and tumors), autoimmune (self-reactive T cells), to those that suppress other T cells (e.g., regulatory T cells). CD3E is a part of the TCR-CD3 complex on the surface of T lymphocytes, and its basic immune function plays a vital role in the adaptive immune response. When antigen-presenting cells activate T cell receptors, TCR-mediated signals are transmitted across the cell membrane through the CD3 chain CD3D, CD3E, CD3G, and CD3Z, thereby activating downstream signaling pathways. In addition to the role of signal transduction in T cell activation, CD3E also plays a vital role in correct T cell development. The TCR-CD3 complex assembly is initiated by forming two heterodimers CD3D/CD3E and CD3G/CD3E. It also participates in the internalization of the TCR-CD3 complex and the down-regulation of the cell surface through the endocytosis sequence present in the cytoplasmic region of CD3E (49, 63). CD3E also participates in proper T cell development. TCR-CD3 complex assembly is initiated by the formation of two heterodimers: CD3D/CD3E and CD3G/CD3E.

Additionally, CD3E participates in the internalization of TCR-CD3 complexes and cell surface down-regulation by endocytic sequences present in the cytoplasmic region of CD3E (49, 63, 64). The relationship between the abundance of tumor infiltrating lymphocytes and the expression, copy number, methylation, or mutation of *CD3E* in LGG is shown in **Figure S1**.

In LGG patients, the higher the expression of *CD3E* signified the worse the patient's survival. It may be attributed to immune cells with high *CD3E* expression promoting anti-tumor immunity, except regulatory T cells. Similarly, CD3E acts as a T cell receptor. Its high expression in many cancers indicates better clinical results (longer survival), with the lone exception of LGG (65). This may be related to the cause of LGG and the immune environment of the brain, or it may be due to the interconnection between isocitrate dehydrogenase and the TME (66–68). In CD3E knockdown experiments, we found down-regulated CD3E expression significantly restrained LGG cells proliferation and invasion capacities, thereby further reducing the malignant biological behaviors and aggressive progression of LGG, which may be closely related to the functional involvement of CD3E in TME of LGG. Studies have shown that combining CD3E antibodies with antibodies that bind to mutant epidermal growth factor receptor variant III can effectively treat mice with gliomas (69). Therefore, *CD3E* may play a dual role in tumors,

**TABLE 1 |** Clinicopathological characteristics in relation to CD3E expression level in AHYMUM cohort.

| Characteristics | AHYMUN cohort | CD3E expression | | $\chi^2$ | P |
|---|---|---|---|---|---|
| | (N=100) | Low IHC score (N = 50) | High IHC score (N = 50) | | |
| N (%) | | | | | |
| Age | | | | 4.889 | **0.027** |
| <60 years | 55 (0.55) | 33 (0.60) | 22 (0.40) | | |
| ≥60 years | 45 (0.45) | 17 (0.38) | 28 (0.72) | | |
| Gender | | | | 0.271 | 0.603 |
| Male | 82 (0.82) | 40 (0.49) | 42 (0.51) | | |
| Female | 18 (0.18) | 10 (0.56) | 8 (0.44) | | |
| Grade | | | | 14.924 | **<0.001** |
| G2 | 69 (0.69) | 39 (0.57) | 30 (0.43) | | |
| G3 | 31 (0.31) | 11 (0.35) | 20 (0.65) | | |
| Seizure history | | | | 12.148 | **<0.001** |
| yes | 61 (0.61) | 39 (0.64) | 22 (0.36) | | |
| no | 39 (0.39) | 11 (0.28) | 28 (0.72) | | |
| Microvascular invasion | | | | 6.828 | **0.009** |
| Absent | 55 (0.55) | 34 (0.62) | 21 (0.38) | | |
| Present | 45 (0.45) | 16 (0.36) | 29 (0.64) | | |
| Capsular invasion | | | | 1.961 | 0.161 |
| Absent | 51 (0.51) | 29 (0.57) | 22 (0.43) | | |
| Present | 49 (0.49) | 21 (0.43) | 28 (0.57) | | |
| Karnofsky score | | | | 9.180 | **0.002** |
| ≥80 | 61 (0.61) | 36 (0.59) | 21 (0.41) | | |
| <80 | 39 (0.39) | 14 (0.36) | 29 (0.64) | | |

IHC, immunohistochemistry; AHYMUN, Affiliated Hospital of YouJiang Medical University for Nationalities.
P value less than 0.05 was considered as statistical significance and marked in bold.

**TABLE 2 |** Multivariate Cox regression analysis of DFS and OS in AHYMUM cohorts.

| Covariates | OS | | | DFS | | |
|---|---|---|---|---|---|---|
| | HR | 95% CI | *P* value | HR | 95% CI | *P* value |
| Grade (ref. G2) | 1.97 | 2.25-3.68 | **0.043** | 2.31 | 1.94-4.02 | **0.037** |
| Microvascular invasion (ref. Absent) | 1.52 | 1.61-2.54 | **0.024** | 1.98 | 1.73-3.64 | **0.031** |
| Capsular invasion (ref. Absent) | 1.63 | 2.17-3.21 | **0.016** | 1.54 | 2.31-3.16 | **0.017** |
| Karnofsky score (ref. >80) | 1.46 | 2.31-3.27 | **0.023** | 1.56 | 1.66-2.64 | **0.044** |
| CD3E expression (ref. low) | 3.32 | 2.48-9.91 | **0.001** | 4.33 | 2.64-12.21 | **<0.001** |

DFS, disease-free survival; OS, overall survival.
P value less than 0.05 was considered as statistical significance and marked in bold.

either promoting survival or inducing apoptosis. In our Western blot and CCK8 experiments, we found that the higher the expression of CD3E represented the higher the invasion of tumor cells. This is one of the reasons why the higher the expression of CD3E, the worse the survival of LGG patients.

In addition, in the TME of glioma, the proliferation of malignant cells is enhanced, the pool of undifferentiated glioma cells increases, and macrophage expression exceeds microglial expression (65–68). Still, it is an interesting question that *CD3E* may have a completely opposite prognostic effect in gliomas than that in most other tumors. In this study, *CD3E* was selected because it had the most significant prognostic value (HR=1.552, *P*<0.001) of LGG. DEGs screened according to *CD3E* expression were mainly involved in stromal related activities. Additionally, significantly increased *CD3E* expression was found in 100 LGG samples from a validation cohort compared with adjacent normal brain tissues. High *CD3E* expression could serve as an independent prognostic indicator

for OS and DFS of LGG. CD3E normally plays an important role in the formation of the TCR and participates in multiple signaling pathways in T cell-regulated immune deficiency. After a literature review and pan-cancer statistical tests, we found that *CD3E* may have a completely opposite prognostic effect in gliomas than in most other tumors (**Figure 8C**), except for Uveal Melanoma (**Figure S2**) and LGG. In our research, we found that CD3E is highly expressed in T cells. Through bioinformatics and immunohistochemistry studies, we found that CD3E is also highly expressed in LGG. Therefore, we studied the expression of CD3E in pan-cancer cell lines (**Figure S7**), and we found that the expression of CD3E in all tumors is not the highest in gliomas. However, in the above studies, we found that the higher the expression of CD3E, the worse the prognosis of LGG, which is completely opposite to tumors such as liver cancer and breast cancer. We considered that CD3E plays an active role in most TMEs and passed It binds to T cell surface receptors in the form of a complex to regulate T
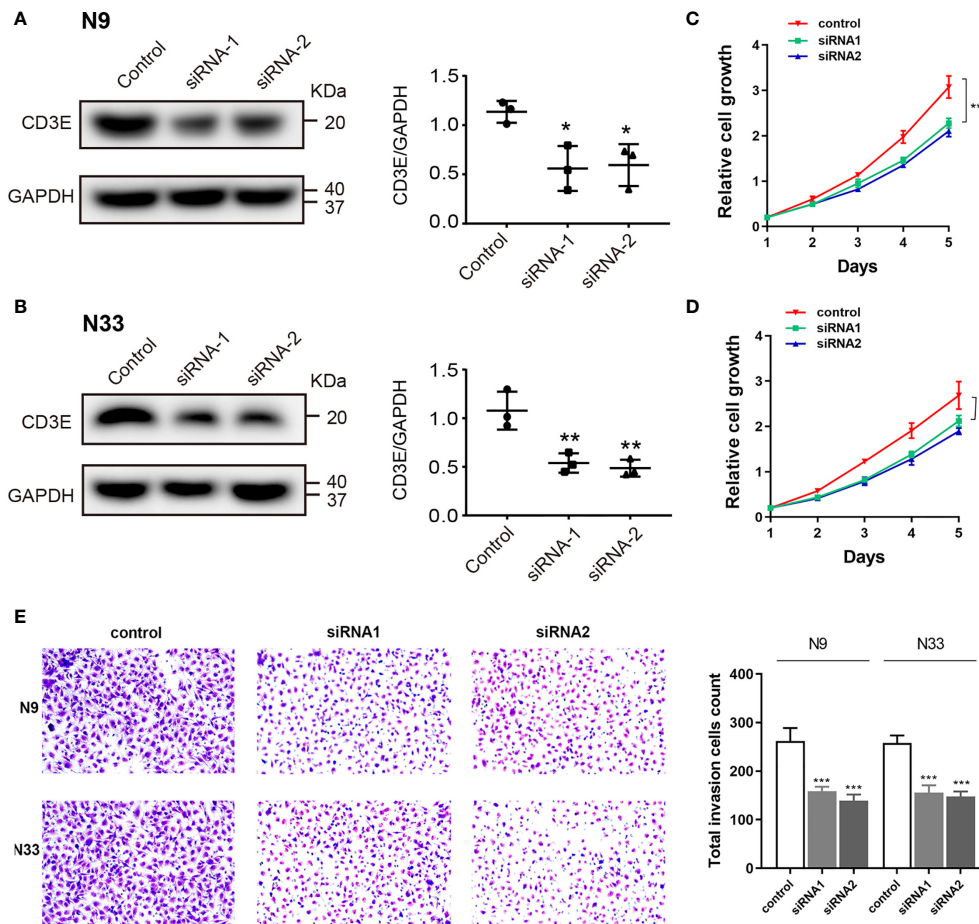
**FIGURE 13** | Down-regulation of CD3E inhibits cell proliferation and invasion abilities in LGG cells. **(A, B)** Western blot showed that CD3E protein expression was markedly decreased after siRNA-CD3E transfection. **(C, D)** CCK8 assay showed that the decreased CD3E expression significantly inhibited cell proliferation in N9 and N33 cells. **(E)** Transwell assay showed that when expression of CD3E was inhibited, the invasion ability of N9 and N33 cell lines was significantly reduced.

cell-mediated anti-tumor immune evasion. The immune system is usually limited to the brain. The activation of various immune cells in LGG makes TME different from other solid tumors. Therefore, we hypothesized that CD3E, as one of the main regulatory elements of the LGG immune microenvironment, may play an important role in LGG immune evasion and the shaping of the immunosuppressive microenvironment. In the previous bioinformatics analysis, we found through single cell analysis of brain tumors that the expression of CD3E is particularly prominent in CD8^{+} T cells. Therefore, we hypothesized that CD3E may promote the immune evasion mechanism of brain tumors by causing T cell dysfunction in the immune cell population. In subsequent experiments, we found that the higher the expression of CD3E in tumor cells, the stronger the invasion ability of LGG. We know that the cells and molecules in TME are in a process of dynamic changes at any time. Stromal cells and immune cells jointly promote the proliferation, apoptosis, metastasis and immune escape of cancer cells (70); while tumor invasion and infiltration are often time-sensitive, influencing TME all the time. Therefore, we made an audacious hypothesis that the reason why CD3E can be used as an independent molecular marker to test the prognosis of LGG patients is because it affects both immune cells and tumor cells. It can be said that in LGG, CD3E is the key gene for tumor cells and TME to influence each other, and it is the bridge between the two. Further studies would focus on the underlying mechanism of CD3E in immune microenvironment of LGG.

Our GSEA results also suggested that high *CD3E* expression enriched stromal related signaling pathways, such as B/T cell receptor signaling pathways and chemokine signaling pathways. These results indicate that *CD3E* may be involved in the transition of the TME from immune-based to metabolic-based. An increasing number of studies show that *CD3E* is related to tumor treatment (71–73). Our research also found that the balance between tumor pathways, sugar metabolism, and lactic acid formation can affect the immune status of LGG. Therefore, we suspect that in the development of LGG, the up-regulation of *CD3E* promotes the decline of tumor purity. Simultaneously, the transition of the TME from immune-based to metabolic-based further promotes the deterioration of LGG.

We also found that positive regulation of voltage-gated potassium channel activity is related to LGG. MicroRNAs (miRNAs) can reportedly promote the development of invasive nonfunctional pituitary adenomas (74, 75). Current knowledge suggests that voltage-gated potassium channels play a fundamental role in the generation and transmission of action potential (76), but their role in tumors has not been deeply studied. Whether genes can affect the tumor immune microenvironment through action potential is an area of further research. We found that positive regulation of potassium ion transmembrane transporter activity is related to LGG as well, so we can confirm that potassium ions play an important role in LGG. Previous studies have found that DNA methylation promotes the invasion and development of osteosarcoma through potassium ion transmembrane transporter activity (77). Perhaps DNA methylation is associated with ion channels and the immune microenvironment, and *CD3E* is a bridge between the three. There are many studies on the regulation of miRNA transcription by RNA pol II and glioma. Some studies have found that overexpression of EGR-1 may participate in the recruitment of RNA pol II to the GDNF promoter in a non-binding manner, and thus is involved in the regulation of GDNF transcription in glioma cells. This regulation depends on histone hyperacetylation of the GDNF promoter (78). Whether *CD3E* is related to this will be the focus of future investigations. Some studies have found that the ion glutamatergic synapse is associated with medulloblastoma in children (78, 79), while miR-375 also affects the occurrence and development of gastric cancer (80). Therefore, we speculate that *CD3E* and miRNAs may affect the invasion of glioma through the ion glutamate synapse. Some scientists have found that rotenone sensitive NADH ubiquinone oxidoreductase is a key regulatory step in controlling oxidative phosphorylation during the growth period in rat glioma cells (81). Based on the abovementioned bioinformatics analyses of *CD3E*-related core genes in LGG, we found that *CD3E* may be a core gene that can affect the immune microenvironment and tumor purity of LGG in combination with miRNAs, cell respiration, ion channels, and DNA methylation. The role of *CD3E* in brain tumors is completely different from that of extracranial tumors. This may be because *CD3E*, as a core gene, regulates the tumor immune microenvironment in a completely different manner than that of extracranial tumors. However, malignant behavior of CD3E in progression of glioma cell was not elucidated in this study. In follow-up research, we could devote ourselves to exploring the biological malignant function of CD3E and its regulatory mechanism on the tumor immune microenvironment in *in vitro* cell lines, *in vivo* animals, and large-scale multicenter LGG patients.

Overall, we used the ESTIMATE algorithm to determine the TME-related genes in LGG by analyzing LGG samples in TCGA datasets. Through the analysis of LGG samples in GEO, we identified prognostic-related genes in LGG. In our current study, there are still many shortcomings. The first is that the LGG samples we collected are still single-center, the sample size is also small, and they are all Asian patients. We will further expand the samples in the next research. Additionally, we will conduct research on LGG patients in Europe, Africa and other places. The second is that this experiment lacks research on the expression of CD3E in different cell populations in tumor samples. In the next work, we will focus on this direction. The abovementioned studies confirmed that *CD3E* is not only a potential prognostic factor for LGG patients, but also a driving factor for the TME to transform from an immune state to a metabolic state. In the next study, we intend to study the expression of CD3E in different cell populations in LGG to clarify the cell types that express CD3E, as well as how the expression of CD3E in different cell populations affects TME.

## CONCLUSION

In conclusion, tumor purity has a considerable impact on clinical, genomic and biological status of LGG. *CD3E*, novel membrane immune biomarker deeply affecting tumor purity, may help to evaluate the prognosis and develop individual immunotherapy strategies for LGG patients. Evaluating the ratio of different tumor purity and *CD3E* expression may provide novel insights into the complex structure of the LGG microenvironment and targeted drug development.

## DATA AVAILABILITY STATEMENT

The original contributions presented in the study are included in the article/**Supplementary Material**. Further inquiries can be directed to the corresponding authors.

## ETHICS STATEMENT

All of the study designs and test procedures were performed in accordance with the Helsinki Declaration II. The Ethics approval and participation consent of this study was approved and agreed by the ethics committee of Affiliated Hospital of Youjiang Medical College for Nationalities (Baise, Guangxi province, China).

## AUTHOR CONTRIBUTIONS

HNH, WL, and CL came up with the design and conception. The data analysis and visualization were conducted by WX, HDH, and XL. YW and WL conducted cell line experiments. The original writing of the draft and its editing were by SC, JW,

WL, and HZ. All authors contributed to the article and approved the submitted version.

## SUPPLEMENTARY MATERIAL

The Supplementary Material for this article can be found online at: https://www.frontiersin.org/articles/10.3389/fonc.2021.676124/full#supplementary-material

**Supplementary Figure 1 |** The relationship between *CD3E* expression and survival of UVM patients was shown.

**Supplementary Figure 2 |** The differential expression of cd3e was investigated according to the histological subtypes of LGG. The expression of CD3E in astrocytoma (n = 194) was significantly higher than that in oligoastrocytoma (n = 130, P = 6.436000e-04) or oligodendroglioma (n = 130, P = 6.418700e-04).

**Supplementary Figure 3 |** A subgroup analysis of different clinical characteristics on clinical data to eliminate clinical bias was performed.

**Supplementary Figure 4 |** Relations between abundance of tumor-infiltrating lymphocytes and expression, copy number, methylation, or mutation of *CD3E*.

**Supplementary Figure 5 |** The relationship between the abundance of tumor infiltrating lymphocytes and the expression, copy number, and methylation or mutation of CD3E in LGG was analyzed.

**Supplementary Figure 6 |** TIDE algorithm to study the effect of CD3E on LGG patients receiving immune checkpoint inhibitor therapy.

**Supplementary Figure 7 |** The expression distribution of CD3E gene in different tumor tissues was shown. The horizontal axis represented different groups of samples, and the vertical axis represented the expression distribution of the gene.

## REFERENCES

1. Ceccarelli M, Barthel FP, Malta TM, Sabedot TS, Salama SR, Murray BA, et al. Molecular Profiling Reveals Biologically Discrete Subsets and Pathways of Progression in Diffuse Glioma. *Cell* (2016) 164(3):550–63. doi: 10.1016/j.cell.2015.12.028

2. Davis ME. Glioblastoma: Overview of Disease and Treatment. *Clin J Oncol Nurs* (2016) 20(5 Suppl):S2–8. doi: 10.1188/16.CJON.S1.2-8

3. Schwartzbaum JA, Fisher JL, Aldape KD, Wrensch M. Epidemiology and Molecular Pathology of Glioma. *Nat Clin Pract Neurol* (2006) 2(9):494–503; quiz 1 p following 516. doi: 10.1038/ncpneuro0289

4. Diwanji TP, Engelman A, Snider JW, Mohindra P. Epidemiology, Diagnosis, and Optimal Management of Glioma in Adolescents and Young Adults. *Adolesc Health Med Ther* (2017) 8:99–113. doi: 10.2147/AHMT.S53391

5. Louis DN, Perry A, Reifenberger G, von Deimling A, Figarella-Branger D, Cavenee WK, et al. The 2016 World Health Organization Classification of Tumors of the Central Nervous System: A Summary. *Acta Neuropathol* (2016) 131(6):803–20. doi: 10.1007/s00401-016-1545-1

6. Kesari S, Schiff D, Drappatz J, LaFrankie D, Doherty L, Macklin EA, et al. Phase II Study of Protracted Daily Temozolomide for Low-Grade Gliomas in Adults. *Clin Cancer Res* (2009) 15(1):330–7. doi: 10.1158/1078-0432.CCR-08-0888

7. McCormack BM, Miller DC, Budzilovich GN, Voorhees GJ, Ransohoff J. Treatment and Survival of Low-Grade Astrocytoma in Adults–1977-1988. *Neurosurgery* (1992) 31(4):636–42; discussion 642. doi: 10.1227/00006123-199210000-00004

8. Turkoglu E, Gurer B, Sanli AM, Dolgun H, Gurses L, Oral NA, et al. Clinical Outcome of Surgically Treated Low-Grade Gliomas: A Retrospective Analysis of a Single Institute. *Clin Neurol Neurosurg* (2013) 115(12):2508–13. doi: 10.1016/j.clineuro.2013.10.010

9. Rathore S, Niazi T, Iftikhar MA, Chaddad A. Glioma Grading Via Analysis of Digital Pathology Images Using Machine Learning. *Cancers (Basel)* (2020) 12(3). doi: 10.3390/cancers12030578

10. Liu W, Xu W, Li C, Xu J, Huang K, Hu R, et al. Network Pharmacological Systems Study of Huang-Lian-Tang in the Treatment of Glioblastoma Multiforme. *Oncol Lett* (2021) 21(1):18. doi: 10.3892/ol.2020.12279

11. Liu WR, Li CY, Xu WH, Liu XJ, Tang HD, Huang HN. Genome-Wide Analyses of the Prognosis-Related mRNA Alternative Splicing Landscape and Novel Splicing Factors Based on Large-Scale Low Grade Glioma Cohort. *Aging (Albany NY)* (2020) 12(13):13684–700. doi: 10.18632/aging.103491

12. Zheng J, Xu W, Liu W, Tang H, Lu J, Yu K, et al. Traditional Chinese Medicine Bu-Shen-Jian-Pi-Fang Attenuates Glycolysis and Immune Escape in Clear Cell Renal Cell Carcinoma: Results Based on Network Pharmacology. *Biosci Rep* (2021) 41(6). doi: 10.1042/BSR20204421

13. Huang S, Wang Y, Zhou Z, Yu Q, Yu Y, Yang Y, et al. Distribution Atlas of COVID-19 Pneumonia on Computed Tomography: A Deep Learning Based Description. *Phenomics* (2021) 1(2):62–72. doi: 10.1007/s43657-021-00011-4

14. Li Y, Ma Y, Wang K, Zhang M, Wang Y, Liu X, et al. Using Composite Phenotypes to Reveal Hidden Physiological Heterogeneity in High-Altitude Acclimatization in a Chinese Han Longitudinal Cohort. *Phenomics* (2021) 1(1):3–14. doi: 10.1007/s43657-020-00005-8

15. Qiu Y, Liu X, Sun Y, Li S, Wei Y, Tian C, et al. In Situ Saturating Mutagenesis Screening Identifies a Functional Genomic Locus That Regulates Ucp1 Expression. *Phenomics* (2021) 1(1):15–21. doi: 10.1007/s43657-020-00006-7

16. Wang Q, Li P, Wu W. A Systematic Analysis of Immune Genes and Overall Survival in Cancer Patients. *BMC Cancer* (2019) 19(1):1225. doi: 10.1186/s12885-019-6414-6

17. Wood SL, Pernemalm M, Crosbie PA, Whetton AD. The Role of the Tumor-Microenvironment in Lung Cancer-Metastasis and its Relationship to Potential Therapeutic Targets. *Cancer Treat Rev* (2014) 40(4):558–66. doi: 10.1016/j.ctrv.2013.10.001

18. Quail DF, Joyce JA. Microenvironmental Regulation of Tumor Progression and Metastasis. *Nat Med* (2013) 19(11):1423–37. doi: 10.1038/nm.3394

19. Jangra S, Chaudhary V, Yadav RC, Yadav NR. High-Throughput Phenotyping: A Platform to Accelerate Crop Improvement. *Phenomics* (2021) 1(2):31–53. doi: 10.1007/s43657-020-00007-6

20. Bussard KM, Mutkus L, Stumpf K, Gomez-Manzano C, Marini FC. Tumor-Associated Stromal Cells as Key Contributors to the Tumor Microenvironment. *Breast Cancer Res* (2016) 18(1):84. doi: 10.1186/s13058-016-0740-2

21. Gajewski TF, Schreiber H, Fu YX. Innate and Adaptive Immune Cells in the Tumor Microenvironment. *Nat Immunol* (2013) 14(10):1014–22. doi: 10.1038/ni.2703

22. Quail DF, Joyce JA. The Microenvironmental Landscape of Brain Tumors. *Cancer Cell* (2017) 31(3):326–41. doi: 10.1016/j.ccell.2017.02.009

23. Roesch S, Rapp C, Dettling S, Herold-Mende C. When Immune Cells Turn Bad-Tumor-Associated Microglia/Macrophages in Glioma. *Int J Mol Sci* (2018) 19(2). doi: 10.3390/ijms19020436

24. Xu WH, Wu J, Wang J, Wan FN, Wang HK, Cao DL, et al. Screening and Identification of Potential Prognostic Biomarkers in Adrenocortical Carcinoma. *Front Genet* (2019) 10:821. doi: 10.3389/fgene.2019.00821

25. Rizvi NA, Mazières J, Planchard D, Stinchcombe TE, Dy GK, Antonia SJ, et al. Activity and Safety of Nivolumab, an anti-PD-1 Immune Checkpoint Inhibitor, for Patients With Advanced, Refractory Squamous Non-Small-Cell Lung Cancer (CheckMate 063): A Phase 2, Single-Arm Trial. *Lancet Oncol* (2015) 16(3):257–65. doi: 10.1016/s1470-2045(15)70054-9

26. Carbone DP, Reck M, Paz-Ares L, Creelan B, Horn L, Steins M, et al. First-Line Nivolumab in Stage IV or Recurrent Non-Small-Cell Lung Cancer. *N Engl J Med* (2017) 376(25):2415–26. doi: 10.1056/NEJMoa1613493

27. Zhang C, Cheng W, Ren X, Wang Z, Liu X, Li G, et al. Tumor Purity as an Underlying Key Factor in Glioma. *Clin Cancer Res* (2017) 23(20):6279–91. doi: 10.1158/1078-0432.CCR-16-2598

28. Bacac M, Fauti T, Sam J, Colombetti S, Weinzierl T, Ouaret D, et al. A Novel Carcinoembryonic Antigen T-Cell Bispecific Antibody (Cea TCB) for the Treatment of Solid Tumors. *Clin Cancer Res* (2016) 22(13):3286–97. doi: 10.1158/1078-0432.CCR-15-1696

29. Gaffney SG, Perry EB, Chen PM, Greenstein A, Kaech SM, Townsend JP. The Landscape of Novel and Complementary Targets for Immunotherapy: an Analysis of Gene Expression in the Tumor Microenvironment. *Oncotarget* (2019) 10(44):4532–45. doi: 10.18632/oncotarget.27027

30. Ryan M, Wong WC, Brown R, Akbani R, Su X, Broom B, et al. TcgaspliceSeq a Compendium of Alternative mRNA Splicing in Cancer. *Nucleic Acids Res* (2016) 44(D1):D1018–22. doi: 10.1093/nar/gkv1288

31. Barrett T, Wilhite SE, Ledoux P, Evangelista C, Kim IF, Tomashevsky M, et al. Ncbi GEO: Archive for Functional Genomics Data Sets–Update. *Nucleic Acids Res* (2013) 41(Database issue):D991–5. doi: 10.1093/nar/gks1193

32. Chan BKC. Data Analysis Using R Programming. *Adv Exp Med Biol* (2018) 1082:47–122. doi: 10.1007/978-3-319-93791-5_2

33. Gentles AJ, Newman AM, Liu CL, Bratman SV, Feng W, Kim D, et al. The Prognostic Landscape of Genes and Infiltrating Immune Cells Across Human Cancers. *Nat Med* (2015) 21(8):938–45. doi: 10.1038/nm.3909

34. Chakraborty H, Hossain A. R Package to Estimate Intracluster Correlation Coefficient With Confidence Interval for Binary Data. *Comput Methods Programs BioMed* (2018) 155:85–92. doi: 10.1016/j.cmpb.2017.10.023

35. Newman AM, Liu CL, Green MR, Gentles AJ, Feng W, Xu Y, et al. Robust Enumeration of Cell Subsets From Tissue Expression Profiles. *Nat Methods* (2015) 12(5):453–7. doi: 10.1038/nmeth.3337

36. Varghese F, Bukhari AB, Malhotra R, De A. Ihc Profiler: An Open Source Plugin for the Quantitative Evaluation and Automated Scoring of Immunohistochemistry Images of Human Tissue Samples. *PloS One* (2014) 9(5):e96801. doi: 10.1371/journal.pone.0096801

37. Smyth GK, Michaud J, Scott HS. Use of Within-Array Replicate Spots for Assessing Differential Expression in Microarray Experiments. *Bioinformatics* (2005) 21(9):2067–75. doi: 10.1093/bioinformatics/bti270

38. Zhao C, Sahni S. String Correction Using the Damerau-Levenshtein Distance. *BMC Bioinf* (2019) 20(Suppl 11):277. doi: 10.1186/s12859-019-2819-0

39. Wu G, Feng X, Stein L. A Human Functional Protein Interaction Network and Its Application to Cancer Data Analysis. *Genome Biol* (2010) 11(5):R53. doi: 10.1186/gb-2010-11-5-r53

40. Gene Ontology Consortium: Going Forward. *Nucleic Acids Res* (2015) 43 (Database issue):D1049–56. doi: 10.1093/nar/gku1179

41. Kanehisa M, Goto S. KEGG: Kyoto Encyclopedia of Genes and Genomes. *Nucleic Acids Res* (2000) 28(1):27–30. doi: 10.1093/nar/28.1.27

42. Subramanian A, Kuehn H, Gould J, Tamayo P, Mesirov JP. Gsea-P: A Desktop Application for Gene Set Enrichment Analysis. *Bioinformatics* (2007) 23 (23):3251–3. doi: 10.1093/bioinformatics/btm369

43. Duerr JS. *Immunohistochemistry*. *Wormbook*. (2006). pp. 1–61. doi: 10.1895/wormbook.1.105.1

44. Yu SC, Qi X, Hu YH, Zheng WJ, Wang QQ, Yao HY. Overview of Multivariate Regression Model Analysis and Application. *Zhonghua Yu Fang Yi Xue Za Zhi* (2019) 53(3):334–6. doi: 10.3760/cma.j.issn.0253-9624.2019.03.020

45. Morris TP, Jarvis CI, Cragg W, Phillips PPJ, Choodari-Oskooei B, Sydes MR. Proposals on Kaplan-Meier Plots in Medical Research and a Survey of Stakeholder Views: Kmunicate. *BMJ Open* (2019) 9(9):e030215. doi: 10.1136/bmjopen-2019-030215

46. Ritchie ME, Phipson B, Wu D, Hu Y, Law CW, Shi W, et al. Limma Powers Differential Expression Analyses for RNA-Sequencing and Microarray Studies. *Nucleic Acids Res* (2015) 43(7):e47. doi: 10.1093/nar/gkv007

47. Xu W, Zheng J, Liu W, Tang H, Lu J, Yu K, et al. Traditional Chinese Medicine Bu-Shen-Jian-Pi-Fang Attenuates Glycolysis and Immune Escape in Clear Cell Renal Cell Carcinoma: Results Based on Network Pharmacology. *Biosci Rep* (2021). doi: 10.1042/bsr20204421

48. Ni W, Zhang S, Jiang B, Ni R, Xiao M, Lu C, et al. Identification of Cancer-Related Gene Network in Hepatocellular Carcinoma by Combined Bioinformatic Approach and Experimental Validation. *Pathol Res Pract* (2019) 215(6):152428. doi: 10.1016/j.prp.2019.04.020

49. Barber EK, Dasgupta JD, Schlossman SF, Trevillyan JM, Rudd CE, et al. The CD4 and CD8 Antigens Are Coupled to a Protein-Tyrosine Kinase (p56lck) That Phosphorylates the CD3 Complex. *Proc Natl Acad Sci USA* (1989) 86 (9):3277–81. doi: 10.1073/pnas.86.9.3277

50. Kreso A, Dick JE. Evolution of the Cancer Stem Cell Model. *Cell Stem Cell* (2014) 14(3):275–91. doi: 10.1016/j.stem.2014.02.006

51. Brat DJ, Verhaak RG, Aldape KD, Yung WK, Salama SR, Cooper LA, et al. Comprehensive, Integrative Genomic Analysis of Diffuse Lower-Grade Gliomas. *N Engl J Med* (2015) 372(26):2481–98. doi: 10.1056/NEJMoa1402121

52. Lawrence MS, Stojanov P, Mermel CH, Robinson JT, Garraway LA, Golub TR, et al. Discovery and Saturation Analysis of Cancer Genes Across 21 Tumour Types. *Nature* (2014) 505(7484):495–501. doi: 10.1038/nature12912

53. Capelle L, Fontaine D, Mandonnet E, Taillandier L, Golmard JL, Bauchet L, et al. Spontaneous and Therapeutic Prognostic Factors in Adult Hemispheric World Health Organization Grade II Gliomas: A Series of 1097 Cases: Clinical Article. *J Neurosurg* (2013) 118(6):1157–68. doi: 10.3171/2013.1.Jns121

54. Verburg N, de Witt Hamer PC. State-of-the-Art Imaging for Glioma Surgery. *Neurosurg Rev* (2021) 44(3):1331–43. doi: 10.1007/s10143-020-01337-9

55. Chang J, Wang Y, Guo R, Guo X, Lu Y, Ma W, et al. The Effect of Operations in Patients With Recurrent Diffuse Low-Grade Glioma: A Qualitative Systematic Review. *Clin Neurol Neurosurg* (2020) 196:105973. doi: 10.1016/j.clineuro.2020.105973

56. Belykh E, Shaffer KV, Lin C, Byvaltsev VA, Preul MC, Chen L. Blood-Brain Barrier, Blood-Brain Tumor Barrier, and Fluorescence-Guided Neurosurgical Oncology: Delivering Optical Labels to Brain Tumors. *Front Oncol* (2020) 10:739. doi: 10.3389/fonc.2020.00739

57. Lim M, Xia Y, Bettegowda C, Weller M. Current State of Immunotherapy for Glioblastoma. *Nat Rev Clin Oncol* (2018) 15(7):422–42. doi: 10.1038/s41571-018-0003-5

58. McGranahan T, Therkelsen KE, Ahmad S, Nagpal S. Current State of Immunotherapy for Treatment of Glioblastoma. *Curr Treat Options Oncol* (2019) 20(3):24. doi: 10.1007/s11864-019-0619-4

59. Huang B, Zhang H, Gu L, Ye B, Jian Z, Stary C, et al. Advances in Immunotherapy for Glioblastoma Multiforme. *J Immunol Res* (2017) 2017:3597613. doi: 10.1155/2017/3597613

60. Yoshihara K, Shahmoradgoli M, Martínez E, Vegesna R, Kim H, Torres-Garcia W, et al. Inferring Tumour Purity and Stromal and Immune Cell Admixture From Expression Data. *Nat Commun* (2013) 4:2612. doi: 10.1038/ncomms3612

61. Mao Y, Feng Q, Zheng P, Yang L, Liu T, Xu Y, et al. Low Tumor Purity Is Associated With Poor Prognosis, Heavy Mutation Burden, and Intense Immune Phenotype in Colon Cancer. *Cancer Manag Res* (2018) 10:3569–77. doi: 10.2147/CMAR.S171855

62. Fischer A, de Saint Basile G, Le Deist F. CD3 Deficiencies. *Curr Opin Allergy Clin Immunol* (2005) 5(6):491–5. doi: 10.1097/01.all.0000191886.12645.79

63. Martin-Blanco N, Jiménez Teja D, Bretones G, Borroto A, Caraballo M, Screpanti I, et al. Cd3ε Recruits Numb to Promote TCR Degradation. *Int Immunol* (2016) 28(3):127–37. doi: 10.1093/intimm/dxv060

64. Borroto A, Lama J, Niedergang F, Dautry-Varsat A, Alarcón B, Alcover A. The CD3 Epsilon Subunit of the TCR Contains Endocytosis Signals. *J Immunol* (1999) 163(1):25–31.

65. Bacolod MD, Barany F, Pilones K, Fisher PB, de Castro RJ. Pathways- and Epigenetic-Based Assessment of Relative Immune Infiltration in Various Types of Solid Tumors. *Adv Cancer Res* (2019) 142:107–43. doi: 10.1016/bs.acr.2019.01.003

66. Venteicher AS, Tirosh I, Hebert C, Yizhak K, Neftel C, Filbin MG, et al. Decoupling Genetics, Lineages, and Microenvironment in IDH-Mutant Gliomas by Single-Cell RNA-Seq. *Science* (2017) 355(6332). doi: 10.1126/science.aai8478

67. Zhang Y, Chen K, Sloan SA, Bennett ML, Scholze AR, O'Keeffe S, et al. An RNA-sequencing Transcriptome and Splicing Database of Glia, Neurons, and Vascular Cells of the Cerebral Cortex. *J Neurosci* (2014) 34(36):11929–47. doi: 10.1523/JNEUROSCI.1860-14.2014

68. Matcovitch-Natan O, Winter DR, Giladi A, Vargas Aguilar S, Spinrad A, Sarrazin S, et al. Microglia Development Follows a Stepwise Program to Regulate Brain Homeostasis. *Science* (2016) 353(6301):aad8670. doi: 10.1126/science.aad8670

69. Schaller TH, Snyder DJ, Spasojevic I, Gedeon PC, Sanchez-Perez L, Sampson JH. First in Human Dose Calculation of a Single-Chain Bispecific Antibody Targeting Glioma Using the MABEL Approach. *J Immunother Cancer* (2020) 8(1). doi: 10.1136/jitc-2019-000213

70. Fridman WH, Zitvogel L, Sautès-Fridman C, Kroemer G. The Immune Contexture in Cancer Prognosis and Treatment. *Nat Rev Clin Oncol* (2017) 14(12):717–34. doi: 10.1038/nrclinonc.2017.101

71. Chen Y, Ma D, Wang X, Fang J, Liu X, Song J, et al. Calnexin Impairs the Antitumor Immunity of CD4(+) and CD8(+) T Cells. *Cancer Immunol Res* (2019) 7(1):123–35. doi: 10.1158/2326-6066.CIR-18-0124

72. Bacolod MD, Talukdar S, Emdad L, Das SK, Sarkar D, Wang XY, et al. Immune Infiltration, Glioma Stratification, and Therapeutic Implications. *Transl Cancer Res* (2016) 5(Suppl 4):S652–6. doi: 10.21037/tcr.2016.10.69

73. Berger MF, Mardis ER. The Emerging Clinical Relevance of Genomics in Cancer Medicine. *Nat Rev Clin Oncol* (2018) 15(6):353–65. doi: 10.1038/s41571-018-0002-6

74. Wu S, Gu Y, Huang Y, Wong TC, Ding H, Liu T, et al. Novel Biomarkers for Non-Functioning Invasive Pituitary Adenomas Were Identified by Using Analysis of Micrornas Expression Profile. *Biochem Genet* (2017) 55(3):253–67. doi: 10.1007/s10528-017-9794-9

75. Xu W, Liu WR, Xu Y, Tian X, Anwaier A, Su JQ, et al. Hexokinase 3 Dysfunction Promotes Tumorigenesis and Immune Escape by Upregulating Monocyte/Macrophage Infiltration Into the Clear Cell Renal Cell Carcinoma Microenvironment. *Int J Biol Sci* (2021) 17(9):2205–22. doi: 10.7150/ijbs.58295

76. Kim DM, Nimigean CM. Voltage-Gated Potassium Channels: A Structural Examination of Selectivity and Gating. *Cold Spring Harb Perspect Biol* (2016) 8(5). doi: 10.1101/cshperspect.a029231

77. Chen XG, Ma L, Xu JX. Abnormal DNA Methylation may Contribute to the Progression of Osteosarcoma. *Mol Med Rep* (2018) 17(1):193–9. doi: 10.3892/mmr.2017.7869

78. Zhang BL, Guo TW, Gao LL, Ji GQ, Gu XH, Shao YQ, et al. Egr-1 and RNA Pol II Facilitate Glioma Cell GDNF Transcription Induced by Histone Hyperacetylation in Promoter II. *Oncotarget* (2017) 8(28):45105–16. doi: 10.18632/oncotarget.15126

79. Huang P, Guo YD, Zhang HW. Identification of Hub Genes in Pediatric Medulloblastoma by Multiple-Microarray Analysis. *J Mol Neurosci* (2020) 70(4):522–31. doi: 10.1007/s12031-019-01451-4

80. Chen X, Li B, Luo R, Cai S, Zhang C, Cao X. Analysis of the Function of microRNA-375 in Humans Using Bioinformatics. *BioMed Rep* (2017) 6(5):561–6. doi: 10.3892/br.2017.889

81. Pasdois P, Deveaud C, Voisin P, Bouchaud V, Rigoulet M, Beauvoit B. Contribution of the Phosphorylable Complex I in the Growth Phase-Dependent Respiration of C6 Glioma Cells In Vitro. *J Bioenerg Biomembr* (2003) 35(5):439–50. doi: 10.1023/a:1027391831382

# Disparities in Reported Testing for 1p/19q Codeletion in Oligodendroglioma and Oligoastrocytoma Patients: An Analysis of the National Cancer Database

Jad Zreik[1], Panagiotis Kerezoudis[2], Mohammed Ali Alvi[2], Yagiz U. Yolcu[2] and Sani H. Kizilbash[3]*

[1] College of Medicine, Central Michigan University, Mount Pleasant, MI, United States, [2] Department of Neurologic Surgery, Mayo Clinic, Rochester, MN, United States, [3] Department of Medical Oncology, Mayo Clinic, Rochester, MN, United States

**Purpose:** A chromosomal 1p/19q codeletion was included as a required diagnostic component of oligodendrogliomas in the 2016 World Health Organization (WHO) classification of central nervous system tumors. We sought to evaluate disparities in reported testing for 1p/19q codeletion among oligodendroglioma and oligoastrocytoma patients before and after the guidelines.

**Methods:** The National Cancer Database (NCDB) was queried for patients with histologically-confirmed WHO grade II/III oligodendroglioma or oligoastrocytoma from 2011-2017. Adjusted odds of having a reported 1p/19q codeletion test for patient- and hospital-level factors were calculated before (2011-2015) and after (2017) the guidelines. The adjusted likelihood of receiving adjuvant treatment (chemotherapy and/or radiotherapy) based on reported testing was also evaluated.

**Results:** Overall, 6,404 patients were identified. The reported 1p/19q codeletion testing rate increased from 45.8% in 2011 to 59.8% in 2017. From 2011-2015, lack of insurance (OR 0.77; 95% CI 0.62-0.97;p=0.025), lower zip code-level educational attainment (OR 0.62; 95% CI 0.49-0.78;p<0.001), and Northeast (OR 0.68; 95% CI 0.57-0.82;p<0.001) or Southern (OR 0.62; 95% CI 0.49-0.79;p<0.001) facility geographic region were negatively associated with reported testing. In 2017, Black race (OR 0.49; 95% CI 0.26-0.91;p=0.024) and Northeast (OR 0.50; 95% CI 0.30-0.84;p=0.009) or Southern (OR 0.42; 95% CI 0.22-0.78;p=0.007) region were negatively associated with reported testing. Patients with a reported test were more likely to receive adjuvant treatment (OR 1.73; 95% CI 1.46-2.04;p<0.001).

**Conclusion:** Despite the 2016 WHO guidelines, disparities in reported 1p/19q codeletion testing by geographic region persisted while new disparities in race/ethnicity were identified, which may influence oligodendroglioma and oligoastrocytoma patient management.

Keywords: 1p/19q codeletion, molecular testing, oligodendroglioma, oligoastrocytoma, disparities, adjuvant treatment

# INTRODUCTION

Chromosomal 1p/19q codeletion status plays an important role in tumor diagnosis for patients with a histological diagnosis of oligodendroglioma or oligoastrocytoma. As the characteristic molecular signature of oligodendrogliomas, 1p/19q codeletion has been associated with improved overall and progression-free survival (1, 2). Randomized clinical trials have identified this mutation as a marker of enhanced response to chemoradiotherapy in anaplastic oligodendrogliomas (3, 4). Additionally, an isocitrate dehydrogenase (IDH) mutation has been previously shown to occur in nearly all gliomas harboring a 1p/19q codeletion (5, 6). As a result of these associations, the 2016 WHO classification of CNS tumors included the presence of an IDH mutation and 1p/19q codeletion as required criteria for diagnosing an oligodendroglioma in WHO grade II and grade III diffuse gliomas (7).

A number of studies have described inequitable access to neuro-oncological care among glioma patients. Factors such as race, socioeconomic status, and geography have been previously shown to influence receipt of treatment, access to high-volume facilities, and overall survival (OS) (8–11). Despite the increasing emphasis on molecular diagnostics, it is unknown whether similar disparities exist in testing for 1p/19q codeletion. Analyzing whether past disparities have been maintained despite the 2016 WHO guidelines may also better inform targets for quality improvement initiatives. Therefore, we sought to evaluate the trends, disparities, and potential impact of a reported 1p/19q codeletion test among oligodendroglioma and oligoastrocytoma patients before and after implementation of the 2016 WHO guidelines.

# METHODS AND MATERIALS

## Data Source and Patient Selection

The National Cancer Database (NCDB) was queried for this study. The NCDB, a joint program between the Commission on Cancer (CoC) of the American College of Surgeons and American Cancer Society, is a clinical oncology outcomes database used to evaluate trends in cancer care, establish benchmarks for participating hospitals, and serve as a basis for quality improvement (12). The registry captures approximately 70% of all newly diagnosed cancer cases in the United States from over 1,500 CoC-accredited facilities (13). Given that patient data in the registry is deidentified, this study was exempt from Institutional Review Board (IRB) approval.

Patients were identified using International Classification of Diseases for Oncology, third revision (ICD-O-3) codes

indicating a histological diagnosis of Grade II or Grade III oligodendroglioma (9450, 9451) or mixed oligoastrocytoma (9382) in the CNS (ICD-O-3 topography codes: C70.1-C72.9). Identified patients were also adults (age ≥18 years) who had positive histologic diagnostic confirmation (based on microscopic tissue examination). Patients diagnosed from 2011-2017 were initially included for an analysis of trends in reported 1p/19q codeletion testing rates. Then, the cohort was stratified into groups diagnosed from 2011-2015 or 2017 in order to evaluate disparities before and after implementation of the 2016 WHO classification of CNS tumors. A diagnosis in 2011 was chosen as the early cutoff since the NCDB Participant User File (PUF) notes that reporting of 1p/19q codeletion is likely underrepresented in 2010, the variable's first year of reporting (14). Cases with missing values for patient demographics, except for facility setting and geographic region, were excluded. Unknown facility setting and geographic region were not excluded in order to attenuate potential selection bias given that the NCDB suppresses these variables for patients aged <40 (14).

## Primary Outcome

Reported 1p/19q codeletion tests were identified using the *CS Site Specific Factor 5* (Chromosome 1p: Loss of Heterozygosity) and *CS Site Specific Factor 6* (Chromosome 19q: Loss of Heterozygosity) variables. Patients who were reported as testing positive or negative for loss of heterozygosity for both variables were identified as having a reported 1p/19q codeletion test. Those documented as "test not done (test not ordered or not performed)" or "not documented in patient record" for at least one of the variables were identified as having an unreported 1p/19q codeletion test. The remaining patients, indicated as "test ordered, results not in chart", were excluded since it was unclear whether a 1p/19q codeletion test was ultimately performed.

## Patient Characteristics

Patient characteristics included patient demographics, tumor properties, and cancer-directed therapies administered during the initial course of treatment, as defined in the NCDB PUF and detailed in **Supplementary Table 1** (14). Tumor location was classified as supratentorial, infratentorial, or not otherwise specified (NOS) or other CNS according to the ICD-O-3 topography code for the primary site. Tumor size was dichotomized as <5cm or ≥5cm in accordance with the previous literature (15, 16). Extent of resection (EOR) was categorized as biopsy only, subtotal resection (STR), or gross total resection (GTR) according to the American College of

Surgeons CoC Facility Oncology Registry Data System manual (17).

## Statistical Analysis

The unadjusted annual percentage of patients with a reported test for codeletion from 2011-2017 was calculated and plotted. The Cochran-Armitage test was performed to evaluate the presence of statistically significant temporal trends. The cohort was subsequently divided into two groups to be independently analyzed: patients diagnosed from 2011-2015 and patients diagnosed in 2017. For both groups, patient characteristics were summarized using frequencies with proportions for categorical variables or medians with interquartile ranges (IQRs) for continuous variables. Comparisons were made between those with reported and unreported 1p/19q codeletion tests using Pearson's chi-squared test for categorical variables or the two-sample t-test for continuous variables. In order to elucidate predictors of a reported 1p/19q test, unadjusted and adjusted odds ratios were calculated.

After merging the two patient groups, the adjusted odds of a reported 1p/19q codeletion test in 2017 versus 2011-2015 was calculated for all patients and for each patient subgroup. Finally, the unadjusted and adjusted odds of receiving adjuvant treatment based on reported testing for 1p/19q codeletion were evaluated. An interaction analysis between EOR and reported testing revealed a statistically significant interaction term for both receipt of chemotherapy (p=0.038) and receipt of radiotherapy (p=0.017). Therefore, for this analysis, adjuvant treatment was dichotomized as receipt of any adjuvant treatment (chemotherapy and/or radiotherapy) or no adjuvant treatment (neither chemotherapy nor radiotherapy). Given that the significant interactions occurred specifically with a GTR, the EOR variable was also dichotomized as a GTR or other resection.

Unadjusted and adjusted odds ratios were calculated using univariate and multivariable logistic regression, respectively. For all regression analyses, univariate logistic regression was initially performed, then variables with p<0.10 were included in the subsequent multivariable logistic regression model. Collinearity between covariates in the multivariable models was assessed using the variance inflation factor. Analyses were performed using R version 3.6.1 (18). P-values were two-sided and values <0.05 were considered statistically significant.

## RESULTS

### Trends in Testing

A total 6,404 patients were included in the analysis following exclusions. From 2011 to 2017, the percentage of patients in the NCDB with a reported test for 1p/19q codeletion increased from 45.8% to 59.8% (p<0.001). The Cochran-Armitage test also identified a statistically significant increasing trend for most patient subgroups. However, Hispanic White (p=0.922), Black (p=0.218), Medicaid/Other (p=0.154), and uninsured (p=0.462) patients did not experience a significant increase in reported codeletion testing over the study period (**Figure 1**).

## Disparities Before 2016 WHO Guidelines

A total of 4,931 patients diagnosed from 2011-2015 were identified; of which, 47.6% (n=2,349) had a reported 1p/19q codeletion test while 52.4% (n=2,582) did not. The median age was 44 years (IQR: 34-55) with 56.0% (n=2,763) being male. Non-Hispanic White, Hispanic White, Black, and other race/ethnicity patients had reported codeletion tests in 48.5%, 44.9%, 40.7%, and 44.7% of cases, respectively (p=0.034). Privately insured, Medicare, Medicaid/Other, and uninsured patients had reported testing rates of 49.4%, 43.0%, 47.3%, and 40.4%, respectively (p<0.001). Patients residing in a zip code in the top, second, third, and bottom quartiles of educational attainment had reported testing rates of 51.9%, 50.6%, 45.5%, and 39.95, respectively (p<0.001). Based on geographic region, a codeletion test was reported in 41.9%, 52.4%, 37.5%, and 55.3% of patients at Northeastern, Midwestern, Southern, and Western facilities, respectively (p<0.001). Significant differences in the rates of reported codeletion tests were also identified based on EOR (p<0.001) and receipt of adjuvant treatment (p<0.001) (**Table 1**).

On univariate analysis, Black (OR 0.73; 95% CI 0.57-0.93; p=0.011) and Medicare (OR 0.77; 95% CI 0.65-0.92; p=0.004) patients were significantly less likely to have a reported 1p/19q codeletion test; however, this significance was not retained after inclusion in the multivariable model. On multivariable analysis, factors including uninsured status (OR 0.77; CI 0.62-0.97; p=0.025), educational attainment in the third (OR 0.76; 95% CI 0.63-0.93; p=0.006) or bottom (OR 0.62; 95% CI 0.49-0.78; p<0.001) quartile, and hospital location in the Northeast (OR 0.68; 95% CI 0.57-0.82; p<0.001) and South (OR 0.62; 95% CI 0.49-0.79; p<0.001) compared to the Midwest were negatively associated with a reported 1p/19q codeletion test. Tumors with oligoastrocytoma histology were also less likely to have a reported codeletion test (OR 0.83; 95% CI 0.73-0.93; p=0.002) (**Table 2**).

## Disparities After 2016 WHO Guidelines

A total of 719 glioma patients diagnosed in 2017 were identified; of which, 59.8% (n=430) had a reported 1p/19q codeletion test while 40.2% (n=289) did not. The median age was 45 years (IQR: 35-56) with 53.7% (n=386) being male. Non-Hispanic White, Hispanic White, Black, and other race/ethnicity patients had reported codeletion tests in 61.6%, 50.6%, 42.6%, and 72.5% of cases, respectively (p=0.008). Based on geographic region, a codeletion test was reported in 53.7%, 70.5%, 47.8%, and 68.9% of patients at Northeastern, Midwestern, Southern, and Western facilities, respectively (p=0.001). Patients with WHO grade III tumors (64.6%) were also more likely to have a reported codeletion test compared to WHO grade II tumors (56.5%) (p=0.030) (**Table 3**).

On multivariable analysis, Black race (OR 0.49; 95% CI 0.26-0.91; p=0.024) and reporting from hospitals in the Northeast (OR 0.50; 95% CI 0.30-0.84; p=0.009) and South (OR 0.42; 95% CI 0.22-0.78; p=0.007) compared to the Midwest were negatively associated with a reported 1p/19q codeletion test. Patients with WHO grade III tumors (OR 1.37; 95% CI 1.01-1.89; p=0.049) were significantly more likely to have a reported test (**Table 4**).
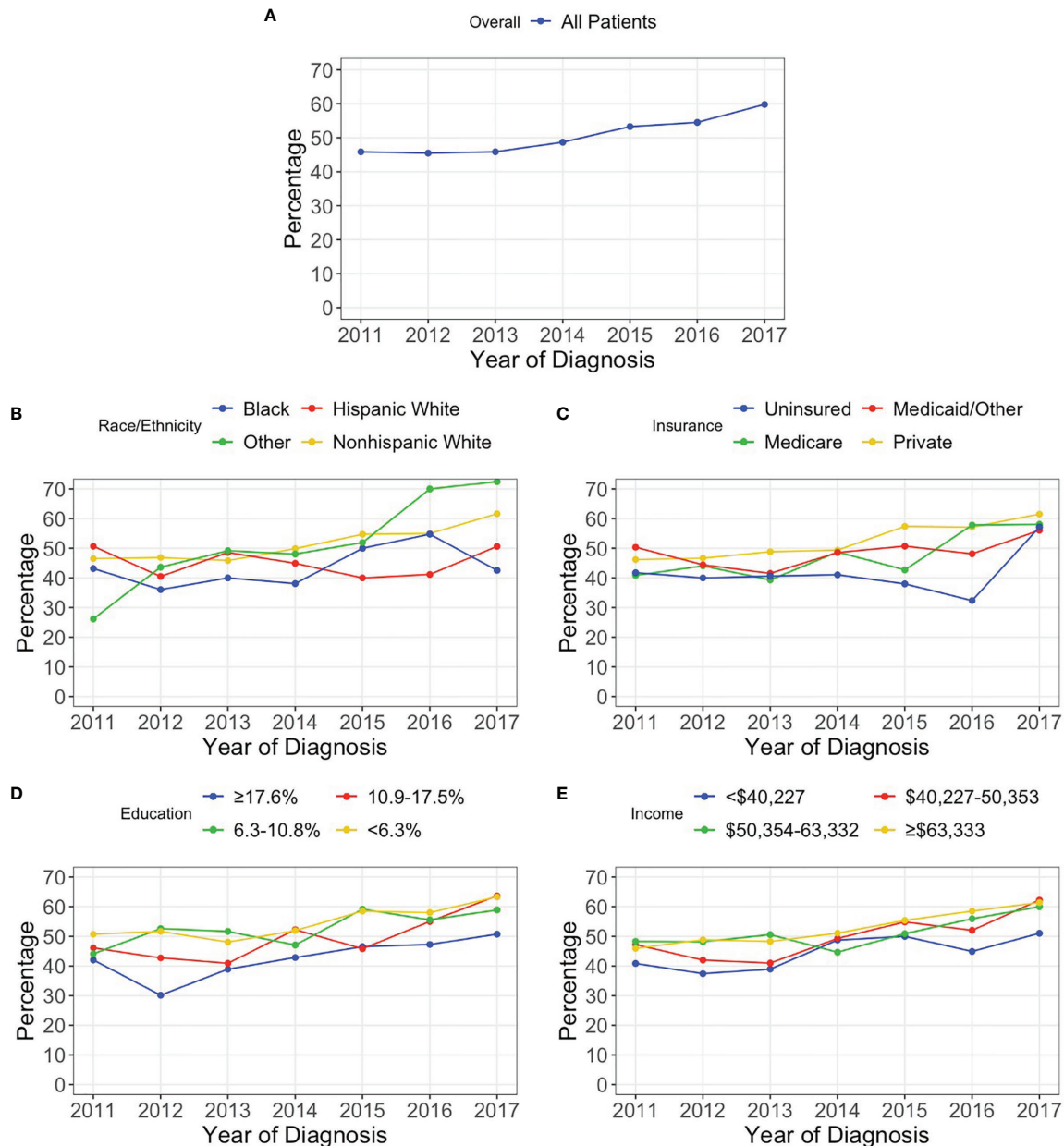
**FIGURE 1** | Percentage of patients with a reported 1p/19q codeletion test for **(A)** all patients and stratified by **(B)** race/ethnicity, **(C)** insurance status, **(D)** percentage of adults without a high school degree in patient's zip code, and **(E)** median household income in patient's zip code.

## Disparities in 2017 Versus 2011-2015

Overall, patients were significantly more likely to have a reported 1p/19q codeletion test in 2017 versus 2011-2015 (OR 1.57; 95% CI 1.33-1.86; p<0.001). This trend was mirrored for most patient subgroups. However, Hispanic White patients (OR 1.28; 95% CI 0.77-2.11; p=0.341), Black patients (OR 1.04; 95% CI 0.54-1.94; p=0.915), rural residents (OR 1.20; 95% CI 0.33-4.46; p=0.783), and patients in the bottom quartile of household income (OR 1.31; 95% CI 0.85-2.03; p=0.228) were not statistically more likely to have a reported test in 2017 versus 2011-2015 (**Table 5**).

## 1p/19q Codeletion Testing and Adjuvant Treatment

On univariate analysis, reported testing was associated with an increased likelihood of receiving adjuvant treatment (OR 1.35; 95% CI 1.20-1.51; p<0.001). An interaction analysis identified GTR as a significant confounding variable. After adjusting for GTR and other relevant confounders, a reported 1p/19q codeletion test was found to be independently associated with increased odds of receiving adjuvant treatment (OR 1.73; 95% CI 1.46-2.04; p<0.001). The interaction between a reported

**TABLE 1 |** Characteristics of patients with and without a reported 1p/19q codeletion test diagnosed from 2011-2015. Frequencies and proportions are row-based.

| Variable | Unreported 1p/19q test N = 2,582 | Reported 1p/19q test N = 2,349 | P-value |
|---|---|---|---|
| Age, median (IQR) | 44 (34-56) | 44 (33-54) | **0.004** |
| Sex | | | 0.256 |
| Male (n=2,763) | 1427 (51.6%) | 1336 (48.4%) | |
| Female (n=2,168) | 1155 (53.3%) | 1013 (46.7%) | |
| Race/Ethnicity | | | **0.034** |
| Non-Hispanic White (4,033) | 2075 (51.5%) | 1958 (48.5%) | |
| Hispanic White (n=356) | 196 (55.1%) | 160 (44.9%) | |
| Black (n=280) | 166 (59.3%) | 114 (40.7%) | |
| Other (n=262) | 145 (55.3%) | 117 (44.7%) | |
| Insurance | | | **<0.001** |
| Private (n=3,233) | 1635 (50.6%) | 1598 (49.4%) | |
| Medicare (n=609) | 347 (57.0%) | 262 (43.0%) | |
| Medicaid/Other (n=713) | 376 (52.7%) | 337 (47.3%) | |
| Uninsured (n=376) | 224 (59.6%) | 152 (40.4%) | |
| Median household income in zip code | | | **0.010** |
| <$40,227 (n=797) | 455 (57.1%) | 342 (42.9%) | |
| $40,227-50,353 (n=1,033) | 553 (53.5%) | 480 (46.5%) | |
| $50,354-63,332 (n=1,182) | 609 (51.5%) | 573 (48.5%) | |
| ≥$63,333 (n=1,919) | 965 (50.3%) | 954 (49.7%) | |
| Adults without high school degree in zip code | | | **<0.001** |
| ≥17.6% (n=972) | 584 (60.1%) | 388 (39.9%) | |
| 10.9%-17.5% (n=1,177) | 641 (54.5%) | 536 (45.5%) | |
| 6.3%-10.8% (n=1,434) | 709 (49.4%) | 725 (50.6%) | |
| <6.3% (n=1,348) | 648 (48.1%) | 700 (51.9%) | |
| Charlson-Deyo Comorbidity Score | | | 0.552 |
| 0 (n=4,092) | 2140 (52.3%) | 1952 (47.7%) | |
| 1 (n=569) | 307 (54.0%) | 262 (46.0%) | |
| 2+ (n=270) | 135 (50.0%) | 135 (50.0%) | |
| Residential Region | | | 0.472 |
| Metropolitan (n=4,159) | 2183 (52.5%) | 1976 (47.5%) | |
| Urban (n=695) | 364 (52.4%) | 331 (47.6%) | |
| Rural (n=77) | 35 (45.5%) | 42 (54.5%) | |
| Geographic Region | | | **<0.001** |
| Northeast (n=1,123) | 653 (58.1%) | 470 (41.9%) | |
| Midwest (n=832) | 396 (47.6%) | 436 (52.4%) | |
| South (n=451) | 282 (62.5%) | 169 (37.5%) | |
| West (n=604) | 270 (44.7%) | 334 (55.3%) | |
| Unknown (n=1,921) | 981 (51.1%) | 940 (48.9%) | |
| Facility Setting | | | 0.113 |
| Academic (n=1,734) | 902 (52.0%) | 832 (48.0%) | |
| Non-academic (n=1,276) | 699 (54.8%) | 577 (45.2%) | |
| Unknown | 981 (51.1%) | 940 (48.9%) | |
| Distance travelled (miles), median (IQR) | 14.8 (6.2-36.4) | 17.5 (7.2-42.9) | 0.368 |
| 1p/19q status | | | NA |
| Co-deleted | NA | 1464 | |
| Not co-deleted | NA | 885 | |
| Histology | | | **0.005** |
| Oligodendroglioma (n=3,253) | 1657 (50.9%) | 1596 (49.1%) | |
| Oligoastrocytoma (n=1,678) | 925 (55.1%) | 753 (44.9%) | |
| WHO grade | | | 0.224 |
| 2 (n=2,859) | 1476 (51.6%) | 1106 (53.4%) | |
| 3 (n=2,072) | 1383 (48.4%) | 966 (46.6%) | |
| Tumor location | | | **0.033** |
| Supratentorial (n=4,707) | 2446 (52.0%) | 2261 (48.0%) | |
| Infratentorial (n=68) | 43 (63.2%) | 25 (36.8%) | |
| NOS or other CNS (n=156) | 93 (59.6%) | 63 (40.4%) | |
| Tumor size | | | **0.002** |
| <5 cm (n=1,934) | 996 (51.5%) | 938 (48.5%) | |
| ≥5 cm (n=1,690) | 848 (50.2%) | 842 (49.8%) | |
| Unknown (n=1,307) | 738 (56.5%) | 569 (43.5%) | |
| Extent of resection | | | **<0.001** |
| Biopsy only (n=498) | 305 (61.2%) | 193 (38.8%) | |
| STR (n=2,471) | 1309 (53.0%) | 1162 (47.0%) | |

*(Continued)*

**TABLE 1 |** Continued

| Variable | Unreported 1p/19q test N = 2,582 | Reported 1p/19q test N = 2,349 | P-value |
|---|---|---|---|
| GTR (n=1,929) | 946 (49.0%) | 983 (51.0%) | |
| Unknown (n=33) | 22 (66.7%) | 11 (33.3%) | |
| Chemotherapy | | | **<0.001** |
| Yes (n=2,459) | 1182 (48.1%) | 1277 (51.9%) | |
| No (n=2,280) | 1277 (56.0%) | 1003 (44.0%) | |
| Unknown (n=192) | 123 (64.1%) | 69 (35.9%) | |
| Radiotherapy | | | 0.070 |
| Yes (n=2,389) | 1218 (51.0%) | 1171 (49.0%) | |
| No (n=2,492) | 1335 (53.6%) | 1157 (46.4%) | |
| Unknown (n=50) | 29 (58.0%) | 21 (42.0%) | |
| Adjuvant treatment | | | **<0.001** |
| Chemotherapy alone (n=578) | 244 (42.2%) | 334 (57.8%) | |
| Radiotherapy alone (n=476) | 260 (54.6%) | 216 (45.4%) | |
| Chemotherapy+Radiotherapy (n=1,874) | 936 (49.9%) | 938 (50.1%) | |
| Neither (n=1,783) | 1005 (56.4%) | 778 (43.6%) | |
| Unknown (n=220) | 137 (62.3%) | 83 (37.7%) | |

*Bold values indicate statistical significance (p < 0.05).*
*NA, not applicable.*

**TABLE 2 |** Univariate and multivariable logistic regression evaluating factors associated with reporting of a 1p/19q codeletion test for patients diagnosed from 2011-2015.

| Variable | Reference | Univariate | | Multivariable | |
|---|---|---|---|---|---|
| | | OR (95% CI) | P-value | OR (95% CI) | P-value |
| Age | Continuous | 0.99 (0.99-1.00) | **0.004** | 0.99 (0.98-1.00) | **0.026** |
| Race/Ethnicity | Non-Hispanic White | | | | |
| Hispanic White | | 0.87 (0.70-1.08) | 0.192 | 0.99 (0.78-1.24) | 0.906 |
| Black | | 0.73 (0.57-0.93) | **0.011** | 0.82 (0.64-1.06) | 0.138 |
| Other | | 0.86 (0.66-1.10) | 0.222 | 0.85 (0.66-1.10) | 0.231 |
| Insurance | Private | | | | |
| Medicare | | 0.77 (0.65-0.92) | **0.004** | 0.93 (0.76-1.15) | 0.527 |
| Medicaid/Other | | 0.92 (0.78-1.08) | 0.300 | 0.98 (0.83-1.16) | 0.795 |
| Uninsured | | 0.69 (0.56-0.86) | **<0.001** | 0.77 (0.62-0.97) | **0.025** |
| Residential region | Metropolitan | | | | |
| Urban | | 1.00 (0.86-1.18) | 0.955 | – | – |
| Rural | | 1.33 (0.84-2.09) | 0.222 | – | – |
| Charlson-Deyo Comorbidity score | 0 | | | | |
| 1 | | 0.94 (0.78-1.12) | 0.458 | – | – |
| 2+ | | 1.10 (0.86-1.40) | 0.464 | – | – |
| Adults without high school degree in zip code | <6.3% | | | | |
| 6.3%-10.8% | | 0.95 (0.82-1.10) | 0.470 | 0.94 (0.80-1.10) | 0.425 |
| 10.9%-17.5% | | 0.77 (0.66-0.91) | **0.001** | 0.76 (0.63-0.93) | **0.006** |
| ≥17.6% | | 0.62 (0.52-0.73) | **<0.001** | 0.62 (0.49-0.78) | **<0.001** |
| Median household income in zip code | <$40,227 | | | | |
| $40,227-50,353 | | 1.15 (0.96-1.39) | 0.130 | 0.97 (0.79-1.18) | 0.742 |
| $50,354-63,332 | | 1.25 (1.04-1.50) | **0.015** | 0.92 (0.75-1.13) | 0.431 |
| ≥$63,333 | | 1.32 (1.11-1.55) | **0.001** | 0.88 (0.71-1.10) | 0.274 |
| Geographic region | Midwest | | | | |
| Northeast | | 0.65 (0.55-0.78) | **<0.001** | 0.68 (0.57-0.82) | **<0.001** |
| South | | 0.54 (0.43-0.69) | **<0.001** | 0.62 (0.49-0.79) | **<0.001** |
| West | | 1.12 (0.91-1.39) | 0.278 | 1.19 (0.96-1.48) | 0.112 |
| Unknown | | 0.87 (0.74-1.02) | 0.094 | 0.77 (0.61-0.97) | **0.026** |
| Facility setting | Academic | | | | |
| Nonacademic | | 0.89 (0.77-1.03) | 0.133 | - | - |
| Unknown | | 1.04 (0.91-1.18) | 0.566 | – | – |
| WHO grade | Grade II | | | | |
| Grade III | | 0.93 (0.83-1.04) | 0.224 | – | – |
| Histology | Oligodendroglioma | | | | |
| Oligoastrocytoma | | 0.85 (0.75-0.95) | **0.005** | 0.83 (0.73-0.93) | **0.002** |

*Bold values indicate statistical significance (p < 0.05).*

TABLE 3 | Characteristics of patients with and without a reported 1p/19q codeletion test diagnosed in 2017. Frequencies and proportions are row-based.

| Variable | Unreported 1p/19q test N = 289 | Reported 1p/19q test N = 430 | P-value |
|---|---|---|---|
| Age, median (IQR) | 44 (35-55) | 45 (36-56) | 0.756 |
| Sex | | | 0.778 |
| Male (n=386) | 157 (40.7%) | 229 (59.3%) | |
| Female (n=333) | 132 (39.6%) | 201 (60.4%) | |
| Race/Ethnicity | | | **0.008** |
| Non-Hispanic White (n=555) | 213 (38.4%) | 342 (61.6%) | |
| Hispanic White (n=77) | 38 (49.4%) | 39 (50.6%) | |
| Black (n=47) | 27 (57.4%) | 20 (42.6%) | |
| Other (n=40) | 11 (27.5%) | 29 (72.5%) | |
| Insurance | | | 0.670 |
| Private (n=452) | 174 (38.5%) | 278 (61.5%) | |
| Medicare (n=93) | 39 (41.9%) | 54 (58.1%) | |
| Medicaid/Other (n=132) | 58 (43.9%) | 74 (56.1%) | |
| Uninsured (n=42) | 18 (42.9%) | 24 (57.1%) | |
| Median household income in zip code | | | 0.294 |
| <$40,227 (n=96) | 47 (49.0%) | 49 (51.0%) | |
| $40,227-50,353 (n=135) | 51 (37.8%) | 84 (62.2%) | |
| $50,354-63,332 (n=185) | 74 (40.0%) | 111 (60.0%) | |
| ≥$63,333 (n=303) | 117 (38.6%) | 186 (61.4%) | |
| Adults without high school degree in zip code | | | 0.080 |
| ≥17.6% (n=134) | 66 (49.3%) | 68 (50.7%) | |
| 10.9%-17.5% (n=176) | 64 (36.4%) | 112 (63.6%) | |
| 6.3%-10.8% (n=202) | 83 (41.1%) | 119 (58.9%) | |
| <6.3% (n=207) | 76 (36.7%) | 131 (63.3%) | |
| Charlson-Deyo Comorbidity Score | | | 0.382 |
| 0 (n=602) | 242 (40.2%) | 360 (59.8%) | |
| 1 (n=83) | 30 (36.1%) | 53 (63.9%) | |
| 2+ (n=34) | 17 (50.0%) | 17 (50.0%) | |
| Residential Region | | | 0.565 |
| Metropolitan (n=606) | 248 (40.9%) | 358 (59.1%) | |
| Urban (n=99) | 35 (35.4%) | 64 (64.6%) | |
| Rural (n=14) | 6 (42.9%) | 8 (57.1%) | |
| Geographic Region | | | **0.001** |
| Northeast (n=162) | 75 (46.3%) | 87 (53.7%) | |
| Midwest (n=122) | 36 (29.5%) | 86 (70.5%) | |
| South (n=69) | 36 (52.2%) | 33 (47.8%) | |
| West (n=106) | 33 (31.1%) | 73 (68.9%) | |
| Unknown (n=260) | 109 (41.9%) | 151 (58.1%) | |
| Facility Setting | | | 0.330 |
| Academic (n=245) | 91 (37.1%) | 154 (62.9%) | |
| Non-academic (n=214) | 89 (41.6%) | 125 (58.4%) | |
| Unknown (n=260) | 109 (41.9%) | 151 (58.1%) | |
| Distance travelled (miles), median (IQR) | 13.9 (7.2-29.6) | 16.8 (7.1-37.0) | 0.387 |
| 1p/19q status | | | NA |
| Co-deleted | NA | 380 | |
| Not co-deleted | NA | 50 | |
| Histology | | | 0.627 |
| Oligodendroglioma (n=678) | 274 (40.4%) | 404 (59.6%) | |
| Oligoastrocytoma (n=41) | 15 (36.6%) | 26 (63.4%) | |
| WHO grade | | | **0.030** |
| 2 (n=428) | 186 (43.5%) | 242 (56.5%) | |
| 3 (n=291) | 103 (35.4%) | 188 (64.6%) | |
| Tumor location | | | 0.697 |
| Supratentorial (n=636) | 254 (39.9%) | 382 (60.1%) | |
| Infratentorial (n=0) | 0 | 0 | |
| NOS or other CNS (n=83) | 35 (42.2%) | 48 (57.8%) | |
| Tumor size | | | 0.805 |
| <5 cm (n=257) | 96 (37.4%) | 161 (62.6%) | |
| ≥5 cm (n=263) | 101 (38.4%) | 162 (61.6%) | |
| Unknown | 92 (46.2%) | 107 (53.8%) | |
| Extent of resection | | | 0.112 |
| Biopsy only (n=65) | 28 (43.1%) | 37 (56.9%) | |
| STR (n=329) | 144 (43.8%) | 185 (56.2%) | |

*(Continued)*

**TABLE 3 |** Continued

| Variable | Unreported 1p/19q test N = 289 | Reported 1p/19q test N = 430 | P-value |
|---|---|---|---|
| GTR (n=320) | 115 (35.9%) | 205 (64.1%) | |
| Unknown (n=5) | 2 (40.0%) | 3 (60.0%) | |
| Chemotherapy | | | 0.187 |
| Yes (n=471) | 181 (38.4%) | 290 (61.6%) | |
| No (n=222) | 97 (43.7%) | 125 (56.3%) | |
| Unknown (n=26) | 11 (42.3%) | 15 (57.7%) | |
| Radiotherapy | | | 0.261 |
| Yes (n=449) | 173 (38.5%) | 276 (61.5%) | |
| No (n=264) | 113 (42.8%) | 151 (57.2%) | |
| Unknown (n=6) | 3 (50.0%) | 3 (50.0%) | |
| Adjuvant treatment | | | 0.522 |
| Chemotherapy alone (n=59) | 25 (42.4%) | 34 (57.6%) | |
| Radiotherapy alone (n=32) | 15 (46.9%) | 17 (53.1%) | |
| Chemotherapy+Radiotherapy (n=412) | 156 (37.9%) | 256 (62.1%) | |
| Neither (n=186) | 80 (43.0%) | 106 (57.0%) | |
| Unknown (n=30) | 13 (43.3%) | 17 (56.7%) | |

*Bold values indicate statistical significance (p < 0.05).*
*NA, not applicable.*

**TABLE 4 |** Univariate and multivariable logistic regression evaluating factors associated with reporting of a 1p/19q codeletion test for patients diagnosed in 2017.

| Variable | Reference | Univariate | | Multivariable | |
|---|---|---|---|---|---|
| | | OR (95% CI) | P-value | OR (95% CI) | P-value |
| Age | Continuous | 1.00 (0.99-1.01) | 0.756 | – | – |
| Race/Ethnicity | Non-Hispanic White | | | | |
| Hispanic White | | 0.64 (0.40-1.03) | 0.067 | 0.68 (0.40-1.15) | 0.149 |
| Black | | 0.46 (0.25-0.84) | **0.012** | 0.49 (0.26-0.91) | **0.024** |
| Other | | 1.64 (0.83-3.50) | 0.174 | 1.66 (0.82-3.60) | 0.174 |
| Insurance | Private | | | | |
| Medicare | | 0.87 (0.55-1.37) | 0.536 | – | – |
| Medicaid/Other | | 0.80 (0.54-1.18) | 0.261 | – | – |
| Uninsured | | 0.83 (0.44-1.60) | 0.580 | – | – |
| Residential region | Metropolitan | | | | |
| Urban | | 1.27 (0.82-1.99) | 0.295 | – | – |
| Rural | | 0.92 (0.32-2.84) | 0.884 | – | – |
| Charlson-Deyo Comorbidity score | 0 | | | | |
| 1 | | 1.19 (0.74-1.93) | 0.479 | – | – |
| 2+ | | 0.67 (0.33-1.35) | 0.260 | – | – |
| Adults without high school degree in zip code | <6.3% | | | | |
| 6.3%-10.8% | | 0.83 (0.56-1.24) | 0.364 | 0.88 (0.57-1.34) | 0.543 |
| 10.9%-17.5% | | 1.02 (0.67-1.54) | 0.943 | 1.27 (0.76-2.12) | 0.361 |
| ≥17.6% | | 0.60 (0.38-0.93) | **0.022** | 0.86 (0.47-1.60) | 0.641 |
| Median household income in zip code | <$40,227 | | | | |
| $40,227-50,353 | | 1.58 (0.93-2.69) | 0.091 | 1.31 (0.74-2.33) | 0.348 |
| $50,354-63,332 | | 1.44 (0.88-2.37) | 0.151 | 1.16 (0.66-2.05) | 0.605 |
| ≥$63,333 | | 1.52 (0.96-2.42) | 0.074 | 1.21 (0.66-2.23) | 0.539 |
| Geographic region | Midwest | | | | |
| Northeast | | 0.49 (0.29-0.79) | **0.004** | 0.50 (0.30-0.84) | **0.009** |
| South | | 0.38 (0.21-0.70) | **0.002** | 0.42 (0.22-0.78) | **0.007** |
| West | | 0.93 (0.53-1.63) | 0.790 | 0.92 (0.51-1.65) | 0.776 |
| Unknown | | 0.58 (0.36-0.91) | **0.020** | 0.62 (0.38-0.99) | **0.047** |
| Facility setting | Academic | | | | |
| Nonacademic | | 0.83 (0.57-1.21) | 0.331 | – | – |
| Unknown | | 0.82 (0.57-1.17) | 0.273 | – | – |
| WHO grade | Grade II | | | | |
| Grade III | | 1.40 (1.03-1.91) | **0.031** | 1.37 (1.01-1.89) | **0.049** |
| Histology | Oligodendroglioma | | | | |
| Oligoastrocytoma | | 1.18 (0.62-2.31) | 0.628 | – | – |

*Bold values indicate statistical significance (p < 0.05).*

**TABLE 5 |** Adjusted odds of a reported test for patients diagnosed in 2017 versus 2011-2015.

| Variable | OR (95% CI) | P-value |
|---|---|---|
| Overall | 1.57 (1.33-1.86) | **<0.001** |
| Race/Ethnicity | | |
| Non-Hispanic White | 1.61 (1.33-1.94) | **<0.001** |
| Hispanic White | 1.28 (0.77-2.11) | 0.341 |
| Black | 1.04 (0.54-1.94) | 0.915 |
| Other | 3.26 (1.57-7.22) | **0.002** |
| Insurance | | |
| Private | 1.54 (1.25-1.90) | **<0.001** |
| Medicare | 1.84 (1.18-2.91) | **0.007** |
| Medicaid/Other | 1.46 (1.00-2.16) | 0.054 |
| Uninsured | 1.80 (0.93-3.53) | 0.082 |
| Residential region | | |
| Metropolitan | 1.51 (1.26-1.81) | **<0.001** |
| Urban | 2.22 (1.42-3.53) | **<0.001** |
| Rural | 1.20 (0.33-4.46) | 0.783 |
| Adults without high school degree in zip code | | |
| <6.3% | 1.56 (1.15-2.12) | **0.004** |
| 6.3%-10.8% | 1.32 (0.97-1.79) | 0.081 |
| 10.9%-17.5% | 2.07 (1.48-2.91) | **<0.001** |
| ≥17.6% | 1.44 (0.99-2.09) | 0.058 |
| Median household income in zip code | | |
| <$40,227 | 1.31 (0.85-2.03) | 0.228 |
| $40,227-50,353 | 1.93 (1.33-2.83) | **<0.001** |
| $50,354-63,332 | 1.59 (1.15-2.22) | **0.006** |
| ≥$63,333 | 1.61 (1.25-2.08) | **<0.001** |
| Geographic region | | |
| Northeast | 1.58 (1.12-2.23) | **0.009** |
| Midwest | 2.05 (1.34-3.20) | **0.001** |
| South | 1.42 (0.84-2.38) | 0.187 |
| West | 1.61 (1.03-2.56) | **0.042** |
| Facility setting | | |
| Academic | 1.86 (1.39-2.50) | **<0.001** |
| Nonacademic | 1.47 (1.08-1.99) | **0.013** |
| WHO grade | | |
| Grade II | 1.34 (1.08-1.66) | **0.007** |
| Grade III | 2.03 (1.56-2.66) | **<0.001** |
| Histology | | |
| Oligodendroglioma | 1.54 (1.30-1.83) | **<0.001** |
| Oligoastrocytoma | 2.39 (1.25-4.76) | **0.009** |

*Bold values indicate statistical significance (p < 0.05).*

codeletion test and GTR was found to be significantly associated with decreased odds of receiving adjuvant treatment (OR 0.63; 95% CI 0.49-0.82; p<0.001) (**Table 6**).

## DISCUSSION

In an analysis of a national oncology registry, we evaluated disparities in reported testing for 1p/19q codeletion in patients with a histological diagnosis of either oligodendroglioma or oligoastrocytoma given the marker's inclusion as a mandatory component of diagnosis in the 2016 WHO classification of CNS tumor guidelines. A 14.0% increase in reported testing was identified from 2011 to 2017. However, the rise was not equitable among all patient subgroups. While disparities among uninsured patients and those in zip codes with lower educational attainment dissipated from 2011-2015 to 2017, geographic regional disparities

were maintained. Black patients were also found to have an insignificant change in testing rates from 2011-2015 to 2017. Subsequently, they were also found to have disproportionately lower odds of testing following the new WHO guidelines. The likelihood of receiving adjuvant treatment was also found to be independently associated with reported codeletion testing status.

Although the precise mechanisms behind these disparities could not be ascertained in our analysis, these are likely multifactorial in nature. Laboratory capabilities such as fluorescence *in situ* hybridization, most commonly used to detect codeletion, may not be available onsite at hospitals with smaller case volumes (19). Inequities in access to high-volume facilities among Black, Hispanic, and lower socioeconomic status patients undergoing brain tumor craniotomy have been extensively documented (8, 10, 20). Heterogeneous geographic disparities in care and a lower likelihood of travelling large distances to high-volume hospitals, previous observations among these patient populations, may compound financial and/or logistical barriers to centralized neuro-oncological care (21–23). Socioeconomic status is often intertwined with race/ethnicity and has also been shown to influence outcomes and access to treatments for glioma patients (9, 11, 24). In our analysis, the Northeast and South were highlighted as geographic regions in the United States that should garner additional focus for addressing disparities in testing. Additionally, the insignificant improvement in testing rates among Black patients was especially concerning given the increased likelihood of testing for most other demographic subgroups. Future studies are needed to more specifically identify how these disparities arise in order to develop targeted initiatives that promote more equitable access to care.

There remains conflicting evidence with regard to the impact of race/ethnicity on OS among oligodendroglioma and oligoastrocytoma patients. Analyses from the Central Brain Tumor Registry of the United States (CBRTUS) and Surveillance, Epidemiology, and End Results (SEER) registry have previously noted a lower incidence of primary oligodendroglial tumors among Black patients, but similar or higher OS, compared to White patients (25, 26). In contrast, Shin et al. evaluated anaplastic oligodendroglioma patients in the NCDB and found that Black patients had significantly lower OS compared to non-Black patients, even after only selecting patients who received chemoradiotherapy (27). However, molecular profile was not evaluated in any of these studies. While it has been suggested that patient race may predispose gliomas to molecular profiles that are associated with discrepancies in survival, the causes of the molecular heterogeneity of gliomas remain poorly understood (28, 29). More likely, the aforementioned inequities in access to care, such as for molecular testing, play a substantial role in influencing differences in patient management and survival.

Studies on the epidemiology of oligodendroglioma diagnoses and testing for O-6-Methylguanine-DNA Methyltransferase (MGMT) promoter methylation in glioblastoma (GBM) patients may provide further insights into disparities in molecular testing rates. An analysis of the CBTRUS identified that the incidence of oligodendroglioma significantly declined from 2000-2013 for

TABLE 6 | Univariate and multivariable logistic regression evaluating factors associated with receipt of adjuvant treatment.

| Variable | Reference | Univariate | | Multivariable | |
|---|---|---|---|---|---|
| | | OR (95% CI) | P-value | OR (95% CI) | P-value |
| 1p/19q testing | Unreported test | | | | |
|   Reported test | | 1.35 (1.20-1.51) | **<0.001** | 1.73 (1.46-2.04) | **<0.001** |
| GTR | No | | | | |
|   Yes | | 0.62 (0.55-0.69) | **<0.001** | 0.63 (0.49-0.82) | **<0.001** |
|   1p/19q testing * GTR | Unreported test or no GTR | | | | |
|   Reported test and GTR | | – | – | | |
| Year of Diagnosis | 2011-2015 | | | | |
|   2017 | | 1.65 (1.38-1.97) | **<0.001** | 2.04 (1.67-2.51) | **<0.001** |
| Age | Continuous | 1.02 (1.02-1.02) | **<0.001** | 0.99 (0.98-1.00) | 0.113 |
| Race | Non-Hispanic White | | | | |
|   Hispanic White | | 0.87 (0.71-1.08) | 0.205 | 0.95 (0.74-1.23) | 0.706 |
|   Black | | 0.79 (0.63-1.07) | 0.054 | 0.92 (0.70-1.21) | 0.555 |
|   Other | | 0.95 (0.74-1.22) | 0.678 | 0.97 (0.73-1.30) | 0.846 |
| Insurance | Private | | | | |
|   Medicare | | 1.04 (0.88-1.23) | 0.666 | 0.68 (0.54-0.86) | **0.001** |
|   Medicaid/Other | | 1.09 (0.93-1.28) | 0.288 | 1.09 (0.90-1.31) | 0.396 |
|   Uninsured | | 0.74 (0.60-0.91) | **0.004** | 0.80 (0.63-1.03) | 0.080 |
| Residential region | Metropolitan | | | | |
|   Urban | | 0.96 (0.82-1.13) | 0.635 | – | - |
|   Rural | | 1.48 (0.94-2.43) | 0.104 | – | - |
| Charlson-Deyo Comorbidity score | 0 | | | | |
|   1 | | 1.03 (0.87-1.23) | 0.726 | – | - |
|   2+ | | 1.06 (0.83-1.37) | 0.639 | – | - |
| Adults without high school degree in zip code | <6.3% | | | | |
|   6.3%-10.8% | | 0.96 (0.83-1.11) | 0.572 | 0.90 (0.75-1.07) | 0.237 |
|   10.9%-17.5% | | 0.98 (0.84-1.14) | 0.769 | 1.03 (0.83-1.27) | 0.810 |
|   ≥17.6% | | 0.78 (0.66-0.91) | **0.002** | 0.79 (0.62-1.02) | 0.067 |
| Median household income in zip code | <$40,227 | | | | |
|   $40,227-50,353 | | 1.24 (1.03-1.50) | **0.020** | 1.24 (0.99-1.54) | 0.059 |
|   $50,354-63,332 | | 1.19 (0.99-1.42) | 0.062 | 1.03 (0.82-1.30) | 0.768 |
|   ≥$63,333 | | 1.15 (0.97-1.35) | 0.102 | 0.97 (0.76-1.24) | 0.809 |
| Geographic region | Midwest | | | | |
|   Northeast | | 0.73 (0.61-0.89) | **0.002** | 0.70 (0.56-0.87) | **0.001** |
|   South | | 0.48 (0.38-0.61) | **<0.001** | 0.48 (0.36-0.62) | **<0.001** |
|   West | | 0.74 (0.59-0.92) | **0.007** | 0.68 (0.53-0.87) | **0.002** |
|   Unknown | | 0.38 (0.32-0.46) | **<0.001** | 0.34 (0.26-0.44) | **<0.001** |
| Facility setting* | Academic | | | | |
|   Nonacademic | | 1.24 (1.06-1.44) | **0.006** | – | - |
|   Unknown | | 0.56 (0.49-0.64) | **<0.001** | – | - |
| WHO grade | II | | | | |
|   III | | 6.36 (5.55-7.29) | **<0.001** | 7.17 (6.20-8.30) | **<0.001** |
| Histology | Oligodendroglioma | | | | |
|   Oligoastrocytoma | | 1.20 (1.07-1.36) | **0.003** | 1.22 (1.06-1.41) | **0.006** |

*Facility setting was not included in the multivariable model due to collinearity with geographic region.
Bold values indicate statistical significance (p < 0.05).

White and Asian/Pacific Islander patients, but not Black patients (26). The increasing emphasis on using 1p/19q codeletion status for diagnosis during this time period, including recommendations for testing in tumors with an oligodendroglial component from the National Comprehensive Cancer Network, suggest that this epidemiological variation may be due to differences in utilization of molecular diagnostics between races (30). In addition, Lamba et al. performed an analysis of the NCDB from 2010-2016 and found that GBM patients of lower socioeconomic status, including insurance and median household income, were disproportionately less likely to be tested for MGMT methylation status. However, patient race/ethnicity was not identified as a significant predictor. MGMT-tested patients were also more likely to receive

chemotherapy compared to untested patients, which is comparable to our findings on adjuvant treatment for oligodendroglioma/ oligoastrocytoma patients (31). As a potential consequence of inequitable molecular testing, racial, socioeconomic, and geographic disparities may exacerbate pre-existing barriers to clinical trial enrollment since molecular profile has become an increasingly emphasized criterion for screening patients with primary CNS tumors (32–34).

A primary concern regarding disparities in testing rates is the potential for inferior patient outcomes, especially for heterogeneously managed tumors like oligodendrogliomas and oligoastrocytomas. Our analysis indicated that having a reported 1p/19q codeletion test was independently associated with receiving

adjuvant treatment. In the literature, differences in patient survival based on adjuvant management of these tumors have been previously noted. Two randomized clinical trials published in 2013 demonstrated an enhanced response to radiotherapy with the addition of adjuvant procarbazine, lomustine, and vincristine (PCV) in anaplastic oligodendroglioma patients with a 1p/19q codeletion compared to those without the mutation (3, 4). Additionally, while we await the results from the ongoing CODEL trial comparing temozolomide with radiotherapy and PCV with radiotherapy for codeleted WHO grade III oligodendrogliomas, results from the initial study design demonstrated superior progression-free survival for patients receiving temozolomide with radiotherapy as compared to temozolomide alone (35). In our study cohort, it is likely that patients without a reported test are comprised of both 1p/19q intact and codeleted patients. Given the impact of reported testing rates on adjuvant management and the influence of molecular profile on tumor treatment response, disparities in molecular testing may influence outcomes for oligodendroglioma and oligoastrocytoma patients.

There are some limitations to this study. The retrospective study design may subject the cohort to selection bias. Variables included in the analysis were limited to those available in the database. Notably, IDH status is not collected in NCDB (14). Although 1p/19q codeletions predominately co-occur with IDH mutations, the most complete evaluation of the 2016 WHO guidelines would include both markers. The analytical technique and timing of codeletion testing was also lacking, limiting our interpretation on optimal integration of testing into clinical practice. Furthermore, the extent of missing data on facility setting and region, since these variables are suppressed for patients aged <40, should be considered when evaluating the results. The potential for miscoding of ICD-O-3 codes should also be acknowledged. Given that the NCDB only captures patients from CoC-accredited hospitals, the study cohort was not population-based. In addition, our analysis is contextualized as evaluating the reported testing rates for codeletion in the NCDB, rather than the actual testing rate. The NCDB PUF acknowledges the likelihood that case coverage of site-specific factors, including 1p/19q codeletion, may be limited in the database (14). This may be due to factors including data availability at the time of abstraction. However, other site-specific factors, like WHO grade, are extensively coded throughout the study period.

## CONCLUSION

Routine molecular profiling of histological oligodendrogliomas and oligoastrocytomas serves as an opportunity to more accurately classify these tumors, better inform prognosis, and optimize patient management. Despite the 2016 WHO guidelines, disparities in facility geographic region persisted and new disparities in race/ethnicity were identified for reported 1p/19q codeletion testing. Since the likelihood of receiving adjuvant treatment was found to be associated with reported testing, these disparities may further influence patient outcomes. These findings highlight the need for more targeted research efforts to identify mechanisms behind these disparities as well as initiatives to promote more equitable access to testing.

## DATA AVAILABILITY STATEMENT

The data analyzed in this study is subject to the following licenses/restrictions: NCDB PUFs are only available through an application process to investigators associated with CoC-accredited cancer programs. Requests to access these datasets should be directed to https://www.facs.org/quality-programs/cancer/ncdb/puf.

## ETHICS STATEMENT

Ethical review and approval was not required for the study on human participants in accordance with the local legislation and institutional requirements. Written informed consent for participation was not required for this study in accordance with the national legislation and the institutional requirements.

## AUTHOR CONTRIBUTIONS

All authors listed have made a substantial, direct, and intellectual contribution to the work and approved it for publication.

## FUNDING

## SUPPLEMENTARY MATERIAL

The Supplementary Material for this article can be found online at: https://www.frontiersin.org/articles/10.3389/fonc.2021.746844/full#supplementary-material

## REFERENCES

1. Zhao J, Ma W, Zhao H. Loss of Heterozygosity 1p/19q and Survival in Glioma: A Meta-Analysis. *Neuro-Oncology* (2013) 16(1):103–12. doi: 10.1093/neuonc/not145
2. Aquilanti E, Miller J, Santagata S, Cahill DP, Brastianos PK. Updates in Prognostic Markers for Gliomas. *Neuro-Oncology* (2018) 20(suppl_7):vii17–26. doi: 10.1093/neuonc/noy158
3. Cairncross G, Wang M, Shaw E, Jenkins R, Brachman D, Buckner J, et al. Phase III Trial of Chemoradiotherapy for Anaplastic Oligodendroglioma: Long-Term Results of RTOG 9402. *J Clin Oncol* (2013) 31(3):337–43. doi: 10.1200/JCO.2012.43.2674
4. van den Bent MJ, Brandes AA, Taphoorn MJ, Kros JM, Kouwenhoven MC, Delattre JY, et al. Adjuvant Procarbazine, Lomustine, and Vincristine Chemotherapy in Newly Diagnosed Anaplastic Oligodendroglioma:

Long-Term Follow-Up of EORTC Brain Tumor Group Study 26951. *J Clin Oncol* (2013) 31(3):344–50. doi: 10.1200/JCO.2012.43.2229

5. Labussière M, Idbaih A, Wang XW, Marie Y, Boisselier B, Falet C, et al. All the 1p19q Codeleted Gliomas Are Mutated on IDH1 or IDH2. *Neurology* (2010) 74(23):1886–90. doi: 10.1212/WNL.0b013e3181e1cf3a

6. Eckel-Passow JE, Lachance DH, Molinaro AM, Walsh KM, Decker PA, Sicotte H, et al. Glioma Groups Based on 1p/19q, IDH, and TERT Promoter Mutations in Tumors. *N Engl J Med* (2015) 372(26):2499–508. doi: 10.1056/NEJMoa1407279

7. Louis DN, Perry A, Reifenberger G, von Deimling A, Figarella-Branger D, Cavenee WK, et al. The 2016 World Health Organization Classification of Tumors of the Central Nervous System: A Summary. *Acta Neuropathol* (2016) 131(6):803–20. doi: 10.1007/s00401-016-1545-1

8. Curry WTJr., Barker FG2nd. Racial, Ethnic and Socioeconomic Disparities in the Treatment of Brain Tumors. *J Neurooncol* (2009) 93(1):25–39. doi: 10.1007/s11060-009-9840-5

9. Brown DA, Himes BT, Kerezoudis P, Chilinda-Salter YM, Grewal SS, Spear JA, et al. Insurance Correlates With Improved Access to Care and Outcome Among Glioblastoma Patients. *Neuro Oncol* (2018) 20(10):1374–82. doi: 10.1093/neuonc/noy102

10. Mukherjee D, Zaidi HA, Kosztowski T, Chaichana KL, Brem H, Chang DC, et al. Disparities in Access to Neuro-Oncologic Care in the United States. *Arch Surg* (2010) 145(3):247–53. doi: 10.1001/archsurg.2009.288

11. Bower A, Hsu FC, Weaver KE, Yelton C, Merrill R, Wicks R, et al. Community Economic Factors Influence Outcomes for Patients With Primary Malignant Glioma. *Neurooncol Pract* (2020) 7(4):453–60. doi: 10.1093/nop/npaa010

12. Bilimoria KY, Stewart AK, Winchester DP, Ko CY. The National Cancer Data Base: A Powerful Initiative to Improve Cancer Care in the United States. *Ann Surg Oncol* (2008) 15(3):683–90. doi: 10.1245/s10434-007-9747-3

13. Boffa DJ, Rosen JE, Mallin K, Loomis A, Gay G, Palis B, et al. Using the National Cancer Database for Outcomes Research: A Review. *JAMA Oncol* (2017) 3(12):1722–8. doi: 10.1001/jamaoncol.2016.6905

14. American College of Surgeons. *National Cancer Database Participant User File: 2017 Data Dictionary 2017*. Available at: https://www.facs.org/-/media/files/quality-programs/cancer/ncdb/puf_data_dictionary_2017.ashx.

15. Garton ALA, Kinslow CJ, Rae AI, Mehta A, Pannullo SC, Magge RS, et al. Extent of Resection, Molecular Signature, and Survival in 1p19q-Codeleted Gliomas. *J Neurosurg* (2020) 134(5):1357–67. doi: 10.3171/2020.2.JNS192767

16. Schomas DA, Laack NN, Rao RD, Meyer FB, Shaw EG, O'Neill BP, et al. Intracranial Low-Grade Gliomas in Adults: 30-Year Experience With Long-Term Follow-Up at Mayo Clinic. *Neuro Oncol* (2009) 11(4):437–45. doi: 10.1215/15228517-2008-102

17. American College of Surgeons. *Facility Oncology Registry Data Standards: Revised for 2016*. Available at: https://www.facs.org/-/media/files/quality-programs/cancer/ncdb/fords-2016.ashx.

18. R Core Team. *R: A Language and Environment for Statistical Computing*. Vienna, Austria: R Foundation for Statistical Computing (2019). Available at: https://www.R-project.org/.

19. Woehrer A, Hainfellner JA. Molecular Diagnostics: Techniques and Recommendations for 1p/19q Assessment. *CNS Oncol* (2015) 4(5):295–306. doi: 10.2217/cns.15.28

20. Trinh VT, Davies JM, Berger MS. Surgery for Primary Supratentorial Brain Tumors in the United States, 2000-2009: Effect of Provider and Hospital Caseload on Complication Rates. *J Neurosurg* (2015) 122(2):280–96. doi: 10.3171/2014.9.JNS131648

21. Lu VM, Lewis CT, Esquenazi Y. Geographic and Socioeconomic Considerations for Glioblastoma Treatment in the Elderly at a National Level: A US Perspective. *Neurooncol Pract* (2020) 7(5):522–30. doi: 10.1093/nop/npaa029

22. Lu VM, Shah AH, Eichberg DG, Quinones-Hinojosa A, Esquenazi Y, Komotar RJ, et al. Geographic Disparities in Access to Glioblastoma Treatment Based on Hispanic Ethnicity in the United States: Insights From a National Database. *J Neurooncol* (2020) 147(3):711–20. doi: 10.1007/s11060-020-03480-1

23. Lopez Ramos C, Brandel MG, Steinberg JA, Wali AR, Rennert RC, Santiago-Dieppa DR, et al. The Impact of Traveling Distance and Hospital Volume on Post-Surgical Outcomes for Patients With Glioblastoma. *J Neuro-Oncology* (2019) 141(1):159–66. doi: 10.1007/s11060-018-03022-w

24. Chandra A, Rick JW, Dalle Ore C, Lau D, Nguyen AT, Carrera D, et al. Disparities in Health Care Determine Prognosis in Newly Diagnosed Glioblastoma. *Neurosurg Focus* (2018) 44(6):E16. doi: 10.3171/2018.3.FOCUS1852

25. Ostrom QT, Cote DJ, Ascha M, Kruchko C, Barnholtz-Sloan JS. Adult Glioma Incidence and Survival by Race or Ethnicity in the United States From 2000 to 2014. *JAMA Oncol* (2018) 4(9):1254–62. doi: 10.1001/jamaoncol.2018.1789

26. Achey RL, Khanna V, Ostrom QT, Kruchko C, Barnholtz-Sloan JS. Incidence and Survival Trends in Oligodendrogliomas and Anaplastic Oligodendrogliomas in the United States From 2000 to 2013: A CBTRUS Report. *J Neurooncol* (2017) 133(1):17–25. doi: 10.1007/s11060-017-2414-z

27. Shin JY, Yoon JK, Diaz AZ. Racial Disparities in Anaplastic Oligodendroglioma: An Analysis on 1643 Patients. *J Clin Neurosci* (2017) 37:34–9. doi: 10.1016/j.jocn.2016.12.003

28. Wu M, Miska J, Xiao T, Zhang P, Kane JR, Balyasnikova IV, et al. Race Influences Survival in Glioblastoma Patients With KPS ≥ 80 and Associates With Genetic Markers of Retinoic Acid Metabolism. *J Neurooncol* (2019) 142(2):375–84. doi: 10.1007/s11060-019-03110-5

29. Heath EI, Lynce F, Xiu J, Ellerbrock A, Reddy SK, Obeid E, et al. Racial Disparities in the Molecular Landscape of Cancer. *Anticancer Res* (2018) 38(4):2235–40. doi: 10.21873/anticanres.12466

30. Nabors LB, Ammirati M, Bierman PJ, Brem H, Butowski N, Chamberlain MC, et al. Central Nervous System Cancers. *J Natl Compr Canc Netw* (2013) 11(9):1114–51. doi: 10.6004/jnccn.2013.0132

31. Lamba N, Chukwueke UN, Smith TR, Ligon KL, Aizer A, Reardon DA, et al. Socioeconomic Disparities Associated With MGMT Promoter Methylation Testing for Patients With Glioblastoma. *JAMA Oncol* (2020) 6(12):1972–4. doi: 10.1001/jamaoncol.2020.4937

32. Lee EQ, Chukwueke UN, Hervey-Jumper SL, de Groot JF, Leone JP, Armstrong TS, et al. Barriers to Accrual and Enrollment in Brain Tumor Trials. *Neuro Oncol* (2019) 21(9):1100–17. doi: 10.1093/neuonc/noz104

33. Morshed RA, Reihl SJ, Molinaro AM, Kakaizada S, Young JS, Schulte JD, et al. The Influence of Race and Socioeconomic Status on Therapeutic Clinical Trial Screening and Enrollment. *J Neurooncol* (2020) 148(1):131–9. doi: 10.1007/s11060-020-03503-x

34. Taha B, Winston G, Tosi U, Hartley B, Hoffman C, Dahmane N, et al. Missing Diversity in Brain Tumor Trials. *Neurooncol Adv* (2020) 2(1):vdaa059. doi: 10.1093/noajnl/vdaa059

35. Jaeckle KA, Ballman KV, van den Bent M, Giannini C, Galanis E, Brown PD, et al. CODEL: Phase III Study of RT, RT + Temozolomide (TMZ), or TMZ for Newly-Diagnosed 1p/19q Codeleted Oligodendroglioma. Analysis From the Initial Study Design. *Neuro Oncol* (2020) 23(3):457–67. doi: 10.1093/neuonc/noaa168

Check for updates

# Retrospective Study on the Application of Enhanced Recovery After Surgery Measures to Promote Postoperative Rehabilitation in 50 Patients With Brain Tumor Undergoing Craniotomy

SongShan Feng[1,2], Bo Xie[1], ZhenYan Li[1], XiaoXi Zhou[1], Quan Cheng[1], ZhiXiong Liu[1], ZiRong Tao[3*] and MingYu Zhang[1,2*]

[1] Department of Neurosurgery, Xiangya Hospital, Central South University, Changsha, China, [2] National Clinical Research Center for Geriatric Disorders, Xiangya Hospital, Central South University, Changsha, China, [3] Teaching and Research Section of Clinical Nursing, Xiangya Hospital, Central South University, Changsha, China

**Objective:** To investigate whether enhanced recovery after surgery (ERAS) can promote rehabilitation of patients after neurosurgical craniotomy.

**Methods:** The clinical data of 100 patients with brain tumor undergoing craniotomy in the Department of Neurosurgery, Xiangya Hospital, Central South University, from January 2018 to August 2020 were collected, including 50 patients in the ERAS group and 50 patients in the control group. t-Test, Wilcoxon's rank sum test, and chi-square analysis were used to compare the clinical characteristics, prognosis, and hospitalization time between the two groups.

**Results:** There was no significant difference in gender, age, and other general clinical data between the two groups ($p > 0.05$). The days of antiemetic drugs applied in the ERAS group were less than those in the control group (1.00 $vs$. 2.00 days, $p = 0.003$), and the proportion of patients requiring analgesics was lower than that of the control group (30% $vs$. 52%, OR = 0.41, 95% CI 0.18–0.93, $p = 0.031$). The time of urinary catheter removal and that of patients starting ambulation in the ERAS group were shorter than those in the control group (16.00 $vs$. 24.00 h, and 1.00 $vs$. 2.00 days, $p < 0.001$, respectively); and the hospital length of stay (LOS) in the ERAS group was shorter than that in the control group (Total LOS, 13.00 $vs$. 15.50 days; Postoperative LOS, 7.00 $vs$. 10.00 days, $p < 0.001$). By analyzing the prognosis of patients in the ERAS group and control group, we found that there was no significant difference in postoperative complications and Karnofsky Performance Status (KPS) score 1 month after operation between the two groups.

**Conclusion:** The application of ERAS in craniotomy can accelerate the postoperative recovery of patients without increasing the perioperative risk, which is worthy of wide application. However, whether the ERAS measures can reduce the postoperative complications and improve the prognosis of patients still needs more large-scale case validation and multicenter collaborative study.

**Keywords:** brain tumor, ERAS, craniotomy, postoperative rehabilitation, prognosis

# 1 INTRODUCTION

The concept of enhanced recovery after surgery (ERAS) was first proposed by Professor Kehlet of Denmark (1), which refers to the adoption of a series of perioperative optimization measures supported by evidence-based medical evidence to accelerate patients' rehabilitation and reduce postoperative complications. Surgeons had achieved remarkable results in shortening hospital stay and reducing hospital expenses by applying the ERAS protocols (2). ERAS has been popularized and applied in many surgical fields, including general surgery and orthopedics. In recent years, the European ERAS society has continuously issued ERAS operation guidelines for many disciplines (3–5). Previously, it was believed that neurosurgical craniotomy required a number of invasive monitoring methods, and most postoperative patients needed to enter intensive care unit and recovered slowly (6). Therefore, there are few reports on the application of ERAS in neurosurgery. However, with the development of microsurgical technique, the continuous progress of multimodal imaging, neuro-navigation, brain function monitoring and other technologies, and the deepening of multidisciplinary cooperation, the postoperative recovery time of patients undergoing craniotomy has been greatly shortened (7). Hagan et al. proposed 17 accelerated rehabilitation measures for craniotomy in 2016, including preoperative counseling, minimally invasive craniotomies, and postoperative artificial nutrition (8). Wang et al. reported a prospective randomized controlled study on the application of accelerated rehabilitation measures in craniotomy in 2018. They believe that ERAS can shorten the hospital length of stay (LOS) and does not increase the perioperative risk (9). However, the ERAS system for craniotomy that can be popularized and applied on a large scale is still limited. This study retrospectively analyzed the clinical data of 100 patients with brain tumors who underwent craniotomy in the Department of Neurosurgery of Xiangya Hospital from January 2018 to August 2020, explored the promoting effect of the ERAS measures on postoperative rehabilitation, and provided evidence for the establishment of the ERAS system for patients with brain tumors accepting craniotomy.

# 2 MATERIALS AND METHODS

## 2.1 Patient Recruitment

This study collected the clinical data of 100 patients with brain tumor hospitalized in the Department of Neurosurgery of Xiangya Hospital from January 2018 to August 2020, including 50 patients accepting accelerated rehabilitation treatment (ERAS group) and 50 patients accepting routine surgical treatment (Control group). The inclusion criteria were as follows: 1) 18–65 years old; 2) preoperative diagnosis was brain tumor; 3) there was no obvious neurological and cognitive impairment before operation; and 4) there were no serious concomitant diseases that may affect the prognosis (such as heart failure and chronic renal insufficiency).

The general clinical data collected included patient name, hospitalization number, gender, age, body mass index (BMI), concomitant disease, smoking and drinking history, and preoperative albumin value; the tumor pathology, tumor location, tumor size, blood loss during surgery, and intraoperative blood transfusion; and hospital LOS, hospitalization expenses, postoperative complications, and Karnofsky Performance Status (KPS) score.

## 2.2 Enhanced Recovery After Surgery Protocol and Clinical Data Collection

The accelerated rehabilitation measures taken by the ERAS group include the following: 1) preoperative evaluation of vomiting risk and application of antiemetics to prevent postoperative vomiting was performed; 2) 200 ml of carbohydrates was taken orally 2 h before operation, and oral feeding was resumed as early as possible after operation; 3) preoperative thrombosis risk assessment and postoperative thrombosis prevention were performed; 4) scalp nerve block and local infiltration anesthesia with ropivacaine were used to reduce postoperative pain; 5) indwelling wound drainage tube during operation was avoided; 6) the urinary catheter was removed as soon as possible after operation; and 7) early ambulation training was performed with the help of nurses after operation. The perioperative management of patients in the control group was mainly based on the personal experience of surgeons and anesthesiologists in our institution.

The data collected included preoperative postoperative nausea and vomiting (PONV) score, preoperative PONV prophylaxis, and the days of postoperative use of antiemetic drugs; postoperative feeding time, proton pump inhibitor application time, and intravenous infusion volume; preoperative thrombosis risk assessment (Caprini score), postoperative thrombosis prophylaxis measures, and whether venous thrombosis occurred; postoperative pain assessment applying Visual Analogue Scale (VAS) score and whether analgesics were used; whether the wound drainage tube was retained during the operation; urinary catheter removal time after surgery; and ambulation time after surgery.

## 2.3 Compliance With Ethical Standards

The study was approved by the Ethics Committee of Xiangya Hospital (Ethics approval No. 2018111102). All participants signed written informed consent.

## 2.4 Statistical Analysis

The measurement data conforming to the normal distribution are represented by "mean ± SD," and the measurement data not conforming to the normal distribution are represented by "median (interquartile spacing)." Student's t-test was used for the comparison between the two groups of measurement data conforming to normal distribution, and Wilcoxon's rank sum test was used for the comparison between that not conforming to normal distribution. Categorical data were described by rate, and chi-square test was used for inter-group comparison. $p < 0.05$ was considered statistically significant. SPSS 25.0 (IBM Corp.) was used for data statistics and analysis.

# 3 RESULTS

## 3.1 Characteristics of Clinical Data

Fifty patients were included in the ERAS group and control group. The average ages of the two groups were $48.12 \pm 11.89$ and $48.10 \pm 15.26$ years, respectively ($p = 0.994$). There were 29 female cases (58%) in the ERAS group and 27 female cases (54%) in the control group ($p = 0.687$). There was no significant difference in BMI, concomitant diseases (including cardiovascular system, respiratory system, digestive system, diabetes, and multiple complications), smoking history, drinking history, and preoperative serum albumin level between the two groups (**Table 1**).

Patients in both groups accepted craniotomy. There was no significant difference in tumor characteristics between the two groups (**Table 2**). The tumor pathological diagnosis was mainly meningioma and glioma. There were 13 cases (26%) diagnosed as glioma in the ERAS group and 18 cases (36%) in the control group ($p = 0.280$). For meningioma, the data were 16 cases (32%) and 15 cases (30%), respectively ($p = 0.829$). The tumors were mainly supratentorial. There were 45 supratentorial cases (90%) in the ERAS group and 46 supratentorial cases (92%) in the control group ($p = 0.727$). The maximum tumor diameter of the two groups was 3.65 (2.63) and 3.00 (2.00) cm ($p = 0.453$). The median blood loss in both groups was 200.00 ml ($p = 0.261$), and the number of blood transfusion patients was four cases (8%) and five cases (10%), respectively ($p = 0.727$).

## 3.2 Measures and Effects of Enhanced Recovery After Surgery Protocols

### 3.2.1 Preoperative Antiemetic Drugs Were Used to Prevent Postoperative Vomiting

PONV score was used to evaluate the risk of postoperative vomiting in the ERAS group and control group before operation. There was no significant difference in PONV score between the two groups (**Table 3**). The proportion of patients accepting PONV prophylaxis in the ERAS group was significantly higher than that in the control group (58% *vs.* 0%,

$p < 0.001$), and the days of using antiemetics after operation were significantly less than those in the control group (1.00 *vs.* 2.00 days, $p = 0.003$).

### 3.2.2 200 ml of Carbohydrates Was Taken Orally 2 h Before Operation, and Oral Feeding Was Resumed Early After Operation

All patients in the ERAS group took 200 ml of carbohydrates orally 2 h before operation and started oral feeding as soon as possible after operation. The patients in the control group followed routine fasting for 8 h before operation. The postoperative water intake time, liquid food intake time, and solid food intake time in the ERAS group were 6.00 (2.00), 12.00 (0), and 24.00 (0) h, respectively; and the corresponding time in the control group was 6.00 (1.00), 14.00 (2.00), and 25.00 (2.00) h, respectively, with $p$-values all less than 0.05. The application time of proton pump inhibitors in the two groups was 1.00 (1.00) and 2.00 (1.00) days ($p < 0.001$). On the first day, the second day, and the third day after operation, the intravenous infusion volume in the ERAS group was 2,300.00 (400.00), 800.00 (250.00), and 375.00 (162.50) ml, respectively; and the corresponding infusion volume in the control group was 2,400.00 (300.00), 1,200.00 (200.00), and 600.00 (125.00) ml, respectively, with $p$-values of 0.147, <0.001, and <0.001, respectively (**Table 3**).

### 3.2.3 Preoperative Thrombosis Risk Assessment and Postoperative Thrombosis Prophylaxis

The risk of thrombosis was assessed by Caprini score before operation in both the ERAS group and control group, and there was no significant difference between the two groups. In the ERAS group, 19 patients (38%), 19 patients (38%), 10 patients (20%), and two patients (4%) were assessed as low, middle, high, and extremely high risk of venous thrombosis, respectively, while in the control group, 22 patients (44%), 19 patients (38%), seven patients (14%), and two patients (4%) were assessed, respectively, with $p$-values greater than 0.05 (**Table 4**). All patients in both groups were treated with lower limbs active/passive activities to prevent thrombosis

**TABLE 1** | Clinical characteristics of 100 patients who underwent craniotomy.

|  | ERAS group | Control group | *p*-Value |
|---|---|---|---|
| No. of patients | 50 | 50 | |
| Average age (years) | $48.12 \pm 11.89$ | $48.10 \pm 15.26$ | 0.994 |
| Gender | | | 0.687 |
|   Male, no. (%) | 21 (42%) | 23 (46%) | |
|   Female, no. (%) | 29 (58%) | 27 (54%) | |
| Average BMI value | $23.28 \pm 3.26$ | $22.79 \pm 2.89$ | 0.429 |
| Concomitant disease, no. (%) | | | |
| Cardiovascular system | 8 (16%) | 6 (12%) | 0.564 |
|   Respiratory system | 1 (2%) | 2 (4%) | 0.558 |
|   Digestive system | 4 (8%) | 4 (8%) | 1.000 |
|   Diabetes | 4 (8%) | 3 (6%) | 0.695 |
| Multiple | 2 (4%) | 1 (2%) | 0.558 |
| (≥2 systems) | | | |
| Smoking history, no. (%) | 6 (12%) | 4 (8%) | 0.505 |
| Drinking history, no. (%) | 3 (6%) | 1 (2%) | 0.307 |
| Preoperative albumin value (g) | $41.25 \pm 2.92$ | $40.91 \pm 3.35$ | 0.583 |

*ERAS, enhanced recovery after surgery; BMI, body mass index.*

**TABLE 2 |** Summary of tumor and operation related details.

|  | ERAS group | Control group | *p*-Value |
|---|---|---|---|
| Tumor pathology |  |  |  |
| Glioma, no. (%) | 13 (26%) | 18 (36%) | 0.280 |
| Meningioma, no. (%) | 16 (32%) | 15 (30%) | 0.829 |
| Others, no. (%) | 21 (42%) | 17 (34%) | 0.410 |
| Lesion location |  |  | 0.727 |
| Supratentorial, no. (%) | 45 (90%) | 46 (92%) |  |
| Subtentorial, no. (%) | 5 (10%) | 4 (8%) |  |
| Maximum tumor diameter (cm) median (interquartile spacing) | 3.6 (2.63) | 3.00 (2.00) | 0.453 |
| Craniotomy, no. (%) | 50 (100%) | 50 (100%) | 1.000 |
| Median blood loss during surgery in ml median (interquartile spacing) | 200.00 (162.50) | 200.00 (200.00) | 0.261 |
| RBC transfusion during surgery, no. (%) | 4 (8%) | 5 (10%) | 0.727 |

*ERAS, enhanced recovery after surgery; RBC, red blood cell.*

(n = 50, 100%). The patients in the ERAS group concurrently received mechanical prevention (intermittent pneumatic compression) (n = 50, 100%), and patients in the control group did not receive mechanical prevention ($p < 0.001$). The patients with postoperative deep venous thrombosis in the two groups were one case (2%) and two cases (4%) ($p = 0.558$).

### 3.2.4 Intraoperative Scalp Nerve Block and Local Infiltration Anesthesia Were Applied to Reduce Postoperative Pain

The intravenous anesthetics and inhaled anesthetics were the same in the two groups. Patients in the ERAS group were treated with scalp nerve block and local infiltration anesthesia with ropivacaine at surgical incision to reduce postoperative pain (n = 50, 100%), and patients in the control group did not accept this handling (**Table 4**). The number of patients with postoperative mild pain (VAS 0–3), moderate pain (VAS 4–6), and severe pain (VAS 7–10) in the ERAS group was 38 (76%), 9 (18%), and 3 (6%); and the corresponding number of patients in the control group was 24 (48%), 19 (38%), and 7 (14%). *p*-Values were 0.004, 0.026, and 0.182, respectively. The proportion of patients receiving postoperative analgesic drugs in the ERAS group was significantly lower than that in the control group (30% *vs.* 52%, OR = 0.41, 95% CI 0.18–0.93, $p = 0.031$).

### 3.2.5 Other Enhanced Recovery After Surgery Protocols

Other ERAS protocols include avoiding indwelling wound drainage tube during operation, removing urinary catheter as soon as possible, and early ambulation training with the help of nurses after operation (**Table 5**). In this study, there was only one patient (2%) accepting wound drainage tube in both the ERAS group and control group. The median time of urinary catheter removal after surgery in the ERAS group was 16.00 (12.00) h, and the time was 24.00 (2.25) h in the control group ($p < 0.001$). The median time of patients in the ERAS group starting to ambulate after surgery was 1.00 (1.00) day, and the time was 2.00 (1.25) days in the control group ($p < 0.001$).

**TABLE 3 |** The first part of ERAS measures and effects.

|  | ERAS group | Control group | *p*-Value |
|---|---|---|---|
| 1. Preoperative antiemetic drugs were used to prevent postoperative vomiting |  |  |  |
| Preop PONV score |  |  |  |
| 0, no. (%) | 4 (8%) | 2 (4%) | 0.400 |
| 1, no. (%) | 17 (34%) | 21 (42%) | 0.410 |
| 2, no. (%) | 29 (58%) | 27 (54%) | 0.687 |
| Preop PONV prophylaxis, no. (%) | 29 (58%) | 0 | <0.001 |
| Days of using antiemetic drugs after operation |  |  |  |
| Median (interquartile spacing) | 1.00 (1.00) | 2.00 (1.00) | 0.003 |
| 2. 200 ml of carbohydrates was taken orally 2 h before operation, and oral feeding was resumed early after operation |  |  |  |
| Preop oral carbohydrate, no. (%) | 50 (100%) | 0 | <0.001 |
| Postop diet Median (interquartile spacing) |  |  |  |
| Postop water intake time (h) | 6.00 (2.00) | 6.00 (1.00) | 0.001 |
| Postop liquid food intake time (h) | 12.00 (0) | 14.00 (2.00) | <0.001 |
| Postop solid food intake time (h) | 24.00 (0) | 25.00 (2.00) | <0.001 |
| Postop application time of proton pump inhibitors (days) | 1.00 (1.00) | 2.00 (1.00) | <0.001 |
| Postop intravenous infusion volume |  |  |  |
| Median (interquartile spacing) |  |  |  |
| Intravenous infusion volume on Postop day 1 (ml) | 2,300.00 (400.00) | 2,400.00 (300.00) | 0.147 |
| Intravenous infusion volume on Postop day 2 (ml) | 800.00 (250.00) | 1,200.00 (200.00) | <0.001 |
| Intravenous infusion volume on Postop day 3 (ml) | 375.00 (162.50) | 600.00 (125.00) | <0.001 |

*ERAS, enhanced recovery after surgery; PONV, postoperative nausea and vomiting.*

**TABLE 4 |** The second part of ERAS measures and effects.

| | ERAS group | Control group | *p*-Value |
|---|---|---|---|
| 3. Preoperative thrombus risk assessment and postoperative thrombus prophylaxis | | | |
| Thrombus risk assessment | | | |
|     Low risk (Caprini score 0–1), no. (%) | 19 (38%) | 22 (44%) | 0.542 |
|     Middle risk (Caprini score 2), no. (%) | 19 (38%) | 19 (38%) | 1.000 |
|     High risk (Caprini score 3–4), no. (%) | 10 (20%) | 7 (14%) | 0.424 |
|     Extremely high risk (Caprini score ≥ 5), no. (%) | 2 (4%) | 2 (4%) | 1.000 |
| Lower limbs active/passive activity, no. (%) | 50 (100%) | 50 (100%) | |
| Mechanical prophylaxis (intermittent pneumatic compression), no. (%) | 50 (100%) | 0 | <0.001 |
| Patients developing thrombus postoperatively, no. (%) | 1 (2%) | 2 (4%) | 0.558 |
| 4. Intraoperative scalp nerve block and local infiltration anesthesia to reduce postoperative pain | | | |
| Patients receiving intraoperative scalp nerve block and local infiltration anesthesia, no. (%) | 50 (100%) | 0 | <0.001 |
| Postoperative pain assessment | | | |
|     Mild (VAS 0–3), no. (%) | 38 (76%) | 24 (48%) | 0.004 |
|     Moderate (VAS 4–6), no. (%) | 9 (18%) | 19 (38%) | 0.026 |
|     Severe (VAS 7–10), no. (%) | 3 (6%) | 7 (14%) | 0.182 |
| Patients receiving postoperative analgesic drugs, no. (%) | 15 (30%) | 26 (52%) | 0.031 |

*ERAS, enhanced recovery after surgery; VAS, Visual Analogue Scale.*

## 3.3 Hospital Length of Stay and Expenses

The total hospital LOS and postoperative LOS in the ERAS group were 13.00 (3.00) and 7.00 (1.00) days, respectively; and the corresponding time in the control group was 15.50 (3.00) and 10.00 (3.00) days ($p < 0.001$). The hospitalization expenses of the ERAS group and control group were 58,146.35 (7,688.28) and 64,815.91 (12,257.06) yuan, respectively ($p < 0.001$) (**Table 6**).

## 3.4 Postoperative Complications and Patient Prognosis

The postoperative complications include intracranial complications and systemic complications. The complications caused by intracranial factors in the ERAS group included one case of intracranial infection (2%), two cases of neurological dysfunction (4%), and one case of epilepsy (2%). The corresponding complications in the control group were two cases of intracranial infection (4%), two cases of neurological dysfunction (4%), and one case of epilepsy (2%). The *p*-values were all greater than 0.05 (**Table 6**). The systemic complications in the ERAS group included two cases of pulmonary infection (4%) and one case of lower extremity deep venous thrombosis (2%), and the corresponding complications in the control group were two cases of pulmonary infection (4%) and two cases of lower extremity deep venous thrombosis (4%). The *p*-values were both greater than 0.05. The 1-month follow-up data after surgery showed that the number of patients with KPS score ≥80 in the

ERAS group was 46 (92%), the number of patients with a score of 50–70 was 4 (8%), and the corresponding number of patients in the control group was 45 (90%) and five cases (10%) ($p = 0.727$).

## 4 DISCUSSION

The implementation of ERAS in multiple surgeries has been proved to shorten hospitalization time, reduce hospitalization expenses, and accelerate rehabilitation of patients, but it is rarely used in neurosurgery. We summarized the ERAS protocols and outcome measures applied in elective craniotomy in the past studies (**Table 7**). Wang et al. reported a prospective randomized controlled study on the application of the ERAS measures in craniotomy in 2018, and they proposed a multidisciplinary management process from preoperative evaluation, intraoperative management to postoperative rehabilitation measures. The conclusion shows that the application of the ERAS measures in patients undergoing elective craniotomy can accelerate the rehabilitation of patients with safety and effectiveness (9). The concept of ERAS emphasizes to minimize the patient's stress response and restore patient's normal physiological functions as soon as possible. Therefore, this study put forward seven important ERAS measures based on this concept, which aim to reduce postoperative stress reactions such as pain and vomiting and to restore normal physiological

**TABLE 5 |** The third part of ERAS measures and effects.

| | ERAS group | Control group | *p*-Value |
|---|---|---|---|
| 5. Avoiding indwelling wound drainage tube during operation | | | |
| Patient accepting wound drainage tube, no. (%) | 1 (2%) | 1 (2%) | 1.000 |
| 6. Remove the urinary catheter as soon as possible after operation | | | |
| Median time of urinary catheter removal after surgery (h) | 16.00 (12.00) | 24.00 (2.25) | <0.001 |
| 7. Early ambulation after operation | | | |
| The median time to ambulate after surgery (days) | 1.00 (1.00) | 2.00 (1.25) | 0.001 |

*ERAS, enhanced recovery after surgery.*

**TABLE 6** | Analysis of median hospital LOS, cost of hospitalization, and prognosis of patients.

| | ERAS group | Control group | *p*-Value |
|---|---|---|---|
| Hospital LOS median (interquartile spacing) | | | |
| Total LOS (days) | 13.00 (3.00) | 15.50 (3.00) | <0.001 |
| Postop LOS (days) | 7.00 (1.00) | 10.00 (3.00) | <0.001 |
| Cost of hospitalization (yuan) median (interquartile spacing) | 58,146.35 (7,688.28) | 64,815.91 (12,257.06) | <0.001 |
| Intracranial complications, no. (%) | | | |
| Intracranial infection | 1 (2%) | 2 (4%) | 0.558 |
| Neurological dysfunction | 2 (4%) | 2 (4%) | 1.000 |
| Epilepsy | 1 (2%) | 1 (2%) | 1.000 |
| Systemic complications, no. (%) | | | |
| Pulmonary infection | 2 (4%) | 2 (4%) | 1.000 |
| Deep venous thrombosis | 1 (2%) | 2 (4%) | 0.558 |
| 1-month follow-up KPS score after surgery | | | 0.727 |
| ≥80, no. (%) | 46 (92%) | 45 (90%) | |
| 50–70, no. (%) | 4 (8%) | 5 (10%) | |

LOS, length of stay; ERAS, enhanced recovery after surgery; KPS, Karnofsky Performance Status.

functions such as oral eating and ambulation as soon as possible, so as to accelerate rehabilitation of patients.

PONV are common adverse reactions, which will delay the recovery of patients (11). For patients undergoing craniotomy, postoperative vomiting may increase intracranial pressure and cause serious complications such as brain edema and intracerebral hemorrhage. Therefore, we evaluated the risk of PONV by Apfel adult PONV risk score (12), and we applied preventive measures for patients with a score ≥2. The preventive drug is the combination of dexamethasone and serotonin receptor antagonist (8, 9). In this study, 29 patients in the ERAS group were treated with preventive measures (58%) before operation, and the median antiemetic drug application time after operation was 1.00 day. There were no patients receiving preventive measures in the control group according to the traditional processing method, and the median antiemetic drug application time after operation was 2.00 days, which was significantly longer than that in the ERAS group (*p* = 0.003).

Previous studies have shown that compared with long-term fasting before surgery, oral carbohydrate 2 h before surgery can reduce patients' insulin resistance; improve patients' subjective feelings of thirst, hunger, and fatigue after operation; and do not increase the occurrence of postoperative vomiting (8, 13). In this study, all patients in the ERAS group took 200 ml of carbohydrates orally 2 h before surgery, and there was no aspiration or vomiting during operation. Except for patients with consciousness disorder after operation, craniotomy generally does not affect the digestive tract function of patients. Therefore, we encourage patients to resume oral feeding early after operation and to reduce the amount of intravenous infusion and the use of proton pump inhibitors. Our results show that this measure can quickly restore the postoperative gastrointestinal function and accelerate the perioperative rehabilitation.

The prevention of deep venous thrombosis in the perioperative period of craniotomy is mainly based on mechanical prevention, but drug prevention can also be considered when the risk of bleeding is

**TABLE 7** | Summarization of the ERAS protocols and outcome measures applied in elective craniotomy in the past studies.

| Authors | Study design | Key ERAS protocols | Outcome measures |
|---|---|---|---|
| Yuan Wang et al. (9) | Prospective randomized controlled trial | PONV management, preop fasting and carb loading, scalp incision anesthetic with ropivacaine, intravenous antibiotics given before incision, surgical incision suturing, evaluation and prophylactic antithrombotic therapy, urinary drainage, postop diet, adherence to ambulation | Median total hospital LOS from admission to discharge, median hospital LOS from end of procedure to discharge, 30-day all-cause readmission rate, reoperation rate for any indication within 30 days, total cost of hospitalization in RMB, surgical complication, nonsurgical complication, functional recovery |
| Anirudh Elayat et al. (10) | Non-randomized controlled trial | Family education, complex-carbohydrate drink, flupirtine, scalp blocks, limited opioids, rigorous fluid and temperature regulation, flupirtine, early mobilization, removal of catheters, initiation of feeds | Length of ICU stay, pain scores in ICU, opioid requirement, glycemic control, hospital stay duration |
| Katherine B. Hagan et al. (8) | Literature review | Preoperative counseling, preoperative smoking and alcohol consumption, preoperative enteral nutrition and perioperative oral immunonutrition, preoperative fasting and carbohydrate loading, anti-thrombotic prophylaxis, antimicrobial prophylaxis and skin preparation, scalp blocks, anesthetic protocol, non-opioid analgesia, PONV, minimally invasive craniotomies and endoscopic skull base approaches, avoiding hypothermia, fluid balance, urinary drainage, postoperative artificial nutrition, early mobilization, audit | NA |

ERAS, enhanced recovery after surgery; LOS, length of stay; ICU, ICU, intensive care unit; PONV, postoperative nausea and vomiting.
NA, Not Available.

low (14). The mechanical prevention is applied as the ERAS measure previously, including intermittent pneumatic compression and graduated compression stockings (8, 9). All patients in this study received lower limb active/passive activities to prevent thrombosis, but only patients in the ERAS group received mechanical prevention concurrently (intermittent pneumatic compression). In the study conducted by Wang, there was no patient suffering from deep venous thrombosis in the ERAS group, while there were two patients suffering from deep venous thrombosis in the control group (3%). Although the $p$-value was greater than 0.05, the authors believed that mechanical prevention could effectively reduce the incidence of perioperative deep venous thrombosis (9). In our study, the numbers of patient developing postoperative deep venous thrombosis in the ERAS group and control group were one (2%) and two (4%), respectively; and the $p$-value was also greater than 0.05. However, we believe that it may be due to the small sample size and because perioperative mechanical prevention can effectively reduce the formation of deep venous thrombosis.

Pain management of craniotomy is an important part of the ERAS process. Reducing postoperative pain can accelerate rehabilitation and improve comfort and satisfaction of patients. Scalp nerve block and incision infiltration anesthesia can effectively reduce postoperative pain and the use of analgesic drugs (8, 15), which are implemented by anesthesiologists and surgeons, respectively. Qu et al. showed that scalp infiltration anesthesia with ropivacaine in the ERAS group could effectively reduce the degree and time of postoperative pain (16). In our study, all patients in the ERAS group were treated with scalp nerve block and infiltration anesthesia before scalp incision. The results showed that the degree of pain was significantly lower and the application of analgesic drugs was less in the ERAS group than in the control group.

Prolonged indwelling of urinary catheter after operation may lead to urinary tract infection and may restrict patient's mobilization (17). Therefore, we emphasize early removal of urinary catheter after operation to restore normal physiological function as soon as possible. In this study, the urinary catheter was removed about 16 h after operation in the ERAS group, and there were no patients developing urinary tract infection. It has been reported that early postoperative ambulation can improve patients' cardiopulmonary function and reduce the incidence of postoperative venous thrombosis (18, 19). In this study, patients in the ERAS group began to ambulate on the first day after operation, which we believe can accelerate the process of postoperative rehabilitation.

By comparing and analyzing the prognosis of patients in the ERAS group and control group, we found that there was no significant difference in surgical complications and KPS score at 1 month after surgery between the two groups. We believe that it may be related to the small sample size, and ERAS measures can reduce postoperative complications and improve prognosis of patients, which is consistent with the conclusion of Wang's research (9). In addition, the results showed that the total hospital LOS, postoperative LOS, and hospitalization expenses of the ERAS group were significantly lower than those of the control group, suggesting the effectiveness and economic benefits of the ERAS measures.

# 5 CONCLUSION

Here, we provide our experience in the application of ERAS in craniotomy. We believe that the application of the ERAS measures in craniotomy can accelerate the postoperative rehabilitation of patients without additional perioperative risk, which is worthy of widespread promotion and application. However, whether the ERAS measures can reduce postoperative complications and improve patients' prognosis requires more large-scale case validation and multicenter collaborative research.

# DATA AVAILABILITY STATEMENT

The original contributions presented in the study are included in the article/supplementary material. Further inquiries can be directed to the corresponding authors.

# ETHICS STATEMENT

The studies involving human participants were reviewed and approved by Medical Ethics Committee of Xiangya Hospital. The patients/participants provided their written informed consent to participate in this study.

# AUTHOR CONTRIBUTIONS

SSF, BX, QC, and XXZ prepared the manuscript, analyzed the data, and performed the experiments. ZYL and ZXL designed the experiments. MYZ modified the manuscript. ZRT and MYZ designed the project and finally approved the manuscript to be published. All authors contributed to the article and approved the submitted version.

# FUNDING

# ACKNOWLEDGMENTS

# REFERENCES

1. Kehlet H. Multimodal Approach to Control Postoperative Pathophysiology and Rehabilitation. *Br J Anaesth* (1997) 78(5):606–17. doi: 10.1093/bja/78.5.606

2. Lemanu DP, Singh PP, Stowers MD, Hill AG. A Systematic Review to Assess Cost Effectiveness of Enhanced Recovery After Surgery Programmes in Colorectal Surgery. *Colorectal Dis* (2014) 16(5):338–46. doi: 10.1111/codi.12505

3. Gustafsson UO, Scott MJ, Hubner M, Nygren J, Demartines N, Francis N, et al. Guidelines for Perioperative Care in Elective Colorectal Surgery: Enhanced Recovery After Surgery (ERAS((R))) Society Recommendations: 2018. *World J Surg* (2019) 43(3):659–95. doi: 10.1007/s00268-018-4844-y

4. Lassen K, Coolsen MM, Slim K, Carli F, de Aguilar-Nascimento JE, Schafer M, et al. Guidelines for Perioperative Care for Pancreaticoduodenectomy: Enhanced Recovery After Surgery (ERAS(R)) Society Recommendations. *Clin Nutr* (2012) 31(6):817–30. doi: 10.1016/j.clnu.2012.08.011

5. Mortensen K, Nilsson M, Slim K, Schafer M, Mariette C, Braga M, et al. Consensus Guidelines for Enhanced Recovery After Gastrectomy: Enhanced Recovery After Surgery (ERAS(R)) Society Recommendations. *Br J Surg* (2014) 101(10):1209–29. doi: 10.1002/bjs.9582

6. Weissman C, Klein N. Who Receives Postoperative Intensive and Intermediate Care? *J Clin Anesth* (2008) 20(4):263–70. doi: 10.1016/j.jclinane.2007.11.005

7. Venkatraghavan L, Bharadwaj S, Au K, Bernstein M, Manninen P. Same-Day Discharge After Craniotomy for Supratentorial Tumour Surgery: A Retrospective Observational Single-Centre Study. *Can J Anaesth* (2016) 63(11):1245–57. doi: 10.1007/s12630-016-0717-8

8. Hagan KB, Bhavsar S, Raza SM, Arnold B, Arunkumar R, Dang A, et al. Enhanced Recovery After Surgery for Oncological Craniotomies. *J Clin Neurosci* (2016) 24:10–6. doi: 10.1016/j.jocn.2015.08.013

9. Wang Y, Liu B, Zhao T, Zhao B, Yu D, Jiang X, et al. Safety and Efficacy of a Novel Neurosurgical Enhanced Recovery After Surgery Protocol for Elective Craniotomy: A Prospective Randomized Controlled Trial. *J Neurosurg* (2018) 1:1–12. doi: 10.3171/2018.1.JNS171552

10. Elayat A, Jena SS, Nayak S, Sahu RN, Tripathy S. Enhanced Recovery After Surgery - ERAS in Elective Craniotomies-A Non-Randomized Controlled Trial. *BMC Neurol* (2021) 21(1):127. doi: 10.1186/s12883-021-02150-7

11. Cao X, White PF, Ma H. An Update on the Management of Postoperative Nausea and Vomiting. *J Anesth* (2017) 31(4):617–26. doi: 10.1007/s00540-017-2363-x

12. Obrink E, Jildenstal P, Oddby E, Jakobsson JG. Post-Operative Nausea and Vomiting: Update on Predicting the Probability and Ways to Minimize Its Occurrence, With Focus on Ambulatory Surgery. *Int J Surg* (2015) 15:100–6. doi: 10.1016/j.ijsu.2015.01.024

13. Wang ZG, Wang Q, Wang WJ, Qin HL. Randomized Clinical Trial to Compare the Effects of Preoperative Oral Carbohydrate Versus Placebo on Insulin Resistance After Colorectal Surgery. *Br J Surg* (2010) 97(3):317–27. doi: 10.1002/bjs.6963

14. Faraoni D, Comes RF, Geerts W, Wiles MD, Esa Vte Guidelines Task Force. European Guidelines on Perioperative Venous Thromboembolism Prophylaxis: Neurosurgery. *Eur J Anaesthesiol* (2018) 35(2):90–5. doi: 10.1097/EJA.0000000000000710

15. Guilfoyle MR, Helmy A, Duane D, Hutchinson PJ. Regional Scalp Block for Postcraniotomy Analgesia: A Systematic Review and Meta-Analysis. *Anesth Analg* (2013) 116(5):1093–102. doi: 10.1213/ANE.0b013e3182863c22

16. Qu L, Liu B, Zhang H, Sankey EW, Chai W, Wang B, et al. Management of Postoperative Pain After Elective Craniotomy: A Prospective Randomized Controlled Trial of a Neurosurgical Enhanced Recovery After Surgery (ERAS) Program. *Int J Med Sci* (2020) 17(11):1541–9. doi: 10.7150/ijms.46403

17. Trickey AW, Crosby ME, Vasaly F, Donovan J, Moynihan J, Reines HD. Using NSQIP to Investigate SCIP Deficiencies in Surgical Patients With a High Risk of Developing Hospital-Associated Urinary Tract Infections. *Am J Med Qual* (2014) 29(5):381–7. doi: 10.1177/1062860613503363

18. Schram A, Ferreira V, Minnella EM, Awasthi EM, Carli EM, Scheede-Bergdahl EM. In-Hospital Resistance Training to Encourage Early Mobilization for Enhanced Recovery Programs After Colorectal Cancer Surgery: A Feasibility Study. *Eur J Surg Oncol* (2019) 45(9):1592–7. doi: 10.1016/j.ejso.2019.04.015

19. Yip VS, Dunne DF, Samuels S, Tan CY, Lacasia C, Tang J, et al. Adherence to Early Mobilisation: Key for Successful Enhanced Recovery After Liver Resection. *Eur J Surg Oncol* (2016) 42(10):1561–7. doi: 10.1016/j.ejso.2016.07.015

# Biopsy Artifact in Laser Interstitial Thermal Therapy: A Technical Note

Thomas Noh[1]*, Parikshit Juvekar[2], Raymond Huang[3], Gunnar Lee[1],
Christian T. Ogasawara[1] and Alexandra J. Golby[2]

[1] Division of Neurosurgery, John A Burns School of Medicine, Honolulu, HI, United States, [2] Department of Neurosurgery, Brigham and Women's Hospital, Harvard Medical School, Boston, MA, United States, [3] Department of Radiology, Brigham and Women's Hospital, Harvard Medical School, Boston, MA, United States

**Purpose:** The safety and effectiveness of laser interstitial thermal therapy (LITT) relies critically on the ability to continuously monitor the ablation based on real-time temperature mapping using magnetic resonance thermometry (MRT). This technique uses gradient recalled echo (GRE) sequences that are especially sensitive to susceptibility effects from air and blood. LITT for brain tumors is often preceded by a biopsy and is anecdotally associated with artifact during ablation. Thus, we reviewed our experience and describe the qualitative signal dropout that can interfere with ablation.

**Methods:** We retrospectively reviewed all LITT cases performed in our intraoperative MRI suite for tumors between 2017 and 2020. We identified a total of 17 LITT cases. Cases were reviewed for age, sex, pathology, presence of artifact, operative technique, and presence of blood/air on post-operative scans.

**Results:** We identified six cases that were preceded by biopsy, all six had artifact present during ablation, and all six were noted to have air/blood on their post-operative MRI or CT scans. In two of those cases, the artifactual signal dropout qualitatively interfered with thermal damage thresholds at the borders of the tumor. There was no artifact in the 11 non-biopsy cases and no obvious blood or air was noted on the post-ablation scans.

**Conclusion:** Additional consideration should be given to pre-LITT biopsies. The presence of air/blood caused an artifactual signal dropout effect in cases with biopsy that was severe enough to interfere with ablation in a significant number of those cases. Additional studies are needed to identify modifying strategies.

Keywords: laser interstitial thermal therapy, LITT, magnetic resonance thermometry, MRT, brain tumors, biopsy, artifact, signal dropout

## INTRODUCTION

Laser interstitial thermal therapy (LITT) is a minimally invasive therapeutic option for treatment of brain tumors. The safety and effectiveness of LITT rely critically on the ability to continuously monitor the ablation in real time based on accurate temperature mapping of the region of interest. Currently, this is achieved by measuring phase change using a magnetic resonance imaging

technique called MR thermometry (MRT) (1, 2), which uses a gradient recalled echo (GRE) sequence to leverage six temperature-sensitive MR parameters, namely, the proton resonance frequency (PRF), the diffusion coefficient (D), T1 and T2 relaxation times, magnetization transfer, and proton density. The temperature measurement is then used to estimate tissue damage using a thermal damage threshold (TDT) model that utilizes temperature and time in a non-linear manner to quantify the damage by relating it to an equivalent heating time at 43°C (**Figure 1A**) (3). This allows the operator to determine when the tumor has been sufficiently ablated without injuring the surrounding normal brain.

LITT for brain tumors is often preceded by a biopsy for histologic and molecular characterization. We have anecdotally found biopsies to be associated with artifact during ablation and thus sought to review the incidence in our series and describe the qualitative signal dropout that can interfere with TDT assessment during LITT ablation.

## METHODS

We retrospectively reviewed all LITT cases performed in our intraoperative MRI suite between 2017 and 2020 (IRB number: 2002P001238) using the NeuroBlate system (Plymouth, MN, USA). We identified a total of 17 LITT cases. We identified six patients in which LITT was preceded by biopsy. Two out of six of those cases were noted to have clinically significant ablation artifact as determined by the neurosurgeon performing the procedure. Clinically significant artifact was defined as ablations where grayed-out voxels were present from the onset of ablation on MRT extended outside of the volumetric limits of the contrast-enhancing portion of the tumor. Post-ablation scans were read by a neuroradiologist. None

of the 11 cases without biopsy had ablation artifact and all but one (complicated by IVH) had no obvious blood or air noted on the post-ablation scans (**Table 1**). All ablations were performed in an IMRIS 3T Siemen's Verio scanner (Erlangen, Germany).

## CASE EXAMPLES

Patient 1: A right-handed male in his 30s had a 3-year history of a recurrent glioblastoma multiforme (GBM) initially treated with standard radiation and temozolomide. He had several recurrences including one at 36 months after his initial diagnosis in the right frontal region and elected to undergo biopsy for tumor restaging and LITT. He underwent three biopsies approximately 5 mm into the lesion for frozen section, followed by three more biopsies for permanent pathology using a standard suction aspiration technique; there was no sense that bleeding had occurred. Immediately following biopsy, he underwent laser ablation during which there appeared grayed-out voxels within the resection cavity and difficulty measuring TDT around the margins of the tumor (**Figure 1B**). Post-ablation T1w and T2w MRI scans were noted to have blood and air within the ablated tumor (**Figure 1C**).

Patient 2: A right-handed female in her 60s presented with a large T1w contrast-enhancing bifrontal lesion with extension through the corpus callosum. She initially underwent four biopsies using a standard suction aspiration. To perform molecular analysis, the biopsy catheter was withdrawn 8 mm and 2 more cores were taken. There was no bleeding noted. A laser catheter was carefully exchanged into the deepest part of the tumor. After initial ablation, the catheter was withdrawn 5 mm for additional ablation to cover more of the tumor volume. This occurred two more times and, in each instance, there were
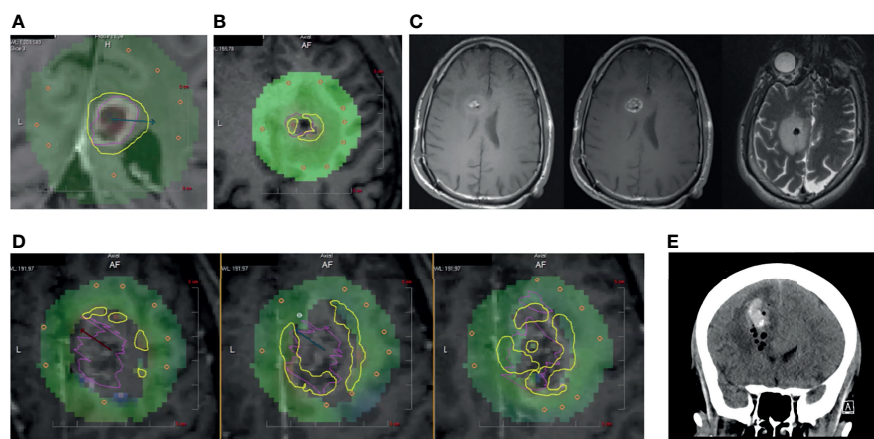


**FIGURE 1** | **(A)** Panel displaying a typical inline view on a contrast-enhanced T1-weighted MRI that is perpendicular to the laser catheter. Yellow TDT lines indicate the areas where tumor (pink) has reached 43°C as measured by MRT. **(B)** Patient 1. Intraoperative ablation showing central zones of signal "dropout" (gray voxels) on MRT and interference with TDT lines at the tumor (pink) borders. **(C)** (left) Unenhanced T1-weighted MRI, (middle) Contrast-enhanced T1-weighted MRI, and (right) T2-weighted MR image showing mixed hyper- and hypo-intensities in biopsy cavity. **(D)** Patient 2. Intraoperative panels showing three sequential inline cuts along the laser catheter with zones of signal dropout and interference with MRT at the tumor (pink) borders. **(E)** Post-operative coronal CT showing air and blood within the ablated tumor.

TABLE 1 | Patients who underwent LITT for brain tumor ablation, with or without preceding biopsy.

| Patient | Age/Sex | Pathology | Blood/air on post-operative scan | # biopsies | Artifact present |
|---------|---------|-----------|----------------------------------|------------|------------------|
| 1 | 30s/M | Recurrent GBM | MRI, yes | 3 | Yes |
| 2 | 60s/F | Recurrent GBM | CT, yes | 6 | Yes |
| 3 | 50s/M | Recurrent GBM | MRI, yes | 4 | Yes |
| 4 | 40s/M | GBM | MRI, yes | 4 | Yes |
| 5 | 60s/M | Small Cell Lung Cancer | MRI, yes | 4 | Yes |
| 6 | 60s/M | Recurrent Metastases | MRI, yes, cystic | 1 | Yes |
| 7 | 50s/M | Recurrent GBM | MRI, no | | No |
| 8 | 50s/M | Recurrent NSCLC metastasis vs necrosis | CT, no | | No |
| 9 | 60s,F | Breast metastases | CT, no | | No |
| 10 | 50s/F | Recurrent GBM | CT, no | | No |
| 11 | 20s/M | Recurrent Grade III astrocytoma | MRI, no | | No |
| 12 | 70s/F | Recurrent GBM | MRI, yes, complicated by IVH | | No |
| 13 | 60s/M | Multiple recurrent metastases | CT, no | | No |
| 14 | 60s/F | Recurrent Small cell metastasis | CT, no | | No |
| 15 | 40s/F | Recurrent GBM | CT, no | | No |
| 16 | 50s/F | Recurrent metastases | MRI, no | | No |
| 17 | 50s/F | Breast metastases | MRI, no | | No |

significant signal dropouts that interfered with MRT and TDT (**Figure 1D**). A post-ablation MRI showed blood and air in the cavity, which was demonstrated as stable on a CT on post-operative day 1 (**Figure 1E**). Histopathology resulted as GBM.

## RESULTS

All patients who underwent biopsy prior to LITT (Patients 1–6) were found to have some degree of artifact during ablation (**Table 1**). Patients 1 and 2 were specifically described as having clinically significant artifact, as defined in the *Methods* section, and thus were discussed as specific case examples. Interestingly, ablation artifacts were observed regardless of the number of biopsies drawn, including for Patient 6, who underwent one single biopsy. For 50% of the cohort (Patients 3–5), four biopsies were obtained. The remaining subjects, Patients 1 and 2, underwent three and six biopsies, respectively. There also does not appear to be correlation with presence of artifact and pathology of lesion. Of the patients in the biopsy cohort, 66% were treated for GBM. The remaining patients were found to have metastatic lesions. However, since this is a low-powered study with a small cohort of patients, trends correlating ablation artifacts with number of biopsies obtained and tumor pathology likely cannot be inferred from this dataset alone.

Importantly, all biopsy patients were found to have either blood or air on their post-ablation scan, whether by MRI or CT. Of the remaining patients who did not undergo biopsy, all but one had no evidence of blood or air on post-ablation imaging. The singular case of LITT without preceding biopsy that did show post-ablative blood on follow up imaging had intraventricular hemorrhage as a confounding factor.

## DISCUSSION

Munier et al. found that when there was artifact present on MRT, the TDT overestimated the cross-sectional ablation area of the

tumor (4). They postulated that the aberrations stemmed from local tissue trauma. Indeed, in our series, we observed this artifact to occur during all LITT cases that were preceded by a biopsy and associated with the presence of blood and air on post-ablation scans in all six cases. Similar to iron within heme molecules, the oxygen content of air is paramagnetic and can cause dephasing in T2*-sensitive MR sequences, resulting in magnitude loss, phase shifts, as well as geometric distortion during MRT (5). Not only does this artifact cause a quantitative overestimation, but we demonstrate two examples of how it can cause qualitative interference particularly at the tumor margins during ablation (**Figures 1B, D**). The signal dropout artifact that occurs during ablation could be detrimental to the patient when artifact extends outside of the tumor (**Figure 1D**). The operator is faced with a dilemma of waiting until a damage estimate line suddenly appears outside the grayed-out voxels or cut the ablation short not knowing where within the voxels the damage has occurred up to.

There is increasing evidence suggesting the clinical benefit of the addition of LITT to biopsy in patients with primary brain tumors (6, 7) which makes finding strategies to avoid this artifact increasingly important. In our anecdotal experience, we find that a slow speed of catheter exchange helps to prevent significant air leaks, and that repositioning the catheter by a few millimeters between ablations may also provide enough of a readjustment of the local environment to restore MRT. Another potential mitigating strategy, particularly for a small lesion in a functional area, may be to add a few milliliters of saline or thrombin (8, 9) to tamponade and restore the local architecture. There are currently no studies to the authors' knowledge that have described using either during LITT.

Although there is currently no understanding of how the artifact affected the software's ability to calculate the ablation zone, there are studies in the literature that have quantified discrepancies between TDT and postoperative MRI contrast-enhancing area.

There are also several newer MRT techniques that may provide a potential solution including spectroscopic imaging and measuring water–fat proton chemical shifts since they do not depend on relative phase shifts (10).

The location of the planned ablation will influence the challenge introduced by the signal dropout. Both patients in whom there was significant loss of MRT data were in non-eloquent brain areas. In cases where lesions may be close to eloquent structures like the corticospinal tracts, the clinician may consider surgical planning with tractography. Future studies should address functional outcomes and factors that influence the degree of artifact such as the size of the lesion, number of biopsies, and novel MRT strategies.

## CONCLUSION

Pre-LITT biopsies should be limited to patients in whom the tissue diagnosis will impact treatment decisions. Although the presence of air/blood in the cavity does not preclude LITT, it caused a qualitatively significant signal dropout effect that interfered with MRT at the tumor's margins.

## REFERENCES

1. de Senneville BD, Mougenot C, Quesson B, Dragonu I, Grenier N, Moonen CTW. MR Thermometry for Monitoring Tumor Ablation. *Eur Radiol* (2007) 17:2401–10. doi: 10.1007/s00330-007-0646-6
2. Patel NV, Mian M, Stafford RJ, Nahed BV, Willie JT, Gross RE, et al. Laser Interstitial Thermal Therapy Technology, Physics of Magnetic Resonance Imaging Thermometry, and Technical Considerations for Proper Catheter Placement During Magnetic Resonance Imaging-Guided Laser Interstitial Thermal Therapy. *Neurosurgery* (2016) 79(Suppl 1):S8–S16. doi: 10.1227/NEU.0000000000001440
3. Peters RD, Chan E, Trachtenberg J, Jothy S, Kapusta L, Kucharczyk W, et al. Magnetic Resonance Thermometry for Predicting Thermal Damage: An Application of Interstitial Laser Coagulation in an *In Vivo* Canine Prostate Model. *Magn Reson Med* (2000) 44:873–83. doi: 10.1002/1522-2594(200012)44:6<873::aid-mrm8>3.0.co;2-x
4. Munier SM, Desai AN, Patel NV, Danish SF. Effects of Intraoperative Magnetic Resonance Thermal Imaging Signal Artifact During Laser Interstitial Thermal Therapy on Thermal Damage Estimate and Postoperative Magnetic Resonance Imaging Ablative Area Concordance. *Oper Neurosurg (Hagerstown)* (2019) 18:524–30. doi: 10.1093/ons/opz182
5. Czervionke LF, Daniels DL, Wehrli FW, Mark LP, Hendrix LE, Strandt JA, et al. Magnetic Susceptibility Artifacts in Gradient-Recalled Echo MR Imaging. *Am J Neuroradiol* (1988) 9:1149–55.
6. Ahluwalia M, Barnett GH, Deng D, Tatter SB, Laxton AW, Mohammadi AM, et al. Laser Ablation After Stereotactic Radiosurgery: A Multicenter Prospective Study in Patients With Metastatic Brain Tumors and Radiation Necrosis. *J Neurosurg* (2018) 130:804–11. doi: 10.3171/2017.11.JNS171273
7. Shah AH, Burks JD, Buttrick SS, Debs L, Ivan ME, Komotar RJ. Laser Interstitial Thermal Therapy as a Primary Treatment for Deep Inaccessible Gliomas. *Neurosurgery* (2019) 84:768–77. doi: 10.1093/neuros/nyy238
8. Chimowitz MI, Barnett GH, Palmer J. Treatment of Intractable Arterial Hemorrhage During Stereotactic Brain Biopsy With Thrombin: Report of Three Patients. *J Neurosurg* (1991) 74:301–3. doi: 10.3171/jns.1991.74.2.0301
9. de Quintana-Schmidt C, Leidinger A, Teixidó JM, Bertrán GC. Application of a Thrombin-Gelatin Matrix in the Management of Intractable Hemorrhage During Stereotactic Biopsy. *World Neurosurg* (2019) 121:180–5. doi: 10.1016/j.wneu.2018.10.053
10. Zhu M, Sun Z, Ng CK. Image-Guided Thermal Ablation With MR-Based Thermometry. *Quant Imaging Med Surg* (2017) 7:356–68. doi: 10.21037/qims.2017.06.06

## DATA AVAILABILITY STATEMENT

The raw data supporting the conclusions of this article will be made available by the authors, without undue reservation.

## ETHICS STATEMENT

## AUTHOR CONTRIBUTIONS

TN: first author. PJ: data gathering and figures. RH: interpretation, writing, and figures. GL: equal contributions. CO: equal contributions. AG: last authorship. All authors contributed to the article and approved the submitted version.

# Radiomics for the Prediction of Epilepsy in Patients With Frontal Glioma

Ankang Gao[1†], Hongxi Yang[2†], Yida Wang[2], Guohua Zhao[1], Chenglong Wang[2], Haijie Wang[2], Xiaonan Zhang[1], Yong Zhang[1], Jingliang Cheng[1*], Guang Yang[2*] and Jie Bai[1*]

[1] Department of MRI, The First Affiliated Hospital of Zhengzhou University, Zhengzhou, China, [2] Shanghai Key Laboratory of Magnetic Resonance, East China Normal University, Shanghai, China

**Objective:** This study was conducted in order to investigate the association between radiomics features and frontal glioma-associated epilepsy (GAE) and propose a reliable radiomics-based model to predict frontal GAE.

**Methods:** This retrospective study consecutively enrolled 166 adult patients with frontal glioma (111 in the training cohort and 55 in the testing cohort). A total 1,130 features were extracted from T2 fluid-attenuated inversion recovery images, including first-order statistics, 3D shape, texture, and wavelet features. Regions of interest, including the entire tumor and peritumoral edema, were drawn manually. Pearson correlation coefficient, 10-fold cross-validation, area under curve (AUC) analysis, and support vector machine were adopted to select the most relevant features to build a clinical model, a radiomics model, and a clinical–radiomics model for GAE. The receiver operating characteristic curve (ROC) and AUC were used to evaluate the classification performance of the models in each cohort, and DeLong's test was used to compare the performance of the models. A two-sided $t$-test and Fisher's exact test were used to compare the clinical variables. Statistical analysis was performed using SPSS software (version 22.0; IBM, Armonk, New York), and $p < 0.05$ was set as the threshold for significance.

**Results:** The classification accuracy of seven scout models, except the wavelet first-order model (0.793) and the wavelet texture model (0.784), was <0.75 in cross-validation. The clinical–radiomics model, including 17 magnetic resonance imaging-based features selected among the 1,130 radiomics features and two clinical features (patient age and tumor grade), achieved better discriminative performance for GAE prediction in both the training [AUC = 0.886, 95% confidence interval (CI) = 0.819–0.940] and testing cohorts (AUC = 0.836, 95% CI = 0.707–0.937) than the radiomics model ($p = 0.008$) with 82.0% and 78.2% accuracy, respectively.

**Conclusion:** Radiomics analysis can non-invasively predict GAE, thus allowing adequate treatment of frontal glioma. The clinical–radiomics model may enable a more precise prediction of frontal GAE. Furthermore, age and pathology grade are important risk factors for GAE.

Keywords: radiomics, glioma, glioma-associated epilepsy, frontal lobe epilepsy, T2 fluid-attenuated inversion recovery

# INTRODUCTION

Glioma-associated epilepsy (GAE) is a common diagnosis of glioma patients, which may be attributed to several factors, including tumor location, peritumoral edema, genetic background, and alterations in the microenvironment (1–3). Currently, there is no broadly acknowledged method for GAE interpretation. The frontal lobe is the most common glioma location associated with epilepsy (4), and frontal glioma is the most common cause for frontal lobe epilepsy (FLE) with lesions (5). FLE impairs the recognition and comprehension of patients, and particularly for frontal GAE, if patients do not receive treatment, there is a risk for status epilepticus (5, 6). Early prediction, increased awareness, and proper treatment of GAEs are vital to protect neurocognitive function and improve the quality of life of the patients (7, 8). With respect to the location of epileptic discharges, the propagation mode, and the experience of the patients, FLE differs from epileptic discharges in extra frontal regions (5); therefore, we independently analyzed frontal GAE in this study.

Radiomics is an emerging method to obtain predictive or prognostic information from medical images by several quantitative image features (9, 10). Although such features are not directly apparent to clinical practitioners, these can potentially produce reliable diagnostic and prognostic models in conjunction with other information sources. Radiomics has been proven helpful for clinical diagnosis, treatment choice, and prognosis assessment based on tomographic imaging (computed tomography, CT; magnetic resonance imaging, MRI; and positron emission tomography, PET) (11–14).

MRI is an essential preoperative examination for patients with glioma, and radiomics based on MRI is one of the focus areas for glioma research. The MRI sequences selected for glioma in previous radiomics research were mostly based on conventional MRI sequencing, such as T2-weighted imaging (T2WI), T2 fluid-attenuated inversion recovery (T2 FLAIR) imaging, apparent diffusion coefficient maps, and contrast-enhanced T1-weighted sequences (15–20). Given its high spatial resolution and the fact that it does not require materials, T2 FLAIR MRI sequences are considered to provide more tumor information than T2WI in glioma research (21). Radiomics analysis in T2WI has been previously applied to GAE (22–24) and has proven effective to predict the occurrence and type of GAE. However, these studies focused on low-grade glioma (LGG) and neglected the influence of brain tumor location on the seizure propagation mode. Therefore, we used the radiomics features extracted from T2 FLAIR imaging to investigate the association between radiomics features and WHO II–IV grade frontal lobe gliomas concurrent with epilepsy.

# MATERIAL AND METHODS

## Patients and Magnetic Resonance Imaging

This retrospective study was approved by the Ethics Committee of Scientific Research and Clinical Experiments of the First Affiliated Hospital of Zhengzhou University, which waived the requirement for written consent. We enrolled 166 consecutive patients with frontal glioma who underwent MRI scanning before surgery at our hospital from August 2016 through August 2019. Inclusion criteria were a) a single tumor and peritumoral edema defined in the frontal lobes by neurosurgery and imaging findings, b) pathologically confirmed single frontal gliomas (WHO II–IV) according to the 2016 WHO criteria, and c) available presurgical T2 FLAIR imaging data. Exclusion criteria were a) satellite tumors of the frontal glioma located beyond the frontal lobe and WHO grade I glioma, b) patients who underwent puncture biopsy and started antitumoral therapy before the MRI scan, and c) frontal glioma patients with other recent lesions that could cause epilepsy, such as cerebral hemorrhage, stroke, and other brain tumors. The preoperative diagnosis of GAE was based on clinical signs, electroencephalography (EEG), and imaging findings (25). According to clinical preoperative diagnosis, the enrolled cases included 89 patients with epilepsy and 77 patients without. The dataset was randomly split into a training cohort ($n = 111$, epilepsy/no epilepsy = 61/50) and a test cohort ($n = 55$, epilepsy/no epilepsy = 28/27). The sex and age of the patients, the tumor grade, and tumor location (left/right/both) were recorded. The whole workflow is illustrated in **Figure 1**.

MR images scanned with 3.0 T MRI scanners (Magnetom Trio TIM/Prisma, Verio or Skyra, Siemens Healthcare; Discovery 750, GE Medical Systems) were retrieved from the Picture Archive and Communication System of the hospital. MRI T2 FLAIR images had a $256 \times 256$-pixel matrix and a $240 \times 240$-mm field of view, inversion time = 2,400–2,500 ms, echo time = 81–135 ms, and repetition time = 8,000–8,500 ms, with section thickness = 5 mm and intersection gap = 1 mm.

## Tumor Masking and Image Preprocessing

One volume of interest (VOI) including the entire tumor and peritumoral edema was manually drawn slice-by-slice on T2 FLAIR images using the ITK-SNAP (version 3.6.0; www.itksnap.org)

**FIGURE 1** | Radiomics workflow.
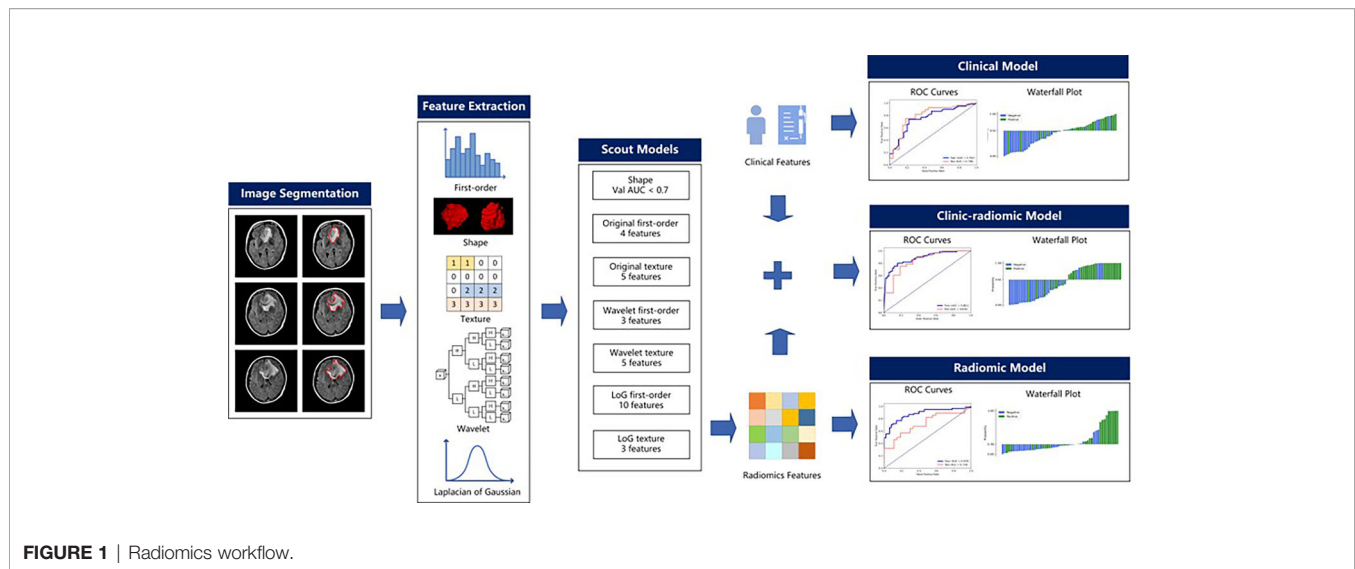
software by a Ph.D. candidate in imaging for medicine (AG, 5 years of experience in neuro-oncology). Next, the segmentation results were reviewed and modified if necessary by a neuroradiologist with 20 years of experience in neuroradiology (JB) using the same software. All images were normalized to a [0, 1] range before feature extraction.

## Radiomics Feature Extraction

Feature extraction was performed with the PyRadiomics (version 3.0) (26) package in Python (3.7.6). For each case, 3D shape features ($n = 14$) were extracted from the VOI before first-order statistics features ($n = 18$); texture features ($n = 75$) were extracted from each of the following image types: 1) original T2 FLAIR images, 2) each of the three Laplacian-of-Gaussian (LoG) filtered images (sigma = 1.0, 3.0, 5.0), and 3) each of the eight sub-bands of 3D wavelet-transformed image sub-bands using the Haar wavelet. The texture features extracted in this study included features based on a gray-level co-occurrence matrix (GLCM), gray-level run length matrix (GLRLM), gray-level size zone matrix (GLSZM), neighboring gray tone difference matrix (NGTDM), and gray-level dependence matrix (GLDM). A total of 1,130 features were extracted for each case.

## Feature Selection and Model Building

To remove the imbalance from the training dataset, upsampling by repeating random cases was applied to balance the GAE and non-GAE group samples.

A total of 1,130 radiomics features were extracted for each case; however, dealing directly with such an extensive feature number limits the robustness and effectiveness of the model. Thus, to reduce the dimensions of the features and select the appropriate ones for radiomics model building, we used a heuristic approach. First, all features were divided into subgroups according to their category, such as first-order, shape, and texture, and a scout model with those features was built for each subgroup using the training dataset. The scout

models were evaluated with a 10-fold cross-validation; the optimal model in each subgroup was selected by its performance on cross-validation with the training cohort. When the area under the receiver operating characteristic curve (AUC) of the optimal scout model on cross-validation was >0.7, all features in the model were used for the final model building. Otherwise, no subgroup features were further used.

To build the scout model, all features were normalized to the [0, 1] range. Thereafter, Pearson correlation coefficient (PCC) values between all feature pairs were calculated, and if the PCC value between two features was >0.99, one of them was removed. To determine the best number of features to be retained in the model, three feature selectors were compared: recursive feature elimination (RFE), which repeatedly builds the model and eliminates the least important feature; relief, which calculates a feature score for every feature and ranks them accordingly; and the Kruskal–Wallis test (KW), which eliminates the most likely feature from the same distribution in both GAE and non-GAE samples. For the classifier, we compared the performance of linear support vector machine (SVM), logistic regression (LR), and random forest (RF) for their good interpretability and demonstrated good performance in diagnosis based on medical imaging.

To find the best model, we tested different combinations of feature selectors and classifiers. Therefore, nine models (three features selectors and three classifiers) were built for a scout model, and the one with the best cross-validation AUC was used. Multimodel building and comparison were implemented semiautomatically with an open-source software, FeAtureExplorer (FAE, version 0.3.3) (27), which uses scikit-learn (version 0.23.2) as backend for machine learning.

As mentioned above, the features retained in qualified scout models were used to build a radiomics model. We also established a clinical model using only clinical variables (sex, age, tumor grade) and a clinical–radiomics model using both selected radiomics features and clinical variables to distinguish

GAE from non-GAE. The process for building the above models was similar to those used in scout model building, but without PCC dimension reduction, due to the relatively small number of input features.

## Performance Evaluation of the Models

The receiver operating characteristic curve (ROC) and AUC were used to evaluate the classification performance of the models in each cohort. DeLong's test was used to observe AUC differences in the models. The accuracy, sensitivity, specificity, positive predictive value (PPV), and negative predictive value (NPV) were also calculated at the cutoff value that maximizes the Youden index value in the training cohort. Calibration curves and decision curve analysis (DCA) (28) served to assess the clinical usefulness of radiomics signatures.

## Statistical Analysis

Age is reported as mean and range, and their difference between the GAE and non-GAE groups was assessed by a two-sided $t$-test. Sex and glioma position and grade were reported as frequency and proportions, and differences between the GAE and non-GAE groups were assessed by Fisher's exact test. Statistical analysis was performed using SPSS software (version 22.0; IBM, Armonk, New York), and $p < 0.05$ was used as the threshold for significance.

## RESULTS

## Demographic and Clinical Data

The main clinical and pathological characteristics of all 166 patients are listed in **Table 1**. There were significant differences between the GAE and non-GAE groups with respect to age, sex, and glioma grade ($p < 0.05$). Thus, younger, male, and LGG patients had a higher risk of GAE. Age distribution and glioma subtypes in the full cohort of patients are listed in **Appendix 1**.

In the GAE group (89/166), 18 patients (18/89) had preoperative EEG [ambulatory EEG ($n = 10$), video EEG ($n = 6$), conventional EEG ($n = 1$), and intracranial EEG ($n = 1$)], and two of them (2/18) showed interictal epileptiform abnormalities (IEAs) in the EEG recording; the others (16/18) had a normal

EEG recording. All patients in the non-GAE group had no EEG recordings.

## Performance of the Models

To find valuable features to build the radiomics model, we divided all radiomics features into seven categories and built a scout model for each. Using the features retained in scout models, we built a final radiomics model. Additionally, a clinical model using clinical variables and a clinical–radiomics model using both radiomics features and clinical variables were built. All models and features are listed in **Appendix 2**.

The performance of all models is listed in **Table 2**. The ROC curves and the predicted probability of clinical, radiomics, and clinical–radiomics models are shown in **Figure 2**. The classification accuracy of the scout models was <0.75 in cross-validation, except the wavelet first-order and wavelet texture models. Among all models, the clinical–radiomics model including 17 radiomics features and two clinical features achieved a performance with a classification accuracy = 0.82 and AUC = 0.886 [95% confidence interval (CI), 0.819–0.940] in the training cohort and a classification accuracy = 0.782 and AUC = 0.836 (95% CI, 0.707–0.937) in the testing cohort. The clinical–radiomics model achieved the best performance on the testing cohort (**Table 3**). DeLong's test showed a $p$-value <0.05 ($p = 0.008$) between the radiomics and clinical–radiomics models (**Table 4**). The calibration curve and DCA for the clinical–radiomics model are shown in **Figures 3A, B**, and its calibration performance, as evaluated with the Brier score, is reported in the legend. **Figure 4** shows a comparison between two representative patient cases with similar image and clinical representation; the clinical–radiomics model effectively distinguished between individuals with GAE and without GAE among glioma patients; the DCA curve revealed that for a high-risk threshold between 0.1 and 0.7, the clinical–radiomics model can be more beneficial than the clinical and radiomics models.

## DISCUSSION

Despite the higher incidence of epilepsy in LGG than in high-grade glioma (HGG) (29, 30), HGG is more common, and

**TABLE 1** | Clinical characteristic of patients in the training and testing cohorts.

| Characteristics | All cohort (n = 166) | | p-value | Training cohort (n = 111) | | p-value | Testing cohort (n = 55) | | p-value |
|---|---|---|---|---|---|---|---|---|---|
| | **Non-GAE group** | **GAE group** | | **Non-GAE group** | **GAE group** | | **Non-GAE group** | **GAE group** | |
| Sample size | 77 | 89 | – | 50 | 61 | – | 27 | 28 | – |
| Male/female | 32/45 | 60/29 | 0.001 | 24/26 | 43/18 | 0.020 | 9/19 | 17/10 | 0.031 |
| Age mean ± SD (range) | 49 ± 12 (15–74) | 41 ± 12 (12–66) | <0.001 | 48 ± 11 (15–73) | 41 ± 12 (12–65) | 0.005 | 50 ± 12 (25–74) | 41 ± 12 (17–66) | 0.014 |
| Glioma position (left/right/both) | 30/26/21 | 35/45/9 | 0.009 | 21/16/12 | 25/30/7 | 0.107 | 8/10/9 | 10/16/2 | 0.051 |
| Glioma grade (WHO II/III/IV) | 22/16/39 | 56/19/14 | <0.001 | 16/10/24 | 38/13/10 | 0.001 | 7/6/14 | 18/6/4 | 0.006 |

*p-values of age are the results of independent-samples t-tests; p-values of gender and tumor grade are the results of Fisher's exact tests.*

| Model | Cohort | AUC (95% CI) | Accuracy | Sensitivity | Specificity | PPV | NPV |
|---|---|---|---|---|---|---|---|
| Clinical model | Training | 0.762 (0.667–0.846) | 0.748 | 0.721 | 0.780 | 0.800 | 0.696 |
| | Testing | 0.799 (0.672–0.917) | 0.782 | 0.750 | 0.815 | 0.808 | 0.759 |
| Radiomics features-combined model | Training | 0.879 (0.805–0.939) | 0.811 | 0.770 | 0.86 | 0.870 | 0.754 |
| | Testing | 0.724 (0.575–0.855) | 0.673 | 0.536 | 0.815 | 0.750 | 0.629 |
| Clinical–radiomics model | Training | 0.886 (0.819–0.940) | 0.820 | 0.803 | 0.840 | 0.860 | 0.778 |
| | Testing | **0.836 (0.707–0.937)** | 0.782 | 0.750 | 0.815 | 0.808 | 0.759 |

*In the process of establishing scout models to select features, only the cross-validation performance was assessed to avoid information leakage. The bold values is optimal value.*
*AUC, area under the curve; PPV, positive predictive value; NPV, negative predictive value.*
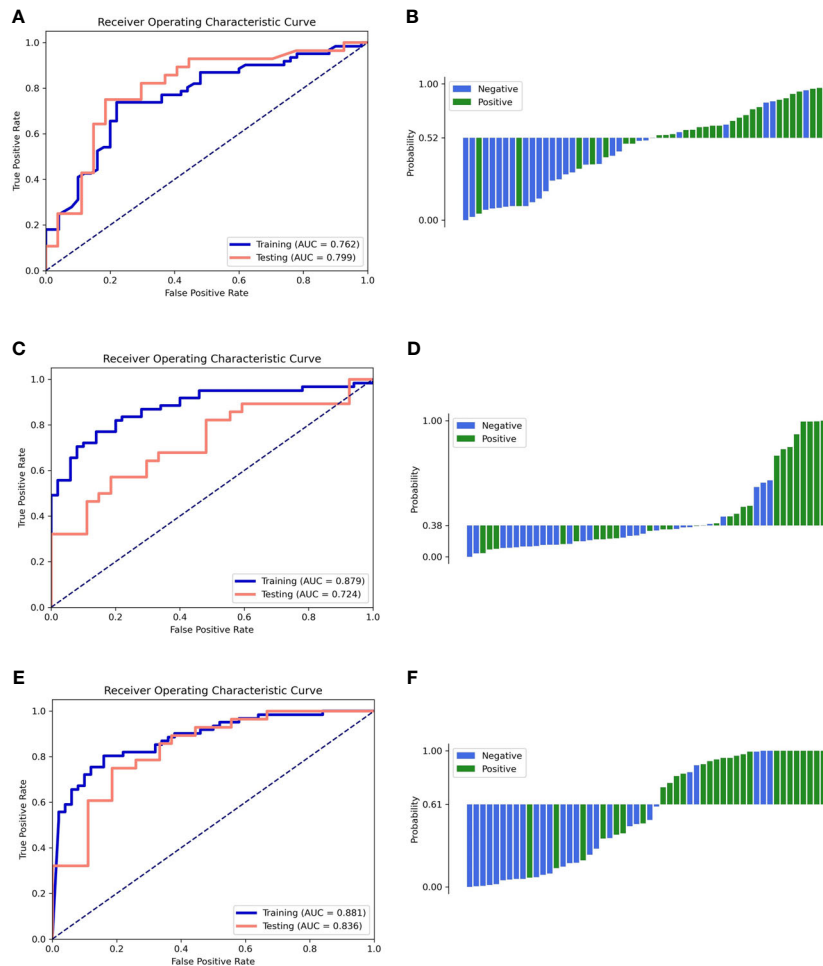


**FIGURE 2 |** ROC curves of the training and testing cohorts (left column) and the waterfall plot of the distribution of prediction probability on the testing cohort (right column). **(A, B)** Clinical model. **(C, D)** Radiomics model. **(E, F)** Clinical–radiomics model.

epilepsy in HGG patients always suggests tumor progression (31). Therefore, a non-invasive way to predict the occurrence of epilepsy in both LGG and HGG patients is needed to improve care, treatment, and timely surgery. Radiomics, which can transform medical images into useful data, has been widely used to classify glioma grade- or subtype-associated mutations and predict tumor proliferation, patient prognosis, etc. (15–20, 22).

In this study, T2 FLAIR-based radiomics was used to automatically extract 1,130 quantitative features, and the optimal model was selected from 10 models for predicting the occurrence of GAE in glioma patients. The best model, which combined clinical and radiomics features, could distinguish GAE patients from glioma patients with satisfying accuracy. Among all scout models, those based on wavelet transform features exhibited better performance than those based on other features, consistent

TABLE 3 | Selected features and the coefficients of features in the clinical–radiomics model.

| Features | Coefficients of SVM |
|---|---|
| Wavelet HHL GLCM correlation | 2.109668663 |
| Wavelet LHL GLCM correlation | 1.729482221 |
| Wavelet LHL GLRLM run variance | 1.691610793 |
| Wavelet HHL GLDM large dependence low gray-level emphasis | 1.618789140 |
| LoG sigma 3.0 mm 3D GLDM dependence non-uniformity normalized | 1.536185789 |
| Wavelet HHL GLDM low gray-level emphasis | 1.513109907 |
| Wavelet HHL first-order kurtosis | 1.398738067 |
| LoG sigma 5.0 mm 3D GLDM dependence non-uniformity normalized | 1.375653827 |
| Wavelet HHL first-order 10 percentile | 1.356330395 |
| Wavelet HHL first-order root mean squared | −1.347183074 |
| Pathological grade | −1.082656461 |
| Original GLDM high gray-level emphasis | 1.032809669 |
| Original GLSZM size zone non-uniformity normalized | −0.836530847 |
| Age | −0.580041869 |
| LoG sigma 1.0 mm 3D GLSZM small area emphasis | −0.444386255 |
| Original first-order mean | 0.363086015 |
| Original first-order 90 percentile | 0.262011650 |
| Original first-order total energy | −0.189844398 |
| LoG sigma 5.0 mm 3D first-order total energy | −0.089783744 |

GLCM, gray-level co-occurrence matrix; GLDM, gray-level dependence matrix; GLRLM, gray-level run length matrix; GLSZM, gray-level size zone matrix; HLL, HHL, LHL, HLH, considering L and H to be a low-pass (i.e. a scaling) and a high-pass (i.e., a wavelet) function; LoG, Laplacian-of-Gaussian.

TABLE 4 | Comparison of the performance of the models.

| Comparison | DeLong's test* (p-value) in the testing cohort | DeLong's test* (p-value) in all cohorts |
|---|---|---|
| Clinical model vs. radiomics model | 0.456 | 0.266 |
| Clinical model vs. clinical–radiomics model | 0.648 | 0.014 |
| Radiomics model vs. clinical–radiomics model | 0.008 | 0.047 |

p-value <0.05 indicated a statistically significant difference. *Test for the comparison of the difference of AUC.
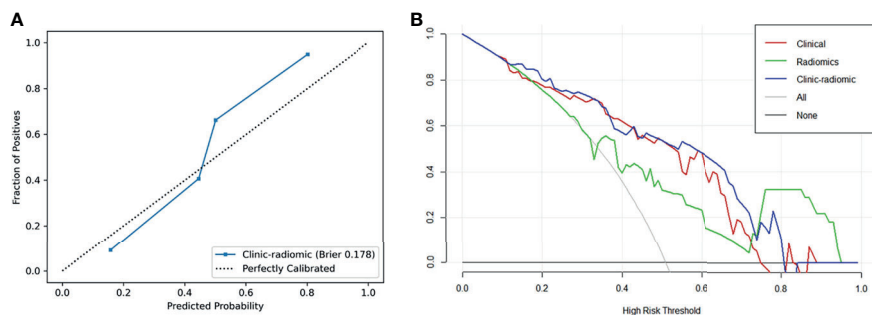


FIGURE 3 | (A) Calibration curve of the clinical–radiomics model. (B) DCA curves of the clinical, radiomics, and clinical–radiomics model.

with the higher weight of wavelet features in the combined models. This suggests the effectiveness of scout models to find useful features. The importance of wavelet features in our models was also consistent with previous research on epilepsy and epilepsy-type prediction in LGG (22, 24). Furthermore, in our study, the features from LoG filtered images were also included and were contributing features in the final models. LoG features are closely related to glioma heterogeneity, tumor microenvironment (10), and personalized tumor information (32) and are widely used in cancer radiomics (11–13).

In the best model, the age of the patients and tumor grade negatively correlated with GAE, which is also consistent with former reports (22, 24). Age is known to be related to a decrease in gamma-aminobutyric acid levels (33), and the metabolism of glioma may increase neuronal activity (7, 34), which implies that older glioma patients are more likely to experience GAE. However, although older patients are more likely to have HGG, LGG is more frequent in younger patients (35, 36). As reported by Englot et al. (1), HGGs have a predilection for white matter, which may preclude epileptogenic development.

**FIGURE 4** | T2 FLAIR images of four patients with or without GAE experience. The blue shadow in the images was manually delineated as the region of VOI. All the clinical characteristics and predicted probabilities of the combined model are presented at the center of the table.
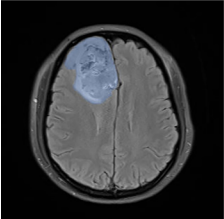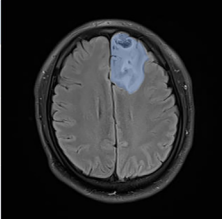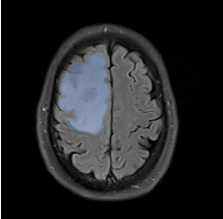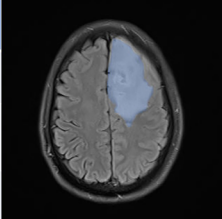
Furthermore, some old patients with malignant tumors may not survive long enough to develop epilepsy or may have other severe symptoms requiring a visit to a doctor before epilepsy develops. Therefore, younger patients have a higher risk of GAE than older patients. Additionally, LGG has a higher IDH mutation rate than HGG (37). Not only is IDH a vital gene for glioma genotyping (37), but IDH mutation type is also associated with GAE (7). Thus, the influence of the age of the patients and tumor grade in GAE is very complex. SVM coefficients of age and tumor grade were not very large; however, the clinical–radiomics model, which used these two variables, still achieved a higher AUC in the test cohort than the radiomics model. Thus, age and tumor grade are necessary features to improve the predictive efficiency of the model.

Tumor location and tumor cell impact on the peritumoral cortex are important factors for epilepsy occurrence, propagation mode, and subtype (1–4, 38), which are used in the research of epilepsy with lesion as critical categorized data (39). It is hard to accurately describe the glioma location in subregions, as there are many FLE-originating subregions, including motor areas and the cingulate gyrus, frontopolar, orbitofrontal, and dorsolateral cortex (40). Furthermore, most gliomas are ill-defined and irregular in shape and involve >1 brain subregion. Liu et al. (22) used the distance from the anterior commissure to the tumor centroid for a quantitative description of the tumor subregional location (22) and demonstrated that the Chebyshev distance significantly contributed to epilepsy prediction. Although no information on subregional tumor location was used in our research, all tumors were located in the frontal lobe and the VOIs included the peritumoral cortex, and our clinical–radiomics model for frontal GAE prediction achieved a slightly better result than that of Liu et al. (22).

The present study has some limitations. First, the diagnosis of GAE was based on clinical presentation rather than EEG analysis. Most GAE patients have an average EEG performance without seizures, and a short preoperative waiting period increases the difficulty of capturing an effective EEG. Second, IDH genotype was not included among the clinical features. In the future, machine learning methods for preoperative glioma IDH genotype prediction may improve the precision of GAE prediction. Third, a multicenter, large-scale prospective clinical trial is required to address the limitation of the small samples originating from a single institution in the present study.

In conclusion, radiomics analysis can non-invasively predict epilepsy to ensure proper treatment of frontal glioma patients. Our results suggest that the clinical–radiomics model may allow for a more precise GAE prediction in frontal glioma. Furthermore, age and pathology grade are important risk factors for GAE.

# DATA AVAILABILITY STATEMENT

The original contributions presented in the study are included in the article/**Supplementary Material**. Further inquiries can be directed to the corresponding authors.

# ETHICS STATEMENT

The studies involving human participants were reviewed and approved by the Ethics Committee of Scientific Research and Clinical Experiments of the First Affiliated Hospital of Zhengzhou University. Written informed consent for participation was not required for this study in accordance with the national legislation and the institutional requirements.

# AUTHOR CONTRIBUTIONS

AG: manuscript preparation, literature research, data acquisition, statistical analysis, and manuscript editing.

HY: manuscript preparation, literature research, data analysis, and statistical analysis. YW: literature research, data analysis, and statistical analysis. GZ, CW, and HW: literature research and data acquisition. XZ and YZ: data analysis and study design. JC, GY, and JB: study concept and design, manuscript review, and guarantor of the integrity of the entire study. All authors contributed to the article and approved the submitted version.

## FUNDING

## SUPPLEMENTARY MATERIAL

The Supplementary Material for this article can be found online at: https://www.frontiersin.org/articles/10.3389/fonc.2021.725926/full#supplementary-material

## REFERENCES

1. Englot DJ, Chang EF, Vecht CJ. Epilepsy and Brain Tumors. *Handb Clin Neurol* (2016) 134:267–85. doi: 10.1016/B978-0-12-802997-8.00016-5
2. Gonen T, Grossman R, Sitt R, Nossek E, Yanaki R, Cagnano E, et al. Tumor Location and IDH1 Mutation may Predict Intraoperative Seizures During Awake Craniotomy. *J Neurosurg* (2014) 121:1133–8. doi: 10.3171/2014.7.JNS132657
3. Stockhammer F, Misch M, Helms HJ, Lengler U, Prall F, von Deimling A, et al. IDH1/2 Mutations in WHO Grade II Astrocytomas Associated With Localization and Seizure as the Initial Symptom. *Seizure* (2012) 21:194–7. doi: 10.1016/j.seizure.2011.12.007
4. Zhang J, Yao L, Peng S, Fang Y, Tang R, Liu J. Correlation Between Glioma Location and Preoperative Seizures: A Systematic Review and Meta-Analysis. *Neurosurg Rev* (2019) 42:603–18. doi: 10.1007/s10143-018-1014-5
5. Giovagnoli AR, Tallarita GM, Parente A, Pastori C, de Curtis M. The Understanding of Mental States and the Cognitive Phenotype of Frontal Lobe Epilepsy. *Epilepsia* (2020) 61:747–57. doi: 10.1111/epi.16457
6. Kerkhof M, Vecht CJ. Seizure Characteristics and Prognostic Factors of Gliomas. *Epilepsia* (2013) 54:12–7. doi: 10.1111/epi.12437
7. Chen H, Judkins J, Thomas C, Wu M, Khoury L, Benjamin CG, et al. Mutant IDH1 and Seizures in Patients With Glioma. *Neurology* (2017) 88:1805–13. doi: 10.1212/WNL.0000000000003911
8. Kemerdere R, Yuksel O, Kacira T, Yeni N, Ozkara C, Tanriverdi T, et al. Low-Grade Temporal Gliomas: Surgical Strategy and Long-Term Seizure Outcome. *Clin Neurol Neurosurg* (2014) 126:196–200. doi: 10.1016/j.clineuro.2014.09.007
9. Bourgier C, Colinge J, Aillères N, Fenoglietto P, Brengues M, Pèlegrin A, et al. Radiomics: Definition and Clinical Development. *Cancer Radiother* (2015) 19:532–7. doi: 10.1016/j.canrad.2015.06.008
10. Gillies RJ, Kinahan PE, Hricak H. Radiomics: Images Are More Than Pictures, They Are Data. *Radiology* (2016) 278:563–77. doi: 10.1148/radiol.2015151169
11. Fiset S, Welch ML, Weiss J, Pintilie M, Conway JL, Milosevic M, et al. Repeatability and Reproducibility of MRI-Based Radiomic Features in Cervical Cancer. *Radiother Oncol* (2019) 135:107–14. doi: 10.1016/j.radonc.2019.03.001
12. Nazari M, Shiri I, Hajianfar G, Oveisi N, Abdollahi H, Deevband MR, et al. Noninvasive Fuhrman Grading of Clear Cell Renal Cell Carcinoma Using Computed Tomography Radiomic Features and Machine Learning. *Radiol Med* (2020) 125:754–62. doi: 10.1007/s11547-020-01169-z
13. Shiri I, Maleki H, Hajianfar G, Abdollahi H, Ashrafinia S, Hatt M, et al. Next-Generation Radiogenomics Sequencing for Prediction of EGFR and KRAS Mutation Status in NSCLC Patients Using Multimodal Imaging and Machine Learning Algorithms. *Mol Imaging Biol* (2020) 22:1132–48. doi: 10.1007/s11307-020-01487-8
14. Han X, Yang J, Luo J, Chen P, Zhang Z, Alu A, et al. Application of CT-Based Radiomics in Discriminating Pancreatic Cystadenomas From Pancreatic Neuroendocrine Tumors Using Machine Learning Methods. *Front Oncol* (2021) 11:606677. doi: 10.3389/fonc.2021.606677
15. Li Z, Wang Y, Yu J, Guo Y, Cao W. Deep Learning Based Radiomics (DLR) and Its Usage in Noninvasive IDH1 Prediction for Low Grade Glioma. *Sci Rep* (2017) 7:5467. doi: 10.1038/s41598-017-05848-2
16. Yu J, Shi Z, Lian Y, Li Z, Liu T, Gao Y, et al. Noninvasive IDH1 Mutation Estimation Based on a Quantitative Radiomics Approach for Grade II Glioma. *Eur Radiol* (2017) 27:3509–22. doi: 10.1007/s00330-016-4653-3
17. Li Y, Liu X, Qian Z, Sun Z, Xu K, Wang K, et al. Genotype Prediction of ATRX Mutation in Lower-Grade Gliomas Using an MRI Radiomics Signature. *Eur Radiol* (2018) 28:2960–8. doi: 10.1007/s00330-017-5267-0
18. Zhang X, Tian Q, Wang L, Liu Y, Li B, Liang Z, et al. Radiomics Strategy for Molecular Subtype Stratification of Lower-Grade Glioma: Detecting IDH and TP53 Mutations Based on Multimodal MRI. *J Magn Reson Imaging* (2018) 48:916–26. doi: 10.1002/jmri.25960
19. Zhang B, Chang K, Ramkissoon S, Tanguturi S, Bi WL, Reardon DA, et al. Multimodal MRI Features Predict Isocitrate Dehydrogenase Genotype in High-Grade Gliomas. *Neuro Oncol* (2017) 19:109–17. doi: 10.1093/neuonc/now121
20. Cho H-H, Park H. Classification of Low-Grade and High-Grade Glioma Using Multi-Modal Image Radiomics Features. *Conf Proc IEEE Eng Med Biol Soc* (2017) 2017:3081–4. doi: 10.1109/EMBC.2017.8037508
21. Jain R, Johnson DR, Patel SH, Castillo M, Smits M, van den Bent MJ, et al. "Real World" Use of a Highly Reliable Imaging Sign: "T2-FLAIR Mismatch" for Identification of IDH Mutant Astrocytomas. *Neuro Oncol* (2020) 22:936–43. doi: 10.1093/neuonc/noaa041
22. Liu Z, Wang Y, Liu X, Du Y, Tang Z, Wang K, et al. Radiomics Analysis Allows for Precise Prediction of Epilepsy in Patients With Low-Grade Gliomas. *NeuroImage Clin* (2018) 19:271–8. doi: 10.1016/j.nicl.2018.04.024
23. Sun K, Liu Z, Li Y, Wang L, Tang Z, Wang S, et al. Radiomics Analysis of Postoperative Epilepsy Seizures in Low-Grade Gliomas Using Preoperative MR Images. *Front Oncol* (2020) 10:1096. doi: 10.3389/fonc.2020.01096
24. Wang Y, Wei W, Liu Z, Liang Y, Liu X, Li Y, et al. Predicting the Type of Tumor-Related Epilepsy in Patients With Low-Grade Gliomas: A Radiomics Study. *Front Oncol* (2020) 10:235. doi: 10.3389/fonc.2020.00235
25. Liang S, Fan X, Zhao M, Shan X, Li W, Ding P, et al. Clinical Practice Guidelines for the Diagnosis and Treatment of Adult Diffuse Glioma-Related Epilepsy. *Cancer Med* (2019) 8:4527–35. doi: 10.1002/cam4.2362
26. van Griethuysen JJM, Fedorov A, Parmar C, Hosny A, Aucoin N, Narayan V, et al. Computational Radiomics System to Decode the Radiographic Phenotype. *Cancer Res* (2017) 77:104–7. doi: 10.1158/0008-5472.CAN-17-0339
27. Song Y, Zhang J, Zhang YD, Hou Y, Yan X, Wang Y, et al. FeAture Explorer (FAE): A Tool for Developing and Comparing Radiomics Models. *PloS One* (2020) 8:e0237587. doi: 10.1371/journal.pone.0237587
28. Vickers AJ, Elkin EB. Decision Curve Analysis: A Novel Method for Evaluating Prediction Models. *Med Decision Making* (2006) 26:565–74. doi: 10.1177/0272989X06295361
29. Pallud J, Audureau E, Blonski M, Sanai N, Bauchet L, Fontaine D, et al. Epileptic Seizures in Diffuse Low-Grade Gliomas in Adults. *Brain* (2014) 137:449–62. doi: 10.1093/brain/awt345

30. Chang EF, Potts MB, Keles GE, Lamborn KR, Chang SM, Barbaro NM, et al. Seizure Characteristics and Control Following Resection in 332 Patients With Low-Grade Gliomas. *J Neurosurg* (2008) 108:227–35. doi: 10.3171/JNS/2008/108/2/0227

31. Chaichana KL, Parker S, Olivi A, Quinones-Hinojosa A. Long -Term Seizure Outcome in Adult Patients Undergoing Primary Resection of Malignant Brain Astrocytomas. *J Neurosurg* (2009) 111:282–92. doi: 10.3171/2009.2.JNS081132

32. Lambin P, van Stiphout RG, Starmans MH, Rios-Velazquez E, Nalbantov G, Aerts HJ, et al. Predicting Outcomes in Radiation Oncology—Multifactorial Decision Support Systems. *Nat Rev Clin Oncol* (2013) 10:27–40. doi: 10.1038/nrclinonc.2012.196

33. Simmonite M, Carp J, Foerster BR, Ossher L, Petrou M, Weissman DH, et al. Age-Related Declines in Occipital GABA Are Associated With Reduced Fluid Processing Ability. *Acad Radiol* (2019) 26:1053–61. doi: 10.1016/j.acra.2018.07.024

34. Schaller B. Influences of Brain Tumor-Associated Ph Changes and Hypoxia on Epileptogenesis. *Acta Neurol Scand* (2005) 111:75–83. doi: 10.1111/j.1600-0404.2004.00355.x

35. Schiff D. Molecular Profiling Optimizes the Treatment of Low-Grade Glioma. *Neuro Oncol* (2016) 18:1593–4. doi: 10.1093/neuonc/now262

36. Avila EK, Chamberlain M, Schiff D, Reijneveld JC, Armstrong TS, Ruda R, et al. Seizure Control as a New Metric in Assessing Efficacy of Tumor Treatment in Low-Grade Glioma Trials. *Neuro Oncol* (2017) 19:12–21. doi: 10.1093/neuonc/now190

37. Chen R, Smith-Cohn M, Cohen AL, Colman H. Glioma Subclassifications and Their Clinical Significance. *Neurotherapeutics* (2017) 14:284–97. doi: 10.1007/s13311-017-0519-x

38. Armstrong TS, Grant R, Gilbert MR, Lee JW, Norden AD. Epilepsy in Glioma Patients: Mechanisms, Management, and Impact of Anticonvulsant Therapy. *Neuro Oncol* (2016) 18:779–89. doi: 10.1093/neuonc/nov269

39. Cendes F, Theodore WH, Brinkmann BH, Sulc V, Cascino GD. Neuroimaging of Epilepsy. *Handb Clin Neurol* (2016) 136:985–1014. doi: 10.1016/B978-0-444-53486-6.00051-X

40. Fisher RS, Cross JH, French JA, Higurashi N, Hirsch E, Jansen FE, et al. Operational Classification of Seizure Types by the International League Against Epilepsy: Position Paper of the ILAE Commission for Classification and Terminology. *Epilepsia* (2017) 58:522–30. doi: 10.1111/epi.13670

# Individualized Cerebral Artery Protection Strategies for the Surgical Treatment of Parasellar Meningiomas on the Basis of Preoperative Imaging

Yang Li[1], XingShu Zhang[1], Jun Su[2], Chaoying Qin[1], Xiangyu Wang[1], Kai Xiao[1] and Qing Liu[1]*

[1] Department of Neurosurgery in Xiangya Hospital, Central South University, Changsha, China, [2] Department of Neurosurgery in Hunan Children's Hospital, Changsha, China

**Objective:** Parasellar meningiomas (PMs) represent a cohort of skull base tumors that are localized in the parasellar region. PMs tend to compress, encase, or even invade the cerebral arteries and their perforating branches. The surgical resection of PMs without damaging neurovascular structures is challenging. This study aimed to analyze functional outcomes in a series of patients who underwent surgery with individualized cerebral artery protection strategies based on preoperative imaging.

**Methods:** A retrospective review was performed on a single surgeon's experience of the microsurgical removal of PMs in 163 patients between January 2012 and March 2020. Individualized approaches with a bidirectional dissection strategy were used. Cerebral artery invasion classification, neurological outcomes, MRC Scale for muscle strength, and Karnofsky performance scale were used to assess tumor vascular invasion, functional outcome, and patient quality-of-life outcomes, respectively.

**Results:** Total resection (Simpson grade I or II) was achieved in 114 patients (69.9%) in our study. A total of 44.7% of patients had improved vision at consecutive follow-ups, 51.1% were stable, and 3.8% deteriorated. Improvements in cranial nerves III, IV, and VI were observed in 41.1%, 36.2%, and 44.8% of patients, respectively. The mean follow-up time was (38.8 ± 27.9) months, and the KPS at the last follow-up was 89.6 ± 8.5. Recurrence was observed in eight patients (13.8%) with cavernous sinus meningiomas, and the recurrence rates in anterior clinoid meningiomas and medial sphenoid wing meningiomas were 3.8% and 2.8%, respectively.

**Conclusions:** Preoperative imaging is important in the selection of surgical approaches. Maximum tumor resection and cerebral artery protection can be achieved concurrently by utilizing the bidirectional dissection technique. Individualized cerebral artery protection strategies provide great utility in improving a patient's quality of life.

Keywords: parasellar meningioma, imaging, perforating artery, skull base surgery, KPS

# INTRODUCTION

Parasellar meningiomas (PMs) are a heterogeneous group of tumors that originate in the parasellar region. They frequently compress, encase, or even invade adjacent neurovascular structures of the anterior and middle skull base, thus making their surgical management challenging for skull base surgeons. However, a clear definition of PMs as a distinct entity is lacking because their multiple definitions and classification. Stirling (1) first described PMs in 1896. Ugrumov (2) divided PMs into three subgroups according to their site of origin: anterior clinoid meningiomas (ACMs), medial sphenoid wing meningiomas (MSWMs), and cavernous sinus meningiomas (CSMs). Recent advances in skull base microsurgery and microanatomy have renewed the understanding of PMs and have contributed to the development of detailed definitions and classifications. Graillon and Mariniello (3, 4) enlarged the definition of PMs and classified them into more subtypes. Individualized surgical strategies were developed and applied to the treatment of PMs on the basis of classifications, to facilitate gross total resection and neurofunction preservation.

In the last 20 years, the widespread use the operating microscope for skull base neurosurgery has allowed neurosurgeons to remove tumors aggressively. However, owing to their localization, PMs often compress, encase, or even invade cranial nerves, skull base bones, cerebral dura mater, cerebral arteries, and their perforating branches, thus resulting in unsatisfactory total tumor resection. The past few years have witnessed the development of stereotactic radiotherapy and molecular targeted therapy for meningiomas, which tempered the enthusiasm for aggressive total resection and influenced surgical strategies to be more conservative. To protect neurovascular structures during operation, the purpose of PM microsurgery is maximal surgical resection followed by adjuvant therapy. The dissection of the cerebral arteries and their perforating branches that are encased or invaded by PMs is the key surgical technique for achieving maximal tumor resection.

The identification of PMs subtypes before surgery is of great significance in individualized cerebral artery protection strategies. With the advances in preoperative neuroimaging, we were able to extend the classification of Ugrumov and classified PMs into ACMs, CMSs, and MSWMs before surgery. These subtypes originate from adjacent regions are difficult to distinguish from each other when they extensively invade surrounding structures. In the current study, we present a method for distinguishing three PMs based on preoperative imaging and through which we can apply the individualized surgical approach to patient. Concurrently, a bidirectional dissection technique was performed to achieving maximum tumor resection while preserving cerebral arteries and their perforating branches.

# METHODS

## Patient Population

We retrospectively analyzed neuroimaging, intraoperative video, and follow-up data from a consecutive series of 163 patients with PMs. The patients included in this study underwent microsurgery between January 2012 and March 2020 in the Department of Neurosurgery, XiangYa Hospital Central South University. The surgery was performed by the senior author Qing Liu. All patients underwent MRI, computed tomography angiography (CTA), KPS, muscle strength grading, and neurological examination before and after surgery. PMs were confirmed again by pathological examination, and the dural origin was observed during the operation. Meningiomas originating from the petroclival region, middle skull base, sellar region, and suprasellar region with secondary involvement of the parasellar region were excluded.

## Imaging and Tumor Classification

All patients underwent routine MRI before surgery, which include T1- and T2-weighted MRI with and without Gd. By using preoperative imaging, we can easily classify PMs into three subtypes (**Figure 1**) according to their growth directions and involved structures. On the basis of imaging classification, an individualized surgical approach and bidirectional dissection technique would be performed. In addition, the degree of resection can be estimated before surgery. For example, the total resection of CSMs with extensive intracavernous extension entails a high risk of cranial nerve injury. Instead of aggressive total resection, we removed the tumor with the goal of maximal resection while preserving the neurofunction. The residual tumor would be required for stereotactic radiotherapy three months after surgery.

We classified these cases as ACMs, CSMs, and MSWMs on the basis of radiological features of preoperative imaging. Consistent with our experience and other reports (5), ACMs originate from the dura covered in the inferior, superior and lateral aspects of the anterior clinoid (6). Coronal MRI images showed that the epicenter of ACMs was located on and around the anterior clinoid and formed a "v" shape. ACMs often extended to the direction which anterior clinoid projected to (**Figure 1A**). By contrast, MSWMs tended to grow perpendicular to the sphenoid ridge and compress the temporal lobe (**Figure 1B**). The other important features of ACMs that we can conclude from CTA or high-resolution computed tomography (HRCT) were the anterior clinoid hyperostosis and optic canal involvement. By contrast, MSWMs and CSMs rarely extended to those structures. CSMs represent a kind of meningiomas that originate from arachnoid granulations localized to the intermembrane space of the lateral wall of the cavernous sinus (7), and CSMs that originate from the outside of the cavernous sinus and those that secondarily invaded into it were excluded. We observed that the CSMs tended to extend within the cavernous sinus in the early stage because of the dense lateral wall (as reflected in the coronal images) and that the CSMs extended perpendicular to the lateral wall of the cavernous sinus (**Figure 1C**). CN III dysfunction in the early stages, along with the radiological features of CSMs, allow surgeon to diagnosed CSMs accurately. Furthermore, large ACMs and MSWMs may secondarily extend to the cavernous sinus via different routes. We observed 20 ACMs invading the cavernous sinus through the oculomotor triangle or infiltrating the roof or lateral wall directly. In contrast to ACMs and CSMs, MSWMs seldom invaded the cavernous sinus instead of compressing its lateral wall.
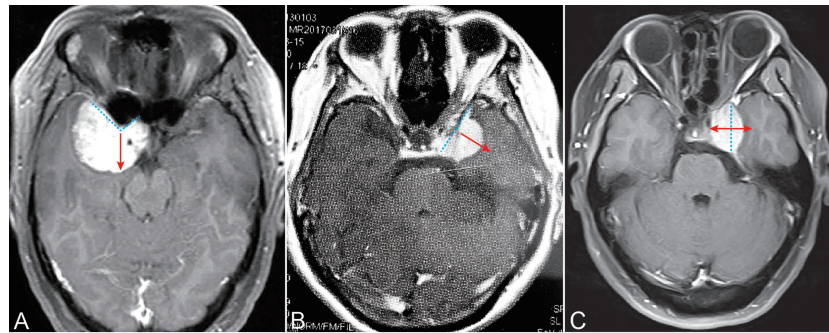
**FIGURE 1** | Extension directions of three typical PCMs. **(A)** ACMs extended to the direction in which the anterior clinoid projected. **(B)** MSWMs grow perpendicular to the sphenoid ridge. **(C)** CSMs extended perpendicular to the lateral wall of the cavernous sinus. Cyan dash line: the base of the tumor. Red arrow: tumor extension directions.

CTA was performed to estimate the relationship between the cerebral arteries and tumors. On the basis of preoperative imaging and intraoperative observation, we divided the cases into three groups: Group A involves tumor-compressed arteries or perforating branches but with the intervening arachnoid plane was intact. Group B involves tumor-displaced or tumor-encased arteries or their perforating branches but with the intervening arachnoid plane was intact; Group C involves tumor-invaded, tumor-encased, or tumor-displaced arteries or their perforating branches, as well as tumors that invaded the adventitia and caused the absence of the intervening arachnoid plane. HRCT was used to evaluate hyperostosis or bone erosion.

## Surgical Approach

The classic pterional approach (frontotemporal approach) has been widely applied to PM surgery for several decades. Our individualized surgical strategies were based on this approach and its modified form. A total of 105 of 163 craniotomies (64.4%) were performed *via* the pterional approach, and the remaining 58 craniotomies were performed using the pretemporal transcavernous approach. A brief overview of our tailored surgical approach based on preoperative imaging is provided below.

When surgery was performed using the pterional subdural approach, the incision was initiated above the palpated zygoma, extending superiorly and then curving anteriorly from the superior temporal line to the limit of the contralateral hairline. Subsequently, a standard frontotemporal craniotomy was performed. The drilling of outer and middle portions of the sphenoid wing was followed tby craniotomy. After the meningoorbital band was transected, drilling was continued to remove the anterior clinoid or optic canal if the tumor invaded those structures. A pterional intradural approach was required to open the dura mater after the extradural steps were completed. The dura was opened in a semicircular incision centered on the Sylvian fissure and extended inferior to the floor of the anterior and middle skull base. The arachnoid membrane over the sphenoid wing was opened to allow the drainage of cerebrospinal fluid (CSF) and the elevation of the temporal lobe. The dissection plane was established using the operation microscope, and the tumor was removed by bipolar coagulation and suction in small parts.

The pretemporal transcavernous approach required the same incision and craniotomy as the pterional subdural approach, but it did not necessitate entry into the subdural space in most cases. The surgery began by dissecting the meningo-orbital band with a microdissector, which can be used to peel off the outer layer of the lateral wall of the cavernous sinus. An incision parallel to the oculomotor or trochlear nerve was made in the inner layer of the lateral wall to provide entry into the cavernous sinus. The tumor within the cavernous sinus was removed by suction. A residual tumor encasing the ICA or its branches was also removed using bidirectional dissection technology. When a tumor that extended to the medial part of the cavernous sinus or petroclival region was encountered, we combined the pterional intradural approach and dissection of the Sylvian fissure. The dura mater of the superior wall of the cavernous sinus was opened, and we were able to access the residual tumor localized to the inner space of the ICA *via* the Dolenc triangle. By following the superior wall and proceeding posteriorly along the tentorial incisura, the tumor extending to the upper part of the petroclival region was removed.

## Bidirectional Dissection

In patients with ACMs and large MSWMs, bidirectional dissection began with extradural anterior clinoidectomy (**Figure 2A**), and the ICA and optic nerve (ON) that localizes to the medial of the anterior clinoid were determined (**Figure 2B**). Forward dissection was performed to expose the proximal ICA. Dissection proceeded from the distal dura ring of the ICA to its bifurcations (**Figure 2C**). Reverse dissection was initiated from the debulking tumor extending to the surface of the Sylvian fissure, and the dissection plane between the tumor and neurovascular structures was identified. The distal MCA branches can be located after splitting the Sylvian fissure. Tumor dissection was started from the MCA toward the ICA by using a microdissector, a microscissor, and a suction in small pieces (**Figure 2D**). When the tumor invaded the adventitia or was too
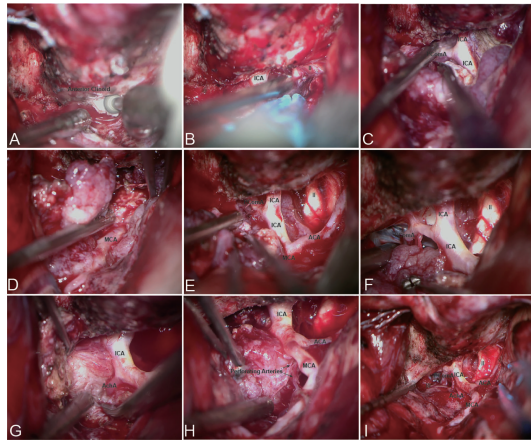
FIGURE 2 | Bidirectional dissection technique applied in ACM. **(A)** Extradural anterior clinoidectomy. **(B)** The proximal ICA can be localized in the medial of the anterior clinoid. **(C)** Forward dissection was started from the identification of the proximal ICA and along the course of the ICA. **(D)** Reverse dissection was initiated after split the Sylvian fissure. **(E–H)** Forward dissection would be applied again after debulking and resection most of the tumor. **(I)** Total resection and artery protection can be achieved by bidirectional dissection.

hard to suction, sharp dissection using a no. 11 blade scalpel was used to remove the tumor covering the arteries. Reverse dissection may be hindered by meningioma calcification or perforating branches, and forward dissection can be applied again to remove the residual tumor (**Figure 2E**). Following the course of the ICA trunk, the MCA, ACA, and anterior choroidal artery (ACHA) can be easily dissected from the residual tumor easily (**Figures 2F, G**). Special care must be taken to identify the perforating branches of the ICA and MCA embedded in the tumor (**Figures 2H, I**).

For patients with CSMs, forward dissection started with the identification of the meningo-orbital band, followed by the peeling of the outer layer of the lateral wall and the incising of the inner layer of the cavernous sinus (**Figure 3A**). Opening the space between the trochlear nerve and the ophthalmic division can expose the posterior bend and horizontal segment of the intracavernous ICA. The abducent nerve coursing through the lateral surface of the ICA should be protected (**Figure 3B**). The posterior bend is a landmark of reverse dissection from which the meningohypophyseal trunk is obtained. The trunk is the most important perforating branch of the intracavernous ICA and should be preserved using the bidirectional dissection technique. The dissection proceeded from the posterior bend forward to the horizontal segment of the ICA *via* suction and microdissection. However, limited by the ICA and trochlear nerve, forward dissection cannot be applied to the resection of the tumor in the inner part of the ICA. Reverse dissection was initiated by opening the Dolenc triangle of the superior wall of the cavernous sinus on the basis of the intradural approach, by localizing the proximal dura ring of the ICA, and by dissecting the tumor from the anterior ascending segment to the anterior bend of the ICA.

## RESULTS

### Patient Population

From January 2012 to March 2020, 163 PMs (63 ACMs, 58 CSMs, and 42 MSWMs) were surgically removed by the senior authors. Among the patients, 113 were female (69%), and 50 were male (31%). The median age was 52.5 years. The most common presenting symptoms were headache (53.2%), visual impairment (42.8%), visual field defect (26.6%), diplopia (17.2%), hemiparesis (6.8%), seizures (5.0%), oculomotor paralysis (14.3%), abducent paralysis (18.1%), and trochlear nerve palsy (12.5%). The mean follow-up time in our study was 38.8 months.

### Imaging and Intraoperative Findings

PM classification was based on preoperative radiological characteristics and intraoperative inspection. A total of 63 tumors with a meningioma epicenter of the anterior clinoid growing toward the direction where the anterior clinoid extends were classified into ACMs (**Figure 1A**). A total of 42 tumors with meningioma originating from the dura of the inner medial sphenoid wing and growing perpendicular to the long axis of the sphenoid wing to compress the medial temporal lobe were grouped into MSWMs (**Figure 1B**). The remaining 58 tumors, which originated within the cavernous sinus or the lateral wall and grew perpendicular to the long axis of the cavernous sinus, were grouped into CSMs (**Figure 1C**).

The prominent imaging and intraoperative findings showed the involvement of the tumor with the ICA, MCA, ACA, ACHA,
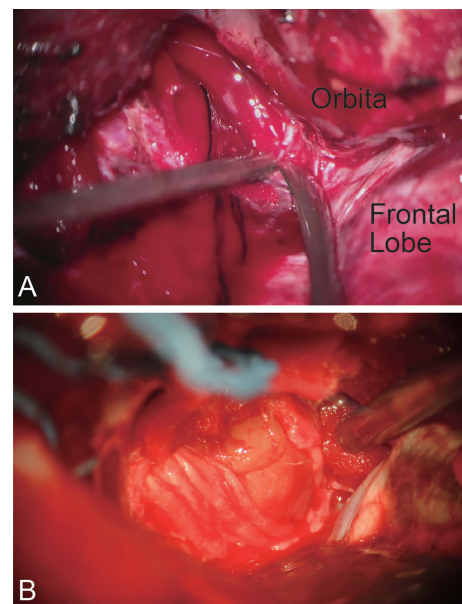


FIGURE 3 | Bidirectional dissection technique applied in CSM. **(A)** Dissection by peeling off the outer layer of the lateral wall and incising the inner layer of the cavernous sinus. **(B)** The cranial nerve coursing through the outer layer of the lateral wall.

and posterior communicating artery (PcomA). According to our preoperative or intraoperative observation, ICA and its branches were encased or invaded in most patients with PMs, whereas ACHA and PcomA were only involved in large PMs (**Table 1**).

The important structures of the parasellar region have also been found to be involved in tumors. ON impressment or encasement and optic canal involvement were found in most ACMs, whereas CSMs and MSWMs seldom invaded them. Cavernous sinus involvement was found in almost all CSMs and in some ACMs that invaded into the cavernous sinus *via* the oculomotor triangle or invaded the wall of the cavernous sinus directly. MSWMs can hardly invade the cavernous sinus, and they tend to compress the lateral wall of this area. The superior orbital fissure was mainly invaded by MSMWs.

## Surgical Results

Tailored approaches were applied according to the preoperative imaging classification. The pterional intradural approach was the most frequently performed approach for 63 ACMs and 42 MSWMs. The pretemporal transcavernous approach was performed in 58 patients with CSMs.

Total resection (Simpson grade I or II) was achieved in 50 patients with ACMs (79.3%), 38 patients with MSWMs (90.5%), and 26 patients with CSMs (44.8%). Subtotal resection (Simpson grade III) and partial resection (Simpson grade IV) were achieved in 13 patients with ACMs (20.7%), 4 patients with MSWMs (9.5%), and 32 patients with CSMs (55.2%) (**Table 2**). The tumor invaded into the cavernous sinus or the adventitia of the artery, and tumor calcification and tumor adherence to the epineurium were the three main reasons for subtotal or partial resection.

Histopathology confirmed that 5 patients (3.1%) had WHO grade II meningiomas, whereas 158 patients (96.9%) had WHO grade I meningiomas. Even though total resection was achieved, the 5 patients with WHO grade II meningioma required radiotherapy after three months.

Postoperative computed tomography scan were performed on all patients after recovery from anesthesia to evaluate the extent of tumor resection and postoperative complications. Postoperative cerebral hemorrhage and severe encephaledema were found in 10(7.7%) and 13(8.0%) patients, respectively, owing to our vascular protection strategy. Patients were required to undergo contrast enhanced MRI to confirm the extent of resection again 72h after the surgery. We suggested that patients with residual tumors initiated stereotactic radiotherapy after three months.

## Neurofunctional Outcome

Postoperative neurofunction outcomes were defined as improved, unchanged, or deteriorated (**Table 3**). Preoperative and postoperative neurofunction was evaluated by ophthalmologic examination or the MRC scale for muscle strength grading at the first follow-up after 3 months.

The visual acuity improvement rates in patients with three types of meningiomas were 41.3%, 46.5%, and 47.6% for ACMs, CSMs, and MSWMs, respectively. However, the vision acuity of most patients remained unchanged at follow-up several months postoperatively.

CN III deterioration was the most common type of CN deterioration in all patients. Four patients with ACMs and two patients with CSMs suffered from transient CN III deterioration, and most of them recovered to unchanged status after a few months. CN IV and CN VI deteriorations were mainly found in five postoperative patients with CSMs (**Table 3**).

## Tumor Recurrence

Overall, 155 patients (95%) underwent long-term follow-up. The actual follow-up time ranges from 11.9–65.7 months. Follow-up was performed with contrast-enhanced MRI. Tumor recurrence or progression was observed in eight patients with CSMs, two patients with ACMs, and one patient with MSWMs. A total of 32

---

**TABLE 1 |** The relationship between the tumor and cerebral arteries in different PMs.
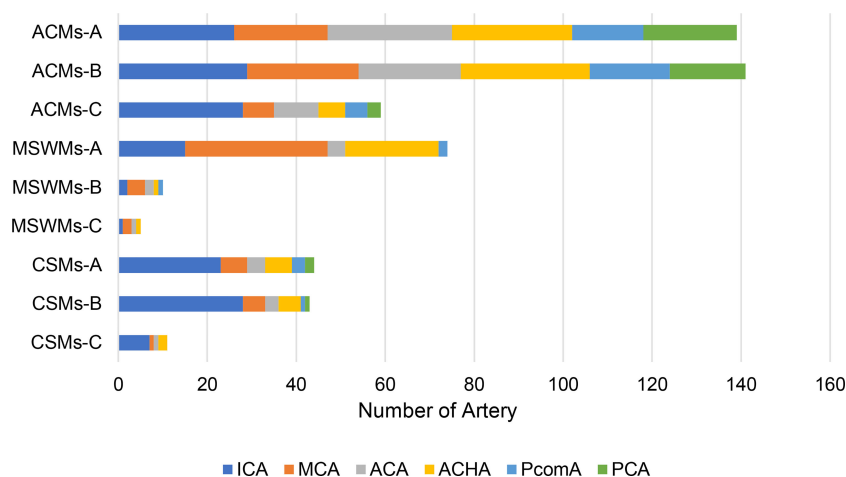


*ICA was involved in most of ACMs and CSMs while MCA tend to be compressed or invaded by most of the MSWMs.*

**TABLE 2 |** Bar graph showing the extent of resection in three types PCMs.
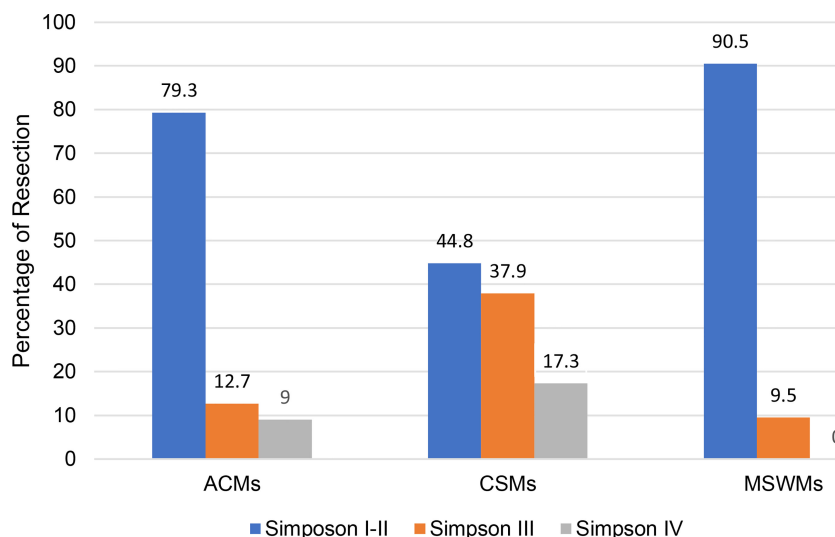


patients with residual tumor within the cavernous sinus or residual tumor that invaded the artery remained stable. The mean KPS performed in patients at follow-up was 89.6 compared with 81.1 preoperatively.

## DISCUSSION

In this study, we improved the classification of Ugrumov (2) and grouped PMs into three subtypes on the basis of preoperative imaging. The classification allowed us to perform individualized surgical approaches and artery protection strategies to achieve maximum tumor resection and minimized mobility. According to Giordano (8), intraoperative MRI allows surgeons to better evaluate the resectability of PCMs. However, in our experiences, we were able to evaluate the resectability of different PCMs before surgery instead of refering to the time-consuming intraoperative MRI.

### Individualized Surgical Strategies

Surgical approaches for removing PMs have been published in many reports. The traditional approach for PM surgery was the

pterional approach which was first described by Dandy (9) in 1942. Dolenc (10) applied the pterional approach to the surgical treatment of cavernous hemangioma of the cavernous sinus. In the last 20 years, pterional approach has been widely applied to the surgical treatment of PMs (5, 11–15), and the pterional approach and extended pterional approach have been centered around the Sylvian fissure with exposure of the temporal and frontal lobes. After removing the bone flap, there are two main routes to the parasellar region. The intradural approach is the most widely used method. After dural opening and CSF drainage, the temporal lobe can be easily elevated to expose the tumor. Another approach is the extradural approach, in which a dural incision is not required. Instead, by removing the sphenoid wing and dissecting the meningo-orbital band, surgeons can easily enter the intermembrane space of the lateral wall of the cavernous sinus to remove the tumor. In this series, we present our experience by combining intradural and extradural approaches to the parasellar region *via* pterional or extended pterional craniotomy.

For ACMs and MSWMs, we drilled the bone constituting the sphenoid wing and transected the meningoorbital band. Thereafter, we elevated the dura from the extradural area and conjugated the arterial supply from the ophthalmic artery, the

**TABLE 3 |** The number of patients with CN function and myodynamia change at the latest follow-up.

|  |  | CN II | CN III | CN IV | CN VI | Myodynamia |
|---|---|---|---|---|---|---|
| ACMs | improved | 26 | 23 | 16 | 29 | 20 |
|  | unchanged | 35 | 36 | 45 | 33 | 43 |
|  | deteriorated | 2 | 4 | 2 | 1 |  |
| CSMs | improved | 20 | 25 | 27 | 29 | 22 |
|  | unchanged | 35 | 31 | 28 | 27 | 36 |
|  | deteriorated | 3 | 2 | 3 | 2 |  |
| MSWMs | improved | 12 | 19 | 16 | 15 | 18 |
|  | unchanged | 29 | 23 | 36 | 27 | 34 |
|  | deteriorated | 1 |  |  |  |  |

anterior branch of the middle meningeal artery and the meningo-orbital artery (13, 16). These techniques have the following advantages: (1) Bone removal and elevation of the dura allow us to identify the ON and ICA from the extradural area. (2) The interruption of the arterial supply from the extradural area alleviates bleeding in the intradural procedures. (3) Bone removal enlarges the operation room and reduces temporal lobe retraction. To alleviate the tension of the brain, we chose to open the dura mater for CSF drainage before tumor resection. A large tumor would be pushed to the surgeon after splitting the Sylvian fissure with the help of the high CSF pressure of the basal arachnoid cisterns. Tumor debulking was initiated from the outside to the inside. By using the bidirectional dissection technique, we can remove the residual tumor that encases the ICA or MCA in small pieces. Anterior clinoidectomy was performed in patients with anterior clinoid hyperostosis or erosion to minimize intraoperative complications. We prefer extradural clinoidectomy because the dura mater acts as a protective screen during dissection or drilling. In addition to this advantage, extradural clinoidectomy allows a section of the falciform ligament to decompress the ON and protect it from the compression of the sharp falciform ligament. Owing to these procedures, visual function deterioration was observed in 2.9% of patients with ACMs and MSMWs.

For CSMs, the bone of the sphenoid wing was drilled to the base of the middle cranial fossa to enlarge the dissection space. Dissection into the cavernous sinus was initiated from the meningo-orbital band, which is located at the apex of the superior orbital fissure (**Figure 3A**). By performing a sharp dissection, a plane between the temporal tip and cavernous sinus lateral wall was established. The outer layer of the lateral wall was peeled away from the anterior aspect of the cavernous sinus (**Figure 3B**). The tumor invading the intermembrane space of the lateral wall can be removed by suction and sharp dissection. An incision parasellar to the CN IV was made in the enlarged space caused by tumor compression superior or inferior to the CN IV to provide entry the cavernous sinus. These maneuvers took advantage of the natural space between the CNs caused by tumor compression and enabled the surgeon to enter the cavernous sinus *via* the shortest routes. Sharp dissection along the cleavage planes within the cavernous sinus minimized injury to the CNs and arteries caused by traction or suction. When the tumor invaded the inner part of the cavernous sinus, we performed the intradural approach and entered the cavernous sinus *via* an incision in its roof. This procedure enabled the total resection of CSMs. When the tumor invaded the adventitia or epineurium of the cavernous sinus, we left the residual tumor in this area and then performed postoperative stereotactic radiotherapy. The recurrence and progression rate of CSMs was 13.7% compared with 7.5%-20% reported in other studies (11–13). A few patients exhibited temporary postoperative cranial dysfunction, and most of them recovered to preoperative levels after several months.

## Bidirectional Dissection

The encasement of the ICA and its branches has been reported in 20%-55% (13, 14). Vessel invasion is dealt with aggressively, and

unintended vessel perforation occurs in 20.8% of patients (6). Sacrificing the middle cerebral artery branches invaded by ACMs resulted in 100% mortality (17). PMs that encase or invade the major cerebral arteries and their perforating branches remain challenging for total surgical resection. However, residual tumor along the arteries is a risk factor for tumor progression. Maximal tumor resection while preserving the arteries is the desired surgical goal. To achieve this goal, we performed a bidirectional dissection technique based on a tailored surgical approach (**Figure 4**).

On the basis of the individualized preoperative classification and approach, we performed this technique in different directions, and one patient suffered from artery perforation. The postoperative hemiparesis rate was 3.1% in patients with PMs. This technique facilitates tumor debulking and differentiation of the feeding artery or perforators. Sharp dissection combined with mild traction is the core technique for bidirectional dissection. Compared with suction and blunt dissection, sharp dissection along the arachnoid plane prevents traction force from injuring CNs and perforating arteries. Once the tumor invaded the adventitia or epineurium, the arachnoid membrane was absent. This led to arteriotomies being indicated on preoperative imaging even though the tumor was small. We chose to leave the tumor tuft along the arteries and their perforating branches.

The bidirectional dissection technique can be applied to the dissection of the ICA, MCA, ACA, ACHA, and PcomA (**Figure 3**). However, it can also be applied to the dissection of perforating branches. Special attention was given to perforating branches that support CNs (**Figure 5**). The arterial supply of the chiasm and ON is mainly from the superior hypophyseal arteries,
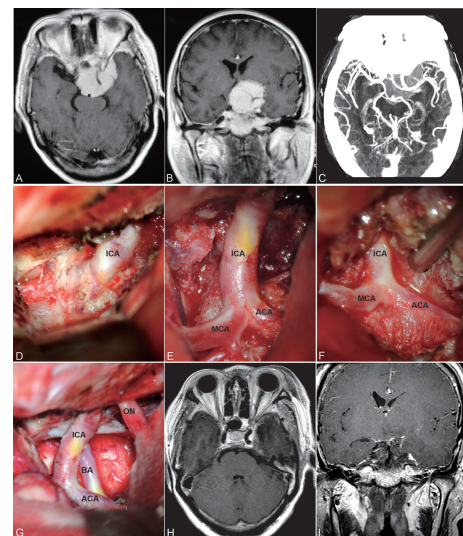


**FIGURE 4** | Contrast-enhanced MRI and CTA images of ACM **(A–C)** preoperative; **H, I** postoperative) and steps of bidirectional dissection technique **(D–G)**. Intradural localization of the ICA **(D)** and dissection along the course of ICA and its branches **(E, F)** to achieve total resection while preserved the ICA and its branches **(G)**.
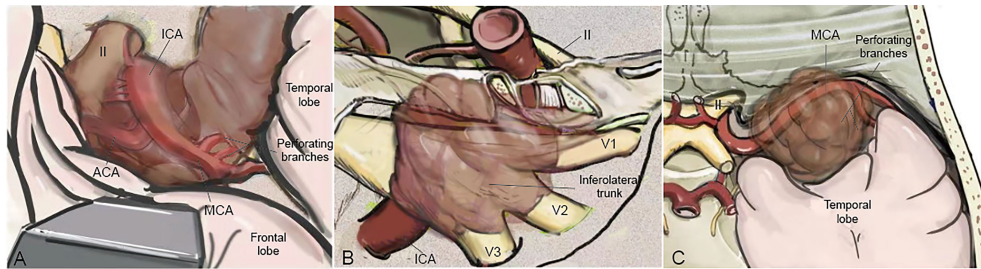
**FIGURE 5** | The cranial artery, perforating branches, and the cranial nerve are involved in the PCMs. The ACA, ICA, MCA, and their perforating branches were involved in ACMs **(A)** while MCA and its perforating branches were the most involved in MSWMs **(C)**. The inferolateral trunk and the meningohypophyseal trunk of the ICA were encased by CSMs **(B)**.

which are often damaged by intraoperative operations, thus resulting in subsequent ON ischemia and visual deficits (18). In the current study, we dissected this branch by finding the entrance point from the posteromedial aspect of the ICA and dissecting it from proximal to distal (**Figure 5A**). The meningohypophyseal trunk and inferolateral trunk are the most important branches of the cavernous ICA and can be located in the posterior and horizontal ICA segments, respectively (**Figure 5B**). The sacrifice of these arteries may cause the dysfunction of CN III, IV, and VI because of the interruption of their blood supply (19). By following their course and using the bidirectional dissection technique, these CNs can be protected while achieving maximal tumor resection. The lenticulostriate arteries are the most important perforating branches of the MCA and may cause hemiparesis, coma or death when damaged (20). The majority of these perforating branches coursed medially and parallel to the M1 supply of the basal ganglia and portions of the internal capsule. Special attention is needed to protect this branch during dissection along the MCA trunk. The dissection of the lenticulostriate arteries was initiated from the MCA trunk followed by tumor decompression to identify the distal end of the lenticulostriate arteries encased in tumors (**Figure 5C**). By using these bidirectional dissection procedures, maximal tumor resection and neurofunctional protection can be achieved.

## Neurofunctional Outcomes at Long-Term Follow-Up

During the past two decades, our surgical goal was to achieve maximal tumor resection while protecting the neurofunction of patients and improving their postoperative quality of life. The individualized surgical techniques mentioned above were used to minimize mobility and morbidity. In our series, the KPS of patients with PMs at the last follow-up was elevated to 89.6 compared with 81.1 preoperatively.

The ON was often involved in PMs and postoperative visual improvement was present in 10%-66.7% of patients according to the previous reports (6, 14, 17). The visual acuity improvement and unchangeability in our series were up to 90.3%. We attributed the good outcome not only to the bidirectional dissection technique but also to the extradural clinoidectomy, the section of the falciform, and the preservation of the

perforating branches that supply the ON and optic chiasm. In our experience, the compression of the nerve directly or its feeding artery was the reason for the deterioration of visual acuity preoperatively. Even in blind patients, efforts should be made to dissect the ON and its feeding arteries from the tumor instead of sacrificing it to achieve maximal tumor resection. Three patients with blind-eye recovery had a sense of light after several months. Another important procedure that may contribute to the improvement of patients is the dissection of the superior hypophyseal arteries, which is the main blood supply of the ON.

CN III, IV, and VI are often encased or invaded by CSMs and large ACMs. Injury to these CNs or injury to their blood supply were the two main reasons for postoperative CN dysfunction. According to previous reports, postoperative CN III, IV, and VI dysfunction from 12.9% to 29% (11–13, 21). The deterioration of nerve function was observed in 9.2% of our patients, and 66.7% recovered to unchanged after follow-up. We attributed these results to the following individualized surgical techniques: (1) A pretemporal transcavernous approach allows the surgeon to identify the plane between the tumor and neurovascular structures within the cavernous sinus. (2) Sharp dissection minimizes the traction to CNs. (3) A bidirectional dissection technique was used to preserve the blood supply of these CNs. The total resection rate of CSMs was 44.8%, which was lower than that of ACMs and MSWMs. The reason was to prevent intraoperative injury to the ICA and CNs when the tumor invaded the adventitia or epineurium. If we remove the residual tumor in the above cases, injury to the ICA or CNs was unavoidable. Owing to the slow growth of the residual tumor (22), we left the residual tumor and performed stereotactic radiotherapy three months after the surgery. The recurrence rate of CSMs was 3.4% during the follow-up.

## Limitations

Most of the results of this study were based on retrospective data. This retrospective aspect may introduce selection bias and misclassification. Prospective studies and multi-organizational research with larger sample sizes are still needed before the surgical techniques and results of this study can be adopted.

## CONCLUSION

PMs are one of the most challenging skull base meningiomas. We modified the classification of Ugrumov (2) and classified PMs into three subtypes on the basis of preoperative imaging, according to which we can perform individualized surgical strategies for patients, including tailored surgical approaches and bidirectional dissection techniques. This technique contributes to the total resection of meningiomas while preserving the cerebral arteries and CNs.

## DATA AVAILABILITY STATEMENT

The original contributions presented in the study are included in the article/**Supplementary Material**. Further inquiries can be directed to the corresponding author.

## ETHICS STATEMENT

The studies involving human participants were reviewed and approved by the Ethics Committee of Xiangya Hospital. The patients/participants provided their written informed consent to participate in this study.

## AUTHOR CONTRIBUTIONS

YL analyzed and interpreted the patient data regarding the PCMs and drafted the article. XZ collected the patient data. CQ and JS provided critical revise. KX and XW draft the figures. QL and other authors were performed the surgeries. All authors contributed to the article and approved the submitted version.

## ACKNOWLEDGMENTS

All contributors to this study are included in the list of authors.

## SUPPLEMENTARY MATERIAL

The Supplementary Material for this article can be found online at: https://www.frontiersin.org/articles/10.3389/fonc.2021.771431/full#supplementary-material

**Supplementary Video 1 |** Forward dissection was performed to expose the proximal ICA. Dissection proceeded from the distal dura ring of the ICA to its bifurcations Reverse dissection was initiated from the debulking tumor extending to the surface of the Sylvian fissure. The distal MCA branches can be located after splitting the Sylvian fissure. When the tumor invaded the adventitia or was too hard to suction, sharp dissection using a no. 11 blade scalpel was used to remove the tumor covering the arteries. Following the course of the ICA trunk, the MCA, ACA, and anterior choroidal artery (ACHA) can be easily dissected from the residual tumor easily.

## REFERENCES

1. Stirling W. Physiology in the French Metropolis. *Br Med J* (1896) 1 (1841):923–4. doi: 10.1136/bmj.1.1841.923
2. Ugrumov VM, Ignatyeva GE, Olushin VE, Tigliev GS, Polenov AL. Parasellar Meningiomas: Diagnosis and Possibility of Surgical Treatment According to the Place of Original Growth. *Acta Neurochir Suppl (Wien)* (1979) 28(2):373–4.
3. Graillon T, Regis J, Barlier A, Brue T, Dufour H, Buchfelder M. Parasellar Meningiomas. *Neuroendocrinology* (2020) 110(9-10):780–96. doi: 10.1159/000509090
4. Mariniello G, de Divitiis O, Bonavolonta G, Maiuri F. Surgical Unroofing of the Optic Canal and Visual Outcome in Basal Meningiomas. *Acta Neurochir (Wien)* (2013) 155(1):77–84. doi: 10.1007/s00701-012-1485-z
5. Pamir MN, Belirgen M, Ozduman K, Kilic T, Ozek M. Anterior Clinoidal Meningiomas: Analysis of 43 Consecutive Surgically Treated Cases. *Acta Neurochir (Wien)* (2008) 150(7):625–35; discussion 35–6. doi: 10.1007/s00701-008-1594-x
6. Al-Mefty O. Clinoidal Meningiomas. *J Neurosurg* (1990) 73(6):840–9. doi: 10.3171/jns.1990.73.6.0840
7. Kehrli P, Maillot C, Wolff Quenot MJ. Sheaths of Cranial Nerves in the Lateral Wall of the Cavernous Sinus. An Embryological and Anatomical Study. *Neurochirurgie* (1995) 41(6):403–12. doi: 10.1179/tns.1993.001
8. Giordano M, Gallieni M, Metwali H, Fahlbusch R, Samii M, Samii A. Can Intraoperative Magnetic Resonance Imaging Be Helpful in the Surgical Resection of Parasellar Meningiomas? A Case Series. *World Neurosurg* (2019) 132:e577–84. doi: 10.1016/j.wneu.2019.08.070

9. Dandy WE. Aneurysm of the Anterior Cerebral Artery. *J Am Med Assoc* (1942) 119(16):1253–4. doi: 10.1001/jama.1942.72830330001005
10. Dolenc V. Direct Microsurgical Repair of Intracavernous Vascular Lesions. *J Neurosurg* (1983) 58(6):824–31. doi: 10.3171/jns.1983.58.6.0824
11. Nanda A, Thakur JD, Sonig A, Missios S. Microsurgical Resectability, Outcomes, and Tumor Control in Meningiomas Occupying the Cavernous Sinus. *J Neurosurg* (2016) 125(2):378–92. doi: 10.3171/2015.3.JNS142494
12. Pichierri A, Santoro A, Raco A, Paolini S, Cantore G, Delfini R. Cavernous Sinus Meningiomas: Retrospective Analysis and Proposal of a Treatment Algorithm. *Neurosurgery* (2009) 64(6):1090–9. doi: 10.1227/01.NEU.0000346023.52541.0A
13. Sindou M, Wydh E, Jouanneau E, Nebbal M, Lieutaud T. Long-Term Follow-Up of Meningiomas of the Cavernous Sinus After Surgical Treatment Alone. *J Neurosurg* (2007) 107(5):937–44. doi: 10.3171/JNS-07/11/0937
14. Attia M, Umansky F, Paldor I, Dotan S, Shoshan Y, Spektor S. Giant Anterior Clinoidal Meningiomas: Surgical Technique and Outcomes. *J Neurosurg* (2012) 117(4):654–65. doi: 10.3171/2012.7.JNS111675
15. Lynch JC, Pereira CE, Goncalves M, Zanon N. Extended Pterional Approach for Medial Sphenoid Wing Meningioma: A Series of 47 Patients. *J Neurol Surg B Skull Base* (2020) 81(2):107–13. doi: 10.1055/s-0039-1677728
16. Yamaki T, Tanabe S, Sohma T, Uede T, Shinya T, Hashi K. Feeding Arteries of Parasellar Meningiomas–Angiographic Study of Medial Sphenoid Ridge and Tuberculum Sellae Meningiomas. *Neurol Med Chir (Tokyo)* (1988) 28(6):553–8. doi: 10.2176/nmc.28.553
17. Goel A, Gupta S, Desai K. New Grading System to Predict Resectability of Anterior Clinoid Meningiomas. *Neurol Med Chir (Tokyo)* (2000) 40(12):610–6; discussion 6-7. doi: 10.2176/nmc.40.610

18. van Overbeeke J, Sekhar L. Microanatomy of the Blood Supply to the Optic Nerve. *Orbit* (2003) 22(2):81–8. doi: 10.1076/orbi.22.2.81.14316

19. Salaud C, Decante C, Ploteau S, Hamel A. Implication of the Inferolateral Trunk of the Cavernous Internal CAROTID Artery in Cranial Nerve Blood Supply: Anatomical Study and Review of the Literature. *Ann Anat* (2019) 226:23–8. doi: 10.1016/j.aanat.2019.07.004

20. Djulejic V, Marinkovic S, Milic V, Georgievski B, Rasic M, Aksic M, et al. Common Features of the Cerebral Perforating Arteries and Their Clinical Significance. *Acta Neurochir (Wien)* (2015) 157(8):1393. doi: 10.1007/s00701-015-2462-0

21. DeMonte F, Smith HK, al-Mefty O. Outcome of Aggressive Removal of Cavernous Sinus Meningiomas. *J Neurosurg* (1994) 81(2):245–51. doi: 10.3171/jns.1994.81.2.0245

22. Hashimoto N, Rabo CS, Okita Y, Kinoshita M, Kagawa N, Fujimoto Y, et al. Slower Growth of Skull Base Meningiomas Compared With Non-Skull Base Meningiomas Based on Volumetric and Biological Studies. *J Neurosurg* (2012) 116(3):574–80. doi: 10.3171/2011.11.JNS11999

# A Continuous Correlation Between Residual Tumor Volume and Survival Recommends Maximal Safe Resection in Glioblastoma Patients: A Nomogram for Clinical Decision Making and Reference for Non-Randomized Trials

Marco Skardelly[1,2]*, Marlene Kaltenstadler[1], Felix Behling[1], Irina Mäurer[3,4], Jens Schittenhelm[5], Benjamin Bender[6], Frank Paulsen[2,7], Jürgen Hedderich[8], Mirjam Renovanz[1,2,3,4,9], Jens Gempt[10], Melanie Barz[10], Bernhard Meyer[10], Ghazaleh Tabatabai[1,2,3,4] and Marcos Soares Tatagiba[1,2]

[1] Department of Neurosurgery, University Hospital Tuebingen, Eberhard Karls University Tuebingen, Tuebingen, Germany, [2] Center for Neuro-Oncology, Comprehensive Cancer Center Tuebingen Stuttgart, University Hospital Tuebingen, Eberhard Karls University of Tuebingen, Tuebingen, Germany, [3] Department of Neurology, Eberhard Karls University of Tuebingen, Tuebingen, Germany, [4] Department Interdisciplinary Neuro-Oncology, Eberhard Karls University of Tuebingen, Tuebingen, Germany, [5] Institute of Pathology and Neuropathology, Division of Neuropathology, University Hospital Tuebingen, Eberhard Karls University Tuebingen, Tuebingen, Germany, [6] Department of Neuroradiology, University Hospital Tuebingen, Eberhard Karls University Tuebingen, Tuebingen, Germany, [7] University Department of Radiation Oncology, University Hospital Tuebingen, Eberhard Karls University of Tuebingen, Tuebingen, Germany, [8] Medistat GmbH, Kiel, Germany, [9] Department of Neurosurgery, University Medical Center, Johannes Gutenberg University Mainz, Mainz, Germany, [10] Department of Neurosurgery, Klinikum rechts der Isar, Technische Universität München, Munich, Germany

**Objective:** The exact role of the extent of resection or residual tumor volume on overall survival in glioblastoma patients is still controversial. Our aim was to create a statistical model showing the association between resection extent/residual tumor volume and overall survival and to provide a nomogram that can assess the survival benefit of individual patients and serve as a reference for non-randomized studies.

**Methods:** In this retrospective multicenter cohort study, we used the non-parametric Cox regression and the parametric log-logistic accelerated failure time model in patients with glioblastoma. On 303 patients (training set), we developed a model to evaluate the effect of the extent of resection/residual tumor volume on overall survival and created a score to estimate individual overall survival. The stability of the model was validated by 20-fold cross-validation and predictive accuracy by an external cohort of 253 patients (validation set).

**Results:** We found a continuous relationship between extent of resection or residual tumor volume and overall survival. Our final accelerated failure time model (pseudo $R^2 = 0.423$; C-index = 0.749) included residual tumor volume, age, $O^6$-methylguanine-

*DNA-methyltransferase* methylation, therapy modality, resectability, and ventricular wall infiltration as independent predictors of overall survival. Based on these factors, we developed a nomogram for assessing the survival of individual patients that showed a median absolute predictive error of 2.78 (mean: 1.83) months, an improvement of about 40% compared with the most promising established models.

**Conclusions:** A continuous relationship between residual tumor volume and overall survival supports the concept of maximum safe resection. Due to the low absolute predictive error and the consideration of uneven distributions of covariates, this model is suitable for clinical decision making and helps to evaluate the results of non-randomized studies.

## INTRODUCTION

Glioblastoma (GBM) is a prognostically unfavorable primary brain tumor with an incidence rate of 3.2 per 100,000 population, representing 14.5% of all primary brain tumors (1). The standard of care remains tumor resection followed by radiation therapy with concomitant and adjuvant temozolomide (TMZ) (2).

Several prognostic factors have been described that significantly influence and predict survival, e.g., methylation of the promoter region of the $O^6$-*methylguanine-DNA-methyltransferase* (MGMT) gene, extent of resection (EOR), treatment regimen, age, and assessment scores as Karnofsky performance status (KPS) (3–7). However, neurosurgeons and neuro-oncologists can only influence the EOR (8, 9) and the treatment regimen (2) to a limited extent. Although the EOR is one of the key elements of treatment in GBM, its exact role is still controversial due to the lack of prospective randomized clinical trials and contradictory retrospective studies and interpretations (3–5, 10–12). Different thresholds for a clinically significant effect were proposed, ranging from about 70% to complete resection of the contrast-enhancing tumor (3, 5, 10–12). More importantly, based on these results, it was concluded that resection might only be indicated if the respective thresholds can be achieved. In contrast, Marko et al. proposed a continuous relationship of EOR and survival times, showing that any degree of tumor resection is beneficial, and concluded that a maximum safe resection is generally indicated (4). Marko et al. were the first group to present data based on a parametric model of survival analysis, the accelerated failure time (AFT) model, instead of the commonly used semiparametric proportional hazard models. They suggested that their model had better explanatory capacity for survival prediction than other published models

based on recursive partitioning analysis or resection thresholds (3, 5, 10–12).

In this study, we wanted to i) validate the concept of a continuous relationship of EOR and survival suggested by the parametric AFT model; ii) extend the introduced AFT model by considering molecular prognostic biomarkers [methylation of MGMT and mutations of *isocitrate dehydrogenase* (IDH)] and radiological/surgical predictors for survival prediction; iii) compare the explanatory power of the AFT model with different Cox proportional hazard models; iv) provide a reliable nomogram for predicting survival; and v) evaluate the model for clinical applicability in an independent cohort.

## METHODS

### Study Design

This is a retrospective multicenter cohort study addressing the relationship of EOR and overall survival (OS) in adult patients with newly diagnosed IDH wild-type GBM. The models were developed on the basis of a patient cohort of one of the three involved centers, which served as a training set (n = 303). The other patients were combined as a cohort to externally validate the final statistical models (validation set, n = 253). The clinical endpoint OS was evaluated by univariate and multivariable Cox regression analyses and AFT model. The different models were cross-validated and compared by their coefficients of determination (pseudo $R^2$) and concordance indices (C-indices). Based on the β-coefficients from the AFT model, a score was derived from convincing predictors by means of a nomogram, and a score-related prediction model for OS was developed.

### Data Collection and Study Population

We included all adult patients (age ≥ 18 years) with newly diagnosed GBM treated at one of the study centers from January 2006 to December 2014. The institutional ethics committees of three universities approved the study. The following variables were obtained for each patient: gender, age

at diagnosis, molecular markers (mutations of IDH and methylation of MGMT), KPS, tumor location, preoperative tumor volume, residual tumor volume (RTV), white matter infiltration related to ventricles (contrast-enhanced tumor infiltration of ventricle wall: yes or no), eloquent brain regions (dominant side of Wernicke's and Broca's speech area and inferior parietal lobule "Geschwind's" region; both sides of the primary motor, sensory, and visual cortices), postoperative deficits on the day of discharge (median d6), treatment modality, use of steroids, time of surgery, time of tumor progression according to Response Assessment in Neuro-Oncology (RANO), death, and last visit. MGMT was determined locally in the different centers without central assessment. MRI within 72 h after surgery assessed RTV by comparing T1-weighted images with and without contrast enhancement. We used Brainlab (BrainLAB AG, Feldkirchen, Germany) for volumetric analyses. Patients with an IDH mutation, incomplete data sets (e.g., missing postoperative MRI and missing molecular markers), or participation in therapy arms of clinical trials were excluded.

## Statistical Analyses

Only patients with complete data sets were included in the analyses; patients with incomplete data sets were excluded. First, we performed univariate Cox regressions to identify potential variables that have an impact on OS. Variables were analyzed using the full spectrum of continuous variables but were also categorized (age, KPS, EOR, and RTV) by classification and regression tree (CART) analyses or by common thresholds according to literature: age (≤50 vs. >50 to >70 vs. >70 years); KPS (≥90 vs. <90); EOR (100%, 98%, 95%, and 80%), and RTV (0, ≤1, 1–10, and >10 cm$^3$). We introduced a new variable called "resectability". We stratified patients into "good" or "bad" resectable with respect to tumor locations that were significantly associated with worse survival in univariate Cox regressions. Tumors were defined as bad resectable if the tumor was in a diencephalic location, a thalamic location, the basal ganglia, or brain stem or if the tumor was multicenter; otherwise, it is was defined as good resectable. Multicollinearity between the identified risk factors was excluded.

Variables that showed hazard ratios (HRs) with p-values ≤0.1 were used to perform multistep Cox regressions with bidirectional elimination. The proportional hazard assumption was confirmed by analyzing Schoenfeld residuals and Rho statistics. Models were internally validated by 20-fold cross-validation. The goodness of fit was assessed by estimating the Cox–Snell pseudo R$^2$, which corresponds to the level of variation that is explained by the regression model. Furthermore, the C-index was determined, which is a generalization of the area under the receiver operating characteristic curve that measures the model's discrimination power (see document, **Supplementary File 1**, which explains the whole development of the statistical models, Model design "1.1–1.3," pp. 1–7).

The most promising EOR model was determined by several multivariable Cox regressions considering different absolute and relative RTV thresholds (see document, **Supplementary File 1**, Appendix—Comparison of different EOR models "4.1–4.9," pp. 22–29).

Log-logistic AFT models were performed based on selected factors from Cox models. The assumption of a log-logistic distribution was tested and confirmed. The AFT model was also internally validated by 20-fold cross-validation. Residuals were calculated for the comparison of the predicted and observed OS (see document, **Supplementary File 1**, Model design 1.4, pp. 8–11). The final AFT model with categorical variables was used to create a score from a nomogram based on the β-coefficients, which was again validated by log-logistic regression (see document, **Supplementary File 1**, Scoring for survival "2," pp. 12–14). Finally, AFT models of a) categorical predictors and b) the derived score were validated by an external patient cohort by comparing the mean and median absolute predictive error (APE), the Cox–Snell pseudo R$^2$, and C-index of models and external validations (see document, **Supplementary File 1**, Model validation on external data "3," pp. 15–18). JMP 12.2 (SAS Institute Inc., Cary, NC; https://www.jmp.com/en_us/home. html) and some functions from R (13) and R package rms (14) were used for the statistical analyses.

# RESULTS

## Patients and Overall Survival

Out of 392 IDH wild-type GBM patients who were treated in our hospitals between 2006 and 2014, 303 patients had complete data sets and were available as a training set for multivariable regressions. Eighty-nine patients were excluded because of missing MRI data (n = 48), inclusion in study arms of prospective studies (n = 36), and missing MGMT status (n = 13). At the time of analysis, 254 patients had died (84%), 26 were still alive (8.5%), and 23 were lost to follow-up (7.5%). Patient characteristics are presented in **Supplementary File 2**. The median OS was 15.0 months (95% CI 13–16), and the median time to progression was 8.4 months (95% CI 7.4–9.2). Estimations of OS rates are shown in **Figure 1** as Kaplan–Meier, Cox regression, and log-logistic regression survival curves; and the table in **Supplementary File 3** illustrates the OS Kaplan–Meier estimates. There is a trend in regression curves towards underestimating longer survival compared with Kaplan–Meier, especially in Cox regression.
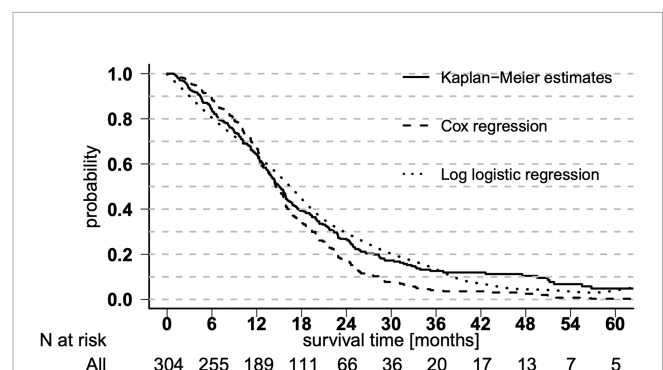


**FIGURE 1** | Overall survival curves. Overall survival shown in Kaplan–Meier estimates and derived from Cox regression and log-logistic regression.

## Relationship Between Residual Tumor Volume and Overall Survival

The parametric AFT model allows the prediction and visualization of the relationship of clinically relevant parameters in addition to point estimates for individual survival times. **Figure 2** illustrates the continuous almost linear relationship between EOR and the median predicted OS. **Table 1** shows the parameters of the logistic regression model. The coefficient of RTV (−0.0127) can be used to calculate the estimated OS as a function of residual tumor size. For example, an RTV of 10 cm$^3$ leads to a shortening in survival time by a factor of 0.88 [exp (−0.0127 × 10)].

## Model Development and Validation

Univariate Cox regressions suggested age, RTV, EOR, methylation of MGMT, KPS, therapy modality, resectability, and white matter infiltration relating to ventricles to be significant predictors of OS. Eloquence, the use of preoperative steroids, and recurrent surgery were, i.a., not significant factors for OS. Multivariable Cox and log-logistic regressions confirmed continuous variables age and RTV and methylation of MGMT, postoperative therapy modality, resectability, and white matter infiltration relating to ventricles as possible predictors of OS. In contrast, KPS was excluded because it had no independent effect on OS. Age and RTV were grouped into three categories. For the complete model development, see document, **Supplementary File 1**, which explains the whole development of the statistical models.

The final AFT model was tested against the null model ($\chi^2$ = 166.09; <0.0001, **Table 2**).

The model demonstrated a pseudo R$^2$ of 0.423, which is the amount of variation of OS that is explained by our regression model, thereby explaining its goodness of fit. The C-index, which is the proportion of all pairs of cases where the case with empirically shorter survival times also has a higher predicted risk (hazard) and thus can be interpreted as a measure of the predictive power of the model, was 0.749, indicating a good model. The internal validation by 20-fold cross-validation shows after correction for optimism a pseudo R$^2$ of 0.428 and a C-index of 0.755, which is very close to the final model demonstrating the stability of the estimates. The median deviation of 0.95 months (mean 0.30 months) is low; i.e., the model applies to the observed data. However, individual deviations can be quite high, and there is a trend towards underestimating longer survival. For external validity assessment, a novel external data set of 253 patients was available, of which 191(76%) had died at the time of analysis and 62 (24%) were still alive or lost to follow-up. Snell's pseudo R$^2$ of this model was 0.271 and C-index 0.686, resulting in a median APE of 2.63 months (mean: 1.81 months).

The parametric AFT model allows the prediction and visualization of the relationship of clinically relevant parameters in addition to point estimates for individual survival times. **Figure 2** illustrates the continuous almost linear relationship between EOR and the median predicted OS.

## The Nomogram Established

A nomogram to estimate individual survival probabilities was built using the final AFT model (**Figure 3**). Median survival and survival rates at 12, 24, and 60 months are obtained from drawing a perpendicular line from the "Total points" axis to the outcome axes. Up to 34 points are possibly given with the best score of 34 and the worst score of 0 points. Alternatively, the score can also be calculated by summing up the score value for each variable (see **Table 3**, showing the scores of each category of predictors for OS) and reading out the survival probabilities in **Figure 4**. For clinical examples, see **Supplementary File 4**.

## DISCUSSION

We evaluated the effects of EOR on survival using non-parametric and parametric survival models, demonstrated the advantages and limitations of the AFT model, and provided an improved nomogram-based prediction model. We also found a continuous relationship between EOR and survival, as suggested by Marko et al. (4). By additionally considering molecular markers (IDH and MGMT), resectability, and the extent of white matter infiltration, we were able to improve the AFT model (pseudo R$^2$ = 0.31 to pseudo R$^2$ = 0.42) and to reduce the APE by about 1.8 months from a median of 4.42 months to a median of 2.63 months compared with the model of Marko et al. (4). We developed a clinically applicable nomogram to predict survival times (C-index = 0.69) with an APE of a median of 2.78 months or a mean of 1.8 months. The developed models show an
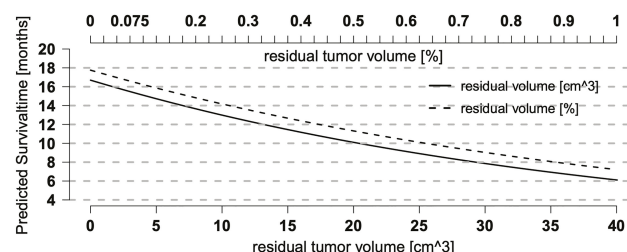


**FIGURE 2** | Relationship between residual tumor volume (RTV) and overall survival (OS). Relationship between predicted OS and RTV or extent of resection (EOR) as single predictors in a log-logistic regression model. Both curves show a continuous, nearly linear relationship and run in parallel with a better prognosis for relative RTV (EOR), suggesting that preoperative tumor size also may have an effect on OS.

**TABLE 1 |** Log-logistic regression model.

| Characteristic | Final AFT model | | |
| --- | --- | --- | --- |
| | Coefficient[§] | SE | p |
| Intercept | 4.1685 | 0.3978 | <0.0001 |
| RTV (cm$^3$) | −0.0127 | 0.0032 | <0.0001 |
| Age (years) | −0.0183 | 0.0050 | 0.0002 |
| MGMT, unmethylated | −0.4316 | 0.0849 | <0.0001 |
| Radiotherapy | 0.1295 | 0.1616 | 0.4229 |
| Radiochemotherapy | 0.3884 | 0.1761 | 0.0274 |
| Resectability, bad | −0.3321 | 0.1095 | 0.0024 |
| Infiltration of vent. Wall | −0.3478 | 0.0823 | <0.0001 |
| Log(scale) | −0.9653 | 0.0528 | <0.0001 |
| Pseudo R$^2$ | 0.404 | | |
| C-index | 0.748 | | |

RTV, residual tumor volume; MGMT, O$^6$-methylguanine-DNA-methyltransferase; AFT, accelerated failure time.

[§] The coefficients in the log-logistic model detect acceleration or deceleration in survival times [acceleration factor (AF)]. The transformation with the exponential function leads to values <1 (delay—disadvantageous) or >1 (acceleration—advantageous). For example, in a patient with a tumor of 80 cm$^3$ with exp(−0.0127 × 80) = 0.36, expected survival is shortened to 36% with biopsy and 94% with subtotal resection, with an RTV of 5 cm$^3$ with exp(−0.0127 × 5) = 0.94, compared with complete resection.

**TABLE 2 |** Final survival model of the prognostic score.

| Characteristic | Final AFT model | | | |
| --- | --- | --- | --- | --- |
| | Coefficient[§] | SE | AF | p |
| Intercept | 3.2403 | 0.2046 | | <0.0001 |
| RTV >10 to ≤20 cm$^3$ | −0.4717 | 0.1905 | 0.624 | 0.0133 |
| RTV >20 cm$^3$ | −0.7840 | 0.1498 | 0.457 | <0.0001 |
| Age >50 to ≤70 | −0.3057 | 0.1169 | 0.734 | 0.0089 |
| Age >70 | −0.4798 | 0.1624 | 0.619 | 0.0031 |
| MGMT, unmethylated | −0.4131 | 0.0834 | 0.662 | <0.0001 |
| Radiotherapy | 0.1512 | 0.1570 | 1.170 | 0.3356 |
| Radiochemotherapy | 0.4905 | 0.1697 | 1.633 | 0.0039 |
| Resectability, bad | −0.2272 | 0.1066 | 0.797 | 0.0330 |
| Infiltration of vent. wall | −0.3274 | 0.0810 | 0.721 | <0.0001 |
| Log(scale) | −0.9845 | 0.0527 | | <0.0001 |
| Pseudo R$^2$ | 0.423 | | | |
| C-index | 0.749 | | | |

RTV, residual tumor volume; MGMT, O$^6$-methylguanine-DNA-methyltransferase; AFT, accelerated failure time.

[§] The coefficients in the log-logistic model detect acceleration or deceleration in survival times [acceleration factor (AF)]. The transformation with the exponential function leads to values <1 (delay—disadvantageous) or >1 (acceleration—advantageous). For example, the factor MGMT with exp(−0.4131) = 0.66 is associated with a survival time for unmethylated versus methylated shortened by a factor of 0.66.

improvement of about 40% compared with the most promising currently established model (4). Finally, we present that despite the further improvement of the model to estimate individual survival times, the model is still not sufficient to reliably predict individual survival times but is suitable to facilitate clinical decision making and to predict the mean/median survival in smaller groups of patients, e.g., for phase 1/2 trials.

## Predictors of Overall Survival in Glioblastoma

To estimate the actual impact of the different predictors of survival, all covariates that affect survival must be identified and integrated into the multivariable regression. Among numerous clinical, radiological, and molecular factors (**Supplementary File 2**), only seven factors demonstrated a significant effect on OS in univariate regressions and were reduced to six factors in our final multivariable models (**Tables 1, 2**). Our data confirm that

younger age at diagnosis, higher EOR or lower RTV, methylated MGMT, and postoperative combined radiochemotherapy or radiotherapy compared with chemotherapy are favorable predictors of survival as previously suggested (4, 7, 15). In contrast to Gittleman et al., KPS and gender had no independent impact on OS in our patient cohort in accordance with the observations of Marko et al. and Gorlia et al. (4, 7, 15). In univariate regression, KPS was also a significant predictor of OS. The multivariate regression showed that KPS was not an independent predictor of survival when the other variables in our model were included. Because it is a multidimensional process, we cannot explain the reason for this precisely but can only speculate. Because most of the other identified variables (age, therapy, extent of resection, MGMT status) are generally also taken into account in other studies, we might speculate that the variable "resectability" newly introduced in our model is responsible. If the differences observed in KPS are explained to a
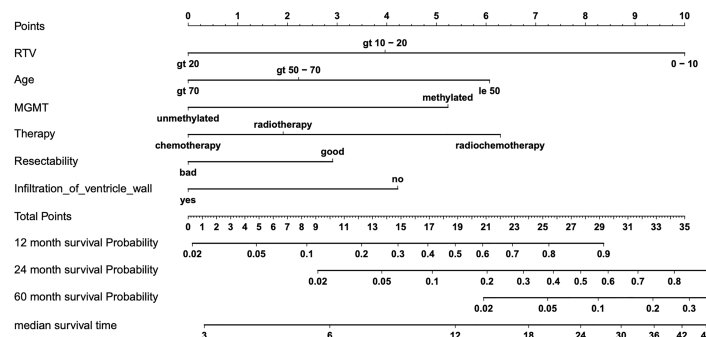
**FIGURE 3** | Nomogram for predicting overall survival (OS). Final nomogram predicting individual median survival times and 12, 24, and 60 months of survival probability based on six predictors of OS, which add up in a summary score from 0 (worst) to 34 (best) total points; for examples, see table, **Supplementary File 4**, with four clinical cases of nomogram-predicted survival versus actual survival.

**TABLE 3** | Scoring for survival.

| Risk factors for overall survival | | | |
| --- | --- | --- | --- |
| **Residual tumor volume (cm$^3$)** | ≤10 | >10 to ≤ 20 cm$^3$ | >20 |
| | **10** | **4** | **0** |
| **Age (years)** | ≤50 | >50 to ≤ 70 | >70 |
| | **6** | **2** | **0** |
| **MGMT** | Methylated | | Unmethylated |
| | **5** | | **0** |
| **Therapy modality** | Radiochemotherapy | Radiotherapy | Chemotherapy |
| | **6** | **2** | **0** |
| **Resectability** | Good | | Bad |
| | **3** | | **0** |
| **Infiltration of ventricular wall** | No | | Yes |
| | **4** | | **0** |

*The "worst" score (with the worst forecast) is thus 0; the best value is 34. The AFT model ($\chi^2$ = 166.95; p < 0.0001, see document, **Supplementary File 1**, Scoring for survival "2," p. 15) of the score demonstrated a pseudo $R^2$ of 0.423 and a C-index of 0.748 and was validated on the independent data set with a pseudo $R^2$ of 0.239 and a C-index of 0.678 resulting in a median APE of 2.78 months (mean: 1.83 months).*
*MGMT, $O^6$-methylguanine-DNA-methyltransferase.*
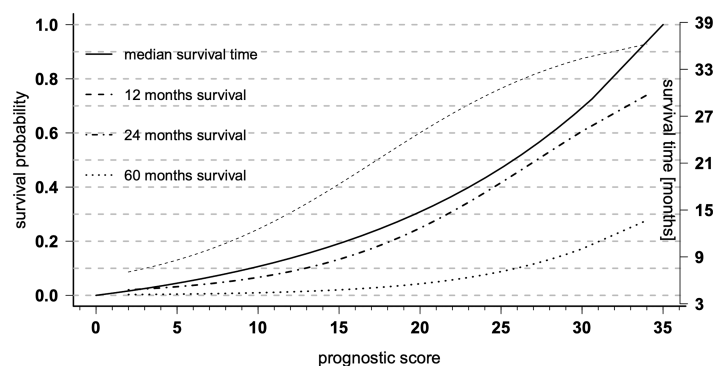


**FIGURE 4** | Prognostic diagrams for overall survival (OS). Prognostic diagrams for the median OS (full line, right y-axis) and 12, 24, and 60 months (dashed lines, left y-axis) survival probability based on the total prognostic scores of the nomogram.

large extent by "resectability", i.e., tumor location, the independent effect of KPS on OS might no longer be large enough to exert a statically significant independent influence on OS. In addition, tumor infiltration beyond the white matter into the ventricular wall had an unfavorable independent effect on OS. This was also observed by Wangaryattawanich et al., who also found deep white matter invasion and ependymal extension as significant predictors of OS (16). In addition, we have introduced a new factor called "resectability" of contrast-enhancing tumor. Tumors stratified as poorly resectable have been shown to be an independent unfavorable predictor of OS in our cohort. Tumor expansion in classic eloquent regions was not a significant predictor of OS, as observed by others (3, 17) because safe tumor removal can now be ensured in these regions through the introduction of electrophysiology and awake surgery.

## Tumor Volume and Survival

We confirmed the continuous inverse relationship between RTV and OS (4), which means that any degree of resection has a benefit of survival. This is in contrast to most studies published in the last two decades that identified different thresholds for a beneficial role of EOR directing different clinical recommendations (3, 5, 10–12). The observed differences in these studies are likely due to the different underlying statistical models. Non-parametric models (e.g., Cox regression) that are commonly used forfeit information by defining dichotomous or categorical thresholds and calculating the median survival by considering the population medians of covariates with semi-quantitative hazards. Interestingly, Lacroix et al. and Grabowski et al. already showed continuous relationships between median OS and increasing thresholds (85%–100%) of EOR (10) or decreasing thresholds of RTVs (25–1 cm$^3$) (17). Instead, Marko et al. used parametric log-logistic regression modeling, which uses the full information of metric data, enabling individual point estimations of survival and providing visualization of the probabilistic relationship of RTV and survival, a concept that was also applied in this study.

The concept of a continuous relationship between RTV and survival rather than postulated thresholds is also supported by the observation that postoperative RTV, determined as gadolinium enhancement within 24–72 h after surgery in all studies, reflects not the true tumor volume. Increasing evidence suggests that tumor volume in GBM is not restricted to gadolinium enhancement (18–20). Suchorska et al. showed that the biological tumor volume (BTV) determined by O-(2-[$^{18}$F]fluoroethyl)-L-tyrosine PET ($^{18}$FET-PET) can be much larger than the volume of gadolinium enhancement and is associated with survival times. They showed that despite complete resection of contrast enhancement, up to 9.5-cm$^3$ BTV could still be detected (19). This has also been supported by studies using 5-aminolevulinic acid (5-ALA) for glioma surgery demonstrating tumor infiltration beyond the gadolinium enhancement in MRI (18). Roessler et al. postulated that 5-ALA is more sensitive for RTV than $^{18}$FET-PET, meaning that GBM extends even beyond BTV in $^{18}$FET-PET (20). These data suggest that the postulated thresholds based on resection of partial tumor volume are unlikely

clinically relevant. Surgeries in patients who were classified as complete resection (5), gross total resection (GTR) of >98% (10), GTR of >78% (3), GTR of >70% (12, 18), etc., have likely more RTV than expected, but patients did, however, benefit from tumor resections. Clinically, these considerations speak against refusing surgery due to the impossibility of obtaining a specific EOR and support the concept of maximum safe resection. This means that surgery is also indicated even in cases of expansive diseases, where only partial tumor resection is safely achievable.

We improved the predictive accuracy of our final regression model and our simplified score model by about 40% compared with the currently established model (4). Although the mean/median APE is small (2.78/1.8 months), individual predictions are still not recommended, as individual deviations can be very high (see document, **Supplementary File 1**, which explains the whole development of the statistical models, Model design, 1.4, p. 11). In contrast, the low APE in our model could be helpful in estimating the effect of therapies in unrandomized studies by considering the combined effect of covariates for each patient and thus compensating for the uneven distribution of risk factors in the different trial groups. This is of particular importance since unrandomized and unstratified retrospective or small prospective phase 1/2 studies do not serve to demonstrate the efficacy of new therapies; patients' covariate risk factors are often unbalanced, distorting the interpretation of survival times.

## Limitations and Strengths of the Study

The main limitation of this study is the retrospective nature; e.g., clinical data as KPS or neurological deficits were collected through medical records and not according to a defined protocol, and MGMT was determined locally without central assessment. The recently identified biomarker CDKN2A, which has been shown to be associated with OS in GBM (21), was not available for analysis. Patients were neither randomized nor stratified by the other predictors of OS to assess the effects of EOR or RTV on OS. However, a prospective study dealing with this question, i.e., randomizing the EOR, would not be ethically acceptable. We consider the unequal distributions of the other covariates through multivariable analysis. After the development of our model, we have internally demonstrated the stability of our model (C-index 0.75) by cross-validation and validated the predictive power and adaptability by an external independent patient cohort. For model and nomogram development, our patient cohorts covered the entire spectrum of clinical GBM cases without limitations of general performance status (i.e., KPS), age, RTV, or postoperative therapy compared with the developed nomograms from specific patient cohorts of prospective clinical trials (7, 15). Another limitation might be the heterogeneity of the patients and data as assessed by the different study centers. At the same time, however, this represents a strength of the study, as it shows the generalizability of the model. However, all patients included in the model come from three German specialized academic centers, which may limit the transfer of the model to other patient cohorts, e.g., from non-academic centers or from other countries.

## CONCLUSIONS

We found a continuous relationship between RTV and OS that supports the concept of maximum safe resection. By considering molecular and radiological markers, we improved the predictive accuracy of previous models by about 40% compared with the most promising established model and developed a clinical applicable score. The developed nomogram helps to estimate the expected survival and the benefit of a more radical surgery. This can be of help to the treating physicians in advising the patients and relatives in the decision for surgery. Nevertheless, individual predictions should only be made with caution on the basis of this model due to the possible high individual deviations. Yet our statistical model could be a very useful tool to estimate the survival effect of retrospective or small prospective phase I/II studies since the median/mean APE is low.

## DATA AVAILABILITY STATEMENT

The raw data supporting the conclusions of this article will be made available by the authors, without undue reservation.

## ETHICS STATEMENT

The studies involving human participants were reviewed and approved by Ethik-Kommission an der Medizinischen Fakultät der Eberhard-Karls-Universität und am Universitätsklinikum Tübingen. Written informed consent for participation was not required for this study in accordance with the national legislation and the institutional requirements.

## AUTHOR CONTRIBUTIONS

Conception and experimental design: MS and MT. Data acquisition: MK, FB, IG-T, JS, BB, FP, MR, JG, and MB. Analysis: MS and JH. Interpretation of the data: MS, MK, JG, MR, JH, MT, and BM. Drafting: MS, GT, and JH. Revision: MK, FB, IG-T, JS, BB, FP, JH, MR, JG, MB, BM, GT, and MT. All authors contributed to the article and approved the submitted version.

## FUNDING

## SUPPLEMENTARY MATERIAL

The Supplementary Material for this article can be found online at: https://www.frontiersin.org/articles/10.3389/fonc.2021.748691/full#supplementary-material

## REFERENCES

1. Ostrom QT, Patil N, Cioffi G, Waite K, Kruchko C, Barnholtz-Sloan JS. CBTRUS Statistical Report: Primary Brain and Other Central Nervous System Tumors Diagnosed in the United States in 2013-2017. *Neuro-Oncology* (2020) 22:iv1–96. doi: 10.1093/neuonc/noaa200

2. Stupp R, Mason WP, van den Bent MJ, Weller M, Fisher B, Taphoorn MJB, et al. Radiotherapy Plus Concomitant and Adjuvant Temozolomide for Glioblastoma. *N Engl J Med* (2005) 352:987–96. doi: 10.1056/nejmoa043330

3. Sanai N, Polley M-Y, McDermott MW, Parsa AT, Berger MS. An Extent of Resection Threshold for Newly Diagnosed Glioblastomas. *J Neurosurg* (2011) 115:3–8. doi: 10.3171/2011.2.jns10998

4. Marko NF, Weil RJ, Schroeder JL, Lang FF, Suki D, Sawaya RE. Extent of Resection of Glioblastoma Revisited: Personalized Survival Modeling Facilitates More Accurate Survival Prediction and Supports a Maximum-Safe-Resection Approach to Surgery. *J Clin Oncol: Off J Am Soc Clin Oncol* (2014) 32:774–82. doi: 10.1200/jco.2013.51.8886

5. Kreth FW, Thon N, Simon M, Westphal M, Schackert G, Nikkhah G, et al. Gross Total But Not Incomplete Resection of Glioblastoma Prolongs Survival in the Era of Radiochemotherapy. *Ann Oncol* (2013) 24:3117–23. doi: 10.1093/annonc/mdt388

6. Hegi ME, Diserens A-C, Gorlia T, Hamou M-F, de Tribolet N, Weller M, et al. MGMT Gene Silencing and Benefit From Temozolomide in Glioblastoma. *N Engl J Med* (2005) 352:997–1003. doi: 10.1056/NEJMoa043331

7. Gorlia T, van den Bent MJ, Hegi ME, Mirimanoff RO, Weller M, Cairncross JG, et al. Nomograms for Predicting Survival of Patients With Newly Diagnosed Glioblastoma: Prognostic Factor Analysis of EORTC and NCIC Trial 26981-22981/CE.3. *Lancet Oncol* (2008) 9:29–38. doi: 10.1016/S1470-2045(07)70384-4

8. Senft C, Bink A, Franz K, Vatter H, Gasser T, Seifert V. Intraoperative MRI Guidance and Extent of Resection in Glioma Surgery: A Randomised, Controlled Trial. *Lancet Oncol* (2011) 12:997–1003. doi: 10.1016/s1470-2045(11)70196-6

9. Stummer W, Pichlmeier U, Meinel T, Wiestler OD, Zanella F, Reulen H-J, et al. Fluorescence-Guided Surgery With 5-Aminolevulinic Acid for Resection of Malignant Glioma: A Randomised Controlled Multicentre Phase III Trial. *Lancet Oncol* (2006) 7:392–401. doi: 10.1016/s1470-2045(06)70665-9

10. Lacroix M, Abi-Said D, Fourney DR, Gokaslan ZL, Shi W, DeMonte F, et al. A Multivariate Analysis of 416 Patients With Glioblastoma Multiforme: Prognosis, Extent of Resection, and Survival. *J Neurosurg* (2001) 95:190–8. doi: 10.3171/jns.2001.95.2.0190

11. Li YM, Suki D, Hess K, Sawaya R. The Influence of Maximum Safe Resection of Glioblastoma on Survival in 1229 Patients: Can We do Better Than Gross-Total Resection? *J Neurosurg* (2016) 124:977–88. doi: 10.3171/2015.5.jns142087

12. Chaichana KL, Jusue-Torres I, Navarro-Ramirez R, Raza SM, Pascual-Gallego M, Ibrahim A, et al. Establishing Percent Resection and Residual Volume Thresholds Affecting Survival and Recurrence for Patients With Newly Diagnosed Intracranial Glioblastoma. *Neuro-Oncology* (2013) 16:113–22. doi: 10.1093/neuonc/not137

13. team RC. *R: A Language and Environment for Statistical Computing*. Available at: https://www.R-project.org/.

14. Harrell FEJr. *Rms: Regression Modeling Strategies*. . *R Package Version 5.1-1*. Available at: https://CRAN.R-project.org/package=rms.

15. Gittleman H, Lim D, Kattan MW, Chakravarti A, Gilbert MR, Lassman AB, et al. An Independently Validated Nomogram for Individualized Estimation of Survival Among Patients With Newly Diagnosed Glioblastoma: NRG Oncology RTOG 0525 and 0825. *Neuro-Oncology* (2016) 19(5):669–77. doi: 10.1093/neuonc/now208

16. Wangaryattawanich P, Hatami M, Wang J, Thomas G, Flanders A, Kirby J, et al. Multicenter Imaging Outcomes Study of The Cancer Genome Atlas Glioblastoma

Patient Cohort: Imaging Predictors of Overall and Progression-Free Survival. *Neuro-Oncology* (2015) 17:1525–37. doi: 10.1093/neuonc/nov117

17. Grabowski MM, Recinos PF, Nowacki AS, Schroeder JL, Angelov L, Barnett GH, et al. Residual Tumor Volume Versus Extent of Resection: Predictors of Survival After Surgery for Glioblastoma. *J Neurosurg* (2014) 121:1115–23. doi: 10.3171/2014.7.jns132449

18. Molina ES, Schipmann S, Stummer W. Maximizing Safe Resections: The Roles of 5-Aminolevulinic Acid and Intraoperative MR Imaging in Glioma Surgery —Review of the Literature. *Neurosurg Rev* (2019) 42(2):197–208. doi: 10.1007/s10143-017-0907-z

19. Suchorska B, Jansen NL, Linn J, Kretzschmar H, Janssen H, Eigenbrod S, et al. Biological Tumor Volume in 18FET-PET Before Radiochemotherapy Correlates With Survival in GBM. *Neurology* (2015) 84:710–9. doi: 10.1212/WNL.0000000000001262

20. Roessler K, Becherer A, Donat M, Cejna M, Zachenhofer I. Intraoperative Tissue Fluorescence Using 5-Aminolevolinic Acid (5-ALA) Is More Sensitive Than Contrast MRI or Amino Acid Positron Emission Tomography ((18)F-FET PET) in Glioblastoma Surgery. *Neurological Res* (2012) 34:314–7. doi: 10.1179/1743132811Y.0000000078

21. Lu VM, O'Connor KP, Shah AH, Eichberg DG, Luther EM, Komotar RJ, et al. The Prognostic Significance of CDKN2A Homozygous Deletion in IDH-Mutant Lower-Grade Glioma and Glioblastoma: A Systematic Review of the Contemporary Literature. *J Neuro Oncol* (2020) 148:221–9. doi: 10.1007/s11060-020-03528-2

# Case Report: Differential Genomics and Evolution of a Meningeal Melanoma Treated With Ipilimumab and Nivolumab

Remberto Burgos[1], Andrés F. Cardona[2,3,4*], Nicolas Santoyo[2], Alejandro Ruiz-Patiño[2,3], Juanita Cure-Casilimas[2], Leonardo Rojas[3,5,6], Luisa Ricaurte[3,4], Álvaro Muñoz[7], Juan Esteban Garcia-Robledo[8], Camila Ordoñez[2,3], Carolina Sotelo[2,3], July Rodríguez[2,3], Zyanya Lucia Zatarain-Barrón[9], Diego Pineda[9] and Oscar Arrieta[10]

[1] Neurosurgery Department, Clínica del Country/Clínica Colsanitas, Bogotá, Colombia, [2] Foundation for Clinical and Applied Cancer Research (FICMAC), Bogotá, Colombia, [3] Molecular Oncology and Biology Systems Research Group (Fox-G), Universidad El Bosque, Bogotá, Colombia, [4] Direction of Research and Education, Luis Carlos Sarmiento Angulo Cancer Treatment and Research Center (CTIC), Bogotá, Colombia, [5] Clinical and Translational Oncology Group, Clínica del Country, Bogotá, Colombia, [6] Clinical Oncology Department, Clínica Colsanitas, Bogotá, Colombia, [7] Radiotherapy Department, Carlos Ardila Lulle Institute of Cancer (ICCAL), Fundación Santa Fe de Bogotá, Bogotá, Colombia, [8] Division of Hematology/Oncology, Mayo Clinic, Phoenix, AZ, United States, [9] Thoracic Oncology Unit and Personalized Oncology Laboratory, National Cancer Institute (INCan), México City, Mexico, [10] Radiology Department, Clinica del County/Resonancia Magnética de Colombia, Bogotá, Colombia

Primary melanocytic tumors of the CNS are extremely rare conditions, encompassing different disease processes including meningeal melanoma and meningeal melanocytosis. Its incidence range between 3-5%, with approximately 0.005 cases per 100,000 people. Tumor biological behavior is commonly aggressive, with poor prognosis and very low survivability, and a high recurrence rate, even after disease remission with multimodal treatments. Specific genetic alterations involving gene transcription, alternative splicing, RNA translation, and cell proliferation are usually seen, affecting genes like BRAF, TERT, GNAQ, SF3B1, and EIF1AX. Here we present an interesting case of a 59-year-old male presenting with neurologic symptoms and a further confirmed diagnosis of primary meningeal melanoma. Multiple therapy lines were used, including radiosurgery, immunotherapy, and chemotherapy. The patient developed two relapses and an evolving genetic makeup that confirmed the disease's clonal origin. We also provide a review of the literature on the genetic basis of primary melanocytic tumors of the CNS.

Keywords: melanoma, radiosurgery, immunotherapy, genomics, GNAQ, TERT, meningeal melanocytic tumor

## INTRODUCTION

Melanocytic tumors that originate in the meninges are rare. These tumors might present as focal (melanomas) or diffuse conditions (melanocytosis). Staging might vary from low grade to high grade malignant stages. These tumors are frequently diagnosed in patients >40 years old and in females. The most common places where it develops include the cervical and thoracic spine and the

posterior fossa (1–4). When its location is the leptomeninges, clinical symptoms and signs are non-specific (5), the gold standard for diagnosis is the evidence of tumor cells present in cerebrospinal fluid, with a sensitivity of CSF cytology of 50% in the first puncture and 98% in repeated punctures (5, 6). Magnetic resonance imaging (MRI) has a sensitivity and specificity of 77%, and a typical leptomeningeal contrast enhancement might be the most frequent finding (5).

Primary meningeal melanocytic neoplasms (PMMs) share genetic and molecular characteristics with uveal melanomas (UMs) (1, 3), which have been found to recur frequently and to have an aggressive behavior with leptomeningeal spread (2). PMMs share mutations with UM. Some of the genes affected include GNAQ/GNA22 or GNA11 (7, 8) (paralogue genes), and to a lesser degree, SF3B1 and EIF1AX (2, 3), while BRAF mutations and TERT promoter mutations are rare (9).

Common mutations have been reported in primary meningeal melanomas with NRAS, SFEB1, and EIF1AX and coexisting with GNAQ or GNA11 (3). Also, the loss of chromosome 3 and BAP1 mutations have been detected in some melanocytic meningeal tumors (2, 3). Therefore, these molecular differences have implications in targeted therapy (3). Meningeal melanomas have specific methylation that allows them to be discriminated from other tumors of the central nervous system. However, there is still no information to establish an adequate primary meningeal tumor profile (2). Understanding the genomic alterations of meningeal melanomas can help improve the diagnosis and treatment.

Among therapies for PMMs, focal radiotherapy, intrathecal and systemic chemotherapy have been proposed, with just a partial benefit. A study assessing radiotherapy's effectiveness combined with checkpoint inhibition using ipilimumab for leptomeningeal melanoma metastases (LMM) showed that complete responses could be achieved (5). LMM and PMMs usually have a poor prognosis with a median overall survival of 2-4 months. Nevertheless, the use of multimodal interventions (surgery, radiotherapy/radiosurgery, targeted therapy, and immunotherapy) has shown a global benefit in managing this type of tumor (10). Here, we present the case of a patient with a PMM considering its clonal evolution throughout various surgical interventions, radiosurgery, the use of adjuvant ipilimumab, the combination of ipilimumab/nivolumab and temozolomide. We also discuss the current evidence on the genomics of PMMs and their treatment and contrast it with the findings taken from our patient. These data provide an insight into new and alternative ways to treat PMMs.

## CASE PRESENTATION

In 2016, a 59-year-old male presented with acute severe headaches, nausea, vomiting, gait instability, and functional limitation. An MRI brain scan showed a bulky solid mass in an extra-axial location, firmly adhered to the right transverse sinus. The solid portion (measuring 38x22x19 mm) coexisted with an intraparenchymal hematoma. The mass effect of the

complex partially collapsed the fourth ventricle causing ascending transtentorial herniation. Additionally, cerebellar tonsil herniation through the foramen magnum was noted (**Figure 1**). The tumor was completely resected, and histology was consistent with a meningeal melanocytic tumor of high-grade malignancy. Histologically, the tumor was moderately pigmented with a lobular architecture associated with prominent vascularization and interconnecting vascular lakes showing melanoma features. A high nuclear-cytoplasmic ratio and prominent nucleoli were observed as well as multinucleation. There were five mitoses per 10 HPF. Areas of hemorrhage and apoptosis were identified, but there was no necrosis. The tumor cells expressed S100, HMB45, and Melan A (**Figure 2**). Ki-67 proliferative index was 15%, and nuclear BAP1 immunohistochemistry expression was utterly negative in melanocytes, with positive staining of endothelial cells (images not available). The clinical, mucosal, and ophthalmological examination did not reveal other melanoma localizations.

**Figure 3** shows the comparative genomic hybridization array (aCGH) analysis of the four samples obtained from surgical resections, including monosomy of chromosome 3 and X, a total gain of chromosome 20, a high-level gain of chromosome 8q, and segmental losses on chromosomes 1p and 6q. The primary melanocytic tumor harbored a somatic mutation in GNAQ (c.626A>T), alteration present in 0.07% of AACR GENIE cases (https://portal.gdc.cancer.gov/), of uveal melanoma, ocular melanoma, cutaneous melanoma, and central nervous system melanoma. Besides, a commutation was found in the eukaryotic translation initiation factor 1A (EIF1A), a gene that encodes a protein that acts as an essential eukaryotic translation initiation factor. The G15D mutation (c.44G> A) is found in up to more than 30% of UMs and in primary melanomas of the meninges, where it usually co-occurs with other mutations in SF3B1, as in the present case (R625H mutation, c.1874G> A) (**Supplementary Data** includes a detailed description of the methods performed for the NGS assessment on the Ion Torrent$^{TM}$ Oncomine$^{TM}$ Comprehensive Assay Plus). As previously reported, the primary tumor's genomic analysis did not reveal mutations in BAP1, BRAF, NRAS, HRAS, KIT, and TERT. Neither microsatellite instability was evidenced, and Tumor Mutation Burden (TMB) was estimated at 3 Mut/Mb.

Postoperatively, patient underwent radiosurgery (gamma knife 16 Gy) on the cerebellar cavity, without complications, followed by four cycles of intravenous ipilimumab 10 mg/kg administered every three weeks for four doses, and then every 12 weeks until one year of treatment. After four cycles of ipilimumab, he developed moderate ipilimumab-induced hepatitis successfully treated with high dose PO corticosteroids (prednisone 1 mg/kg/day for ten days) subsequent tapering.

After 23 months, the patient presented with recurrent symptoms. Follow-up imaging showed vasogenic edema involving the right cerebellar hemisphere and the vermis, with a small marginal nodule visible on MRI and PET/CT (SUVmax 3.2) (**Figure 4**). In March 2018, he was taken to an optimal secondary surgery that confirmed recurrent melanoma with an expression of Melan A, HMB45, S100, SOX10, and MITF. Ki-67
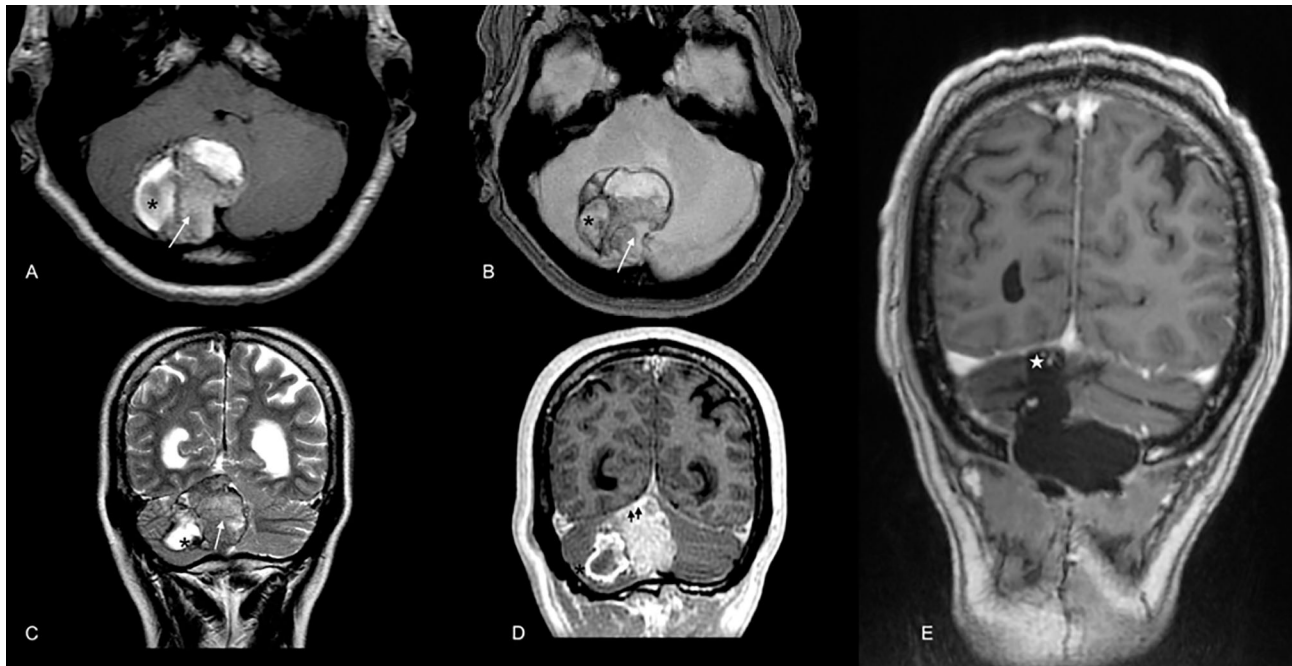
FIGURE 1 | Brain MRI scan at diagnosis in 2016. Extra-axial bulky solid mass with a hypercellular solid component in the right paravermian location depicted by the arrow in **(A)** (axial T1WI), **(B)** (GRE), and C (T2WI). Note the hypointense components in T2WI **(C)** and blooming effect in GRE **(B)** highly suspicious for melanic or pigmented components. Also, note the coexistent intraparenchymal hematoma [* in **(A–D)**]. Mass was firmly attached to dural surface compressing right transverse dural sinus (doble arrowhead in D, postcontrast T1WI). In the post-operative scan [**(E)**, T1 WI postcontrast], no macroscopic evidence of residual disease in the surgical cavity was noted [white star in **(E)**].
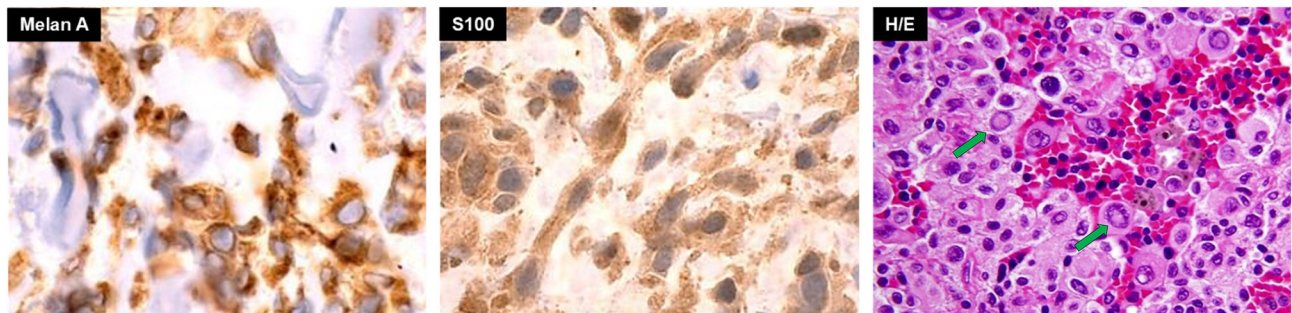


FIGURE 2 | Basal pathology of meningeal hyperpigmented lesion from the posterior fossa compatible with a primary melanoma of the meninges. Green arrows in H/E image show large nucleoli in cells with a high nucleus-cytoplasm ratio.

was quantified at 30%. The second sample's genetic analysis revealed five new alterations in the TERT promoter (C228T), SDE, PDRX2, CHIT1, and TNIP genes. As a complication, he had a CSF cyst plus bacterial meningitis that delayed the execution of new radiosurgery with gamma knife (16 Gy). Then, he was started on nivolumab, achieving a progression-free survival (PFS) of 7.2 months. He developed meningeal progression with new nodules and meningeal thickening attached to the torcula causing partial compression of the right transverse sinus (**Figures 5A, B**). A cfDNA analysis was carried

out by NGS in the cerebrospinal fluid, finding only the TERT promoter's mutation. In parallel, he started with ipilimumab (1 mg/kg) plus Nivolumab (3 mg/kg) every three weeks following data from the CheckMate 511 phase IIIb/IV trial. Initially, no limiting toxicity was found; however, he had a recurrence of grade 3 hepatitis just after the fourth cycle when steroids were administered again. Subsequently, he received 15 cycles of Nivolumab 480 mg every 28 days until February 2020. An irregular nodular enhancement focus was then found in the right paravermian cerebellar postsurgical cavity, related to local
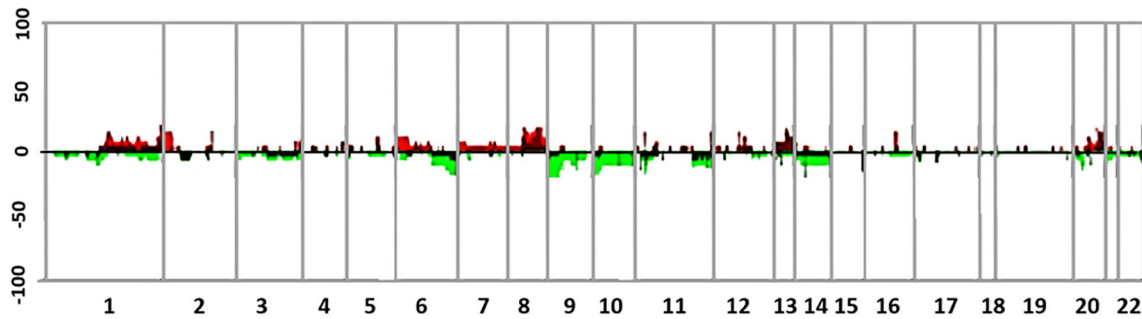
**FIGURE 3** | Summary of genomic profiles of four different samples from the case. Samples correspond to the meningeal melanoma at diagnosis and its three further recurrences with their chromosomal alterations. The recurrence of CNAs across the samples in segmented data (y-axis) is plotted for each probe (4) evenly aligned along the x-axis in chromosomal order. The percentage of samples harboring gains, amplifications, losses, and deletions for each locus is depicted according to the following scheme: dark red (gains with a $log_2$ ratio >=0.15) and green (loss with a $log_2$ ratio <=−0.15) and are plotted along with bright red (amplifications with a $log_2$ ratio ≥ 0.4) and bright green (deletions with $log_2$ ratio ≤−0.4).
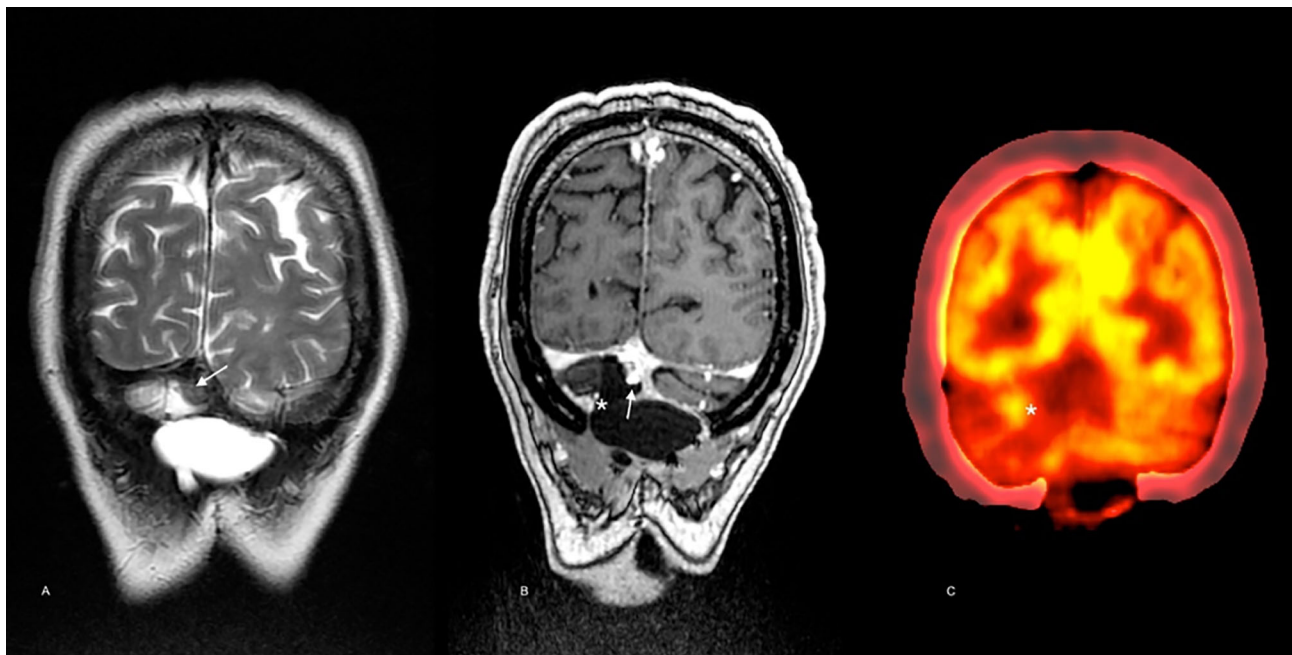


**FIGURE 4** | Imaging follow-up 23 months after diagnosis. Brain MRI scan showed a solid nodule below the torcular Herophili at the midline [arrow in **(A)**, T2WI, and **(B)**, postcontrast T1WI]. Note the low signal in the nodule in A (T2WI) and the avid contrast enhancement in B (postcontrast T1WI) in a similar pattern as in the pre-operative scan. In the medial margin of the surgical cavity [* in **(C)**] contrast enhancement may be noted matching the hypermetabolic focus seen on PET-CT [* in **(D)**] consistent with local recurrence.

tumor relapse with perilesional vasogenic edema (**Figure 5C**). He was taken to a third neurosurgical intervention without complications but with greater neurological involvement concerning slight ataxia and dysmetria.

After finding persistence of the GNAQ and TERT alterations in tumor tissue, he began treatment with temozolomide on the 5/28 schedule, maintaining the response to date. At that time, he completed 58 months of survival. **Figure 6** describes the timeline from diagnosis to the present, including the different genomic

findings. Decision of initial and subsequent therapies were made based on progression development. No targeted therapies were used.

## DISCUSSION

In this case, a patient with non-specific neurological symptoms is presented. Due to their persistence, an MRI is performed where a

**FIGURE 5** | Brain MRI scan after secondary resection. A similar low signal nodule in the surgical cavity is depicted [arrow in **(A)**, T2WI]. According to new onset of cephalalgia, the torcula's extrinsic compression was demonstrated [double arrowhead in **(B)**, venous-phase angio-MRI]. In **(C)** (postcontrast T1WI), meningeal and surgical cavity enhancement is also noted (star).
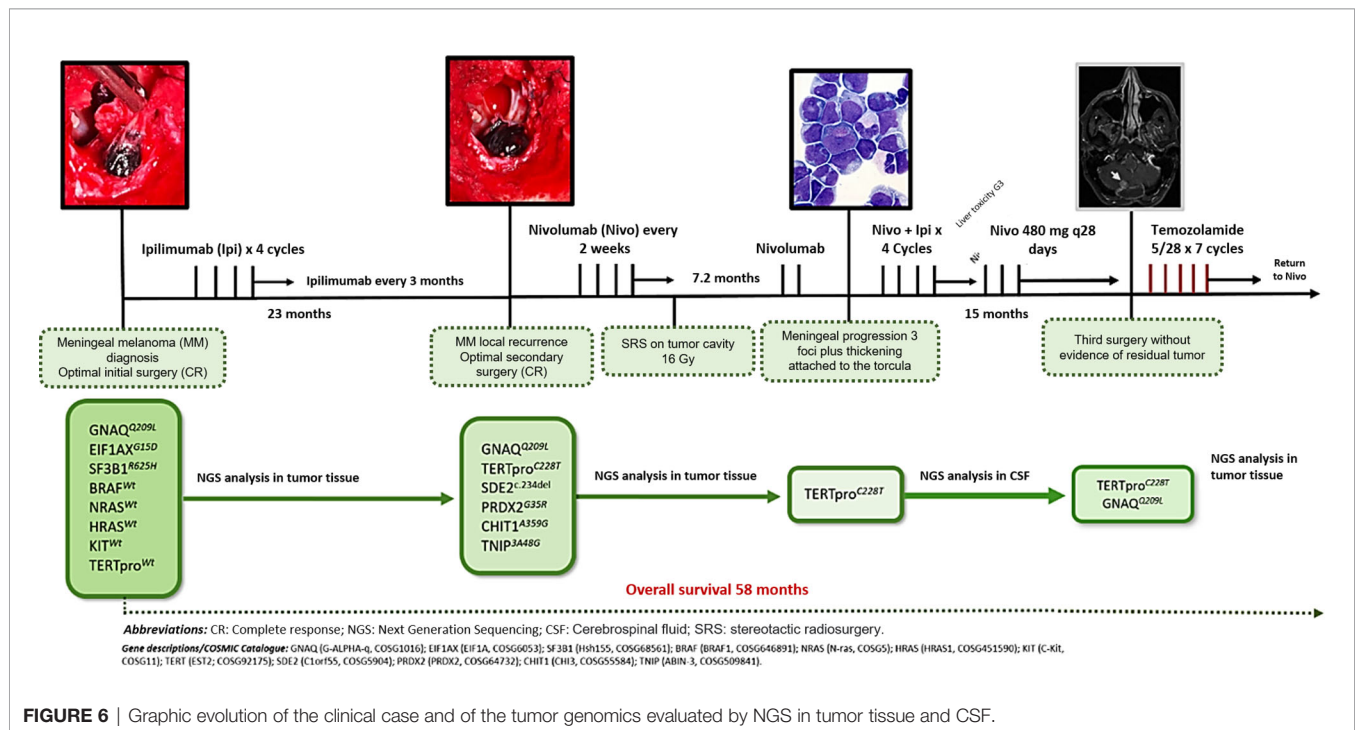


**FIGURE 6** | Graphic evolution of the clinical case and of the tumor genomics evaluated by NGS in tumor tissue and CSF.

heterogeneous lesion of extra-axial location and adhere to the transverse sinus with cerebellar involvement is evident; surgical intervention was done early, showing a malignant melanoma macroscopically. Immunohistochemical findings showed the expression of Melan-A, HMB, S100, and MITF and negativity for AE1/AE3. At diagnosis, the presence of BRAF, NRAS, HRAS and KIT mutations was ruled out, and during disease evolution, several alterations were found in GNAQ, EIF1AX, SF3B1, SDE2,

PRDX2, CHIT1, TNIP, and TERT. Treatment included radiosurgery and checkpoint inhibition with ipilimumab and nivolumab with an adequate response.

The development of extracutaneous primary melanomas results from malignant transformation of neural crest cells that might have scattered throughout mucous membranes, eyes, and the leptomeninges during cell migration in embryogenesis (4, 11). PMM is a rare type of tumor. Its presentation is associated with focal/spread meningeal lesions or metastases. Evidence regarding the biology and clinical features of this condition is scarce; however, specific analyses have shown that these types of tumors present with a particular genetic makeup that allows for an adequate and comprehensive therapeutic approach. The first case of PMM was described by Virchow in 1859, with very few cases reported later. PMMs are usually seen in adults, with a higher prevalence among those over the fourth decade of life. Pediatric patients are extremely rare, accounting for approximately 0.1% of all pediatric central nervous system tumors (4).

These tumors have an uncertain biological behavior; most of them are aggressive, although they depend on their genetic background (12). These tumors' behavior is not well defined either; however, prognostic markers such as BAP1 mutations and chromosome loss have been proposed (2, 9). Copy number variations such as 6p gain, 6q loss, chromosome 8 gain, 1p loss, and 1q gain have been reported in some meningeal melanocytic tumors. This becomes important given that they have predictive value, as the gain of chromosome 8 and loss of 1p is associated with a worse prognosis (9).

A cerebrospinal fluid sample, in some cases, may be the first and only sample necessary to make the diagnosis of meningeal melanoma, as different diagnostic biomarkers like Melan A, HMB-45, and MITF can be found in this fluid (13). Mutations in GNAQ and GNA11 are commonly found in adults with PMM, while children usually present with NRAS$^{Q61K}$ (4).

This NRAS mutation is most probably developed during embryogenesis, throughout the post-zygotic stage of neural crest cells, before migration to the skin and leptomeninges, which could condition NRAS mosaicism (4). In a case series, Küsters-Vandevelde et al. showed NRAS mutations in a patient with a melanocytic CNS tumor and congenital melanocytic nevus, with an SF3B1 mutation only in the CNS tumor but not in the melanocytic nevus. On the other hand, some cases of melanocytomas with meningeal seeding plus SF3B1 mutations and associated GNAQ were reported (3). A point mutation in EIF1AX was also reported in five primary meningeal melanomas (3). Consistently, EIF1AX mutations were mutually exclusive with SF3B1 mutations but coexisted with GNAQ or GNA11 alterations suggesting that they occur in the late phase of tumorigenesis (3, 14). SF3B1 gene mutations in PMMs occur mainly at codons 625 or 634. They are regularly associated with a disomy for chromosome 3, accompanied by GNAQ or GNA11 mutations and overexpression, and to a lesser extent with NRAS mutations (3). The GNAQ, GNA11, and NRAS mutations are believed to play a critical role in the initiation of PMMs tumorigenesis, while the SF3B1 conversion seems to be a later event (3). Curiously, in our case, the baseline coexistence of the

GNAQ$^{Q209L}$, EIF1AX$^{G15D}$, and SF3B1$^{R625H}$ mutations was found, a profile that had not been previously described in PMMs, or their uveal counterparts. **Figure 7** integrates GNAQ-related signaling pathways in PMMs. Griewank et al. analyzed a large set of CNS melanocytic tumors using techniques like mutation analysis, copy number alterations and DNA methylation profiling. They included PMMs, UMs, CNS cutaneous melanoma metastases and blue nevus-like melanomas. They found that EIF1AX, SF3B1, and BAP1 mutations in UM are associated with favorable, intermediate, and poor prognosis, respectively. They also showed that EIF1AX, SF3B1, and BAP1 mutations in PMMs don't seem to match accordingly with an expected histologic pattern, this might explain why in our patient, there were no BAP1 mutations but a negative expression in IHC. The researchers also demonstrated that PMMs harboring chromosome 3 loss and BAP1 alterations (mutations or IHC loss), should be considered as high risk, with a high malignant potential. This is in fact the situation of our patient. Also, when there are no alterations in EIF1AX, SF3B1, and BAP1, or there are only mutations in EIF1AX with wild-type versions of SF3B1 and BAP1, the prognosis is favorable (15).

Additionally, in our case, a mutation of the somatic telomerase reverse transcriptase gene (TERT) was identified. This mutation has been evidenced in approximately 80% of cases of patients with sporadic and familial melanoma (12, 16); although this mutation is rare in PMMs, it is very pervasive, and it is believed to increase gene expression, generating a positive selection of malignant cells. Besides, a joint expression has been shown with BRAF and NRAS, which activate melanoma oncogenesis, and TERT activation is believed to enhance melanocyte immortalization (12, 16, 17). TERT promoter mutations are found more frequently in sun-exposed sites and show mutations that could be consistent with UV-induced cytidine-to-thymidine transitions (6), it has been suggested that these mutations might occur early in the development of cutaneous melanoma. As the primary melanoma occurred on sun-exposed skin, it is somewhat surprising that a UV-induced TERT promoter was not detected in the primary lesion. However, as C228T mutations are also frequently found in UV-protected internal malignancies, it is possible that the melanoma acquired its TERT promoter mutation after metastasizing (6, 18). Alternatively, the C228T mutant cells could have been present as a small subset of the primary lesion, which was not detected by initial gene sequencing, but then became the dominant cell type by the time the melanoma was progressive.

Leptomeningeal melanoma remains a devastating complication, and its control is a tremendous unmet clinical need since progression results in rapid neurological decline and death. The diagnosis can be difficult and is often made on radiological findings without confirmation of CSF cytology. Arasaratnam et al. recently reported the outcomes of fourteen patients with extracranial melanomas and meningeal involvement (10). Almost all had BRAF mutations (79%). The median time from diagnosis of metastatic melanoma to confirmed leptomeninges' involvement was 5.7 months, and all but one patient received local therapy, systemic therapy, or both. The median overall survival (OS) from
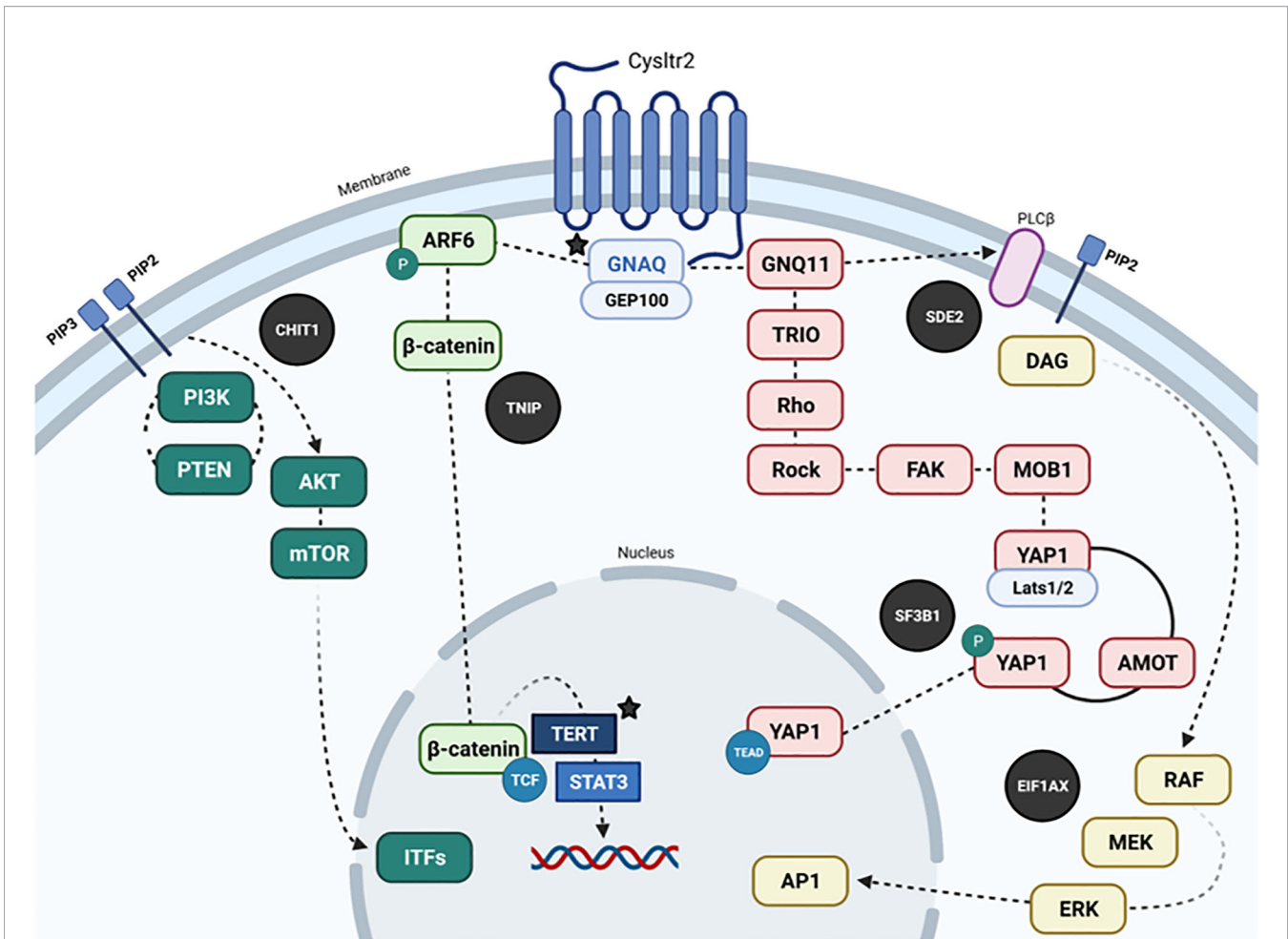
**FIGURE 7** | Dysregulated pathways in PMMs (in black circles, other mutated genes are highlighted with their protein representation, and colocalization parallel to the main signaling pathways). Recurrent mutations in GNAQ, PLCβ4, and CYSLTR2 are mutually exclusive and trigger Gαq signaling and related pathways (Akt/mTOR, Wnt/β-catenin, Yes-associated protein (YAP), and MAPK pathways). In brief, GNAQ mediates signals between the G protein-coupled receptor (GPCR) and downstream effectors. Receptor activation by ligand binding causes the activation of GNAQ by catalyzing the release of GDP and binding of GTP. In its active form, GTP-bound GNAQ causes the release of the beta and gamma subunits of the heterotrimeric G-protein. GTP-GNAQ and beta and gamma subunits transfer the receptor-mediated signal to downstream effectors through secondary messengers, which participate in diverse signaling pathways to evoke different effectors. The known effectors for GNAQ include PLC beta, p63-RhoGEF, Trio, and Duet. GNAQ has been shown to activate the MAP kinase pathway, possibly *via* DAG-mediated activation of protein kinase C isoforms. GNAQ has an intrinsic GTPase domain at the C terminus, which causes the hydrolysis of GTP to GDP, and the G-alpha-GDP re-associates with G-beta and G-gamma subunits. Somatic mutations in GNAQ have been described in uveal and meningeal melanocytic neoplasias. In uveal melanoma, 97% of the hotspot mutations cause the amino acid substitution Q209L (data similar to rare cases originating in the meninges); the other 3% of mutations generate amino acid change R183Q. The Glutamine 209 of GNAQ is similar to residue 61 of RAS protein. The Q209 and R183 mutations cause a complete or partial loss of intrinsic GTPase activity, thereby locking the protein in a constitutively active form. Q209 and R183 mutations occur in a mutually exclusive pattern in human neoplasia. Mutations in GNAQ are also mutually exclusive from the hotspot mutations in GNA11, which belongs to the same family and shares 90% sequence homology. GNAQ mutations are not concurrent with other common oncogenic mutations in BRAF, NRAS, or KIT found in common melanomas. CYSLTR2, Cysteinyl leukotriene receptor 2; PIP3, Phosphatidylinositol, 3,4,5)-trisphosphate; PIP2, Phosphatidylinositol 4,5-bisphosphate; GNAQ, G protein subunit alpha q; ARF6, ADP-ribosylation factor 6; GNQ11, G protein subunit alpha 11; GEP100, ADP-Ribosylation Factor - Guanine nucleotide-Exchange Protein; PI3K, Phosphatidylinositol 3-kinase; PTEN, phosphatase and tensin homolog; AKT, AKT serine/threonine kinase; mTOR, mechanistic target of rapamycin kinase; CHIT1, Chitinase 1; TNIP, TNFAIP3 interacting protein; TRIO, Triple functional domain protein; Rho, Rho factor; Rock, Rho kinase; FAK, PTK2 protein; MOB1, MOB kinase 1A; YAP, Yes-associated protein 1; AMOT, Angiomotin; TERT, Telomerase reverse transcriptase; RAF, RAF kinase; MEK, Mitogen-activated protein kinase; ERK, extracellular signal-regulated kinase; STAT3, Signal transducer and activator of transcription 3; SF3B1, Splicing factor 3B subunit 1; EIF1AX, Eukaryotic translation initiation factor 1A.

diagnosis of meningeal disease was 5.2 months, and 12-month OS was 21%. Additionally, immunotherapy was administered to 64% of patients (two ipilimumab, five anti-PD1 antibodies, and one both) with a median OS for those who received ipilimumab of 3.0 months.

The patients that received anti-PD-1 antibodies appeared to live longer than those that did not (median OS 7.1 months vs. 2.9 months) (10). Central nervous system involvement in patients with UMs is extremely rare and only five cases has been described in the

literature to date (19). Patients with UM leptomeningeal disease typically have a median OS of ~10 weeks and derive benefit from intrathecal interleukin-2 (IT IL-2), whole brain radiation and ipilimumab (20).

Given the biological similarity between UMs and PMMs, the therapeutic results on the former might be extrapolated. Previously, Heppt et al. identified and analyzed seven expanded access programs (EAPs) (n=162), 4 phase II trials (n=171), and 1 phase Ib trial of immunotherapeutic interventions in UM patients (21). Ipilimumab monotherapy was assessed at 3 mg/kg in 5 trials (n=186) with a 0 to 5% response rate. Besides, two reports investigated ipilimumab at 10 mg/kg (n=45) with radiological responses observed in 0 to 6.5%. The median progression-free survival (PFS) was below 3 months in both groups, and the median OS was 5.2-9.8 months. Similarly, two studies investigated pembrolizumab or nivolumab with overall response rates (ORRs) of 30% and 6%, respectively. Data on combined ipilimumab and PD-1 inhibition were available from one EAP, but no response was observed with a median PFS of 2.9 months (21). Even though UMs and PMMs share a wide array of driver mutations, treatment outcomes might vary, this is mainly due to the physiological immune privilege of the eye (22).

The systematic characterization of the immune profile of UMs made it possible to find that tumors with the greatest potential for response to immunotherapy were those that showed a higher level of CD3+, CD8+, FoxP3- T cells, and CD68+ macrophages. Also, the analysis of RNAseq expression profiles by NanoString revealed significant differences in a set of immune markers between responders, including a group of genes relevant to the interferon-γ signature, particularly, the suppressor of cytokine signaling-1 (identified as a marker potentially contributing to the response to immunotherapy (23). Paradoxically, recurrence-free survival (RFS) in patients with UMs seems to be related to higher PD-L1 expression and fewer tumor-infiltrating lymphocytes (TILs). However, the cellular response to PD-1 inhibitors and disease control in UMs does appear to be dependent on IFN-γ levels (24). This information has not been extrapolated to PMMs, but it could be used in the future as a factor to stratify the population of patients who are candidates for combination immunotherapy. In our case, the patient had adequate control of the disease after the use of adjuvant ipilimumab (10 mg/kg), and with ipilimumab/nivolumab after recurrence. Other recent reports have demonstrated the value of immunotherapy in patients with primary leptomeningeal melanomatosis and melanomas (25).

Notably, other strategies were developed, considering that the typical mutations in GNAQ/GNA11 in UMs and PMMs lead to constitutive activation of the MAPK and PI3K/AKT pathways (26). Thus, logical approaches considered downstream targeted therapies against effector proteins, such as MEK and AKT. Some clinical trials were developed based on this rationale of inhibition of downstream Gαq (**Supplementary Table 1**). In this context, selumetinib (an oral selective MEK1/2 inhibitor) was tested against chemotherapy (temozolomide or dacarbazine) in a phase 2 trial, and in combination with dacarbazine in the phase 3, multicenter, and randomized SUMIT trial. Unfortunately, both

studies showed limited clinical activity (ORR 14% and 3%, respectively) in advanced UM patients (27, 28). Subsequently, the MEK inhibition trametinib was tested alone or in combination with the AKT inhibitor GSK2141795 in a phase 2 trial, including patients with advanced UM (29). The combination did not improve the clinical outcomes since patients in the trametinib arm ($n = 18$) achieved an ORR of 5.5% compared to 4.8% in the combined arm ($n = 21$). The median PFS was 3.6 months in both groups. Based on the concept that UMs (and probably PMMs) normally synthesize and secrete vascular endothelial growth factor (VEGF), an additional targeted therapy tested was the oral multi-kinase inhibitor sunitinib (30). Scheulen et al. developed a phase 2 trial recruiting 118 chemonaive patients with metastatic UM. Unfortunately, only two cases had a partial response (1.7%), 78 had a stable disease (66.1%), and the median PFS was 5.5 months (31).

## CONCLUSIONS

In conclusion, although PMM is a rare entity and its presentation is aggressive in most cases, understanding gene expression, signaling pathways, and determining cancer genomics enables better performance in targeted treatments; however, more studies are still required better to understand the pathogenesis and early treatment of this pathology. Furthermore, the comprehensive and integrated approach with neurosurgery, radiotherapy, pathology, clinical oncology, and the early initiation of medications is fundamental to improve survival, prognosis and decrease disease recurrences (32).

## DATA AVAILABILITY STATEMENT

The original contributions presented in the study are included in the article/**Supplementary Material**. Further inquiries can be directed to the corresponding author.

## ETHICS STATEMENT

Written informed consent was obtained from the individual(s) for the publication of any potentially identifiable images or data included in this article.

## AUTHOR CONTRIBUTIONS

RB, AC, and OA were in charge of ideation, analysis, writing and correction. NS, AR-P, JC-C, LeR, LuR, AM, JEG-R, CO, CS, JR, ZZ-B, and DP also participated in analysis, writing and correction. All authors approved the final version of the manuscript before submission.

## ACKNOWLEDGMENTS

## REFERENCES

1. Küsters-Vandevelde HVN, Germans MR, Rabbie R, Rashid M, Ten Broek R, Blokx WAM, et al. Whole-Exome Sequencing of a Meningeal Melanocytic Tumour Reveals Activating CYSLTR2 and EIF1AX Hotspot Mutations and Similarities to Uveal Melanoma. *Brain Tumor Pathol* (2018) 35:127–30. doi: 10.1007/s10014-018-0308-1

2. Küsters-Vandevelde HVN, Kruse V, Van Maerken T, Boterberg T, Pfundt R, Creytens D, et al. Copy Number Variation Analysis and Methylome Profiling of a GNAQ-Mutant Primary Meningeal Melanocytic Tumor and Its Liver Metastasis. *Exp Mol Pathol* (2017) 102:25–31. doi: 10.1016/j.yexmp.2016.12.006

3. Küsters-Vandevelde HVN, Creytens D, van Engen-van Grunsven ACH, Jeunink M, Winnepennickx V, Groenen PJT, et al. SF3B1 and EIF1AX Mutations Occur in Primary Leptomeningeal Melanocytic Neoplasms; Yet Another Similarity to Uveal Melanomas. *Acta Neuropathol Commun* (2016) 4:5. doi: 10.1186/s40478-016-0272-0

4. Angelino G, De Pasquale MD, De Sio L, Serra A, Massimi L, De Vito R, et al. NRASQ61K Mutated Primary Leptomeningeal Melanoma in a Child: Case Presentation and Discussion on Clinical and Diagnostic Implications. *BMC Cancer* (2016) 16:512. doi: 10.1186/s12885-016-2556-y

5. Geukes Foppen MH, Brandsma D, Blank CU, van Thienen JV, Haanen JB, Boogerd W. Targeted Treatment and Immunotherapy in Leptomeningeal Metastases From Melanoma. *Ann Oncol* (2016) 27:1138–42. doi: 10.1093/annonc/mdw134

6. Iles MM, Bishop DT, Taylor JC, Hayward NK, Brossard M, Cust AE, et al. The Effect on Melanoma Risk of Genes Previously Associated With Telomere Length. *JNCI J Natl Cancer Inst* (2014) 106:dju267. doi: 10.1093/jnci/dju267

7. Van Raamsdonk CD, Bezrookove V, Green G, Bauer J, Gaugler L, O'Brien JM, et al. Frequent Somatic Mutations of GNAQ in Uveal Melanoma and Blue Naevi. *Nature* (2009) 457:599–602. doi: 10.1038/nature07586

8. Van Raamsdonk CD, Griewank KG, Crosby MB, Garrido MC, Vemula S, Wiesner T, et al. Mutations in GNA11 in Uveal Melanoma. *N Engl J Med* (2010) 363:2191–9. doi: 10.1056/NEJMoa1000584

9. Hosler GA, Davoli T, Mender I, Litzner B, Choi J, Kapur P, et al. A Primary Melanoma and Its Asynchronous Metastasis Highlight the Role of BRAF, CDKN2A, and TERT. *J Cutan Pathol* (2015) 42:108–17. doi: 10.1111/cup.12444

10. Arasaratnam M, Hong A, Shivalingam B, Wheeler H, Guminksi AD, Long GV, et al. Leptomeningeal Melanoma—A Case Series in the Era of Modern Systemic Therapy. *Pigment Cell Melanoma Res* (2018) 31:120–4. doi: 10.1111/pcmr.12652

11. Urtatiz O, Cook C, Huang JL-Y, Yeh I, Van Raamsdonk CD. GNAQQ209L Expression Initiated in Multipotent Neural Crest Cells Drives Aggressive Melanoma of the Central Nervous System. *Pigment Cell Melanoma Res* (2020) 33:96–111. doi: 10.1111/pcmr.12843

12. Read J, Wadt KAW, Hayward NK. Melanoma Genetics. *J Med Genet* (2016) 53:1–14. doi: 10.1136/jmedgenet-2015-103150

13. Kolin DL, Geddie WR, Ko HM. CSF Cytology Diagnosis of NRAS-Mutated Primary Leptomeningeal Melanomatosis With Neurocutaneous Melanosis. *Cytopathology* (2017) 28:235–8. doi: 10.1111/cyt.12366

14. Knappe UJ, Tischoff I, Tannapfel A, Reinbold W-D, Möller I, Sucker A, et al. Intraventricular Melanocytoma Diagnosis Confirmed by Gene Mutation Profile. *Neuropathol Off J Jpn Soc Neuropathol* (2018) 38:288–92. doi: 10.1111/neup.12443

15. Griewank KG, Koelsche C, van de Nes JAP, Schrimpf D, Gessi M, Möller I, et al. Integrated Genomic Classification of Melanocytic Tumors of the Central Nervous System Using Mutation Analysis, Copy Number Alterations, and DNA Methylation Profiling. *Clin Cancer Res Off J Am Assoc Cancer Res* (2018) 24:4494–504. doi: 10.1158/1078-0432.CCR-18-0763

16. Horn S, Figlp A, Rachakonda pS, Fischer C, Sucker A, Gast A, et al. TERT Promoter Mutations in Familial and Sporadic Melanoma. *Science* (2013) 339:959–61. doi: 10.1126/science.1230062

17. Huang FW, Hodis E, Xu MJ, Kryukov GV, Chin L, Garraway LA. Highly Recurrent TERT Promoter Mutations in Human Melanoma. *Science* (2013) 339:957–9. doi: 10.1126/science.1229259

18. Heidenreich B, Nagor E, Rachakonda PS, Garcia-Casado Z, Requena C, Traves V, et al. Telomerase Reverse Transcriptase Promoter Mutations in Primary Cutaneous Melanoma. *Nat Commun* (2014) 5:3401. doi: 10.1038/ncomms4401

19. Glitza IC, Reddy ST, Patel SP. Leptomeningeal Disease in Uveal Melanoma: A Case Series. *J Neurooncol* (2018) 139:503–5. doi: 10.1007/s11060-018-2878-5

20. Glitza IC, Rohlfs M, Guha-Thakurta N, Bassett RL, Bernatchez C, Diab A, et al. Retrospective Review of Metastatic Melanoma Patients With Leptomeningeal Disease Treated With Intrathecal Interleukin-2. *ESMO Open* (2018) 3:e000283. doi: 10.1136/esmoopen-2017-000283

21. Heppt MV, Steeb T, Schlager JG, Rosumeck S, Dressler C. Immune Checkpoint Blockade for Unresectable or Metastatic Uveal Melanoma: A Systematic Review. *Cancer Treat Rev* (2017) 60:44–52. doi: 10.1016/j.ctrv.2017.08.009

22. Taylor AW. Ocular Immune Privilege and Transplantation. *Front Immunol* (2016) 7:37. doi: 10.3389/fimmu.2016.00037

23. Qin Y, Bollin K, de Macedo MP, Carapeto F, Kim KB, Roszik J, et al. Immune Profiling of Uveal Melanoma Identifies a Potential Signature Associated With Response to Immunotherapy. *J Immunother Cancer* (2020) 8:e000960. doi: 10.1136/jitc-2020-000960

24. Singh L, Singh M, Kenney MC, Jager MJ, Rizvi MA, Meel R, et al. Prognostic Significance of PD-1/PD-L1 Expression in Uveal Melanoma: Correlation With Tumor-Infiltrating Lymphocytes and Clinicopathological Parameters. *Cancer Immunol Immunother CII* (2021) 70:1291–303. doi: 10.1007/s00262-020-02773-8

25. Misir Krpan A, Rakusic Z, Herceg D. Primary Leptomeningeal Melanomatosis Successfully Treated With PD-1 Inhibitor Pembrolizumab: A Case Report. *Med (Baltimore)* (2020) 99:e22928. doi: 10.1097/MD.0000000000022928

26. Curley CT, Stevens AD, Mathew AS, Stasiak K, Garrison WJ, Miller GW, et al. Immunomodulation of Intracranial Melanoma in Response to Blood-Tumor Barrier Opening With Focused Ultrasound. *Theranostics* (2020) 10:8821–33. doi: 10.7150/thno.47983

27. Carvajal RD, Sosman JA, Quevedo JF, Milhem MM, Joshua AM, Kudchakar RR, et al. Effect of Selumetinib vs Chemotherapy on Progression-Free Survival in Uveal Melanoma: A Randomized Clinical Trial. *JAMA* (2014) 311:2397–405. doi: 10.1001/jama.2014.6096

28. Carvajal RD, Piperno-Neumann S, Kapiteijn E, Chapman PB, Frank S, Joshua AM, et al. Selumetinib in Combination With Dacarbazine in Patients With Metastatic Uveal Melanoma: A Phase III, Multicenter, Randomized Trial (SUMIT). *J Clin Oncol* (2018) 36:1232–9. doi: 10.1200/JCO.2017.74.1090

29. Shoushtari AN, Kudchadkar RR, Panageas K, Murthy RK, Jung M, Shah R, et al. A Randomized Phase 2 Study of Trametinib With or Without GSK2141795 in Patients With Advanced Uveal Melanoma. *J Clin Oncol* (2016) 34:9511–1. doi: 10.1200/JCO.2016.34.15_suppl.9511

30. Castet F, Garcia-Mulero S, Sanz-Pamplona R, Cuellar A, Casanovas O, Caminal JM, et al. Uveal Melanoma, Angiogenesis and Immunotherapy, Is There Any Hope? *Cancers* (2019) 11:834. doi: 10.3390/cancers11060834

31. Scheulen ME, Kaempgen E, Keilholz U, Heinzerling L, Ochsenreither S, Abendroth A, et al. STREAM: A Randomized Discontinuation, Blinded, Placebo-Controlled Phase II Study of Sorafenib (S) Treatment of Chemonaïve Patients (Pts) With Metastatic Uveal Melanoma (MUM). *J Clin Oncol* (2017) 35(15_suppl):9511. doi: 10.1200/JCO.2017.35.15_suppl.9511

32. Glitza IC, Smalley KSM, Brastianos PK, Davies MA, McCutcheon I, Liu JKC, et al. Leptomeningeal Disease in Melanoma Patients: An Update to

## SUPPLEMENTARY MATERIAL

The Supplementary Material for this article can be found online at: https://www.frontiersin.org/articles/10.3389/fonc.2021.691017/full#supplementary-material

Treatment, Challenges, and Future Directions. *Pigment Cell Melanoma Res* (2020) 33:527–41. doi: 10.1111/pcmr.12861

# The Road to CAR T-Cell Therapies for Pediatric CNS Tumors: Obstacles and New Avenues

Ian Burns[1†], William D. Gwynne[2†], Yujin Suk[1,3], Stefan Custers[3], Iqra Chaudhry[3], Chitra Venugopal[2] and Sheila K. Singh[2*]

[1] Michael G. DeGroote School of Medicine, McMaster University, Hamilton, ON, Canada, [2] Department of Surgery, McMaster University, Hamilton, ON, Canada, [3] Department of Biochemistry and Biomedical Sciences, Faculty of Health Sciences, McMaster University, Hamilton, ON, Canada

Pediatric central nervous system (CNS) tumors are the most common solid tumors diagnosed in children and are the leading cause of pediatric cancer-related death. Those who do survive are faced with the long-term adverse effects of the current standard of care treatments of chemotherapy, radiation, and surgery. There is a pressing need for novel therapeutic strategies to treat pediatric CNS tumors more effectively while reducing toxicity – one of these novel modalities is chimeric antigen receptor (CAR) T-cell therapy. Currently approved for use in several hematological malignancies, there are promising pre-clinical and early clinical data that suggest CAR-T cells could transform the treatment of pediatric CNS tumors. There are, however, several challenges that must be overcome to develop safe and effective CAR T-cell therapies for CNS tumors. Herein, we detail these challenges, focusing on those unique to pediatric patients including antigen selection, tumor immunogenicity and toxicity. We also discuss our perspective on future avenues for CAR T-cell therapies and potential combinatorial treatment approaches.

**Keywords: chimeric antigen receptor T-cell, pediatric brain tumor, immunotherapy, CNS tumor, combinatorial immunotherapy**

## INTRODUCTION

Pediatric central nervous system (CNS) tumors are the most common solid tumors diagnosed in children (1). Despite advances in the molecular characterization of these tumors and the fine-tuning of multimodal therapies, numerous patients experience high rates of tumor recurrence and mortality (2, 3). In fact, CNS tumors are the leading cause of pediatric cancer-related death, recently surpassing leukemia (1, 4). Those who survive face lifelong challenges associated with the standard of care (SoC) treatment, which usually consists of surgery, chemotherapy and/or local or craniospinal irradiation. Chemotherapy leaves patients with off-target organ damage and often neurocognitive deficits (5), and radiation causes debilitating damage to the developing brain (6). Given this persistent mortality and morbidity, there is an urgent need for novel therapies that effectively eradicate CNS tumors in children, providing durable remissions while minimizing treatment-related toxicity.

Recent developments in cancer immunotherapy have unveiled targeted treatment strategies that can prevent tumor recurrence and negate long-term neurotoxic sequalae caused by

cytotoxic therapies. Immune checkpoint inhibition with antibodies targeting programmed cell death protein 1 (PD-1) and CTLA4 demonstrates superior efficacy in comparison to the SoC in several cancers (7, 8). In many children with relapsed and treatment-refractory leukemia, treatment with Chimeric Antigen Receptor (CAR) T-cells has led to durable remission (9, 10). CAR T-cells are generated by engineering patient T-cells to express the hybrid CAR protein, which contains an extracellular antibody-like domain that recognizes a cancer-specific antigen and intracellular signalling components that trigger an immune response (11). Each new generation of CAR T-cell has comprised more sophisticated co-stimulatory signalling domains, including CD28 and 4-1BB, and other genetic modifications, such as transgenes for cytokine secretion, to optimize anti-tumor activity (12). Currently, CAR T-cells are approved for use in hematological malignancies including relapsed/refractory non-Hodgkin lymphoma, multiple myeloma, and pediatric relapsed acute lymphoblastic leukemia (13). Solid tumors have emerged as the next frontier for CAR T-cell therapies.

Pre-clinical and early clinical trial data have suggested that CAR T-cells could play an important role in the treatment of pediatric CNS tumors, including medulloblastomas (MB), atypical rhabdoid teratoid tumors (ATRT), high grade gliomas (HGG) and ependymomas (14–16). Many obstacles remain, however, to the successful development of CAR T-cell therapies in pediatric CNS tumors. The paucity of targetable antigens and the unfavourable immunological characteristics of these tumors present unique challenges, and children have unique and poorly understood vulnerabilities to treatment-related toxicities. Herein, we review the major challenges associated with developing CAR T-cell therapies specifically for pediatric CNS tumors and present our perspective on possible avenues for the future development of more effective CAR T-cell and combinatorial immunotherapies.

## CHALLENGES

### Antigen Selection

Whereas adult CNS tumors display an abundance of neoantigens that arise from high mutational burden, there is a marked paucity of neoantigens on pediatric CNS tumors (17, 18). Children are exposed to fewer environmental factors that contribute to DNA damage and the resultant lack of neoantigens presents a unique challenge for pediatric immunotherapy target selection. Target antigens should have tumor-specific (little to no expression in normal cells) or tumor-associated (overexpressed in tumor tissue) expression to spare the developing brain from off-tumor toxicity (19). One promising strategy to overcome the paucity of true neoantigens is to target oncofetal antigens, a class of cell surface markers normally expressed exclusively during prenatal tissue development that can become re-expressed during neoplastic transformation (20). For example, CAR T-cells have been developed to target tumor-specific exons of the oncofetal antigen cerebroglycan GPC2 (21, 22). Alternatively, they can be made to target tumor-specific antigen epitopes. CAR T-cells targeting the

epidermal growth factor receptor (EGFR) 806 epitope that is uniquely expressed on the surface of tumor cells can effectively eradicate glioblastoma (GBM) cells while sparing EGFR-expressing human fetal astrocytes (23).

In addition to a reduced neoantigen abundance, there is extensive intratumoral phenotypic heterogeneity among pediatric CNS tumor cells (24). Brain tumor initiating cells (BTICs) are an infrequent subpopulation of tumor cells CAR T-cell that share properties with normal stem cells, including the capacity for limitless self-renewal and proliferation. BTICs are resistant to chemotherapy (25) and radiation (26) and seed pediatric CNS tumor recurrence and leptomeningeal metastasis (27, 28). The identification of a target that selectively marks BTICs may provide an effective means to eradicate therapy refractory tumor cells, thus delaying or preventing recurrence. Unfortunately, existing BTIC markers amenable to immunotherapy in adult gliomas, such as prominin 1 (PROM1; CD133), are also expressed by human neural stem and progenitor cells (29).

Selection of tumor cells with reduced target antigen expression throughout the course of treatment will also induce temporal heterogeneity. This antigen escape is an impediment to effective CAR T-cell treatment (24, 30). Multivalent CARs are a potential way to improve targeting of tumors with heterogenous antigen expression. Bielamowicz et al. demonstrated improved anti-tumor efficacy in GBM models using trivalent CAR T-cells targeting ephrin A receptor 2, human epidermal growth factor receptor 2 (HER2) and interleukin-13 receptor alpha-2 (IL13Rα2) (30). With the same trivalent design, a significant survival benefit was observed in patient-derived xenograft (PDX) models of MB and ependymoma. Notably, modest expression of HER2 and IL13Rα2 on patient samples in this study suggests additional, more highly expressed targets are needed (15).

Currently, there are a limited number of CAR T-cell clinical trials for children with CNS tumors, all at phase I. Targets include HER2, B7 homolog 3 (B7H3), EGFR806, the disialoganglioside GD2 and IL13Rα2 (**Table 1**).

### Delivery

In comparison to hematological malignancies, solid tumors and especially CNS tumors situated behind the blood brain barrier (BBB) present unique physical challenges that hinder effective delivery of CAR T-cells. While peripherally infused CAR T-cells have been found to modestly cross the BBB (31–33), numerous pre-clinical studies evaluating the comparative efficacy of intravenous (IV), intratumoral (IT) and intraventricular (ICV) delivery of CAR T-cells targeting CNS tumors have produced compelling evidence favoring locoregional administration via surgically-inserted catheter (IT or ICV). Locoregional delivery is associated with more effective tumor infiltration, improved anti-tumor efficacy, and reduced systemic toxicity (16, 34–36). For example, Theruvath et al. tested B7H3 CAR T-cells against ATRT patient-derived xenografts in mice and showed dramatically more rapid tumor homing and expansion with locoregional delivery, in comparison to the far higher doses of CAR T-cells delivered via IV. Additionally, significantly higher levels of systemic inflammatory cytokines were detected upon IV

| NCT# | Target | Tumors | Delivery | Ages eligible (years) | Trial location |
|------|--------|--------|----------|------------------------|----------------|
| 04510051 | IL13Rα2 | IL13Rα2-positive recurrent/refractory CNS tumors | ICV | 4-25 | City of Hope Medical Centre |
| 04185038 | B7H3 | DIPG, DMG, recurrent/refractory CNS tumors | IT, ICV | 1-26 | Seattle Children's Hospital |
| 03638167 | EGFR806 | EGFR-positive recurrent/refractory CNS tumors | IT, ICV | 1-26 | Seattle Children's Hospital |
| 04099797 | GD2 | GD2-positive CNS tumors including HGG, DIPG, MB | IV | 1-18 | Texas Children's Hospital |
| 04196413 | GD2 | H3K27M-mutated DIPG or spinal DMG | IV | 2-30 | Stanford University |
| 03500991 | HER2 | HER2-positive recurrent/refractory CNS tumors | IT, ICV | 1-26 | Seattle Children's Hospital |
| 04903080 | HER2 | HER2-positive recurrent/refractory ependymoma | IV | 1-21 | Texas Children's Hospital |
| 02442297 | HER2 | HER2-positive recurrent/refractory primary CNS tumors or HER2-positive tumors metastatic to CNS | IT, ICV | ≥3 | Texas Children's Hospital |

*DIPG, Diffuse intrinsic pontine glioma; DMG, diffuse midline glioma; MB, medulloblastoma; ICV, intraventricular; IT, intratumoral; IV, intravenous.*
*All trials are in Phase 1.*

delivery (16). Notably, ICV delivery may be superior to IT in cases of leptomeningeal spread, as CAR T-cells are able to more freely traffic throughout the CNS (34). In current pediatric clinical trials, locoregional delivery is the preferred method (**Table 1**).

## Homing and Persistence

Other important challenges impeding the development of effective CAR T-cells for pediatric CNS tumors include CAR T-cell homing and persistence. To improve homing to tumor sites, CAR T-cells expressing chemokine receptors have been developed (37, 38). Once CAR T-cells reach target sites, they must be capable of exerting an antitumoral response prior to exhaustion. Should exhaustion occur prior to tumor clearance, CAR T-cell efficacy drops dramatically. A recent study found that co-expression of AP1 transcription factor, c-Jun, in CAR T-cells led to an increased capacity for expansion, and diminished terminal differentiation. These exhaustion-resistant CAR T-cells also exhibit a dramatic increase in antitumoral efficacy (39).

Additional strategies to improve CAR T-cell persistence and reduce exhaustion include optimizing T-cell activation and co-stimulation signalling and interfering with molecules that impair T-cell activation (40). For example, CAR T-cells engineered to express pro-inflammatory cytokines such as IL-12 and IL-18 and those with constitutively active IL-15 and IL-7 have increased anti-tumor efficacy and improved persistence in solid tumors (41–44). Particularly in immunologically "cold" pediatric CNS tumors, additional inflammatory cytokine secretion by CAR T-cells could also augment local immune cell activation. This benefit must be balanced with local and systemic toxicity associated with increased cytokine production (40). Finally, issues of CAR-T cell persistence can be addressed by optimizing the timing of their delivery. For example, the use of small, frequent (usually weekly) dosing regimens may help maximize the therapeutic window while minimizing infusion-associated toxicity (37). It is unclear, however, whether frequent CAR T-cell dosing translates to improved anti-tumor efficacy in comparison to infrequent or one-time dosing.

## Toxicity

Cytokine release syndrome (CRS), a systemic inflammatory response following excess cytokine production by endogenous immune cells and/or CAR T-cells, and the toxic encephalopathy known as immune effector cell-associated neurotoxicity syndrome (ICANS) that often follows, are major systemic side effects of CAR T-cell therapies targeting hematological malignancies (45). Relatively little is known regarding these toxicities in the context of CAR T-cells for CNS tumors, especially in pediatrics. Nevertheless, the locoregional delivery strategies currently employed with many CNS-targeting CAR T-cell therapies reduce much of the concern for systemic toxicity, which is known to be a dose-dependent (46) manifestation of the systemic administration and peripheral activation of CAR T-cells (16, 45). This is in keeping with the CRS reported by Goff et al. after IV infusion of only the highest dose of EGFRvIII-targeting CAR T-cells in a GBM patient (47), and that most trials with CAR T-cells targeting CNS tumors have shown few adverse events (48). There is, however, reasonable concern for excess cytokine production leading to local CNS toxicity following locoregional delivery. Promisingly, 3 pediatric patients recently treated with locally-infused CAR T-cells targeting HER2 experienced no dose limiting toxicity while still showing local CNS immune activation (49). Interestingly, CRS and ICANS were not predicted by pre-clinical studies of CD19-targeting CAR T-cells (45) – perhaps similarly unexpected toxicities will emerge through the development of CAR T-cells for CNS tumors.

Given that CAR T-cell dosing, antigen affinity and other design factors remain largely empiric, off-target and particularly on-target/off-tumor toxicity are major concerns. Illustrating this concern, Richman et al. showed that high-affinity CAR T-cells targeting GD2 caused fatal encephalitis after acting on normal brain tissues expressing GD2 in a neuroblastoma mouse model (50). It has also been observed that ICV-administered CAR T-cells migrate effectively into the periphery (16), suggesting that even with locoregional delivery strategies, off-tumor toxicity within the periphery must be considered.

In creating CAR T-cells for the pediatric population, attention must be drawn to the fact that the childhood brain and other tissues are still developing and also have different antigen expression in comparison to adults. This is particularly relevant with CAR T-cells targeting known or potential stem cell antigens. For example, CD133 is expressed on neural stem cells (51) and hematopoietic stem cells (52). Hence, while treatment with CD133-targeting CAR T-cells may be tolerated in adults with GBM, this target may not be appropriate in pediatric patients. Preclinical development of novel targets

must ensure proper examination of appropriate control tissues, such as human neural stem cells and fetal tissue arrays, to get insights into potential toxicities. Building inducible control into CAR T-cells provides clinicians with the ability to rapidly regulate CAR T-cell activity during treatment and in case of anticipated or unanticipated toxicities. These include suicide genes such as inducible Caspase 9 and herpes simplex virus tyrosine kinase, and cell surface elimination markers that allow for antibody-mediated control (53).

## Tumor Immune Microenvironment

Tumors comprise a distinct network of tumor cells, immune cells, stromal cells, and extracellular matrix proteins, a spectrum collectively termed the tumor immune microenvironment (TIME). Immunologically "hot" tumors comprise high numbers of tumor-infiltrating lymphocytes (TILs) and increased PD-1 ligand expression, whereas immunologically "cold" tumors have low numbers of TILs and reduced PD-1 expression. Pediatric CNS tumors are immunologically cold due to their low mutational burden and a lack of neoantigen expression (54, 55). Cold tumors respond poorly to immune checkpoint inhibition (56) and are associated with poor clinical outcomes (18, 57). Colder tumors are also less responsive to adoptive T-cell and CAR T-cell therapies (58, 59). In such cases, administered CAR T-cells must be capable of activation and infiltration, where endogenous T-cells are unable to do the same. To overcome the cold TIMEs of pediatric CNS tumors, novel CAR T-cell engineering approaches can be applied to optimize their function in these environments. Potential tools include cytokine switch receptors, which transform an inhibitory signal into a growth-inducing signal, and optimization of CAR T-cell metabolism in the hypoxic and reactive oxygen species-filled microenvironment (40).

In addition to being immunologically cold, there is substantial heterogeneity in the TIME between and among pediatric CNS tumor types. To develop effective immunotherapies, this heterogeneity must be understood and exploited. Grabovska et al. analyzed genome-wide DNA methylation data from >6,000 pediatric CNS tumors – interestingly, the immune infiltrate subgroups that they identified exist independent of molecular subgroup and are predictive of outcomes in multiple pediatric tumor types. They also showed that specific molecular drivers like H3.3G34 mutations in HGG are associated with characteristic immune infiltrates independent of tumor subtype (18). In MB, several studies have shown that Sonic Hedgehog tumors have an increased proportion of T-cells in comparison to other subgroups, rendering them promising candidates for immunotherapy (18, 60). Notably, pediatric midline gliomas are exceptionally immunologically cold and have very low inflammatory cytokine expression (61). In comparison to normal brain tissue, Diffuse Intrinsic Pontine Glioma (DIPG) tumors do not display increased macrophage or T-cell infiltration, or PD1L expression (62).

Looking forward, a deeper understanding of the heterogenous and cold TIMEs of pediatric CNS tumors will allow for the development of novel treatment approaches that help overcome these unfavorable environments. In addition to novel CAR T-cell design, combining CAR T-cells with other immunotherapies or small molecules may allow for the induction of a potent inflammatory response and improve outcomes.

## COMBINATORIAL THERAPIES

Agents, including small-molecule drugs and other immunotherapies, that can prime CAR T-cells to overcome immunosuppressive effects of tumor cells or those that can convert a cold TIME into a hot TIME may act in combination with CAR T-cell therapies to elicit a more powerful antitumoral response in the pediatric CNS (63). Inhibition of the PD-1/PD-1 ligand immune checkpoint axis, which tumor cells exploit to avoid detection from host immune cells, is a strategy that may enhance the activity of CAR T-cells through increased target engagement (63). The development of small molecules capable of targeting PD-1 have been hindered, however, in part due to the hydrophobic PD-1/PDL-1 interface. The use of cytotoxic/cytolytic agents like cisplatin chemotherapy (64, 65), or oncolytic viruses such as HSV-1 G207 (66), can also enhance the effectiveness of immunotherapy by releasing tumor-associated antigens and cytosolic DNA that promote the conversion of a typically cold pediatric TIME into a hot TIME. The latter presents a potential treatment window of opportunity in pediatric CNS brain tumor patients that are treated with chemoradiotherapy. Researchers have exploited a metabolic vulnerability of immunosuppressive regulatory T-cells (T-reg) to overcome their immunosuppressive nature. Small molecule inhibitors of Indoleamine-pyrrole 2,3-dioxygenase (IDO1) reduce T-reg activity in the TIME and increase immunotherapy efficacy (67).

The capacity for small molecules to be administered systemically, penetrate the BBB, and modulate intracellular targets provides combinatorial immunotherapeutic opportunities for small-molecule agents that monoclonal antibodies and other larger molecules cannot fulfill. Cytotoxic and cytolytic agents also have the potential to greatly enhance the efficacy of CAR T-cell therapies. These combinatorial treatment approaches may be the key to overcoming the challenges presented by solid pediatric CNS tumors.

## DISCUSSION

CAR T-cell therapies for hematological malignancies represent major breakthroughs in cancer research and adapting CAR T-cells to target solid tumors represents the next frontier. Here we have reviewed the unique physical and biological challenges associated with developing CAR T-cells for pediatric CNS tumors, and highlighted promising avenues of current and future research (**Figure 1**). The paucity of targetable antigens, intratumoral heterogeneity, and the co-expression of many

**FIGURE 1** | Challenges and potential solutions for development of effective CAR T-cell therapies for pediatric CNS tumors. Infographic depicting the challenges (red) associated with immunotherapies for malignant pediatric CNS tumors, and the proposed solutions (green) that might mitigate them. TIME, tumor immune microenvironment; BTIC, brain tumor initiating cell; NSC, neural stem cell; IT, intrathecal; ICV, intraventricular. Figured created with BioRender.com.

potential antigens in normal and developing tissues are all fundamental challenges. Potential solutions include using appropriate preclinical controls, exploring BTIC-specific antigens and novel CAR T-cell engineering strategies such as multivalent CARs. In terms of CAR T-cell administration, IT and ICV methods improve delivery and reduce systemic toxicity. There are also many unknowns regarding the local and systemic toxicity of CAR T-cell therapies for pediatric brain tumors and therefore, a cautious approach guided by an awareness of the potential unique susceptibilities of the pediatric brain is called for. It is unclear how treatment of CNS tumors with CAR T-cells may impact brain development. Other novel approaches are also necessary to improve the homing and persistence of administered cells. Finally, the cold and heterogeneous TIMEs of some pediatric CNS tumors necessitate the development and application of novel combinatorial therapies to support CAR T-cells in generating an immune response sufficient to eradicate tumor cells. With creative use of existing and novel therapies and

continued innovation in CAR T-cell design, there is potential for a new era of improved outcomes and reduced toxicity for children with CNS tumors.

## DATA AVAILABILITY STATEMENT

The original contributions presented in the study are included in the article/supplementary material. Further inquiries can be directed to the corresponding author.

## AUTHOR CONTRIBUTIONS

IB, WG, YS, SC, and IC contributed to the conception and drafting of the manuscript. All authors reviewed and approved the final version.

# REFERENCES

1. Ostrom QT, Patil N, Cioffi G, Waite K, Kruchko C, Barnholtz-Sloan JS. CBTRUS Statistical Report: Primary Brain and Other Central Nervous System Tumors Diagnosed in the United States in 2013-2017. *Neuro Oncol* (2020) 22 (12 Suppl 2):iv1–iv96. doi: 10.1093/neuonc/noaa200

2. Girardi F, Allemani C, Coleman MP. Worldwide Trends in Survival From Common Childhood Brain Tumors: A Systematic Review. *J Global Oncol* (2019) 5):1–25. doi: 10.1200/jgo.19.00140

3. Hill RM, Richardson S, Schwalbe EC, Hicks D, Lindsey JC, Crosier S, et al. Time, Pattern, and Outcome of Medulloblastoma Relapse and Their Association With Tumour Biology at Diagnosis and Therapy: A Multicentre Cohort Study. *Lancet Child Adolesc Health* (2020) 4(12):865–74. doi: 10.1016/S2352-4642(20)30246-7

4. Withrow DR, Berrington de Gonzalez A, Lam CJK, Warren KE, Shiels MS. Trends in Pediatric Central Nervous System Tumor Incidence in the United States 1998-2013. *Cancer Epidemiol Biomark Prev* (2019) 28(3):522–30. doi: 10.1158/1055-9965.Epi-18-0784

5. Askins MA, Moore BD. Preventing Neurocognitive Late Effects in Childhood Cancer Survivors. *J Child Neurol* (2008) 23(10):1160–71. doi: 10.1177/0883073808321065

6. Radcliffe J, Packer RJ, Atkins TE, Bunin GR, Schut L, Goldwein JW, et al. Three- and Four-Year Cognitive Outcome in Children With Noncortical Brain Tumors Treated With Whole-Brain Radiotherapy. *Ann Neurol* (1992) 32(4):551–4. doi: 10.1002/ana.410320411

7. Wolchok JD, Chiarion-Sileni V, Gonzalez R, Rutkowski P, Grob J-J, Cowey CL, et al. Overall Survival With Combined Nivolumab and Ipilimumab in Advanced Melanoma. *N Engl J Med* (2017) 377(14):1345–56. doi: 10.1056/NEJMoa1709684

8. Motzer RJ, Tannir NM, McDermott DF, Arén Frontera O, Melichar B, Choueiri TK, et al. Nivolumab Plus Ipilimumab Versus Sunitinib in Advanced Renal-Cell Carcinoma. *N Engl J Med* (2018) 378(14):1277–90. doi: 10.1056/NEJMoa1712126

9. Maude SL, Frey N, Shaw PA, Aplenc R, Barrett DM, Bunin NJ, et al. Chimeric Antigen Receptor T Cells for Sustained Remissions in Leukemia. *N Engl J Med* (2014) 371(16):1507–17. doi: 10.1056/NEJMoa1407222

10. Maude SL, Laetsch TW, Buechner J, Rives S, Boyer M, Bittencourt H, et al. Tisagenlecleucel in Children and Young Adults With B-Cell Lymphoblastic Leukemia. *N Engl J Med* (2018) 378(5):439–48. doi: 10.1056/NEJMoa1709866

11. Sadelain M, Brentjens R, Rivière I. The Basic Principles of Chimeric Antigen Receptor Design. *Cancer Discov* (2013) 3(4):388–98. doi: 10.1158/2159-8290.Cd-12-0548

12. Subklewe M, von Bergwelt-Baildon M, Humpe A. Chimeric Antigen Receptor T Cells: A Race to Revolutionize Cancer Therapy. *Transfus Med Hemother* (2019) 46(1):15–24. doi: 10.1159/000496870

13. Goldsmith SR, Ghobadi A, DiPersio JF. Hematopoietic Cell Transplantation and CAR T-Cell Therapy: Complements or Competitors?. *Front Oncol* (2020) 10:608916–608916. doi: 10.3389/fonc.2020.608916

14. Wang SS, Bandopadhayay P, Jenkins MR. Towards Immunotherapy for Pediatric Brain Tumors. *Trends Immunol* (2019) 40(8):748–61. doi: 10.1016/j.it.2019.05.009

15. Donovan LK, Delaidelli A, Joseph SK, Bielamowicz K, Fousek K, Holgado BL, et al. Locoregional Delivery of CAR T Cells to the Cerebrospinal Fluid for Treatment of Metastatic Medulloblastoma and Ependymoma. *Nat Med* (2020) 26(5):720–31. doi: 10.1038/s41591-020-0827-2

16. Theruvath J, Sotillo E, Mount CW, Graef CM, Delaidelli A, Heitzeneder S, et al. Locoregionally Administered B7-H3-Targeted CAR T Cells for Treatment of Atypical Teratoid/Rhabdoid Tumors. *Nat Med* (2020) 26 (5):712–9. doi: 10.1038/s41591-020-0821-8

17. Hutzen B, Ghonime M, Lee J, Mardis ER, Wang R, Lee DA, et al. Immunotherapeutic Challenges for Pediatric Cancers. *Mol Ther Oncolyt* (2019) 15:38–48. doi: 10.1016/j.omto.2019.08.005

18. Grabovska Y, Mackay A, O'Hare P, Crosier S, Finetti M, Schwalbe EC, et al. Pediatric Pan-Central Nervous System Tumor Analysis of Immune-Cell Infiltration Identifies Correlates of Antitumor Immunity. *Nat Commun* (2020) 11(1): 4324. doi: 10.1038/s41467-020-18070-y

19. Robinson GW, Orr BA, Wu G, Gururangan S, Lin T, Qaddoumi I, et al. Vismodegib Exerts Targeted Efficacy Against Recurrent Sonic Hedgehog-Subgroup Medulloblastoma: Results From Phase II Pediatric Brain Tumor Consortium Studies PBTC-025B and PBTC-032. *J Clin Oncol* (2015) 33 (24):2646–54. doi: 10.1200/jco.2014.60.1591

20. Wepsic HT. Overview of Oncofetal Antigens in Cancer. *Ann Clin Lab Sci* (1983) 13(4):261–6.

21. Bosse KR, Raman P, Zhu Z, Lane M, Martinez D, Heitzeneder S, et al. Identification of GPC2 as an Oncoprotein and Candidate Immunotherapeutic Target in High-Risk Neuroblastoma. *Cancer Cell* (2017) 32(3):295–309.e212. doi: 10.1016/j.ccell.2017.08.003

22. Li N, Torres MB, Spetz MR, Wang R, Peng L, Tian M, et al. CAR T Cells Targeting Tumor-Associated Exons of Glypican 2 Regress Neuroblastoma in Mice. *Cell Rep Med* (2021) 2(6):100297. doi: 10.1016/j.xcrm.2021.100297

23. Ravanpay AC, Gust J, Johnson AJ, Rolczynski LS, Cecchini M, Chang CA, et al. EGFR806-CAR T Cells Selectively Target a Tumor-Restricted EGFR Epitope in Glioblastoma. *Oncotarget* (2019) 10:7080–95. doi: 10.18632/oncotarget.27389

24. Kabir TF, Kunos CA, Villano JL, Chauhan A. Immunotherapy for Medulloblastoma: Current Perspectives. *Immunotargets Ther* (2020) 9:57–77. doi: 10.2147/ITT.S198162

25. Beier D, Schriefer B, Brawanski K, Hau P, Weis J, Schulz JB, et al. Efficacy of Clinically Relevant Temozolomide Dosing Schemes in Glioblastoma Cancer Stem Cell Lines. *J Neurooncol* (2012) 109(1):45–52. doi: 10.1007/s11060-012-0878-4

26. Bao S, Wu Q, McLendon RE, Hao Y, Shi Q, Hjelmeland AB, et al. Glioma Stem Cells Promote Radioresistance by Preferential Activation of the DNA Damage Response. *Nature* (2006) 444(7120):756–60. doi: 10.1038/nature05236

27. Vanner RJ, Remke M, Gallo M, Selvadurai HJ, Coutinho F, Lee L, et al. Quiescent Sox2(+) Cells Drive Hierarchical Growth and Relapse in Sonic Hedgehog Subgroup Medulloblastoma. *Cancer Cell* (2014) 26(1):33–47. doi: 10.1016/j.ccr.2014.05.005

28. Kahn SA, Wang X, Nitta RT, Gholamin S, Theruvath J, Hutter G, et al. Notch1 Regulates the Initiation of Metastasis and Self-Renewal of Group 3 Medulloblastoma. *Nat Commun* (2018) 9(1):4121. doi: 10.1038/s41467-018-06564-9

29. Vora P, Venugopal C, Salim SK, Tatari N, Bakhshinyan D, Singh M, et al. The Rational Development of CD133-Targeting Immunotherapies for Glioblastoma. *Cell Stem Cell* (2020) 26(6):832–44.e836. doi: 10.1016/j.stem.2020.04.008

30. Bielamowicz K, Fousek K, Byrd TT, Samaha H, Mukherjee M, Aware N, et al. Trivalent CAR T Cells Overcome Interpatient Antigenic Variability in Glioblastoma. *Neuro Oncol* (2018) 20(4):506–18. doi: 10.1093/neuonc/nox182

31. Davila ML, Brentjens RJ. CD19-Targeted CAR T Cells as Novel Cancer Immunotherapy for Relapsed or Refractory B-Cell Acute Lymphoblastic Leukemia. *Clin Adv Hematol Oncol* (2016) 14(10):802–8.

32. Gust J, Hay KA, Hanafi L-A, Li D, Myerson D, Gonzalez-Cuyar LF, et al. Endothelial Activation and Blood-Brain Barrier Disruption in Neurotoxicity After Adoptive Immunotherapy With CD19 CAR-T Cells. *Cancer Discov* (2017) 7(12):1404–19. doi: 10.1158/2159-8290.CD-17-0698

33. O'Rourke DM, Nasrallah MP, Desai A, Melenhorst JJ, Mansfield K, Morrissette JJD, et al. A Single Dose of Peripherally Infused EGFRvIII-Directed CAR T Cells Mediates Antigen Loss and Induces Adaptive Resistance in Patients With Recurrent Glioblastoma. *Sci Trans Med* (2017) 9(399):eaaa0984. doi: 10.1126/scitranslmed.aaa0984

34. Brown CE, Aguilar B, Starr R, Yang X, Chang WC, Weng L, et al. Optimization of IL13Rα2-Targeted Chimeric Antigen Receptor T Cells for Improved Anti-Tumor Efficacy Against Glioblastoma. *Mol Ther* (2018) 26 (1):31–44. doi: 10.1016/j.ymthe.2017.10.002

35. Priceman SJ, Tilakawardane D, Jeang B, Aguilar B, Murad JP, Park AK, et al. Regional Delivery of Chimeric Antigen Receptor-Engineered T Cells Effectively Targets HER2(+) Breast Cancer Metastasis to the Brain. *Clin Cancer Res An Off J Am Assoc Cancer Res* (2018) 24(1):95–105. doi: 10.1158/1078-0432.CCR-17-2041

36. Mulazzani M, Fräßle SP, von Mücke-Heim I, Langer S, Zhou X, Ishikawa-Ankerhold H, et al. Long-Term In Vivo Microscopy of CAR T Cell Dynamics During Eradication of CNS Lymphoma in Mice. *Proc Natl Acad Sci USA* (2019) 116(48):24275–84. doi: 10.1073/pnas.1903854116

37. Akhavan D, Alizadeh D, Wang D, Weist MR, Shepphird JK, Brown CE. CAR T Cells for Brain Tumors: Lessons Learned and Road Ahead. *Immunol Rev* (2019) 290(1):60–84. doi: 10.1111/imr.12773

38. Jin L, Tao H, Karachi A, Long Y, Hou AY, Na M, et al. CXCR1- or CXCR2-Modified CAR T Cells Co-Opt IL-8 for Maximal Antitumor Efficacy in Solid Tumors. *Nat Commun* (2019) 10(1):4016. doi: 10.1038/s41467-019-11869-4

39. Lynn RC, Weber EW, Sotillo E, Gennert D, Xu P, Good Z, et al. C-Jun Overexpression in CAR T Cells Induces Exhaustion Resistance. *Nature* (2019) 576(7786):293–300. doi: 10.1038/s41586-019-1805-z

40. Wagner J, Wickman E, DeRenzo C, Gottschalk S. CAR T Cell Therapy for Solid Tumors: Bright Future or Dark Reality? *Mol Ther* (2020) 28(11):2320–39. doi: 10.1016/j.ymthe.2020.09.015

41. Koneru M, Purdon TJ, Spriggs D, Koneru S, Brentjens RJ. IL-12 Secreting Tumor-Targeted Chimeric Antigen Receptor T Cells Eradicate Ovarian Tumors. *Vivo Oncoimmunol* (2015) 4(3):e994446. doi: 10.4161/2162402x.2014.994446

42. Hurton LV, Singh H, Najjar AM, Switzer KC, Mi T, Maiti S, et al. Tethered IL-15 Augments Antitumor Activity and Promotes a Stem-Cell Memory Subset in Tumor-Specific T Cells. *Proc Natl Acad Sci USA* (2016) 113(48):E7788–e7797. doi: 10.1073/pnas.1610544113

43. Hu B, Ren J, Luo Y, Keith B, Young RM, Scholler J, et al. Augmentation of Antitumor Immunity by Human and Mouse CAR T Cells Secreting IL-18. *Cell Rep* (2017) 20(13):3025–33. doi: 10.1016/j.celrep.2017.09.002

44. Shum T, Omer B, Tashiro H, Kruse RL, Wagner DL, Parikh K, et al. Constitutive Signaling From an Engineered IL7 Receptor Promotes Durable Tumor Elimination by Tumor-Redirected T Cells. *Cancer Discov* (2017) 7 (11):1238–47. doi: 10.1158/2159-8290.Cd-17-0538

45. Morris EC, Neelapu SS, Giavridis T, Sadelain M. Cytokine Release Syndrome and Associated Neurotoxicity in Cancer Immunotherapy. *Nat Rev Immunol* (2021). doi: doi: 10.1038/s41577-021-00547-6

46. Hay KA, Hanafi LA, Li D, Gust J, Liles WC, Wurfel MM, et al. Kinetics and Biomarkers of Severe Cytokine Release Syndrome After CD19 Chimeric Antigen Receptor-Modified T-Cell Therapy. *Blood* (2017) 130(21):2295–306. doi: 10.1182/blood-2017-06-793141

47. Goff SL, Morgan RA, Yang JC, Sherry RM, Robbins PF, Restifo NP, et al. Pilot Trial of Adoptive Transfer of Chimeric Antigen Receptor-Transduced T Cells Targeting EGFRvIII in Patients With Glioblastoma. *J Immunother (Hagerstown Md 1997)* (2019) 42(4):126–35. doi: 10.1097/CJI.0000000000000260

48. Maggs L, Cattaneo G, Dal AE, Moghaddam AS, Ferrone S. CAR T Cell-Based Immunotherapy for the Treatment of Glioblastoma. *Front Neurosci* (2021) 15:662064(535). doi: 10.3389/fnins.2021.662064

49. Vitanza NA, Johnson AJ, Wilson AL, Brown C, Yokoyama JK, Künkele A, et al. Locoregional Infusion of HER2-Specific CAR T Cells in Children and Young Adults With Recurrent or Refractory CNS Tumors: An Interim Analysis. *Nat Med* (2021) 27:1544–52. doi: 10.1038/s41591-021-01404-8

50. Richman SA, Nunez-Cruz S, Moghimi B, Li LZ, Gershenson ZT, Mourelatos Z, et al. High-Affinity GD2-Specific CAR T Cells Induce Fatal Encephalitis in a Preclinical Neuroblastoma Model. *Cancer Immunol Res* (2018) 6(1):36–46. doi: 10.1158/2326-6066.Cir-17-0211

51. Schwartz PH, Bryant PJ, Fuja TJ, Su H, O'Dowd DK, Klassen H. Isolation and Characterization of Neural Progenitor Cells From Post-Mortem Human Cortex. *J Neurosci Res* (2003) 74(6):838–51. doi: 10.1002/jnr.10854

52. Handgretinger R, Kuçi S. CD133-Positive Hematopoietic Stem Cells: From Biology to Medicine. *Adv Exp Med Biol* (2013) 777:99–111. doi: 10.1007/978-1-4614-5894-4_7

53. Brandt LJB, Barnkob MB, Michaels YS, Heiselberg J, Barington T. Emerging Approaches for Regulation and Control of CAR T Cells: A Mini Review. *Front Immunol* (2020) 11:326(326). doi: 10.3389/fimmu.2020.00326

54. Gröbner SN, Worst BC, Weischenfeldt J, Buchhalter I, Kleinheinz K, Rudneva VA, et al. The Landscape of Genomic Alterations Across Childhood Cancers. *Nature* (2018) 555(7696):321–7. doi: 10.1038/nature25480

55. Abedalthagafi M, Mobark N, Al-Rashed M, AlHarbi M. Epigenomics and Immunotherapeutic Advances in Pediatric Brain Tumors. *NPJ Precis Oncol* (2021) 5(1):34. doi: 10.1038/s41698-021-00173-4

56. Maleki Vareki S. High and Low Mutational Burden Tumors Versus Immunologically Hot and Cold Tumors and Response to Immune Checkpoint Inhibitors. *J Immunother Cancer* (2018) 6(1):157. doi: 10.1186/s40425-018-0479-7

57. Yang I, Tihan T, Han SJ, Wrensch MR, Wiencke J, Sughrue ME, et al. CD8+ T-Cell Infiltrate in Newly Diagnosed Glioblastoma Is Associated With Long-Term Survival. *J Clin Neurosci* (2010) 17(11):1381–5. doi: 10.1016/j.jocn.2010.03.031

58. Galon J, Rossi J, Turcan S, Danan C, Locke FL, Neelapu SS, et al. Characterization of Anti-CD19 Chimeric Antigen Receptor (CAR) T Cell-Mediated Tumor Microenvironment Immune Gene Profile in a Multicenter Trial (ZUMA-1) With Axicabtagene Ciloleucel (Axi-Cel, KTE-C19). *J Clin Oncol* (2017) 35(15_suppl):3025–5. doi: 10.1200/JCO.2017.35.15_suppl.3025

59. Spranger S, Dai D, Horton B, Gajewski TF. Tumor-Residing Batf3 Dendritic Cells Are Required for Effector T Cell Trafficking and Adoptive T Cell Therapy. *Cancer Cell* (2017) 31(5):711–23.e714. doi: 10.1016/j.ccell.2017.04.003

60. Bockmayr M, Mohme M, Klauschen F, Winkler B, Budczies J, Rutkowski S, et al. Subgroup-Specific Immune and Stromal Microenvironment in Medulloblastoma. *Oncoimmunology* (2018) 7(9):e1462430. doi: 10.1080/2162402x.2018.1462430

61. Bailey CP, Wang R, Figueroa M, Zhang S, Wang L, Chandra J. Computational Immune Infiltration Analysis of Pediatric High-Grade Gliomas (pHGGs) Reveals Differences in Immunosuppression and Prognosis by Tumor Location. *Comput Syst Oncol* (2020) n/a(n/a):e1016. doi: 10.1002/cso2.1016

62. Lieberman NAP, DeGolier K, Kovar HM, Davis A, Hoglund V, Stevens J, et al. Characterization of the Immune Microenvironment of Diffuse Intrinsic Pontine Glioma: Implications for Development of Immunotherapy. *Neuro Oncol* (2019) 21(1):83–94. doi: 10.1093/neuonc/noy145

63. Yang J, Hu L. Immunomodulators Targeting the PD-1/PD-L1 Protein-Protein Interaction: From Antibodies to Small Molecules. *Med Res Rev* (2019) 39 (1):265–301. doi: 10.1002/med.21530

64. Galluzzi L, Buqué A, Kepp O, Zitvogel L, Kroemer G. Immunological Effects of Conventional Chemotherapy and Targeted Anticancer Agents. *Cancer Cell* (2015) 28(6):690–714. doi: 10.1016/j.ccell.2015.10.012

65. Krombach J, Hennel R, Brix N, Orth M, Schoetz U, Ernst A, et al. Priming Anti-Tumor Immunity by Radiotherapy: Dying Tumor Cell-Derived DAMPs Trigger Endothelial Cell Activation and Recruitment of Myeloid Cells. *Oncoimmunology* (2019) 8(1):e1523097. doi: 10.1080/2162402x.2018.1523097

66. Friedman GK, Johnston JM, Bag AK, Bernstock JD, Li R, Aban I, et al. Oncolytic HSV-1 G207 Immunovirotherapy for Pediatric High-Grade Gliomas. *N Engl J Med* (2021) 384(17):1613–22. doi: 10.1056/NEJMoa2024947

67. Prendergast GC, Mondal A, Dey S, Laury-Kleintop LD, Muller AJ. Inflammatory Reprogramming With IDO1 Inhibitors: Turning Immunologically Unresponsive 'Cold' Tumors 'Hot'. *Trends Cancer* (2018) 4(1):38–58. doi: 10.1016/j.trecan.2017.11.005

# The Clinical and Prognostic Impact of the Choice of Surgical Approach to Fourth Ventricular Tumors in a Single-Center, Single-Surgeon Cohort of 92 Consecutive Pediatric Patients

Nicola Onorini[1], Pietro Spennato[1], Valentina Orlando[1,2], Fabio Savoia[3], Camilla Calì[3], Carmela Russo[4], Lucia De Martino[5], Maria Serena de Santi[1], Giuseppe Mirone[1], Claudio Ruggiero[1], Lucia Quaglietta[5] and Giuseppe Cinalli[1*]

[1] Department of Pediatric Neurosciences, Pediatric Neurosurgery Unit, Santobono-Pausilipon Children's Hospital, Naples, Italy, [2] Division of Neurosurgery, Department of Neurosciences, Reproductive and Odontostomatological Sciences, Università degli Studi di Napoli Federico II, Naples, Italy, [3] Evaluative Epidemiology-Childhood Cancer Registry of Campania, Santobono-Pausilipon Children's Hospital, Naples, Italy, [4] Department of Pediatric Neurosciences, Pediatric Neuroradiology Unit, Santobono-Pausilipon Children's Hospital, Naples, Italy, [5] Department of Pediatric Neurosciences, Pediatric Neuro-Oncology Unit, Santobono-Pausilipon Children's Hospital, Naples, Italy

**Objective:** A single-institution cohort of 92 consecutive pediatric patients harboring tumors involving the fourth ventricle, surgically treated *via* the telovelar or transvermian approach, was retrospectively reviewed in order to analyze the impact of surgical route on surgery-related outcomes and cumulative survival.

**Methods:** Clinical, radiological, surgical, and pathology details were retrospectively analyzed. We selected n = 6 surgery-related clinical and radiological outcomes: transient and permanent neurological deficits, duration of assisted ventilation, postoperative new onset medical events, postoperative cerebellar mutism, and extent of resection. We built univariate and multivariate logistic models to analyze the significance of relationships between the surgical routes and the outcomes. Cumulative survival (CS) was estimated by the cohort approach.

**Results:** There were 53 girls and 39 boys (mean age, 83 months). Telovelar approach was performed in 51 cases and transvermian approach in 41 cases. Early postoperative MRI studies showed complete removal in 57 cases (62%) and measurable residual tumor in 35 cases (38%). The average tumor residual volume was 1,316 cm$^3$ (range, 0.016–4.231 cm$^3$; median value, 0.9875 cm$^3$). Residual disease was more often detected on immediate postop MRI after telovelar approach, but the difference was not significant. Cerebellar mutism was observed in 10 cases (11%). No significant difference in the onset of cerebellar mutism was detected between telovelar and transvermian approach.

The choice of surgical approach did not significantly modify any other postoperative outcome and 1-/3-year CS of high-grade surgically treated tumors.

**Conclusions:** With the limitation of a single-center, single-surgeon retrospective series, our findings offer significant data to reconsider the real impact of the choice of the surgical route to the fourth ventricle on the incidence of cerebellar mutism and surgery-related morbidity. This seems to be in line with some recent reports in the literature. Surgical approach to the fourth ventricle should be individualized according to the location of the tumor, degree of vermian infiltration, and lateral and upward extension. Telovelar and transvermian approaches should not be considered alternative but complementary. Pediatric neurosurgeons should fully master both approaches and choose the one that they consider the best for the patient based on a thorough and careful evaluation of pre-operative imaging.

Keywords: fourth ventricle, telovelar, transvermian, cerebellar mutism, children

# INTRODUCTION

The surgical strategy to access the fourth ventricle has evolved over time in order to minimize the surgical invasiveness and maximize the degree of surgical resection (1–5). Along this line, the telovelar approach (6–11) was introduced to avoid the anatomical damage of the classic transvermian route (3, 4, 8) and the potential consequences in terms of postoperative cerebellar mutism (12, 13).

The aim of our study was to analyze the impact of the choice of the surgical route to the fourth ventricle on the incidence of cerebellar mutism (CM) and surgery-related morbidity in children.

# MATERIALS AND METHODS

## Patient Population: Criteria of Inclusion/Exclusion

From January 2007 to June 2018, 215 patients below 18 years of age were operated for neoplasms of the posterior fossa at the Department of Pediatric Neurosurgery of Santobono-Pausilipon Children's Hospital of Naples. The patient was considered eligible for this study if 1) there is primary diagnosis without previous surgeries, 2) the tumor was located into the fourth ventricle, 3) it invaded the fourth ventricle from adjacent anatomical structure, or 4) its removal required surgical approach to the fourth ventricle.

Exclusion criteria were the following: 1) relapsed or progressing cases first treated before January 2007, 2) cerebellar hemispheric tumors, 3) brainstem tumors without predominant (>50%) exophytic component into the fourth ventricle, 4) tumors of the cerebellopontine angle without fourth ventricular involvement, 5) pineal tumor, and 6) purely aqueductal tumors.

The retrospective analysis of our study covers a period from January 2007 to June 2018. The Senior author started using the telovelar approach from 2001. The tumors of the fourth ventricle treated from 2001 to 2006 were excluded from our analysis in order to avoid the bias of the possible conversion from the telovelar to the transvermian approach.

The selected cases were classified in the following six main groups: (A) intraventricular, (B) mesencephalo-aqueductal tumors, (C) cerebellar/vermian tumors, (D) cerebellopontine angle tumors extending to the fourth ventricle, (E) brainstem tumors with exophytic fourth ventricular component, and (F) large tumors with extensive posterior fossa involvement, including the fourth ventricle (**Figure 1**).

## Clinical and Neuroimaging Data

Medical records, neuroimaging studies, and operative and pathological reports were retrospectively analyzed.

Clinical and neurological status before surgery and new transient (<1 year after surgery) or permanent (>1 year after surgery) postoperative neurological deficits and cerebrospinal fluid (CSF)-related complications were identified. Postoperative infections, new onset medical conditions, days of mechanical ventilation, and intensive care unit length of stay were also analyzed.

Before 2016, we identified CM in cases of muteness with delayed onset and limited duration, following posterior fossa surgery, usually presenting with other neurological sings/symptoms: emotional lability, hypotonia, ataxia, long tract sings, and cranial nerve palsy. Since 2016, the Iceland Delphi Group diagnostic criteria (14) for CM have been adopted in our Institution.

All patients with postoperative CM underwent early postoperative neuropsychological assessment (<72 h) exploring: attention, memory, executive functions, processing speed, and cognitive efficiency (although in absence of a standardized institutional protocol) and also full preoperative and late postoperative (1, 3, and 12 months) complete neuropsychological assessment.

All patients were studied using brain CT scan and/or brain and spinal cord contrast-enhanced MRI scan on a 1.5-T machine. MRI sequences used for anatomical classification were T1w without and with injection, T2w turbo spin-echo, T2w fast spin-echo, DRIVE, and balanced fast-field echo (B-FFE). These sequences allowed to classify uni- or bilateral involvement of the foramina of
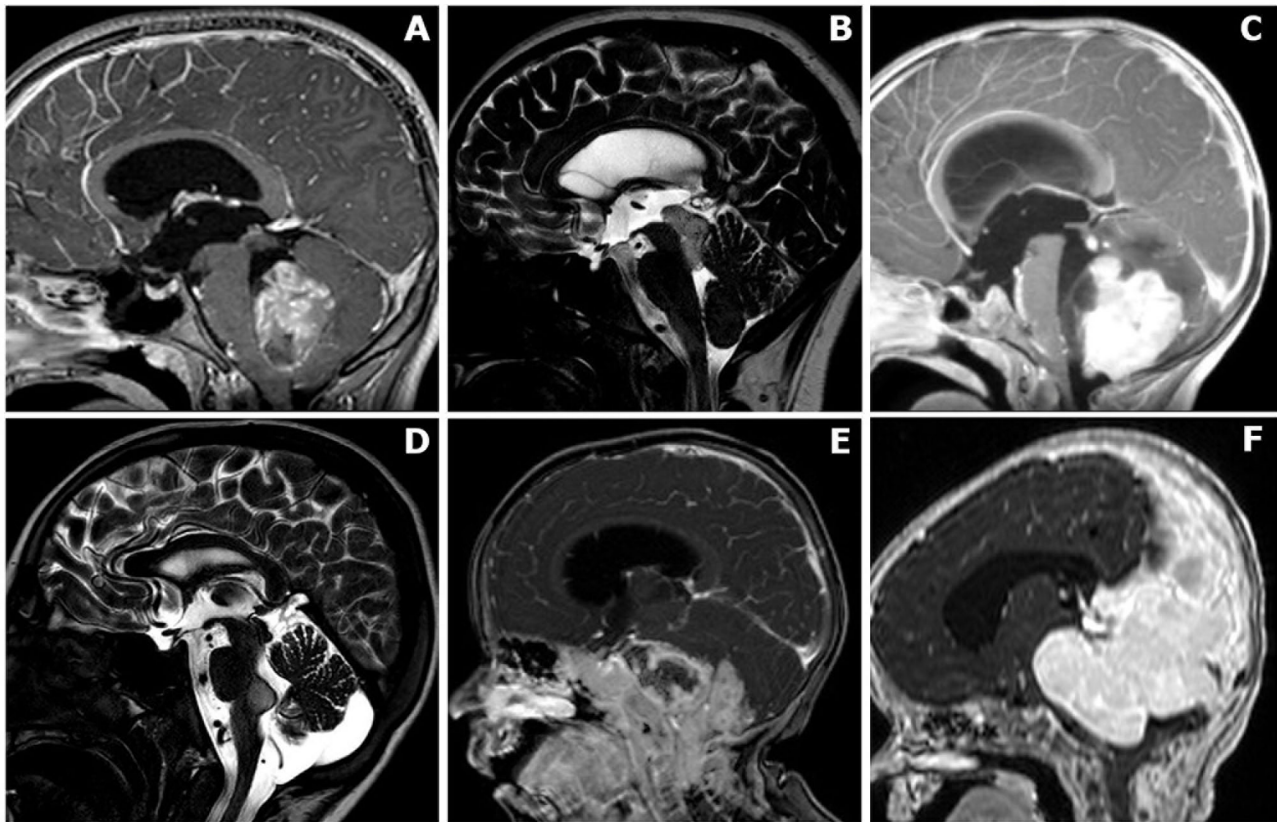
**FIGURE 1** | Anatomical classification of posterior fossa tumors requiring surgical access to the fourth ventricle. **(A)** Mainly/purely intraventricular, without evident brainstem infiltration or extensive vermian infiltration. **(B)** Midbrain/intra-aqueductal tumor with significant bulging in the upper part of the fourth ventricle. **(C)** Cerebellar/vermian tumor with extensive parenchymal/vermian infiltration and secondary bulging into the fourth ventricle. **(D)** Cerebellopontine angle tumors extending into the fourth ventricle through the Luschka foramen/foramina. **(E)** Brainstem tumors with dorsally exophytic fourth ventricular component. **(F)** Giant tumors with extensive posterior fossa involvement, including a significant fourth ventricle component..

Luschka, caudal extension through the foramen of Magendie, vermian and brainstem infiltration, and cerebellar tonsillar herniation below the foramen magnum.

All patients received postoperative MRI within 24 h to assess the following: extent of resection (EOR%), residual tumor volume (cm$^3$) and location, and postoperative complications. Flow void sign through the endoscopic third ventriculostomy (ETV) was sought on T2-w sagittal cuts.

Tumor preoperative volume (cm$^3$) and tumor residual volume (cm$^3$) were calculated for each patient independently by two authors (NO and VO) using 3D volumetric sequences in Horos TM 3.3.5 (GNU General Public License, version 3.0) on the basis of axial sections on 3D T1-w FFE contrast-enhanced images. In case of computational disagreement, an arbitrary difference of 5% of the largest calculation was set as the limit for revision by a third author (CR). Preoperative tumor volumes were split into three homogeneous groups using two tertiles.

## Surgery

Every attempt was done not to open the posterior fossa in the presence of untreated hydrocephalus. Endoscopic third ventriculostomy (ETV), external ventricular drain (EVD), or ventriculoperitoneal (VP) shunt were performed, if necessary, at presentation by the neurosurgeon on call at the time of admission in agreement with senior author indications, depending on clinicoradiological features (age, metastases, clinical conditions, anatomy of third ventricle floor, and available surgical theater).

All patients were operated in the prone position through a median suboccipital craniotomy. The senior author decided the surgical approach on preoperative neuroimaging without randomization.

Intraoperative macroscopic evidence of vermian and/or brainstem infiltration and extension of cervical laminectomy/laminotomy, dural opening, and closing of posterior fossa dural defect were noted. Anesthesia records provided information on clinical parameters during surgery.

Surgical microscope was used in all cases, and all procedures were recorded (Zeiss® OPMI®/NC4 microscope; Zeiss® OPMI®/Pentero® 800 microscope).

Since 2009, intraoperative neuronavigation system was routinely used (Medtronic® StealthStation Treon Plus® Surgical Navigation System; Medtronic® StealthStation S7® and S8® Surgical Navigation System). The CUSA® Excel® ultrasonic aspiration

system was used in all cases, changing the irrigation, aspiration, amplitude, and tissue select modes in relation to the specific situation. Self-retaining flexible retractors are adopted in all procedures.

Neurophysiological intraoperative monitoring (IOM) was used in case of dorsal exophytic brainstem tumor, brainstem infiltration, fourth ventricle tumor with cerebellopontine angle (CPA) involvement, and tumor extending through the foramen magnum.

## Follow-Up and Adjuvant Therapy

All follow-up MRI studies were retrospectively reviewed to assess the presence and timing of recurrence or regrowth of residual tumor. The timing of follow-up MRI was adapted according to pathological results and intercurrent modifications of neurological status. We considered as the most recent follow-up the date of the last MRI study and consequent neurosurgical/oncological examination.

Patients enrolled in this study were all evaluated by a multidisciplinary team and treated according to national guidelines. Treatment protocols of the Italian Society of Pediatric Oncology were followed for adjuvant treatment in case of medulloblastoma, ependymoma, and AT-RT. Standard treatment options for childhood low-grade gliomas included follow-up and surgery in case of residual tumor or recurrence; radiotherapy was rarely indicated and only in case of failure of surgery to achieve complete resection or if surgery was considered too dangerous for neurological function.

## Statistical Analysis

Six post-surgical outcomes were analyzed: transient and permanent neurological deficits (respectively: <1 and >1 year after surgery), duration of assisted ventilation (two groups with 48 h cut-off), postoperative new onset medical events (yes–no), postoperative CM (yes–no), and extent of resection (three groups: no residual disease, residual volume <1.5 or > 1.5 cm$^3$).

We built univariate and multivariate logistic models for every outcome. We calculated odds ratios (OR) and 95% confidence interval (95% CI), and we analyzed the significance of relationships between the outcomes and the covariate variables ($p < 0.05$ was considered significant). In logistic regression, the maximum likelihood estimation suffered from small-sample bias, so in our analysis, we choose to use the penalized maximum likelihood estimation proposed by Firth: always in multivariate analysis and in the univariate analysis when one of the number of events resulted equal to zero. The postoperative tumor residual volume is an ordinal outcome, so the ordered logistic model was applied to estimate its relationship with the set of covariates (both in univariate and multivariate analysis).

Cumulative survival (CS) was estimated by the cohort approach. One- and 3-year cumulative survival was analyzed in relation to histological grading (WHO 1–2 vs. WHO 3–4), histological subtype (medulloblastoma, pilocytic astrocytoma, and ependymomas), and surgical approach (telovelar approach–transvermian approach for high-grade tumors) and was calculated using the Kaplan–Meier method. The confidence intervals (95% CI) of the survivor functions were obtained using Greenwood's formula. The survival distributions were compared using the log-rank test ($p < 0.05$ was considered significant). For the surgical approach, the power of predicting factors (surgical approach and postoperative residual tumor volume) was evaluated in a Cox proportional hazard model.

The analyses were performed using a commercially available software (Stata 15/MP2).

# RESULTS

## Clinical Presentation, Radiology, and Pathology

Ninety-two patients met the inclusion criteria. There were 53 girls (58%) and 39 boys (42%). The mean age at the time of diagnosis was 83 months (range, 1 month–17.3 years). Thirty-four tumors were low grade (WHO grade 1–2), and 58 tumors were high grade (WHO 3–4). Details of clinical and radiological presentation and tumor anatomical features are shown in **Table 1**.

Brain MRI was performed in 89 patients (3 not performed due to emergency surgery). In six patients, tumor volume was not computable due to lack of the specific postop MRI volumetric sequences. In the remaining 86 patients, median tumor volume was 25.21 cm$^3$ (range, 0.529–137.696 cm$^3$). Tumor volumes were classified into three homogeneous groups: <15, 15–26, and >26 cm$^3$, using the two tertiles.

The main differences in the choice of the approach were dictated by the anatomical pattern of the tumor: telovelar was chosen exclusively for tumors of the aqueduct bulging in the fourth ventricle and intraventricular extension of CPA tumors and almost exclusively for dorsally exophytic brainstem tumors. For pure intraventricular tumors or for tumors expanding into the cisterna magna or in the cervical canal, the telovelar approach was predominantly chosen. The only group where the choice of transvermian was predominant was the group with extensive vermian infiltration. Telovelar approach was also preferred when the tumor was <15 cm$^3$ (**Table 1**). Telovelar approach was more frequently chosen for all ependymoma subtype and for AT-RT (**Table 1**).

## Surgery

Telovelar approach was performed in 51 cases and transvermian approach in 41 cases. Details of operative features are listed in **Table 2**. Twenty-eight children (30%) were re-operated for progressing and/or relapsing disease. Multiple surgical procedures were performed in nine patients (range, 2–4 procedures for each patient).

Early postoperative MRI studies showed complete removal in 57 cases (62%) and measurable residual tumor in 35 cases (38%). The volume of residual disease could be measured in 33 cases (missing MRI sequences in two cases). The average tumor residual volume was 1.316 cm$^3$ (range, 0.016–4.231 cm$^3$; median value, 0.9875 cm$^3$). Large residuals (>1.5 cm$^3$) were equally distributed between telovelar (6) and transvermian approaches (4), whereas smaller residuals (<1.5 cm$^3$) where more frequently left using the telovelar (15 cases) than the transvermian approach (8 cases), but these

| | | Total No. (%) | Telovelar No. (%) | Transvermian No. (%) |
|---|---|---|---|---|
| **Age at diagnosis** | <6 months | 7 (7) | 6 (86) | 1 (14) |
| | 6 months–5 years | 21 (23) | 14 (67) | 7 (33) |
| | >5 years | 64 (70) | 31 (48) | 33 (52) |
| **Incidental diagnosis** | | 3 (3) | 3 | 0 |
| **Neurological assessment**[1] | ICH | 81 (91) | 43 (53) | 38 (47) |
| | Cerebellar syndrome | 34 (38) | 15 (47) | 18 (53) |
| | CN palsy | 29 (33) | 16 (55) | 13 (45) |
| | Various[2] | 36 (39) | 19 (52) | 17 (48) |
| **Anatomical pattern** | Fourth ventricle (pure) | 23 (25) | 14 (61) | 9 (39) |
| | + Mes./Aq. | 4 (4) | 4 | 0 |
| | + Verm./Cerebell. | 48 (53) | 16 (33) | 32 (67) |
| | + CPA | 4 (4) | 4 | 0 |
| | + BS dorsally exophytic | 12 (13) | 11 (92) | 1 (8) |
| | + Entire PCF | 1 (1) | 1 | 0 |
| **Lateral extension** | No | 39 (42) | 18 (46) | 21 (54) |
| | Unilateral | 34 (37) | 21 (62) | 13 (38) |
| | Bilateral | 19 (21) | 12 (63) | 7 (37) |
| **Caudal extension** | No | 23 (25) | 12 (52) | 11 (48) |
| | Magendie | 37 (40) | 15 (42) | 22 (58) |
| | + Cisterna magna | 20 (22) | 15 (75) | 5 (25) |
| | + Cervical spinal canal | 12(13) | 9 (75) | 3 (25) |
| **BS involvement** | No | 52 (57) | 25 (48) | 27 (52) |
| | BS infiltration | 28 (30) | 15 (54) | 13 (46) |
| | BS dorsally exophytic | 12 (13) | 11 (92) | 1 (8) |
| **Hydrocephalus** | No | 22 (24) | 15 (68) | 7 (32) |
| | Yes | 70 (76) | 36 (51) | 34 (49) |
| **Tumor volume**[3] | <15 cm$^3$ | 28 (33) | 20 (71) | 8 (29) |
| | 15–26 cm$^3$ | 30 (34) | 15 (50) | 15 (50) |
| | >26 cm$^3$ | 28 (33) | 14 (50) | 14 (50) |
| **Histological subtypes**[4] | Medulloblastoma | 37 (40) | 16 (43) | 21 (57) |
| | Pilocytic astrocytoma | 28 (30) | 13 (46) | 15 (54) |
| | Ependymoma | 7 (8) | 4 (57) | 3 (43) |
| | Anaplastic ependymoma | 6 (7) | 5 (83) | 1 (17) |
| | ATRT | 6 (7) | 5 (83) | 1 (17) |
| | Various | 8 (8) | 8 (8) | 0 |
| **Oncogenic syndromes** | NF-1 | 4 (4) | 2 (50) | 2 (50) |
| | Turcot syndrome | 1 (1) | 0 | 1 |
| **Gene mutations** | ALC-RET | 1 (1) | 1 | 0 |
| | AUTS2 | 1 (1) | 0 | 1 |

CN, cranial nerve; Mes., mesencephalic; Aq., aqueductal; Ver., vermian; Cerebell, cerebellar; CPA, cerebellopontine angle; BS, brainstem; ICH, intracranial hypertension; PCF, posterior cranial fossa; CE, contrast enhancement; ATRT, atypical teratoid/rhabdoid tumor; NF-1, neurofibromatosis type 1; ALC-RET, ALC-RET gene mutation; AUTS2, AUTS2 gene mutation.
[1]Most patients presented with more than one sign/symptom.
[2]Various: torticollis, evolutive macrocrania, diffuse hypotonia, opisthotonic posturing, irritability.
[3]We used two tertiles to split volumetric data into three groups. N = 86 computable MRI sequences for volumetric analysis.
[4]According to the 2016 WHO Classification of Tumors of the Central Nervous System.

differences were not significant. Details of extension of resection (EOR%), volumetric quantification of residual disease (cm$^3$), and specific locations of residual disease are listed in **Table 2**.

## Surgery-Related Complications

Postoperative radiological adverse events were identified on 18 postoperative MRI (20%) (**Table 2**), and only 2 of these events required surgical treatment: within 48 h in one case (cerebellar swelling, treated with EVD) and beyond 48 h in another one case (epidural hematoma from Mayfield pin).

Postoperative CSF-related complications are described in **Table 2**. Pseudomeningocele was resolved by lumbar puncture in almost all cases (mean number, n = 2; range, 1–4) except in two patients who required lumbar spinal drainage.

## Management of Hydrocephalus

Hydrocephalus at onset required CSF-diversion procedures in 65 cases (93%). Early radiological signs of ETV failure were detected in 10 cases (26%). Among treated cases, 14 children (22%) developed postoperative hydrocephalus.

Seven cases of mild preoperative hydrocephalus were referred directly to surgery within 24 h and developed early postoperative hydrocephalus in two cases. Seven patients without preoperative hydrocephalus required CSF-diversion procedures.

Overall, in the long term, 23 children of our population required permanent VP shunt (25%). Patients treated preoperatively by ETV required permanent VP shunt in 19% of the cases, whereas patients treated with pre- or intraoperative EVD required permanent VP shunt in 8% of the cases. Other differences in hydrocephalus

**TABLE 2 |** Surgery and postoperative clinical/radiological assessment.

| | Total No. (%) | Missing data | Telovelar No. (%) | Transvermian No. (%) |
|---|---|---|---|---|
| **C1 laminectomy** | 80 (88) | n = 1 | 51 (64) | 29 (36) |
| **C1 + C2 laminotomy** | 3 (3) | n = 1 | 3 | 0 |
| **Intraoperative changes of CVP** | 13 (16) | n = 11 | 11 (85) | 2 (15) |
| **Macroscopic evidence of BS involvement** | 38 (43) | n = 1 | 26 (68) | 12 (32) |
| **Macroscopic evidence of CV infiltration** | 48 (53) | n = 1 | 15 (31) | 33 (69) |
| **Transient neurological deficit [1]** | 48 (53) | n = 1 | 26 (54) | 22 (46) |
| Cerebellar syndrome | 25 (28) | | 16 (64) | 9 (36) |
| Upper CN palsy | 23 (26) | | 14 (61) | 9 (39) |
| Pyramidal syndrome | 14 (16) | | 8 (57) | 6 (43) |
| Cerebellar mutism | 10 (11) | | 4 (40) | 6 (60) |
| Dysphagia | 7 (8) | | 4 (57) | 3 (43) |
| Dysphonia | 3 (3) | | 3 | 0 |
| **Permanent neurological deficit[1]** | 25 (31) | n = 11 [2] | 16 (64) | 9 (36) |
| CN palsy | 16 (20) | | 10 (63) | 6 (47) |
| Cerebellar syndrome | 14 (18) | | 7 (50) | 7 (50) |
| Pyramidal syndrome | 9 (11) | | 5 (56) | 4 (44) |
| Dysphagia | 2 (3) | | 1 (50) | 1 (50 |
| **Mechanical ventilation** | | n = 1 | | |
| <48 h | 80 (88) | | 41 (51) | 39 (49) |
| >48 h | 11 (12) | | 8 (73) | 3 (27) |
| **Medical morbidity** | 19 (21) | | 14 (74) | 5 (26) |
| **CSF-related complications** | | | | |
| Pseudomeningocele | 21 (23) | | 9 (43) | 12 (57) |
| CSF leak | 7 (8) | | 4 (57) | 3 (43) |
| CSF infections <1 month | 4 (4) | | 2 (50) | 2 (50) |
| CSF infections >1 month | 1 (1) | | 0 | 1 (50) |
| **Residual disease volume** | | n = 2 | | |
| No residual disease | 57 (63) | | 28 (49) | 29 (51) |
| <1.5 cm$^3$ | 23 (26) | | 15 (65) | 8 (35) |
| >1.5 cm$^3$ | 10 (11) | | 6 (60) | 4 (40) |
| **EOR[3]** | | n = 2 | | |
| Total | 57 (63) | | 29 (51) | 28 (49) |
| Subtotal (>90%) | 21 (24) | | 13 (62) | 8 (38) |
| Partial (<90%) | 12 (13) | | 8 (67) | 4 (43) |
| **Location of residual disease[3]** | 33 | n = 2 | | |
| Brainstem/floor of the fourth ventricle | 18 (55) | | 12 (67) | 6 (33) |
| Fastigium/CV | 10 (30) | | 6 (60) | 4 (40) |
| Various | 8 (42) | | 4 (50) | 4 (50) |
| **Radiological adverse events** | 18 (20) | | | |
| Intraventricular blood clots | 8 (9) | | 2 (25) | 6 (75) |
| Pericerebellar fluid collections | 6 (7) | | 2 (33) | 4 (67) |
| Ischemia (PICA territory) | 1 (1) | | 1 | 0 |
| Epidural hematoma | 1 (1) | | 0 | 1 |
| Cerebellar swelling | 1 (1) | | 1 | 0 |
| **CSF-diversion procedures[4]** | 65 (93) | | | |
| ETV | 43 (66) | | 22 (51) | 21 (49) |
| EVD | 13 (20) | | 5 (38) | 8 (62) |
| VPS | 9 (14) | | 8(89) | 1 (11) |
| **Postoperative ETV patency (<48 h)** | 29 (74) | n = 4 | 14 (48) | 15 (52) |
| **Postoperative ETV failure (<48 h)** | 10 (26) | n = 4 | 6 (60) | 4 (40) |
| **Postoperative hydrocephalus** | | | | |
| Preop. CSF-diversion procedures | 14 (22[4]) | | 9 (64) | 5 (36) |
| No preop. CSF-diversion procedures | 2 (40[4]) | | 0 | 2 |
| No hydrocephalus at onset | 7 (32[4]) | | 5 (71) | 2 (29) |
| **Permanent VPS** | 23 (25) | | 17 (74) | 6 (26) |

*CVP, cardiovascular parameters; CT, computed tomography; BS, brainstem; CV, cerebellar vermis; CN, cranial nerve; CSF, cerebrospinal fluid; EOR, extension of resection; ETV, endoscopic third ventriculostomy; EVD, external ventricular drainage; VPS, ventriculo-peritoneal shunt; preop., preoperative.*
*[1]Most patients presented with more than one sign/symptom.*
*[2]n = 11 patients died before 1 year of follow-up.*
*[3]n = 3 cases of multiple location.*
*[4]n = 65 (93%) of n = 70 patients with hydrocephalus at onset were treated with CSF-diversion procedures; n = 5 (7%) patients with hydrocephalus were referred directly to surgery; in n = 22 cases, preoperative hydrocephalus was not detected (see Table 1).*

treatment and outcome between the two groups are shown in **Table 2**.

## Postoperative Course

According to the aforementioned diagnostic criteria, cerebellar mutism was identified in 10 children (11%) (**Table 2**). In all cases, the onset of speech loss appeared within 4 days after surgery. The duration of mute phase lasted up to 15 days in eight cases (80%) and up to 30 days in two cases (20%); nine patients (90%) exhibited dysarthria after remission of mutism, with long-term persistence of motor speech deficits in six cases (60%).

When considering the approach chosen, no significant difference in the onset of CM was detected between telovelar and transvermian approach (**Table 3**).

Postoperative new-onset transient neurological deficits were assessed in 48 cases (53% of 91 cases analyzed; multiple deficits in 69%) and are listed in **Table 2**. No differences were found between the two approaches (**Table 3**).

Postoperative permanent neurological deficits (persistent >1 year of follow-up) were assessed in 25 patients (31% of 81 patients: 11 patients died before 1 year of follow-up; multiple permanent deficits in 56%) (see **Table 2**). This incidence was not modified by the choice of the approach (**Table 3**).

Postoperative new onset medical events and duration of mechanical ventilation following the first surgery are shown in **Table 2**, and both were not influenced by the surgical approach (**Table 3**).

Average intensive care unit length of stay, consequent to the first surgery, was 3 days (range, 1–26 days), and no differences were found between the two approaches (**Table 3**).

Residual disease was more often detected on immediate postop MRI after telovelar approach, but the difference was not significant (**Table 3**).

Overall, in univariate and multivariate analyses, neither telovelar nor transvermian approach modified significantly any postoperative outcome analyzed.

## Follow-Up and Adjuvant Therapy

Mean clinical–radiological follow-up was 55.5 months (range, 0–136 months). In detail, during radiological surveillance after first radical surgery (n = 57 cases of no residual disease), 43 cases (75%) remained stable without relapse, and 14 cases relapsed (25%). Among the cases with residual disease (n = 35), 18 cases (51%) did not progress, 14 cases (40%) progressed, and 3 cases (9%) progressed and, then, after surgical resection, relapsed. Twenty-one cases (23%) suffered from tumoral dissemination or metastasis.

According to the last clinical examination and radiological evaluation, we categorized our patients in three main groups: ANED (alive with no evidence of disease), n = 45 cases (49%); AWED (alive with evidence of disease), n = 24 cases (26%); and DOD (died of disease), n = 23 cases (25%).

Two patients died due to chemotherapy complications. One patient, suffering from tumor predisposition syndrome, died due to leukemia.

**TABLE 3 |** Surgical approach and postoperative outcomes.

| | Transient deficit | | | | | | | | | |
|---|---|---|---|---|---|---|---|---|---|---|
| | Yes | | No | | Univariate analysis | | | Multivariate analysis* | | |
| | n | % | n | % | OR | 95% CI | p | OR | 95% CI | p |
| Telovelar | 26 | 52 | 24 | 48 | | | | | | |
| Transvermian | 22 | 54 | 19 | 45 | 1.07 | 0.47–2.44 | 0.88 | 1.28 | 0.39–4.15 | 0.68 |
| **Permanent deficits** | | | | | | | | | | |
| | Yes | | No | | | | | | | |
| Telovelar | 16 | 36 | 28 | 64 | | | | | | |
| Transvermian | 9 | 24 | 28 | 76 | 0.56 | 0.21–1.48 | 0.25 | 0.86 | 0.21–3.43 | 0.83 |
| **Ventilation** | | | | | | | | | | |
| | >48 h | | <48 h | | | | | | | |
| Telovelar | 8 | 16 | 41 | 84 | | | | | | |
| Transvermian | 3 | 7 | 39 | 93 | 0.39 | 0.10–1.59 | 0.19 | 1.26 | 0.17–9.61 | 0.82 |
| **Cerebellar mutism** | | | | | | | | | | |
| | Yes | | No | | | | | | | |
| Telovelar | 4 | 8 | 46 | 92 | | | | | | |
| Transvermian | 6 | 15 | 35 | 85 | 1.97 | 0.52–7.51 | 0.32 | 0.81 | 0.16–4.12 | 0.81 |
| **Medical events** | | | | | | | | | | |
| | Yes | | No | | | | | | | |
| Telovelar | 14 | 28 | 36 | 72 | | | | | | |
| Transvermian | 5 | 12 | 37 | 88 | 0.35 | 0.11–1.06 | 0.06 | 0.26 | 0.06–1.23 | 0.09 |

| | Residual disease | | | | | | | | | | | |
|---|---|---|---|---|---|---|---|---|---|---|---|---|
| | No | | <1.5 cm³ | | >1.5 cm³ | | Univariate analysis** | | | Multivariate analysis** | | |
| | n | % | n | % | n | % | OR | 95% CI | p | OR | 95% CI | p |
| Telovelar | 28 | 57 | 15 | 31 | 6 | 12 | | | | | | |
| Transvermian | 29 | 71 | 8 | 19 | 4 | 10 | 0,58 | 0.24–1.37 | 0.21 | 0.44 | 0.12–1.60 | 0.22 |

*Penalized maximum likelihood estimation.*
**Ordered logistic model.**

No intraoperative death was documented. Eleven children died before 1 year from the diagnosis; of these, 1 perioperatory death was assessed (a child admitted in coma and bilateral mydriasis), 1 patient died of postoperative respiratory complications, and 9 deaths were related to the aggressive tumor behavior.

One- and 3-year CS were analyzed in relation to histological grading (WHO 1–2 vs. WHO 3–4), showing, as expected, a better 1- and 3-year CS for low-grade group (log-rank test, p = 0.0001) (see **Figure 2A**).

One- and 3-year CS for medulloblastoma, pilocytic astrocytoma, ependymomas, and anaplastic ependymomas are reported in **Figure 2B** (log-rank test, p = 0.03).

Considering the choice of surgical approach for high-grade tumors (58 cases), we found a better 1- and 3-year CS of tumors
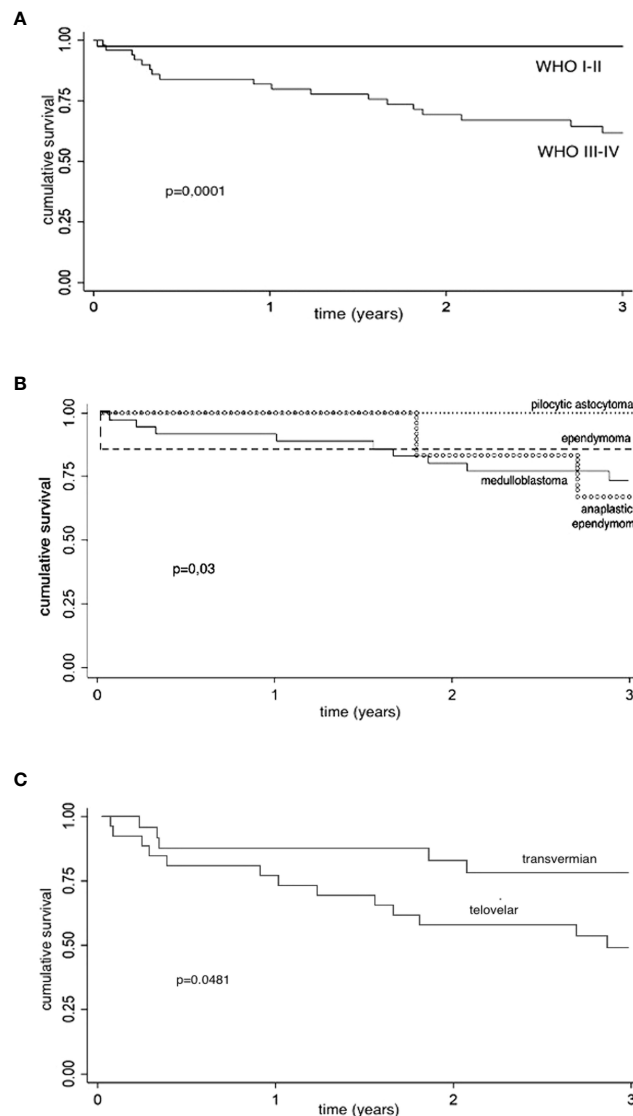


**FIGURE 2** | Kaplan–Meier survival estimates. CS, cumulative survival; CI, confidence interval; y, year. **(A)** Kaplan–Meier survival estimates (histological grading): 1- and 3-year CS are analyzed in relation to histological grading (WHO 1–2 vs. WHO 3–4), showing a better 1- and 3-year CS for low-grade group (log-rank test, p = 0.0001). Low-grade tumors: 1-year CS, 97.6% (95% CI: 83.9%–99.7%); 3-year CS, 97.6% (95% CI: 83.9%–99.7%). High-grade tumors: 1-year CS, 82% (95% CI: 68.2%–90.2%); 3-year CS: 62% (95% CI: 46.4%–74.2%). **(B)** Kaplan-Meier survival estimates (histology): 1- and 3-year CS are analyzed in relation to histology (log-rank test, p = 0.03). Pilocytic astrocytoma: 1- and 3-year CS, 100%. Non-anaplastic ependymomas: 1-y CS, 85.7% (95% CI: 33.4%–97.9%); 3-year CS, 85.7% (95% CI, 33.4%–97.9%). Medulloblastomas: 1-year CS, 91.9% (95% CI, 76.9%–97.3%); 3-year CS, 73.6% (95% CI: 55.1%–85.4%). Anaplastic ependymomas: 1-year CS, 100%; 3-year CS, 66.7% (95% CI: 19.5%–90.4%). **(C)** Kaplan–Meier survival estimates (surgical approach for high-grade tumors): Considering the choice of surgical approach for high-grade tumors (WHO 3–4), we found better 1- and 3-years CS of transvermian approach when compared to telovelar approach with statistical significance (log-rank test, p = 0.048). Telovelar approach: 1-year CS, 76.9% (95% CI: 55.7%–88,9%); 3-year CS, 48.8% (95% CI, 28.5%–66.4%). Transvermian approach: 1-year CS, 87.5% (95% CI: 66.1%–95.8%); 3-year CS, 78% (95% CI, 54.8%–90.3%). The power of predicting factors (surgical approach for high-grade tumors and residual tumor volume) is evaluated in a Cox proportional hazard model (**Table 4**).

operated through a transvermian approach when compared with tumors operated through the telovelar with statistical significance (log-rank test, p = 0.0481) (**Figure 2C**). The power of predicting factors (surgical approach and postoperative residual tumor volume), evaluated in a Cox proportional hazard model, show that higher scores on postoperative residual tumor volume are associated with poorer prognosis (HR, 2.53). This is statistically significant (p = 0.003) (**Table 4**).

## DISCUSSION

The goals of fourth ventricular tumors surgery are to 1) obtain the largest possible safe tumor resection, 2) restore CSF circulation releasing the fourth ventricle outlets, 3) decompress the brainstem, and 4) obtain tissue sample for pathological and molecular analysis (4). Historically, the oldest and the most intuitive route to the fourth ventricle was to remove part of a cerebellar hemisphere (1). Dandy stated that the inferior cerebellar vermis could be incised at its center and split on the cerebellar suboccipital surface without any significant functional consequence, taking care to avoid excessive surgical manipulation and damage to the dentate nuclei (3).

Since Dandy's original report (3), the transvermian route has been the most used approach to access the fourth ventricle (13). Dailey (12) and other authors (15–24) considered the vermian incision by default as the main responsible for cerebellar mutism, although clear evidence of this is still lacking. Moreover, the reported more limited control of the laterality offered by this approach motivated some authors (5–11) to explore the natural corridor of the cerebellomedullary fissure (CMF) opening of the tela choroidea and the inferior medullary velum, to avoid any incision of cerebellar parenchyma. Matsushima described three main ways to dissect the CMF, approaching it on its medial or lateral side, or both (5–11).

The medial variant of the CMF opening is the so-called "telovelar approach" and was developed for intra-CMF and/or intraventricular lesions extending also into the cerebellomedullary cistern (CMC), approached *via* the midline suboccipital route (5, 6, 8, 9, 11). In cadaveric specimens, the telovelar approach allows a better operative control of the lateral aspects of the fourth ventricle (25, 26), and C1 laminectomy nullifies the advantage of the transvermian approach in terms of operative working angle when accessing the rostral fourth ventricle (26). These findings are coherent with our surgical experience.

The choice of surgical route (telovelar vs. transvermian) may depend on thorough evaluation of preoperative imaging, intraoperative features, and surgeon's preference/experience.

**TABLE 4 |** Cox regression (High-grade tumors).

|  | HR | z | p>\|z\| | 95% CI |
|---|---|---|---|---|
| Surgery | 0.47 | −1.39 | 0.165 | 0.16–1.37 |
| Residual volume (cm$^3$) | 2.53 | 2.99 | 0.003 | 1.38–4.64 |

*HR, hazard ratio; CI, confidence interval; p, p-value.*

The trend of recent literature considers the telovelar approach protective towards cerebellar mutism attributed to the vermian incision and splitting (20–24), leading us to investigate this topic in our cohort.

Postoperative CM [reported incidence, 8–32% (14, 27, 28)] is characterized by delayed onset mutism (24–48 h after surgery), reduced speech, limited duration and spontaneous recovery, usually associated with other deficits of cognitive, affective, and motor functions (13, 14, 29, 30).

Immediately after the transient mute phase, almost all children experience dysarthria (30, 31), as we have also seen in our patients (90% of 10 CM cases, in our cohort), with long-term persistence of motor speech deficits in 60% of our cases, according to other reports (30).

There are two main types of motor speech deficits: 1) a pure dysarthria with normal cognitive functions and 2) an apraxic language disorder with more complex neuropsychological correlates (30).

The severity of associated neuropsychological deficits after surgery was found to be a negative prognostic factor for long-term motor speech deficits, in terms of clinical/neuropsychological impact (30). Full recovery is often incomplete in cases of apraxic dysarthria (30, 31).

However, there is no substantial consensus regarding other prognostic factors, such as the age of onset, for long-term sequelae of CM (30).

Many surgical series, focused exclusively on the telovelar approach, show the beneficial result of this approach in preventing or reducing CM (15–24, 32). When the telovelar approach is compared with the transvermian approach (33, 34), it seems to be protective for postoperative CM and neurological morbidity, although statistical significance was only reported by Ferguson et al. (33) in a mixed adult/child series. The work of Ebrahim et al. (34) does not include adequate statistical analysis.

However, when considering larger series in everyday clinical practice, the reported advantages of telovelar approach are less evident.

Cobourn et al. (35) reported that in pediatric medulloblastomas, vermian incision seems to be a risk factor for CM.

In a retrospective multicenter analysis of 263 pediatric patients harboring posterior fossa tumors, Renne et al. (36) reported no statistical correlation between the surgical approach and postoperative CM.

Recently, Toescu et al. (37) retrospectively analyzed 167 fourth ventricle tumors in a case series of only pediatric patients, showing no significant difference in the rate of CM between telovelar or transvermian approach and no statistically significant relationships between cerebellar mutism syndrome and surgical approach.

Among the few purely pediatric fourth ventricular tumor case series published in the literature (**Table 5**), a retrospective head-to-head comparison between telovelar and transvermian approach was carried out only in one case (Toescu et al. (37). In Cobourn et al. (35), the frequency of telovelar approach was not reported. In all other studies, the impact of the surgical approach on CM has been retrospectively analyzed only in

**TABLE 5** | Surgery of fourth ventricle tumors: published pediatric case series.

| Authors, year | No of patients | Telovelar approach (%) | Transvermian approach (%) | CMS (%) | GTR (%) |
|---|---|---|---|---|---|
| Kellogg & Piatt, 1997 (15) | 11 | 100 | 0 | 0 | 81.2 |
| Rajesh et al., 2007 (18) | 15 | 100 | 0 | 13.3 | 93.3 |
| Zaheer& Wood, 2010 (19) | 20 | 100 | 0 | 30 | 70 |
| Qiu et al., 2016 (22) | 26 | 100 | 0 | 7.7 | 84.6 |
| Eissa, 2018 (24) | 40 | 100 | 0 | 2.5 | 45 |
| Atallah et al., 2019 (32) | 44 | 100 | 0 | 13.6 | 84.1 |
| Cobourn et al., 2020 (35) | 63 | * | 53.8 | 10.8 | NR |
| Toescu et al., 2020 (37) | 167 | 33.0 | 64.1 | 28.7 | 70.7 |
| *current series* | *92* | *55* | *45* | *11* | *62* |

CMS, cerebellar mutism syndrome; GTR, gross total removal; NR, not reported.
*Frequency of telovelar approach: not reported.

children treated *via* the telovelar route, showing a wide variability in incidence of mutism (0–30%) (**Table 5**).

When the telovelar approach fails to reduce the incidence of CM, other explanations are proposed (30, 38).

In our series, the two approaches were not randomized and were not considered as alternative but complementary, with specific indications for each approach only based on careful and thorough evaluation of preoperative imaging.

Transvermian approach was chosen for midline fourth ventricular tumors associated with extensive lower vermian infiltration and/or rostral extension up to the fastigium and upper vermis infiltration. The telovelar approach was chosen for tumors filling only the fourth ventricle and/or bulging in the cisterna magna through an enlarged Magendie, with little or no vermian infiltration, lateral extension, and CPA extension (**Table 1**). Using these criteria, the overall incidence of CM remained in the lower range (n = 10 cases; 11%) of those reported in the literature (27, 28, 36–38) regardless of the approach used (**Table 5**).

According to our data, the development of CM after posterior fossa surgery in children appears to be a more complex phenomenon, requiring a combination of 1) surgery-unrelated factors (e.g., location of the tumor, medulloblastoma histology, brainstem infiltration) and 2) surgery-related factors (e.g., surgical manipulation near the dentate nuclei or the superior/middle cerebellar peduncles causing injury to the dento-rubro-thalamo-cortical pathways, inadequate use of self-retaining retractors and ultrasonic aspiration) (28, 35, 36, 38, 39). The risk factors identified in most papers (28) are mainly surgery unrelated: midline location (vermis and/or fourth ventricle), brainstem infiltration/compression, medulloblastoma histology with higher risk for 3–4 molecular subgroups (40), and tumor size (41, 42).

The choice of surgical approach did not significantly modify any considered postoperative outcome (**Table 3**), in contrast with that of Ferguson et al. (33) and according to the recent findings of Toescu et al. (37).

Our data show transient neurological deficits in 53% of children and permanent neurological morbidity in 31% of cases (**Table 2**) with prevalence of motor/cerebellar deficits and cranial nerve impairment. In a mixed adult/child retrospective series of 55 surgically treated fourth ventricular tumors, Ferguson et al. (33) describe neurological complications in 76% of cases. Toescu et al. (37) report postoperative morbidity in

70.7% of 167 children with fourth ventricular tumors. Despite the differences in data collection and classification, our findings are similar to those presented in previous series.

Radiological adverse events (20% of cases in our cohort, see **Table 2**) required neurosurgical treatment only in two cases (see *Results*). The low incidence of postoperative neurosurgical complications requiring reoperation is in line with Toescu et al. (37).

It could be hypothesized that telovelar approach could offer less good visibility or less comfortable working angles in the area of the fastigium and fourth ventricle roof, but in fact, the measurable postoperative residual tumor was left adherent to the brainstem or in the fastigium area indifferently from the approach used.

The senior surgeon operating and/or closely supervising all the surgeries trained in the 1990s in the transvermian era but started to use progressively the telovelar in the early 2000s after the publication of Mussi (7), so he could be considered skilled enough also in the telovelar approach at the early time of recruitment of this study, canceling the possible bias of different learning curve.

The finding that high-grade tumors operated on through the transvermian approach have a better CS than those operated on through the telovelar approach should only be considered as a confirmation that, in our series, the choice of the surgical approach was highly dependent on anatomical presentation and the typology of tumor and the telovelar being mainly chosen in two aggressive histologies (AT-RT, anaplastic ependymoma). Moreover, the significant impact of the choice of surgical approach (**Figure 2C**) should be reconsidered when the factor of postoperative residual tumor volume is taken into account (**Table 4**).

Therefore, in this unicentric, single-surgeon retrospective series, when surgical approach was chosen only on the basis of a rational and thorough examination of preoperative images, cerebellar mutism remained approximately 11% whatever the approach used. In our hands, none of the two surgical approaches proved to be superior to the other in terms of quality of resection and postoperative complications. For these reasons and due to the inconsistency of the current literature relative to this subject, we will continue to choose the approach on the basis of the preoperative MRI anatomical features and intraoperative characteristics until further evidence will become available. Telovelar approach will be preferred whenever

anatomically suitable for its higher anatomical respect of cerebellar parenchyma, but transvermian approach will continue to be part of our surgical armamentarium in cases where extensive vermian infiltration or unusual dorsal extension will lead us to consider the latter approach safer for the patient.

## CONCLUSION

In our experience, the choice of the surgical approach (telovelar vs. transvermian) to fourth ventricular tumors in children did not significantly modify any considered postoperative outcome, including the incidence of postoperative CM.

Our findings offer significant data to reconsider the real impact of the choice of surgical route to the fourth ventricle on the incidence of CM and surgery-related morbidity. Surgical approach to the fourth ventricle, like all surgical approaches, should be individualized according to the location of the tumor, degree of vermian infiltration, and lateral and upward extension. Surgeons should fully master both approaches and choose the one that they consider the best for the patient according preoperative imaging evaluation.

## DATA AVAILABILITY STATEMENT

The raw data supporting the conclusions of this article will be made available by the authors, without undue reservation.

## ETHICS STATEMENT

The present study was approved by the Cardarelli-Santobono Hospitals Ethics Committee (Cod.Reg. RGP2020 - Prot.N. 00022209 - 21/09/2020).Written informed consent from the participants' legal guardian/next of kin was not required to participate in this study in accordance with the national legislation and the institutional requirements.

## AUTHOR CONTRIBUTIONS

NO and GC: study design and manuscript conception. NO: data collection. NO and GC: data revision and interpretation and manuscript drafting and revision. FS, CC, and NO: statistical analysis. CR, GC, and NO: imaging data interpretation. NO, VO, and CR: volumetric analysis. LDM, LQ, MdS, and NO: oncological follow-up data analysis. NO, GC, PS, CRu, and GM: surgical videos and operative reports interpretation. All authors contributed to the article and approved the submitted version.

## FUNDING

## REFERENCES

1. Frazier CH. Remarks Upon the Surgical Aspects of Tumors of the Cerebellum. *NY State J Med* (1905) 18:272–280, 332–337.
2. Craig WM, Kernohan JW. Tumors of the Fourth Ventricle. *JAMA* (1938) 111 (26):2370–7. doi: 10.1001/jama.1938.02790520026006
3. Dandy WE. Surgery of the Brain. In: D Lewis, editor. *Practice of Surgery. Vol 12*. Hagerstown, Md: WF Prior (1932). p. 625–31.
4. Özek MM, Cinalli G, Maixner W, Sainte-Rose C. *Posterior Fossa Tumors in Children*. Switzerland: Springer International Publishing (2015), 948. doi: 10.1007/978-3-319-11274-9
5. Matsushima T. Microsurgical Anatomy of the Cerebellomedullary Fissure and Variations of the Transcerebellomedullary Fissure Approach. In: T Matsushima, editor. *Microsurgical Anatomy and Surgery of the Posterior Cranial Fossa*. Tokyo: Springer (2015). p. 73–99. doi: 10.1007/978-4-431-54183-7_7
6. Matsushima T, Rhoton ALJr., Lenkey C. Microsurgery of the Fourth Ventricle: Part 1. Microsurgical Anatomy. *Neurosurgery* (1982) 11(5):631–67. doi: 10.1227/00006123-198211000-00008
7. Mussi AC, Rhoton ALJr. Telovelar Approach to the Fourth Ventricle: Microsurgical Anatomy. *J Neurosurg* (2000) 92(5):812–23. doi: 10.3171/jns.2000.92.5.0812
8. Matsushima T, Abe H, Kawashima M, Inoue T. Exposure of the Wide Interior of the Fourth Ventricle Without Splitting the Vermis: Importance of Cutting Procedures for the Tela Choroidea. *Neurosurg Rev* (2012) 35(4):563–72. doi: 10.1007/s10143-012-0384-3
9. Matsushima T, Inoue T, Inamura T, Natori Y, Ikezaki K, Fukui M. Transcerebellomedullary Fissure Approach With Special Reference to Methods of Dissecting the Fissure. *J Neurosurg* (2001) 94(2):257–64. doi: 10.3171/jns.2001.94.2.0257

10. Mussi AC, Matushita H, Andrade FG, Rhoton AL. Surgical Approaches to IV Ventricle-Anatomical Study. *Childs Nerv Syst* (2015) 31(10):1807–14. doi: 10.1007/s00381-015-2809-0
11. Matsushima T, Rutka J, Matsushima K. Evolution of Cerebellomedullary Fissure Opening: Its Effects on Posterior Fossa Surgeries From the Fourth Ventricle to the Brainstem. *Neurosurg Rev* (2021) 44(2):699–708. doi: 10.1007/s10143-020-01295-2
12. Dailey AT, McKhann GM2nd, Berger MS. The Pathophysiology of Oral Pharyngeal Apraxia and Mutism Following Posterior Fossa Tumor Resection in Children. *J Neurosurg* (1995) 83(3):467–75. doi: 10.3171/jns.1995.83.3.0467
13. Pollack IF, Polinko P, Albright AL, Towbin R, Fitz C. Mutism and Pseudobulbar Symptoms After Resection of Posterior Fossa Tumors in Children: Incidence and Pathophysiology. *Neurosurgery* (1995) 37(5):885–93. doi: 10.1227/00006123-199511000-00006
14. Gudrunardottir T, Morgan AT, Lux AL, Walker DA, Walsh KS, Wells EM, et al. Consensus Paper on Post-Operative Pediatric Cerebellar Mutism Syndrome: The Iceland Delphi Results. *Childs Nerv Syst* (2016) 32(7):1195–203. doi: 10.1007/s00381-016-3093-3
15. Kellogg JX, Piatt JHJr. Resection of Fourth Ventricle Tumors Without Splitting the Vermis: The Cerebellomedullary Fissure Approach. *Pediatr Neurosurg* (1997) 27(1):28–33. doi: 10.1159/000121221
16. Gök A, Alptekin M, Erkutlu I. Surgical Approach to the Fourth Ventricle Cavity Through the Cerebellomedullary Fissure. *Neurosurg Rev* (2004) 27 (1):50–4. doi: 10.1007/s10143-003-0286-5
17. El-Bahy K. Telovelar Approach to the Fourth Ventricle: Operative Findings and Results in 16 Cases. *Acta Neurochir (Wien)* (2005) 147(2):137–42. doi: 10.1007/s00701-004-0407-0
18. Rajesh BJ, Rao BR, Menon G, Abraham M, Easwer HV, Nair S. Telovelar Approach: Technical Issues for Large Fourth Ventricle Tumors. *Childs Nerv Syst* (2007) 23(5):555–8. doi: 10.1007/s00381-006-0295-0

19. Zaheer SN, Wood M. Experiences With the Telovelar Approach to Fourth Ventricular Tumors in Children. *Pediatr Neurosurg* (2010) 46(5):340–3. doi: 10.1159/000321539

20. Han S, Wang Z, Wang Y, Wu A. Transcerebellomedullary Fissure Approach to Lesions of the Fourth Ventricle: Less Is More? *Acta Neurochir (Wien)* (2013) 155(6):1011–6. doi: 10.1007/s00701-013-1689-x

21. Tomasello F, Conti A, Cardali S, La Torre D, Angileri FF. Telovelar Approach to Fourth Ventricle Tumors: Highlights and Limitations. *World Neurosurg* (2015) 83(6):1141–7. doi: 10.1016/j.wneu.2015.01.039

22. Qiu BO, Wang Y, Wang W, Wang C, Wu P, Bao Y, et al. Microsurgical Management of Pediatric Ependymomas of the Fourth Ventricle *via* the Trans-Cerebellomedullary Fissure Approach: A Review of 26 Cases. *Oncol Lett* (2016) 11(6):4099–106. doi: 10.3892/ol.2016.4507

23. Winkler EA, Birk H, Safaee M, Yue JK, Burke JF, Viner JA, et al. Surgical Resection of Fourth Ventricular Ependymomas: Case Series and Technical Nuances. *J Neurooncol* (2017) 130(2):341–349. doi: 10.1007/s11060-016-2198-6

24. Eissa EM. The Role of the Telovelar Approach in Fourth Ven- Tricular Surgery: A New Perspective. *Turk Neurosurg* (2018) 28(4):523–9. doi: 10.5137/1019-5149.JTN.21209-17.1

25. Tanriover N, Ulm AJ, Rhoton ALJr, Yasuda A. Comparison of the Transvermian and Telovelar Approaches to the Fourth Ventricle. *J Neurosurg* (2004) 101(3):484–98. doi: 10.3171/jns.2004.101.3.0484

26. Deshmukh VR, Figueiredo EG, Deshmukh P, Crawford NR, Preul MC, Spetzler RF. Quantification and Comparison of Telovelar and Transvermian Approaches to the Fourth Ventricle. *Neurosurgery* (2006) 58(4 Suppl 2):ONS–202-6; discussion ONS-206-7. doi: 10.1227/01.NEU.0000207373.26614.BF

27. Robertson PL, Muraszko KM, Holmes EJ, Sposto R, Packer RJChildren's Oncology Group. Incidence and Severity of Postoperative Cerebellar Mutism Syndrome in Children With Medulloblastoma: A Prospective Study by the Children's Oncology Group. *J Neurosurg* (2006) 105(6 Suppl):444–51. doi: 10.3171/ped.2006.105.6.444

28. Catsman-Berrevoets CE, Patay Z. Cerebellar Mutism Syndrome. In: M Manto, TAGM Huisman, editors. *Handbook of Clinical Neurology Vol 155 (3rd Series) The Cerebellum: Disorders and Treatment*. Oxford, United Kingdom: Elsevier B.V (2018). p. 273–88.

29. Rekate HL, Grubb RL, Aram DM, Hahn JF, Ratcheson RA. Muteness of Cerebellar Origin. *Arch Neurol* (1985) 42(7):697–8. doi: 10.1001/archneur.1985.04060070091023

30. Tamburrini G, Frassanito P, Chieffo D, Massimi L, Caldarelli M, Di Rocco C. Cerebellar Mutism. *Childs Nerv Syst* (2015) 31(10):1841–51. doi: 10.1007/s00381-015-2803-6

31. Paquier PF, Walsh KS, Docking KM, Hartley H, Kumar R, Catsman-Berrevoets C. Post-Operative Cerebellar Mutism Syndrome: Rehabilitation Issues. *Childs Nerv Syst* (2020) 36:1215–22. doi: 10.1007/s00381-019-04229-6

32. Atallah A, Rady MR, Kamal HM, El-Mansy NFM, Alsawy N, Hegazy A, et al. Telovelar Approach to Pediatric Fourth Ventricle Tumors: Feasibility and Outcome. *Turk Neurosurg* (2019) 29(4):497–505. doi: 10.5137/1019-5149.JTN.24078-18.3

33. Ferguson SD, Levine NB, Suki D, Tsung AJ, Lang FF, Sawaya R, et al. The Surgical Treatment of Tumors of the Fourth Ventricle: A Single-Institution Experience. *J Neurosurg* (2018) 128(2):339–51. doi: 10.3171/2016.11.JNS161167

34. Ebrahim KS, Toubar AF. Telovelar Approach Versus Transvermian Approach in Management of Fourth Ventricular Tumors. *Egypt J Neurosurg* (2019) 34:10. doi: 10.1186/s41984-019-0036-9

35. Cobourn K, Marayati F, Tsering D, Ayers O, Myseros JS, Magge SN, et al. Cerebellar Mutism Syndrome: Current Approaches to Minimize Risk for CMS. *Childs Nerv Syst* (2020) 36(6):1171–9. doi: 10.1007/s00381-019-04240-x

36. Renne B, Radic J, Agrawal D, Albrecht B, Bonfield CM, Cohrs G, et al. Cerebellar Mutism After Posterior Fossa Tumor Resection in Children: A Multicenter International Retrospective Study to Determine Possible Modifiable Factors. *Childs Nerv Syst* (2019) 36(6):1159–69. doi: 10.1007/s00381-019-04058-7

37. Toescu SM, Samarth G, Layard Horsfall H, Issitt R, Margetts B, Phipps KP, et al. Fourth Ventricle Tumors in Children: Complications and Influence of Surgical Approach. *J Neurosurg Pediatr* (2020) 23:1–10. doi: 10.3171/2020.6.PEDS2089

38. Avula S, Mallucci C, Kumar R, Pizer B. Posterior Fossa Syndrome Following Brain Tumour Resection: Review of Pathophysiology and a New Hypothesis on its Pathogenesis. *Childs Nerv Syst* (2015) 10:1859–67. doi: 10.1007/s00381-015-2797-0

39. Schmahmann JD. Neuroanatomy of Pediatric Postoperative Cerebellar Cognitive Affective Syndrome and Mutism. *Neurology* (2019) 93(16):693–4. doi: 10.1212/WNL.0000000000008311

40. Jabarkheel R, Amayiri N, Yecies D, Huang Y, Toescu S, Nobre L, et al. Molecular Correlates of Cerebellar Mutism Syndrome in Medulloblastoma. *Neuro Oncol* (2020) 22(2):290–7. doi: 10.1093/neuonc/noz158

41. Catsman-Berrevoets CE, Van Dongen HR, Mulder PG, Paz y Geuze D, Paquier PF, Lequin MH. Tumour Type and Size are High Risk Factors for the Syndrome of "Cerebellar" Mutism and Subsequent Dysarthria. *J Neurol Neurosurg Psychiatry* (1999) 6):755–7. doi: 10.1136/jnnp.67.6.755

42. Pols SYCV, van Veelen MLC, Aarsen FK, Gonzalez Candel A, Catsman-Berrevoets CE. Risk Factors for Development of Postoperative Cerebellar Mutism Syndrome in Children After Medulloblastoma Surgery. *J Neurosurg Pediatr* (2017) 1):35–41. doi: 10.3171/2017.2.PEDS16605

# Intracranial Metastatic Disease: Present Challenges, Future Opportunities

Alyssa Y. Li [1†], Karolina Gaebe [1†], Katarzyna J. Jerzak [1,2], Parneet K. Cheema [3], Arjun Sahgal [1,4] and Sunit Das [1,5*]

[1] Institute of Medical Science, Faculty of Medicine, University of Toronto, Toronto, ON, Canada, [2] Division of Oncology, Department of Medicine, Sunnybrook Health Sciences Centre, University of Toronto, Toronto, ON, Canada, [3] Division of Oncology, William Osler Health System, Brampton, ON, Canada, [4] Department of Radiation Oncology, Sunnybrook Health Sciences Centre, University of Toronto, Toronto, ON, Canada, [5] Division of Neurosurgery, St. Michael's Hospital, University of Toronto, Toronto, ON, Canada

Intracranial metastatic disease (IMD) is a prevalent complication of cancer that significantly limits patient survival and quality of life. Over the past half-century, our understanding of the epidemiology and pathogenesis of IMD has improved and enabled the development of surveillance and treatment algorithms based on prognostic factors and tumor biomolecular characteristics. In addition to advances in surgical resection and radiation therapy, the treatment of IMD has evolved to include monoclonal antibodies and small molecule antagonists of tumor-promoting proteins or endogenous immune checkpoint inhibitors. Moreover, improvements in the sensitivity and specificity of imaging as well as the development of new serological assays to detect brain metastases promise to revolutionize IMD diagnosis. In this review, we will explore current treatment principles in patients with IMD, including the emerging role of targeted and immunotherapy in select primary cancers, and discuss potential areas for further investigation.

**Keywords: intracranial metastatic disease (IMD), brain metastases, targeted therapy, immunotherapy, neurosurgery, minimally invasive surgery, radiation therapy, screening**

## 1 INTRODUCTION

The development of intracranial metastatic disease (IMD) is a frequent and serious complication of cancer, affecting nearly 30% of cancer patients [1]. The incidence of IMD is expected to increase as our population ages and as advancements in primary cancer therapy result in longer disease survival [1]. IMD has been observed to disproportionately affect patients with certain primary cancers, including lung cancer (19.6%), melanoma (6.4%), renal cell carcinoma (4.2%), breast cancer (3.1%), and colorectal cancer (1.4%), reflecting possible organotropy in IMD or successes with local disease control [2]. Indeed, among patients with brain metastases (BrM), lung cancer, breast cancer, and melanoma account for nearly 60%, 11%, and 6% of all primary cancers in some studies [2].

The impact of IMD on morbidity and mortality of patients with cancer is significant. The median time to diagnosis of IMD has been reported to be 5.2 months following primary cancer diagnosis, suggesting that a large proportion of patients may already have BrM at the time their primary cancer is diagnosed [2]. Given the high prevalence of IMD and the short median survival of 3.7 months

following IMD diagnosis, there is interest in developing screening strategies and tools to identify patients with IMD (2). Magnetic resonance imaging (MRI) remains the most commonly used modality for the diagnosis of BrM and leptomeningeal disease (3). Historically, MRI evaluation has been prompted by the development of neurological symptoms, including headache, seizure, and altered mental status, in patients with cancer. Several algorithms have since been created to identify asymptomatic, high-risk patients who would benefit from MRI screening at the time of their primary cancer diagnosis (3). Imaging and serum biomarkers of IMD to allow for earlier and more cost-effective diagnosis of IMD are under investigation, however, their role in IMD surveillance remains to be fully elucidated (4, 5).

At present, the most common local treatments for IMD are surgical resection, whole brain radiation therapy (WBRT), and stereotactic radiosurgery (SRS). The Graded Prognostic Assessment (GPA) is often used to estimate survival for patients with BrM and is based on prognostic factors including Karnofsky performance score (KPS), age, presence of extracranial metastases, number of BrM, and tumor subtype, depending on the primary tumor histology (6). In some treatment algorithms, patients with greater IMD burden or poorer performance status are directed toward WBRT, while younger patients with fewer intracranial metastases may be directed toward treatment with surgical resection or SRS (7). Advances in surgical technique and delivery of radiation have resulted in improved survival estimates for patients with IMD from less than six months over fifteen years ago to 8-16 months today (6, 8–11).

Recent data have supported a role for systemic targeted therapies and immunotherapies in the treatment of select patients with IMD, including but not limited to those with non-small cell lung cancer (NSCLC), breast cancer, and malignant melanoma (12, 13). There remains, however, a clear clinical need for further investigation to develop more effective screening and treatment for IMD. In this review, we outline and describe recent and current efforts to improve outcomes in patients with IMD of the brain through novel therapeutics, improved surveillance, and prevention.

## 2 EMERGING TREATMENTS FOR IMD

Traditionally, prognosis for patients with IMD has been extremely poor. However, modern treatments have significantly improved survival and quality of life (QoL) in these patients. The main goals of IMD therapy include lengthening survival, diminishing or controlling IMD burden, minimizing adverse events associated with IMD development and treatment, as well as improving cognition and QoL.

### 2.1 Surgical Resection and Minimally Invasive Surgery

Surgery has been a long-standing modality in the treatment of BrM. In contrast to other forms of IMD management, surgical resection can offer immediate relief of mass effect and neurological symptoms caused by compression and edema, while providing tissue for diagnostic purposes (14, 15). Risks associated with neurosurgery include iatrogenic neurological injury, hemorrhage, infection, and seizure (16, 17). Recent literature has also confirmed a long-standing concern that surgery holds a risk of leptomeningeal disease recurrence, likely related to unintentional local cell seeding during the process of surgical resection (18). However, with modern techniques, surgical resection is typically safe and recovery from surgery often short, making surgery an appealing option, particularly for patients with a large brain lesion, limited number of BrM, and well controlled systemic disease (19). In the 1990s, two landmark randomized controlled trials (RCTs) demonstrated that surgical resection compared with needle biopsy or no surgery prior to WBRT decreased local recurrence, improved median survival, and resulted in more rapid and sustained functional independence (20, 21). In contrast, a similar study by Mintz et al., which included many patients with progressive extracranial disease and lower performance status, found no survival benefit with the addition of surgical resection to WBRT (22). A recent systematic review and meta-analysis found that the literature supports surgical resection followed by postoperative WBRT in patients with good performance status (KPS ≥ 70), controlled systemic disease, and a single brain lesion (23).

While surgical resection of a single BrM in patients with well controlled systemic disease is well-established in clinical practice, the role of surgery in the treatment of patients with limited BrM (2-4 lesions) or deep BrM remains a topic of debate (22, 24). In current clinical practice, these patients are more often treated with SRS. A few retrospective studies have reported equivalence of outcomes between groups treated with surgery and SRS for limited BrM (25–27). SRS is less effective for larger lesions and is associated with delayed treatment effect, differences that have become more significant as improvements in systemic therapies have led to prolonged overall survival (OS) and highlighted the importance of achieving adequate IMD control to maintain QoL (24, 28). These factors, as well as the significant benefits observed with surgical resection in the management of single brain lesions, have prompted investigation into the role of surgery in patients with limited BrM or deep, large lesions (29–31).

Advances in surgical technique and intraoperative technologies may expand indications for surgical resection. Improvements in microsurgery, for example, through improved microscopic and endoscopic visualization, the use of "keyhole" techniques, and evolution away from the use of fixed retractors during surgery, have greatly reduced surgical morbidity and mortality, with recent studies reporting a complication rate between 2-9% (32–36). Further, the development of minimally invasive parafascicular surgery (MIPS), based on the use of a minimal-access tubular retractor advanced into the brain using stereotactic guidance, has allowed surgeons access to deep-seated lesions, while minimizing the iatrogenic injury that has been historically the cost of reaching these areas (37). Even in the setting of high-risk brain lesions,

minimal complications were reported by Gassie et al. with the use of MIPS in 15 patients with deep-seated brain tumors: only one patient had decreased postoperative KPS and no patients developed local complications, such as stroke, infection, hemorrhage, or seizure (38). These results imply that surgical management of deep-seated, high-risk brain lesions may be feasible, however, clinical efficacy in comparison with other treatment approaches remains to be studied.

## 2.2 Radiation Therapy

WBRT has been a mainstay for the treatment of IMD since the middle of the 20th century (39–41). Gains in patient survival with improvements in systemic therapies, however, have brought mounting concerns regarding the late toxicities of WBRT, particularly on neurocognitive function (42). Several modifications to the delivery of WBRT have since been investigated, for example, techniques that spare exposure to the hippocampus, or concurrent delivery of a neuroprotective agent (43–46). In current practice, WBRT remains the preferred treatment option for patients with multiple BrM, widely disseminated metastatic disease, or short life expectancy, and is used as prophylactic therapy for patients with small cell lung cancer (SCLC) in the absence of IMD (47).

### 2.2.1 The Evolution of SRS in the Treatment of IMD

A major improvement in the treatment of BrM has been SRS, which allows for focal delivery of high doses of radiation. For patients with limited (1–4) BrM, SRS has been shown to be an effective treatment to achieve local control of lesions within the cerebrum, cerebellum, and brainstem (48, 49). A secondary analysis of an RCT designed to investigate the addition of WBRT to SRS or surgical resection showed similar rates of local control following surgical resection and WBRT, compared with WBRT followed by cavity radiation with SRS (50). At present, we do not have RCT data that directly compare surgical resection and SRS in the setting of a single or limited BrM. Multiple studies, however, have investigated 1) the utility of adding SRS to WBRT; and 2) treatment with SRS as an alternative to WBRT.

Two seminal RCTs by Andrews et al. and Kodziolka et al. investigated the benefit of SRS boost following WBRT for patients with limited or multiple BrM. Both trials found that SRS improved OS (6.5 vs. 4.9 months, p=0.39; and 11.0 vs. 7.5 months, p=0.03) as well as local control (51, 52). Given the neurotoxicity associated with WBRT, Aoyama et al. then asked if SRS was sufficient as a treatment for patients with limited BrM. One hundred thirty-two patients were randomized to SRS alone (n=65) or WBRT and SRS (n=67). Although higher rates of local tumor control were observed at 1 year in the group treated with WBRT and SRS compared with standalone SRS treatment (88.7% vs 72.5%, p=0.002), the addition of WBRT did not confer a statistically significant benefit on survival (median 7.5 vs. 8.0 months, p=0.42) (53). A subsequent RCT by Chang et al. to evaluate neurocognitive decline in patients with limited BrM treated with SRS or WBRT plus SRS was halted prematurely when an interim analysis showed that patients randomized to receive WBRT plus SRS were at a significantly increased risk for

neurocognitive decline at four months (54). Notably, their findings again showed a dissociation between achievement of local control and OS: both 1-year freedom from recurrence and risk of death were higher with combined WBRT and SRS (hazard ratio (HR) 2.47, p=0.0036; 27% vs. 73%, p=0.0003). The finding in this study that treatment with SRS alone conferred a greater survival benefit than bimodality treatment has received criticism as an artifact of higher burden of extracranial and intracranial disease in the WBRT plus SRS arm (55). Overall, these studies highlight the fact that many of these patients succumb to progression of their systemic disease.

A study by the European Organization for Research and Treatment of Cancer (EORTC) similarly found that WBRT improved local control at 2 years compared with observation only after SRS (31% vs. 19%, p=0.040). In line with the findings by Aoyama and colleagues, however, no OS difference was observed between the SRS alone and WBRT plus SRS arms (SRS only: 10.7 months, WBRT plus SRS: 10.9 months, p=0.89). Further, improved tumor control with the addition of WBRT did not lengthen the median duration of functional independence (SRS only: 10.0 months, WBRT plus SRS: 9.5 months, p=0.71) (56). In fact, QoL was better in the SRS-only arm (57). In a separative analysis of this trial, Kim et al. found that, compared with upfront WBRT, SRS alone was more cost-effective in patients with one to three IMD lesions (58). Meta-analyses by Tsao et al. and Sahgal et al. concluded that, while WBRT improved local and distant brain control compared with SRS alone (HR 2.61, p<0.0001, and HR 2.15, p<0.00001, respectively), treatment with SRS alone is associated with longer survival in patients age ≤ 50 years (13.6 vs. 8.2 months), and that there is no difference in survival with the addition of WBRT to SRS in patients age > 50 years, compared to SRS alone (10.1 vs. 8.6 months, respectively) (59, 60). A subsequent trial in which patients with limited melanoma BrM treated with SRS were randomized to adjuvant WBRT showed no clinical benefit with the addition of WBRT to local therapy on distant intracranial control, survival, or preservation of performance status (61). Consequently, in a statement released by the American Society for Radiation Oncology as part of its Choosing Wisely campaign, addition of WBRT to SRS is no longer recommended for patients with limited number of BrM (62). Conversely, WBRT remains standard of care in patients with multiple (≥ 4 BrM). More recent data have supported a possible role for SRS in the treatment of patients with multiple (≤ 10) BrM. A prospective observational study of nearly 1200 Japanese patients found similar rates of OS in patients treated with SRS for two to four lesions compared with SRS for five to ten lesions (HR 0.79, p=0.78) (63).

### 2.2.2 Late Adverse Effects Following SRS

Although SRS is generally well-tolerated, patients can experience adverse effects, most notably radiation necrosis, which negatively affects QoL and morbidity. Radiation necrosis develops in 5-25% of patients following SRS treatment and constitutes a late adverse treatment effect that can occur months to years after SRS has been completed (64–70). Patients affected by radiation necrosis can present with a variety of symptoms ranging from asymptomatic to symptoms of increased intracranial pressure,

including headaches, seizures, or cognitive/neurological decline (71). Diagnosis of radiation necrosis is challenging, as radiation necrosis and recurrent tumor lesions present with similar features on conventional imaging. Ultimately, biopsies of suspicious lesions are required to establish a definite diagnosis. While glial cell and vascular injury have been postulated as potential underlying etiologies for radiation necrosis, damage following SRS is directly related to radiation dose per fraction administered (72–74). Additional risk factors include prior radiation (in particular SRS) to the same site, larger lesion size, or receipt of targeted or immunotherapy (64, 75–77). In one study, SRS to the same lesion was associated with an increased risk of radiation necrosis at 1 year when compared with prior WBRT, concurrent WBRT, or no prior radiation (20%, 4%, 8%, and 3%, respectively) (77). Blonigen et al. also demonstrated that the risk of radiation necrosis was higher when the volume of brain parenchyma receiving more than 10 Gy or 12 Gy exceeded 10.5 cm$^3$ or 7.9 cm$^3$, respectively (64). In another study of 480 patients secondary to NSCLC, melanoma, or renal cell carcinoma, the risk of radiation necrosis following SRS treatment was 2.5 times higher in patients who received prior immunotherapy, further illustrating the multi-faceted nature of radiation necrosis (78). Management of radiation necrosis can be conservative in the absence of symptoms, or can involve corticosteroids, bevacizumab, surgical resection, or laser interstitial therapy for symptom control (79–82). Radiation necrosis is a challenging complication of SRS treatment and should be considered as a potential complication following SRS.

### 2.2.3 Approaches to Limit Cognitive Impacts of WBRT

Given the neurotoxicity associated with WBRT, several strategies to limit the cognitive impacts of WBRT have been investigated. Our advancing understanding of the mechanisms underlying radiation-induced injury has led to the development of pharmacological agents that modulate the brain's sensitivity to radiation-induced effects. One such agent is memantine, a drug that is used in the treatment of Alzheimer's dementia and that helps prevent vascular injury. The efficacy of memantine in preventing radiation-induced cognitive dysfunction was investigated in a RCT (RTOG 0614) of 508 patients treated with WBRT and either memantine (20 mg/day) or placebo, both initiated within three days of WBRT for 24 weeks. There were no differences in OS and progression-free survival (PFS) between the two arms, and memantine did not cause additional toxicity. Although no statistically significant differences in terms of the Hopkins Verbal Learning Test–Revised Delayed Recall (HVLT-R DL) were observed at 24 weeks (memantine median decline: 0, placebo median decline: -2, p=0.059), participants treated with memantine showed delayed time to cognitive decline (HR 0.78, 95% CI 0.62-0.99, p=0.01) and superior executive function at 8 (p=0.008) and 16 weeks (p=0.0041), as well as superior processing speed (p=0.0137) and delayed recognition (p=0.0149) at 24 weeks (43). Following these results, the National Cancer Comprehensive Network (NCCN) incorporated the use of memantine along with WBRT into their consensus guidelines. Despite this, routine use of

memantine for patients receiving WBRT has not yet been established; future health policy strategies should develop ways in which memantine can be more quickly adopted into routine therapy (83). Other agents, such as the donepezil, renin-angiotensin system blockers, or *Ginkgo biloba*, have also been investigated (84–87).

The decline in memory function observed following WBRT may be a consequence of radiation-induced injury to the hippocampus, a region which is involved in neurocognitive functions, including memory, learning, and spatial information processing (88). Given the low frequency of BrM in the hippocampus, this region could represent a dose-limiting structure (89). Early data to support this hypothesis stems from a single-arm, multi-institutional phase II study (RTOG 0933) that showed superior cognitive preservation (as measured by the HVLT-R DR) with the use of hippocampal avoidance WBRT (HA-WBRT) compared with historical data from WBRT-treated controls (mean relative decline from baseline to 4 months 7% vs. 30%, p<0.001) (45).

Given the success observed with memantine, a more recent phase III trial investigating the addition of memantine to HA-WBRT showed significantly lower risk of cognitive failure after HA-WBRT plus memantine compared with HA-WBRT alone (HR 0.74, 95% CI 0.58-0.95) (90). Treatment efficacy in terms of intracranial PFS (iPFS) and OS did not differ between the two arms, suggesting that HA-WBRT plus memantine should be considered as standard of care for patients scheduled to receive WBRT with no BrM in the hippocampal region. As patients experience longer survival, neurological sequalae from radiation treatment will become increasingly important. Anatomical avoidance and pharmacotherapy are promising ways for clinicians to preserve cognitive function in patients receiving WBRT.

### 2.2.4 Radiation Therapy in the Setting of SCLC

WBRT does remain the standard of care for patients with SCLC in the form of prophylactic cranial irradiation (PCI). As many as 40-60% of patients with SCLC will develop IMD during the course of their disease, with rates of IMD 1.3-2 times higher than in patients with NSCLC (91). Notably, this standard is being challenged by mounting evidence from retrospective studies and meta-analyses on the lack of survival benefit in the extensive stage setting and additional neurotoxicity of PCI in patients with SCLC (92–94). As patients with SCLC have been historically excluded from trials for SRS, data comparing SRS and WRBT alone, or SRS and WBRT + boost, in this patient population is uniformly retrospective. A propensity score-matched observational study by Rusthoven et al. found that, as for other malignancies, the addition of WBRT to SRS improved intracranial control (time to central nervous system (CNS) progression HR 0.28, p<0.001), but not survival (median OS 5.2 months for WBRT vs. 6.5 months for SRS, p=0.79), in patients with SCLC (95). Similarly, a phase III trial found equivalent OS and intracranial control with WBRT with hippocampal sparing (HA-WBRT) compared to conventional WBRT, with prolonged preservation of neurocognitive function in the HA-WBRT arm (96). These findings suggest a trend away from conventional WBRT as PCI for patients with SCLC toward

treatments aligned to achieve IMD control while maintaining QoL and cognition.

## 2.3 Pharmacological Therapies for IMD

Although surgery and radiation therapy remain the cornerstone of treatment for patients with IMD, recent data support a role for targeted systemic therapies and immunotherapy with immune check point inhibitors in certain patient subgroups.

### 2.3.1 Targeted Therapies

Advances in genetic and genomic analyses have enabled the discovery of genetic alterations that promote tumor growth and proliferation. In a subset of patients with breast cancer, for example, amplification of the human epidermal growth factor receptor 2 (HER2/neu) has been shown to drive cancer propagation (97–99). The development of small molecule or antibody-based agents to target these molecular drivers of cancer and their associated signalling pathways has revolutionized the treatment of patients with HER2-positive breast cancer, epidermal growth factor receptor (EGFR)-mutant or anaplastic lymphoma kinase (ALK)-rearranged NSCLC, and BRAF-mutant melanoma (**Table 1**).

#### 2.3.1.1 Targeted Therapies in Breast Cancer

As IMD is a frequent complication in patients with breast cancer, a large body of literature is available that describes current efforts to identify and evaluate targeted therapy in HER2-positive breast cancer, hormone receptor (HR)-positive breast cancer, and triple negative breast cancer (TNBC).

*2.3.1.1.1 HER2-Positive Breast Cancer.* The addition of trastuzumab, a monoclonal antibody against the HER2 receptor, has been shown to prolong OS and PFS in patients with HER2-positive breast cancer (100). While trastuzumab therapy has been demonstrated to improve systemic disease control, population-based studies identified an increased incidence of IMD in patients treated with trastuzumab, likely resulting from the prolongation in survival and limited penetration of drug across the blood-brain barrier (BBB), rendering the brain a "sanctuary site" for cancer cells (150–152). Notably, HER2-positive breast cancer patients treated with palliative chemotherapy and trastuzumab were more likely to develop BrM than patients who received palliative chemotherapy alone (37.8% vs. 25.0%, p=0.028); conversely, median time to death (TTD) measured from the development of IMD was significantly longer for patients treated with palliative chemotherapy and trastuzumab, compared to those treated with palliative chemotherapy alone (14.9 vs. 4.0 months, p=0.0005), suggesting that trastuzumab might exert some biological effect, even if partial, on IMD (101). Supporting this hypothesis, studies have similarly found that trastuzumab prolongs median OS in HER2-positive breast cancer patients with IMD (102–104).

Lapatinib, an inhibitor of HER2 and EGFR, was subsequently developed to treat HER2-positive breast cancer that had progressed on all previous lines of therapy. From the perspective of IMD, lapatinib was theorized to have better BBB penetrance than trastuzumab, given its smaller molecular weight.

Initial phase II trial results in HER2-positive breast cancer patients with progressive IMD despite WBRT or SRS demonstrated modest antitumor activity with either lapatinib alone (CNS objective response rate (ORR): 2.6-6%) or in combination with capecitabine (CNS ORR: 20%) (105, 106). Subsequent work has suggested that the combination of lapatinib and capecitabine increases median OS from the time of IMD development in HER2-positive breast cancer patients previously treated with anthracycline, trastuzumab, and a taxane, compared with patients receiving anthracycline, trastuzumab, and a taxane only (27.9 vs. 16.7 months, p=0.01) (107). The combination of lapatinib and capecitabine also demonstrated high antitumor activity (CNS ORR: 65.9%) in HER2-positive breast cancer patients with previously untreated IMD in the LANDSCAPE trial, though the impact of treatment on OS was not explicitly determined and concerns regarding treatment toxicity and delays in accessing radiotherapy were raised (108).

Following the development of lapatinib, additional small molecule candidates have been engineered. Neratinib, an irreversible inhibitor of HER1, HER2, and HER4, has been demonstrated to have good antitumor activity in combination with capecitabine in lapatinib-naive or lapatinib-treated patients with IMD secondary to HER2-positive breast cancer (CNS ORR: 49% and 33%, respectively). Among these two patient cohorts, median PFS was 5.5 and 3.1 months, respectively, and median OS was 13.3 and 15.1 months, respectively, though no direct comparisons between groups were reported (109). When compared head-to-head with lapatinib and capecitabine (L+C) in a recent RCT, neratinib and capecitabine (N+C) showed a substantial though not statistically significant effect on OS (13.9 vs. 2.4 months, HR 0.90, p=0.635) and PFS (5.6 vs. 4.3 months, HR 0.66, p=0.074) in HER2-positive breast cancer patients with IMD who have previously failed at least two anti-HER2 therapies (110). The lack of statistical significance may have been due to small sample sizes. Of 621 patients enrolled, 101 (16.3%) had known CNS metastases at baseline (N+C: $n = 51$; L+C: $n = 50$); 81 had received prior CNS-directed radiotherapy or surgery. In the CNS subgroup, mean PFS through 24 months was 7.8 months with N+C versus 5.5 months with L+C (HR 0.66, 95% CI 0.41–1.05), and mean OS through 48 months was 16.4 vs. 15.4 months (HR 0.90, 95% CI 0.59–1.38). At 12 months, cumulative incidence of interventions for CNS disease was 25.5% for the N+C group vs. 36.0% for the L+C group, and cumulative incidence of progressive CNS disease was 26.2% versus 41.6%, respectively. In patients with target CNS lesions at baseline ($n = 32$), confirmed intracranial ORR (iORR) were 26.3% and 15.4%, respectively.

A third HER2 inhibitor, tucatinib, demonstrated excellent antitumor activity in combination with trastuzumab and capecitabine in HER2-positive breast cancer patients with IMD, compared to trastuzumab and capecitabine alone (iORR 47.3% vs. 20%, p=0.03), and prolonged median OS (18.1 vs. 12.0 months, HR 0.58, p=0.005) and median PFS (9.9 vs. 4.2 months, HR 0.32, p<0.0001) (111).

Multiple small studies have shown signal for intracranial activity in patients with metastatic HER2-positive breast cancer

**TABLE 1 |** Summary of studies investigating targeted therapies for IMD secondary to breast cancer, NSCLC, and melanoma.

| | Drug | Trial/Study | Study design | Total participants (n) | Study arms | Median OS (months) | Findings |
|---|---|---|---|---|---|---|---|
| Breast cancer | Trastuzumab | Slamon et al. (100) | RCT | 469 | Standard chemotherapy ± trastuzumab in all breast cancer patients | 25.1 vs. 20.3 (p=0.046) | Relative risk reduction of death at 30-month follow-up: 20% |
| | | Park et al. (101) | Retrospective cohort study | 251 | Palliative chemotherapy ± trastuzumab in all breast cancer patients | 31.7 vs. 16.7 (p=0.001) | Incidence of BrM: 37.8 vs. 25% (p=0.028) TTD from BrM: 14.9 vs. 4.0 months (p=0.0005) |
| | | Park et al. (102) | Retrospective cohort study | 78 | Trastuzumab after BrM diagnosis vs. trastuzumab before BrM diagnosis only vs. no trastuzumab | 13.6 vs. 5.5 vs. 4.0 (p<0.001) | Median TTP of BrM: 7.8 vs. 3.9 vs. 2.9 months (p=0.006) HR for death in patients with BrM: 0.5 (p=0.017) |
| | | Okita et al. (103) | Retrospective cohort study | 62 | Trastuzumab vs. no trastuzumab | 38.4 vs 8.4 (p=0.0005) | Median second brain metastatic-free survival time: 7.0 vs. 5.6 months (p=0.057) |
| | | Dawood et al. (104) | Retrospective cohort study | 598 | Trastuzumab vs. no trastuzumab vs. HER2-negative | 11.6 vs. 6.1 vs. 6.3 (p<0.0001) | – |
| | Lapatinib | Lin et al. (105) | Single-arm clinical trial | 39 | Lapatinib | – | CNS ORR: 2.6% |
| | | Lin et al. (106) | Single-arm clinical trial | 242 | Lapatinib, lapatinib and capecitabine (n = 50) | – | CNS ORR: 6% (lapatinib alone), 20% (with capecitabine) ≥20% BrM volume reduction: 21% (lapatinib alone), 40% (with capecitabine) |
| | | Metro et al. (107) | Retrospective cohort study | 30 | Lapatinib and capecitabine | 27.9 vs. 16.7 (p=0.01) | CNS ORR: 31.8% Disease stabilization: 27.3% |
| | | Bachelot et al. (108) | Single-arm clinical trial | 45 | Lapatinib and capecitabine | 17.0 | Median TTP: 5.5 months CNS ORR: 65.9% Disease stabilization: 36% |
| | Neratinib | Freedman et al. (109) | Single-arm clinical trial | 49 | Neratinib and capecitabine in lapatinib-naïve and lapatinib-treated patients | 13.3 and 15.1 | CNS ORR: 49% and 33% Median PFS: 5.5 and 3.1 months |
| | | Hurvitz et al. (110) | RCT | 101 | Neratinib and capecitabine vs. lapatinib and capecitabine | 13.9 vs. 12.4 (p=0.635) | Median PFS: 5.6 vs. 4.3 months (p=0.074) |
| | Tucatinib | Lin et al. (111) | RCT | 291 | Trastuzumab and capecitabine with or without tucatinib | 18.1 vs. 12.0 (p=0.005) | Median PFS: 9.9 vs. 4.2 months, HR 0.32, P<0.0001 iORR: 47.3% vs. 20%, p=0.03 |
| | Trastuzumab emtansine (T-DM1) | Bartsch et al. (112) | Retrospective cohort study | 10 | T-DM1 | – | iORR: 30% |
| | | Jacot et al. (113) | Single-arm clinical trial | 2002 | T-DM1 | – | – |
| | | Krop et al. (114) | RCT | 991 | T-DM1 vs. capecitabine and laptinib | 26.8 vs. 12.9 (HR 0.38, p=0.008) | Median PFS: 5.9 vs. 5.7 months (HR 1.00, p=1.0) |
| | | Montemurro et al. (115) | Single-arm clinical trial | 2002 | T-DM1 | 18.9 | Median PFS: 5.5 months ORR: 21.4% |
| | Trastuzumab deruxtecan (T-DXd) | Barsch et al. (116) | Single-arm clinical trial | 10 | T-DXd | – | CNS ORR: 83.3% |
| | | Jerusalem et al. (117) | Single-arm clinical trial | 24 | T-DXd | – | Median PFS: 18.1 months ORR: 58.3% CNS ORR: 50% |
| | Abemaciclib | Tolaney et al. (118) | Non-randomized clinical trial | 104 | Abemaciclib ± hormone therapy | 12.5 | CNS ORR: 5.2% |
| | | | | | Abemaciclib and trastuzumab | 10.1 | CNS ORR: 0% Median intracranial PFS: 2.7 months |
| | Palbociclib | Brastianos et al. (119) | Single-arm clinical trial | 15 | Palbociclib | 6.4 | Intracranial disease benefit rate: 53.3% |
| | Iniparib | Anders et al. (120) | Single-arm clinical trial | 37 | Iniparib and irinotecan | 7.83 | CNS ORR: 12% |
| | Talazoparib | Litton et al. (121) | RCT | 431 | Talazoparib vs. chemotherapy | | – |

*(Continued)*

**TABLE 1 |** Continued

| | Drug | Trial/Study | Study design | Total participants (n) | Study arms | Median OS (months) | Findings |
|---|---|---|---|---|---|---|---|
| | | | | | | – (HR 0.671, 95% CI 0.366-1.229) | |
| NSCLC | Crizotinib | Solomon et al. (122) | RCT | 343 | Crizotinib vs. pemetrexed + platinum-based chemotherapy | – | Median PFS: 9.0 vs. 4.0 months, HR 0.40, P<0.001<br>iORR: 77% vs. 28%, p<0.001 |
| | Ceritinib | Crinò et al. (123) | Single-arm clinical trial | 140 | Ceritinib | – | Median PFS: 5.4 months<br>Intracranial ORR: 33% |
| | Alectinib | Gadgeel et al. (124) | Single-arm clinical trial | 47 | Alectinib | – | iORR: 52% |
| | | Peters et al. (125) | RCT | 303 | Alectinib vs. crizotinib | – | PFS rate: 12% vs. 45%, HR 0.51, p<0.001 |
| | Brigatinib | Camidge et al. (126) | RCT | 275 | Brigatinib vs. crizotinib | – | 12-month PFS rate: 67% vs. 21%, HR 0.27<br>Intracranial median TTP: HR 0.30<br>iORR: 78% vs. 29%, OR 10.42 |
| | Lorlatinib | Shaw et al. (127) | RCT | 296 | Lorlatinib vs. crizotinib | – | 12-month PFS rate: 96% vs. 60%, HR 0.07<br>iORR: 82% vs. 23%, OR 16.83 |
| | | Shaw et al. (128) | Single-arm clinical trial | 364 | Lorlatinib | – | CNS ORR (TKI-naive): 64%<br>CNS ORR (previous crizotinib): 50% |
| | Ensartinib | Horn et al. (129) | RCT | 290 | Ensartinib vs. crizotinib | – | Median PFS (baseline BrM): 11.8 vs. 7.5 months (HR 0.55, p=0.05)<br>Median PFS (no baseline BrM): NR vs. 16.6 months (HR 0.46, p=0.003) |
| | Lazertinib | Ahn et al. (130) | Single-arm clinical trial | 127 | Lazertinib | – | CNS ORR: 44% |
| | | Cho et al. (131) | Single-arm clinical trial | 78 | Lazertinib | – | CNS ORR: 85.7% |
| | Furmonertinib | Shi et al. (132) | Single-arm clinical trial | 130 | Furmonertinib | – | Median PFS: 9.9 months<br>CNS ORR: 58.8% |
| | | Shi et al. (133) | Single-arm clinical trial | 220 | Furmonertinib | – | CNS ORR (measurable BrM): 66%<br>CNS ORR (measurable/non-measurable BrM): 34%<br>Median PFS (measurable/non-measurable BrM): 11.6 months |
| | Amivantamab | Park et al. (134) | Single-arm clinical trial | 81 | Amivantamab | – | ORR: 39% |
| | Gefitinib | Ceresoli et al. (135) | Single-arm clinical trial | 41 | Gefitinib | – | Median PFS: 3.0 months<br>iORR: 10%<br>DCR: 27% |
| | | Hotta et al. (136) | Retrospective cohort study | 57 | Gefitinib | – | iORR: 42.9% |
| | | Lee et al. (137) | Single-arm clinical trial | 37 | Gefitinib | – | iORR: 70% |
| | | Chiu et al. (138) | Single-arm clinical trial | 76 | Gefitinib | – | iORR: 33.3%<br>DCR: 63.2% |
| | | Kim et al. (139) | Double-arm clinical trial | 23 | Gefitinib or erlotinib | 18.8 | Median PFS: 7.1 months<br>iORR: 73.9%<br>Overall ORR: 69.6%<br>Overall DCR: 82.6% |
| | | Park et al. (140) | Double-arm clinical trial | 28 | Gefitinib or erlotinib | 15.9 | Median PFS: 6.6 months<br>Overall ORR: 83%<br>Overall DCR: 93% |
| | Osimertinib | Mok et al. (141) | RCT | 419 | Osimertinib vs. pemetrexed with platinum-based chemotherapy | – | Median PFS: 8.5 vs. 4.2 months, HR 0.32 |
| | | Soria et al. (142) | RCT | 456 | Osimertinib vs. erlotinib or gefitinib | – | Median PFS: 15.2 vs. 9.6 months, HR 0.47, p<0.001 |
| | Sotorasib | Skoulidis et al. (143) | Single-arm clinical trial | 126 | Sotorasib in all KRAS$^{G12C}$-positive patients | 12.5 | Median PFS: 6.8 months<br>Overall ORR: 37.1% |

*(Continued)*

**TABLE 1 |** Continued

| | Drug | Trial/Study | Study design | Total participants (n) | Study arms | Median OS (months) | Findings |
|---|---|---|---|---|---|---|---|
| | Selpercatinib | Drilon et al. (144) | Single-arm clinical trial | 105 | Selpercatinib | – | CNS ORR: 91% |
| | Pralsetinib | Gainor et al. (145) | Single-arm clinical trial | 233 | Pralsetinib | – | CNS ORR: 56% |
| | Repotrectinib | Drilon et al. (146) | Single-arm clinical trial | – | Repotrectinib | – | – |
| | Tepotinib | Paik et al. | Single-arm clinical trial | 152 | Tepotinib | – | Median PFS: 10.0 months ORR: 55% |
| | Capmatinib | Wolf et al. | Single-arm clinical trial | 364 | Capmatinib | – | CNS ORR: 53.8% |
| | Laprotrectinib | Hong et al. | Single-arm clinical trial | 159 | Laprotrectinib | – | CNS ORR: 66.7% |
| | Entrectinib | John et al. | Single-arm clinical trial | 16 | Entrectinib | – | CNS ORR (measurable BrM): 62.5% CNS ORR (measurable/non-measurable BrM): 50% |
| Melanoma | Dabrafenib | Long et al. (147) | Single-arm clinical trial | 172 | Dabrafenib in BRAF$^{V600E}$-positive melanoma patients with treatment-naïve IMD or progressive IMD | 7.64 and 7.25 | Median PFS: 3.72 and 3.83 months iORR: 39.2% and 30.8% |
| | | Davies et al. (148) | Single-arm clinical trial | 125 | Dabrafenib and trametinib in BRAF$^{V600E}$-positive melanoma patients with treatment-naïve IMD or progressive IMD | 10.8 and 24.3 | Median PFS: 5.6 and 7.2 months iORR: 58% and 56% |
| | Vemurafenib | McArthur et al. (149) | Single-arm clinical trial | 146 | Vemurafenib in BRAF$^{V600}$-positive melanoma patients with treatment-naïve IMD or progressive IMD | 8.9 and 9.6 | Median PFS: 3.7 and 4.0 months iORR: 18% and 18% |

*Median overall survival marked with a dash if the data was 1) not reported or 2) reported for the entire population, including patients without IMD.*

*BrM, brain metastases; CI, confidence interval; CNS, central nervous system; DCR, disease control rate; HER2, human epidermal growth factor 2; HR, hazard ratio; IMD, intracranial metastatic disease; iORR, intracranial ORR; NR, not reached; NSCLC, non-small cell lung cancer; OR, odds ratio; ORR, objective response rate; OS, overall survival; PFS, progression-free survival; RCT, randomized control trial; T-DM1, trastuzumab emtansine; T-DXd, trastuzumab deruxtecan; TKI, tyrosine kinase inhibitor; TTD, time to death; TTP, time to progression.*

with the antibody-drug conjugate trastuzumab emtansine (T-DM1) (112, 113); secondary analysis has further shown T-DM1 to improve OS in patients with trastuzumab-resistant advanced metastatic breast cancer and asymptomatic BrM previously treated with radiotherapy, compared with lapatinib plus capecitabine (114). An exploratory final analysis of the ongoing KAMILLA trial, an international, single-arm, open-label, phase IIIb study evaluating the safety and efficacy of T-DM1 in patients with previously treated, HER2-positive advanced breast cancer, showed a high CNS-specific ORR, including a CNS-specific ORR of ~50% in a subgroup of 67 patients who had not received prior radiation therapy for BrM (115).

Similar to T-DM1, trastuzumab deruxtecan (T-DXd) is an antibody-drug conjugate that has been shown to demonstrate potential therapeutic benefits for HER2-positive breast cancer patients with BrM in early analyses of multiple phase II/III trials, although these analyses have only been reported in abstracts. For example, a preliminary analysis of an ongoing phase II trial, TUXEDO-1, demonstrated an initial iORR of 83.3% in participants enrolled in the first stage of the study (116), while a subgroup analysis of DESTINY-Breast01, another currently

active phase II study, found an ORR of 58.3% and median PFS of 18.1 months (95% CI 6.7-18.1) in 24 patients treated with T-DXd (117). Encouraging results were recently presented by Hurvitz and colleagues in a subgroup analysis of DESTINY-Breast03 (NCT03529110), an ongoing phase III trial, comparing T-DXd and T-DM1 in HER2-positive breast cancer patients previously treated with trastuzumab and taxane-based chemotherapy, and we eagerly await publication of their abstract/full-text article.

While the availability of multiple treatment regimens consisting of single and combination agents has broadened the treatment of HER2-positive breast cancer with BrM, most studies in this area have historically excluded IMD patients. In addition to the identification and validation of new agents, current efforts are aimed at understanding the therapeutic efficacy and toxicities of these targeted therapies, and future studies should focus on the possibility of combining these agents with brain-directed radiation therapies to treat BrM.

*2.3.1.1.2 Hormone Receptor-Positive Breast Cancer.* HR-positive, HER2-negative breast cancers represent a subtype of breast cancers that do not respond to HER2 inhibitors, such as

trastuzumab. Historically, treatment of HR-positive cancer has been limited to hormonal therapies, including aromatase inhibitors, selective estrogen receptor modulators, and estrogen receptor downregulators. Recent efforts in drug development have identified three cyclin-dependent kinase 4/6 (CDK4/6) inhibitors to enhance the management of HR-positive breast cancer. However, the landmark trials investigating CDK 4/6 inhibitors, such MONARCH 1-3, MONALEESA-2, and PALOMA-1, have excluded patients with BrM (153, 154). Among HR-positive, HER2-negative breast cancer patients with BrM, abemaciclib demonstrated an iORR of 5.2% and median OS of 12.5 months (95% CI 9.3-16.4) in one phase II trial (118). In the same trial, the combination of abemaciclib and trastuzumab did not demonstrate objective intracranial responses in patients with HR-positive, HER2-positive breast cancer. Patients who received abemaciclub and trastuzumab had a median OS of 10.1 months (95% 4.2-14.3) and median iPFS of 2.7 months (95% CI 1.4-4.0) (118). A second CDK4/6 inhibitor, palbociclib, demonstrated an intracranial benefit rate of 53.3% and median OS of 6.4 months (90% CI 2.8-6.8) in a small prospective trial of patients with BrM secondary to breast cancer, melanoma, NSCLC, and esophageal cancer (119). Specific outcomes of the 3/15 patients with HR-positive, HER2-negative breast cancer were not reported, limiting our ability to draw conclusions on the effectiveness of palbociclib in patients with HR-positive, HER2-negative breast cancer. Several clinical trials have been launched to investigate the role of CDK4/6 inhibitors in patients with HR-positive breast cancer patients with BrM (NCT04791384, NCT04923542, and NCT04227327).

*2.3.1.1.3 Triple-Negative Breast Cancer.*    Approximately 50% of patients with TNBC are diagnosed with BrM (155). In this patient population, the survival prognosis following BrM diagnosis remains guarded given the lack of molecular targets compared with HER2-positive and HR-positive breast cancer. Poly (ADP-ribose) polymerase (PARP) inhibitors have been investigated in TNBC patients with BrM. The combination of the PARP inhibitor iniparib and the anti-cancer agent irinotecan demonstrated an iORR of 12.0% and median OS of 7.83 months (95% CI 5.10-10.2) (120). A second PARP inhibitor talazoparib was evaluated in the phase III EMBRACA trial and did not significantly prolong OS in a subgroup of TNBC patients with a history of BrM (HR 0.671, 95% CI 0.366-1.229) (121). Given treatment challenges with targeted therapies, there is a trend toward immunotherapies in TNBC, which will be discussed in the appropriate section of this review.

### 2.3.1.2 Targeted Therapies in NSCLC
IMD is a frequent complication of NSCLC. Here, we discuss current targeted therapy efforts for three common genetic alterations associated with NSCLC: ALK, EGFR, and Kirsten rat sarcoma virus (KRAS).

*2.3.1.2.1 ALK Rearrangements in NSCLC.*    BrM have been reported to occur in 15-35% of patients with ALK-positive NSCLC, and up to 60% of these patients develop IMD after first-line therapy (156). In the PROFILE 104 trial, the first-generation

ALK inhibitor crizotinib improved median PFS in patients with ALK-positive NSCLC with IMD when administered as a single agent compared with platinum-based chemotherapy (9.0 vs. 4.0 months, HR 0.40, p<0.001), however, likely due to low CNS penetration of crizotinib, approximately half of patients suffered CNS progression (122). First line treatment for ALK-positive NSCLC has therefore shifted to next generation ALK TKIs that offer longer PFS and have greater activity within the CNS. In the ASCEND-2 trial, 100/140 enrolled ALK-positive NSCLC patients with IMD and previously treated with crizotinib and another regimen, received ceritinib (123). Of these patients, 33% achieved an ORR with a median PFS of 5.4 months. The median OS for this subset of patients with IMD was not reported (123). Similarly, alectinib was found to demonstrate adequate anti-tumor activity in 52% of crizotinib-resistant, ALK-positive NSCLC patients with IMD in an early single-arm phase II trial (124).

These findings were supported by the ALEX trial, which demonstrated IMD progression in 12% of untreated ALK-positive NSCLC patients with IMD receiving alectinib compared with 45% of patients receiving crozitinb (HR 0.51, p<0.001) (125). In ALK-positive NSCLC patients with measurable IMD and no previous ALK inhibitor treatment, patients randomized to treatment with brigatinib demonstrated an iORR of 78% compared with an iORR of 29% in patients randomized to receive crizotinib (OR 10.42) (126). Collectively, these results suggest that second generation ALK inhibitors effectively reduce IMD progression and death in patients with IMD secondary to ALK-positive NSCLC, compared with crizotinib.

The recent CROWN RCT investigated the third generation ALK inhibitor lorlatinib in ALK-positive NSCLC patients with measurable IMD and no prior systemic therapies. Adequate intracranial anti-tumor activity was reported in 82% of patients receiving lorlatinib compared with 23% of patients receiving crizotinib (OR 16.83) (127). The 12-month iPFS rate among patients treated with lorlatinib was 96%, compared with 60% in patients treated with crizotinib (HR 0.07, 95% CI 0.03-0.l17) (127). Ensartinib, another ALK-inhibitor, has also been demonstrated to have high therapeutic efficacy among patients with ALK-positive NSCLC and BrM in the eXalt3 trial (129). Among patients with baseline BrM, those treated with ensartinib had higher median PFS compared to those treated with crizotinib (11.8 vs. 7.5 months, HR 0.55, 95% 0.30-1.01, p=0.05). A similar trend in median PFS was observed among patients without baseline BrM receiving ersartinib versus crizotinib (NR vs. 16.6 months, HR 0.46, 95% CI 0.27-0.77, p=0.003). Of note, the incidence of BrM was lower in patients receiving ersantinib compared with those receiving crozitinib at 12-months follow-up (cause-specific HR 0.32, 95% 0.16-0.63, p=0.001) (129). These findings suggest that ALK inhibitors may be effective as monotherapies in patients with ALK-positive NSCLC patients and IMD.

Notably, these trials were all designed with intent to allow for study of drug effect on IMD. First, the trials described above allowed entry of patients that had untreated asymptomatic BrM.

Second, all trials required that patient undergo MRI of the brain at accrual, regardless of IMD status, then mandated routine surveillance MRI while patients remained on trial. This approach allowed investigators to measure "prevention" of BrM. Finally, all three trials were compared the study drug to crizotinib, a systemically effective agent with poor CNS activity. This design could serve as a model for future trials designed to include the study of intracranial disease.

*2.3.1.2.2 EGFR Mutations in NSCLC.* Activating mutations in EGFR are present in 14-47% of NSCLC cases, and 2-63% of patients with EGFR-mutant NSCLC develop IMD during the course of their disease, accounting for a significant proportion of NSCLC-IMD cases, especially in East Asian populations (157). The first generation EGFR inhibitors, erlotinib and gefitinib, demonstrated increased efficacy compared with systemic chemotherapy in patients with EGFR-mutant NSCLC (157). Among patients with IMD secondary to EGFR-mutant NSCLC and previous chemotherapy or WBRT, treatment with gefitinib resulted in a partial response in about 10% of patients, and the overall disease control rate and median PFS were found to be 27% and 3 months, respectively (135). Similar results were obtained in subsequent single-arm clinical trials (136–138). Non-comparative trials with EGFR-mutant NSCLC patients with IMD receiving erlotinib or gefitinib as first-line therapy report an iORR of 73.9%, median OS of 18.8 months, and PFS of 7.1 months (139). These results have since been reproduced with no statistically significant differences in OS found between erlotinib and gefitinib (140). The second-generation agent, afatinib, has shown similarly low activity in the CNS.

Of more clinical relevance is the third-generation agent, osimertinib, given its high efficacy in treatment-resistant, EGFR-mutant NSCLC and high CNS activity (158). In EGFR-mutant NSCLC patients with IMD and known or likely resistance to first- and second-generation EGFR inhibitors, osimertinib was found to be more effective than pemetrexed-based chemotherapy regimens (median PFS 8.5 vs. 4.2 months, HR 0.32, 95% CI 0.21-0.49) (141). The benefits of osimertinib were more pronounced in untreated patients with EGFR-mutant NSCLC and IMD when compared with the first-generation EGFR inhibitors erlotinib and gefitinib (median PFS 15.2 vs. 9.6 months, HR 0.47, p<0.001) (142). Given its effectiveness in delaying intracranial progression and death, osimeritinib has become the first-line treatment for patients with EGFR-mutant NSCLC (159).

In addition to osimeritinib, several third-generation agents have been investigated. In two phase I/II trials, lazertinib demonstrated an iORR of 44-85.7% in patients with BrM secondary to EGFR-mutant NSCLC (130, 131). Furmonertinib (formerly, alflutinib) exhibited good treatment efficacy in a phase I/II trial involving 17 EGFR-mutant NSCLC patients with BrM (iORR: 58.8%; median PFS: 9.9 months) (132). These findings were replicated in a phase IIb trial involving 105 EGFR-mutant NSCLC patients with BrM: In 29 patients with one or more measurable BrM, treatment with alflutinib achieved an iORR of 66%, while among the 87 patients in the complete analysis dataset, iORR was 34% and median PFS was 11.6 months

(95% CI 8.3-13.8). Across both cohorts, the intracranial disease control rate ranged from 98-100% (133). Several clinical trials have also reported encouraging unpublished results, including a phase 2 expansion of the APOLLO trial (NCT02981108) on the efficacy of almonertinib in metastatic EGFR-mutant NSCLC. Further trials (NCT04808752, NCT04870190) are currently active to clarify the therapeutic efficacy of almonertinib. Third-generation mutant EGFR inhibitors, such as rezivertinib and abivertinib (formerly, avitinib), have been investigated in patients with NSCLC. However, outcomes in subpopulations of patients with BrM have yet to be reported in published formats.

In addition to third-generation EGFR inhibitors, amivantamab, a bispecific antibody directed against EGFR and mesenchymal-epithelial transition (MET) receptor, has been investigated for the treatment of exon 20 insertion-EGFR-mutant NSCLC. Initial phase I trial data from CHRYSALIS was encouraging: an ORR of 39% was achieved in patients with a history of IMD (134). A new clinical trial, MARIPOSA (NCT04487080), has recently been launched to compare the therapeutic efficacy of the combination of amivantamab and lazertinib with the efficacy of osimertinib in patients with untreated EGFR-mutant NSCLC.

### 2.3.1.3 Emerging Targeted Therapies in NSCLC

Mutations in the proto-oncogene KRAS have been reported in 25-30% of patients with NSCLC and, therefore, represent the most prevalent genomic driver of malignancy in the disease (160). As of December 2021, a single small molecule inhibitor of KRAS, sotorasib, has been developed and approved for the treatment of patients with $KRAS^{G12C}$-positive NSCLC who have previously failed standard therapies; however, its clinical efficacy in the context of IMD remains to be determined (143). Selpercatinib and pralsetinib, inhibitors of the RET pathway, have shown promising systemic and CNS activity in RET fusion-positive disease (144, 145). Repotrectinib and lorlatinib have also been shown to have efficacy and CNS activity in patients with ROS1-positive NSCLC (128, 146). Tepotinib and capmatinib have demonstrated efficacy with good CNS activity in patients in NSCLC with MET exon 14 skipping mutations (161, 162). Finally, larotrectinib exhibited complete or partial intracranial responses in 2/3 patients with BrM secondary to TRK fusion-positive cancers (163). Similar intracranial efficacy was demonstrated with entrectinib in patients with BrM secondary to TRK fusion-positive cancers (iORR 50-62.5%) (164). The therapeutic efficacy of larotrectinib and entrectinib in TRK fusion-positive NSCLC specifically remains unclear, however, since these trials did not stratify patient outcomes by primary cancer type (163, 164).

### 2.3.1.4 Targeted Therapies in Melanoma

Studies have suggested that half of patients with metastatic melanoma will develop IMD, with a median OS of 4.7 months (165). Of note, genetic alterations in BRAF, including the activating mutations $BRAF^{V600E}$ and $BRAF^{V600K}$, have been identified in 47% of patients with melanoma and in 24% of melanoma patients with IMD, making BRAF mutations a likely target in the treatment of IMD secondary to melanoma (166).

In the landmark BREAK-MB trial, dabrafenib, a small molecule inhibitor of BRAF$^{V600E}$, demonstrated adequate anti-tumor activity in 39.2% of BRAF$^{V600E}$-positive melanoma patients with treatment-naïve IMD and 30.8% of BRAF$^{V600E}$-positive melanoma patients with progressive IMD (147). Median OS was 33.1 weeks and 31.4 weeks in BRAF$^{V600E}$-positive melanoma patients with treatment-naïve IMD and progressive IMD, respectively, and median PFS was 16.1 and 16.6 weeks in the same treatment groups. Intracranial response rates, median OS, and median PFS were lower for patients with BRAF$^{V600K}$-positive melanoma with progressive IMD than with treatment-naïve IMD, though no explicit comparisons were made between cohorts (147). A second BRAF$^{V600}$ inhibitor, vemurafenib, demonstrated adequate anti-tumor activity in 18% of patients with BRAF$^{V600}$-positive melanoma with either untreated or progressive IMD (149). Median OS was 8.9 months in patients with untreated IMD and 9.6 months in patients with previously treated IMD, however, no comparisons were made with dabrafenib (149).

In the COMBI-MB trial, the combination of dabrafenib and the mitogen-activated protein kinase kinase (MEK) inhibitor trametinib demonstrated adequate intracranial tumor control in 58% of BRAF$^{V600E}$-positive melanoma patients with treatment-naïve, asymptomatic IMD, 56% of BRAF$^{V600E}$-positive melanoma patients with progressive, asymptomatic IMD, 44% of BRAF$^{V600D/K/R}$-positive melanoma patients with asymptomatic IMD, and 59% of BRAF$^{V600E/D/K/R}$-positive melanoma with symptomatic IMD (148). Median OS was 10.8 and 24.3 months in BRAF$^{V600E}$-positive melanoma patients with treatment-naïve IMD and progressive IMD, respectively. Median PFS was 5.6 and 7.2 months in the same cohorts (148). Several additional single or combination agents, including vemurafenib and the MEK inhibitor cobimetinib or the BRAF inhibitor encorafenib and MEK inhibitor binimetinib, have been described to be effective in treating IMD secondary to BRAF-mutant melanoma. While these discussions have been thus far limited to case series and conference abstracts, early data suggest that multidrug targeted drug regimens for IMD secondary to BRAF-mutant melanoma may be future treatments for patients with BRAF-mutant melanoma and IMD.

## 2.3.2 Immunotherapies

Immune-checkpoint inhibitors (ICIs) include large monoclonal antibody-based therapies and small molecule inhibitors that upregulate the immune system and its antitumor activity (167, 168). Initial trials with ICIs have supported their use in patients with IMD secondary to NSCLC and melanoma. Additional trials are now underway to study their efficacy in patients with IMD secondary to other primary cancers, including breast cancer. For example, an early phase II trial studying ipilimumab, an anti-cytotoxic T-lymphocyte-associated antigen 4 (CLTA-4) antibody that promotes T lymphocyte destruction of cancer cells, demonstrated that 16% of melanoma patients with asymptomatic IMD receiving ipilimumab and 5% of melanoma patients with symptomatic IMD receiving corticosteroids and ipilimumab achieved an intracranial objective response (169). In the same study, median OS was 7 months in melanoma patients

with asymptomatic IMD receiving ipilimumab and 4 months in melanoma patients with symptomatic IMD receiving corticosteroids and ipilimumab.

In addition to CLTA-4, programmed cell death protein (PD-1), which acts as a negative immune inhibitor, has emerged as a potential anti-cancer target. In an early phase II trial studying the anti-PD-1 antibody pembrolizumab, 22% of melanoma patients with IMD and 33% of NSCLC patients with IMD treated with pembrolizumab monotherapy demonstrated an intracranial objective response (170). A slightly lower iORR was found with the administration of the anti-PD-1 antibody nivolumab in patients with NSCLC and IMD (17%) (171). Both studies support the hypothesis that anti-PD-1 antibodies are active in patients with IMD and present future therapy options. The combination of ipilimumab and nivolumab was investigated in Checkmate 204, which demonstrated an iORR in 53.5% of melanoma patients with asymptomatic IMD and 16.7% of melanoma patients with symptomatic IMD. In the same study, median PFS was reported to be 39.3 months and 1.2 months, respectively (172, 173). Finally, the RELATIVITY-047 trial recently reported prolonged PFS in patients with untreated or unresectable melanoma treated with a combination of nivolumab and lymphocyte-activation gene 3 (LAG-3) inhibitor relatlimab compared to those treated with nivolumab alone (HR 0.75, 95% CI 0.62-0.92, p=0.006) (174). A subgroup analysis of patients with BrM and associated intracranial outcomes is necessary to clarify the role of this promising drug combination in the setting of IMD secondary to melanoma.

Monoclonal antibodies against programmed cell death-ligand 1 (PD-L1) have also been investigated. In patients with IMD secondary to TNBC studied in the Impassion130 RCT, the combination of atezolizumab and nab-paclitaxel did not significantly improve median PFS (HR 0.86, 95% CI 0.50-1.49) or median OS (HR 1.34, 95% CI 0.72-2.48) compared with placebo and nab-paclitaxel (175, 176). Additional prospective trials, including NCT03483012 and NCT04303988, may further clarify the role of PD-L1 inhibitors in patients with IMD and TNBC.

Further investigations are necessary to clarify the role of immunotherapy for IMD in patients receiving concurrent targeted therapies (**Table 2**).

## 2.3.3 Immunotherapy in Combination With Radiation Therapy

Results from studies investigating the combined administration of radiation and immunotherapies suggest a biological synergy between the two modalities (182, 183). Yet, evidence on the treatment of IMD with radiation and ICI is conflicting and limited to retrospective analyses. Knisley et al., for example, reported a median OS of 21.3 months in 27 patients with melanoma and BrM who received ipilimumab in combination with radiosurgery, compared with 4.9 months in 50 patients treated with radiosurgery alone (p=0.03) (178). These findings have been corroborated in another single-institution case series (median OS 18.3 vs. 5.3 months, HR 0.43, p=0.005) (179). On the other hand, investigators from New York University found no improvement in median OS when SRS was administered

together with ipilimumab (n=25) compared with SRS as a stand-alone therapy (n=33) in patients with patients with melanoma and BrM (180). Several case reports also describe the combined administration of WBRT and immunotherapies, but evidence from larger cohort studies or RCTs is lacking (184, 185).

There is emerging evidence supporting the use of SRS and nivolumab: Minniti and colleagues reported that nivolumab was more effective in preventing intracranial disease progression and prolonging OS than ipilimumab when either agent was combined with SRS (median PFS 10 vs. 6 months, p=0.02; median OS 22.0 vs. 14.7 months, p=0.015) (181). In a study of patients with renal cell carcinoma and IMD, the PFS benefits of nivolumab were enhanced by prior SRS or WBRT (median iPFS 2.7 vs. 4.8 months, HR 0.49, p=0.0277) (177). Caution needs to be exercised around the current level of evidence, however. One 2013 RCT for example that compared WBRT plus SRS alone versus WBRT plus SRS in combination with temozolomide or erlotinib for NSCLC patients with limited number of metastases showed higher rates of grade 3 to 5 toxicities in the combination arms (11%, 41%, and 49%, respectively, p<0.001) (186). Moreover, BrM may harbour a distinct set of genetic alterations compared with the primary lesion, and thus responses to targeted therapies may be limited (187). Given the success of immunotherapies in the treatment of IMD and the already-established utility of radiation therapy, these combined approaches are promising avenues for the future. Further research is required before these approaches can be reliably translated into clinical practice (**Table 2**).

# 3 EMERGING CONSIDERATIONS FOR SECONDARY PREVENTION

Given its impact on survival and QoL, there is clinical interest in early identification of IMD in patients with high-risk primary cancer types. Understanding the pathobiology of IMD may enable the development of new clinical tools to detect early IMD and initiate appropriate treatments in patients with lower systemic metastatic disease burden.

## 3.1 Screening for IMD
Experience from screening efforts for breast, prostate, and lung cancer have shown that early cancer detection and treatment results in improved disease control and prolonged survival (188–190). To date, IMD diagnosis has depended on imaging, either for staging or screening purposes, or to assess patients who manifest neurological symptoms concerning for brain metastases (7). Default intracranial imaging for all cancer patients would be structurally and financially infeasible; further, given the finding in observational studies that nearly 4% of asymptomatic individuals harbor an intracranial "incidentaloma", this approach would likely lead to overdiagnosis and unintentional overtreatment (191, 192). Instead, many current efforts have focused on screening of patients who are at high risk for the development of IMD (193). A recent review of studies reporting on the incidence of IMD in

patients with metastatic and non-metastatic breast cancer found a significantly higher incidence of IMD in patients with metastatic HER2-positive (22-36%) and metastatic TNBC (15-37%) compared with other forms of metastatic breast cancer (approximately 10%) and non-metastatic breast cancer (annual incidence of IMD as first site of recurrence ≤3% for all identified studies) (193). Findings from this review indicate that patients with metastatic HER2-positive and TNBC are at a sufficiently high risk for development of IMD to warrant routine screening. The American Society of Clinical Oncology (ASCO) and the NCCN currently do not recommend routine screening for IMD in women with metastatic breast cancer; conversely, the 2021 European Association of Neuro-Oncology (EANO)/European Society for Medical Oncology (ESMO) guidelines indicate that screening at diagnosis is "potentially justified" in patients with metastatic HER2-positive and TNBC [EANO: IV, n/a; ESMO: IV, B] (194). To clarify the risks and benefits of routine screening in these patients, multiple studies are currently randomizing patients with HER2-positive or TNBC, both subgroups with a well-defined higher risk of IMD, to either receive regularly scheduled MRI brain imaging or standard of care alone (NCT03881605; NCT04030507; NCT03617341) (193, 195). It remains to be determined if these efforts will result in improved outcomes for patients.

Overall, the reliance on imaging, and particularly MRI, has been a profound limitation to efforts for IMD screening, early detection, and treatment. There has been significant interest in development tools for IMD screening that circumvent intracranial imaging, for example, liquid biopsy (196). The concept of liquid biopsy rests on the assumption that different elements of tumor material, such as tumor-specific DNA, RNA, proteins, and exosomes, and circulating tumor cells, can be identified in blood or cerebrospinal fluid (CSF) as a surrogate for cancer burden. To date, these efforts have been limited by the need to isolate and enrich cancer markers in blood to enable sequencing for genomic approaches, which results in technical error and false biological signals, leading to high false-negative results. There are also valid concerns that spillage of intracranial tumor into the systemic circulation may be limited, which could mandate study of CSF rather than blood (a much more invasive process which requires lumbar puncture) to assess intracranial disease (197).

## 3.2 Understanding the Biology of Brain Metastases
There has been significant interest in delineating the biological processes that underlie metastatic progression in cancer and, in particular, mediate the development of IMD (198). Multiple studies have shown that BrM are derived from cancer subclones that are distinct from dominant populations in the systemic cancer cell pool (199, 200). This finding raises the possibility that primary tumor profiling could identify patients who harbor subclones that are organotypic for the brain and are thus at risk of IMD (201). Further, this finding promises the likelihood of novel pathways, both cell-intrinsic and environmental, that are critical for IMD development and that could be targets for IMD prevention (187, 202, 203).

**TABLE 2 |** Summary of studies investigating immunotherapies for IMD.

| Trial/ Study | Drug | Radiation | Study design | Total participants (n) | Cohorts | Median OS (months) | Median PFS (months) | Findings |
|---|---|---|---|---|---|---|---|---|
| Margolin et al. (169) | Ipilimumab | – | Single-arm clinical trial | 72 | Asymptomatic IMD | 7 | – | iORR: 16% |
| | | | | | | | | Intracranial DCR: 24% |
| | | | | | Symptomatic IMD + corticosteroids | 4 | – | iORR: 5% |
| | | | | | | | | Intracranial DCR: 10% |
| Goldberg et al. (170) | Pembrolizumab | – | Single-arm clinical trial | 52 | Melanoma | NR | – | iORR: 22% |
| | | | | | NSCLC | 7.7 | – | iORR: 33% |
| Crinò et al. (171) | Nivolumab | – | Single-arm clinical trial | 1588 | – | 8.6 | 3.0 | Overall ORR: 17% |
| | | | | | | | | Overall DCR: 39% |
| Flippot et al. (177) | Nivolumab | – | Single-arm clinical trial | 73 | Untreated IMD | – | 2.4 | iORR: 12% |
| | | | | | | | | Intracranial DCR: 50% |
| | | | | | | | | Intracranial PFS: 2.7 months |
| | | | | | Previously treated IMD (SRS/WBRT) | – | 2.5 | Intracranial PFS: 4.8 months, HR 0.49, p=0.0277 |
| Tawbi et al. (172) | Ipilimumab + nivolumab | – | Single-arm clinical trial | 94 | – | – | – | iORR: 55% |
| | | | | | | | | Intracranial DCR: 57% |
| Tawbi et al. (173) | Ipilimumab + nivolumab | – | Single-arm clinical trial | 165 | Asymptomatic IMD | – | 39.3 | iORR: 53.5% |
| | | | | | | | | Intracranial DCR: 57.4% |
| | | | | | Symptomatic IMD | – | 1.2 | iORR: 16.7% |
| | | | | | | | | Intracranial DCR: 16.7% |
| Tawbi et al. (174) | Relatlimab + nivolumab | – | RCT | 714 | Relatlimab + nivolumab | – | – | – |
| | | | | | Nivolumab | – | – | – |
| Schmid et al. (175) | Atezolizumab + nab-paclitaxel | – | RCT | 451 | Atezolizumab + nab-paclitaxel | – | 4.9 (HR 0.86, 95% CI 0.50-1.49) | – |
| | | | | | Placebo + nab-paclitaxel | – | 4.4 | – |
| Schmid et al. (176) | Atezolizumab + nab-paclitaxel | – | RCT | 902 | Atezolizumab + nab-paclitaxel | 14.3 (HR 1.34, 95% CI 0.72-2.48) | – | – |
| | | | | | Placebo + nab-paclitaxel | 16.2 | – | – |
| Knisely et al. (178) | Ipilimumab | SRS | Retrospective cohort study | 77 | SRS + ipilimumab | 21.3 | – | – |
| | | | | | SRS only | 4.9 (HR 0.48, p=0.03) | – | – |
| Silk et al. (179) | Ipilimumab | SRS | Retrospective cohort study | 70 | SRS + ipilimumab | 18.3 | 2.7 | – |
| | | | | | SRS only | 5.3 (HR 0.43, p=0.005) | 3.3 | – |
| Mathew et al. (180) | Ipilimumab | SRS | Retrospective cohort study | 58 | SRS + ipilimumab | 56% in 6 months | – | – |
| | | | | | SRS only | 45% in 6 months (p=0.18) | – | – |
| Minniti et al. (181) | Nivolumab or ipilimumab | SRS | Retrospective cohort study | 80 | Nivolumab + SRS | 22.0 | 10 | iORR: 76% |
| | | | | | Ipilimumab + SRS | 14.7 (p=0.015) | 6 (p=0.02) | iORR: 60% |

*Median overall survival marked with a dash if the data was 1) not reported or 2) reported for the entire population, including patients without IMD.*
*CI, confidence interval; DCR, disease control rate; HR, hazard ratio; IMD, intracranial metastatic disease; iORR, intracranial ORR; NR, not yet reached; NSCLC, non-small cell lung cancer; ORR, objective response rate; OS, overall survival; PFS, progression-free survival; RCT, randomized control trial; SRS, stereotactic radiosurgery; WBRT, whole-brain radiotherapy.*

# 4 CONCLUSION

Diagnosis of IMD places a significant burden on patient survival and QoL. Over the past several decades, technical innovations and an advancing understanding of tumor biology have enabled physicians to optimize treatment outcomes for these patients. While WBRT initially formed the mainstay of localized treatment for IMD, surgical resection and SRS have become established treatment approaches for patients with limited intracranial disease burden and are increasingly considered for a wider patient spectrum. Several molecular drivers have also been identified as targets for systemic therapy. While most of these agents historically had limited application for treatment of IMD, mounting evidence suggests that some targeted therapy drugs may retain activity in the brain, especially in patients with IMD due to single driver-mediated breast cancer, NSCLC, and melanoma. Early investigations into the efficacy of immunotherapies and their combination with radiation therapy may further form future avenues of treatment. These advances promise to improve outcomes patients with cancer and IMD.

## AUTHOR CONTRIBUTIONS

## FUNDING

## REFERENCES

1. Scoccianti S, Ricardi U. Treatment of Brain Metastases: Review of Phase III Randomized Controlled Trials. *Radiother Oncol* (2012) 102(2):168–79. doi: 10.1016/j.radonc.2011.08.041

2. Habbous S, Forster K, Darling G, Jerzak K, Holloway CMB, Sahgal A, et al. Incidence and Real-World Burden of Brain Metastases From Solid Tumors and Hematologic Malignancies in Ontario: A Population-Based Study. *Neurooncol Adv* (2021) 3(1):vdaa178. doi: 10.1093/noajnl/vdaa178

3. Zakaria R, Das K, Bhojak M, Radon M, Walker C, Jenkinson MD. The Role of Magnetic Resonance Imaging in the Management of Brain Metastases: Diagnosis to Prognosis. *Cancer Imaging* (2014) 14(1):8. doi: 10.1186/1470-7330-14-8

4. Winther-Larsen A, Hviid CVB, Meldgaard P, Sorensen BS, Sandfeld-Paulsen B. Neurofilament Light Chain as A Biomarker for Brain Metastases. *Cancers* (2020) 12(10):2852. doi: 10.3390/cancers12102852

5. Bhatia A, Birger M, Veeraraghavan H, Um H, Tixier F, McKenney AS, et al. MRI Radiomic Features Are Associated With Survival in Melanoma Brain Metastases Treated With Immune Checkpoint Inhibitors. *Neuro-Oncology* (2019) 21(12):1578–86. doi: 10.1093/neuonc/noz141

6. Sperduto PW, Mesko S, Li J, Cagney D, Aizer A, Lin NU, et al. Survival in Patients With Brain Metastases: Summary Report on the Updated Diagnosis-Specific Graded Prognostic Assessment and Definition of the Eligibility Quotient. *J Clin Oncol* (2020) 38(32):3773–84. doi: 10.1200/JCO.20.01255

7. Suh JH, Kotecha R, Chao ST, Ahluwalia MS, Sahgal A, Chang EL. Current Approaches to the Management of Brain Metastases. *Nat Rev Clin Oncol* (2020) 17(5):279–99. doi: 10.1038/s41571-019-0320-3

8. Borgelt B, Gelber R, Kramer S, Brady LW, Chang CH, Davis LW, et al. The Palliation of Brain Metastases: Final Results of the First Two Studies by the Radiation Therapy Oncology Group. *Int J Radiat Oncol Biol Phys* (1980) 6(1):1–9. doi: 10.1016/0360-3016(80)90195-9

9. Mehta MP, Rodrigus P, Terhaard CH, Rao A, Suh J, Roa W, et al. Survival and Neurologic Outcomes in a Randomized Trial of Motexafin Gadolinium and Whole-Brain Radiation Therapy in Brain Metastases. *J Clin Oncol* (2003) 21(13):2529–36. doi: 10.1200/JCO.2003.12.122

10. Suh JH, Stea B, Nabid A, Kresl JJ, Fortin A, Mercier JP, et al. Phase III Study of Efaproxiral as an Adjunct to Whole-Brain Radiation Therapy for Brain Metastases. *J Clin Oncol* (2006) 24(1):106–14. doi: 10.1200/JCO.2004.00.1768

11. Sperduto PW, Deegan BJ, Li J, Jethwa KR, Brown PD, Lockney N, et al. Estimating Survival for Renal Cell Carcinoma Patients With Brain Metastases: An Update of the Renal Graded Prognostic Assessment Tool. *Neuro Oncol* (2018) 20(12):1652–60. doi: 10.1093/neuonc/noy099

12. Niranjan A, Lunsford LD, Ahluwalia MS. Targeted Therapies for Brain Metastases. *Prog Neurol Surg* (2019) 34:125–37. doi: 10.1159/000493057

13. Erickson AW, Habbous S, Wright F, Lofters AK, Jerzak KJ, Das S. Assessing the Association of Targeted Therapy and Intracranial Metastatic Disease. *JAMA Oncol* (2021) 7(8):1220–4. doi: 10.1001/jamaoncol.2021.1600

14. Kanner AA, Bokstein F, Blumenthal DT, Ram Z. Surgical Therapies in Brain Metastasis. *Semin Oncol* (2007) 34(3):197–205. doi: 10.1053/j.seminoncol.2007.03.011

15. Kuo T, Recht L. Optimizing Therapy for Patients With Brain Metastases. *Semin Oncol* (2006) 33(3):299–306. doi: 10.1053/j.seminoncol.2006.03.005

16. Sawaya R, Hammoud M, Schoppa D, Hess KR, Wu SZ, Shi WM, et al. Neurosurgical Outcomes in a Modern Series of 400 Craniotomies for Treatment of Parenchymal Tumors. *Neurosurgery* (1998) 42(5):1044–55; discussion 55-6. doi: 10.1097/00006123-199805000-00054

17. Redmond KJ, De Salles AAF, Fariselli L, Levivier M, Ma L, Paddick I, et al. Stereotactic Radiosurgery for Postoperative Metastatic Surgical Cavities: A Critical Review and International Stereotactic Radiosurgery Society (ISRS) Practice Guidelines. *Int J Radiat Oncol Biol Phys* (2021) 111(1):68–80. doi: 10.1016/j.ijrobp.2021.04.016

18. Prabhu RS, Turner BE, Asher AL, Marcrom SR, Fiveash JB, Foreman PM, et al. A Multi-Institutional Analysis of Presentation and Outcomes for Leptomeningeal Disease Recurrence After Surgical Resection and Radiosurgery for Brain Metastases. *Neuro Oncol* (2019) 21(8):1049–59. doi: 10.1093/neuonc/noz049

19. DeAngelis LM, Posner JB. *Neurologic Complications of Cancer*. New York City, NY, USA: Oxford University Press (2009).

20. Patchell RA, Tibbs PA, Walsh JW, Dempsey RJ, Maruyama Y, Kryscio RJ, et al. A Randomized Trial of Surgery in the Treatment of Single Metastases to the Brain. *N Engl J Med* (1990) 322(8):494–500. doi: 10.1056/NEJM199002223220802

21. Vecht CJ, Haaxma-Reiche H, Noordijk EM, Padberg GW, Voormolen JH, Hoekstra FH, et al. Treatment of Single Brain Metastasis: Radiotherapy Alone or Combined With Neurosurgery? *Ann Neurol* (1993) 33(6):583–90. doi: 10.1002/ana.410330605

22. Mintz AH, Kestle J, Rathbone MP, Gaspar L, Hugenholtz H, Fisher B, et al. A Randomized Trial to Assess the Efficacy of Surgery in Addition to Radiotherapy in Patients With a Single Cerebral Metastasis. *Cancer* (1996) 78(7):1470–6. doi: 10.1002/(SICI)1097-0142(19961001)78:7<1470::AID-CNCR14>3.0.CO;2-X

23. Gaspar LE, Mehta MP, Patchell RA, Burri SH, Robinson PD, Morris RE, et al. The Role of Whole Brain Radiation Therapy in the Management of Newly Diagnosed Brain Metastases: A Systematic Review and Evidence-Based Clinical Practice Guideline. *J Neurooncol* (2010) 96(1):17–32. doi: 10.1007/s11060-009-0060-9

24. Kalkanis SN, Kondziolka D, Gaspar LE, Burri SH, Asher AL, Cobbs CS, et al. The Role of Surgical Resection in the Management of Newly Diagnosed Brain Metastases: A Systematic Review and Evidence-Based Clinical Practice Guideline. *J Neurooncol* (2010) 96(1):33–43. doi: 10.1007/s11060-009-0061-8

25. Garell PC, Hitchon PW, Wen BC, Mellenberg DE, Torner J. Stereotactic Radiosurgery Versus Microsurgical Resection for the Initial Treatment of Metastatic Cancer to the Brain. *J Radiosurg* (1999) 2(1):1–5. doi: 10.1023/A:1022914932190

26. O'Neill BP, Iturria NJ, Link MJ, Pollock BE, Ballman KV, O'Fallon JR. A Comparison of Surgical Resection and Stereotactic Radiosurgery in the Treatment of Solitary Brain Metastases. *Int J Radiat Oncol Biol Phys* (2003) 55(5):1169–76. doi: 10.1016/S0360-3016(02)04379-1

27. Schödel P, Schebesch K-M, Brawanski A, Proescholdt MA. Surgical Resection of Brain Metastases—Impact on Neurological Outcome. *Int J Mol Sci* (2013) 14(5):8708–18. doi: 10.3390/ijms14058708

28. Kondziolka D, Kano H, Harrison GL, Yang HC, Liew DN, Niranjan A, et al. Stereotactic Radiosurgery as Primary and Salvage Treatment for Brain Metastases From Breast Cancer. *Clin article J Neurosurg* (2011) 114(3):792–800. doi: 10.3171/2010.8.JNS10461

29. Gazzeri R, Nalavenkata S, Teo C. Minimally Invasive Key-Hole Approach for the Surgical Treatment of Single and Multiple Brain Metastases. *Clin Neurol Neurosurg* (2014) 123:117–26. doi: 10.1016/j.clineuro.2014.05.010

30. Iwadate Y, Namba H, Yamaura A. Significance of Surgical Resection for the Treatment of Multiple Brain Metastases. *Anticancer Res* (2000) 20(1b):573–7.

31. Salvati M, Tropeano MP, Maiola V, Lavalle L, Brogna C, Colonnese C, et al. Multiple Brain Metastases: A Surgical Series and Neurosurgical Perspective. *Neurol Sci* (2018) 39(4):671–7. doi: 10.1007/s10072-017-3220-2

32. Baker CM, Glenn CA, Briggs RG, Burks JD, Smitherman AD, Conner AK, et al. Simultaneous Resection of Multiple Metastatic Brain Tumors With

Multiple Keyhole Craniotomies. *World Neurosurg* (2017) 106:359–67. doi: 10.1016/j.wneu.2017.06.118

33. Eroglu U, Shah K, Bozkurt M, Kahilogullari G, Yakar F, Dogan İ, et al. Supraorbital Keyhole Approach: Lessons Learned From 106 Operative Cases. *World Neurosurg* (2019) 124:e667–74. doi: 10.1016/j.wneu.2018.12.188

34. Gazzeri R, Nishiyama Y, Teo C. Endoscopic Supraorbital Eyebrow Approach for the Surgical Treatment of Extraaxialand Intraaxial Tumors. *Neurosurg Focus* (2014) 37(4):E20. doi: 10.3171/2014.7.FOCUS14203

35. Phang I, Leach J, Leggate JRS, Karabatsou K, Coope D, D'Urso PI. Minimally Invasive Resection of Brain Metastases. *World Neurosurg* (2019) 130:e362–e7. doi: 10.1016/j.wneu.2019.06.091

36. Raza SM, Garzon-Muvdi T, Boaehene K, Olivi A, Gallia G, Lim M, et al. The Supraorbital Craniotomy for Access to the Skull Base and Intraaxial Lesions: A Technique in Evolution. *Minim Invasive Neurosurg* (2010) 53(1):1–8. doi: 10.1055/s-0030-1247504

37. Wang JL, Elder JB. Techniques for Open Surgical Resection of Brain Metastases. *Neurosurg Clin N Am* (2020) 31(4):527–36. doi: 10.1016/j.nec.2020.06.003

38. Gassie K, Alvarado-Estrada K, Bechtle P, Chaichana KL. Surgical Management of Deep-Seated Metastatic Brain Tumors Using Minimally Invasive Approaches. *J Neurol Surg A Cent Eur Neurosurg* (2019) 80(3):198–204. doi: 10.1055/s-0038-1676575

39. Chao JH, Phillips R, Nickson JJ. Roentgen-Ray Therapy of Cerebral Metastases. *Cancer* (1954) 7(4):682–9. doi: 10.1002/1097-0142(195407)7:4<682::AID-CNCR2820070409>3.0.CO;2-S

40. Order SE, Hellmän S, Essen CFV, Kligerman MM. Improvement in Quality of Survival Following Whole-Brain Irradiation for Brain Metastasis. *Radiology* (1968) 91(1):149–53. doi: 10.1148/91.1.149

41. Patchell RA, Tibbs PA, Regine WF, Dempsey RJ, Mohiuddin M, Kryscio RJ, et al. Postoperative Radiotherapy in the Treatment of Single Metastases to the Brain: A Randomized Trial. *Jama* (1998) 280(17):1485–9. doi: 10.1001/jama.280.17.1485

42. Tallet AV, Azria D, Barlesi F, Spano JP, Carpentier AF, Gonçalves A, et al. Neurocognitive Function Impairment After Whole Brain Radiotherapy for Brain Metastases: Actual Assessment. *Radiat Oncol* (2012) 7:77. doi: 10.1186/1748-717X-7-77

43. Brown PD, Pugh S, Laack NN, Wefel JS, Khuntia D, Meyers C, et al. Memantine for the Prevention of Cognitive Dysfunction in Patients Receiving Whole-Brain Radiotherapy: A Randomized, Double-Blind, Placebo-Controlled Trial. *Neuro-Oncology* (2013) 15(10):1429–37. doi: 10.1093/neuonc/not114

44. Gondi V, Deshmukh S, Brown PD, Wefel JS, Tome W, Armstrong T, et al. NRG Oncology CC001: A Phase III Trial of Hippocampal Avoidance (HA) in Addition to Whole-Brain Radiotherapy (WBRT) Plus Memantine to Preserve Neurocognitive Function (NCF) in Patients With Brain Metastases (BM). *Am Soc Clin Oncol* (2019) 37(15 suppl):2009. doi: 10.1200/JCO.2019.37.15_suppl.2009

45. Gondi V, Pugh SL, Tome WA, Caine C, Corn B, Kanner A, et al. Preservation of Memory With Conformal Avoidance of the Hippocampal Neural Stem-Cell Compartment During Whole-Brain Radiotherapy for Brain Metastases (RTOG 0933): A Phase II Multi-Institutional Trial. *J Clin Oncol* (2014) 32(34):3810–6. doi: 10.1200/JCO.2014.57.2909

46. Meyers CA, Smith JA, Bezjak A, Mehta MP, Liebmann J, Illidge T, et al. Neurocognitive Function and Progression in Patients With Brain Metastases Treated With Whole-Brain Radiation and Motexafin Gadolinium: Results of a Randomized Phase III Trial. *J Clin Oncol* (2004) 22(1):157–65. doi: 10.1200/JCO.2004.05.128

47. Soffietti R, Abacioglu U, Baumert B, Combs SE, Kinhult S, Kros JM, et al. Diagnosis and Treatment of Brain Metastases From Solid Tumors: Guidelines From the European Association of Neuro-Oncology (EANO). *Neuro Oncol* (2017) 19(2):162–74. doi: 10.1093/neuonc/now241

48. Gerosa M, Nicolato A, Foroni R, Tomazzoli L, Bricolo A. Analysis of Long-Term Outcomes and Prognostic Factors in Patients With Non-Small Cell Lung Cancer Brain Metastases Treated by Gamma Knife Radiosurgery. *J Neurosurg* (2005) 102 Suppl:75–80. doi: 10.3171/jns.2005.102.s_supplement.0075

49. Hussain A, Brown PD, Stafford SL, Pollock BE. Stereotactic Radiosurgery for Brainstem Metastases: Survival, Tumor Control, and Patient Outcomes. *Int J Radiat Oncol Biol Phys* (2007) 67(2):521–4. doi: 10.1016/j.ijrobp.2006.08.081

50. Churilla TM, Chowdhury IH, Handorf E, Collette L, Collette S, Dong Y, et al. Comparison of Local Control of Brain Metastases With Stereotactic Radiosurgery vs Surgical Resection: A Secondary Analysis of a Randomized Clinical Trial. *JAMA Oncol* (2019) 5(2):243–7. doi: 10.1001/jamaoncol.2018.4610

51. Andrews DW, Scott CB, Sperduto PW, Flanders AE, Gaspar LE, Schell MC, et al. Whole Brain Radiation Therapy With or Without Stereotactic Radiosurgery Boost for Patients With One to Three Brain Metastases: Phase III Results of the RTOG 9508 Randomised Trial. *Lancet* (2004) 363 (9422):1665–72. doi: 10.1016/S0140-6736(04)16250-8

52. Kondziolka D, Patel A, Lunsford LD, Kassam A, Flickinger JC. Stereotactic Radiosurgery Plus Whole Brain Radiotherapy Versus Radiotherapy Alone for Patients With Multiple Brain Metastases. *Int J Radiat Oncol Biol Phys* (1999) 45(2):427–34. doi: 10.1016/S0360-3016(99)00198-4

53. Aoyama H, Shirato H, Tago M, Nakagawa K, Toyoda T, Hatano K, et al. Stereotactic Radiosurgery Plus Whole-Brain Radiation Therapy vs Stereotactic Radiosurgery Alone for Treatment of Brain Metastases: A Randomized Controlled Trial. *Jama* (2006) 295(21):2483–91. doi: 10.1001/jama.295.21.2483

54. Chang EL, Wefel JS, Hess KR, Allen PK, Lang FF, Kornguth DG, et al. Neurocognition in Patients With Brain Metastases Treated With Radiosurgery or Radiosurgery Plus Whole-Brain Irradiation: A Randomised Controlled Trial. *Lancet Oncol* (2009) 10(11):1037–44. doi: 10.1016/S1470-2045(09)70263-3

55. Weiss SE, Kelly PJ. Neurocognitive Function After WBRT Plus SRS or SRS Alone. *Lancet Oncol* (2010) 11(3):220–1. doi: 10.1016/S1470-2045(09)70387-0

56. Kocher M, Soffietti R, Abacioglu U, Villà S, Fauchon F, Baumert BG, et al. Adjuvant Whole-Brain Radiotherapy Versus Observation After Radiosurgery or Surgical Resection of One to Three Cerebral Metastases: Results of the EORTC 22952-26001 Study. *J Clin Oncol* (2011) 29(2):134–41. doi: 10.1200/JCO.2010.30.1655

57. Soffietti R, Kocher M, Abacioglu UM, Villa S, Fauchon F, Baumert BG, et al. A European Organisation for Research and Treatment of Cancer Phase III Trial of Adjuvant Whole-Brain Radiotherapy Versus Observation in Patients With One to Three Brain Metastases From Solid Tumors After Surgical Resection or Radiosurgery: Quality-of-Life Results. *J Clin Oncol* (2013) 31 (1):65–72. doi: 10.1200/JCO.2011.41.0639

58. Kim H, Rajagopalan MS, Beriwal S, Smith KJ. Cost-Effectiveness Analysis of Stereotactic Radiosurgery Alone Versus Stereotactic Radiosurgery With Upfront Whole Brain Radiation Therapy for Brain Metastases. *Clin Oncol (R Coll Radiol)* (2017) 29(10):e157–e64. doi: 10.1016/j.clon.2017.05.001

59. Sahgal A, Aoyama H, Kocher M, Neupane B, Collette S, Tago M, et al. Phase 3 Trials of Stereotactic Radiosurgery With or Without Whole-Brain Radiation Therapy for 1 to 4 Brain Metastases: Individual Patient Data Meta-Analysis. *Int J Radiat Oncol Biol Phys* (2015) 91(4):710–7. doi: 10.1016/j.ijrobp.2014.10.024

60. Tsao M, Xu W, Sahgal A. A Meta-Analysis Evaluating Stereotactic Radiosurgery, Whole-Brain Radiotherapy, or Both for Patients Presenting With a Limited Number of Brain Metastases. *Cancer* (2012) 118(9):2486–93. doi: 10.1002/cncr.26515

61. Hong AM, Fogarty GB, Dolven-Jacobsen K, Burmeister BH, Lo SN, Haydu LE, et al. Adjuvant Whole-Brain Radiation Therapy Compared With Observation After Local Treatment of Melanoma Brain Metastases: A Multicenter, Randomized Phase III Trial. *J Clin Oncol* (2019) 37 (33):3132–41. doi: 10.1200/JCO.19.01414

62. ASTRO. *Don't Routinely Add Adjuvant Whole Brain Radiation Therapy to Stereotactic Radiosurgery for Limited Brain Metastases*. Philadelphia: ABIM Foundation (2014). Available at: https://www.choosingwisely.org/clinician-lists/american-society-radiation-oncology-adjuvant-whole-brain-radiation-therapy/.

63. Yamamoto M, Serizawa T, Shuto T, Akabane A, Higuchi Y, Kawagishi J, et al. Stereotactic Radiosurgery for Patients With Multiple Brain Metastases (JLGK0901): A Multi-Institutional Prospective Observational Study. *Lancet Oncol* (2014) 15(4):387–95. doi: 10.1016/S1470-2045(14)70221-9

64. Blonigen BJ, Steinmetz RD, Levin L, Lamba MA, Warnick RE, Breneman JC. Irradiated Volume as a Predictor of Brain Radionecrosis After Linear Accelerator Stereotactic Radiosurgery. *Int J Radiat Oncol Biol Phys* (2010) 77(4):996–1001. doi: 10.1016/j.ijrobp.2009.06.006

65. Chin LS, Ma L, DiBiase S. Radiation Necrosis Following Gamma Knife Surgery: A Case-Controlled Comparison of Treatment Parameters and Long-Term Clinical Follow Up. J Neurosurg (2001) 94(6):899–904. doi: 10.3171/jns.2001.94.6.0899

66. Kohutek ZA, Yamada Y, Chan TA, Brennan CW, Tabar V, Gutin PH, et al. Long-Term Risk of Radionecrosis and Imaging Changes After Stereotactic Radiosurgery for Brain Metastases. J Neuro-Oncol (2015) 125(1):149–56. doi: 10.1007/s11060-015-1881-3

67. Minniti G, Clarke E, Lanzetta G, Osti MF, Trasimeni G, Bozzao A, et al. Stereotactic Radiosurgery for Brain Metastases: Analysis of Outcome and Risk of Brain Radionecrosis. Radiat Oncol (2011) 6(1):1–9. doi: 10.1186/1748-717X-6-48

68. Varlotto JM, Flickinger JC, Niranjan A, Bhatnagar AK, Kondziolka D, Lunsford LD. Analysis of Tumor Control and Toxicity in Patients Who Have Survived at Least One Year After Radiosurgery for Brain Metastases. Int J Radiat Oncol Biol Phys (2003) 57(2):452–64. doi: 10.1016/S0360-3016(03)00568-6

69. Fujimoto D, von Eyben R, Gibbs IC, Chang SD, Li G, Harsh GR, et al. Imaging Changes Over 18 Months Following Stereotactic Radiosurgery for Brain Metastases: Both Late Radiation Necrosis and Tumor Progression can Occur. J Neuro-Oncol (2018) 136(1):207–12. doi: 10.1007/s11060-017-2647-x

70. Strenger V, Lackner H, Mayer R, Sminia P, Sovinz P, Mokry M, et al. Incidence and Clinical Course of Radionecrosis in Children With Brain Tumors. Strahlenther und Onkologie (2013) 189(9):759–64. doi: 10.1007/s00066-013-0408-0

71. Chi D, Béhin A, Delattre J-Y. Neurologic Complications of Radiation Therapy. In: Cancer Neurology in Clinical Practice. Totowa, NJ: Humana Press (2008). p. 259–86.

72. Rahmathulla G, Marko NF, Weil RJ. Cerebral Radiation Necrosis: A Review of the Pathobiology, Diagnosis and Management Considerations. J Clin Neurosci (2013) 20(4):485–502. doi: 10.1016/j.jocn.2012.09.011

73. Ruben JD, Dally M, Bailey M, Smith R, McLean CA, Fedele P. Cerebral Radiation Necrosis: Incidence, Outcomes, and Risk Factors With Emphasis on Radiation Parameters and Chemotherapy. Int J Radiat Oncol Biol Phys (2006) 65(2):499–508. doi: 10.1016/j.ijrobp.2005.12.002

74. Nedzi LA, Kooy H, Alexander E, Gelman RS, Loeffler JS. Variables Associated With the Development of Complications From Radiosurgery of Intracranial Tumors. Int J Radiat OncolBiolPhys (1991) 21(3):591–9. doi: 10.1016/0360-3016(91)90675-T

75. Colaco RJ, Martin P, Kluger HM, Yu JB, Chiang VL. Does Immunotherapy Increase the Rate of Radiation Necrosis After Radiosurgical Treatment of Brain Metastases? J Neurosurg (2016) 125(1):17–23. doi: 10.3171/2015.6.JNS142763

76. Kim JM, Miller JA, Kotecha R, Xiao R, Juloori A, Ward MC, et al. The Risk of Radiation Necrosis Following Stereotactic Radiosurgery With Concurrent Systemic Therapies. J Neurooncol (2017) 133(2):357–68. doi: 10.1007/s11060-017-2442-8

77. Sneed PK, Mendez J, Vemer-van den Hoek JG, Seymour ZA, Ma L, Molinaro AM, et al. Adverse Radiation Effect After Stereotactic Radiosurgery for Brain Metastases: Incidence, Time Course, and Risk Factors. J Neurosurg (2015) 123(2):373–86. doi: 10.3171/2014.10.JNS141610

78. Martin AM, Cagney DN, Catalano PJ, Alexander BM, Redig AJ, Schoenfeld JD, et al. Immunotherapy and Symptomatic Radiation Necrosis in Patients With Brain Metastases Treated With Stereotactic Radiation. JAMA Oncol (2018) 4(8):1123–4. doi: 10.1001/jamaoncol.2017.3993

79. Levin VA, Bidaut L, Hou P, Kumar AJ, Wefel JS, Bekele BN, et al. Randomized Double-Blind Placebo-Controlled Trial of Bevacizumab Therapy for Radiation Necrosis of the Central Nervous System. Int J Radiat Oncol Biol Phys (2011) 79(5):1487–95. doi: 10.1016/j.ijrobp.2009.12.061

80. McPherson CM, Warnick RE. Results of Contemporary Surgical Management of Radiation Necrosis Using Frameless Stereotaxis and Intraoperative Magnetic Resonance Imaging. J Neurooncol (2004) 68(1):41–7. doi: 10.1023/B:NEON.0000024744.16031.e9

81. Newman WC, Goldberg J, Guadix SW, Brown S, Reiner AS, Panageas K, et al. The Effect of Surgery on Radiation Necrosis in Irradiated Brain Metastases: Extent of Resection and Long-Term Clinical and Radiographic Outcomes. J Neurooncol (2021) 153(3):507–18. doi: 10.1007/s11060-021-03790-y

82. Ahluwalia M, Barnett GH, Deng D, Tatter SB, Laxton AW, Mohammadi AM, et al. Laser Ablation After Stereotactic Radiosurgery: A Multicenter Prospective Study in Patients With Metastatic Brain Tumors and Radiation Necrosis. J Neurosurg (2018) 130(3):804–11. doi: 10.3171/2017.11.JNS171273

83. Lamba N, Mehanna E, Kearney RB, Catalano PJ, Brown PD, Haas-Kogan DA, et al. Prescription of Memantine During Non-Stereotactic, Brain-Directed Radiation Among Patients With Brain Metastases: A Population-Based Study. J Neuro-Oncol (2020) 148(3):509–17. doi: 10.1007/s11060-020-03542-4

84. Attia A, Rapp SR, Case LD, D'Agostino R, Lesser G, Naughton M, et al. Phase II Study of Ginkgo Biloba in Irradiated Brain Tumor Patients: Effect on Cognitive Function, Quality of Life, and Mood. J Neurooncol (2012) 109(2):357–63. doi: 10.1007/s11060-012-0901-9

85. Rapp SR, Case LD, Peiffer A, Naughton MM, Chan MD, Stieber VW, et al. Donepezil for Irradiated Brain Tumor Survivors: A Phase III Randomized Placebo-Controlled Clinical Trial. J Clin Oncol (2015) 33(15):1653–9. doi: 10.1200/JCO.2014.58.4508

86. Shaw MG, Ball DL. Treatment of Brain Metastases in Lung Cancer: Strategies to Avoid/Reduce Late Complications of Whole Brain Radiation Therapy. Curr Treat Options Oncol (2013) 14(4):553–67. doi: 10.1007/s11864-013-0258-0

87. Robbins ME, Payne V, Tommasi E, Diz DI, Hsu FC, Brown WR, et al. The AT1 Receptor Antagonist, L-158,809, Prevents or Ameliorates Fractionated Whole-Brain Irradiation-Induced Cognitive Impairment. Int J Radiat Oncol Biol Phys (2009) 73(2):499–505. doi: 10.1016/j.ijrobp.2008.09.058

88. Monje ML, Mizumatsu S, Fike JR, Palmer TD. Irradiation Induces Neural Precursor-Cell Dysfunction. Nat Med (2002) 8(9):955–62. doi: 10.1038/nm749

89. Ghia A, Tomé WA, Thomas S, Cannon G, Khuntia D, Kuo JS, et al. Distribution of Brain Metastases in Relation to the Hippocampus: Implications for Neurocognitive Functional Preservation. Int J Radiat Oncol Biol Phys (2007) 68(4):971–7. doi: 10.1016/j.ijrobp.2007.02.016

90. Brown PD, Gondi V, Pugh S, Tome WA, Wefel JS, Armstrong TS, et al. Hippocampal Avoidance During Whole-Brain Radiotherapy Plus Memantine for Patients With Brain Metastases: Phase III Trial NRG Oncology Cc001. J Clin Oncol (2020) 38(10):1019–29. doi: 10.1200/JCO.19.02767

91. Rusthoven CG, Camidge DR, Robin TP, Brown PD. Radiosurgery for Small-Cell Brain Metastases: Challenging the Last Bastion of Preferential Whole-Brain Radiotherapy Delivery. J Clin Oncol (2020) 38(31):3587–91. doi: 10.1200/JCO.20.01823

92. Higgins KA, Simone CB2nd, Amini A, Chetty IJ, Donington J, Edelman MJ, et al. American Radium Society Appropriate Use Criteria on Radiation Therapy for Extensive-Stage SCLC. J Thorac Oncol (2021) 16(1):54–65. doi: 10.1016/j.jtho.2020.09.013

93. Takahashi T, Yamanaka T, Seto T, Harada H, Nokihara H, Saka H, et al. Prophylactic Cranial Irradiation Versus Observation in Patients With Extensive-Disease Small-Cell Lung Cancer: A Multicentre, Randomised, Open-Label, Phase 3 Trial. Lancet Oncol (2017) 18(5):663–71. doi: 10.1016/S1470-2045(17)30230-9

94. Yin X, Yan D, Qiu M, Huang L, Yan SX. Prophylactic Cranial Irradiation in Small Cell Lung Cancer: A Systematic Review and Meta-Analysis. BMC Cancer (2019) 19(1):95. doi: 10.1186/s12885-018-5251-3

95. Rusthoven CG, Yamamoto M, Bernhardt D, Smith DE, Gao D, Serizawa T, et al. Evaluation of First-Line Radiosurgery vs Whole-Brain Radiotherapy for Small Cell Lung Cancer Brain Metastases: The FIRE-SCLC Cohort Study. JAMA Oncol (2020) 6(7):1028–37. doi: 10.1001/jamaoncol.2020.1271

96. Rodriguez de Dios N, Counago F, Murcia-Mejia M, Rico-Oses M, Calvo-Crespo P, Samper P, et al. Randomized Phase III Trial of Prophylactic Cranial Irradiation With or Without Hippocampal Avoidance for Small-Cell Lung Cancer (PREMER): A GICOR-GOECP-SEOR Study. J Clin Oncol (2021) 39(28):3118–27. doi: 10.1200/JCO.21.00639

97. Bendell JC, Domchek SM, Burstein HJ, Harris L, Younger J, Kuter I, et al. Central Nervous System Metastases in Women Who Receive Trastuzumab-

Based Therapy for Metastatic Breast Carcinoma. *Cancer* (2003) 97 (12):2972–7. doi: 10.1002/cncr.11436

98. Lin NU, Winer EP. Brain Metastases: The HER2 Paradigm. *Clin Cancer Res* (2007) 13(6):1648–55. doi: 10.1158/1078-0432.CCR-06-2478

99. Kennecke H, Yerushalmi R, Woods R, Cheang MC, Voduc D, Speers CH, et al. Metastatic Behavior of Breast Cancer Subtypes. *J Clin Oncol* (2010) 28 (20):3271–7. doi: 10.1200/JCO.2009.25.9820

100. Slamon DJ, Leyland-Jones B, Shak S, Fuchs H, Paton V, Bajamonde A, et al. Use of Chemotherapy Plus a Monoclonal Antibody Against HER2 for Metastatic Breast Cancer That Overexpresses Her2. *N Engl J Med* (2001) 344(11):783–92. doi: 10.1056/NEJM200103153441101

101. Park YH, Park MJ, Ji SH, Yi SY, Lim DH, Nam DH, et al. Trastuzumab Treatment Improves Brain Metastasis Outcomes Through Control and Durable Prolongation of Systemic Extracranial Disease in HER2-Overexpressing Breast Cancer Patients. *Br J Cancer* (2009) 100(6):894–900. doi: 10.1038/sj.bjc.6604941

102. Park IH, Ro J, Lee KS, Nam BH, Kwon Y, Shin KH. Trastuzumab Treatment Beyond Brain Progression in HER2-Positive Metastatic Breast Cancer. *Ann Oncol* (2009) 20(1):56–62. doi: 10.1093/annonc/mdn539

103. Okita Y, Narita Y, Suzuki T, Arita H, Yonemori K, Kinoshita T, et al. Extended Trastuzumab Therapy Improves the Survival of HER2-Positive Breast Cancer Patients Following Surgery and Radiotherapy for Brain Metastases. *Mol Clin Oncol* (2013) 1(6):995–1001. doi: 10.3892/mco.2013.162

104. Dawood S, Broglio K, Esteva FJ, Ibrahim NK, Kau SW, Islam R, et al. Defining Prognosis for Women With Breast Cancer and CNS Metastases by HER2 Status. *Ann Oncol* (2008) 19(7):1242–8. doi: 10.1093/annonc/mdn036

105. Lin NU, Carey LA, Liu MC, Younger J, Come SE, Ewend M, et al. Phase II Trial of Lapatinib for Brain Metastases in Patients With Human Epidermal Growth Factor Receptor 2-Positive Breast Cancer. *J Clin Oncol* (2008) 26 (12):1993–9. doi: 10.1200/JCO.2007.12.3588

106. Lin NU, Diéras V, Paul D, Lossignol D, Christodoulou C, Stemmler HJ, et al. Multicenter Phase II Study of Lapatinib in Patients With Brain Metastases From HER2-Positive Breast Cancer. *Clin Cancer Res* (2009) 15(4):1452–9. doi: 10.1158/1078-0432.CCR-08-1080

107. Metro G, Foglietta J, Russillo M, Stocchi L, Vidiri A, Giannarelli D, et al. Clinical Outcome of Patients With Brain Metastases From HER2-Positive Breast Cancer Treated With Lapatinib and Capecitabine. *Ann Oncol* (2011) 22(3):625–30. doi: 10.1093/annonc/mdq434

108. Bachelot T, Romieu G, Campone M, Diéras V, Cropet C, Dalenc F, et al. Lapatinib Plus Capecitabine in Patients With Previously Untreated Brain Metastases From HER2-Positive Metastatic Breast Cancer (LANDSCAPE): A Single-Group Phase 2 Study. *Lancet Oncol* (2013) 14(1):64–71. doi: 10.1016/S1470-2045(12)70432-1

109. Freedman RA, Gelman RS, Anders CK, Melisko ME, Parsons HA, Cropp AM, et al. TBCRC 022: A Phase II Trial of Neratinib and Capecitabine for Patients With Human Epidermal Growth Factor Receptor 2-Positive Breast Cancer and Brain Metastases. *J Clin Oncol* (2019) 37(13):1081–9. doi: 10.1200/JCO.18.01511

110. Hurvitz SA, Saura C, Oliveira M, Trudeau ME, Moy B, Delaloge S, et al. Efficacy of Neratinib Plus Capecitabine in the Subgroup of Patients With Central Nervous System Involvement From the NALA Trial. *Oncologist* (2021) 26(18):e1327–38 doi: 10.1002/onco.13830

111. Lin NU, Borges V, Anders C, Murthy RK, Paplomata E, Hamilton E, et al. Intracranial Efficacy and Survival With Tucatinib Plus Trastuzumab and Capecitabine for Previously Treated HER2-Positive Breast Cancer With Brain Metastases in the HER2CLIMB Trial. *J Clin Oncol* (2020) 38 (23):2610–9. doi: 10.1200/JCO.20.00775

112. Bartsch R, Berghoff AS, Vogl U, Rudas M, Bergen E, Dubsky P, et al. Activity of T-DM1 in Her2-Positive Breast Cancer Brain Metastases. *Clin Exp Metastasis* (2015) 32(7):729–37. doi: 10.1007/s10585-015-9740-3

113. Jacot W, Pons E, Frenel JS, Guiu S, Levy C, Heudel PE, et al. Efficacy and Safety of Trastuzumab Emtansine (T-DM1) in Patients With HER2-Positive Breast Cancer With Brain Metastases. *Breast Cancer Res Treat* (2016) 157 (2):307–18. doi: 10.1007/s10549-016-3828-6

114. Krop IE, Lin NU, Blackwell K, Guardino E, Huober J, Lu M, et al. Trastuzumab Emtansine (T-DM1) Versus Lapatinib Plus Capecitabine in Patients With HER2-Positive Metastatic Breast Cancer and Central Nervous

System Metastases: A Retrospective, Exploratory Analysis in EMILIA. *Ann Oncol* (2015) 26(1):113–9. doi: 10.1093/annonc/mdu486

115. Montemurro F, Delaloge S, Barrios CH, Wuerstlein R, Anton A, Brain E, et al. Trastuzumab Emtansine (T-DM1) in Patients With HER2-Positive Metastatic Breast Cancer and Brain Metastases: Exploratory Final Analysis of Cohort 1 From KAMILLA, a Single-Arm Phase IIIb Clinical Trial(). *Ann Oncol* (2020) 31(10):1350–8. doi: 10.1016/j.annonc.2020.06.020

116. Bartsch R, Berghoff AS, Furtner J, Bergen ES, Roider-Schur S, Marhold M, et al. 280p Intracranial Activity of Trastuzumab-Deruxtecan (T-DXd) in HER2-Positive Breast Cancer Patients With Active Brain Metastases: Results From the First Stage of the Phase II TUXEDO-1 Trial. *Ann Oncol* (2021) 32: S486. doi: 10.1016/j.annonc.2021.08.563

117. Jerusalem GHM, Park YH, Yamashita T, Hurvitz SA, Modi S, Andre F, et al. Trastuzumab Deruxtecan (T-DXd) in Patients With HER2+ Metastatic Breast Cancer With Brain Metastases: A Subgroup Analysis of the DESTINY-Breast01 Trial. *J Clin Oncol* (2021) 39(15_suppl):526–. doi: 10.1200/JCO.2021.39.15_suppl.526

118. Tolaney SM, Sahebjam S, Le Rhun E, Bachelot T, Kabos P, Awada A, et al. A Phase II Study of Abemaciclib in Patients With Brain Metastases Secondary to Hormone Receptor–Positive Breast Cancer. *Clin Cancer Res* (2020) 26 (20):5310. doi: 10.1158/1078-0432.CCR-20-1764

119. Brastianos PK, Kim AE, Wang N, Lee EQ, Ligibel J, Cohen JV, et al. Palbociclib Demonstrates Intracranial Activity in Progressive Brain Metastases Harboring Cyclin-Dependent Kinase Pathway Alterations. *Nat Cancer* (2021) 2(5):498–502. doi: 10.1038/s43018-021-00198-5

120. Anders C, Deal AM, Abramson V, Liu MC, Storniolo AM, Carpenter JT, et al. TBCRC 018: Phase II Study of Iniparib in Combination With Irinotecan to Treat Progressive Triple Negative Breast Cancer Brain Metastases. *Breast Cancer Res Treat* (2014) 146(3):557–66. doi: 10.1007/s10549-014-3039-y

121. Litton JK, Hurvitz SA, Mina LA, Rugo HS, Lee KH, Gonçalves A, et al. Talazoparib Versus Chemotherapy in Patients With Germline BRCA1/2-Mutated HER2-Negative Advanced Breast Cancer: Final Overall Survival Results From the EMBRACA Trial. *Ann Oncol* (2020) 31(11):1526–35. doi: 10.1016/j.annonc.2020.08.2098

122. Solomon BJ, Cappuzzo F, Felip E, Blackhall FH, Costa DB, Kim DW, et al. Intracranial Efficacy of Crizotinib Versus Chemotherapy in Patients With Advanced ALK-Positive Non-Small-Cell Lung Cancer: Results From PROFILE 1014. *J Clin Oncol* (2016) 34(24):2858–65. doi: 10.1200/JCO.2015.63.5888

123. Crinò L, Ahn M-J, De Marinis F, Groen HJM, Wakelee H, Hida T, et al. Multicenter Phase II Study of Whole-Body and Intracranial Activity With Ceritinib in Patients With ALK-Rearranged Non–Small-Cell Lung Cancer Previously Treated With Chemotherapy and Crizotinib: Results From ASCEND-2. *J Clin Oncol* (2016) 34(24):2866–73. doi: 10.1200/JCO.2015.65.5936

124. Gadgeel SM, Gandhi L, Riely GJ, Chiappori AA, West HL, Azada MC, et al. Safety and Activity of Alectinib Against Systemic Disease and Brain Metastases in Patients With Crizotinib-Resistant ALK-Rearranged Non-Small-Cell Lung Cancer (AF-002JG): Results From the Dose-Finding Portion of a Phase 1/2 Study. *Lancet Oncol* (2014) 15(10):1119–28. doi: 10.1016/S1470-2045(14)70362-6

125. Peters S, Camidge DR, Shaw AT, Gadgeel S, Ahn JS, Kim DW, et al. Alectinib Versus Crizotinib in Untreated ALK-Positive Non-Small-Cell Lung Cancer. *N Engl J Med* (2017) 377(9):829–38. doi: 10.1056/NEJMoa1704795

126. Camidge DR, Kim HR, Ahn MJ, Yang JC, Han JY, Lee JS, et al. Brigatinib Versus Crizotinib in ALK-Positive Non-Small-Cell Lung Cancer. *N Engl J Med* (2018) 379(21):2027–39. doi: 10.1056/NEJMoa1810171

127. Shaw AT, Bauer TM, De Marinis F, Felip E, Goto Y, Liu G, et al. First-Line Lorlatinib or Crizotinib in Advanced ALK-Positive Lung Cancer. *N Engl J Med* (2020) 383(21):2018–29. doi: 10.1056/NEJMoa2027187

128. Shaw AT, Solomon BJ, Chiari R, Riely GJ, Besse B, Soo RA, et al. Lorlatinib in Advanced ROS1-Positive Non-Small-Cell Lung Cancer: A Multicentre, Open-Label, Single-Arm, Phase 1-2 Trial. *Lancet Oncol* (2019) 20 (12):1691–701. doi: 10.1016/S1470-2045(19)30655-2

129. Horn L, Wang Z, Wu G, Poddubskaya E, Mok T, Reck M, et al. Ensartinib vs Crizotinib for Patients With Anaplastic Lymphoma Kinase-Positive Non-Small Cell Lung Cancer: A Randomized Clinical Trial. *JAMA Oncol* (2021) 7 (11):1617–25. doi: 10.1001/jamaoncol.2021.3523

130. Ahn MJ, Han JY, Lee KH, Kim SW, Kim DW, Lee YG, et al. Lazertinib in Patients With EGFR Mutation-Positive Advanced Non-Small-Cell Lung Cancer: Results From the Dose Escalation and Dose Expansion Parts of a First-in-Human, Open-Label, Multicentre, Phase 1-2 Study. *Lancet Oncol* (2019) 20(12):1681–90. doi: 10.1016/S1470-2045(19)30504-2

131. Cho BC, Han JY, Kim SW, Lee KH, Cho EK, Lee YG, et al. A Phase 1/2 Study of Lazertinib 240 Mg in Patients With Advanced EGFR T790M-Positive NSCLC After Previous EGFR Tyrosine Kinase Inhibitors. *J Thorac Oncol* (2021). doi: 10.1016/j.jtho.2021.11.025

132. Shi Y, Zhang S, Hu X, Feng J, Ma Z, Zhou J, et al. Safety, Clinical Activity, and Pharmacokinetics of Alflutinib (AST2818) in Patients With Advanced NSCLC With EGFR T790M Mutation. *J Thorac Oncol* (2020) 15(6):1015–26. doi: 10.1016/j.jtho.2020.01.010

133. Shi Y, Hu X, Zhang S, Lv D, Wu L, Yu Q, et al. Efficacy, Safety, and Genetic Analysis of Furmonertinib (AST2818) in Patients With EGFR T790M Mutated Non-Small-Cell Lung Cancer: A Phase 2b, Multicentre, Single-Arm, Open-Label Study. *Lancet Respir Med* (2021) 9(8):829–39. doi: 10.1016/S2213-2600(20)30455-0

134. Park K, Haura EB, Leighl NB, Mitchell P, Shu CA, Girard N, et al. Amivantamab in EGFR Exon 20 Insertion-Mutated Non-Small-Cell Lung Cancer Progressing on Platinum Chemotherapy: Initial Results From the CHRYSALIS Phase I Study. *J Clin Oncol* (2021) 39(30):3391–402. doi: 10.1200/JCO.21.00662

135. Ceresoli GL, Cappuzzo F, Gregorc V, Bartolini S, Crinò L, Villa E. Gefitinib in Patients With Brain Metastases From Non-Small-Cell Lung Cancer: A Prospective Trial. *Ann Oncol* (2004) 15(7):1042–7. doi: 10.1093/annonc/mdh276

136. Hotta K, Kiura K, Ueoka H, Tabata M, Fujiwara K, Kozuki T, et al. Effect of Gefitinib ('Iressa', ZD1839) on Brain Metastases in Patients With Advanced Non-Small-Cell Lung Cancer. *Lung Cancer* (2004) 46(2):255–61. doi: 10.1016/j.lungcan.2004.04.036

137. Lee DH, Han J-Y, Lee HG, Lee JJ, Lee EK, Kim HY, et al. Gefitinib as a First-Line Therapy of Advanced or Metastatic Adenocarcinoma of the Lung in Never-Smokers. *Clin Cancer Res* (2005) 11(8):3032–7. doi: 10.1158/1078-0432.CCR-04-2149

138. Chiu C-H, Tsai C-M, Chen Y-M, Chiang S-C, Liou J-L, Perng R-P. Gefitinib is Active in Patients With Brain Metastases From Non-Small Cell Lung Cancer and Response is Related to Skin Toxicity. *Lung Cancer* (2005) 47(1):129–38. doi: 10.1016/j.lungcan.2004.05.014

139. Kim J-E, Lee DH, Choi Y, Yoon DH, Kim S-W, Suh C, et al. Epidermal Growth Factor Receptor Tyrosine Kinase Inhibitors as a First-Line Therapy for Never-Smokers With Adenocarcinoma of the Lung Having Asymptomatic Synchronous Brain Metastasis. *Lung Cancer* (2009) 65(3):351–4. doi: 10.1016/j.lungcan.2008.12.011

140. Park SJ, Kim HT, Lee DH, Kim KP, Kim SW, Suh C, et al. Efficacy of Epidermal Growth Factor Receptor Tyrosine Kinase Inhibitors for Brain Metastasis in Non-Small Cell Lung Cancer Patients Harboring Either Exon 19 or 21 Mutation. *Lung Cancer* (2012) 77(3):556–60. doi: 10.1016/j.lungcan.2012.05.092

141. Mok TS, Wu YL, Ahn MJ, Garassino MC, Kim HR, Ramalingam SS, et al. Osimertinib or Platinum-Pemetrexed in EGFR T790M-Positive Lung Cancer. *N Engl J Med* (2017) 376(7):629–40. doi: 10.1056/NEJMoa1612674

142. Soria JC, Ohe Y, Vansteenkiste J, Reungwetwattana T, Chewaskulyong B, Lee KH, et al. Osimertinib in Untreated EGFR-Mutated Advanced Non-Small-Cell Lung Cancer. *N Engl J Med* (2018) 378(2):113–25. doi: 10.1056/NEJMoa1713137

143. Skoulidis F, Li BT, Dy GK, Price TJ, Falchook GS, Wolf J, et al. Sotorasib for Lung Cancers With KRAS P.G12C Mutation. *N Engl J Med* (2021) 384(25):2371–81. doi: 10.1056/NEJMoa2103695

144. Drilon A, Oxnard GR, Tan DSW, Loong HHF, Johnson M, Gainor J, et al. Efficacy of Selpercatinib in RET Fusion-Positive Non-Small-Cell Lung Cancer. *N Engl J Med* (2020) 383(9):813–24. doi: 10.1056/NEJMoa2005653

145. Gainor JF, Curigliano G, Kim DW, Lee DH, Besse B, Baik CS, et al. Pralsetinib for RET Fusion-Positive Non-Small-Cell Lung Cancer (ARROW): A Multi-Cohort, Open-Label, Phase 1/2 Study. *Lancet Oncol* (2021) 22(7):959–69. doi: 10.1016/S1470-2045(21)00247-3

146. Drilon A, Ou SI, Cho BC, Kim DW, Lee J, Lin JJ, et al. Repotrectinib (TPX-0005) Is a Next-Generation ROS1/TRK/ALK Inhibitor That Potently Inhibits ROS1/TRK/ALK Solvent-Front Mutations. *Cancer Discov* (2018) 8(10):1227–36. doi: 10.1158/2159-8290.CD-18-0484

147. Long GV, Trefzer U, Davies MA, Kefford RF, Ascierto PA, Chapman PB, et al. Dabrafenib in Patients With Val600Glu or Val600Lys BRAF-Mutant Melanoma Metastatic to the Brain (BREAK-MB): A Multicentre, Open-Label, Phase 2 Trial. *Lancet Oncol* (2012) 13(11):1087–95. doi: 10.1016/S1470-2045(12)70431-X

148. Davies MA, Saiag P, Robert C, Grob JJ, Flaherty KT, Arance A, et al. Dabrafenib Plus Trametinib in Patients With BRAF(V600)-Mutant Melanoma Brain Metastases (COMBI-MB): A Multicentre, Multicohort, Open-Label, Phase 2 Trial. *Lancet Oncol* (2017) 18(7):863–73. doi: 10.1016/S1470-2045(17)30429-1

149. McArthur GA, Maio M, Arance A, Nathan P, Blank C, Avril MF, et al. Vemurafenib in Metastatic Melanoma Patients With Brain Metastases: An Open-Label, Single-Arm, Phase 2, Multicentre Study. *Ann Oncol* (2017) 28(3):634–41. doi: 10.1093/annonc/mdw641

150. Arvanitis CD, Ferraro GB, Jain RK. The Blood-Brain Barrier and Blood-Tumour Barrier in Brain Tumours and Metastases. *Nat Rev Cancer* (2020) 20(1):26–41. doi: 10.1038/s41568-019-0205-x

151. Musolino A, Ciccolallo L, Panebianco M, Fontana E, Zanoni D, Bozzetti C, et al. Multifactorial Central Nervous System Recurrence Susceptibility in Patients With HER2-Positive Breast Cancer. *Cancer* (2011) 117(9):1837–46. doi: 10.1002/cncr.25771

152. Pestalozzi BC, Brignoli S. Trastuzumab in CSF. *J Clin Oncol* (2000) 18(11):2349–51. doi: 10.1200/JCO.2000.18.11.2349

153. Nguyen LV, Searle K, Jerzak KJ. Central Nervous System-Specific Efficacy of CDK4/6 Inhibitors in Randomized Controlled Trials for Metastatic Breast Cancer. *Oncotarget* (2019) 10(59):6317–22. doi: 10.18632/oncotarget.27238

154. Schlam I, Tolaney SM. Is There a Role for CDK 4/6 Inhibitors in Breast Cancer Brain Metastases? *Oncotarget* (2021) 12(9):873–5. doi: 10.18632/oncotarget.27904

155. Lin NU, Claus E, Sohl J, Razzak AR, Arnaout A, Winer EP. Sites of Distant Recurrence and Clinical Outcomes in Patients With Metastatic Triple-Negative Breast Cancer: High Incidence of Central Nervous System Metastases. *Cancer* (2008) 113(10):2638–45. doi: 10.1002/cncr.23930

156. Guérin A, Sasane M, Zhang J, Culver KW, Dea K, Nitulescu R, et al. Brain Metastases in Patients With ALK+ Non-Small Cell Lung Cancer: Clinical Symptoms, Treatment Patterns and Economic Burden. *J Med Economics* (2015) 18(4):312–22. doi: 10.3111/13696998.2014.1003644

157. Kelly WJ, Shah NJ, Subramaniam DS. Management of Brain Metastases in Epidermal Growth Factor Receptor Mutant Non-Small-Cell Lung Cancer. *Front Oncol* (2018) 8:208. doi: 10.3389/fonc.2018.00208

158. Jänne PA, Yang JC, Kim DW, Planchard D, Ohe Y, Ramalingam SS, et al. AZD9291 in EGFR Inhibitor-Resistant Non-Small-Cell Lung Cancer. *N Engl J Med* (2015) 372(18):1689–99. doi: 10.1056/NEJMoa1411817

159. Melosky B, Banerji S, Blais N, Chu Q, Juergens R, Leighl NB, et al. Canadian Consensus: A New Systemic Treatment Algorithm for Advanced EGFR-Mutated Non-Small-Cell Lung Cancer. *Curr Oncol* (2020) 27(2):e146–e55. doi: 10.3747/co.27.6007

160. Tomasini P, Walia P, Labbe C, Jao K, Leighl NB. Targeting the KRAS Pathway in Non-Small Cell Lung Cancer. *Oncologist* (2016) 21(12):1450–60. doi: 10.1634/theoncologist.2015-0084

161. Paik PK, Felip E, Veillon R, Sakai H, Cortot AB, Garassino MC, et al. Tepotinib in Non-Small-Cell Lung Cancer With MET Exon 14 Skipping Mutations. *N Engl J Med* (2020) 383(10):931–43. doi: 10.1056/NEJMoa2004407

162. Wolf J, Seto T, Han JY, Reguart N, Garon EB, Groen HJM, et al. Capmatinib in MET Exon 14-Mutated or MET-Amplified Non-Small-Cell Lung Cancer. *N Engl J Med* (2020) 383(10):944–57. doi: 10.1056/NEJMoa2002787

163. Hong DS, DuBois SG, Kummar S, Farago AF, Albert CM, Rohrberg KS, et al. Larotrectinib in Patients With TRK Fusion-Positive Solid Tumours: A Pooled Analysis of Three Phase 1/2 Clinical Trials. *Lancet Oncol* (2020) 21(4):531–40. doi: 10.1016/S1470-2045(19)30856-3

164. John T, Chiu CH, Cho BC, Fakih M, Farago AF, Demetri GD, et al. 364o Intracranial Efficacy of Entrectinib in Patients With NTRK Fusion-Positive Solid Tumours and Baseline CNS Metastases. *Ann Oncol* (2020) 31:S397–S8. doi: 10.1016/j.annonc.2020.08.473

165. Davies MA, Liu P, McIntyre S, Kim KB, Papadopoulos N, Hwu W-J, et al. Prognostic Factors for Survival in Melanoma Patients With Brain Metastases. *Cancer* (2011) 117(8):1687–96. doi: 10.1002/cncr.25634

166. Jakob JA, Bassett RL, Ng CS, Curry JL, Joseph RW, Alvarado GC, et al. NRAS Mutation Status Is an Independent Prognostic Factor in Metastatic Melanoma. *Cancer* (2012) 118(16):4014–23. doi: 10.1002/cncr.26724

167. Wilson EH, Weninger W, Hunter CA. Trafficking of Immune Cells in the Central Nervous System. *J Clin Invest* (2010) 120(5):1368–79. doi: 10.1172/JCI41911

168. Prins RM, Vo DD, Khan-Farooqi H, Yang MY, Soto H, Economou JS, et al. NK and CD4 Cells Collaborate to Protect Against Melanoma Tumor Formation in the Brain. *J Immunol* (2006) 177(12):8448–55. doi: 10.4049/jimmunol.177.12.8448

169. Margolin K, Ernstoff MS, Hamid O, Lawrence D, McDermott D, Puzanov I, et al. Ipilimumab in Patients With Melanoma and Brain Metastases: An Open-Label, Phase 2 Trial. *Lancet Oncol* (2012) 13(5):459–65. doi: 10.1016/S1470-2045(12)70090-6

170. Goldberg SB, Gettinger SN, Mahajan A, Chiang AC, Herbst RS, Sznol M, et al. Pembrolizumab for Patients With Melanoma or Non-Small-Cell Lung Cancer and Untreated Brain Metastases: Early Analysis of a Non-Randomised, Open-Label, Phase 2 Trial. *Lancet Oncol* (2016) 17(7):976–83. doi: 10.1016/S1470-2045(16)30053-5

171. Crinò L, Bronte G, Bidoli P, Cravero P, Minenza E, Cortesi E, et al. Nivolumab and Brain Metastases in Patients With Advanced Non-Squamous Non-Small Cell Lung Cancer. *Lung Cancer* (2019) 129:35–40. doi: 10.1016/j.lungcan.2018.12.025

172. Tawbi HA, Forsyth PA, Algazi A, Hamid O, Hodi FS, Moschos SJ, et al. Combined Nivolumab and Ipilimumab in Melanoma Metastatic to the Brain. *N Engl J Med* (2018) 379(8):722–30. doi: 10.1056/NEJMoa1805453

173. Tawbi HA, Forsyth PA, Hodi FS, Algazi AP, Hamid O, Lao CD, et al. Long-Term Outcomes of Patients With Active Melanoma Brain Metastases Treated With Combination Nivolumab Plus Ipilimumab (CheckMate 204): Final Results of an Open-Label, Multicentre, Phase 2 Study. *Lancet Oncol* (2021) 22(12):1692–704. doi: 10.1016/S1470-2045(21)00545-3

174. Tawbi HA, Schadendorf D, Lipson EJ, Ascierto PA, Matamala L, Castillo Gutiérrez E, et al. Relatlimab and Nivolumab Versus Nivolumab in Untreated Advanced Melanoma. *N Engl J Med* (2022) 386(1):24–34. doi: 10.1056/NEJMoa2109970

175. Schmid P, Adams S, Rugo HS, Schneeweiss A, Barrios CH, Iwata H, et al. Atezolizumab and Nab-Paclitaxel in Advanced Triple-Negative Breast Cancer. *N Engl J Med* (2018) 379(22):2108–21. doi: 10.1056/NEJMoa1809615

176. Schmid P, Rugo HS, Adams S, Schneeweiss A, Barrios CH, Iwata H, et al. Atezolizumab Plus Nab-Paclitaxel as First-Line Treatment for Unresectable, Locally Advanced or Metastatic Triple-Negative Breast Cancer (IMpassion130): Updated Efficacy Results From a Randomised, Double-Blind, Placebo-Controlled, Phase 3 Trial. *Lancet Oncol* (2020) 21(1):44–59. doi: 10.1016/S1470-2045(19)30689-8

177. Flippot R, Dalban C, Laguerre B, Borchiellini D, Gravis G, Négrier S, et al. Safety and Efficacy of Nivolumab in Brain Metastases From Renal Cell Carcinoma: Results of the GETUG-AFU 26 NIVOREN Multicenter Phase II Study. *J Clin Oncol* (2019) 37(23):2008–16. doi: 10.1200/JCO.18.02218

178. Knisely JP, Yu JB, Flanigan J, Sznol M, Kluger HM, Chiang VL. Radiosurgery for Melanoma Brain Metastases in the Ipilimumab Era and the Possibility of Longer Survival. *J Neurosurg* (2012) 117(2):227–33. doi: 10.3171/2012.5.JNS111929

179. Silk AW, Bassetti MF, West BT, Tsien CI, Lao CD. Ipilimumab and Radiation Therapy for Melanoma Brain Metastases. *Cancer Med* (2013) 2(6):899–906. doi: 10.1002/cam4.140

180. Mathew M, Tam M, Ott PA, Pavlick AC, Rush SC, Donahue BR, et al. Ipilimumab in Melanoma With Limited Brain Metastases Treated With Stereotactic Radiosurgery. *Melanoma Res* (2013) 23(3):191–5. doi: 10.1097/CMR.0b013e32835f3d90

181. Minniti G, Anzellini D, Reverberi C, Cappellini GCA, Marchetti L, Bianciardi F, et al. Stereotactic Radiosurgery Combined With Nivolumab or Ipilimumab for Patients With Melanoma Brain Metastases: Evaluation of Brain Control and Toxicity. *J ImmunoTher Cancer* (2019) 7(1):102. doi: 10.1186/s40425-019-0588-y

182. Okwan-Duodu D, Pollack BP, Lawson D, Khan MK. Role of Radiation Therapy as Immune Activator in the Era of Modern Immunotherapy for Metastatic Malignant Melanoma. *Am J Clin Oncol* (2015) 38(1):119–25. doi: 10.1097/COC.0b013e3182940dc3

183. Seung SK, Curti BD, Crittenden M, Walker E, Coffey T, Siebert JC, et al. Phase 1 Study of Stereotactic Body Radiotherapy and Interleukin-2–Tumor and Immunological Responses. *Sci Transl Med* (2012) 4(137):137ra74. doi: 10.1126/scitranslmed.3003649

184. Bot I, Blank CU, Brandsma D. Clinical and Radiological Response of Leptomeningeal Melanoma After Whole Brain Radiotherapy and Ipilimumab. *J Neurol* (2012) 259(9):1976–8. doi: 10.1007/s00415-012-6488-4

185. Mueller-Brenne T, Rudolph B, Schmidberger H, Grabbe S, Loquai C. Successful Therapy of a Cerebral Metastasized Malign Melanoma by Whole-Brain-Radiation and Therapy With Ipilimumab. In: *Journal Der Deutschen Dermatologischen Gesellschaft*. 350 MAIN ST, MALDEN 02148, MA USA: WILEY-BLACKWELL COMMERCE PLACE (2011).

186. Sperduto PW, Wang M, Robins HI, Schell MC, Werner-Wasik M, Komaki R, et al. A Phase 3 Trial of Whole Brain Radiation Therapy and Stereotactic Radiosurgery Alone Versus WBRT and SRS With Temozolomide or Erlotinib for Non-Small Cell Lung Cancer and 1 to 3 Brain Metastases: Radiation Therapy Oncology Group 0320. *Int J Radiat Oncol Biol Phys* (2013) 85(5):1312–8. doi: 10.1016/j.ijrobp.2012.11.042

187. Brastianos PK, Carter SL, Santagata S, Cahill DP, Taylor-Weiner A, Jones RT, et al. Genomic Characterization of Brain Metastases Reveals Branched Evolution and Potential Therapeutic Targets. *Cancer Discov* (2015) 5(11):1164–77. doi: 10.1158/2159-8290.CD-15-0369

188. Luo YH, Luo L, Wampfler JA, Wang Y, Liu D, Chen YM, et al. 5-Year Overall Survival in Patients With Lung Cancer Eligible or Ineligible for Screening According to US Preventive Services Task Force Criteria: A Prospective, Observational Cohort Study. *Lancet Oncol* (2019) 20(8):1098–108. doi: 10.1016/S1470-2045(19)30329-8

189. Schunemann HJ, Lerda D, Quinn C, Follmann M, Alonso-Coello P, Rossi PG, et al. Breast Cancer Screening and Diagnosis: A Synopsis of the European Breast Guidelines. *Ann Intern Med* (2020) 172(1):46–56. doi: 10.7326/M19-2125

190. Carroll PH, Mohler JL. NCCN Guidelines Updates: Prostate Cancer and Prostate Cancer Early Detection. *J Natl Compr Canc Netw* (2018) 16(5S):620–3. doi: 10.6004/jnccn.2018.0036

191. Vernooij MW, Ikram MA, Tanghe HL, Vincent AJ, Hofman A, Krestin GP, et al. Incidental Findings on Brain MRI in the General Population. *N Engl J Med* (2007) 357(18):1821–8. doi: 10.1056/NEJMoa070972

192. O'Sullivan JW, Muntinga T, Grigg S, Ioannidis JPA. Prevalence and Outcomes of Incidental Imaging Findings: Umbrella Review. *BMJ* (2018) 361:k2387. doi: 10.1136/bmj.k2387

193. Komorowski AS, Warner E, MacKay HJ, Sahgal A, Pritchard KI, Jerzak KJ. Incidence of Brain Metastases in Nonmetastatic and Metastatic Breast Cancer: Is There a Role for Screening? *Clin Breast Cancer* (2020) 20(1):e54–64. doi: 10.1016/j.clbc.2019.06.007

194. Le Rhun E, Guckenberger M, Smits M, Dummer R, Bachelot T, Sahm F, et al. EANO-ESMO Clinical Practice Guidelines for Diagnosis, Treatment and Follow-Up of Patients With Brain Metastasis From Solid Tumours. *Ann Oncol* (2021) 32(11):1332–47. doi: 10.1016/j.annonc.2021.07.016

195. Kuksis M, Gao Y, Tran W, Hoey C, Kiss A, Komorowski AS, et al. The Incidence of Brain Metastases Among Patients With Metastatic Breast Cancer: A Systematic Review and Meta-Analysis. *Neuro Oncol* (2021) 23(6):894–904. doi: 10.1093/neuonc/noaa285

196. Boire A, Brandsma D, Brastianos PK, Le Rhun E, Ahluwalia M, Junck L, et al. Liquid Biopsy in Central Nervous System Metastases: A RANO Review and Proposals for Clinical Applications. *Neuro Oncol* (2019) 21(5):571–84. doi: 10.1093/neuonc/noz012

197. Seoane J, De Mattos-Arruda L, Le Rhun E, Bardelli A, Weller M. Cerebrospinal Fluid Cell-Free Tumour DNA as a Liquid Biopsy for Primary Brain Tumours and Central Nervous System Metastases. *Ann Oncol* (2019) 30(2):211–8. doi: 10.1093/annonc/mdy544

198. Shih DJH, Nayyar N, Bihun I, Dagogo-Jack I, Gill CM, Aquilanti E, et al. Genomic Characterization of Human Brain Metastases Identifies Drivers of Metastatic Lung Adenocarcinoma. *Nat Genet* (2020) 52(4):371–7. doi: 10.1038/s41588-020-0592-7

199. Iwamoto T, Niikura N, Ogiya R, Yasojima H, Watanabe KI, Kanbayashi C, et al. Distinct Gene Expression Profiles Between Primary Breast Cancers and Brain Metastases From Pair-Matched Samples. *Sci Rep* (2019) 9(1):13343. doi: 10.1038/s41598-019-50099-y

200. Fischer GM, Jalali A, Kircher DA, Lee WC, McQuade JL, Haydu LE, et al. Molecular Profiling Reveals Unique Immune and Metabolic Features of Melanoma Brain Metastases. *Cancer Discov* (2019) 9(5):628–45. doi: 10.1158/2159-8290.CD-18-1489

201. Hanssen A, Riebensahm C, Mohme M, Joosse SA, Velthaus JL, Berger LA, et al. Frequency of Circulating Tumor Cells (CTC) in Patients With Brain Metastases: Implications as a Risk Assessment Marker in Oligo-Metastatic Disease. *Cancers (Basel)* (2018) 10(12):527. doi: 10.3390/cancers10120527

202. Zeng Q, Michael IP, Zhang P, Saghafinia S, Knott G, Jiao W, et al. Synaptic Proximity Enables NMDAR Signalling to Promote Brain Metastasis. *Nature* (2019) 573(7775):526–31. doi: 10.1038/s41586-019-1576-6

203. Gril B, Paranjape AN, Woditschka S, Hua E, Dolan EL, Hanson J, et al. Reactive Astrocytic S1P3 Signaling Modulates the Blood-Tumor Barrier in Brain Metastases. *Nat Commun* (2018) 9(1):2705. doi: 10.1038/s41467-018-05030-w

frontiers
in Oncology

# The Subventricular Zone in Glioblastoma: Genesis, Maintenance, and Modeling

Jamison Beiriger [1,2], Ahmed Habib [1,2], Nicolina Jovanovich [1,2], Chowdari V. Kodavali [1,2], Lincoln Edwards [1,2], Nduka Amankulor [1,2] and Pascal O. Zinn [1,2]*

[1] Department of Neurosurgery, University of Pittsburgh Medical Center, Pittsburgh, PA, United States,
[2] Hillman Cancer Center, University of Pittsburgh Medical Center, Pittsburgh PA, United States

Glioblastoma (GBM) is a malignant tumor with a median survival rate of 15-16 months with standard care; however, cases of successful treatment offer hope that an enhanced understanding of the pathology will improve the prognosis. The cell of origin in GBM remains controversial. Recent evidence has implicated stem cells as cells of origin in many cancers. Neural stem/precursor cells (NSCs) are being evaluated as potential initiators of GBM tumorigenesis. The NSCs in the subventricular zone (SVZ) have demonstrated similar molecular profiles and share several distinctive characteristics to proliferative glioblastoma stem cells (GSCs) in GBM. Genomic and proteomic studies comparing the SVZ and GBM support the hypothesis that the tumor cells and SVZ cells are related. Animal models corroborate this connection, demonstrating migratory patterns from the SVZ to the tumor. Along with laboratory and animal research, clinical studies have demonstrated improved progression-free survival in patients with GBM after radiation to the ipsilateral SVZ. Additionally, key genetic mutations in GBM for the most part carry regulatory roles in the SVZ as well. An exciting avenue towards SVZ modeling and determining its role in gliomagenesis in the human context is human brain organoids. Here we comprehensively discuss and review the role of the SVZ in GBM genesis, maintenance, and modeling.

Keywords: SVZ, glioblastoma, modeling, ventricular, organoid

## INTRODUCTION

Glioblastoma (GBM) is the most common and most aggressive malignant glial tumor found in adults (1, 2). While prognosis varies with factors such as age and specific mutations (2–4), GBM remains an incurable tumor with a median survival of 9 months without treatment and 15-16 months with treatment (5–7). However, a small percentage of patients achieve long-term survival (>2.5yrs) (8, 9). Cases of longer-term survival and response to treatment provide hope that increasing knowledge of the disease pathology can lead to treatments with improved survival. Conventional treatment for GBM includes surgical resection followed by concurrent radiotherapy and temozolomide (TMZ) and subsequently, 6-12 cycles of TMZ (6, 10, 11). Aggressive tumor cell migration and growth preclude complete surgical resection, resulting in a near 100% relapse

rate (12–15). Incomplete resection, post-operative recovery time, and neurologic deficits may delay subsequent treatment, thus, leading to GBM progression early within weeks of surgery or delayed within 2 years for a majority of patients (16, 17).

Cancer stem-like cells have been suggested as the origin of many cancers (18). Neural stem/precursor cells (NSCs), in particular, have been linked to cancer (19). Molecular evidence establishes a strong link between stem cells and cancer stem cells (20). Animal studies have corroborated this link, supporting a hypothesis of tumor origination from neural precursor cells (19, 21–23). Furthermore, a clinical report of neural precursor transplantation leading to the formation of donor cell-derived tumors demonstrates a possible stem cell origin of cancer in humans (24). Altogether, these findings provide strong support for NSCs as one of the cells of origin for cancer. Specifically, NSCs in the subventricular zone are implicated (25).

The subventricular zone (SVZ) is a 3-5mm layer between the lateral ventricle, corpus callosum, and striatum (26–28) that harbors the largest population of NSCs in the brain (3, 4, 29–32). The SVZ in humans is characterized by an astrocytic ribbon that is separated from a layer of ependymal cells by a hypocellular layer (33). The SVZ in animals differs in cellular composition and structure from the SVZ in humans (33–35).

Disease modeling towards identifying specific therapies for numerous cancers has been described (36). While numerous models have been developed for GBM research, faithfully recapitulating the microenvironment, structure, and molecular characteristics (36), GBM modeling has remained a challenge. Each model is unique and complex with benefits and drawbacks. Models range from *in vitro* cellular tumor systems to animal models (36). The recent advent of 3D models has increased the ability to effectively model the brain and associated tumors in the human context (37). These models more effectively simulate and maintain tumor structure compared to 2D models. However, challenges remain to model GBM, those include a lack of regionalized organoids and the underdevelopment of an immunological/inflammatory response, as well as the presence of only primitive vascular systems (37). It follows that utilizing a combination of models may be most apt for developing novel and effective therapeutic interventions.

Recent research has shed new light on the role of the SVZ in GBM (38, 39). This review addresses current hypotheses in SVZ involvement in gliomagenesis, maintenance, and modeling standards, as well as the capacity of current models to incorporate these hypotheses.

## GLIOBLASTOMA CELL OF ORIGIN

Cancer cells expressing stem cell surface markers reside in brain tumors, comprising between < 1% of cancer cells in low-grade tumors and over 25% of cancer cells in high-grade tumors (40, 41). A connection between glioblastoma initiating cells (GICs) and NSCs has been identified, but the specific lineages downstream of GICs remain understudied (42). The GBM

stem cell and the astrocyte dedifferentiation theory are the two prevailing hypotheses for the origin of GBM (43, 44).

Both of these theories serve to explain the presence of cancer stem cells within the tumor (45, 46). The astrocyte dedifferentiation theory relies on the multi-step process of tumorigenesis leading a mature astrocyte to dedifferentiate to become a malignant stem-like cell. This model is supported by recent experiments demonstrating the formation of tumors that are histologically similar to GBM after activation of oncogenes and suppression of tumor suppressor genes in astrocytes (47). These experiments show that genetic manipulation of astrocytes can lead to tumorigenesis. To induce GBM formation, both tumor suppressors and oncogenes must be manipulated in astrocytes, whereas progenitor cells only require oncogene activation (44, 47). This manipulation in astrocytes results in their acquisition of stem cell-like characteristics, offering one possible explanation for the similarities between GICs and stem cells (48, 49).

The glioblastoma stem cell theory proposes that GICs are derived from NSCs. NSCs are self-renewing, multipotent cells in the brain responsible for differentiating into neurons, astrocytes, and oligodendrocytes (50–52). These cells are most active during development; however, recent evidence has suggested small populations in specific stem-cell niches remain functional in the adult brain (53–57). As such, neurogenesis in the human brain continues throughout life (58, 59). The glioblastoma stem cell theory is based on a longstanding hypothesis that cancers arise from a stem-like cell population, and thus, that tumors contain a subset of multipotent cells with stem cell characteristics. In the case of GBM, partially differentiated glial cells including oligodendrocyte precursor cells (OPCs) and astrocyte precursor cells may contribute to or be responsible for tumorigenesis (38). Lee et al (38) proposed that the most likely pathogenesis involves driver mutations in NSCs that contribute to tumorigenesis after differentiation into the oligodendrocyte cell line. The presence of cells with stem cell-like characteristics has been identified in many cancers (60), including brain tumors (41, 44, 61). Clinical evidence supporting this theory includes the formation of a donor-derived brain tumor after NSCs were injected intracerebrally and intrathecally into an Ataxia Telangiectasia patient (24). This case example demonstrates a stem cell to tumor transition in the human brain. Considering the heterogeneity of GBM, each of these theories may contribute a portion of the total tumor population included in the category of GBM.

## NEURAL STEM CELLS AND GLIOBLASTOMA STEM CELLS ARE MOLECULARLY RELATED

Many molecular characteristics are shared between GBM stem cells (GSCs) and NSCs. Genome-Wide CRISPR-Cas9 screens of NSCs and GSCs identified several genetic commonalities (20). SOCS3, a modulatory protein that is responsible for maintaining stemness in NSCs (62), was identified as a top-scoring

GBM-specific fitness gene (20). Loss of function of SOCS3 leads to downregulation of multiple GSC fitness genes, upregulation of neuronal progenitor markers, and ultimately GSC differentiation (20). SOX2, another important NSC factor (63), is also a high-scoring fitness gene for both NSCs and GBM (20). Other genes with similar fitness scores in NSCs and GSCs include SQLE, CDK6, and DOT1L (20). Similar fitness scores in these genes provide evidence that developmental growth patterns are reactivated in GBM (20). Some genes with high fitness scores in GBM had low fitness scores in NSCs, including JUN and SOX9 (20). This could suggest that GBM-specific gene activation promotes the maintenance of GSCs (20). Stem cell gene networks, similar to those of non-transformed NSCs, generate and maintain GSCs (20).

Proteomic analysis similarly highlights the relationship between NSCs and GSCs (64–71). Of 108 proteins differentially expressed in GSC, NSC, and other tumor tissues, 22 were overexpressed in GSC and NSC but not tumor tissue. Most of these genes are involved in chromatin, mRNA, and DNA processing (64). Pathways necessary for self-renewal properties are common between NSCs and GSCs (66–72). One of the proteins overexpressed in GSCs and NSCs is vimentin (64, 73). Hepatoma-derived growth factor (HDGF), an angiogenesis-promoting factor, is expressed at normal levels in NSCs but is overexpressed and secreted in GSCs (64), indicating a potential oncogenic alteration of a normal NSC process. Overexpression of HDGF is implicated in various cancers (74–80) including GBM (64). In addition to HDGF, other growth factors associated with development are produced in GSCs including vascular endothelial growth factor (VEGF), basic fibroblast growth factor (bFGF), transforming growth factor-alpha (TGFα), and stromal-derived factor 1 (SDF1) (64, 81–84). A study specifically examining chromosome 19 proteins in GSCs found upregulation of multiple molecular patterns related to stemness and development (85). These molecular markers highlight the relationship between NSCs and GSCs, as well as the potential avenues for the transformation of NSCs to GSCs.

# SUBVENTRICULAR ZONE

## Human Subventricular Zone

The SVZ is the largest neural stem cell niche in the adult brain. In humans, the SVZ is divided into four regions comprised of different cell types. The ependymal layer (Layer I) is the cellular layer closest to the ventricle common to all areas of SVZ within the brain. The hypocellular layer (Layer II) borders the ependymal layer and consists of basal processes of ependymal cells, astrocyte processes, and diffuse astrocyte cell bodies. Opposite the hypocellular gap from the ependymal layer is the astrocytic ribbon of cells (Layer III). This is the proliferative region where astrocyte-like cells act as stem cells (33, 86). Layer IV is the transitional zone to the brain parenchyma. Myelinated neuronal processes and neuron bodies are abundant in this area (87) (**Figure 1**). The cytoarchitecture of the human SVZ is unlike any other studied mammals. Cell types present in this region include astrocytes, NSCs, neurons, ependymal cells, oligodendrocytes, OPCs, and neuroblasts with transitory amplifying progenitors noticeably missing (39). The human subventricular zone is unique in its organization and cellular composition making it difficult to translate research from animals to humans.

## Subventricular Zone in Humans vs. Subventricular Zone in Animals

Structurally, the SVZ in studied animals differs quite significantly from the human SVZ. The SVZ in rodents is not separated into four distinct layers; in fact, no hypocellular zone exists in adult mice (34). The hypocellular zone is only reported in humans and bovines (88), with all other mammalian models having close contact between ependymal cells and NSCs (35). Another unique characteristic of the human SVZ is the astrocytic ribbon containing proliferative cells previously thought to be NSCs (33, 89). No progenitor cells or migration has been observed from this region, calling into question the activity of these "NSCs" (89). However, when cultured *in vitro*, astrocytes from



**FIGURE 1** | A schematic illustration depicting a coronal view of the subventricular zone (SVZ) neurogenic niche in the adult human brain.
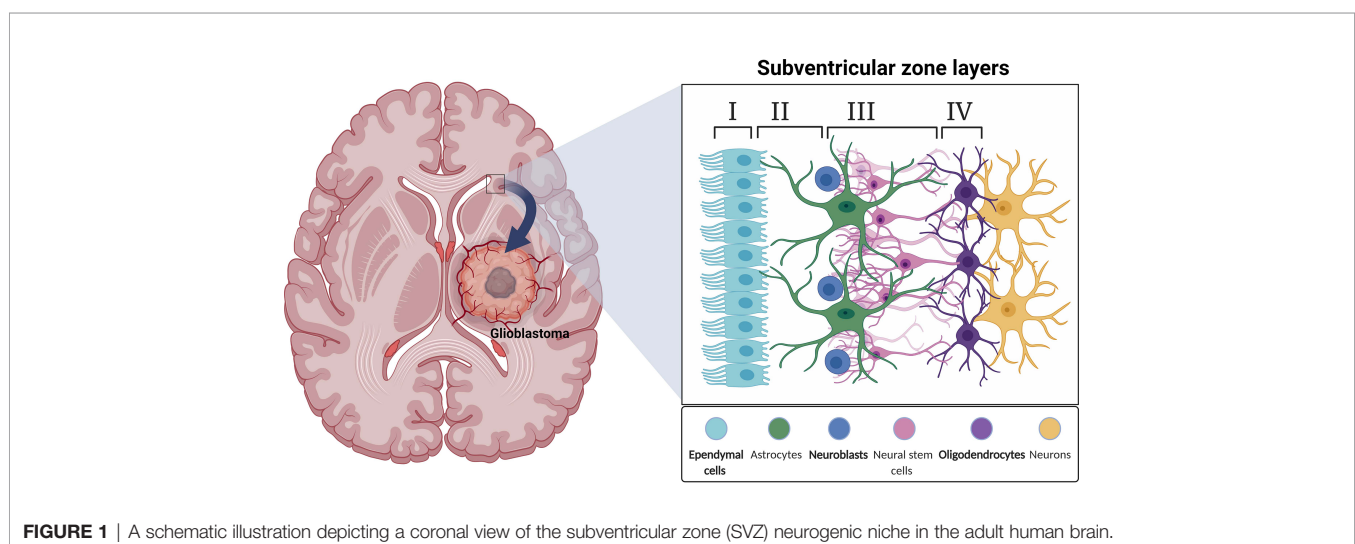
this region have the capacity to form neurospheres consisting of astrocytes, oligodendrocytes, and neurons (90) potentially indicative of function in the human SVZ. Regardless of function, the astrocytic ribbon is an aspect of the SVZ unique to humans.

Cytoarchitecture also differs. The rodent SVZ includes four cell types based on electron microscopic analysis of ultrastructural characteristics. Unlike in humans, the only cell types are astrocytes, transitory amplifying progenitors (type C cells), neuroblasts, neurons, and ependymal cells (35, 91). NSCs have a radial morphology similar to radial glial cells, their predecessors. NSCs are capable of giving rise to type C cells (29) and ependymal cells (92, 93). Type C cells, located near the blood vessels, are rapidly dividing cells that give rise to OPCs, neuroblasts and astrocytes (94–98). Neuroblasts migrate from the SVZ to the olfactory bulb (OB) where they can undergo neurogenesis (27, 99–101). The rodent SVZ is characterized by a much higher number of neurons than the human SVZ (33, 35, 87). The number of proliferating cells in the human SVZ is also much lower than that seen in rodents (33, 87, 102). While the rodent SVZ has more neuroblasts and increased proliferation, GFAP+, nestin+ radial glia observed in the human third ventricle SVZ are absent from the corresponding third ventricle SVZ in mice (34). Lastly, the rodent SVZ contains chains of migrating neuroblasts, which the human SVZ lacks (103). Migration from the SVZ in adult humans remains controversial (33, 58, 102, 104). In postnatal humans, migration from the SVZ occurs but quickly declines (105). In addition to the rostral migratory stream, a medial migratory stream was identified in humans leading from the SVZ to the prefrontal cortex (58). The medial migratory stream is absent from postnatal mice (58). In rodents, neural progenitor cells differentiate into local interneurons, granule cells, and periglomerular cells after migrating to the OB (106–110). Despite a much lower rate of neurogenesis, the adult human SVZ retains the ability to regenerate neurons (58, 111, 112). Neurogenesis in the SVZ can be regulated by GABAergic, dopaminergic, serotonergic, cholinergic, and nitric oxide-releasing neurons (113–116). Specific circumstances, including depression and Parkinson's disease, increase neurogenesis from insignificant to noticeable levels (117, 118).

Studies over the past five decades have demonstrated cellular proliferation in the SVZ in multiple species including mice, rats, rabbits, voles, dogs, cows, monkeys, and humans (33, 87, 88, 119–126). Rodent and other model SVZs share characteristics with the human SVZ, yet there are structural and functional differences (127). One major difference is the destination of new neurons from the SVZ. In humans, the rostral migratory stream contains only a small number of migratory neuroblasts that do not form the chains observed in rodents. These neuroblasts express immature neuron and proliferation signals similar to those in rodents but do not migrate to the OB, a major destination for neuroblasts in rodents and monkeys (119). Carbon 14 analysis of cells in the human OB confirms negligible post-developmental neuronal proliferation in this area (128). Rather, the striatum seems a much more likely target for neuroblast migration in humans. Located adjacent to

the SVZ, the striatum has cells co-expressing the neuroblast markers DCX and PSA-NCAM, indicating migration to this region (129). Carbon dating of a subpopulation of DARP23-negative interneurons in striatum demonstrates a 2.7% turnover rate, significantly higher than that of the OB (< 1% over 100 years). Furthermore, recently developed striatal neurons and neuroblasts co-express the markers calretinin and neuropeptide Y, supporting an SVZ origin for striatal neurogenesis (129). Other animals demonstrate decreased striatal neurogenesis compared to humans (130–135). Research in mice found Notch-dependent local astrocyte-mediated neurogenesis in the striatum (136). It is unclear the extent to which this occurs in humans (135). These differences highlight the challenges involved with translating animal research to humans in this area.

## Additional Elements of the Subventricular Zone

The following elements of the SVZ have been established in non-human mammals, but the extent to which they are present in the human SVZ is unclear. The SVZ stem cell niche is comprised of various cellular and acellular components along with the major cell types. Blood vessels influence differentiation and migration patterns in this niche. Brain-derived neurotropic factor (BDNF) signaling guides neuroblast migration parallel to blood vessels adjacent to the SVZ (92, 137, 138). The SVZ has a leaky blood-brain barrier, permitting neural progenitor cells (NPCs) of the SVZ to respond to signals in the blood more readily (95). SVZ cells are drawn to blood vessels by molecules secreted by endothelial cells (139). Endothelial cells also promote neuroblast proliferation (94, 95, 140) and influence cell migration to and from the niche through SDF1/CXCR4 signaling (139). An extensive basal lamina contacts nearly every cell in the SVZ providing an avenue for molecular signaling to the entire niche (141, 142). These extracellular matrix structures, called fractones, bind growth factors and modulate NSC proliferation in the SVZ (143). Fractones are fractal-like structures consisting of laminins, collagens II and XVIII, nidogen, HSPGs, and perlecan (143). Laminin constructs both NSC and cancer stem cell (CSC) niches (144, 145) and supports stem cell renewal (146). Additionally, laminin interaction with integrin α-6 is important for the maintenance of NSCs and CSCs (147). Non-stem tumor cells produce laminin α-2, which permits GBM stem cell growth (148).

Macro-structure of the SVZ also facilitates signaling and subsequent cellular responses. Viewed from the ventral surface, the SVZ is organized in pinwheel structural units composed of ependymal cells spiraled around astrocytic processes. Cells in the pinwheels are connected by adherens junctions. Adherens junctions allow one daughter cell to remain a stem cell while the other differentiates into a progenitor. The pinwheel structure is important for stem cell proliferation and is characteristic of other stem cell niches in the body (149).

Gliogenesis is prominent in the developing SVZ from embryonic day (E) 90 until after E125. The SVZ serves as the origin of many of the glial cells in the mammalian brain (150–152). Studies examining multiple sclerosis and the rodent

OB indicate that gliogenesis in the SVZ continues in adults (153, 154) and evidence indicates that injury in the adult brain leads to increased gliogenesis from the SVZ (155, 156). Galectin-3 (Gal-3), up-regulated in brain injury, inflammation, and cancer, has a suggested role in modulating both neurogenesis and gliogenesis in the adult SVZ (157).

# NEURAL STEM CELLS IN THE SUBVENTRICULAR ZONE IMPLICATION IN THE ORIGIN OF GLIOBLASTOMA

## Subventricular Zone Neural Stem Cells Play a Role in Tumorigenesis

Genomic and proteomic analyses of GBM and the SVZ have supported an association between the two. Recent molecular and genetic analysis of human GBM by Lee et al. (38) backs the theory that GBM develops from NSCs in the SVZ. They described direct molecular and genetic evidence from glioblastoma patients' tissue and mouse models that there were astrocyte-like NSCs in the SVZ that could be the cell of origin. These cells contain the main driver mutations known to form GBM in humans. In their experiment, they performed sequencing of patient-matched tissues types (normal SVZ tissue, tumor tissue, and normal brain cortex or blood) from 28 patients with variable genetic profiles including isocitrate dehydrogenase-1 wild type (IDH-WT). They concluded that low-level driver mutations of GBM were present in the non-tumor SVZ tissue in 56.3% of IDH wild-type patients. Furthermore, single-cell sequencing and laser microdissection analysis of the obtained brain tissue as well as genome editing of their mouse model showed astrocyte-like NSCs carry driver mutations that lead to the development of high-grade gliomas (38). Additionally, extensive analysis of 28 tumors from both adults and children by Neftel et al. (158), indicates the presence of four cellular states that drive GBM malignant cells heterogeneity. These cellular states are associated with cycling cells representing mostly NPC-like and OPC-like states, particularly in pediatric tumors. Earlier reports of lineage tracing methods (159) also revealed significant aberrant growth prior to malignancy in OPCs. These findings suggest OPCs could be the major source of malignancy though initial mutations could occur in NSCs. This highlights the importance of analyzing premalignant stages to identify the cancer cell of origin.

SVZ-related markers, such as GFAP and vimentin, are upregulated in GBM (160). This association supports the hypothesis that tumor cells in GBM are most related to the SVZ cells (160). Specifically, neuroblasts in GBM contain high levels of c-Myc, implicating the population of SVZ cells with high c-Myc expression in oncogenic transformation (160). In fact, overexpression of c-Myc may play a role in tumorigenesis and migration as it is expressed in SVZ cells with migratory potential (160).

Furthermore, restriction of proteases in GBM inhibits tumorigenesis, providing support for the theory of long-distance migration of GBM pathogenesis. Genomic

investigation of SVZ-associated GBM supports this analysis, identifying genes commonly altered in SVZ and GBM (161). Differences between SVZ+ (SVZ-associated GBM) and SVZ- (Non-SVZ-associated GBM) GBM have also been observed (161). Notch signaling upregulation in SVZ+ GBM is correlated with Notch upregulation in the SVZ. The differential expression of various Notch signaling molecules is associated with predictable prognostic factors, including overall survival (OS) and progression-free survival (PFS) (162).

Proteome analysis of SVZ+ serum and tissue shows increased acute-phase proteins, lipid carrying proteins, and increased regulatory proteins potentially implicated in increased SVZ+ aggressiveness (163). CD133 expression, which is associated with a shorter time to distant recurrence, is greater in SVZ+ tumors (determined by imaging) than in SVZ- tumors (164). Additionally, the prognosis for GBM is strongly associated with the intracranial location in relation to the SVZ. Tumors contacting the SVZ have worse OS and PFS compared to more distant GBM (165). Furthermore, recurrence of GBM is significantly associated with neurogenic regions (12). The niche factors secreted by the SVZ promote proliferation and migration of GBM progenitor cells, promoting tumor growth and progression (166, 167). In contrast, the hippocampus is often spared from GBM invasion, possibly due to a less compatible extracellular matrix (ECM) (168). Furthermore, NSCs in the hippocampus are less likely involved in tumorigenesis. There are a few factors that differentiate NSCs in the SVZ from hippocampal NSCs in the subgranular zone (SGZ). Like NSCs in the SVZ, hippocampal NSCs have an apical process that contacts blood vessels; however, their basal process contacts neurons and glial cells (169, 170). These stem cells lack CSF contact which is normally a source of factors moderating proliferation for NSCs in the SVZ (25, 171). Abnormal signaling from the CSF is a potential mechanism for malignant transformation (25). Additionally, NSCs in the SGZ only differentiate into local granule neurons. The SGZ niche promotes differentiation without migration, whereas the SVZ promotes proliferation and migration while restricting differentiation (25).

Commonalities of GSCs and NSCs in the SVZ include nestin expression, proliferation capability, high motility, diverse progeny, association with vasculature, and communication with other niche components (25, 172). Much like NSCs (173, 174), GSCs rely on endothelial cells for factors promoting self-renewal, tumorigenicity, and survival (175–177). GSCs are also able to recruit microglia through cytokine production (178–180), which in turn promote tumor growth through angiogenesis and trophic factors (181). Much like in the tumor niche, NSCs and microglia regulate each other in the SVZ (182). Additionally, astrocytes and ECM proteins support the proliferation of both GSCs and NSCs (183–186). These similarities highlight the likeness the tumor niche displays for the SVZ. One notable difference is the lack of CSF within close proximity to cells within the tumor niche, which may contribute to the tumor pathology due to absence of regulation from CSF signaling (25).

Tumorigenesis experimentation in mice supports the theory that GBM-like invasive tumors originate in the SVZ. High-grade tumors are formed from NSCs/NPCs in mouse models after

migration. Migration occurs following the leader cell creation of an infiltrative path. Most infiltrations occur along blood vessels, fiber tracts, or over the surface *via* the subarachnoid space (187). In mice, SVZ cell migration occurs through the rostral migratory stream to many areas including the OB, hippocampus, and striatum. These cells have more migratory potential than other NPC niches, traveling further and to more locations (153). Neuroblasts have been identified in high numbers between the SVZ and the tumor in mice models, indicating SVZ cell migration to the tumor. Upregulation of neural precursors in the ipsilateral SVZ in mice with tumors contributes to this hypothesis (188). Follistatin secretion from NPCs decreases tumor growth and can even inhibit tumor growth *in vitro* (189). Follistatin expression by NPCs in the SVZ may explain why migration occurs before tumorigenesis. Neural precursor cell migration from the SVZ to the tumor zone is a critical finding in the pathogenesis of GBM tumors. This pathway represents an important target of future therapy and more models are needed to further investigate this relationship.

## Common Genes Implicated in Glioblastoma Play a Role in the Subventricular Zone

There are several common mutations associated with human GBM. Primary GBM is classified by *de novo* mutations without evidence of a prior lesion (160). Primary GBM typically results from epidermal growth factor receptor (EGFR) amplification and loss of PTEN (190), while secondary GBMs result from IDH1 or IDH2 mutations (191, 192). Inactivation of TP53 (23), PTEN (193), and mutations in telomerase reverse transcriptase (TERT) (194, 195) are also commonly thought to contribute to the pathogenesis of GBM. Each of these genes, with the exception of IDH1, is known to be involved in the control of the SVZ NSCs (160). Matarredona and Pastor (25) recently reviewed some of the most common genetic mutations and their involvement in implicating the SVZ in GBM development.

Epidermal Growth Factor (EGF) induces proliferation and inhibits differentiation of NSCs in the SVZ (196–198). Amplification of the EGFR gene has been proposed as a potential mechanism for the development of GBM because of its role in the SVZ (160, 199). Both TP53 and PTEN are tumor suppressor genes. TP53, which modulates cell division, differentiation, and proliferation in the SVZ, is commonly mutated in both primary and secondary GBM (23, 190, 200–202). PTEN is involved in regulating migration, apoptosis, and proliferation for NSCs in the SVZ (203, 204). Knockout of TP53 or PTEN induces proclivity towards oncogenic transformation (193, 205). In adult mammals, telomerase expression is restricted to the OB and the SVZ (206), where it permits the growth and survival of NSCs (207). TERT is frequently upregulated in cancers (208), including more than half of GBMs (194, 209). In a study of human GBM mutations in IDH1 wild-type, the tumor-free SVZ had TERT promoter mutations, suggesting this could be an early mutation in the progression from NSC to GBM (38, 194).

While IDH1 has no known direct influence on the SVZ, IDH1 mutation is correlated with platelet-derived growth factor (PDGF) expression in GBM (210). PDGF promotes the proliferation of NSCs in the SVZ (211). Some other factors and pathways commonly altered in GBM and SVZ include c-Met, FoxO3, the Wnt pathway, and the sonic hedgehog pathway (160, 172, 212–216). These mutations provide strong evidence that SVZ NSCs are the origin of GBM in humans and accentuate pathways that could be targeted with therapeutics.

## Clinical Significance of the Subventricular Zone in Glioblastoma

Understanding the role of the SVZ in GBM provides significant clinical value. Proposed therapy for GBM includes administering radiation to the SVZ to prevent tumor reoccurrence. So far, the reported effect of SVZ irradiation on outcomes in GBM patients has been inconsistent. In a meta-analysis of four studies observing the effects of high vs lose dose radiation on prognosis, increased radiation dose to the ipsilateral SVZ significantly increased PFS while failing to significantly improve OS (217). Irradiation dose to the contralateral SVZ did not significantly improve PFS. Contralateral SVZ radiation dose effect on OS was not analyzed as it did not meet the study's inclusion criteria. Higher cutoffs for "high dose irradiation" in the various studies correlated with increased PFS and OS as compared to lower cutoffs (217). Gupta et al. (218) found increased OS with increased radiation to the ipsilateral SVZ but decreased OS with increased radiation to the contralateral SVZ. Consistent with the results described above, Rizzo et al. (219) showed that increasing bilateral SVZ radiation dose directly correlates with increased PFS and OS. Furthermore, they found that a high radiation dose to the ipsilateral SVZ is associated with increased PFS and that there is no correlation between the dose administered to the contralateral SVZ and OS or PFS (219).

Gross total resection (GTR) may account for some of the variations in the results, as Chen et al. (220) found that high dose irradiation of the SVZ improves PFS only in patients with GTR, not in patients with subtotal resection or biopsy. In patients with GTR, PFS and OS were both improved with high-dose irradiation when compared to low-dose irradiation. This suggests that residual tumors may be responsible for recurrence in irradiated patients without GTR, and therefore, that irradiation may potentially prevent GBM recurrence originating from the SVZ (220). CXCL12 mediated upregulation of mesenchymal traits protects GSCs located in the SVZ from radiation, potentially explaining the increased effectiveness of higher doses of radiation (221). These data point to promising evidence that links radiation of areas of the SVZ to increased measures of survival and highlight the importance of studying GBM in the context of the SVZ. By means of human cerebral organoid SVZ models, we hope to expand on the research that has highlighted this relationship between the SVZ and GBM prognosis (**Figure 2**).

## MODELS

There are several different methods of modeling GBM. Robertson et al. (36) organize GBM models into five separate categories: Patient-derived glioblastoma cell lines are cultured
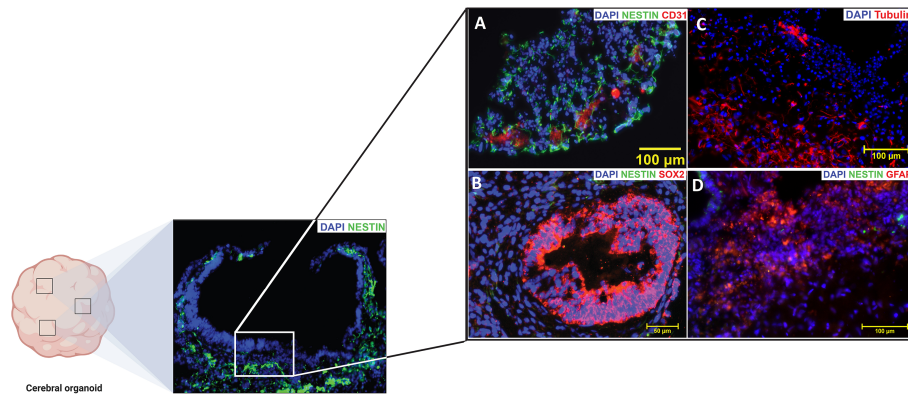
**FIGURE 2** | The subventricular zone (SVZ) of a mature cortical organoid highly resembles the (SVZ) of an adult human brain. Positive immunofluorescence signatures of the common (SVZ) markers are represented in **(A–D)**. NESTIN (Green) is an intermediate filament protein that is expressed by neural stem cells (NSCs) in the subventricular zone (SVZ) and it is generally recognized as a marker of undifferentiated nervous system cells. CD31 [Red, **(A)**] also known as Platelet endothelial cell adhesion molecule-1 (PECAM-1), is a glycoprotein highly expressed on endothelial cells and it is generally recognized as blood vessel markers. SOX-2 [Red, **(B)**] is an HMG-Box transcription factor that is expressed in neural progenitor cells and is considered as a marker of high pluripotency. Beta-Tubulin III [Red, **(C)**] an essential structural protein of the neural microtubule network that correlates with the earliest phases of neuronal differentiation. GFAP [Red, **(D)**] is a marker for the glial fibrillary acidic protein expressed by astrocytes and ependymal cells during development. (Source Zinn lab).

directly from patient tumors; engineered GBM-like cell lines are cells genetically manipulated to represent GBM; *ex vivo* models study animal tissue in relation to GBM; *in vivo* tumor transplantation models involve human tumor implantation in animal models, and genetically engineered mouse models (GEMMs) involve the introduction of GBM through germline genetic manipulation. Organoid models are 3D patient-derived suspensions discussed separately. Each model has unique benefits and drawbacks in the study of GBM.

## Patient-Derived Glioblastoma Cell Lines

*In vitro* models are often the simplest models. They involve culturing and experimenting on cell lines meant to represent GBM. Investigators have the choice of experimenting on widely used highly passaged 'classic' cell lines or patient-derived models such as low passage primary cell lines or tumor tissue slice cultures. The reliability of classically used cell lines, and the tumors they produce, have been called into question because they have assumed a differentiated state that may no longer reflect the GSCs intended to be represented. Tumors resulting from orthotopic transplantation of the classic cell lines that are grown in serum adherent to plates in 2D culture settings, often do not resemble GBM, but rather grow as an encapsulated tumor in the mouse brain, resembling the growth pattern of brain metastasis (65). One of the most popularly studied cell lines, U87MG, is genetically different in many respects and no longer matches the original culture (222, 223). Even without these issues, *in vitro* cell models using classic cell lines, have limited utility for simple mechanistic studies and likely should be moved away from (36, 222, 224).

Unlike classic cell lines, patient-derived GBM cell models retain the genetic and transcriptional state of the parent tumor, when cultured in similar conditions, long term (41, 61, 65, 225, 226). Cultures are deemed viable for long-term self-renewal after 10

passages which equate to at least 2 months in culture and can be frozen for long-term preservation (227). In one study, eight out of nine patient-derived models that lasted at least 8 passages were still viable after 50 passages (228). However, in practice low passage cultures are always archived. Patient-derived GBM cell models were originally grown as neurospheres in suspension culture, but the suspension is not necessary for survival and expansion. Adherent cultures are viable, permitting easier experimentation with these models (147, 229, 230). Additionally, adherent cultures were effective in deriving new cell lines in >90% of cases when using IDH-WT GBM cell lines (36, 224, 226). While adherent cultures are often easier to manipulate and study, suspension cultures can be developed into organoid models. These models are discussed more in a later section.

## Engineered Glioblastoma-Like Cell Lines

GBM can also be engineered *in vitro*. Introduction of driver mutations stepwise into NSCs or other cells, *in vitro*, can cause these cells to transform phenotypically into cancer cells. They can then be transplanted and studied *in vivo* (36). Various methods such as plasmid transfection, lentiviral or retroviral transduction (48), and CRISPR/Cas9 technology (231) are used to induce these mutations and produce a GBM-like phenotype. CRISPR/Cas9 technology enables gene knock-out/in and more precise insertions/deletions compared to previous methods. It also allows for more experimental control through novel genetic screening techniques *in vitro* and *in vivo* (232, 233). CRISPR is effective for genetic manipulation of both human and mouse NSCs and could be used in a variety of future experiments towards this (36, 234). Additionally, it has been used to induce tumorigenesis in organoid models by knocking out tumor suppressor genes. The resulting tumor cells are molecularly similar to GBM and can be implanted into mice to grow into tumors (235, 236).

## *Ex Vivo* Animal Models

*Ex vivo* modeling is a popular neuroscience procedure adapted for GBM study (36, 237). Mice are the most common model due to their short breeding times, relatively low cost, easy genetic manipulation, and mammalian organ systems (36). Both slice culture methods and whole animal models can be studied. Slice culture methods allow an accurate microanatomical analysis of tissue-tumor interaction, which has provided insight into the interaction between GBM and the SVZ (238). However, whole animal models are often necessary as comprehensive disease-relevant models (36). Both tumor cell transplantation and genetically manipulated *de novo* tumors are viable methods of tumor induction of GBM *in vivo*.

## *In Vivo* Tumor Transplantation Models

Tumor cells are directly transplanted into the brain or the skin in *in vivo* tumor transplantation models *via* orthotopic or subcutaneous injections. Orthotopic grafts are preferred due to spatial and temporal selectivity which allows for the induction of similar tumor physiology in multiple mice (36). Some drawbacks of orthotopic grafts include the technical challenge of implantation, lack of control over engraftment and seeding, and disruption of normal tissue architecture where the injury is caused by the injection procedure. Subcutaneous grafts are easier to introduce but lack the specific brain microenvironment and infiltration characteristic of GBM (239). Patient-derived orthotopic xenografts (PDOX) models involve the implantation of human tumor cells into immunocompromised mice, potentially simulating the tumor microenvironment of human GBM (36). Golebiewska et al. (240) reported the generation of a unique set of organoids and patient-derived xenografts of various glioma subtypes and corresponding longitudinal PDOX from primary and recurrent tumors. The model they presented captured a wide spectrum of the molecular genotypes of GBM that highlights the potential of these models for precision medicine. The mutations described in their models include: IDH1, ATRX, TP53, MDM2/4, amplification of EGFR, PDGFRA, MET, CDK4/6, MDM2/4, and of CDKN2A/B deletion, PTCH, and PTEN. With regards to the corresponding PDOX model, they found that it recapitulates the limited genetic evolution of gliomas in patients following treatment. The model they presented showed a clinically relent response to TMZ and targeted therapies and could be used as starting point to develop more advanced models that may help develop a therapeutically effective GBM precision treatment modality.

## Genetically Engineered Mouse Models

GEMMs are created by introducing germline genetic mutations of tumor suppressors and oncogenes. This can occur *via* mutagen exposure (241), Cre-lox recombination (19), lentivirus administration (242), or CRISPR- technology (36, 243). Selective breeding allows for the maintenance of mice litters with reproducible, mutated genotypes that are more susceptible to developing tumors and are useful for experimentation (36). These models provide insight into initiation events and driver mutations for GBM. A GEMM study revealed NF1 as a driver mutation for malignant astrocytoma (244), contributing to the subsequent discovery of NF1 as a driver mutation in GBM (245). Other work with GEMMs supports the theory that GBM derives from NSCs in the SVZ (242, 246–248). These studies found that NSCs are easier to transform to tumor cells than astrocytes are (242, 246, 248) and that expression of an IDH1 mutation in the adult SVZ can model gliomagenesis (247).

## Organoids

Three-dimensional organoid models are some of the most useful models for studying GBM. Lancaster et al. (249) developed the first organoid model in 2013 by creating neuroectoderm tissue from induced pluripotent stem cells (iPSCs) and then suspending this tissue in a rotating bioreactor to enhance growth. These models recapitulate the cellular heterogeneity and structure seen *in vivo* (249). Organoids can either represent a brain structure or a tumor cytoarchitecture by culturing iPSCs or GSCs respectively (250). Eventually, the model develops to contain differentiated cells of various populations, mirroring the microenvironment of the brain, or tumor, structure. Organoid models allow cells representing a large spectrum of differentiation to coexist within a model (250). Additionally, primary tumors are able to grow to size in organoid models allowing expression of necrotic and hypoxic features of human tumors (250). These features can create a relatively realistic experimental model of a tumor in the human context; however, there are limitations to this model system. Cerebral organoid models take months to culture and can be highly variable, as well as often lack functional vasculature or immune responses (36). Despite these drawbacks, we believe human cerebral organoid technology is an excellent adjunct model system to the current models described above. Other models remain important as adherent cultures are used when a more reductionist model is needed and suspension cultures are used when a more comprehensive heterogenic model is necessary.

Azzarelli et al. (37), identified five different methods developed to create organoid models: (1) adding minced GBM specimen to Matrigel (250), (2) culturing extracted tumor into a matrigel-free serum-free environment on an orbital shaker (251), (3) nucleofecting embryonic stem cell brain organoids (235, 236), (4) adding 2D cultured patient-derived GSCs to embryonic stem cell brain organoids (236, 252), (5) and 3D bioprinting of GBM and endothelial cells with added ECM components (253). Preference for 3D organoid models stems from their ability to potentially recapitulate *in vivo* response to therapy more accurately than other models such as 2D cultures and PDOXs (235, 250, 252). Additionally, organoids are advantageous because they are able to culture a heterogeneous population of cells in the same environment (37). This allows CSC heterogeneity and development to be studied in the proper environment surrounded by a heterogeneous population of cells (37, 254). Recent techniques have enabled the creation of organoid models within 1-2 weeks (251), dramatically reducing the previous procedural time of multiple months (235, 236, 250, 252). This time reduction is key for therapeutic relevance because patients may begin treatment 1-2 weeks after surgical resection (37).

Some future challenges for 3D models include maintaining tumor complexity, establishing a microenvironment to mimic

inflammatory responses, and reducing variability (255). A combination of models that takes advantage of each model's strengths may be most beneficial (37). In some cases, tumors were unable to develop despite genetic alterations consistent with pathogenesis (255). Regionalized organoids for the area of origin of a particular tumor may be required to solve this problem (255–258). It follows, that if human cerebral organoids do demonstrate a relatively faithful microarchitecture and presence of various differentiated cell types, that organoids may be an ideal model to study the human SVZ and how it relates to gliomagenesis.

## Subventricular Zone Organoid Models

Organoid models have a variety of uses at various stages of research. Kim et al (259) reasons that organoid research is useful in four capacities: basic research, biobanking, disease modeling, and precision medicine. Given the clinical and basic science evidence supporting an association between the SVZ and GBM, an organoid model that accurately resembles the SVZ would be extremely valuable for the study of GBM. In the basic research sense, such a model may provide a comprehensive picture of gliomagenesis from driver mutations to tumor formation, unlike any other model. Biobanking is critical to improving standardization of study, allowing for research on tumors from patients with naturally developed tumors. Ideally, this model should reliably mimic both structural and cytoarchitectural components of the human SVZ to allow for analysis of the involvement of various niche components in GBM formation and maintenance. Heterogeneity in organoids permits additional factors such as immunologic response to be incorporated to judge their influence on the tumor within the simulated environment (260). Using an SVZ model, therapeutic strategies can be tailored to and tested on tumors in the early stages of development. Organoid models have the advantage of being created using iPSCs from a patient in just a few weeks to allow for the personalization of the treatment regimens for a tumor with specific mutations (261). The SVZ, in particular, is important to study in this context as this is where the earliest

mutations are hypothesized to occur meaning this could be the earliest therapeutic target.

Current regional organoid models for the SVZ have some difficulties for GBM research purposes. The Qian et al. (262) model includes SVZ specific cells but lacks non-neurally differentiated structures important to GBM pathology like vasculature and meninges. Lack of vasculature severely limits the size of the organoid. Hypoxia and the absence of nutrients for cells more than 300-500 µm from the surface result in a necrotic core. Due to size limitations, this model only mirrors the human fetal cerebral cortex up to the second trimester, rendering it ineffective for studying tumor pathology in adults (262). Linkous et al. (252) created a model that includes SVZ zone markers, but for the developing brain only. Additionally, no structural or cytoarchitectural analysis of the region confirms an accurately simulated human SVZ (252). Other cerebral organoid models do not demonstrate the presence of a subventricular zone-like region altogether (235, 236, 250, 251, 253, 263). A model that accurately recapitulates the structure, cytoarchitecture, and molecular patterns of the SVZ is necessary for a more comprehensive understanding of GBM initiation and recurrence (**Figure 3**).

## FINAL REMARKS/CONCLUSION

The recent evidence is in support of NSCs in the SVZ as the cells of origin of GBM, however, the astrocyte dedifferentiation hypothesis has not been rejected and in fact, gliomagenesis can certainly be a combination of oncogenic differentiation and dedifferentiation events. In addition to the site of origin, the SVZ may be involved in the recurrence of GBM as evidenced by improved PFS with radiation therapy to the ipsilateral SVZ (217). Modeling of this region could provide great insight into the pathology of GBM. Such a model could enable therapeutic testing *in vivo*, allowing for the creation of an individualized treatment profile specifically targeting the culprit cells for recurrence (264). Organoid modeling is an all-humanoid and
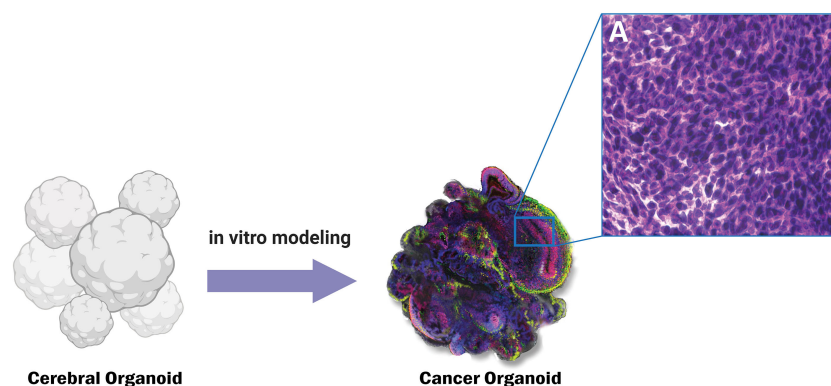


**FIGURE 3** | Genetically engineered cancer organoids show histopathological similarity to CNS tumors such as Glioblastoma. Panel A shows the characteristic histopathological features of cancerous tissue such as increased nuclear to cytoplasmic ratio.

3D system, an intriguing adjunct model system for brain cancers as opposed to xenotransplantation in animal models and 2D cultures (37). In this review we discuss the role of the subventricular zone in glioblastoma genesis, maintenance, and modeling. We also pointed out the potential impact of introducing novel iPSC-based cerebral organoid SVZ models in the study of gliomagenesis. This is an exciting field of research and may lead to a more personalized approach since iPSC-based models can readily be patient-tailored. It is certain that the SVZ in general and particularly its role in cancer is not entirely understood to date; and it will remain of great interest across various fields of study such as neuroscience, neurodegeneration, and cancer research.

## REFERENCES

1. Ostrom QT, Gittleman H, Farah P, Ondracek A, Chen Y, Wolinsky Y, et al. CBTRUS Statistical Report: Primary Brain and Central Nervous System Tumors Diagnosed in the United States in 2006-2010. *Neuro Oncol* (2013) 15:ii1–56. doi: 10.1093/neuonc/not151

2. Louis DN, Perry A, Reifenberger G, von Deimling A, Figarella-Branger D, Cavenee WK, et al. The 2016 World Health Organization Classification of Tumors of the Central Nervous System: A Summary. *Acta Neuropathol* (2016) 131:803–20. doi: 10.1007/s00401-016-1545-1

3. Taylor MD, Poppleton H, Fuller C, Su X, Liu Y, Jensen P, et al. Radial Glia Cells Are Candidate Stem Cells of Ependymoma. *Cancer Cell* (2005) 8:323–35. doi: 10.1016/j.ccr.2005.09.001

4. Castillo M. Stem Cells, Radial Glial Cells, and a Unified Origin of Brain Tumors. *Am J Neuroradiol* (2010) 31:389–90. doi: 10.3174/ajnr.A1674

5. Koshy M, Villano JL, Dolecek TA, Howard A, Mahmood U, Chmura SJ, et al. Improved Survival Time Trends for Glioblastoma Using the SEER 17 Population-Based Registries. *J Neurooncol* (2012) 107:207–12. doi: 10.1007/s11060-011-0738-7

6. Stupp R, Mason WP, van den Bent MJ, Weller M, Fisher B, Taphoorn MJB, et al. Radiotherapy Plus Concomitant and Adjuvant Temozolomide for Glioblastoma. *N Engl J Med* (2005) 352:987–96. doi: 10.1056/NEJMoa043330

7. Bi WL, Beroukhim R. Beating the Odds: Extreme Long-Term Survival With Glioblastoma. *Neuro-Oncology* (2014) 16:1159–60. doi: 10.1093/neuonc/nou166

8. Smoll NR, Schaller K, Gautschi OP. The Cure Fraction of Glioblastoma Multiforme. *Neuroepidemiology* (2012) 39:63–9. doi: 10.1159/000339319

9. Smoll NR, Schaller K, Gautschi OP. Long-Term Survival of Patients With Glioblastoma Multiforme (GBM). *J Clin Neurosci* (2013) 20:670–5. doi: 10.1016/j.jocn.2012.05.040

10. Stupp R, Tonn JC, Brada M, Pentheroudakis G. High-Grade Malignant Glioma: ESMO Clinical Practice Guidelines for Diagnosis, Treatment and Follow-Up. *Ann Oncol* (2010) 21:v190–3. doi: 10.1093/annonc/mdq187

11. Macdonald DR, Kiebert G, Prados M, Yung A, Olson J. Benefit of Temozolomide Compared to Procarbazine in Treatment of Glioblastoma Multiforme at First Relapse: Effect on Neurological Functioning, Performance Status, and Health Related Quality of Life. *Cancer Invest* (2005) 23:138–44. doi: 10.1081/CNV-200050453

12. Chen L, Chaichana KL, Kleinberg L, Ye X, Quinones-Hinojosa A. Glioblastoma Recurrence Patterns Near Neural Stem Cell Regions. *Radiother Oncol* (2015) 116:294–300. doi: 10.1016/j.radonc.2015.07.032

13. Bette S, Barz M, Huber T, Straube C, Schmidt-Graf F, Combs SE, et al. Retrospective Analysis of Radiological Recurrence Patterns in Glioblastoma, Their Prognostic Value and Association to Postoperative Infarct Volume. *Sci Rep* (2018) 8:4561. doi: 10.1038/s41598-018-22697-9

14. Oh J, Sahgal A, Sanghera P, Tsao MN, Davey P, Lam K, et al. Glioblastoma: Patterns of Recurrence and Efficacy of Salvage Treatments. *Can J Neurol Sci* (2011) 38:621–5. doi: 10.1017/S0317167100012166

15. Stupp R, Hegi ME, Mason WP, van den Bent MJ, Taphoorn MJ, Janzer RC, et al. Effects of Radiotherapy With Concomitant and Adjuvant Temozolomide Versus Radiotherapy Alone on Survival in Glioblastoma in a Randomised Phase III Study: 5-Year Analysis of the EORTC-NCIC Trial. *Lancet Oncol* (2009) 10:459–66. doi: 10.1016/S1470-2045(09)70025-7

16. Bastiancich C, Vanvarenberg K, Ucakar B, Pitorre M, Bastiat G, Lagarce F, et al. Lauroyl-Gemcitabine-Loaded Lipid Nanocapsule Hydrogel for the Treatment of Glioblastoma. *J Cont Rel* (2016) 225:283–93. doi: 10.1016/j.jconrel.2016.01.054

17. Pinel S, Thomas N, Boura C, Barberi-Heyob M. Approaches to Physical Stimulation of Metallic Nanoparticles for Glioblastoma Treatment. *Adv Drug Deliv Rev* (2019) 138:344–57. doi: 10.1016/j.addr.2018.10.013

18. Bjerkvig R, Tysnes BB, Aboody KS, Najbauer J, Terzis AJA. The Origin of the Cancer Stem Cell: Current Controversies and New Insights. *Nat Rev Cancer* (2005) 5:899–904. doi: 10.1038/nrc1740

19. Alcantara Llaguno S, Chen J, Kwon C-H, Jackson EL, Li Y, Burns DK, et al. Malignant Astrocytomas Originate From Neural Stem/Progenitor Cells in a Somatic Tumor Suppressor Mouse Model. *Cancer Cell* (2009) 15:45–56. doi: 10.1016/j.ccr.2008.12.006

20. MacLeod G, Bozek DA, Rajakulendran N, Monteiro V, Ahmadi M, Steinhart Z, et al. Genome-Wide CRISPR-Cas9 Screens Expose Genetic Vulnerabilities and Mechanisms of Temozolomide Sensitivity in Glioblastoma Stem Cells. *Cell Rep* (2019) 27:971–86.e9. doi: 10.1016/j.celrep.2019.03.047

21. Wang Y, Yang J, Zheng H, Tomasek GJ, Zhang P, McKeever PE, et al. Expression of Mutant P53 Proteins Implicates a Lineage Relationship Between Neural Stem Cells and Malignant Astrocytic Glioma in a Murine Model. *Cancer Cell* (2009) 15:514–26. doi: 10.1016/j.ccr.2009.04.001

22. Yang ZJ, Ellis T, Markant SL, Read T-A, Kessler JD, Bourboulas M, et al. Medulloblastoma Can Be Initiated by Deletion of Patched in Lineage-Restricted Progenitors or Stem Cells. *Cancer Cell* (2008) 14:135–45. doi: 10.1016/j.ccr.2008.07.003

23. Zheng H, Ying H, Yan H, Kimmelman AC, Hiller DJ, Chen A-J, et al. P53 and Pten Control Neural and Glioma Stem/Progenitor Cell Renewal and Differentiation. *Nature* (2008) 455:1129–33. doi: 10.1038/nature07443

24. Amariglio N, Hirshberg A, Scheithauer BW, Cohen Y, Loewenthal R, Trakhtenbrot L, et al. Donor-Derived Brain Tumor Following Neural Stem Cell Transplantation in an Ataxia Telangiectasia Patient. *PloS Med* (2009) 6:e1000029. doi: 10.1371/journal.pmed.1000029

25. Matarredona ER, Pastor AM. Neural Stem Cells of the Subventricular Zone as the Origin of Human Glioblastoma Stem Cells. Therapeutic Implications. *Front Oncol* (2019) 9:779. doi: 10.3389/fonc.2019.00779

26. Kishi K. Golgi Studies on the Development of Granule Cells of the Rat Olfactory Bulb With Reference to Migration in the Subependymal Layer. *J Comp Neurol* (1987) 258:112–24. doi: 10.1002/cne.902580109

27. Luskin MB. Restricted Proliferation and Migration of Postnatally Generated Neurons Derived From the Forebrain Subventricular Zone. *Neuron* (1993) 11:173–89. doi: 10.1016/0896-6273(93)90281-U

28. Lois C, Alvarez-Buylla A. Long-Distance Neuronal Migration in the Adult Mammalian Brain. *Science* (1994) 264:1145–8. doi: 10.1126/science.8178174

29. Doetsch F, Caillé I, Lim DA, García-Verdugo JM, Alvarez-Buylla A. Subventricular Zone Astrocytes Are Neural Stem Cells in the Adult Mammalian Brain. *Cell* (1999) 97:703–16. doi: 10.1016/S0092-8674(00)80783-7

30. Vescovi AL, Galli R, Reynolds BA. Brain Tumour Stem Cells. *Nat Rev Cancer* (2006) 6:425–36. doi: 10.1038/nrc1889

31. Pilkington GJ. Cancer Stem Cells in the Mammalian Central Nervous System. *Cell Prolif* (2005) 38:423–33. doi: 10.1111/j.1365-2184.2005.00358.x

32. Dirks PB. Brain Tumor Stem Cells: Bringing Order to the Chaos of Brain Cancer. *J Clin Oncol Off J Am Soc Clin Oncol* (2008) 26:2916–24. doi: 10.1200/JCO.2008.17.6792

33. Sanai H, Tramontin AD, Quinones-Hinojosa A, Barbaro NM, Gupta N, Kunwar S, et al. Unique Astrocyte Ribbon in Adult Human Brain Contains Neural Stem Cells But Lacks Chain Migration. *Nature* (2004) 427:740–4. doi: 10.1038/nature02301

34. Dahiya S, Lee DY, Gutmann DH. Comparative Characterization of the Human and Mouse Third Ventricle Germinal Zones. *J Neuropathol Exp Neurol* (2011) 70:622–33. doi: 10.1097/NEN.0b013e31822200aa

35. Doetsch F, Garcìa-Verdugo JM, Alvarez-Buylla A. Cellular Composition and Three-Dimensional Organization of the Subventricular Germinal Zone in the Adult Mammalian Brain. *J Neurosci* (1997) 17:5046–61. doi: 10.1523/JNEUROSCI.17-13-05046.1997

36. Robertson FL, Marqués-Torrejón MA, Morrison GM, Pollard SM. Experimental Models and Tools to Tackle Glioblastoma. *DMM Dis Models Mech* (2019) 12. doi: 10.1242/dmm.040386

37. Azzarelli R. Organoid Models of Glioblastoma to Study Brain Tumor Stem Cells. *Front Cell Dev Biol* (2020) 8. doi: 10.3389/fcell.2020.00220

38. Lee JH, Lee JE, Kahng JY, Kim SH, Park JS, Yoon SJ, et al. Human Glioblastoma Arises From Subventricular Zone Cells With Low-Level Driver Mutations. *Nature* (2018) 560:243–7. doi: 10.1038/s41586-018-0389-3

39. Altmann C, Keller S, Schmidt MHH. The Role of Svz Stem Cells in Glioblastoma. *Cancers (Basel)* (2019) 11:448. doi: 10.3390/cancers11040448

40. Bardella C, Al-Shammari AR, Soares L, Tomlinson I, O'Neill E, Szele FG. The Role of Inflammation in Subventricular Zone Cancer. *Prog Neurobiol* (2018) 170:37–52. doi: 10.1016/j.pneurobio.2018.04.007

41. Singh SK, Clarke ID, Terasaki M, Bonn VE, Hawkins C, Squire J, et al. Identification of a Cancer Stem Cell in Human Brain Tumors. *Cancer Res* (2003) 63:5821–8.

42. Kawamura Y, Takouda J, Yoshimoto K, Nakashima K. New Aspects of Glioblastoma Multiforme Revealed by Similarities Between Neural and Glioblastoma Stem Cells. *Cell Biol Toxicol* (2018) 34:425–40. doi: 10.1007/s10565-017-9420-y

43. Goffart N, Kroonen J, Rogister B. Glioblastoma-Initiating Cells: Relationship With Neural Stem Cells and the Micro-Environment. *Cancers (Basel)* (2013) 5:1049–71. doi: 10.3390/cancers5031049

44. Stiles CD, Rowitch DH. Glioma Stem Cells: A Midterm Exam. *Neuron* (2008) 58:832–46. doi: 10.1016/j.neuron.2008.05.031

45. Lan X, Jorg DJ, Cavalli FMG, Richards LM, Nguyen LV, Vanner RJ, et al. Fate Mapping of Human Glioblastoma Reveals an Invariant Stem Cell Hierarchy. *Nature* (2017) 549:227–32. doi: 10.1038/nature23666

46. Patel AP, Tirosh I, Trombetta JJ, Shalek AK, Gillespie SM, Wakimoto H, et al. Single-Cell RNA-Seq Highlights Intratumoral Heterogeneity in Primary Glioblastoma. *Science (80)* (2014) 344:1396–401. doi: 10.1126/science.1254257

47. Friedmann-Morvinski D, Bushong EA, Ke E, Soda Y, Marumoto T, Singer O, et al. Dedifferentiation of Neurons and Astrocytes by Oncogenes can Induce Gliomas in Mice. *Science (80)* (2012) 338:1080–4. doi: 10.1126/science.1226929

48. Bachoo RM, Maher EA, Ligon KL, Sharpless NE, Chan SS, You MJ, et al. Epidermal Growth Factor Receptor and Ink4a/Arf: Convergent Mechanisms Governing Terminal Differentiation and Transformation Along the Neural Stem Cell to Astrocyte Axis. *Cancer Cell* (2002) 1:269–77. doi: 10.1016/S1535-6108(02)00046-6

49. Krivtsov AV, Twomey D, Feng Z, Stubbs MC, Wang Y, Faber J, et al. Transformation From Committed Progenitor to Leukaemia Stem Cell Initiated by MLL-Af9. *Nature* (2006) 442:818–22. doi: 10.1038/nature04980

50. Das S, Srikanth M, Kessler JA. Cancer Stem Cells and Glioma. *Nat Clin Pract Neurol* (2008) 4:427–35. doi: 10.1038/ncpneuro0862

51. Joyner AL, Zervas M. Genetic Inducible Fate Mapping in Mouse: Establishing Genetic Lineages and Defining Genetic Neuroanatomy in the Nervous System. *Dev Dynamics* (2006) 235:2376–85. doi: 10.1002/dvdy.20884

52. Simitzi C, Ranella A, Stratakis E. Controlling the Morphology and Outgrowth of Nerve and Neuroglial Cells: The Effect of Surface Topography. *Acta Biomater* (2017) 51:21–52. doi: 10.1016/j.actbio.2017.01.023

53. Vessal M, Darian-Smith C. Adult Neurogenesis Occurs in Primate Sensorimotor Cortex Following Cervical Dorsal Rhizotomy. *J Neurosci* (2010) 30:8613–23. doi: 10.1523/JNEUROSCI.5272-09.2010

54. Mitchell BD, Emsley JG, Magavi SSP, Arlotta P, Macklis JD. Constitutive and Induced Neurogenesis in the Adult Mammalian Brain: Manipulation of Endogenous Precursors Toward CNS Repair. *Dev Neurosci* (2004) 26:101–17. doi: 10.1159/000082131

55. Gould E. How Widespread Is Adult Neurogenesis in Mammals? *Nat Rev Neurosci* (2007) 8:481–8. doi: 10.1038/nrn2147

56. Boldrini M, Fulmore CA, Tartt AN, Simeon LR, Pavlova I, Poposka V, et al. Human Hippocampal Neurogenesis Persists Throughout Aging. *Cell Stem Cell* (2018) 22:589–99.e5. doi: 10.1016/j.stem.2018.03.015

57. Fowler CD, Liu Y, Wang Z. Estrogen and Adult Neurogenesis in the Amygdala and Hypothalamus. *Brain Res Rev* (2008) 57:342–51. doi: 10.1016/j.brainresrev.2007.06.011

58. Sanai N, Nguyen T, Ihrie RA, Mirzadeh Z, Tsai H-H, Wong M, et al. Corridors of Migrating Neurons in the Human Brain and Their Decline During Infancy. *Nature* (2011) 478:382–6. doi: 10.1038/nature10487

59. Wang C, Liu F, Liu Y-Y, Zhao C-H, You Y, Wang L, et al. Identification and Characterization of Neuroblasts in the Subventricular Zone and Rostral Migratory Stream of the Adult Human Brain. *Cell Res* (2011) 21:1534–50. doi: 10.1038/cr.2011.83

60. Reya T, Morrison SJ, Clarke MF, Weissman IL. Stem Cells, Cancer, and Cancer Stem Cells. *Nature* (2001) 414:105–11. doi: 10.1038/35102167

61. Galli R, Binda E, Orfanelli U, Cipelletti B, Gritti A, De Vitis S, et al. Isolation and Characterization of Tumorigenic, Stem-Like Neural Precursors From Human Glioblastoma. *Cancer Res* (2004) 64:7011–21. doi: 10.1158/0008-5472.CAN-04-1364

62. Cao F, Hata R, Zhu P, Ma Y-J, Tanaka J, Hanakawa Y, et al. Overexpression of SOCS3 Inhibits Astrogliogenesis and Promotes Maintenance of Neural Stem Cells. *J Neurochem* (2006) 98:459–70. doi: 10.1111/j.1471-4159.2006.03890.x

63. Zhang S. Sox2, a Key Factor in the Regulation of Pluripotency and Neural Differentiation. *World J Stem Cells* (2014) 6:305. doi: 10.4252/wjsc.v6.i3.305

64. Thirant C, Galan-Moya E, Dubois LG, Pinte S, Chafey P, Broussard C, et al. Differential Proteomic Analysis of Human Glioblastoma and Neural Stem Cells Reveals HDGF as a Novel Angiogenic Secreted Factor. *Stem Cells* (2012) 30:845–53. doi: 10.1002/stem.1062

65. Lee J, Kotliarova S, Kotliarov Y, Li A, Su Q, Donin NM, et al. Tumor Stem Cells Derived From Glioblastomas Cultured in bFGF and EGF More Closely Mirror the Phenotype and Genotype of Primary Tumors Than Do Serum-Cultured Cell Lines. *Cancer Cell* (2006) 9:391–403. doi: 10.1016/j.ccr.2006.03.030

66. Gangemi RMR, Griffero F, Marubbi D, Perera M, Capra MC, Malatesta P, et al. SOX2 Silencing in Glioblastoma Tumor-Initiating Cells Causes Stop of Proliferation and Loss of Tumorigenicity. *Stem Cells* (2009) 27:40–8. doi: 10.1634/stemcells.2008-0493

67. Zbinden M, Duquet A, Lorente-Trigos A, Ngwabyt S-N, Borges I. NANOG Regulates Glioma Stem Cells and is Essential *In Vivo* Acting in a Cross-Functional Network With GLI1 and P53. *EMBO J* (2010) 29:2659–74. doi: 10.1038/emboj.2010.137

68. Clement V, Sanchez P, de Tribolet N, Radovanovic I, Ruiz i Altaba A. HEDGEHOG-GLI1 Signaling Regulates Human Glioma Growth, Cancer Stem Cell Self-Renewal, and Tumorigenicity. *Curr Biol* (2007) 17:165–72. doi: 10.1016/j.cub.2006.11.033

69. Bar EE, Chaudhry A, Lin A, Fan X, Schreck K, Matsui W, et al. Cyclopamine-Mediated Hedgehog Pathway Inhibition Depletes Stem-Like Cancer Cells in Glioblastoma. *Stem Cells* (2007) 25:2524–33. doi: 10.1634/stemcells.2007-0166

70. Xu Q, Yuan X, Liu G, Black KL, Yu JS. Hedgehog Signaling Regulates Brain Tumor-Initiating Cell Proliferation and Portends Shorter Survival for

Patients With PTEN-Coexpressing Glioblastomas. *Stem Cells* (2008) 26:3018–26. doi: 10.1634/stemcells.2008-0459

71. Fareh M, Turchi L, Virolle V, Debruyne D, Almairac F, de-la-Forest Divonne S, et al. The miR 302-367 Cluster Drastically Affects Self-Renewal and Infiltration Properties of Glioma-Initiating Cells Through CXCR4 Repression and Consequent Disruption of the SHH-GLI-NANOG Network. *Cell Death Differ* (2012) 19:232–44. doi: 10.1038/cdd.2011.89

72. Hu Q, Zhang L, Wen J, Wang S, Li M, Feng R, et al. The Egf Receptor-Sox2-Egf Receptor Feedback Loop Positively Regulates the Self-Renewal of Neural Precursor Cells. *Stem Cells* (2010) 28:279–86. doi: 10.1002/stem.246

73. Ayuso-Sacido A, Roy NS, Schwartz TH, Greenfield JP, Boockvar JA. Long-Term Expansion of Adult Human Brain Subventricular Zone Precursors. *Neurosurgery* (2008) 62:223–31. doi: 10.1227/01.NEU.0000311081.50648.4C

74. Shetty A, Dasari S, Banerjee S, Gheewala T, Zheng G, Chen A, et al. Hepatoma-Derived Growth Factor: A Survival-Related Protein in Prostate Oncogenesis and a Potential Target for Vitamin K2. *Urol Oncol Semin Orig Investig* (2016) 34:483.e1–8. doi: 10.1016/j.urolonc.2016.05.027

75. Uyama H, Tomita Y, Nakamura H, Nakamori S, Zhang B, Hoshida Y, et al. Hepatoma-Derived Growth Factor Is a Novel Prognostic Factor for Patients With Pancreatic Cancer. *Clin Cancer Res* (2006) 12:6043–8. doi: 10.1158/1078-0432.CCR-06-1064

76. Tsai HE, Wu J-C, Kung M-L, Liu L-F, Kuo L-H, Kuo H-M, et al. Up-Regulation of Hepatoma-Derived Growth Factor Facilities Tumor Progression in Malignant Melanoma. *PloS One* (2013) 8:e59345. doi: 10.1371/journal.pone.0059345

77. Ren H, Tang X, Lee JJ, Feng L, Everett AD, Hong WK, et al. Expression of Hepatoma-Derived Growth Factor Is a Strong Prognostic Predictor for Patients With Early-Stage Non-Small-Cell Lung Cancer. *J Clin Oncol* (2004) 22:3230–7. doi: 10.1200/JCO.2004.02.080

78. Yamamoto S, Tomita Y, Hoshida Y, Takiguchi S, Fujiwara Y, Yasuda T, et al. Expression of Hepatoma-Derived Growth Factor Is Correlated With Lymph Node Metastasis and Prognosis of Gastric Carcinoma. *Clin Cancer Res* (2006) 12:117–22. doi: 10.1158/1078-0432.CCR-05-1347

79. Hu TH, Huang C-C, Liu L-F, Lin P-R, Liu S-Y, Chang H-W, et al. Expression of Hepatoma-Derived Growth Factor in Hepatocellular Carcinoma: A Novel Prognostic Factor. *Cancer* (2003) 98:1444–56. doi: 10.1002/cncr.11653

80. Lin YW, Huang S-T, Wu J-C, Chu T-H, Huang S-C, Lee C-C, et al. Novel HDGF/HIF-1α/VEGF Axis in Oral Cancer Impacts Disease Prognosis. *BMC Cancer* (2019) 19:1083. doi: 10.1186/s12885-019-6229-5

81. Bao S, Wu Q, Sathornsumetee S, Hao Y, Li Z, Hjelmeland AB, et al. Stem Cell-Like Glioma Cells Promote Tumor Angiogenesis Through Vascular Endothelial Growth Factor. *Cancer Res* (2006) 66:7843–8. doi: 10.1158/0008-5472.CAN-06-1010

82. Li G, et al. Autocrine Factors Sustain Glioblastoma Stem Cell Self-Renewal. *Oncol Rep* (2009) 21:419–24. doi: 10.3892/or_00000239

83. Surena AL, de Faria GP, Studler J-M, Peiretti F, Pidoux M, Camonis J, et al. DLG1/SAP97 Modulates Transforming Growth Factor α Bioavailability. *Biochim Biophys Acta - Mol Cell Res* (2009) 1793:264–72. doi: 10.1016/j.bbamcr.2008.09.005

84. Terasaki M, Sugita Y, Arakawa F, Okada Y, Ohshima K, Shigemori M. CXCL12/CXCR4 Signaling in Malignant Brain Tumors: A Potential Pharmacological Therapeutic Target. *Brain Tumor Pathol* (2011) 28:89–97. doi: 10.1007/s10014-010-0013-1

85. Lichti CF, Liu H, Shavkunov AS, Mostovenko E, Sulman EP, Ezhilarasan R, et al. Integrated Chromosome 19 Transcriptomic and Proteomic Data Sets Derived From Glioma Cancer Stem-Cell Lines. *J Proteome Res* (2014) 13:191–9. doi: 10.1021/pr400786s

86. Kam M, Curtis MA, McGlashan SR, Connor B, Nannmark U, Faull RLM. The Cellular Composition and Morphological Organization of the Rostral Migratory Stream in the Adult Human Brain. *J Chem Neuroanat* (2009) 37:196–205. doi: 10.1016/j.jchemneu.2008.12.009

87. Quiñones-Hinojosa A, Sanai N, Soriano-Navarro M, Gonzalez-Perez O, Mirzadeh Z. Cellular Composition and Cytoarchitecture of the Adult Human Subventricular Zone: A Niche of Neural Stem Cells. *J Comp Neurol* (2006) 494:415–34. doi: 10.1002/cne.20798

88. Rodríguez-Pérez LM, Pérez-Martín M, Jiménez AJ, Fernández-Llebrez P. Immunocytochemical Characterisation of the Wall of the Bovine Lateral Ventricle. *Cell Tissue Res* (2003) 314:325–35. doi: 10.1007/s00441-003-0794-1

89. Lim DA, Alvarez-Buylla A. The Adult Ventricular–Subventricular Zone (V-SVZ) and Olfactory Bulb (OB) Neurogenesis. *Cold Spring Harb Perspect Biol* (2016) 8:a018820. doi: 10.1101/cshperspect.a018820

90. Quiñones-Hinojosa A, Sanai N, Gonzalez-Perez O, Garcia-Verdugo JM. The Human Brain Subventricular Zone: Stem Cells in This Niche and Its Organization. *Neurosurg Clin North Am* (2007) 18:15–20. doi: 10.1016/j.nec.2006.10.013

91. García-Verdugo JM, Doetsch F, Wichterle H, Lim DA, Alvarez-Buylla A. Architecture and Cell Types of the Adult Subventricular Zone: In Search of the Stem Cells. *J Neurobiol* (1998) 18:234–48. doi: 10.1002/(SICI)1097-4695(199808)36:2<234::AID-NEU10>3.0.CO;2-E

92. Luo J, Daniels SB, Lennington JB, Notti RQ, Conover JC. The Aging Neurogenic Subventricular Zone. *Aging Cell* (2006) 5:139–52. doi: 10.1111/j.1474-9726.2006.00197.x

93. Luo J, Shook BA, Daniels SB, Conover JC. Subventricular Zone-Mediated Ependyma Repair in the Adult Mammalian Brain. *J Neurosci* (2008) 28:3804–13. doi: 10.1523/JNEUROSCI.0224-08.2008

94. Shen Q, Wang Y, Kokovay E, Lin G, Chuang S-M, Goderie SK, et al. Adult SVZ Stem Cells Lie in a Vascular Niche: A Quantitative Analysis of Niche Cell-Cell Interactions. *Cell Stem Cell* (2008) 3:289–300. doi: 10.1016/j.stem.2008.07.026

95. Tavazoie M, van der Veken L, Silva-Vargas V, Louissaint M, Colonna L, Zaidi B, et al. A Specialized Vascular Niche for Adult Neural Stem Cells. *Cell Stem Cell* (2008) 3:279–88. doi: 10.1016/j.stem.2008.07.025

96. Hu H, Tomasiewicz H, Magnuson T, Rutishauser U. The Role of Polysialic Acid in Migration of Olfactory Bulb Interneuron Precursors in the Subventricular Zone. *Neuron* (1996) 3:279–88. doi: 10.1016/S0896-6273(00)80094-X

97. Wichterle H, García-Verdugo JM, Alvarez-Buylla A. Direct Evidence for Homotypic, Glia-Independent Neuronal Migration. *Neuron* (1997) 18:779–91. doi: 10.1016/S0896-6273(00)80317-7

98. Maki T, Liang AC, Miyamoto N, Lo EH, Arai K. Mechanisms of Oligodendrocyte Regeneration From Ventricular-Subventricular Zone-Derived Progenitor Cells in White Matter Diseases. *Front Cell Neurosci* (2013) 7. doi: 10.3389/fncel.2013.00275

99. Doetsch F, Alvarez-Buylla A. Network of Tangential Pathways for Neuronal Migration in Adult Mammalian Brain. *Proc Natl Acad Sci USA* (1996) 93:14895–900. doi: 10.1073/pnas.93.25.14895

100. Lois C, García-Verdugo JM, Alvarez-Buylla A. Chain Migration of Neuronal Precursors. *Science (80)* (1996) 271:978–81. doi: 10.1126/science.271.5251.978

101. Imayoshi I, Sakamoto M, Ohtsuka T, Takao K, Miyakawa T, Yamaguchi M, et al. Roles of Continuous Neurogenesis in the Structural and Functional Integrity of the Adult Forebrain. *Nat Neurosci* (2008) 11:1153–61. doi: 10.1038/nn.2185

102. Sanai N, Berger MS, Garcia-Verdugo JM, Alvarez-Buylla A. Comment on 'Human Neuroblasts Migrate to the Olfactory Bulb *via* a Lateral Ventricular Extension'. *Science* (2007) 318:393–393. doi: 10.1126/science.1145011

103. Van Strien ME, Van Den Berge SA, Hol EM. Migrating Neuroblasts in the Adult Human Brain: A Stream Reduced to a Trickle. *Cell Res* (2011) 21:1523–5. doi: 10.1038/cr.2011.101

104. Curtis MA, Kam M, Nannmark U, Anderson MF, Axell MZ, Wikkelso C, et al. Human Neuroblasts Migrate to the Olfactory Bulb *via* a Lateral Ventricular Extension. *Science (80)* (2007) 315:1243–9. doi: 10.1126/science.1136281

105. Yang Z, Ming GL, Song H. Postnatal Neurogenesis in the Human Forebrain: From Two Migratory Streams to Dribbles. *Cell Stem Cell* (2011) 9:385–6. doi: 10.1016/j.stem.2011.10.007

106. Lazarini F, Gabellec M-M, Moigneu C, de Chaumont F, Olivo-Marin J-C. Adult Neurogenesis Restores Dopaminergic Neuronal Loss in the Olfactory Bulb. *J Neurosci* (2014) 34:14430–42. doi: 10.1523/JNEUROSCI.5366-13.2014

107. Gheusi G, Lepousez G, Lledo PM. Adult-Born Neurons in the Olfactory Bulb: Integration and Functional Consequences. *Curr Top Behav Neurosci* (2012) 15:49–72. doi: 10.1007/7854_2012_228

108. Sakamoto M, Kageyama R, Imayoshi I. The Functional Significance of Newly Born Neurons Integrated Into Olfactory Bulb Circuits. *Front Neurosci* (2014) 8:121. doi: 10.3389/fnins.2014.00121

109. Merkle FT, Fuentealba LC, Sanders TA, Magno L, Kessaris N, Alvarez-Buylla A. Adult Neural Stem Cells in Distinct Microdomains Generate Previously

Unknown Interneuron Types. *Nat Neurosci* (2014) 17:207–14. doi: 10.1038/nn.3610

110. Alvarez-Buylla A, Garcia-Verdugo JM. Neurogenesis in Adult Subventricular Zone. *J Neurosci* (2002) 22:629–34. doi: 10.1523/JNEUROSCI.22-03-00629.2002

111. Ernst A, Frisén J. Adult Neurogenesis in Humans- Common and Unique Traits in Mammals. *PloS Biol* (2015) 136:e1002045. doi: 10.1371/journal.pbio.1002045

112. Knoth R, Singec I, Ditter M, Pantazis G, Capetian P, Meyer RP, et al. Murine Features of Neurogenesis in the Human Hippocampus Across the Lifespan From 0 to 100 Years. *PloS One* (2010) 5:e8809. doi: 10.1371/journal.pone.0008809

113. Paez-Gonzalez P, Asrican B, Rodriguez E, Kuo CT. Identification of Distinct ChAT+ Neurons and Activity-Dependent Control of Postnatal SVZ Neurogenesis. *Nat Neurosci* (2014) 17:934–42. doi: 10.1038/nn.3734

114. Pilz GA, Jessberger S. ChAT Me Up: How Neurons Control Stem Cells. *Nat Neurosci* (2014) 17:897–8. doi: 10.1038/nn.3746

115. Tong CK, Chen J, Cebrian-Silla A, Mirzadeh Z, Obernier K, CD G, et al. Axonal Control of the Adult Neural Stem Cell Niche. *Cell Stem Cell* (2014) 14:500–11. doi: 10.1016/j.stem.2014.01.014

116. Young SZ, Taylor MM, Bordey A. Neurotransmitters Couple Brain Activity to Subventricular Zone Neurogenesis. *Eur J Neurosci* (2011) 33:1123–32. doi: 10.1111/j.1460-9568.2011.07611.x

117. Huisman E, Uylings HBM, Hoogland PV. A 100% Increase of Dopaminergic Cells in the Olfactory Bulb May Explain Hyposmia in Parkinson's Disease. *Mov Disord* (2004) 19:687–92. doi: 10.1002/mds.10713

118. Maheu ME, Devorak J, Freibauer A, Davoli MA, Turecki G, Mechawar N. Increased Doublecortin (DCX) Expression and Incidence of DCX-Immunoreactive Multipolar Cells in the Subventricular Zone-Olfactory Bulb System of Suicides. *Front Neuroanat* (2015) 9. doi: 10.3389/fnana.2015.00074

119. Kornack DR, Rakic P. The Generation, Migration, and Differentiation of Olfactory Neurons in the Adult Primate Brain. *Proc Natl Acad Sci USA* (2001) 104:423–33. doi: 10.1073/pnas.081074998

120. Blakemore WF. The Ultrastructure of the Subependymal Plate in the Rat. *J Anat* (1969) 217:947–5. doi: 10.1038/217974a0

121. Lewis PD. Mitotic Activity in the Primate Subependymal Layer and the Genesis of Gliomas. *Nature* (1968) 1:69–84. doi: 10.1038/217974a0

122. Blakemore WF, Jolly RD. The Subependymal Plate and Associated Ependyma in the Dog. An Ultrastructural Study. *J Neurocytol* (1972) 57:269–77. doi: 10.1007/BF01098647

123. McDermott KWG, Lantos PL. Cell Proliferation in the Subependymal Layer of the Postnatal Marmoset, Callithrix Jacchus. *Dev Brain Res* (1990) 4:1313–7. doi: 10.1016/0165-3806(90)90053-2

124. Eriksson PS, Perfilieva E, Bjork-Eriksson T, Alborn A-M, Nordborg C, Peterson DA, et al. Neurogenesis in the Adult Human Hippocampus. *Nat Med* (1998) 36:410–20. doi: 10.1038/3305

125. Huang L, DeVries GJ, Bittman EL. Photoperiod Regulates Neuronal Bromodeoxyuridine Labeling in the Brain of a Seasonally Breeding Mammal. *J Neurobiol* (1998) 286:548–52. doi: 10.1002/(SICI)1097-4695(19980905)36:3<410::AID-NEU8>3.0.CO;2-Z

126. Gould E, Reeves AJ, Graziano MSA, Gross CG. Neurogenesis in the Neocortex of Adult Primates. *Science (80)* (1999) 98:4752–7. doi: 10.1126/science.286.5439.548

127. Lenting K, Verhaak R, Ter Laan M, Wesseling P, Leenders W. Glioma: Experimental Models and Reality. *Acta Neuropathol* (2017) 133:263–82. doi: 10.1007/s00401-017-1671-4

128. Bergmann O, Liebl J, Bernard S, Alkass K, Yeung MSY, Steier P, et al. The Age of Olfactory Bulb Neurons in Humans. *Neuron* (2012) 74:634–9. doi: 10.1016/j.neuron.2012.03.030

129. Ernst A, Alkass K, Bernard S, Salehpour M, Perl S, Tisdale J, et al. Neurogenesis in the Striatum of the Adult Human Brain. *Cell* (2014) 156:1072–83. doi: 10.1016/j.cell.2014.01.044

130. Bédard A, Cossette M, Lévesque M, Parent A. Proliferating Cells can Differentiate Into Neurons in the Striatum of Normal Adult Monkey. *Neurosci Lett* (2002) 328:213–6. doi: 10.1016/S0304-3940(02)00530-X

131. Dayer AG, Cleaver KM, Abouantoun T, Cameron HA. New GABAergic Interneurons in the Adult Neocortex and Striatum Are Generated From

132. Tonchev AB, Yamashima T, Sawamoto K, Okano H. Enhanced Proliferation of Progenitor Cells in the Subventricular Zone and Limited Neuronal Production in the Striatum and Neocortex of Adult Macaque Monkeys After Global Cerebral Ischemia. *J Neurosci Res* (2005) 81:776–88. doi: 10.1002/jnr.20604

133. Luzzati F, De Marchis S, Fasolo A, Peretto P. Neurogenesis in the Caudate Nucleus of the Adult Rabbit. *J Neurosci* (2006) 26:609–21. doi: 10.1523/JNEUROSCI.4371-05.2006

134. Inta D, Alfonso J, von Engelhardt J, Kreuzberg MM, Meyer AH, van Hooft JA, et al. Neurogenesis and Widespread Forebrain Migration of Distinct GABAergic Neurons From the Postnatal Subventricular Zone. *Proc Natl Acad Sci USA* (2008) 105:20994–9. doi: 10.1073/pnas.0807059105

135. Bergmann O, Spalding KL, Frisén J. Adult Neurogenesis in Humans. *Cold Spring Harb Perspect Med* (2015) 7:a018994. doi: 10.1101/cshperspect.a018994

136. Magnusson JP, Goritz C, Tatarishvili J, DO D, Smith EMK, Lindvall O, et al. A Latent Neurogenic Program in Astrocytes Regulated by Notch Signaling in the Mouse. *Science (80)* (2014) 346:237–41. doi: 10.1126/science.346.6206.237

137. Baker KL, Daniels SB, Lennington JB, Lardaro T, Czap A, Notti RQ, et al. Neuroblast Protuberances in the Subventricular Zone of the Regenerative MRL/MpJ Mouse. *J Comp Neurol* (2006) 498:747–61. doi: 10.1002/cne.21090

138. Snapyan M, Lemasson M, Brill MS, Blais M, Massouh M, Ninkovic J, et al. Vasculature Guides Migrating Neuronal Precursors in the Adult Mammalian Forebrain *via* Brain-Derived Neurotrophic Factor Signaling. *J Neurosci* (2009) 29:4172–88. doi: 10.1523/JNEUROSCI.4956-08.2009

139. Kokovay E, Goderie S, Wang Y, Lotz S, Lin G, Sun Y, et al. Adult Svz Lineage Cells Home to and Leave the Vascular Niche *via* Differential Responses to SDF1/CXCR4 Signaling. *Cell Stem Cell* (2010) 7:163–173. doi: 10.1016/j.stem.2010.05.019

140. Shen Q, Goderie SK, Jin L, Karanth N, Sun Y, Abramova N, et al. Endothelial Cells Stimulate Self-Renewal and Expand Neurogenesis of Neural Stem Cells. *Science (80)* (2004) 7:163–73. doi: 10.1126/science.1095505

141. Kerever A, Schnack J, Vellinga D, Ichikawa N, Moon C, Arikawa-Hirasawa E, et al. Novel Extracellular Matrix Structures in the Neural Stem Cell Niche Capture the Neurogenic Factor Fibroblast Growth Factor 2 From the Extracellular Milieu. *Stem Cells* (2007) 25:2146–51. doi: 10.1634/stemcells.2007-0082

142. Mercier F, Kitasako JT, Hatton GI. Anatomy of the Brain Neurogenic Zones Revisited: Fractones and the Fibroblast/Macrophage Network. *J Comp Neurol* (2002) 451:170–88. doi: 10.1002/cne.10342

143. Mercier F. Fractones: Extracellular Matrix Niche Controlling Stem Cell Fate and Growth Factor Activity in the Brain in Health and Disease. *Cell Mol Life Sci* (2016) 73:4661–74. doi: 10.1007/s00018-016-2314-y

144. Lathia JD, Patton B, Eckley DM, Magnus T, Mughal MR, Sasaki T, et al. Patterns of Laminins and Integrins in the Embryonic Ventricular Zone of the CNS. *J Comp Neurol* (2007) 505:630–43. doi: 10.1002/cne.21520

145. Belousov A, Titov S, Shved N, Garbuz M, Malykin G, Gulaia V, et al. The Extracellular Matrix and Biocompatible Materials in Glioblastoma Treatment. *Front Bioeng Biotechnol* (2019) 7. doi: 10.3389/fbioe.2019.00341

146. Imbeault S, Gauvin LG, Toeg HD, Pettit A, Sorbara CD, Migahed L, et al. The Extracellular Matrix Controls Gap Junction Protein Expression and Function in Postnatal Hippocampal Neural Progenitor Cells. *BMC Neurosci* (2009) 10:13. doi: 10.1186/1471-2202-10-13

147. Sun Y, et al. Long-Term Tripotent Differentiation Capacity of Human Neural Stem (NS) Cells in Adherent Culture. *Mol Cell Neurosci* (2008) 38:245–58. doi: 10.1016/j.mcn.2008.02.014

148. Lathia JD, Li M, Hall PE, Gallagher J, Hale JS, Wu Q, et al. Laminin Alpha 2 Enables Glioblastoma Stem Cell Growth. *Ann Neurol* (2012) 72:766–78. doi: 10.1002/ana.23674

149. Mirzadeh Z, Merkle FT, Soriano-Navarro M, Garcia-Verdugo JM, Alvarez-Buylla A. Neural Stem Cells Confer Unique Pinwheel Architecture to the Ventricular Surface in Neurogenic Regions of the Adult Brain. *Cell Stem Cell* (2008) 3:265–78. doi: 10.1016/j.stem.2008.07.004

150. Rash BG, Duque A, Morozov YM, Arellano JI, Micali N, Rakic P. Gliogenesis in the Outer Subventricular Zone Promotes Enlargement and Gyrification of

Different Precursors. *J Cell Biol* (2005) 168:415–27. doi: 10.1083/jcb.200407053

the Primate Cerebrum. *Proc Natl Acad Sci USA* (2019) 116:7089–94. doi: 10.1073/pnas.1822169116

151. Azevedo FAC, Carvalho LRB, Grinberg LT, Farfel JM, Ferretti REL, Leite REP, et al. Equal Numbers of Neuronal and Nonneuronal Cells Make the Human Brain an Isometrically Scaled-Up Primate Brain. *J Comp Neurol* (2009) 513:532–41. doi: 10.1002/cne.21974

152. Gabi M, Collins CE, Wong P, Torres LB, Kaas JH, Herculano-Houzel S. Cellular Scaling Rules for the Brains of an Extended Number of Primate Species. *Brain Behav Evol* (2010) 76:32–44. doi: 10.1159/000319872

153. Aguirre A, Gallo V. Postnatal Neurogenesis and Gliogenesis in the Olfactory Bulb From NG2-Expressing Progenitors of the Subventricular Zone. *J Neurosci* (2004) 24:10530–41. doi: 10.1523/JNEUROSCI.3572-04.2004

154. Nait-Oumesmar B, Picard-Riéra N, Kerninon C, Baron-Van Evercooren A. The Role of SVZ-Derived Neural Precursors in Demyelinating Diseases: From Animal Models to Multiple Sclerosis. *J Neurol Sci* (2008) 265:26–31. doi: 10.1016/j.jns.2007.09.032

155. Christie KJ, Turnley AM. Regulation of Endogenous Neural Stem/Progenitor Cells for Neural Repair - Factors That Promote Neurogenesis and Gliogenesis in the Normal and Damaged Brain. *Front Cell Neurosci* (2012) 6. doi: 10.3389/fncel.2012.00070

156. Romanko MJ, et al. Roles of the Mammalian Subventricular Zone in Cell Replacement After Brain Injury. *Prog Neurobiol* (2004) 74:77–99. doi: 10.1016/j.pneurobio.2004.07.001

157. Al-Dalahmah O, Campos Soares L, Nicholson J, Draijer S, Mundim M, Lu VM, et al. Galectin-3 Modulates Postnatal Subventricular Zone Gliogenesis. *Glia* (2020) 68:435–50. doi: 10.1002/glia.23730

158. Neftel C, Laffy J, Filbin MG, Hara T, Shore ME, Rahme GJ, et al. An Integrative Model of Cellular States, Plasticity, and Genetics for Glioblastoma. *Cell* (2019) 178:835–49.e21. doi: 10.1016/j.cell.2019.06.024.

159. Liu C, Sage JC, Miller MR, Verhaak RGW, Hippenmeyer S, Vogel H, et al. Mosaic Analysis With Double Markers Reveals Tumor Cell of Origin in Glioma. *Cell* (2011) 146:209–21. doi: 10.1016/j.cell.2011.06.014

160. Haskins WE, Zablotsky BL, Foret MR, Ihrie RA, Alvarez-Buylla A, Eisenman RN, et al. Molecular Characteristics in MRI-Classified Group 1 Glioblastoma Multiforme. *Front Oncol* (2013) 3. doi: 10.3389/fonc.2013.00182

161. Lin C-HA, Rhodes CT, Lin C, Phillips JJ, Berger MS. Comparative Analyses Identify Molecular Signature of MRI-Classified SVZ-Associated Glioblastoma. *Cell Cycle* (2017) 16:765–75. doi: 10.1080/15384101.2017.1295186

162. Jungk C, Mock A, Exner J, Geisenberger C, Warta R, Capper D, et al. Spatial Transcriptome Analysis Reveals Notch Pathway-Associated Prognostic Markers in IDH1 Wild-Type Glioblastoma Involving the Subventricular Zone. *BMC Med* (2016) 14:1–16. doi: 10.1186/s12916-016-0710-7

163. Gollapalli K, Ghantasala S, Kumar S, Srivastava R, Rapole S, Moiyadi A, et al. Subventricular Zone Involvement in Glioblastoma – A Proteomic Evaluation and Clinicoradiological Correlation. *Sci Rep* (2017) 7:1449. doi: 10.1038/s41598-017-01202-8

164. Yamaki T, Shibahra I, Matsuda K, Kanemura Y, Konta T, Kanamori M, et al. Relationships Between Recurrence Patterns and Subventricular Zone Involvement or CD133 Expression in Glioblastoma. *J Neurooncol* (2020) 146:489–99. doi: 10.1007/s11060-019-03381-y

165. Adeberg S, Bostel T, Konig L, Welzel T, Debus J, Combs SE. A Comparison of Long-Term Survivors and Short-Term Survivors With Glioblastoma, Subventricular Zone Involvement: A Predictive Factor for Survival? *Radiat Oncol* (2014) 9:95. doi: 10.1186/1748-717X-9-95

166. Willard N, Kleinschmidt-DeMasters BK. Massive Dissemination of Adult Glioblastomas. *Clin Neuropathol* (2015) 34:310–42. doi: 10.5414/NP300882

167. Iacoangeli M, Rienzo D, Colasanti R, Gladi M, Alvaro L, et al. Endoscopy-Verifed Occult Subependymal Dissemination of Glioblastoma and Brain Metastasis Undetected by MRI: Prognostic Significance. *Onco Targets Ther* (2012) 5:449. doi: 10.2147/OTT.S39429

168. Mughal AA, Zhang L, Fayzullin A, Server A, Li Y, Wu Y, et al. Patterns of Invasive Growth in Malignant Gliomas—The Hippocampus Emerges as an Invasion-Spared Brain Region. *Neoplasia (United States)* (2018) 20:643–56. doi: 10.1016/j.neo.2018.04.001

169. Palmer TD, Willhoite AR, Gage FH. Vascular Niche for Adult Hippocampal Neurogenesis. *J Comp Neurol* (2000) 425:479–94. doi: 10.1002/1096-9861(20001002)425:4<479::AID-CNE2>3.0.CO;2-3

170. Seri B, García-Verdugo JM, Collado-Morente L, McEwen BS, Alvarez-Buylla A. Cell Types, Lineage, and Architecture of the Germinal Zone in the Adult Dentate Gyrus. *J Comp Neurol* (2004) 478:359–78. doi: 10.1002/cne.20288

171. Codega P, Silva-Vargas V, Paul A, Maldonado-Soto AR, DeLeo AM, Pastrana E, et al. Prospective Identification and Purification of Quiescent Adult Neural Stem Cells From Their *In Vivo* Niche. *Neuron* (2014) 82:545–559. doi: 10.1016/j.neuron.2014.02.039

172. Sanai N, Alvarez-Buylla A, Berger MS. Neural Stem Cells and the Origin of Gliomas. *N Engl J Med* (2005) 353:811–22. doi: 10.1056/nejmra043666

173. Goldman SA, Chen Z. Perivascular Instruction of Cell Genesis and Fate in the Adult Brain. *Nat Neurosci* (2011) 14:1382–9. doi: 10.1038/nn.2963

174. Goldberg JS, Hirschi KK. Diverse Roles of the Vasculature Within the Neural Stem Cell Niche. *Regener Med* (2009) 4:879–97. doi: 10.2217/rme.09.61

175. Zhu TS, Costello MA, Talsma CE, Flack CG, Crowley JG, Hamm LL, et al. Endothelial Cells Create a Stem Cell Niche in Glioblastoma by Providing NOTCH Ligands That Nurture Self-Renewal of Cancer Stem-Like Cells. *Cancer Res* (2011) 71:6061–72. doi: 10.1158/0008-5472.CAN-10-4269

176. Infanger DW, Cho Y, Lopez BS, Mohanan S, Liu SC, Gursel D, et al. Glioblastoma Stem Cells Are Regulated by Interleukin-8 Signaling in a Tumoral Perivascular Niche. *Cancer Res* (2013) 73:7079–89. doi: 10.1158/0008-5472.CAN-13-1355

177. Galan-Moya EM, Le Guelte A, Lima-Fernandes E, Thirant C, Dwyer J, Bidere N, et al. Secreted Factors From Brain Endothelial Cells Maintain Glioblastoma Stem-Like Cell Expansion Through the mTOR Pathway. *EMBO Rep* (2011) 12:470–6. doi: 10.1038/embor.2011.39

178. Imai Y, Kohsaka S. Intracellular Signaling in M-CSF-Induced Microglia Activation: Role of Iba1. *GLIA* (2002) 40:164–74. doi: 10.1002/glia.10149

179. Held-Feindt J, Hattermann K, Muerkoster SS, Wedderkopp H, Knerlich-Lukoschus F, Ungefroren H, et al. CX3CR1 Promotes Recruitment of Human Glioma-Infiltrating Microglia/Macrophages (GIMs). *Exp Cell Res* (2010) 316:1553–66. doi: 10.1016/j.yexcr.2010.02.018

180. Forstreuter F, Lucius R, Mentlein R. Vascular Endothelial Growth Factor Induces Chemotaxis and Proliferation of Microglial Cells. *J Neuroimmunol* (2002) 132:93–8. doi: 10.1016/S0165-5728(02)00315-6

181. Sarkar S, Yong VW. The Battle for the Brain. *Oncoimmunology* (2014) 3: e28047. doi: 10.4161/onci.28047

182. Matarredona ER, Talaverón R, Pastor AM. Interactions Between Neural Progenitor Cells and Microglia in the Subventricular Zone: Physiological Implications in the Neurogenic Niche and After Implantation in the Injured Brain. *Front Cell Neurosci* (2018) 12. doi: 10.3389/fncel.2018.00268

183. Ulrich TA, De Juan Pardo EM, Kumar S. The Mechanical Rigidity of the Extracellular Matrix Regulates the Structure, Motility, and Proliferation of Glioma Cells. *Cancer Res* (2009) 69:4167–74. doi: 10.1158/0008-5472.CAN-08-4859

184. Hallal S, Mallawaaratchy DM, Wei H, Ebrahimkhani S, Stringer BW, Day BW, et al. Extracellular Vesicles Released by Glioblastoma Cells Stimulate Normal Astrocytes to Acquire a Tumor-Supportive Phenotype *via* P53 and MYC Signaling Pathways. *Mol Neurobiol* (2019) 56:4566–81. doi: 10.1007/s12035-018-1385-1

185. Gengatharan A, Bammann RR, Saghatelyan A. The Role of Astrocytes in the Generation, Migration, and Integration of New Neurons in the Adult Olfactory Bulb. *Front Neurosci* (2016) 10:149. doi: 10.3389/fnins.2016.00149

186. Theocharidis U, Long KCharles ffrench-Constant, , Faissner A. Regulation of the Neural Stem Cell Compartment by Extracellular Matrix Constituents. *Prog Brain Res* (2014) 3–28. doi: 10.1016/B978-0-444-63486-3.00001-3

187. Sampetrean O, Saga I, Nakanishi M, Sugihara E, Fukaya R, Onishi N, et al. Invasion Precedes Tumor Mass Formation in a Malignant Brain Tumor Model of Genetically Modified Neural Stem Cells. *Neoplasia* (2011) 13:784–91. doi: 10.1593/neo.11624

188. Bexell D, Gunnarsson S, Nordquist J, Bengzon J. Characterization of the Subventricular Zone Neurogenic Response to Rat Malignant Brain Tumors. *Neuroscience* (2007) 147:824–32. doi: 10.1016/j.neuroscience.2007.04.058

189. Staflin K, Zuchner T, Honeth G, Darabi A, Lundberg C. Identification of Proteins Involved in Neural Progenitor Cell Targeting of Gliomas. *BMC Cancer* (2009) 9:206. doi: 10.1186/1471-2407-9-206

190. Ohgaki H, Kleihues P. Genetic Pathways to Primary and Secondary Glioblastoma. *Am J Pathol* (2007) 170:1445–53. doi: 10.2353/ajpath.2007.070011

191. Nobusawa S, Watanabe T, Kleihues P, Ohgaki H. IDH1 Mutations as Molecular Signature and Predictive Factor of Secondary Glioblastomas. *Clin Cancer Res* (2009) 15:6002–7. doi: 10.1158/1078-0432.CCR-09-0715

192. Ohgaki H, Kleihues P. The Definition of Primary and Secondary Glioblastoma. *Clin Cancer Res* (2013) 19:764–72. doi: 10.1158/1078-0432.CCR-12-3002

193. Duan S, Yuan G, Liu X, Ren R, Li J, Zhang W, et al. PTEN Deficiency Reprogrammes Human Neural Stem Cells Towards a Glioblastoma Stem Cell-Like Phenotype. *Nat Commun* (2015) 6:10068. doi: 10.1038/ncomms10068

194. Brennan CW, Verhaak RGW, McKenna A, Campos B, Noushmehr H, Salama SR, et al. The Somatic Genomic Landscape of Glioblastoma. *Cell* (2013) 155:462–77. doi: 10.1016/j.cell.2013.09.034

195. Killela PJ, Reitman ZJ, Jiao Y, Bettegowda C, Agrawal N, Diaz LA, et al. TERT Promoter Mutations Occur Frequently in Gliomas and a Subset of Tumors Derived From Cells With Low Rates of Self-Renewal. *Proc Natl Acad Sci USA* (2013) 110:6021–6. doi: 10.1073/pnas.1303607110

196. Reynolds BA, Tetzlaff W, Weiss S. A Multipotent EGF-Responsive Striatal Embryonic Progenitor Cell Produces Neurons and Astrocytes. *J Neurosci* (1992) 12:4565–74. doi: 10.1523/jneurosci.12-11-04565.1992

197. Craig CG, Tropepe V, Morshead C, Reynolds B, Weiss S, van der Kooy D. *In Vivo* Growth Factor Expansion of Endogenous Subependymal Neural Precursor Cell Populations in the Adult Mouse Brain. *J Neurosci* (1996) 16:2649–58. doi: 10.1523/jneurosci.16-08-02649.1996

198. Doetsch F, Petreanu L, Caille I, Garcia-Verdugo JM, Alvarez-Buylla A. EGF Converts Transit-Amplifying Neurogenic Precursors in the Adult Brain Into Multipotent Stem Cells. *Neuron* (2002) 36:1021–34. doi: 10.1016/S0896-6273(02)01133-9

199. Wechsler-Reya R, Scott MP. The Developmental Biology of Brain Tumors. *Annu Rev Neurosci* (2001) 24:385–428. doi: 10.1146/annurev.neuro.24.1.385

200. Van Lookeren Campagne M, Gill R. Tumor-Suppressor P53 Is Expressed in Proliferating and Newly Formed Neurons of the Embryonic and Postnatal Rat Brain: Comparison With Expression of the Cell Cycle Regulators P21 (Waf1/Cip1), P27(Kip1), P57(Kip2), P16(Ink4a), Cyclin G1, and the Proto-Oncoge. *J Comp Neurol* (1998) 397:181–98. doi: 10.1002/(SICI)1096-9861(19980727)397:2<181::AID-CNE3>3.0.CO;2-X

201. Gil-Perotin S. Loss of P53 Induces Changes in the Behavior of Subventricular Zone Cells: Implication for the Genesis of Glial Tumors. *J Neurosci* (2006) 34:1040–52. doi: 10.1523/JNEUROSCI.3970-05.2006

202. Gil-Perotin S, Haines JD, Kaur J, Marin-Husstege M, Spinetta MJ, Kim K-H, et al. Roles of P53 and P27 Kip1 in the Regulation of Neurogenesis in the Murine Adult Subventricular Zone. *Eur J Neurosci* (2011) 34:1040–52. doi: 10.1111/j.1460-9568.2011.07836.x

203. Li L, Liu F, Salmonsen RA, Turner TK, Litofsky NS, Di Cristofano A, et al. PTEN in Neural Precursor Cells: Regulation of Migration, Apoptosis, and Proliferation. *Mol Cell Neurosci* (2002) 20:21–9. doi: 10.1006/mcne.2002.1115

204. Li L, Liu F, Ross AH. PTEN Regulation of Neural Development and CNS Stem Cells. *J Cell Biochem* (2003) 88:24–8. doi: 10.1002/jcb.10312

205. Leonard JR, D'Sa C, Klocke BJ, Roth KA. Neural Precursor Cell Apoptosis and Glial Tumorigenesis Following Transplacental Ethyl-Nitrosourea Exposure. *Oncogene* (2001) 20:8281–6. doi: 10.1038/sj.onc.1205024

206. Caporaso GL, Lim DA, Alvarez-Buylla A, Chao MV. Telomerase Activity in the Subventricular Zone of Adult Mice. *Mol Cell Neurosci* (2003) 23:693–702. doi: 10.1016/S1044-7431(03)00103-9

207. Ferrón S, Mira H, Franco S, Cano-Jaimez M, Bellmunt E, Ramirez C, et al. Telomere Shortening and Chromosomal Instability Abrogates Proliferation of Adult But Not Embryonic Neural Stem Cells. *Development* (2004) 131:4059–70. doi: 10.1242/dev.01215

208. Mocellin S, Pooley KA, Nitti D. Telomerase and the Search for the End of Cancer. *Trends Mol Med* (2013) 19:125–33. doi: 10.1016/j.molmed.2012.11.006

209. Vinagre J, Almeida A, Populo H, Batista R, Lyra J, Pinto V, et al. Frequency of TERT Promoter Mutations in Human Cancers. *Nat Commun* (2013) 4:2185. doi: 10.1038/ncomms3185

210. Cantanhede IG, De Oliveira JRM. PDGF Family Expression in Glioblastoma Multiforme: Data Compilation From Ivy Glioblastoma Atlas Project Database. *Sci Rep* (2017) 7:15271. doi: 10.1038/s41598-017-15045-w

211. Jackson EL, Garcia-Verdugo JM, Gil-Perotin S, Roy M, Quinones-Hinojosa A. Pdgfrα-Positive B Cells Are Neural Stem Cells in the Adult SVZ That Form Glioma-Like Growths in Response to Increased PDGF Signaling. *Neuron* (2006) 51:187–99. doi: 10.1016/j.neuron.2006.06.012

212. Alvarez-Palazuelos E, Robles-Cervantes MS, Castillo-Velazquez G, Rivas-Souza M, Guzman-Muniz J, Moy-Lopez N, et al. Regulation of Neural Stem Cells in the Human SVZ by Trophic and Morphogenic Factors. *Curr Signal Transduction Ther* (2011) 6:320–6. doi: 10.2174/157436211797483958

213. Nicoleau C, Benzakour O, Agasse F, Thiriet N, Petit J, Prestoz L, et al. Endogenous Hepatocyte Growth Factor Is a Niche Signal for Subventricular Zone Neural Stem Cell Amplification and Self-Renewal. *Stem Cells* (2009) 27:408–19. doi: 10.1634/stemcells.2008-0226

214. Ohba S, Yamada Y, Murayama K, Sandika E, Sasaki H, Yamada S, et al. C-Met Expression Is a Useful Marker for Prognosis Prediction in IDH-Mutant Lower-Grade Gliomas and IDH-Wildtype Glioblastomas. *World Neurosurg* (2019) 126:e1042–9. doi: 10.1016/j.wneu.2019.03.040

215. Renault VM, Rafalski VA, Morgan AA, Salih DAM, Brett JO, Webb AE, et al. FoxO3 Regulates Neural Stem Cell Homeostasis. *Cell Stem Cell* (2009) 5:527–39. doi: 10.1016/j.stem.2009.09.014

216. Qian Z, Ren L, Wu D, Yang X, Zhou Z, Nie Q, et al. Overexpression of FoxO3a Is Associated With Glioblastoma Progression and Predicts Poor Patient Prognosis. *Int J Cancer* (2017) 140:2792–804. doi: 10.1002/ijc.30690

217. Şuşman S, Leucuţa DC, Kacso G, Florian ŞI. High Dose vs Low Dose Irradiation of the Subventricular Zone in Patients With Glioblastoma—A Systematic Review and Meta-Analysis. *Cancer Manage Res* (2019) 11:6741–53. doi: 10.2147/CMAR.S206033

218. Gupta T, Nair V, Paul SN, Kannan S, Moiyadi A, Epari S, et al. Can Irradiation of Potential Cancer Stem-Cell Niche in the Subventricular Zone Influence Survival in Patients With Newly Diagnosed Glioblastoma? *J Neurooncol* (2012) 109:195–203. doi: 10.1007/s11060-012-0887-3

219. Rizzo AE, Yu J, Suh J, Emch T, Murphy E, Ahluwalia M, et al. Investigating the Relationship Between Radiation Dose to Neural Stem Cell Niches and Survival in GBM. *Int J Radiat Oncol* (2014) 90:S283–4. doi: 10.1016/j.ijrobp.2014.05.965

220. Chen L, Quinones-Hinojosa A, Ford E, McNutt T, Kleinberg L, Lim M, et al. Increased Radiation Dose to the SVZ Improves Survival in Patients With GBM. *Int J Radiat Oncol* (2012) 84:S8. doi: 10.1016/j.ijrobp.2012.07.027

221. Goffart N, Lombard A, Lallemand F, Kroonen J, Nassen J, Di Valentin E, et al. CXCL12 Mediates Glioblastoma Resistance to Radiotherapy in the Subventricular Zone. *Neuro Oncol* (2017) 19:66–77. doi: 10.1093/neuonc/now136

222. Allen M, Bjerke M, Edlund H, Nelander S, Westermark B. Origin of the U87MG Glioma Cell Line: Good News and Bad News. *Sci Transl Med* (2016) 8. doi: 10.1126/scitranslmed.aaf6853

223. Pontén J, Macintyre EH. Long Term Culture of Normal and Neoplastic Human Glia. *Acta Pathol Microbiol Scand* (1968) 74:465–86. doi: 10.1111/j.1699-0463.1968.tb03502.x

224. Xie Y, Bergstrom T, Jiang Y, Johansson P, Marinescu VD, Lindberg N, et al. The Human Glioblastoma Cell Culture Resource: Validated Cell Models Representing All Molecular Subtypes. *EBioMedicine* (2015) 2:1351–63. doi: 10.1016/j.ebiom.2015.08.026

225. Hemmati HD, Nakano I, Lazareff JA, Masterman-Smith M, Geschwind DH, Bronner-Fraser M, et al. Cancerous Stem Cells can Arise From Pediatric Brain Tumors. *Proc Natl Acad Sci USA* (2003) 100:15178–83. doi: 10.1073/pnas.2036535100

226. Pollard SM, Yoshikawa K, Clarke ID, Danovi D, Stricker S, Russell R, et al. Glioma Stem Cell Lines Expanded in Adherent Culture Have Tumor-Specific Phenotypes and Are Suitable for Chemical and Genetic Screens. *Cell Stem Cell* (2009) 4:568–80. doi: 10.1016/j.stem.2009.03.014

227. Hasselbach LA, Irtenkauf SM, Lemke NW, Nelson KK, Berezovsky AD, Carlton ET, et al. Optimization of High Grade Glioma Cell Culture From Surgical Specimens for Use in Clinically Relevant Animal Models and 3D Immunochemistry. *J Vis Exp* (2014) 85:e51088. doi: 10.3791/51088

228. Günther HS, Schmidt NO, Phillips HS, Kemming D, Kharbanda S, Soriano R, et al. Glioblastoma-Derived Stem Cell-Enriched Cultures Form Distinct

Subgroups According to Molecular and Phenotypic Criteria. *Oncogene* (2008) 27:2897–09. doi: 10.1038/sj.onc.1210949

229. Conti L, Pollard SM, Gorba T, Reitano E, Toselli M, Biella G, et al. Niche-Independent Symmetrical Self-Renewal of a Mammalian Tissue Stem Cell. *PLoS Biol* (2005) 3:e283. doi: 10.1371/journal.pbio.0030283

230. Pastrana E, Silva-Vargas V, Doetsch F. Eyes Wide Open: A Critical Review of Sphere-Formation as an Assay for Stem Cells. *Cell Stem Cell* (2011) 8:486–98. doi: 10.1016/j.stem.2011.04.007

231. Bressan RB, Dewari PS, Kalantzaki M, Gangoso E, Matjusaitis M, Garcia-Diaz C, et al. Efficient CRISPR/cas9-Assisted Gene Targeting Enables Rapid and Precise Genetic Manipulation of Mammalian Neural Stem Cells. *Development* (2017) 144:635–48. doi: 10.1242/dev.140855

232. Chow RD, Guzman CD, Wang G, Schmidt F, Youngblood MW, Ye L, et al. AAV-Mediated Direct *In Vivo* CRISPR Screen Identifies Functional Suppressors in Glioblastoma. *Nat Neurosci* (2017) 20:1329–41. doi: 10.1038/nn.4620

233. Toledo CM, Ding Y, Hoellerbauer P, Davis RJ, Basom R, Girard EJ, et al. Genome-Wide CRISPR-Cas9 Screens Reveal Loss of Redundancy Between PKMYT1 and WEE1 in Glioblastoma Stem-Like Cells. *Cell Rep* (2015) 13:2425–39. doi: 10.1016/j.celrep.2015.11.021

234. Choi PS, Meyerson M. Targeted Genomic Rearrangements Using CRISPR/Cas Technology. *Nat Commun* (2014) 5:3728. doi: 10.1038/ncomms4728

235. Bian S, Repic M, Guo Z, Kavirani A, Burkard T, Bagley JA, et al. Genetically Engineered Cerebral Organoids Model Brain Tumor Formation. *Nat Methods* (2018) 15:631–9. doi: 10.1038/s41592-018-0070-7

236. Ogawa J, Pao GM, Shokhirev MN, Verma IM. Glioblastoma Model Using Human Cerebral Organoids. *Cell Rep* (2018) 23:1220–9. doi: 10.1016/j.celrep.2018.03.105

237. Humpel C. Organotypic Brain Slice Cultures: A Review. *Neuroscience* (2015) 305:86–98. doi: 10.1016/j.neuroscience.2015.07.086

238. Marques-Torrejon MA, Gangoso E, Pollard SM. Modelling Glioblastoma Tumour-Host Cell Interactions Using Adult Brain Organotypic Slice Co-Culture. *Dis Model Mech* (2018) 11. doi: 10.1242/dmm.031435

239. Liu F, Hon GC, Villa GR, Turner KM, Ikegami S, Yang H, et al. EGFR Mutation Promotes Glioblastoma Through Epigenome and Transcription Factor Network Remodeling. *Mol Cell* (2015) 60:307–18. doi: 10.1016/j.molcel.2015.09.002

240. Golebiewska A, Hau A-C, Oudin A, Stieber D, Yabo YA, Baus V, et al. Patient-Derived Organoids and Orthotopic Xenografts of Primary and Recurrent Gliomas Represent Relevant Patient Avatars for Precision Oncology. *Acta Neuropathol* (2020) 140:919–49. doi:10.1007/s00401-020-02226-7

241. Schiffer D, Giordana MT, Pezzotta S, Lechner C, Paoletti P. Cerebral Tumors Induced by Transplacental ENU: Study of the Different Tumoral Stages, Particularly of Early Proliferations. *Acta Neuropathol* (1978) 41:27–31. doi: 10.1007/BF00689553

242. Marumoto T, Tashiro A, Friedmann-Morvinski D, Scadeng M, Soda Y, Gage FH, et al. Development of a Novel Mouse Glioma Model Using Lentiviral Vectors. *Nat Med* (2009) 15:110–16. doi: 10.1038/nm.1863

243. Pathania M, De Jay N, Maestro N, Harutyunyan AS, Nitarska J, Pahlavan P, et al. H3.3K27M Cooperates With Trp53 Loss and PDGFRA Gain in Mouse Embryonic Neural Progenitor Cells to Induce Invasive High-Grade Gliomas. *Cancer Cell* (2017) 32:110–16. doi: 10.1016/j.ccell.2017.09.014

244. Zhu Y, Guignard F, Zhao D, Liu L, Burns DK, Mason RP, et al. Early Inactivation of P53 Tumor Suppressor Gene Cooperating With NF1 Loss Induces Malignant Astrocytoma. *Cancer Cell* (2005) 8:119–30. doi: 10.1016/j.ccr.2005.07.004

245. McLendon R, Friedman A, Bigner D, Van Meir EG, Brat DJ, Mastrogianakis GM, et al. Comprehensive Genomic Characterization Defines Human Glioblastoma Genes and Core Pathways. *Nature* (2008) 455:1061–8. doi: 10.1038/nature07385

246. Chow LML, Endersby R, Zhu X, Rankin S, Qu C, Zhang J, et al. Cooperativity Within and Among Pten, P53, and Rb Pathways Induces High-Grade Astrocytoma in Adult Brain. *Cancer Cell* (2011) 19:305–16. doi: 10.1016/j.ccr.2011.01.039

247. Bardella C, Al-Dalahmah O, Krell D, Brazauskas P, Al-Qahtani K, Tomkova M, et al. Expression of Idh1R132H in the Murine Subventricular Zone Stem

Cell Niche Recapitulates Features of Early Gliomagenesis. *Cancer Cell* (2016) 30:578–94. doi: 10.1016/j.ccell.2016.08.017

248. Jacques TS, Swales A, Brzozowski MJ, Henriquez NV, Linehan JM, Mirzadeh Z, et al. Combinations of Genetic Mutations in the Adult Neural Stem Cell Compartment Determine Brain Tumour Phenotypes. *EMBO J* (2010) 29:222–35. doi: 10.1038/emboj.2009.327

249. Lancaster MA, Renner M, Martin C-A, Wenzel D, Bicknell LS, Hurles ME, et al. Cerebral Organoids Model Human Brain Development and Microcephaly. *Nature* (2013) 501:373–9. doi: 10.1038/nature12517

250. Hubert CG, Rivera M, Spangler LC, Wu Q, Mack SC, Prager BC, et al. A Three-Dimensional Organoid Culture System Derived From Human Glioblastomas Recapitulates the Hypoxic Gradients and Cancer Stem Cell Heterogeneity of Tumors Found *In Vivo*. *Cancer Res* (2016) 76:2465–77. doi: 10.1158/0008-5472.CAN-15-2402

251. Jacob F, Salinas RD, Zhang DY, Nguyen PTT, Schnoll JG, Wong SZH, et al. A Patient-Derived Glioblastoma Organoid Model and Biobank Recapitulates Inter- and Intra-Tumoral Heterogeneity. *Cell* (2020) 180:188–204.e22. doi: 10.1016/j.cell.2019.11.036

252. Linkous A, Balamatsias D, Snuderl M, Edwards L, Miyaguchi K, Milner T, et al. Modeling Patient-Derived Glioblastoma With Cerebral Organoids. *Cell Rep* (2019) 26:48–63.e6. doi: 10.1016/j.celrep.2019.02.063

253. Yi HG, Jeong YH, Kim Y, Choi Y-J, Moon HE, Park SH, et al. A Bioprinted Human-Glioblastoma-on-a-Chip for the Identification of Patient-Specific Responses to Chemoradiotherapy. *Nat Biomed Eng* (2019) 3:509–19. doi: 10.1038/s41551-019-0363-x

254. Bhaduri A, Di Lullo E, Jung D, Muller S, Crouch EE, Espinosa CS, et al. Outer Radial Glia-Like Cancer Stem Cells Contribute to Heterogeneity of Glioblastoma. *Cell Stem Cell* (2020) 26:48–63.e6. doi: 10.1016/j.stem.2019.11.015

255. Ballabio C, Anderle M, Gianesello M, Lago C, Miele E, Cardano M, et al. Modeling Medulloblastoma *In Vivo* and With Human Cerebellar Organoids. *Nat Commun* (2020) 11583. doi: 10.1038/s41467-019-13989-3

256. Dias C, Guillemot F. Revealing the Inner Workings of Organoids. *EMBO J* (2017) 36:1299–1301. doi: 10.15252/embj.201796860

257. Muguruma K, Nishiyama A, Kawakami H, Hashimoto K, Sasai Y. Self-Organization of Polarized Cerebellar Tissue in 3D Culture of Human Pluripotent Stem Cells. *Cell Rep* (2015) 10:537–50. doi: 10.1016/j.celrep.2014.12.051

258. Renner M, Lancaster MA, Bian S, Choi H, Ku T, Peer A, et al. Self-Organized Developmental Patterning and Differentiation in Cerebral Organoids. *EMBO J* (2017) 36:1316–29. doi: 10.15252/embj.201694700

259. Kim J, Koo BK, Knoblich JA. Human Organoids: Model Systems for Human Biology and Medicine. *Nat Rev Mol Cell Biol* (2020) 21:571–84. doi: 10.1038/s41580-020-0259-3

260. Chen Z, Hambardzumyan D. Immune Microenvironment in Glioblastoma Subtypes. *Front Immunol* (2018) 9. doi: 10.3389/fimmu.2018.01004

261. Li Y, Tang P, Cai S, Peng J, Hua G. Organoid Based Personalized Medicine: From Bench to Bedside. *Cell Regener* (2020) 9:21. doi: 10.1186/s13619-020-00059-z

262. Qian X, Jacob F, Song MM, Nguyen HN, Song H, Ming G. Generation of Human Brain Region–Specific Organoids Using a Miniaturized Spinning Bioreactor. *Nat Protoc* (2018) 13:565–580. doi: 10.1038/nprot.2017.152

263. da Silva B, Mathew RK, Polson ES, Williams J, Wurdak H. Spontaneous Glioblastoma Spheroid Infiltration of Early-Stage Cerebral Organoids Models Brain Tumor Invasion. *SLAS Discov* (2018) 23:862–8. doi: 10.1177/2472555218764623

264. Plummer S, Wallace S, Ball G, Lloyd R, Schiapparelli P, Quinones-Hinojosa A, et al. A Human iPSC-Derived 3D Platform Using Primary Brain Cancer Cells to Study Drug Development and Personalized Medicine. *Sci Rep* (2019) 9:1407. doi: 10.1038/s41598-018-38130-0

**Publisher's Note:** All claims expressed in this article are solely those of the authors and do not necessarily represent those of their affiliated organizations, or those of the publisher, the editors and the reviewers. Any product that may be evaluated in

# Frontiers in
# Oncology

Advances knowledge of carcinogenesis and tumor progression for better treatment and management

The third most-cited oncology journal, which highlights research in carcinogenesis and tumor progression, bridging the gap between basic research and applications to imrpove diagnosis, therapeutics and management strategies.

## Discover the latest Research Topics

See more →

**frontiers** | Research Topics